THE CA3 REGION OF THE HIPPOCAMPUS: HOW IS IT? WHAT IS IT FOR? HOW DOES IT DO IT?

EDITED BY: Enrico Cherubini and Richard Miles
PUBLISHED IN: Frontiers in Cellular Neuroscience

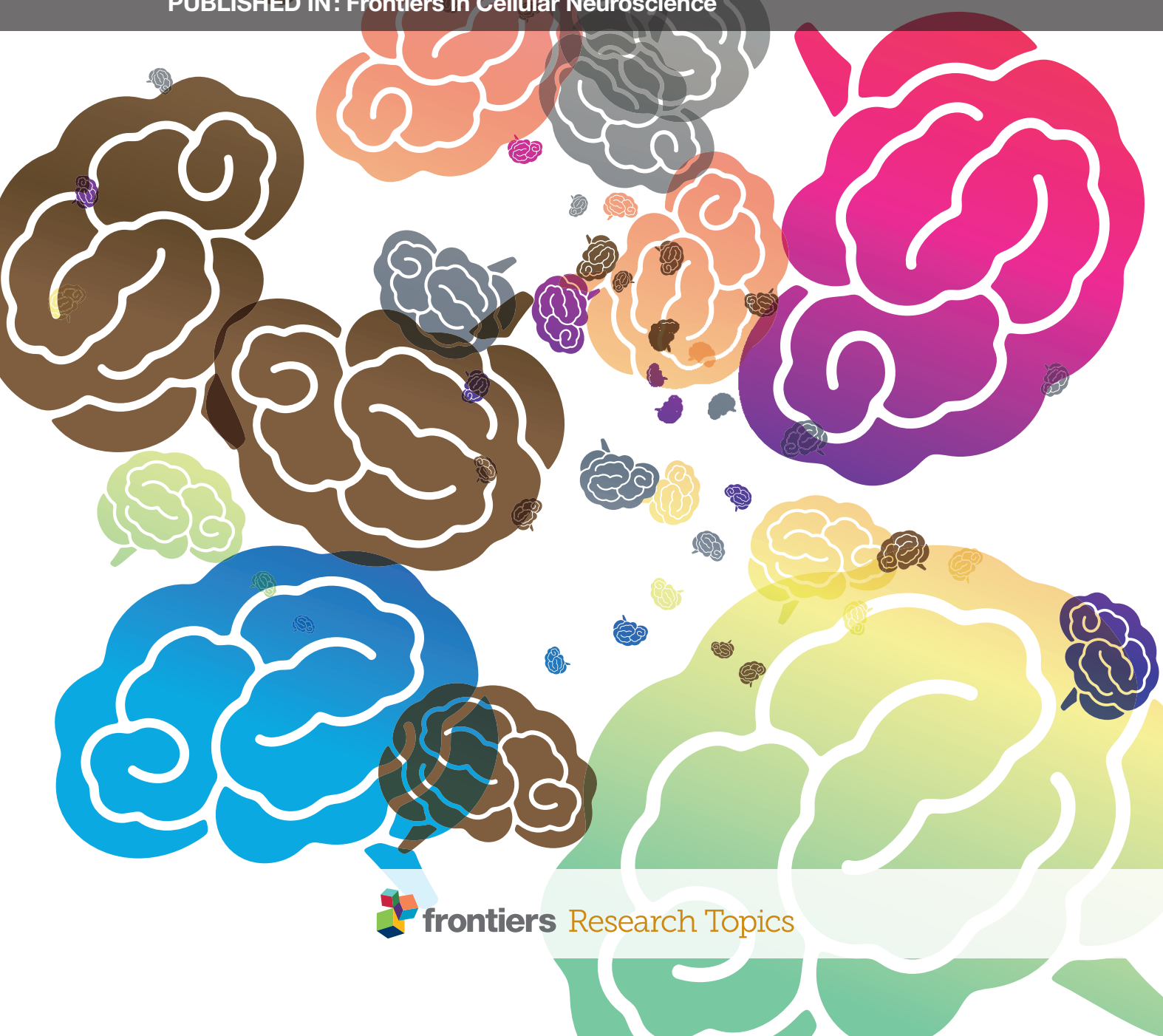

frontiers Research Topics

frontiers

ISSN 1664-8714
ISBN 978-2-88919-631-9
DOI 10.3389/978-2-88919-631-9

About Frontiers

Frontiers is more than just an open-access publisher of scholarly articles: it is a pioneering approach to the world of academia, radically improving the way scholarly research is managed. The grand vision of Frontiers is a world where all people have an equal opportunity to seek, share and generate knowledge. Frontiers provides immediate and permanent online open access to all its publications, but this alone is not enough to realize our grand goals.

Frontiers Journal Series

The Frontiers Journal Series is a multi-tier and interdisciplinary set of open-access, online journals, promising a paradigm shift from the current review, selection and dissemination processes in academic publishing. All Frontiers journals are driven by researchers for researchers; therefore, they constitute a service to the scholarly community. At the same time, the Frontiers Journal Series operates on a revolutionary invention, the tiered publishing system, initially addressing specific communities of scholars, and gradually climbing up to broader public understanding, thus serving the interests of the lay society, too.

Dedication to Quality

Each Frontiers article is a landmark of the highest quality, thanks to genuinely collaborative interactions between authors and review editors, who include some of the world's best academicians. Research must be certified by peers before entering a stream of knowledge that may eventually reach the public - and shape society; therefore, Frontiers only applies the most rigorous and unbiased reviews.
Frontiers revolutionizes research publishing by freely delivering the most outstanding research, evaluated with no bias from both the academic and social point of view.
By applying the most advanced information technologies, Frontiers is catapulting scholarly publishing into a new generation.

What are Frontiers Research Topics?

Frontiers Research Topics are very popular trademarks of the Frontiers Journals Series: they are collections of at least ten articles, all centered on a particular subject. With their unique mix of varied contributions from Original Research to Review Articles, Frontiers Research Topics unify the most influential researchers, the latest key findings and historical advances in a hot research area! Find out more on how to host your own Frontiers Research Topic or contribute to one as an author by contacting the Frontiers Editorial Office: **researchtopics@frontiersin.org**

THE CA3 REGION OF THE HIPPOCAMPUS: HOW IS IT? WHAT IS IT FOR? HOW DOES IT DO IT?

Topic Editors:
Enrico Cherubini, International School for Advanced Studies (SISSA), Trieste, Italy and European Brain Research Institute (EBRI), Rome, Italy
Richard Miles, Institut du Cerveau et de la Moelle, CHU Pitié-Salpêtrière Inserm U1127, CNRS UMR7225, Université Pierre et Marie Curie Paris UMR S1127, France

Citation: Cherubini, E., Miles, R., eds. (2015). The CA3 Region of the Hippocampus: How is it? What is it for? How Does it Do it?. Lausanne: Frontiers Media. doi: 10.3389/978-2-88919-631-9

Table of Contents

frontiers in
CELLULAR NEUROSCIENCE

EDITORIAL
published: 05 February 2015
doi: 10.3389/fncel.2015.00019

The CA3 region of the hippocampus: how is it? What is it for? How does it do it?

Enrico Cherubini*[1,2]* and *Richard Miles*[3]

[1] *Department of Neuroscience, International School for Advanced Studies, Trieste, Italy*
[2] *European Brain Research Institute (EBRI) Rita Levi-Montalcini, Rome, Italy*
[3] *Institut du Cerveau et de la Moelle, CHU Pitié-Salpêtrière Inserm U1127, CNRS UMR7225, Université Pierre et Marie Curie UMR S1127, Paris, France*
**Correspondence: cher@sissa.it; richard.miles@upmc.fr*

Edited and reviewed by:
Egidio D'Angelo, University of Pavia, Italy

Keywords: hippocampus, CA3 subfield, mossy fibers, associative network, theta rhythm, spatial representation, episodic memory, Aβ peptide

The hippocampus, in the temporal lobe, is phylogenetically one of the oldest parts of the brain and forms part of the limbic system. The hippocampus proper is defined by the dentate gyrus and Cornu Ammonis (CA). While the dentate gyrus contains the fascia dentata and the hilus, the CA is anatomically and functionally differentiated into distinct subfields named CA1, CA2, CA3, and CA4. The CA3 region has attracted major attention in recent years for its specific role in memory processes, susceptibility to seizures and neuro-degeneration.

Internal connectivity in the CA3 subfield is more rich than in other hippocampal regions. Recurrent axon collaterals of CA3 pyramidal cells ramify extensively making excitatory contacts with neighboring excitatory and inhibitory neurons (Lorente de Nó, 1934). This circuit is implicated in encoding spatial representations (O'Keefe and Nadel, 1978) and episodic memories (Scoville and Milner, 1957). It generates coherent population synchronies, including gamma, theta and sharp-waves, presumed to associate firing in selected assemblies of cells in different behavioral conditions (Buzsáki et al., 1983). The CA3 region receives inputs from the entorhinal cortex either directly *via* the perforant path or indirectly from the dentate gyrus *via* the mossy fibers (Amaral and Witter, 1983). Mossy fiber connections made with principal or mossy cells terminate with large boutons (5–8 μm) while those with interneurons are targeted by smaller filopodial extensions. The mossy fiber pathway acts as a high-pass filter that translates densely coded cortical signals to a sparse, specific hippocampal code, essential for memory formation.

This e-book aims to highlight recent advances by bringing together experts on the cellular and molecular mechanisms regulating the wiring properties of the CA3 hippocampal microcircuit in both physiological and pathological conditions. The seven reviews and four research articles are organized to follow neuronal information flowing from the dentate gyrus to the CA3 associative network.

Firstly, Münster-Wandowski et al. (2013) (*Inst. Integrative Neuroanatomy, La Charité, Berlin and Instituto Politécnico Nacional, Mexico City*) review recent data showing that MF terminals can transiently release GABA as well as glutamate, both in early post-natal life and after periods of intense activity in adulthood. GABA and glutamate co-release from single identified MF boutons has been recently demonstrated. Mossy fibers apparently form electrical synapses, as well as chemical synapses, with CA3 pyramidal cells potentially permitting a fast excitation to overcome a strong, but delayed, feed-forward inhibition.

Since MF axons of dentate granule cells may be generated post-natally, Pedroni et al. (2014) (*Dept. Neurosci, SISSA, Trieste and European Brain Research Inst, Rome*) studied immature granule cells at P0–P3. At this age, with a clear GABAergic phenotype, granule cells have small somata, few dendritic branches and axons often terminate as growth cones in the CA3 region. Depolarization induces either rudimentary or overshooting sodium spikes and low threshold calcium spikes. Post-synaptic CA3 pyramidal cells participate in spontaneous GDPs driven by synergistic actions of GABA and glutamate. The excitatory actions of GABA released from mossy fiber terminals may be crucial for network synchrony, suggested to refine microcircuits of the CA3 region.

Radial glial cells guide migrating CA3 neurons during development. After characterizing signaling molecules and the temporal sequence of hippocampal development, Belvindrah et al. (2014) (*INSERM U839, Inst. Fer à Moulin, Paris*) review abnormalities of migration linked to human brain malformations: agenesia, lissencephaly, holoprosencephaly, polymicrogyria, heterotopia, and focal cortical dysplasia. Mutations in genes associated with neuronal migration in mouse models result in lamination defects of the CA3 area, a region especially vulnerable to stress and seizure-induced damage. This review links genetic, migration and cellular defects and multiple inherited neurological and psychiatric disorders.

An overview of how CA3 neurons process afferent activity from dentate granule cells is provided by Evstratova and Tóth (2014) (*Dept. Psychiatry and Neuroscience, Université Laval, Quebec City*). They describe how the shape of mossy fiber terminals affects transmission to both CA3 pyramidal cells and interneurons. Transmission exhibits short-term plasticities over different frequencies which vary according to post-synaptic cell type. Granule cells usually fire at 0.01–0.1 Hz, but frequency can increase to 15–50 Hz or even higher when spatial information is coded. At these higher frequencies, glutamate also activates presynaptic autoreceptors, which modulate calcium signaling and release from mossy fiber terminals. These processes, including synaptic plasticity, differ at MF.

Lorente de Nó (1934) suggested that recurrent cortical connections might underly reverberating neuronal discharges as a short-term electrical memory. Le Duigou et al. (2014) (*INSERM U112, Inst. du Cerveau et de la Moelle, Paris*) review recurrent circuits in the CA3 region. CA3 pyramidal cell axons form an associative network associated with sharp waves and other EEG oscillations as well as epileptiform synchrony. Paired records from CA3 pyramidal cells and interneurons have provided data on synaptic contacts and efficacy within recurrent circuits. Connectivity in the associative recurrent CA3 network seems to be spatially more extensive and sparse than in other sensory cortices possibly facilitating representation coding.

Kesner (2013) (*Dept. Psychology, Univ. Utah, Salt Lake City*) reviews contributions from the CA3 region subfields CA3a, b and c in acquiring and encoding spatial information. Mnemonic functions depend on synaptic interactions of CA3 associative networks, operating as an attractor, with inputs from the dentate gyrus and entorhinal cortex (Kesner and Hunsaker, 2010). Fields CA3a and b encode spatial information in short-term memory and also support retrieval by spatial pattern completion. In contrast, the CA3c field may support pattern separation *via* interactions with the DG. The output subfields, CA3a and b process information sequentially communicating with the CA1 region *via* the Schaffer collaterals.

Rolls (2013) (*Centre for Computational Neuroscience, Univ Oxford and Dept. Computer Science, Univ. Warwick*) describes quantitatively how the CA3 region operates and how it contributes to episodic memory. The CA3 system, through its recurrent collateral connections, is presented as a single attractor enabling fast, one trial, associations between any spatial location and an object or reward. A recurrent structure permits memory completion during recall from any subset of acquired links. This theory permits associations between time, objects and rewards to provide the temporal order needed for episodic memory. Neurophysiological tests and supports of the theory are described with novel hypotheses on the advantages of a low recurrent connectivity in CA3.

Cerasti and Treves (2013) (*Cognitive Neuroscience, SISSA, Trieste, Collège de France, Paris and Kavli Inst., Trondheim*) next discuss how self-organizing recurrent connections enable spatial representations to be acquired in the CA3 area. A simplified network model shows that self-organization can lead to the emergence of multiple loosely organized discrete point-like attractors which differ from structures associated with a single, continuous attractor.

The pivotal role of the CA3 region in humans is discussed by Deuker et al. (2014) (*Dept. Epileptology and Center for Neurodegenerative Diseases Univ. Bonn and Donders Inst., Univ. Nijmegen*). They describe how the human CA3 region forms associations during encoding and how during retrieval it reconstructs memory representations with pattern separation and completion based on partial cues (Deuker et al., 2013). Functional properties of different hippocampal subfields can be identified with high resolution fMRI and related to behavioral, and structural alterations associated with mild cognitive impairment in early Alzheimer's disease.

Spatial information is encoded by the phase of principal cell firing during theta oscillations. The hyperpolarization activated cation current I_h is a critical regulator of this phase dependent firing. The research article of Borel et al. (2013) (*Dept. Physiology, Development and Neuroscience, Univ. Cambridge and Dept. Brain and Cognitive Engineering, Korea Univ. Seoul*) asks how I_h controls firing of CA1 and CA3 pyramidal cells. CA1 neurons are suggested to express I_h at higher levels than CA3 pyramidal cells ensuring larger responses to hyperpolarization and thus more prominent resonance peaks. With a strong I_h, excitatory inputs during theta can delay firing, an effect counteracted by phasic inhibitory currents during theta oscillations. Interactions between synaptic inputs and active I_h currents may then account for distinct phase responses of CA1 and CA3 neurons in temporal outputs during theta oscillations.

The final article from Nava-Mesa et al. (2013) (Lab. Neurofisiología y Comportamiento, Univ. Castilla-La Mancha, Ciudad Real and Dept. Fisiología y Farmacología, Univ. Salamanca) shows how the Aβ peptide affects synapses made by fimbrial afferents with CA3 pyramidal cells. Stimulation of the lateral fimbria evokes AMPA-mediated EPSPs followed by early and late IPSPs mediated by distinct GABA receptors. Aβ depolarizes CA3 pyramidal cells, increases their input resistance and decreases the late $GABA_B$-mediated IPSP current. This post-synaptic effect, is mediated via the G protein-gated inwardly rectifying potassium channel GirK. Dysfunction of septo-hippocampal oscillations involving GirK at fimbria-CA3 synapses may account for memory deficits during early stages of Alzheimer's disease.

REFERENCES

Amaral, D. G., and Witter, M. P. (1983). The three-dimensional organization of the hippocampal formation: a review of anatomical data. *Neuroscience* 31, 571–591. doi: 10.1016/0306-4522(89)90424-7

Belvindrah, R., Nosten-Bertrand, M., and Francis, F. (2014). Neuronal migration and its disorders affecting the CA3 region. *Front. Cell. Neurosci.* 8:63. doi: 10.3389/fncel.2014.00063

Borel, M., Guadagna, S., Jang, H. J., Kwag, J., and Paulsen, O. (2013). Frequency dependence of CA3 spike phase response arising from h-current properties. *Front. Cell. Neurosci.* 7:263. doi: 10.3389/fncel.2013.00263

Buzsáki, G., Leung, L. W., and Vanderwolf, C. H. (1983). Cellular bases of hippocampal EEG in the behaving rat. *Brain Res.* 287, 139–171.

Cerasti, E., and Treves, A. (2013). The spatial representations acquired in CA3 by self-organizing recurrent connections. *Front. Cell. Neurosci.* 7:112. doi: 10.3389/fncel.2013.00112

Deuker, L., Doeller, C. F., Fell, J., and Axmacher, N. (2014). Human neuroimaging studies on the hippocampal CA3 region—integrating evidence for pattern separation and completion. *Front. Cell. Neurosci.* 8:64. doi: 10.3389/fncel.2014.00064

Deuker, L., Olligs, J., Fell, J., Kranz, T. A., Mormann, F., Montag, C., et al. (2013). Memory consolidation by replay of stimulus-specific neural activity. *J. Neurosci.* 33, 19373–19383.

Evstratova, A., and Tóth, K. (2014). Information processing and synaptic plasticity at hippocampal mossy fiber terminals. *Front. Cell. Neurosci.* 8:28. doi: 10.3389/fncel.2014.00028

Kesner, R. P. (2013). A process analysis of the CA3 subregion of the hippocampus. *Front. Cell. Neurosci.* 7:78. doi: 10.3389/fncel.2013.00078

Kesner, R. P. and Hunsaker, M. R. (2010). The temporal attributes of episodic memory. *Behav. Brain Res.* 215, 299–309. doi: 10.1016/j.bbr.2009.12.029

Le Duigou, C., Simonnet, J., Teleñczuk, M. T., Fricker, D., and Miles, R. (2014). Recurrent synapses and circuits in the CA3 region of the hippocampus: an associative network. *Front. Cell. Neurosci.* 7:262. doi: 10.3389/fncel.2013.00262

Lorente de Nó, R. (1934). Studies on the structure of the cerebral cortex: continuation of the study of the ammonic system. *J. Psychol. Neurol.* 46, 113–177.

Münster-Wandowski, A., Gómez-Lira, G., and Gutiérrez, R. (2013). Mixed neurotransmission in the hippocampal mossy fibers. *Front. Cell. Neurosci.* 7:210. doi: 10.3389/fncel.2013.00210

Nava-Mesa, M. O., Jiménez-Díaz, L., Yajeya, J., and Navarro-Lopez, J. D. (2013). Amyloid-β induces synaptic dysfunction through G protein-gated inwardly rectifying potassium channels in the fimbria-CA3 hippocampal synapse. *Front. Cell. Neurosci.* 7:117. doi: 10.3389/fncel.2013.00117

O'Keefe, J., and Nadel, L. (1978). *The Hippocampus as a Cognitive Map.* Oxford, UK: Oxford University Press.

Pedroni, A., Minh do, D., Mallamaci, A., and Cherubini, E. (2014). Electrophysiological characterization of granule cells in the dentate gyrus immediately after birth. *Front. Cell. Neurosci.* 8:44. doi: 10.3389/fncel.2014.00044

Rolls, E. T. (2013). A quantitative theory of the functions of the hippocampal CA3 network in memory. *Front. Cell. Neurosci.* 7:98. doi: 10.3389/fncel.2013.00098

Scoville, W. B., and Milner, B. (1957). Loss of recent memory after bilateral hippocampal lesions. *J. Neurol. Neurosurg. Psychiatry* 20, 11–21. doi: 10.1136/jnnp.20.1.11

Conflict of Interest Statement: The authors declare that the research was conducted in the absence of any commercial or financial relationships that could be construed as a potential conflict of interest.

Received: 12 November 2014; accepted: 12 January 2015; published online: 05 February 2015.

Citation: Cherubini E and Miles R (2015) The CA3 region of the hippocampus: how is it? What is it for? How does it do it? Front. Cell. Neurosci. ***9****:19. doi: 10.3389/fncel.2015.00019*

This article was submitted to the journal Frontiers in Cellular Neuroscience.

frontiers in
CELLULAR NEUROSCIENCE

REVIEW ARTICLE
published: 22 November 2013
doi: 10.3389/fncel.2013.00210

Mixed neurotransmission in the hippocampal mossy fibers

Agnieszka Münster-Wandowski[1†], Gisela Gómez-Lira[2†] and Rafael Gutiérrez[2]*

[1] Institute of Integrative Neuroanatomy, Charité-Universitätsmedizin Berlin, Campus Mitte, Berlin, Germany
[2] Department of Pharmacobiology, Centro de Investigación y Estudios Avanzados del Instituto Politécnico Nacional, Mexico City, Mexico

Edited by:
Enrico Cherubini, International School for Advanced Studies, Italy

Reviewed by:
Rosemarie Grantyn, Humboldt University Medical School, Germany
Laura Borodinsky, University of California Davis School of Medicine, USA

***Correspondence:**
Rafael Gutiérrez, Department of Pharmacobiology, Centro de Investigación y Estudios Avanzados del Instituto Politécnico Nacional, Calzada de los Tenorios No. 235, México City, DF 14330, Mexico
e-mail: rafagut@cinvestav.mx

†Agnieszka Münster-Wandowski and Gisela Gómez-Lira have contributed equally to this work.

The hippocampal mossy fibers (MFs), the axons of the granule cells (GCs) of the dentate gyrus, innervate mossy cells and interneurons in the hilus on their way to CA3 where they innervate interneurons and pyramidal cells. Synapses on each target cell have distinct anatomical and functional characteristics. In recent years, the paradigmatic view of the MF synapses being only glutamatergic and, thus, excitatory has been questioned. Several laboratories have provided data supporting the hypothesis that the MFs can transiently release GABA during development and, in the adult, after periods of enhanced excitability. This transient glutamate-GABA co-transmission coincides with the transient up-regulation of the machinery for the synthesis and release of GABA in the glutamatergic GCs. Although some investigators have deemed this evidence controversial, new data has appeared with direct evidence of co-release of glutamate and GABA from single, identified MF boutons. However, this must still be confirmed by other groups and with other methodologies. A second, intriguing observation is that MF activation produced fast spikelets followed by excitatory postsynaptic potentials in a number of pyramidal cells, which, unlike the spikelets, underwent frequency potentiation and were strongly depressed by activation of metabotropic glutamate receptors. The spikelets persisted during blockade of chemical transmission and were suppressed by the gap junction blocker carbenoxolone. These data are consistent with the hypothesis of mixed electrical-chemical synapses between MFs and some pyramidal cells. Dye coupling between these types of principal cells and ultrastructural studies showing the co-existence of AMPA receptors and connexin 36 in this synapse corroborate their presence. A deeper consideration of mixed neurotransmission taking place in this synapse may expand our search and understanding of communication channels between different regions of the mammalian CNS.

Keywords: mossy fibers, dentate gyrus, GABA, co-release, gap junctions, CA3

INTRODUCTION

By the end of the 1800s and early 1900s, research on the nervous system was directed toward defining its conformation, particularly, to answer whether it was constituted by individual entities, neurons (neuronal doctrine championed by Santiago Ramón y Cajal) or by a continuous network (reticular hypothesis, championed by Camilo Golgi).

The debate was even present in the Nobel Lectures, held by those who shared the prize in 1906: Ramón y Cajal (1906) and Golgi (1906), both "in recognition of their work on the structure of the nervous system." The neuronal doctrine prevailed as evidence accumulated, but this issue was not only solved by anatomists. Indeed, physiologists played an important role in defining the concept of neuron while they were discussing about another related issue: whether transmission among nerves and effector organs/muscles was chemical or electrical. The growing evidence in favor of chemical transmission, in turn, supported the growing anatomical evidence of neurons being independent entities.

The groundbreaking work of Loewi and Dale, who demonstrated that stimulation of the nerves of the autonomic nervous system produced the release of "substances" that had inhibitory or excitatory effects on their target organs, established chemical transmission as a "general principle." However, during the 1930s to the 1950s several electrophysiologists, including most notoriously Eccles, argued that in nicotinic synapses the excitation of the nerves generated a current that flowed into the postsynaptic cell and that it could be followed by a residual action mediated by a chemical transmitter such as acetylcholine (Ach). Doubts were dissipated and it became clear that peripheral synapses were of chemical nature, mainly through the work of Bernard Katz and coworkers. Eccles, despite his finally endorsing the chemical synapse in ganglia said: ". . .it would seem expedient to restrict it (the electrical synapse) in the first instance to monosynaptic transmission through the spinal cord, where chemical transmission by ACh seems highly improbable, and where the experimental investigation has been more rigorous than elsewhere in the nervous system" (cited in Cowan et al., 2001). This view, or rather defense of the electrical synapse, prevailed until he and his group discovered synaptic inhibition at the beginning of the 1950s, of course of chemical nature, but the transmitters involved were still to be discovered. So, at that stage, a key question was still open. Are there more chemicals in the central nervous system (CNS) than adrenalin and ACh, shown to act in the autonomic nervous system and, the latter, also in the neuromuscular junction? One thing seemed to be clear: that neurons

released what they produced and contained. And, in this context, Dale (1935) concluded that a neuron functions as a metabolic unit, therefore, a process occurring in the cell influences all of the compartments of that given neuron. In other words, the neuron would release the same neurotransmitter from all its terminals. Unfortunately, this was transformed in the literature to a "principle" stating that "a single cell releases only one neurotransmitter" or that "its action is the same on all its postsynaptic targets."

A whole range of transmitter substances were discovered during the last half of the twentieth century, ranging from amino acids (glutamate, GABA, glycine, etc.) to dopamine (DA), norepinephrine and serotonin and, finally, a long list of neuropeptides. On the other hand, in the 1970s it became evident that the "one neuron, one neurotransmitter" postulate is the exception rather than the rule because many of these substances co-exist and can be simultaneously released from single cells and even segregated so as to be released from different terminals of the same cell. Therefore, it was established that a cell could co-release a fast-acting "classical" neurotransmitter and a modulatory factor, that could be a peptide, nucleotide (e.g., ATP), Zn^{2+}, neurotrophic factor, nitric oxide, or endogenous cannabinoids – among other modulators. By contrast, the co-existence and co-release of two or more "classical" neurotransmitters, each conveying a "principal message," has been less studied. However, during recent years, several research groups have shown that co-release is not that uncommon, and it is now known to occur in a variety of neural systems. In addition, although many populations of adult neurons may not release two classical neurotransmitters under basal conditions, many appear to do so transiently following an established program during early development, or in response to a variety of physiological and pathophysiological stimuli (Gutiérrez, 2009; Dulcis and Spitzer, 2011; Borodinsky et al., 2012).

But what about "co-existence" of electrical and chemical transmission? After years of efforts to prove the chemical nature of synaptic transmission in the CNS, Fatt (1954) pointed out that it was premature to conclude that chemical transmission was in fact universal. Soon enough, Furshpan and Potter (1957) showed that the passage of electrical current accounted for the transmission of information between the presynaptic giant axon and the post-synaptic motor axon in the crayfish nerve cord. Moreover, it was found that electrical communication can also cause inhibition (Furukawa and Furshpan, 1963). The work of Bennett and collaborators established that in most cases the flow of current in electrical synapses can be in either direction and that they were most commonly found in rapidly activated circuits, where reciprocity and speed are important for the synchrony of ensembles of neurons (Bennett, 1972). Finally, Martin and Pilar (1963) discovered that both electrical and chemical communication do coexist in the chick ciliary ganglion. It is now recognized that electrical communication through gap junctions in dendro-dentritic and axo-axonic synapses is more common than originally thought in the mammalian brain (Connors and Long, 2004; Söhl et al., 2005). By contrast, although already detected (for a review see Connors and Long, 2004), mixed electrical-chemical communication involving axo-dendritic contacts is still under scrutiny.

In line with this introduction concerning mixed synaptic transmission, in this review we examine the surprising physiology of the mossy fibers (MFs). Indeed, these axons have proven to be neuronal elements still full of surprises. The traditional working paradigm of those working on MF transmission is that granule cells (GCs) form glutamatergic synapses with pyramidal cells and local inhibitory interneurons of the CA3 area. Thus, activation of the MF provokes monosynaptic excitatory responses in both cell types, and the activation of interneurons, in turn, produces inhibitory responses in pyramidal cells to maintain feedforward inhibition (Lawrence and McBain, 2003). Therefore, activation of GC during the blockade of glutamate-mediated transmission prevents both excitatory and inhibitory responses from appearing in CA3. However, two sets of data that add a twist to this paradigm will be the focus of this review: the possibility of GCs co-releasing glutamate and gamma-aminobutyric acid (GABA) on to their target cells in CA3 area and the possibility of some MFs establishing mixed electrical-chemical synapses among them and some establishing axo-dendritic mixed, electrical-chemical synapses with CA3 pyramidal cells.

DEFINING MARKERS OF GLUTAMATERGIC AND GABAERGIC NEURONS

Glutamatergic and GABAergic neuronal phenotypes have long been considered independent, each being characterized by dedicated molecular components or markers that have a segregated cellular and subcellular localization. However, recent research has challenged these long-standing assumptions, whereby the co-localization of glutamatergic and GABAergic molecular components has been found in both, glutamatergic and GABAergic cells in various brain regions, most notoriously in dentate GCs and the MF system. What does a glutamatergic or a GABAergic cell contain or express to be defined as such?

GLUTAMATE

Glutamate is the major, widely distributed, excitatory neurotransmitter in the mammalian CNS. In addition to its involvement in fast synaptic transmission, it has a role in long-term potentiation, as a proposed molecular substrate for learning and memory (Attwell, 2000). Glutamine and alpha-ketoglutarate, the major precursors of glutamate, are actively taken up into the pre-synaptic terminal via an active, Na^{+}-dependent uptake mechanism (Anderson and Swanson, 2000; Daikhin and Yudkoff, 2000). Glutamine is then transported to mitochondria, where it is converted via phosphate-activated glutaminase to glutamate and ammonia. Alternatively, glutamate may be formed from alpha-ketoglutarate and alanine catalyzed by alanine aminotransferase. The cytoplasmic glutamate is packed into synaptic vesicles by vesicular glutamate transporters (VGLUTs) for future release into the synaptic cleft by a process of vesicular exocytosis (Südhof et al., 1993; Bennett and Scheller, 1994; Söllner and Rothman, 1994). Glutamate is rapidly removed from the cleft by being: (1) actively transported back to the neuron and the glial cells or (2) inactivated by enzymatic degradation (Anderson and Swanson, 2000; Attwell, 2000; Daikhin and Yudkoff, 2000). Glutamate uptake is mediated by plasma membrane glutamate transporters EAAC1/EAAT3 and GLT1/EAAT2, respectively.

In glial cells, glutamate is metabolized to either glutamine via glutamine synthase or α-ketoglutarate by glutamate oxaloacetate transaminase or glutamate dehydrogenase (Meldrum et al., 1999; Anderson and Swanson, 2000). These two precursors, glutamine and α-ketoglutarate are then actively transported out of the glial cells and back into the pre-synaptic axon terminals for subsequent re-synthesis of glutamate (Meldrum et al., 1999).

In GABAergic interneurons glutamate can be synthesized via a different enzymatic route, involving glutamate dehygrogenase (Schmitt and Kugler, 1999), aspartate aminotransferase (Rothe et al., 1995), and glutaminase (Laake et al., 1999; Holten and Gundersen, 2008). This is in line with the fact that there is a significant level of glutamate in GABA nerve terminals, as shown by electron microscopic immunogold technique (Laake et al., 1999; Holten and Gundersen, 2008).

The concentration of glutamate within the vesicle is thought to be ∼100 mmol/L. Release of a single vesicle is believed to produce high concentrations in the cleft to saturate postsynaptic receptors and induce a "quantal-sized" excitatory post-synaptic potential (EPSP) (Meldrum, 2000). The extracellular concentration of glutamate *in vivo* is normally very low (∼1 μM; Anderson and Swanson, 2000; Attwell, 2000), enough to prevent excitotoxicity (Choi, 1992; Rothstein et al., 1996).

GABA

In the mammalian CNS, inhibition is primarily mediated by the amino acids GABA and glycine. GABA is the main inhibitory neurotransmitter in the adult cortex and its synthesis is unique among neurotransmitters, having two separate isoforms of the rate-controlling enzyme, glutamic acid decarboxylase GAD65 and GAD67, that convert excitatory amino acids into GABA. These isoforms differ in their cellular localization and functional properties. GABA synthesized by GAD65 is used for neurotransmission whereas GABA synthesized by GAD67 is used for processes such as synaptogenesis and protection against neuronal injury. GABA is loaded into synaptic vesicles with the help of the vesicular GABA transporter (VGAT) by using the electrochemical gradient of H^+ (Ahnert-Hilger and Jahn, 2011; Riazanski et al., 2011). Additionally, chloride gradients between the vesicle lumen and the presynaptic cytosol may contribute to the vesicular loading of GABA (Ahnert-Hilger and Jahn, 2011; Riazanski et al., 2011). GAD65 and VGAT are functionally linked at the synaptic vesicle membrane and GABA synthesized by GAD65 is preferentially loaded into the synaptic vesicle over GABA synthesized in cytoplasm by GAD67. In a GABAergic synapse it is likely that approximately 80% of the released GABA is transported back into the GABAergic nerve ending, whereas the remaining GABA will be taken up into the astrocytes in the proximity of the synapse (Hertz and Schousboe, 1987).

There have been no functional estimates of intracellular GABA levels until now. Previous studies proposed GABA concentrations ranging from 7 mM in somata (Obata et al., 1970; Otsuka et al., 1971) to 50–150 mM in nerve terminals (Fonnum and Walberg, 1973). These estimates raise the intriguing possibility that VGAT saturation is a prerequisite for efficient refilling of inhibitory vesicles. However, Apostolides and Trussell (2013) found that the endogenous transmitter does not saturate vesicular transporters: dialyzing presynaptic cells with high concentrations of glycine or GABA reduced the efficacy of a fast-off glycine receptor antagonist and potentiated GABAergic transmission.

GLUTAMATE AND GABA TRANSPORTERS

Glutamate and GABA transporters play a major role in the removal of transmitters from the synaptic cleft and the extracellular space, recycling, and repackaging them in synaptic vesicles. On the basis of their structure and site of action, transporters can be divided into two superfamilies: (1) vesicular transporters and (2) plasma membrane transporters.

Glutamate and GABA vesicular transporters

Three isoforms of VGLUTs (VGLUT1, VGLUT2, and VGLUT3) underlie the vesicular uptake of glutamate in CNS neurons and thus represent markers of glutamatergic transmission. They share salient structural and functional characteristics but have differential cellular localization and functional properties, suggesting isoform-specific physiological roles (Fremeau et al., 2004; Chaudhry et al., 2008). In the CNS, VGLUT1, and VGLUT2 show complementary patterns of expression mainly in subset of glutamatergic neurons (Fremeau et al., 2001; Varoqui et al., 2002). VGLUT3, by contrast, is mostly expressed in neurons that were identified as non-glutamatergic. A broader examination of the distribution and functions of VGLUTs subsequently revealed that also VGLUT1 and VGLUT2 can be expressed in non-glutamatergic neurons, in consequence giving the strong indication that glutamate may very well act as a co-transmitter in many types of neurons. The presence of a VGLUT isoform in non-glutamatergic axon terminals indicates that glutamate can be either co-released by these axons or that it may contribute to an increased filling of synaptic vesicles with the primary transmitter, and consequently, increase the release of this transmitter. This has been demonstrated for cholinergic and serotonergic neurons, which contain VGLUT3 (Amilhon et al., 2010), and in dopaminergic neurons (Hnasko et al., 2010) and GABAergic neurons (Zander et al., 2010), which contain VGLUT2.

Only one vesicular transporter for GABA and glycine is known – the vesicular inhibitory amino acid transporter (VIAAT = VGAT; McIntire et al., 1997; Sagne et al., 1997). The transporter is co-expressed with markers for GABAergic and glycinergic synapses including GABA and glycine themselves, the GABA-synthesizing enzymes GAD65 and GAD67, the membrane glycine transporter GlyT2, and GABA membrane transporter (GAT1; Sagne et al., 1997; Chaudhry et al., 1998; Dalby, 2003). In summary, the co-expression of VGAT and the GAD enzymes determines the GABAergic phenotype (Wojcik et al., 2006), whereas, the co-expression of VGAT with the neuronal membrane glycine transporter GlyT2 is responsible for the glycinergic phenotype of a neuron (Gomeza et al., 2003).

Glutamate and GABA membrane transporters

The primary function assigned to the sodium-dependent membrane glutamate transporters (EAATs) is to maintain the extracellular glutamate concentration in the low micromolar

range, allowing glutamate to be used as a signaling molecule in the brain and preventing its cytotoxic effects. Five high-affinity membrane glutamate transporters have been cloned from mammalian tissue: astrocyte-specific glutamate transporter (GLAST), glutamate transporter 1 (GLT1), excitatory amino acid carrier 1 (EAAC1), excitatory amino acid transporter 4 (EAAT4) and 5 (EAAT5). Immunocytochemical studies have revealed that GLAST and GLT1 are localized primarily in astrocytes (Shashidharan and Plaitakis, 1993; Tanaka et al., 1997), while EAAT3 and EAAT4 are distributed in neuronal membranes (Furuta et al., 1997).

GABA membrane transporter (GAT1) was the first of four GABA plasma membrane transporters isolated from rat brain (Radian et al., 1986; Guastella et al., 1990), which recognize GABA as a substrate (Dalby, 2003; Sarup et al., 2003). GAT1 ultrastructural localization is limited to axon terminals form symmetrical synapses (i.e., GABAergic) in the rat cerebral cortex but it can be also be expressed to some extent in proximal astrocytic processes, while the other transporters (GAT2-4) are located in astrocytic processes (Minelli et al., 1995; Ribak et al., 1996; Biedermann et al., 2002).

Transporters mediating reuptake of neurotransmitters have long been considered as selective glutamatergic and GABAergic neuronal markers. However, there is increasing evidence that neurons can co-express membrane transporters for various other transmitters. The key examples are the plasma membrane glutamate EAAT4 and EAAT3 transporter subtypes, which are localized on GABAergic Purkinje cells in the cerebellum (Rothstein et al., 1994; Furuta et al., 1997) and on hippocampal GABAergic neurons, respectively (Raiteri et al., 2002). Conversely, the plasma membrane GABA transporter GAT1 type co-exists with plasma membrane glutamate transporters on glutamatergic nerve terminals in spinal cord (Raiteri et al., 2005).

NEUROTRANSMITTER PHENOTYPE MARKERS PRESENT IN THE GRANULE CELLS AND THEIR MOSSY FIBER

The hippocampal formation consists of GCs in the dentate gyrus and pyramidal cells in the CA1 and CA3 areas. The other type of neurons, the interneurons, are present in all hippocampal areas. The principal cells are interconnected by glutamatergic synapses, forming the "trisynaptic pathway" (Andersen et al., 1971; Storm-Mathisen, 1977). The GCs of the dentate gyrus receive excitatory glutamatergic input from layer II pyramidal cells of the entorhinal cortex (Steward and Scoville, 1976) and project to CA3 pyramidal cells. From there, they project to CA1 cells, which in turn project to the subiculum and back to the entorhinal cortex (Andersen et al., 1971; Amaral et al., 1990). The GCs show highly conserved properties across species (Seress and Frotscher, 1990) and are born continuously throughout life (Altman and Bayer, 1990), a feature that may be related to their role in memory formation (Schmidt-Hieber et al., 2004). There are approximately one million GCs within the rat dentate gyrus, all projecting thin unmyelinated axons into the stratum lucidum of the CA3, adjacent to the cell body layer. MFs form synaptic contacts with complex spines on proximal apical dendrites of CA3 pyramidal cells (Claiborne et al., 1986; Amaral et al., 1990) and various types of interneurones (Acsády et al., 1998).

Mossy fibers display three main types of presynaptic terminal exist along the entire length of the main axon: (1) large mossy boutons (4–10 mm in diameter), (2) filopodial extensions (0.5–2.0 mm) that emerge from the large mossy boutons, and (3) small *en-passant* varicosities (0.5–2.0 mm; Amaral, 1979; Frotscher, 1985; Claiborne et al., 1986; Acsády et al., 1998). The total number of large mossy boutons along a single axon is about 10 in the hilar region and about 12 (range 10–18) in the CA3 region, with the terminals being distributed approximately every 150 mm along the MF axon (Acsády et al., 1998). The large MF terminals, which contain up to 35 individual release sites envelop postsynaptic complex spines ("thorny excrescences") found on the proximal apical dendrite of CA3 pyramidal cells. A single CA3 pyramidal neuron typically receives input from about 50 MF boutons (Amaral et al., 1990). In the hilus, the so called "mossy cells" constitute the principal target of the large mossy terminals. Small filopodial extensions and *en passant* terminals found on the parent axon predominantly innervate inhibitory interneurons in both the hilus and stratum lucidum (Acsády et al., 1998). These terminals form single, often perforated, asymmetric synapses on the cell bodies, dendrites, and spines of GABAergic inhibitory interneurons (McBain, 2008). Although large MF boutons do not typically innervate GABAergic interneurons, they have occasionally been observed to directly contact dendrites interneurons in the guinea pig (Frotscher, 1985). These MF-interneuron synapses recruit feed-forward inhibition onto the CA3 pyramidal cells. Thus, the morphological properties of the MF synapse are consistent with the view that it forms a powerful, but sparse synaptic connection (Rollenhagen and Lübke, 2010).

GLUTAMATE

The primary excitatory neurotransmitter released from MF terminals is glutamate (Crawford and Connor, 1973; Storm-Mathisen, 1981; Storm-Mathisen et al., 1983). MFs-CA3 pyramidal cell synapses are one of the most powerful glutamatergic input, "detonator" synapses (Urban et al., 2001; Henze et al., 2002; Mori et al., 2007). However, the high strength requires some winding up, in the form of frequency dependent facilitation (Henze et al., 2002; Mori et al., 2007) and it is coupled with a very low basal firing rate of GCs *in vivo* (<0.5 Hz). In fact, many GCs appear not to fire action potentials for extended periods of time (Jung and McNaughton, 1993).

GABA AND GAD

Sandler and Smith (1991) found GABA contained in MF terminals that made asymmetric synaptic contact with spines arising from large dendrites of CA3 pyramidal cells. GC bodies, however, did not show GABA immunoreactivity. They also showed the colocalization of GABA and glutamate within the same terminals with electron microscopy. Later, Sloviter et al. (1996) conclusively demonstrated that GABA and its synthesizing enzyme, GAD67, co-existed in the MFs of rats, monkeys, and humans. These authors additionally demonstrated that seizures upregulated the contents of both isoforms of GAD and GABA (Sloviter et al., 1996). Other authors showed that GAD67 and its mRNA (but not GAD65) were transiently upregulated after seizures provoked by kainic acid or

by the kindling method in the rat (Schwarzer and Sperk, 1995; Lehmann et al., 1996; Ramírez and Gutiérrez, 2001; Maqueda et al., 2003). Quantitative immunogold analysis confirmed the co-existence of these amino acids within single MF terminals, and in close relationship with synaptic vesicles, where GABA concentration was found to be lower than that of glutamate (1.5 vs. 7.2 mM, respectively; Bergersen et al., 2003). Recently, Sperk et al. (2012) showed a marked enhancement of the expression of one of the two key enzymes of GABA synthesis – GAD67 – in MFs of epilepsy patients.

Therefore, if the GCs have the necessary enzyme for the synthesis of GABA and GABA itself, the GCs indeed synthesize GABA that could probably be used as a neurotransmitter.

VESICULAR GLUTAMATE TRANSPORTER (VGLUT1 AND VGLUT2) AND VESICULAR GABA TRANSPORTER (VGAT)

Bellocchio et al. (1998) and Takamori et al. (2000) conclusively demonstrated that a protein, previously identified as brain specific Na^+-dependent phosphate transporter (BNPI; Ni et al., 1994) – now known as VGLUT – endows the cells with a functional glutamatergic phenotype. Moreover, these authors showed that the protein was both in the DG and MF terminals. On the other hand, the first evidence of the presence of VGAT mRNA in MF was obtained from an enriched MF synaptosome preparation and from micro slices of the DG, where the possibility of having GABAergic cells could not be ruled out (Lamas et al., 2001). However, in that work, the expression pattern of the mRNA coincided with the upregulation of GAD and appearance of GABA-mediated transmission on MF stimulation (see below). Soon after, with the use of single-cell PCR, Gómez-Lira et al. (2005) conclusively demonstrated that mRNA was contained in the GCs and that it was expressed in a developmental- and activity-dependent manner. Despite the presence of VGAT mRNA, some immunohistological studies failed to detect the VGAT protein in the MFs (Chaudhry et al., 1998; Sperk et al., 2003). Bergersen et al. (2003, 2008), by using an electron microscopic immunogold method, could show that GABA was present together with glutamate in all large MF terminals and that both amino acids were associated with synaptic vesicles.

In a recent work, the presynaptic co-localization of VGLUTs and VGAT proteins in glutamatergic hippocampal MF terminals was conclusively demonstrated (Zander et al., 2010). We found that the GABA transmitter phenotype is preserved in the mature brain as indicated by the presence of GABA synthesizing enzymes GAD65 and GAD67, as well as the VGAT (**Figure 1**). Also, unique co-existence of VGAT and VGLUT was observed in cerebellar MF terminals by absence of VGAT immunoreactivity in other glutamatergic cerebellar parallel fiber (VGLUT1-positive) and climbing fiber (VGLUT2-positive) terminals. These findings provide strong morphological evidence for synaptic co-existence of glutamatergic and GABAergic transporters in adult glutamatergic MF terminals. Furthermore, we carried out postembedding immunogold electron microscopy with vesicular immunoisolation experiments in order to determine vesicular co-localization VGAT and VGLUT in the MF synapse. The immunoisolation experiments from whole brain of adult rats further confirmed that VGLUT1 immunoisolates also contain VGLUT2 and, conversely, VGLUT2 immunoisolates show VGLUT1 immunoreactivity, indicating the vesicular co-localization of both VGLUTs. VGLUT2 immunoisolates harbor, in addition, VGAT and VGAT immunoisolates also contain VGLUT2. Transporter-specific immunoisolations from rat brain at different postnatal stages (P5 and P15) showed a pronounced vesicular co-localization of VGLUT2 and VGAT during these early developmental stages. Transmitter uptake studies using Glu and GABA proved the functional integrity of immunoisolated vesicles. In fact, VGAT immunoisolates were found to concentrate Glu in addition to GABA. Using the specific inhibitor trypan blue we found that VGLUT activity improves GABA, as well as monoamine uptake into synaptic vesicles. Thus, VGLUT activity modulates transmitter storage in a substrate-independent manner. Using immunogold detection and electron microscopy, Zander et al. (2010) proposed that glutamatergic MF terminals contain vesicles co-expressing either VGLUT1 or VGLUT2 and VGAT. This confirms that both vesicle transporters are in the same terminals, which strongly support the hypothesis of co-release of glutamate and GABA. However, direct proof of co-existence of vesicular transporters of different kind in single vesicles cannot be provided by the limitations of the immunogold technique. Although it is possible that both transporters can be expressed by single vesicles, electrophysiological experiments suggest that these vesicular transporters could be sorted to different pools of vesicles (Walker et al., 2001; Beltrán and Gutiérrez, 2012; see, Activation of the MFs Normally Produces Gabaergic Responses During Development).

GABA MEMBRANE TRANSPORTER

It was found that MF terminals from control and epileptic animals capture GABA and nipecotic acid blocks this uptake (Gómez-Lira et al., 2002), suggesting that they normally express GAT-1, further indicating that these cells are actually potentially GABAergic. This has also been confirmed by immunohistological techniques (Frahm et al., 2000; Sperk et al., 2003). These data show another GABAergic marker in the MFs, which allows them to take GABA from the extracellular millieu into the terminals. Its presence, however, is not what determines that MFs release GABA, moreover, blockage of this transporter enhances MF-evoked GABA responses (Vivar and Gutiérrez, 2005).

GABAA RECEPTORS

For a neurotransmitter to exert its action, the corresponding receptor(s) should be in the subsynaptic site. In other words, pyramidal cells of CA3 and interneurons in the hilus and CA3 should have GABAA receptors together with glutamate receptors apposed MF terminals. Bergersen et al. (2003) demonstrated that GABAA receptors coexist with AMPA type glutamate receptors apposed MF terminals using immunogold detection. Moreover, they also detected presynaptic GABAA receptors in the MFs themselves (Bergersen et al., 2003; Ruiz et al., 2003), which can be activated by GABA released from interneurons or even from the MFs themselves (Treviño and Gutiérrez, 2005; Alle and Geiger, 2007), and which can exert strong modulation of MF excitability (Ruiz et al., 2010). Thus, GABA released by the MFs can activate post-synaptic and presynaptic GABAA and B receptors to produce collateral potentiation or

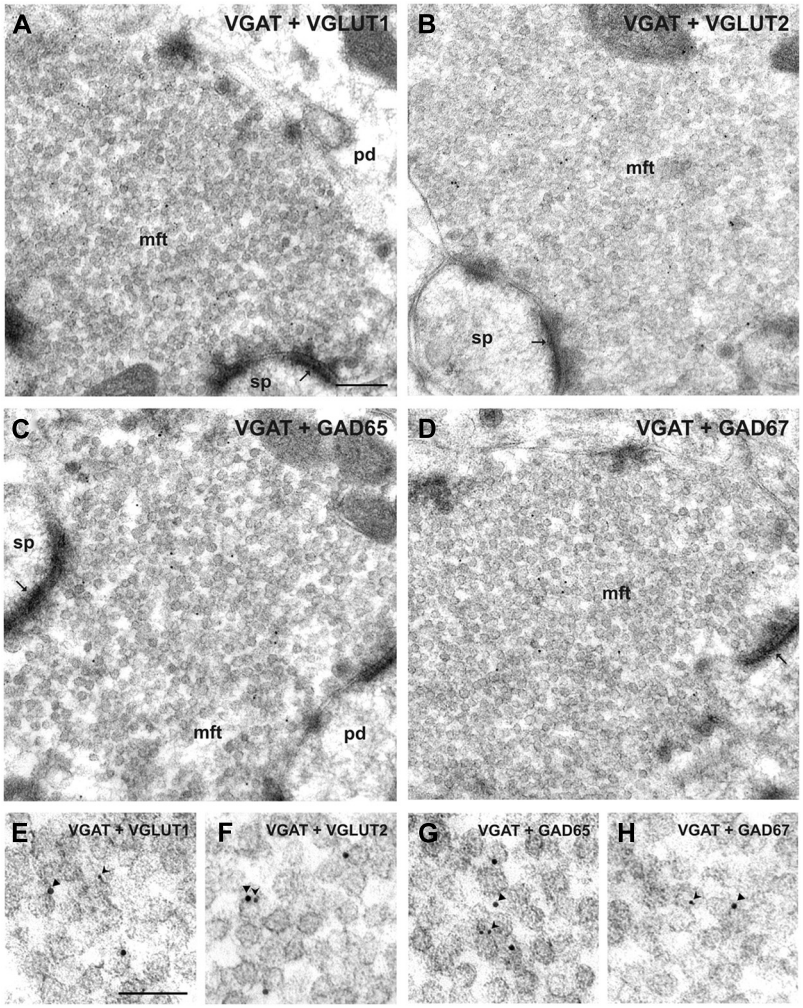

FIGURE 1 | Co-localization of VGAT with either GAD or VGLUT isoforms in hippocampal mossy fiber terminals. (A,B) Mossy fiber terminals (mft) of the CA3 area were double-immunolabeled with the guinea pig antiserum against VGAT (10 nm gold particles, arrowheads in **E**, **F**) and rabbit antisera against either VGLUT1 and VGLUT2 (5 nm gold particles, forked arrowheads in **E**, **F**, respectively). Note the SV exhibiting putatively co-localized immunogold signals for VGAT and VGLUT2 shown in **(F)**. **(C,D)** Mossy fiber terminals were double-immunolabeled with the guinea pig antiserum against VGAT (10 nm gold particles, arrowheads in **G**, **H**) and rabbit antisera against either GAD65 or GAD67 (5 nm gold particles each, forked arrowheads in **G**, **H)**, respectively. **(E–H)** Represents details at higher magnification. pd, pyramidal dendrite; sp, spine; thin arrows indicate asymmetric contacts. Bars given represent: **(A–D)**, 200 nm; **(E–H)**, 100 nm (from Zander et al., 2010).

inhibition (Ruiz et al., 2003, 2010; Treviño and Gutiérrez, 2005; Cabezas et al., 2012).

PHYSIOLOGICAL AND PHARMACOLOGICAL MARKERS

Because MFs neurotransmission is usually studied in the slice preparation, and activation of fibers other than MFs is always a possibility, there is an agreement on three principal characteristics that glutamatergic, and thus GABAergic, synaptic responses of putative MF origin should have to be recognized as true MF responses: (1) strong frequency-dependent potentiation (>300%) in response to modest increases in stimulation frequency; (2) robust NMDA-independent LTP; and (3) depression (>80%) of the responses by activation of mGluR, which are present in the MFs. These and several other physiological characteristics of MF transmission and its plasticity are thoroughly reviewed elsewhere (Henze et al., 2000; Lawrence and McBain, 2003; Nicoll and Schmitz, 2005; Jaffe and Gutiérrez, 2007; Galván et al., 2011; Ruiz and Kullmann, 2013). Moreover, these characteristics are preserved in cultured GCs establishing autapses (Rost et al., 2010) or in synapses made by GCs co-cultured with pyramidal cells and interneurons of CA3 (Osorio et al., 2013).

DOES THE PRESENCE OF ALL THE GABAERGIC MARKERS IN THE GRANULE CELLS AND THEIR MFS MAKE THEM GABAERGIC AND INHIBITORY?

The presence of markers of the GABAergic phenotype in the GCs should not necessarily make them GABAergic and inhibitory. However, evidence has been accumulating in favor of them expressing, besides a glutamatergic phenotype, a GABAergic

phenotype, with inhibitory functions. We will make a comprehensive account of what we now know about the GABAergic signaling of the MFs to be able to orderly attempt to speculate on the outcome of all of the possibilities and their interactions (Mody, 2002).

The first electrophysiological evidence of GABAergic transmission from the MFs to CA3 was in total agreement with the observations that seizures transiently upregulated the expression of the GABAergic markers GAD65 and GAD67 (Schwarzer and Sperk, 1995; Lehmann et al., 1996; Sloviter et al., 1996; Ramírez and Gutiérrez, 2001) and VGAT (Lamas et al., 2001). In accordance with this evidence, Gutiérrez and Heinemann (1997, 2001) and Gutiérrez (2000) found monosynaptic GABA-mediated transmission from the DG to CA3 in kindled epileptic but not in control healthy rats, i.e., activation of the MFs in the presence of glutamatergic blockers evoked fast, m-GluR-sensitive IPSPs with the same latency as the EPSP evoked before blocking glutamatergic transmission, and blocked by bicuculline. By contrast, perfusion of glutamatergic antagonists to slices of healthy animals prevented all synaptic responses, as expected for blockade of monosynaptic, glutamatergic and thus, polysynaptic, GABAergic inhibition. Another group provided independent evidence that strongly supported the hypothesis that MFs corelease glutamate and GABA. In contrast to the aforementioned data, Walker et al. (2001) showed that in non-epileptic, young guinea pigs, minimal stimulation of the MF in the presence of glutamatergic antagonists provoked monosynaptic GABAergic responses with the pharmacological and physiological profile of transmission of MF origin. Because all control animals used in the former experiments were adult Wistar rats (Gutiérrez, 2000), a possible source of discrepancy with the results obtained by Walker et al. (2001) could be attributed to the developmental stage or to the different species used. However, the discrepancy does not seem to arise from the use of different species because there is evidence of the presence of GABA and GAD in the MFs of the rat, guinea pig, and even in human and non-human primates (Sandler and Smith, 1991; Sloviter et al., 1996; Bergersen et al., 2003; Sperk et al., 2012).

ACTIVATION OF THE MFS NORMALLY PRODUCES GABAERGIC RESPONSES DURING DEVELOPMENT

The aforementioned data suggested the possibility that MFs of young rodents may naturally release GABA while adult animals lose this capability. We recorded responses of CA3 pyramidal cells to MF stimulation throughout development in Wistar rats (Gutiérrez et al., 2003) and found that in the developing rat MF stimulation in the presence of glutamatergic blockers normally evoked a monosynaptic GABA-mediated response, which was depressed by activation of mGluR and completely blocked by bicuculline. This response was depolarizing during the first week of life (6 days old), turned to hyperpolarizing from the second week (10 days old) and, from day 21, the number of cells having the MF-GABAergic response declined rapidly until they were no longer detected by day 23–24 (Gutiérrez, 2003).

These data, together with those of Walker et al. (2001) using the young guinea pig, established that MF GABA release was a characteristic of the developing rodent. Moreover, their thorough analysis of the physiological (frequency potentiation, LTP) and pharmacological (mGluR sensitivity) characteristics indicated that the GABAergic monosynaptic responses have indeed their origin in the MFs. Additionally, they suggested that glutamate and GABA should be released from different vesicles because the synaptic events were produced by either activation of glutamate receptors, GABA receptors, or both (Walker et al., 2001; Beltrán and Gutiérrez, 2012). Were both amino acids co-released from the same vesicles, each synaptic event would contain both components. Finally, these characteristics of MF transmission were also corroborated and extended by the group of Cherubini, which provided further evidence for a GABAergic phenotype of the MFs at even earlier ages. They suggested that MF transmission is primarily GABAergic during the first posnatal days, at P0–P6 (Safiulina et al., 2006). From P6, the co-expression of the glutamatergic and GABAergic phenotypes in a single pathway provides an efficient and rapid synergism on their target cells during development (Gutiérrez et al., 2003; Kasyanov et al., 2004). Indeed, it was shown that "pairing" spontaneous GABA-mediated giant depolarizing potentials with MF stimulation, which produces GABAA receptor-mediated synaptic responses, induces a persistent increase in synaptic efficacy at MF–CA3 synapses and proposed that different fibers or boutons release either glutamate or GABA or both (Kasyanov et al., 2004), which has been recently directly proven (Beltrán and Gutiérrez, 2012). The sequence of the development of the initially GABAergic-only, dual GABAergic-glutamatergic, and finally glutamatergic-only phenotype of the MFs is summarized in **Figure 2**.

Additionally, as in the case of glutamatergic signaling, the MF-GABAergic signaling is presynaptically tightly controlled by GABA, kainate and CB1 receptors (Safiulina et al., 2010). Indeed, CB1 receptors, which are expressed in the GCs at very young ages, can be activated by endocannabinoids released by the post-synaptic cells, thus, counteracting enhanced excitability induced by the excitatory action of GABA at that developmental stage (Caiati et al., 2012). It is interesting that activation of type III mGluRs have a much stronger inhibitory effect than that of type II MGluRs on MF GABA responses evoked both in the guinea pig and rat (Walker et al., 2001; Gutiérrez, 2003; Kasyanov et al., 2004) and the glutamate present in the extracellular milieu reaches concentrations that can also strongly inhibit MF release by acting on GluK1 receptors (Caiati et al., 2010; **Figure 2**). Finally, MF-GABA release itself controls subsequent release through activation of GABAB receptors, increasing the number of silent synapses (Safiulina and Cherubini, 2009). Recently, Cabezas et al. (2012) have shown that GAD67-containing MFs of juvenile mice can release GABA to modulate MF excitability by acting on presynaptic GABAB receptors, and suggest that their primary function is instructing the pre-synaptic element. Interestingly, despite detecting the release of GABA from the MF, they could not record GABAA-mediated responses in post-synaptic cells.

GABAA receptors appear before AMPA receptors and GABA provides the necessary depolarization needed to activate CA3 pyramidal cells. During the first postnatal week, GABA has a depolarizing action, as observed by somatic recordings, and

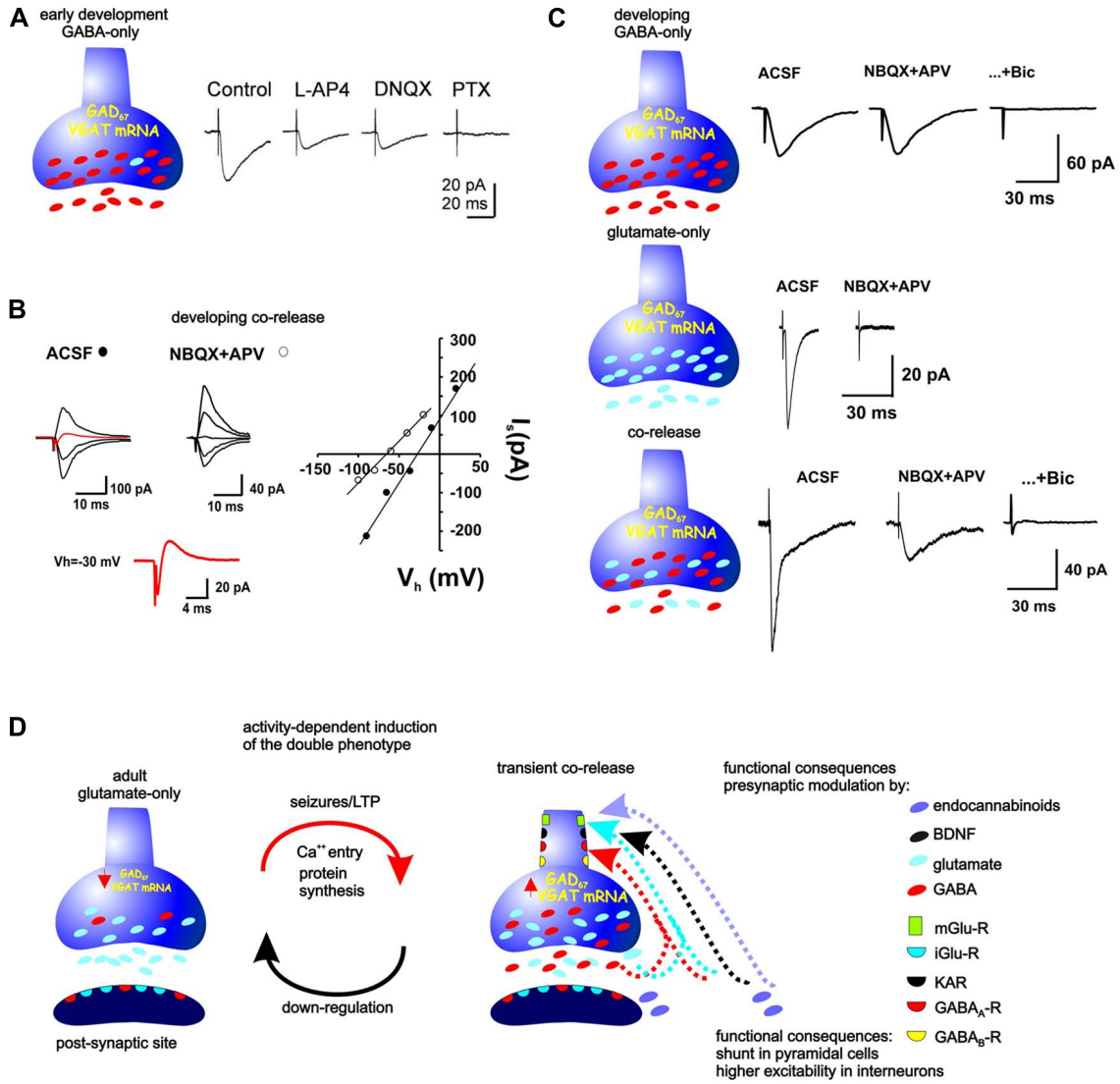

FIGURE 2 | Neurotransmitter phenotype of the MFs during development and its plasticity in the adult. **(A)** During the first 5 days of life, MFs are GABAergic. Minimal stimulation provokes synaptic currents that are partially inhibited by the glutamatergic antagonist DNQX and completely blocked by the GABAA-R antagonist, picrotoxin (modified from Safiulina et al., 2006). **(B)** From postnatal day 5–6 and up to the end of postnatal day 21–22, the synaptic responses evoked by stimulation of MF boutons can consist of inward and outward currents, consistent with co-release of glutamate and GABA (red traces at Vh = 30 mV), whereby their reversal potential is much more positive than that expected for a GABA-R-mediated current or much more negative than that expected for a glutamate-R-mediated current. Block of glutamatergic receptors isolates GABAergic responses, shifting the reversal potential to a more negative value (modified from Beltrán and Gutiérrez, 2012). **(C)** Other responses observed by stimulation of single, identified MF boutons during this period consist of glutamatergic-only or GABAergic-only currents (modified from Beltrán and Gutiérrez, 2012). **(D)** Stimulation of MFs in adult preparations provoke glutamate-R-mediated responses, however, seizures or repeated LTP-like stimulation up-regulate the GABAergic markers and MF activation provokes monosynaptic GABAR-mediated responses in their target cells. The release of glutamate and GABA from the MFs can serve presynaptic modulation of parallel MFs or of the releasing fibers themselves. Mossy fibers as well as the post-synaptic sites contain glutamate and GABA receptors. Moreover, the MFs themselves express these and receptors to BDNF, endocannabinoids, kainite, and metabotropic glutamate and GABAreceptors, which have been shown to modulate both glutamate and GABA release.

has been proposed to exert a trophic effect during development (Ben-Ari et al., 1994, 1997). From the second week of age, GABA exerts hyperpolarizing actions, so what would be the function of MF-GABA after that period and up to the third week of life? Interestingly, it was shown that although GABA actions are hyperpolarizing from the second week, as measured in the soma, MF-GABA still produces a depolarizing actions in the pyramidal cell dendrites until the end of the third week (Romo-Parra et al., 2008). This is explained by a relocation of the NKCC transporter from the somatic to the dendritic region at that developmental stage (Marty et al., 2002). Thus, GABA release from the MFs may contribute, both pre- and postsynaptically, to the refinement of neuronal connectivity before the establishment of the adult neuronal circuit (**Figure 2**).

ACTIVATION OF THE MF IN THE ADULT TRANSIENTLY PRODUCES MIXED GLUTAMATERGIC-GABAERGIC RESPONSES AFTER A PERIOD OF ENHANCED EXCITABILITY

In slices from mature control rats, the perfusion of glutamatergic antagonists blocked all synaptic responses in CA3 to DG stimulation. However, in slices from kindled rats, the perfusion of glutamatergic antagonists blocked the EPSP but a fast monosynaptic inhibitory postsynaptic potential (IPSPs) remained (Gutiérrez and Heinemann, 1997, 2001; Gutiérrez, 2000). This GABAA receptor-mediated response had the same latency as the EPSP obtained previous to its blockage and remained in low Ca^{2+} conditions without modifying its latency. As expected of responses of MF origin, activation of mGluR depresses these monosynaptic GABA responses (Gutiérrez, 2000; Gutiérrez and Heinemann, 2001). Importantly, the presence of these responses was transient because they are not present if the same type of recording is conducted 1 month after the last of several kindled seizures. On the other hand, it was established that the MF-GABAergic responses could be observed after producing a single seizure, which does not constitute a permanent epileptic state. Thus, these data together show that it is not the preexistence of an epileptic condition, nor the possible sprouting of interneurons during its evolution that explains why pyramidal cells responded with a GABAergic response on MF stimulation. Furthermore, the induction of the expression of MF GABA-mediated transmission can also occur after LTP-like stimulation *in vitro* of the perforant path, which demonstrated that this is a presynaptic phenomenon. Moreover, providing the LTP-like stimulation directly over the GCs during blockade of synaptic potentials (with NBQX and APV) also induced the MF GABAergic responses. This evidence rules out activation of interneurons as origin of mGluR-sensitive, GABAergic responses evoked by DG stimulation. Finally, the induction of MF-GABA transmission was shown to depend on protein synthesis (Gutiérrez, 2002; Romo-Parra et al., 2003; **Figure 2**).

As might be expected, the major target cells of the MFs, the interneurons in area CA3 (Acsády et al., 1998), also receive this dual input (Romo-Parra et al., 2003; Safiulina et al., 2006), as do the mossy cells in the hilar region (Bergersen et al., 2003). Whether there are different types of modulation of the MF GABAergic input onto each type of GABAergic interneuron of CA3 is still unknown, however, current data in our laboratory indicates that this is the case. This can be expected given the evidence of compartmentalization of MF actions on different types of target cells (MacCaferri et al., 1998; Galván et al., 2011).

THE GABAERGIC MARKERS ARE TRANSIENTLY UP-REGULATED WHEN GABAERGIC TRANSMISSION FROM THE MFS IS TRANSIENTLY EXPRESSED

As previously noted, the appearance of the GABAA-receptor-mediated monosynaptic responses after kindled or PTZ-induced seizures is transient and coincides with the transient upregulation of GAD (Schwarzer and Sperk, 1995; Sloviter et al., 1996; Ramírez and Gutiérrez, 2001), GABA (Gómez-Lira et al., 2002), and VGAT mRNA (Gómez-Lira et al., 2005). We know that prevention of protein synthesis prevents the MF GABAergic responses to appear, but at this time we do not know which protein is the limiting one for the ultimate release of GABA from the MFs (**Figure 2**). It is interesting that MF boutons in the adult contain detectable levels of GABA and GAD (Sloviter et al., 1996) and still, GABA does not seem to be released in the rat after 22 days of age, unless a period of hyperexcitability is induced.

Other epilepsy models have also shown that GAD and/or GABA are upregulated after seizures (Sloviter et al., 1996; Sirvanci et al., 2005). Finally, although MF GABA synaptic transmission has not been corroborated in human epileptic tissue, the expression of GAD and GABA in epileptic MFs is enhanced as compared to post mortem controls, suggesting the emergence of a compensatory, protecting mechanism against further excitability (Sperk et al., 2012).

FUNCTIONAL RELEVANCE OF THE DUAL GLUTAMATERGIC-GABAERGIC PHENOTPYE OF THE MOSSY FIBERS

We have discussed some of the possible implications of glutamate-GABA corelease from the MFs during development (see activation of the MFs normally produces GABAergic responses during development), most of which have been confirmed by several research groups. The emergence of a GABAergic phenotype in adult, glutamatergic GCs has also been extensively studied. As we have already mentioned, it is not only the presence of the markers of the GABAergic phenotype that makes them GABAergic and inhibitory. A wealth of evidence supports the assumption that, in the adult, MFs actually become inhibitory when they express GABAergic markers. Because MFs release GABA onto both, pyramidal cells and interneurons (Romo-Parra et al., 2003), the overall effect of MF input on CA3 could be disinhibitory, which has been discarded. Moreover, activation of the MF in hippocampal slices from epileptic, but not from control animals, produced GABA-mediated field responses in Stratum lucidum (SL) of CA3, which could be pharmacologically isolated (Treviño and Gutiérrez, 2005) and that were inhibited by mGluR activation and sensitive to change in stimulation frequency. Thus, the MF pathway functions as a GABAergic projection in the hippocampus that can alter CA3 population activity after seizures. Moreover, this GABAergic transmission from the MFs activates presynaptic GABAA receptors located in other MF axons (MFA), producing collateral inhibition. The activation of the DG after applying a kindling-like protocol *in vitro*, or after producing one or several seizures *in vivo*, results in a graded and reversible increase of inhibitory conductances in pyramidal cells, while in Sl-interneurons, an increase of excitatory conductances occurs. Thus, interneurons reach more depolarized membrane potentials on DG activation yielding a high excitatory postsynaptic potential-spike coupling, while the contrary occurs in pyramidal cells. This effective activation of feedforward inhibition is synergized by the emergence of direct DG-mediated inhibition on pyramidal cells. These factors force the synaptic conductance to peak at a potential value close to resting membrane potential, thus producing shunt inhibition and decreasing the responsiveness of CA3 output cells to MF input (Treviño et al., 2011). Therefore, the time-locked interaction of the excitatory and inhibitory conductances in pyramidal cells tends to inhibit spiking activity and may produce a shunting effect of other excitatory inputs (see also Monier et al., 2008). Thus, the contribution of this GABAergic input is consistent with

the hypothesis that shunt inhibition restricts the firing of action potentials, even during a partial build-up of depolarization. On the other hand, spontaneous oscillations of CA3 were analyzed in control and epileptic animals and we found that spontaneous beta-gamma oscillations of this region are tonically suppressed by the MF input and the activation of mGluR relieves this tonic inhibition. By contrast, oscillations observed in slices from control animals were not altered. A second evidence for the MF GABAergic modulation of CA3 oscillatory activity was the lack of effect of inhibition when the MF tract was disrupted (Treviño et al., 2007).

Thus, the emergence of co-release of glutamate and GABA from the MFs in the epileptic brain can reflect the put in play of excitation-restraining, antiepileptic, and neuroprotective actions in response to extreme activity conditions. It has been proposed that the DG serves as a filter (Heinemann et al., 1992) limiting the transfer of information from the entorhinal cortex to the pyramidal layer of the hippocampus. In chronic temporal lobe epilepsy and respective animal models, MF rearrange such that they innervate also neighboring glutamatergic projection cells. Co-release of GABA and glutamate after seizures will thus prevent activation of neighboring cells and may also prevent activation of mossy cells. Reduced activation in these cells may also have impact on the reduced seizure susceptibility which is frequently observed after temporal lobe seizures.

NEWBORN GRANULE CELLS IN THE ADULT CAN REGULATE THE EXPRESSION OF GABAERGIC MARKERS

Because GCs are generated throughout life, and GCs normally express GABA markers during their development, it was reasonable to propose that the newborn neurons in the adult rodent recapitulate the development of the neurotransmitter phenotype of GCs generated during embryonic and early postnatal development. Interestingly, single seizures produce a strong up-regulation of GAD67 in cells located in the infragranular layer of the DG, where most of GCs born in the adult are located (Ramírez and Gutiérrez, 2001), which suggested that GCs born in the adult can express a GABAergic phenotype. Toni et al. (2008) explored this possibility by stimulating MF boutons (light evoked transmitter release) and electrophysiologically recording in the postsynaptic cells. Their analysis, however, was conducted in cells labeled 4 months prior to the experiments, which time is probably beyond the transient period when they express GABAergic markers. If the GABAergic phenotype is transiently expressed, then its markers should be present at younger ages after retroviral infection. We determined that 15–20% of developing GFP^+ GCs expressed GAD67/GABA, while the adult, GFP^+ GCs did not express these markers at 30 days post injection. However, while these results refer to the somatic expression of the GABAergic markers, we observed that GFP^+ MF boutons expressed GAD67 at all ages (Lara et al., 2012). There may be several possible reasons why only this percentage of developing GFP^+ cells expresses GAD67, while adult GFP^+ cells do not. Indeed, it has been shown that many, but not all GCs born perinatally express the GABAergic markers in their somata (Gutiérrez et al., 2003; Maqueda et al., 2003). Also, GCs are born continuously but different cohorts of newborn can be found at a given time (Mathews et al., 2010; Piatti et al., 2011). It is possible that some cohorts do express GAD67 (as found in developing rats; Gutiérrez et al., 2003) and they may be differentially integrated to circuits. Noteworthy, while GFP^+ GCs somata may not express GAD67/GABA, we found that their MFs did express GAD67, as has been shown to occur normally in developing and adult MFs (Lara et al., 2012). A specific GAD67-expressing population of newborn cells may be distributed into distinctive networks to serve a function in cognitive tasks. Thus, the possible existence of reserve pools of neurons that can respecify their neurotransmitter phenotype (Dulcis and Spitzer, 2011), could apply to newborn GCs that can be recruited into dynamic, existing circuits. Interestingly, newborn GCs increase after seizures (Parent et al., 1997) and it has been shown that they overexpress GAD67 (Jiang et al., 2004). Additionally, newborn GCs in culture conditions can express a GABAergic phenotype in a manner dependent on activity, and by kainate or BDNF exposure (Babu et al., 2007), as previously described to occur in cultured adult GCs (Gómez-Lira et al., 2005).

Together, this information suggests that GCs born in the adult may release GABA just before their complete incorporation to the circuitry, probably to act as a trophic factor or to instruct the formation of new synapses. This possibility is supported by the fact that stimulation of the DG in slices of adult rats do not normally evoke synaptic responses in CA3 in the presence of glutamatergic antagonists, though they continue to produce new neurons. On the other hand, applying LTP stimulation over the DG in the presence of glutamatergic antagonists, which does not initially evoke synaptic responses, originates the appearance of GABA-mediated responses in CA3 cells after its repetition (12 times) in a protein synthesis-dependent manner (Gutiérrez, 2002). This excludes the newborn GCs as the source of monosynaptic GABAergic responses. A caveat of these experiments, however, is that no paired recordings were conducted, so short range projections of newborn GCs could not be probed in a selective manner. Future experiments will determine whether the expression of GABAergic markers confer the GCs a true GABAergic phenotype.

EVIDENCE AGAINST AND DIRECT EVIDENCE IN FAVOR OF THE GABAERGIC PHENOTYPE OF THE MFs

The wealth of data here presented strongly suggests that GCs are able to synthesize, vesiculate, and release GABA and glutamate on to their target cells during development and, in the adult GCs, after a period of enhanced excitability. Moreover, the physiological changes observed during the expression of the GABAergic phenotype are consistent with them being also inhibitory. Despite this, some works have appeared with interpretations for the "MF GABA responses" other than co-release. Some of these works do not find evidence of co-release rather than providing evidence against the hypothesis of co-release. Indeed, some reports fail to observe a given GABAergic marker, or a given characteristic of a "true" MF GABAergic response, usually because different experimental conditions have been used.

The first obstacle in accepting that GABA could be released from MFs was the apparent lack of its vesicular transporter, VGAT. Several authors failed to find the protein in the MFs (Sperk et al., 2003; Boulland and Chaudhry, 2012) and our initial

results, although showing the presence of VGAT mRNA in MFs synaptosomes and DG, lacked the specificity so as to ascertain that VGAT was indeed present in GCs (Lamas et al., 2001). We later demonstrated with the use of single-cell PCR that its mRNA was indeed present, that its expression was modulated by age and activity in the adult (Gómez-Lira et al., 2005). Recently, using postembedding immunogold electronmicroscopy, we could reveal the co-localization of VGAT protein with VGLUTs in single MF boutons and the evidence also suggested that they were also in single vesicles (Zander et al., 2010). It has also been suggested that an unidentified GABA transporter may exist, also supported by the evidence that some GABAergic interneurons lack VGAT (Chaudhry et al., 1998; Boulland and Chaudhry, 2012). Finally, the diverging data may be due to technical differences. As derived from this, a direct demonstration of VGAT-dependent release from the MFs is still needed.

Mori et al. (2004) conducted paired recordings of connected GCs and pyramidal cells in cultured slices and did not find GABA-mediated responses in pyramidal cells on activation of GCs. Their conclusion was that the GCs do not release of GABA. We should remember, however, that these experiments were conducted under culture conditions with cells of more than 4 weeks of age. This does not constitute evidence against co-release because the experiments did not meet the conditions where co-release has been determined to occur: during development or in adult GCs, after a period of enhanced excitability. The same holds true for another report by Cabezas et al. (2012), who did not detect GABA-mediated postsynaptic currents in pyramidal cells by activation of coupled GCs in organotypic cultures. Interestingly, they did show that MFs released GABA that can act on GABAB receptors present in the presynaptic terminals, suggesting that GAD expression does not endow the MFs with a GABAergic phenotype, rather GABA's primary function is to instruct the presynaptic element. Cultured slices have the inconvenience that the developmental stage of the cells is difficult to define and both, their excitability conditions and synaptic organization can be strongly affected by the culture method (Gutiérrez and Heinemann, 1999; De Simoni et al., 2003).

Uchigashima et al. (2007) questioned the putative MF origin of the GABAergic responses observed in CA3 on MF stimulation and suggested that they may be brought about, possibly, by stimulation of MF-associated interneurons (Vida and Frotscher, 2000; Losonczy et al., 2004). However, some of the responses they found were mildly sensitive to the activation of type II mGluR with DCG-IV (Uchigashima et al., 2007), while other monosynaptic GABAergic responses that they did observe to be more sensitive to mGluR activation were those in which L-AP4, a type III mGluR agonist, was used. Thus, they leave open the possibility that L-AP4 is indeed a better modulator of MF GABAergic transmission, albeit with reservations or without testing whether this was indeed the case. L-AP4 has been repeatedly shown to be strong inhibitor of MF GABA responses in the rat in comparison to DCG-IV (Gutiérrez, 2002; see also Safiulina et al., 2006; Treviño et al., 2007). Uchigashima et al. (2007) acknowledge that the GABAergic machinery, GAD and GABA, is present in the MF, although they did not detect VGAT (as already mentioned, this protein was, until recently, very difficult to detect with immunohistochemical methods, but postembedding electron microscopy has revealed its presence; Zander et al., 2010). On the other hand, the recognition of L-AP4-sensitive monosynaptic GABAergic responses as not of MF origin may be a false negative interpretation. Indeed, the number of boutons that release GABA or that co-release glutamate and GABA is low (Beltrán and Gutiérrez, 2012). Identical experiments should be done, as the work of Uchigashima et al. (2007) attempted, but without discarding possible positive results without proper controls (for example, there is evidence that L-AP4 is more effective than DCG-IV in inhibiting putative MF-GABA transmission and that L-AP4 does not affect IPSCs evoked by SL interneurons, which were not tested). Although at first sight, Uchigashima et al. (2007) provide evidence that is in contrast to what several groups have shown, there are some methodological differences in their work with respect to others that do not permit to state that they have found evidence against the release of GABA from the MF.

To avoid ascribing synaptic transmission to fibers other than MFs, an excitatory or an inhibitory response should be evoked on a pyramidal cell by an action potential of an identified GC. This task is unlikely to be accomplished using paired recordings on slices. Selective stimulation of MF boutons and recording from a post-synaptic cell in a slice is also a possibility to solve this problem, but because of the difficulty in finding the post-synaptic cell that responds to the bouton being stimulated and because only a number of boutons seem to co-release the amino acids, this second possibility can also be time-consuming and not ideal for these goals (Bischofberger et al., 2006).

We recently provided what constitutes the most direct evidence in favor of the co-release hypothesis using a preparation that avoids sources of "synaptic contamination." In dissociated pyramidal cells, with identified boutons of MFs and boutons of interneurons attached to their apical or basal dendrites, we selectively recorded responses to stimulation of each type of bouton (**Figure 3**). Indeed, in young rats stimulation of a number of boutons identified MFs, but not of interneurons, released glutamate, or GABA or co-release glutamate and GABA and these responses had the signature of transmission of MF origin. By contrast, activation of MF boutons of adult rats did not release GABA (**Figure 3**; Beltrán and Gutiérrez, 2012). These data give us a very important message when considering "the existence or not" of co-release: (1) not all boutons release glutamate or GABA or both; alternantively it is not possible to know which cell one records that receives which type of bouton. (2) The number of MF that make contact with postsynaptic cells is very low. Therefore, the possibility of stimulating a fiber (minimal stimulation), finding a responding cell (or doing a paired recording for that matter), which, additionally happens to have co-releasing boutons, points to low odds of everybody doing the experiment in the same way to find the same responses. Therefore, it is the identification of the molecular switch that turns off GABA release during development or turns off (or preventing) GABA release in the adult after seizures that will prove (for all) that GCs are really capable of being GABAergic.

MOSSY FIBERS EXPRESS GAP JUNCTIONS

Hamzei-Sichani et al. (2007) showed the presence of gap junctions on MFs, which suggests that axo-axonal communication between

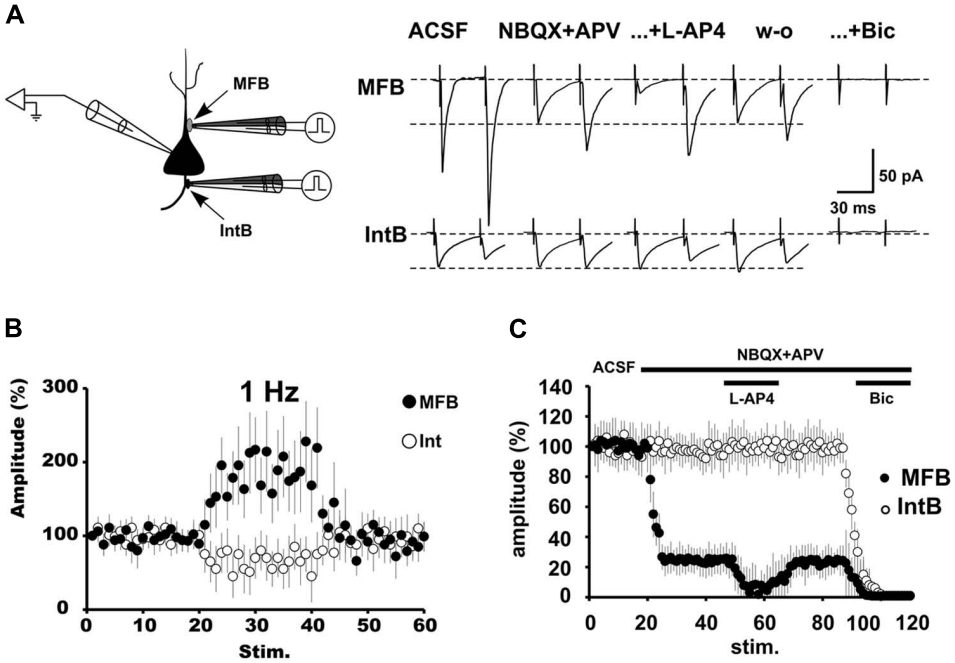

FIGURE 3 | The pharmacologically isolated GABAergic synaptic currents evoked by stimulation of MFBs have the signature of transmission of MF origin. (A) Schematic depiction of an isolated pyramidal cell with a fluorescent MF bouton on the apical dendrite and an interneuronal bouton on the basal dendrite. A bipolar theta glass pipette was used for stimulation of the boutons. Changing the stimulation frequency from 0.05 to 1 Hz produced a strong potentiation (>200%) of the GABAergic synaptic responses (black circles). By contrast stimulation of IntBs (open circles) produced frequency-dependent depression. **(B)** The effect of L-AP4 on the pharmacologically isolated GABAergic current evoked by MF bouton stimulation is presynaptic, as evidenced by the paired-pulse protocol. By contrast, GABAergic responses evoked by interneuronal bouton stimulation were unaffected. **(C)** Group synaptic responses to MF bouton (black circles; $n = 6$) and interneuronal bouton stimulation (open circles; $n = 6$). Responses to MF bouton stimulation were partially blocked by iGluR blockers. The remaining responses were strongly and reversibly depressed by the activation of mGluRs with L-AP4, and completely blocked by bicuculline. Responses to interneuronal bouton stimulation were not affected by the perfusion of iGluR blockers, but completely blocked by bicuculline (from Beltrán and Gutiérrez, 2012).

them can underlie very fast network oscillations. Using transmission electron microscopy and freeze-fracture replica immunogold labeling, they were able to determine the presence of Cx36 as the main constituent of these gap junctions. They proposed that only a few gap junctions per axon were present, which contribute to normal axonal electrical activity and that may also be involved in altered electrical activity in epilepsy. Interestingly, not only were the gap junctions found along the MFA themselves but also in the terminals in CA3. Indeed, Hamzei-Sichani et al. (2012) presented ultrastructural, immunocytochemical and dye coupling evidence for mixed electrical-chemical synapses (**Figure 4**). Cx36 was found in MF boutons in contact with dendritic spines of pyramidal cells, among other types of connections. This has also been observed with immunofluorescence and confocal microscopy, whereby Cx36 co-localized with VGLUT1 in the MF boutons (Nagy, 2012).

EVIDENCE OF ELECTRICAL COMMUNICATION BETWEEN THE MFs

The presence of gap junctions between MFs would enable passage of electrical currents from one axon to the other and, if that is the case, evoking an antidromic action potential in one axon, an electrical spikelet should be seen in another, contiguous cell. Schmitz et al. (2001) provided electrophysiological evidence that coupling potentials were indeed invading a contiguous axon prior to reaching the soma of a nearby cell, and that this effect was blocked by the gap junction blocker carbenoxolone (CBX). This activity provides the basis for an extremely fast communication mechanism and endows the axons with integrative properties, rather than just being a transmission line (Schmitz et al., 2001). Thus, high-frequency network oscillations can have their basis on this type of communication, which allows recruiting principal neurons in a network that generates activity with plastic frequency ranges.

Evidence of electrical communication between MFs and pyramidal cells

A hypothesis that can be immediately derived from the observation of Cx36 in MFs is that its expression may not be confined to the axons, but that it can also occur in their terminals in the adult rat. If this were to be the case, MF-to-pyramidal cell electrical communication should be detected. Moreover, the extremely low coupling of MF-to-MF would suggest that also MF-to-pyramidal cell electrical connectivity would be of very low probability, as we also showed to be the case by dye coupling (**Figure 5**; Hamzei-Sichani et al., 2012). Despite the evidence of gap junctions in the principal cells of the DG, axo-dendritic electrical synapses between two different types of principal cells in the hippocampus have not been reported so far. Moreover, no axo-dendritic

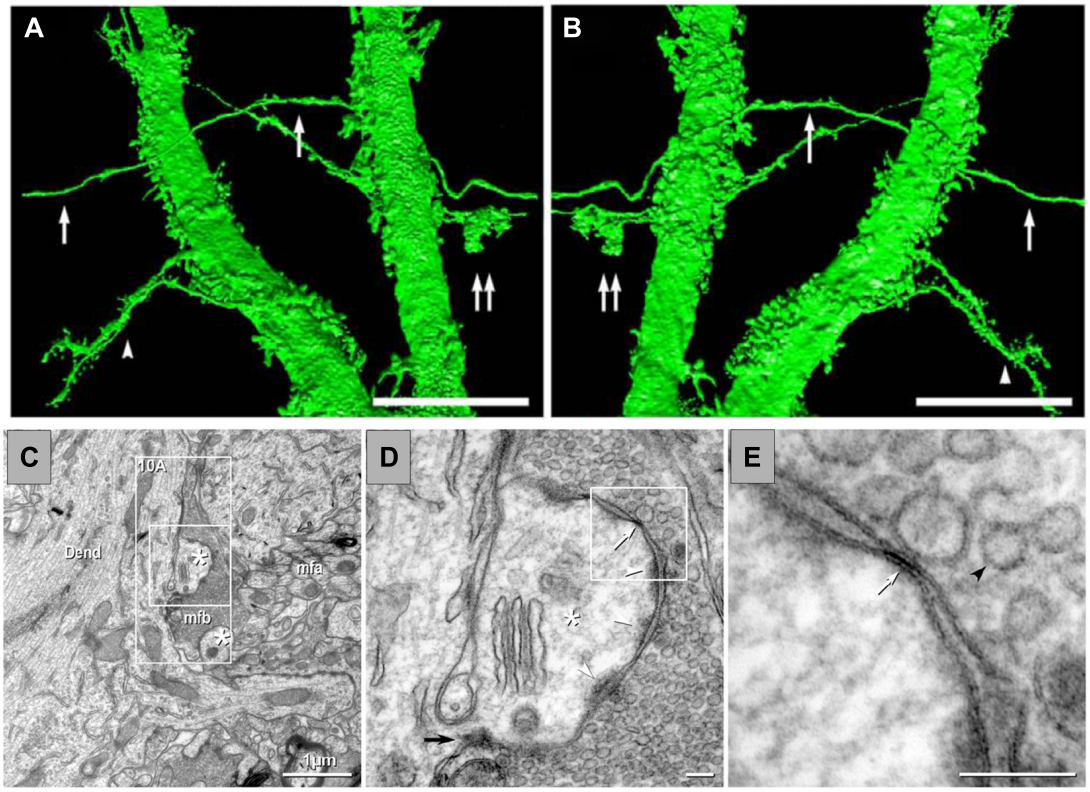

FIGURE 4 | Anatomical evidence of gap junctions between MFs and pyramidal cell dendrites and thin-section TEM evidence for MF – pyramidal cell mixed synapses. (A,B) High-resolution 3D reconstructions (in two opposite *z* directions) of two dendrites of a lucifer yellow-injected pyramidal cell, dye-coupled to MFs (arrows). Double arrows mark a MF bouton. The arrowhead in **(C)** marks two dendrites with spines. **(C)** Image showing part of a dendrite (Dend) with dendritic spines (astrisks) and adjacent MFA . **(D)** Higher magnification of boxed area in **(C)**. A typical large-diameter MF bouton containing synaptic vesicles surrounds a dendritic spine at a synaptic contact containing both close membrane appositions characteristic of gap junctions (white arrows) and wider membrane appositions with asymmetric dense cytoplasmic material (arrowheads) characteristic of postsynaptic densities. **(E)** Higher magnification of boxed area in **(D)** showing the gap junction contact (white arrow) between the MF bouton and the dendritic spine. A synaptic vesicle is marked with a black arrowhead (from Hamzei-Sichani et al., 2012).

electrical synapses have been observed between excitatory axons and principal cell dendrites, in the mammalian telencephalon. We provided the first evidence of electrical coupling between MFs and pyramidal cells, which, as expected, were very few (Vivar et al., 2012). Under blockage of ionotropic glutamate and GABA receptors, stimulation of the DG provoked, in about 5% of pyramidal cells recorded (>700), spikelets of fast kinetics, which were blocked by CBX and potentiated by DA. These data are consistent with electrical coupling. Their latency was shorter than of chemical transmission and their MF specificity can be assessed by two criteria. The probability of recruiting interneurons (by electrical synapses), which in turn, make electrical contacts with pyramidal cells is minimal because the delay that we observed is compatible with the conduction velocity of the MFs; by contrast, direct interneuron activation recruiting a pyramidal cell by an electrical contact would produce a response of extremely short latency (<0.4 ms, Mercer et al., 2006); additionally, intensity produced an all or none response, if higher intensities recruit interneurons, latencies would shift strongly (**Figure 5**). Finally, further evidence in favor of this would be given by mixed electrical-chemical transmission.

Evidence of mixed electrical-chemical communication between MFs and pyramidal cells. Another type of co-transmission of the MFs

As stated above, if electrical communication can be present in a well-known chemical synapse (MF-CA3), then chemical – electrical cotransmission might occur, whereby stimulation of the MFs would evoke an electrical spikelet accompanied by a chemical component. Pharmacological and physiological criteria must then be met to imply that such a response corresponds to transmission of MF origin. We tested this hypothesis and showed that MF activation produced fast spikelets in a number of PCs with an onset latency consistent with MF conduction velocity and were followed by glutamate receptor-mediated excitatory postsynaptic potentials that had the physiological and pharmacological characteristics of MF neurotransmission in the adult rat (Vivar et al., 2012). Moreover, the fast spikelets persisted during blockade of chemical transmission, were potentiated by DA and suppressed by the gap junction blocker CBX. To our knowledge, this constitutes the first evidence of mixed electrical-chemical communication between two principal cells of the mammalian forebrain. We showed that in a number of cells, stimulation of the DG initially produced an EPSP and, when threshold intensity for

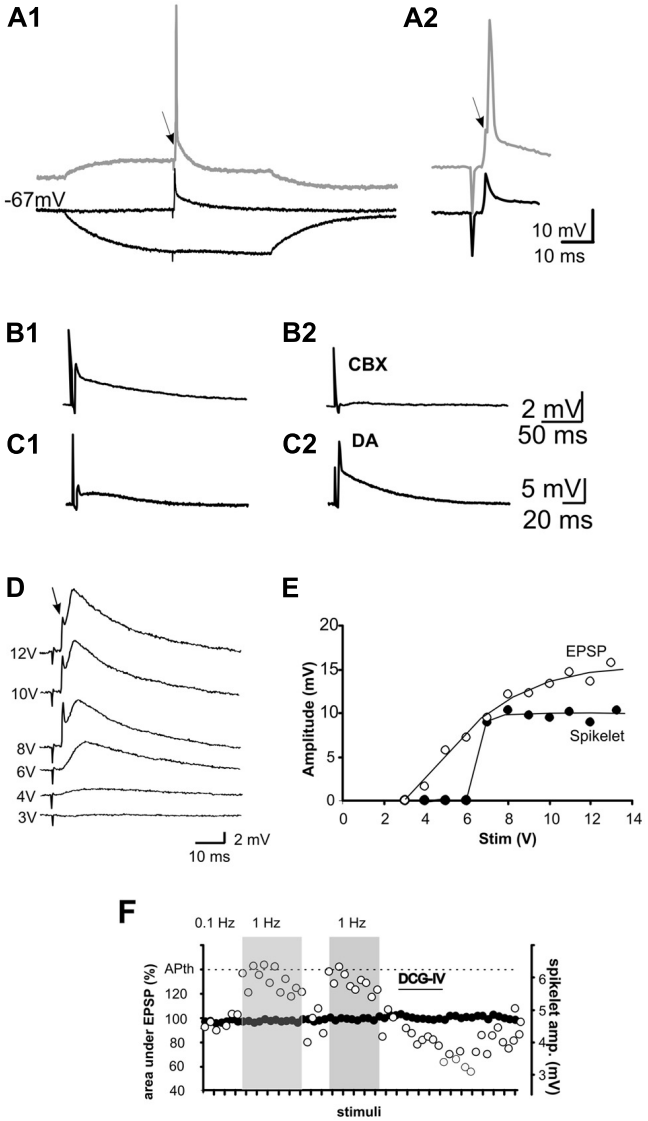

FIGURE 5 | Mossy fiber activation evokes spikelets in some pyramidal cells (5–7%) of CA3. (A1) Spikelets are evoked in an all-or-none fashion at resting membrane potential in the presence of glutamate, GABAA and ACh-M1 receptor antagonists. When stimulation is given at a depolarized membrane potential (displaced trace in **A1** and expanded trace in **A2**, the cell fires an action potential, which is preceded by a notch (arrow) corresponding to an underlying spikelet. By contrast, hyperpolarization of the membrane potential by ± 15 mV suppresses the spikelet **B1,2**). The non-selective gap junction blocker, carbenoxolone (CBX) blocked the spikelet, whereas dopamine (DA) potentiated the spikelet **(C1,2)**. If electrical spikelets appear in the MF synapse, a mixed electrical-chemical transmission is expected. This is shown in **(D)**. Increasing stimulation intensities enhanced the chemical component of the synaptic response, whereas the spikelet was evoked upon reaching threshold intensity and not further modified by increasing the stimulus intensity. **(E)** Input–output curve of the chemical (EPSP) and electrical (spikelet) synaptic components. Note that the spikelet is evoked in an all-or-none fashion. **(F)** Plot of the behavior of the EPSP (area under the curve; left *y*-axis) and spikelet (amplitude; right *y*-axis) at 0.01 and 1 Hz and during the perfusion of DCG-IV. APth, action potential threshold.

activating a MF that established an electric synapse was reached, the EPSP was preceded by a fast spikelet. The amplitude of the EPSP augmented as stimulation intensity was increased, whereas the amplitude of the spikelet was not modified. In other cells, spikelets were readily evoked at the minimal intensity needed to evoke any synaptic response. Furthermore, the chemical component of the response was depressed by DCG-IV and was strongly potentiated when raising the stimulation frequency from 0.1 to 1 Hz, while the electrical spikelet remained unaltered (**Figure 5**; Vivar et al., 2012). Mixed electrical and glutamatergic communication between GCs and some pyramidal cells in CA3 may ensure the activation of sets of pyramidal cells, bypassing the strong action of concurrent feed-forward inhibition that GCs activate.

CONCLUSION

Having reviewed the available data about how the MFs transmit information by different chemicals or by signals of different physical characteristics, one seems to be recollecting the first decades of "modern neuroscience" when "it had to be one or the other." Or are we still living in those years?

Many features of synaptic communication observed at the MF synapses are not usually observed in most cortical synapses, and thus have drawn the attention of many groups studying different aspects of the transmission of information, of which many authoritative reviews have been published. In recent years, the paradigmatic view that the MFs synapses form merely excitatory, glutamatergic contacts with their post-synaptic target cells has been questioned. In addition, the possibility of them communicating with some of their target cells through gap junctions (Cx36), co-localized with the chemical ones (AMPA-R), compels us to add adjectives to this unique synapse. Short after the first evidence of the co-release of GABA and glycine in the spinal cord (Jonas et al., 1998) and of the possibility that GABA could be co-released with glutamate from the MFs (Gutiérrez and Heinemann, 1997, 2001; Gutiérrez, 2000; Walker et al., 2001) several examples of co-release of classical neurotransmitters in different regions of the CNS appeared (reviewed in Gutiérrez, 2009). Studies on how different transmitters can be released from single synapses ought to be conducted, as some kind of selectivity in the release may be expected, i.e., activity-dependent modifications in content and vesiculation may instruct the synapse to release more of one than the other neurotransmitter. Studies performing quantal release should help to disclose this. Another intriguing possibility is that different presynaptic mechanisms may selectively control the release of either neurotransmitter. As for the post-synaptic site, it is possible that activity-dependent release may evoke receptor incorporation or relocation in the membrane that would tip the balance in favor of a response to one rather than to the other neurotransmitter. These and many questions are still open.

On the other hand, although dendro-dendritic and axo-axonic electrical synapses in the mammalian forebrain are well known, axo-dendritic electrical-chemical synapses were just recently revealed in the MF synapse and there is no doubt that more will certainly appear in different regions of the mammalian CNS. As in the case of the study of the co-release of glutamate and GABA,

selective activation of MF boutons should prove true electrical coupling. These experiments, however, are technically difficult because direct stimulation of the bouton can produce an artifact that may obscure the fast electrical component. Despite this, the evidence available is consistent with some MFs establishing electrical coupling with a number of pyramidal cells. This type of contacts in the MF synapse may allow bidirectional, possibly graded communication that can be faster than chemical synapses and which will possibly explain different forms of modulation.

ACKNOWLEDGMENTS

We thank Prof. I. Vida for reading an earlier version of the manuscript. This work was supported by grant I020/193/10 FON.INST.-29-10 to Rafael Gutiérrez from Consejo Nacional de Ciencia y Tecnología, México.

REFERENCES

Acsády, L., Kamondi, A., Sik, A., Freund, T., and Buzsaki, G. (1998). GABAergic cells are the major postsynaptic targets of mossy fibers in the rat hippocampus. *J. Neurosci.* 18, 3386–3403.

Ahnert-Hilger, G., and Jahn, R. (2011). CLC-3 spices up GABAergic synaptic vesicles. *Nat. Neurosci.* 14, 405–407. doi: 10.1038/nn.2786

Alle, H., and Geiger, J. R. (2007). GABAergic spill-over transmission onto hippocampal mossy fiber boutons. *J. Neurosci.* 27, 942–950. doi: 10.1523/JNEUROSCI.4996-06.2007

Altman, J., and Bayer, S. A. (1990). Migration and distribution of two populations of hippocampal granue cell precursors during the perinatal and postnatal periods. *J. Comp. Neurol.* 301, 365–381. doi: 10.1002/cne.903010304

Amaral, D. G. (1979). Synaptic extensions from the mossy fibers of the fascia dentata. *Anat. Embryol.* 155, 241–251. doi: 10.1007/BF00317638

Amaral, D. G., Ishizuka, N., and Claiborne, B. (1990). Neurons, numbers and the hippocampal network. *Prog. Brain Res.* 83, 1–11. doi: 10.1016/S0079-6123(08)61237-6

Amilhon, B., Lepicard, E., Renoir, T., Mongeau, R., Popa, D., Poirel, O., et al. (2010). VGLUT3 (vesicular glutamate transporter type 3) contribution to the regulation of serotonergic transmission and anxiety. *J. Neurosci.* 30, 2198–2210. doi: 10.1523/JNEUROSCI.5196-09.2010

Andersen, P., Bliss, T. V., and Skrede, K. K. (1971). Lamellar organization of hippocampal pathways. *Exp. Brain Res.* 13, 222–238. doi: 10.1007/BF00234087

Anderson, C. M., and Swanson, R. A. (2000). Astrocyte glutamate transport: review of properties, regulation, and physiological functions. *Glia* 32, 1–14. doi: 10.1002/1098-1136(200010)32:1<1::AID-GLIA10>3.0.CO;2-W

Apostolides, P. F., and Trussell, L. O. (2013). Rapid, activity-independent turnover of vesicular transmitter content at a mixed glycine/GABA synapse. *J. Neurosci.* 33, 4768–4781. doi: 10.1523/JNEUROSCI.5555-12.2013

Attwell, D. (2000). Brain uptake of glutamate: food for thought. *J. Nutr.* 130(4S Suppl.), 1023S–1025S.

Babu, H., Cheung, G., Kettenmann, H., Palmer, T. D., and Kempermann, G. (2007). Enriched monolayer precursor cell cultures from micro-dissected adult mouse dentate gyrus yield functional granule cell-like neurons. *PLoS ONE* 4:e388, 1–11. doi: 10.1371/journal.pone.0000388

Bellocchio, E. E., Hu, H., Pohorille, A., Chan, J., Ticket, V. M., and Edwards, R. H. (1998). The localization of the brain-specific inorganic phosphate transporter suggests a specific presynaptic role in glutamatergic transmission. *J. Neurosci.* 18, 8648–8659.

Beltrán, J. Q., and Gutiérrez, R. (2012). Co-release of glutamate and GABA from single, identified mossy fiber giant boutons. *J. Physiol.* 590, 4789–4800. doi: 10.1113/jphysiol.2012.236372

Ben-Ari, Y., Khazipov, R., Leinekugel, X., Caillard, O., and Gaiarsa, J. L. (1997). GABAA, NMDA and AMPA receptors: a developmentally regulated 'ménage a trios.' *Trends Neurosci.* 20, 523–529. doi: 10.1016/S0166-2236(97)01147-8

Ben-Ari, Y., Tseeb, V., Raggozzino, D., Khazipov, R., and Gaiarsa, J. L. (1994). Gamma-aminobutyric acid (GABA): a fast excitatory transmitter, which may regulate the development of hippocampal neurones in early postnatal life. *Prog. Brain Res.* 102, 261–273. doi: 10.1016/S0079-6123(08)60545-2

Bennett, M. V. L. (1972). "A comparison of electrically and chemically mediated transmission," in *Structure and Function of Synapses*, eds G. D. Pappas and D. P. Purpura (New York: Raven Press), 221–256.

Bennett, M. K., and Scheller, R. H. (1994). Molecular correlates of synaptic vesicle docking and fusion. *Curr. Opin. Neurobiol.* 4, 324–329. doi: 10.1016/0959-4388(94)90092-2

Bergersen, L., Ruiz, A., Bjaalie, J. G., Kullmann, D. M., and Gundersen, V. (2003). GABA and GABAA receptors at hippocampal mossy fibre synapses. *Eur. J. Neurosci.* 18, 931–941. doi: 10.1046/j.1460-9568.2003.02828.x

Bergersen, L. H., Storm-Mathisen, J., and Gundersen, V. (2008). Immunogold quantification of amino acids and proteins in complex subcellular compartments. *Nat. Protoc.* 3, 144–152. doi: 10.1038/nprot.2007.525

Biedermann, B., Bringmann, A., and Reichenbach, A. (2002). High-affinity GABA uptake in retinal glial (Müller) cells of the guinea pig: electrophysiological characterization, immunohistochemical localization, and modeling of efficiency. *Glia* 39, 217–228. doi: 10.1002/glia.10097

Bischofberger, J., Engel, D., Li, L., Geiger, J. R., and Jonas, P. (2006). Patch-clamp recording from mossy fiber terminals in hippocampal slices. *Nat. Protoc.* 1, 2075–2081. doi: 10.1038/nprot.2006.312

Borodinsky, L. N., Belgacem, Y. H., Swapna, I., and Sequerra, E. B. (2012). Dynamic regulation of neurotransmitter specification: relevance to nervous system homeostasis. *Neuropharmacology* doi: 10.1016/j.neuropharm.2012.12.005 [Epub ahead of print].

Boulland, J. L., and Chaudhry, F. A. (2012). Ontogenetic changes in the distribution of the vesicular GABA transporter VGAT correlate with the excitation/inhibition shift of GABA action. *Neurochem. Int.* 61, 506–516. doi: 10.1016/j.neuint.2012.03.018

Cabezas, C., Irinopoulou, T., Gauvain, G., and Poncer, J. C. (2012). Presynaptic but not postsynaptic GABA signaling at unitary mossy fiber synapses. *J. Neurosci.* 32, 11835–11840. doi: 10.1523/JNEUROSCI.5543-11.2012

Caiati, M. D., Sivakumaran, S., and Cherubini, E. (2010). In the developing rat hippocampus, endogenous activation of presynaptic kainate receptors reduces GABA release from mossy fiber terminals. *J. Neurosci.* 30, 1750–1759. doi: 10.1523/JNEUROSCI.4566-09.2010

Caiati, M. D., Sivakumaran, S., Lanore, F., Mulle, C., Richard, E., Verrier, D., et al. (2012). Developmental regulation of CB1-mediated spike-time dependent depression at immature mossy fiber-CA3 synapses. *Sci. Rep.* 2, 285. doi: 10.1038/srep00285

Chaudhry, F. A., Edwards, R. H., and Fonnum, F. (2008). Vesicular neurotransmitter transporters as targets for endogenous and exogenous toxic substances. *Annu. Rev. Pharmacol. Toxicol.* 48, 277–301. doi: 10.1146/annurev.pharmtox.46.120604.141146

Chaudhry, F. A., Reimer, R. J., Bellocchio, E. E., Danbolt, N. C., Osen, K. K., Edwards, R. H., et al. (1998). The vesicular GABA transporter, VGAT, localizes to synaptic vesicles in sets of glycinergic as well as GABAergic neurons. *J. Neurosci.* 18, 9733–9750.

Choi, D. W. (1992). Excitotoxic cell death. *J. Neurobiol.* 23, 1261–1276. doi: 10.1002/neu.480230915

Claiborne, B., Amaral, D. G., and Cowan, M. W. (1986). A light and electron microscopic analysis of the mossy fibers of the rat dentate gyrus. *J. Comp. Neurol.* 246, 435–458. doi: 10.1002/cne.902460403

Connors, B. W., and Long, M. A. (2004). Electrical synapses in the mammalian brain. *Annu. Rev. Neurosci.* 27, 393–418. doi: 10.1146/annurev.neuro.26.041002.131128

Cowan, W. M., Südhof, T. C., and Stevens, C. F. (2001). *Synapses.* Baltimore, MD: The Johns Hopkins University Press.

Crawford, I. L., and Connor, J. D. (1973). Localization and release of glutamic acid in relation to the hippocampal mossy fibre pathway. *Nature* 244, 442–443. doi: 10.1038/244442a0

Daikhin, Y., and Yudkoff, M. (2000). Compartmentation of brain glutamate metabolism in neurons and glia. *J. Nutr.* 130(4S Suppl.), 1026S–1031S.

Dalby, N. O. (2003). Inhibition of gamma-aminobutyric acid uptake: anatomy, physiology and effects against epileptic seizures. *Eur. J. Pharmacol.* 479, 127–137. doi: 10.1016/j.ejphar.2003.08.063

Dale, H. H. (1935). Pharmacology and nerve endings. *Proc. R. Soc. Med.* 28, 319–332. doi: 10.1136/bmj.2.3859.1161

De Simoni, A., Griesinger, C. B., and Edwards, F. A. (2003). Development of rat CA1 neurons in acute versus organotypic slices: role of experience in synaptic morphology and activity. *J. Physiol.* 550, 135–147. doi: 10.1113/jphysiol.2003.039099

Dulcis, D., and Spitzer, N. C. (2011). Reserve pool neuron transmitter respecification: novel neuroplasticity. *Dev. Neurobiol.* 72, 465–474. doi: 10.1002/dneu.20920

Fatt, P. (1954). Biophysics of junctional transmission. *Physiol. Rev.* 34, 674–710.

Fonnum, F., and Walberg, F. (1973). The concentration of GABA within inhibitory nerve terminals. *Brain Res.* 62, 577–579. doi: 10.1016/0006-8993(73)90724-5

Frahm, C., Engel, D., Piechotta, A., Heinemann, U., and Draguhn, A. (2000). Presence of γ-aminobutyric acid transporter mRNA in interneurons and principal cells of rat hippocampus. *Neurosci. Lett.* 388, 175–178. doi: 10.1016/S0304-3940(00)01217-9

Fremeau, R. T. Jr., Troyer, M. D., Pahner, I., Nygaard, G. O., Tran, C. H., Reimer, R. J., et al. (2001). The expression of vesicular glutamate transporters defines two classes of excitatory synapse. *Neuron* 31, 247–260. doi: 10.1016/S0896-6273(01)00344-0

Fremeau, R. T., Voglmaier, S., Seal, R. P., and Edwards, R. H. (2004). VGLUTs define subset of excitatory neurons and suggest novel roles for glutamate. *Trends Neurosci.* 27, 98–103. doi: 10.1016/j.tins.2003.11.005

Frotscher, M. (1985). Mossy fibres form synapses with identified pyramidal basket cells in the CA3 region of the guinea-pig hippocampus: a combined Golgi-electron microscope study. *J. Neurocytol.* 14, 245–259. doi: 10.1007/BF01258450

Furshpan, E. J., and Potter, D. D. (1957). Mechanism of nerve impulse transmission at a crayfish synapse. *Nature* 180, 342–343. doi: 10.1038/180342a0

Furukawa, T., and Furshpan, E. J. (1963). Two inhibitory mechanisms in the Mauthner neurons of goldfish. *J. Neurophysiol.* 26, 140–176.

Furuta, A., Martin, L. J., Lin, C. L. G., Dykes-Hoberg, M., and Rothstein, J. D. (1997). Cellular and synaptic localization of the neuronal glutamate transporters excitatory amino acid transporters 3 and 4. *Neuroscience* 81, 1031–1042. doi: 10.1016/S0306-4522(97)00252-2

Galván, E. J., Cosgrove, K. E., and Barrionuevo, G. (2011). Multiple forms of long-term synaptic plasticity at hippocampal mossy fiber synapses on interneurons. *Neuropharmacology* 60, 740–747. doi: 10.1016/j.neuropharm.2010.11.008

Golgi, C. (1906). *The Neuron Doctrine – Theory and Facts.* Available at: http://www.nobelprize.org/nobel_prizes/medicine/laureates/1906/golgi-lecture.pdf

Gomeza, J., Ohno, K., Hülsmann, S., Armsen, W., Eulenburg, V., Richter, D. W., et al. (2003). Deletion of the mouse glycine transporter 2 results in a hyperekplexia phenotype and postnatal lethality. *Neuron* 40, 797–806. doi: 10.1016/S0896-6273(03)00673-1

Gómez-Lira, G., Lamas, M., Romo-Parra, H., and Gutiérrez, R. (2005). Programmed and induced phenotype of the hippocampal granule cells. *J. Neurosci.* 25, 6939–6946. doi: 10.1523/JNEUROSCI.1674-05.2005

Gómez-Lira, G., Trillo, E., Ramírez, M., Asai, M., Sitges, M., and Gutiérrez, R. (2002). The expression of GABA in mossy fiber synaptosomes coincides with the seizure-induced expression of GABAergic transmission in the mossy fiber synapse. *Exp. Neurol.* 177, 276–283. doi: 10.1006/exnr.2002.7986

Guastella, J., Nelson, N., Nelson, H., Czyzyk, L., Keynan, S., Miedel, M. C., et al. (1990). Cloning and expression of a rat brain GABA transporter. *Science* 249, 1303–1306. doi: 10.1126/science.1975955

Gutiérrez, R. (2000). Seizures induce simultaneous GABAergic and glutamatergic neurotransmission in the dentate gyrus – CA3 system. *J. Neurophysiol.* 84, 3088–3090.

Gutiérrez, R. (2002). Activity-dependent expression of simultaneous glutamatergic and GABAergic neurotransmission from the mossy fibers in vitro. *J. Neurophysiol.* 87, 2562–2570.

Gutiérrez, R. (2003). The GABAergic phenotype of the "glutamatergic" granule cells of the dentate gyrus. *Prog. Neurobiol.* 71, 337–358. doi: 10.1016/j.pneurobio.2003.11.004

Gutiérrez, R. (2009). "Co-existence and co-release of classical neurotransmitters," in *Ex Uno Plures*, ed. R. Gutiérrez (New York, NY: Springer Verlag), 15–22.

Gutiérrez, R., and Heinemann, U. (1997). Simultaneous release of glutamate and GABA might be induced in mossy fibers after kindling. *Neurosci. Lett. Suppl.* 48, S23. doi: 10.1016/S0304-3940(97)90092-6

Gutiérrez, R., and Heinemann, U. (1999). Synaptic reorganization in explanted cultures of rat hippocampus. *Brain Res.* 815, 304–316. doi: 10.1016/S0006-8993(98)01101-9

Gutiérrez, R., and Heinemann, U. (2001). Kindling induces transient fast inhibition in the dentate gyrus – CA3 projection. *Eur. J. Neurosci.* 13, 1371–1379. doi: 10.1046/j.0953-816x.2001.01508.x

Gutiérrez, R., Romo-Parra, H., Maqueda, J., Vivar, C., Ramírez, M., Morales M. A., et al. (2003). Plasticity of the GABAergic phenotype of the "glutamatergic" granule cells of the rat dentate gyrus. *J. Neurosci.* 23, 5594–5598.

Hamzei-Sichani, F., Davidson, K. G. V., Yasumura, T., Janssen, W. G. M., Wearne, S. L., Hof, P. R., et al. (2012). Mixed electrical–chemical synapses in adult rat hippocampus are primarily glutamatergic and coupled by connexin-36. *Front. Neuroanat.* 6:13. doi: 10.3389/fnana.2012.00013

Hamzei-Sichani, F., Kamasawa, N., Janssen, W. G., Yasumura, T., Davidson, K. G., Hof, P. R., et al. (2007). Gap junctions on hippocampal mossy fiber axons demonstrated by thin-section electron microscopy and freeze fracture replica immunogold labeling. *Proc. Natl. Acad. Sci. U.S.A.* 104, 12548–12553. doi: 10.1073/pnas.0705281104

Heinemann, U., Beck, H., Dreier, J. P., Ficker, E., Stabel, J., and Zhang, C. L. (1992). The dentate gyrus as a regulated gate for the propagation of epileptiform activity. *Epilepsy Res. Suppl.* 7, 273–280.

Henze, D. A., Urban, N. N., and Barrionuevo, G. (2000). The multifarious hippocampal mossy fiber pathway: a review. *Neuroscience* 98, 407–427. doi: 10.1016/S0306-4522(00)00146-9

Henze, D. A., Wittner, L., and Buzsáki, G. (2002). Single granule cells reliable discharge targets in the hippocampal CA3 network *in vivo*. *Nat. Neurosci.* 5, 790–795. doi: 10.1038/nn887

Hertz, L., and Schousboe, A. (1987). "Primary cultures of gabaergic and glutamatergic neurons as model systems to study neurotransmitter functions I. Differentiated cells," in *Model Systems of Development and Aging of the Nervous System*, eds A. Vernadakis, A. Privat, J. M. Lauder, P. S. Timiras, and E. Giacobini (New York, NY: Springer US), 19–31. doi: 10.1007/978-1-4613-2037-1_2

Hnasko, T. S., Chuhma, N., Zhang, H., Goh, G. Y., Sulzer, D., Palmiter, R. D., et al. (2010). Vesicular glutamate transport promotes dopamine storage and glutamate corelease in vivo. *Neuron* 65, 643–656. doi: 10.1016/j.neuron.2010.02.012

Holten, A. T., and Gundersen, V. (2008). Glutamine as a precursor for transmitter glutamate, aspartate and GABA in the cerebellum: a role for phosphate-activated glutaminase. *J. Neurochem.* 104, 1032–1042. doi: 10.1111/j.1471-4159.2007.05065.x

Jaffe, D. B., and Gutiérrez, R. (2007). Mossy fiber synaptic transmission: communication from the dentate gyrus to area CA3. *Prog. Brain Res.* 163, 109–805. doi: 10.1016/S0079-6123(07)63006-4

Jiang, W., Wang, J.-C., Zhang, Z., Sheerin, A. H., and Zhang, X. (2004). Response of seizure-induced newborn neurons in the dentate gyrus of adult rats to second episode of seizures. *Brain Res.* 1007, 248–252. doi: 10.1016/j.brainres.2004.02.005

Jonas, P., Bischofberger, J., and Sandkühler, J. (1998). Corelease of two fast neurotransmitters at a central synapse. *Science* 281, 419–424. doi: 10.1126/science.281.5375.419

Jung, M. W., and McNaughton, B. L. (1993). Spatial selectivity of unit activity in the hippocampal granular layer. *Hippocampus* 3, 165–182. doi: 10.1002/hipo.450030209

Kasyanov, A. M., Safiulina, V. F., Voronin, L. L., and Cherubini, E. (2004). GABA-mediated giant depolarizing potentials as coincidence detectors for enhancing synaptic efficacy in the developing hippocampus. *Proc. Natl. Acad. Sci. U.S.A.* 101, 3967–3972. doi: 10.1073/pnas.0305974101

Laake, J. H., Takumi, Y., Eidet, J., Torgner, I. A., Roberg, B., Kvamme, E., et al. (1999). Postembedding immunogold labelling reveals subcellular localization and pathway-specific enrichment of phosphate activated glutaminase in rat cerebellum. *Neuroscience* 88, 1137–1151. doi: 10.1016/S0306-4522(98)00298-X

Lamas, M., Gómez-Lira, G., and Gutiérrez, R. (2001). Vesicular GABA transporter mRNA expression in the dentate gyrus and in mossy fiber synaptosomes. *Brain Res. Mol. Brain Res.* 93, 209–214. doi: 10.1016/S0169-328X(01)00202-9

Lara, E., Beltrán, J. Q., Segovia, J., and Gutiérrez, R. (2012). Granule cells born in the adult rat hippocampus can regulate the expression of GABAergic markers. *Exp. Neurol.* 237, 134–141. doi: 10.1016/j.expneurol.2012.06.022

Lawrence, J. J., and McBain, C. J. (2003). Containing the detonation-feedforward inhibition in the CA3 hippocampus. *Trends Neurosci.* 26, 631–640. doi: 10.1016/j.tins.2003.09.007

Lehmann, H., Ebert, U., and Löscher, W. (1996). Immunocytochemical localization of GABA immunoreactivity in dentate granule cells of normal and kindled rats. *Neurosci. Lett.* 212, 41–44. doi: 10.1016/0304-3940(96)12777-4

Losonczy, A., Biró, A. A., and Nusser, Z. (2004). Persistently active cannabinoid receptors mute a subpopulation of hippocampal interneurons. *Proc. Natl. Acad. Sci. U.S.A.* 101, 1362–1367. doi: 10.1073/pnas.0304752101

MacCaferri, G., Tóth, K., and McBain, C. J. (1998). Target-specific expression of presynaptic mossy fiber plasticity. *Science* 279, 1368–1370. doi: 10.1126/science.279.5355.1368

Maqueda, J., Ramírez, M., Lamas, M., and Gutiérrez, R. (2003). Glutamic acid decarboxylase (GAD)67, but not GAD65, is constitutively expressed during development and transiently overexpressed by activity in the mossy fibers. *Neurosci. Lett.* 353, 69–71. doi: 10.1016/j.neulet.2003.08.077

Martin, A. R., and Pilar, G. (1963). Dual mode of synaptic transmission in the avian ciliary ganglion. *J. Physiol.* 168, 443–463.

Marty, S., Wehrle, R., Alvarez-Leefmans, F. J., Gasnier, B., and Sotelo, C. (2002). Postnatal maturation of Na^+, K^+, $2Cl^-$ cotransporter expression and inhibitory synaptogenesis in the rat hippocampus: an immunocytochemical analysis. *Eur. J. Neurosci.* 15, 233–245. doi: 10.1046/j.0953-816x.2001.01854.x

Mathews, E. A., Morgenstern, N. A., Piatti, V. C., Zhao, C., Jessberger, S., Schinder, A. F., et al. (2010). A distinctive layering pattern of mouse dentate granule cells is generated by developmental and adult neurogenesis. *J. Comp. Neurol.* 518, 4479–4490. doi: 10.1002/cne.22489

McBain, C. J. (2008). Differential mechanisms of transmission and plasticity at mossy fiber synapses. *Prog. Brain Res.* 169, 225–240. doi: 10.1016/S0079-6123(07)00013-1

McIntire, S. L., Reimer, R. J., Schuske, K., Edwards, R. H., and Jorgensen, E. M. (1997). Identification and characterization of the vesicular GABA transporter. *Nature* 389, 870–876. doi: 10.1038/39908

Meldrum, B. S. (2000). Glutamate as a neurotransmitter in the brain: review of physiology and pathology. *J. Nutr.* 130, 1007S–1015S.

Meldrum, B. S., Akbar, M. T., and Chapman, A. G. (1999). Glutamate receptors and transporters in genetic and acquired models of epilepsy. *Epilepsy Res.* 36, 189–204. doi: 10.1016/S0920-1211(99)00051-0

Mercer, A., Bannister, A. P., and Thomson, A. M. (2006). Electrical coupling between pyramidal cells in adult cortical regions. *Brain Cell Biol.* 35, 13–27. doi: 10.1007/s11068-006-9005-9

Minelli, A., Brecha, N. C., Karschin, C., DeBiasi, S., and Conti, F. (1995). GAT-1, a high-affinity GABA plasma membrane transporter, is localized to neurons and astroglia in the cerebral cortex. *J. Neurosci.* 15, 7734–7746.

Mody, I. (2002). The GAD-given right of dentate gyrus granule cells to become GABAergic. *Epilepsy Curr.* 2, 143–145. doi: 10.1046/j.1535-7597.2002.00053.x

Monier, C., Fournier, J., and Frégnac, Y. (2008). In vitro and in vivo measures of evoked excitatory and inhibitory conductance dynamics in sensory cortices. *J. Neurosci. Methods* 169, 323–365. doi: 10.1016/j.jneumeth.2007.11.008

Mori, M., Abegg, M. H., Gähwiler, B. H., and Gerber, U. (2004). A frequency-dependent switch from inhibition to excitation in a hippocampal unitary circuit. *Nature* 431, 453–456. doi: 10.1038/nature02854

Mori, M., Gähwiler, B. H., and Gerber, U. (2007). Recruitment of an inhibitory hippocampal network after bursting in a single granule cell. *Proc. Natl. Acad. Sci. U.S.A.* 104, 7640–7645. doi: 10.1073/pnas.0702164104

Nagy, J. I. (2012). Evidence for connexin36 localization at hippocampal mossy fiber terminals suggesting mixed chemical/electrical transmission by granule cells. *Brain Res.* 1487, 107–122. doi: 10.1016/j.brainres.2012.05.064

Ni, B., Rosteck, P. R. Jr., Nadi, N. S., and Paul, S. M. (1994). Cloning and expression of a cDAN encoding a brain-specific Na(+)-dependent inorganic phosphate cotransporter. *Proc. Natl. Acad. Sci. U.S.A.* 91, 5607–5611. doi: 10.1073/pnas.91.12.5607

Nicoll, R. A., and Schmitz, D. (2005). Synaptic plasticity at hippocampal mossy fibre synapses. *Nat. Rev. Neurosci.* 6, 863–876. doi: 10.1038/nrn1786

Obata, K., Otsuka, M., and Tanaka, Y. (1970). Determination of gamma-aminobutyric acid in single nerve cells of cat central nervous system. *J. Neurochem.* 17, 697–698. doi: 10.1111/j.1471-4159.1970.tb00550.x

Osorio, B., León, U., Galván, E. J., and Gutiérrez, R. (2013). Cocultures of GFP^+-granule cells with GFP – pyramidal cells and interneurons for the study of mossy fiber neurotransmission with paired recordings. *Hippocampus* 23, 247–252. doi: 10.1002/hipo.22102

Otsuka, M., Obata, K., Miyata, Y., and Tanaka, Y. (1971). Measurement of gamma-aminobutyric acid in isolated nerve cells of cat central nervous system. *J. Neurochem.* 18, 287–295. doi: 10.1111/j.1471-4159.1971.tb00567.x

Parent, J. M., Yu, T. W., Leibowitz, R. T., Geschwind, D. H., Sloviter, R. S., and Lowenstein, D. H. (1997). Dentate granule cell neurogenesis is increased by seizures and contributes to aberrant network reorganization in the adult rat hippocampus. *J. Neurosci.* 17, 3727–3738.

Piatti, V. C., Davies-Sala, M. G., Espósito, M. S., Mongiat, L. A., Trinchero, M. F., and Schinder, A. F. (2011). The timing of neuronal maturation in the adult hippocampus is modulated by local network activity. *J. Neurosci.* 31, 7715–7728. doi: 10.1523/JNEUROSCI.1380-11.2011

Radian, R., Bendahan, A., and Kanner, B. I. (1986). Purification and identification of the functional sodium- and chloride-coupled gamma-aminobutyric acid transport glycoprotein from rat brain. *J. Biol. Chem.* 261, 15437–15441.

Raiteri, L., Raiteri, M., and Bonanno, G. (2002). Coexistence and function of different neurotransmitter transporters in the plasma membrane of CNS neurons. *Prog. Neurobiol.* 68, 287–309. doi: 10.1016/S0301-0082(02)00059-X

Raiteri, L., Stigliani, S., Patti, L., Usai, C., Bucci, G., Diaspro, A., et al. (2005). Activation of c-aminobutyric acid GAT-1 transporters on glutamatergic terminals of mouse spinal cord mediates glutamate release through anion channels and by transporter reversal. *J. Neurosci. Res.* 80, 424–433. doi: 10.1002/jnr.20437

Ramírez, M., and Gutiérrez, R. (2001). Activity-dependent expression of GAD67 in the granule cells of the rat hippocampus. *Brain Res.* 917, 139–146. doi: 10.1016/S0006-8993(01)02794-9

Ramón y Cajal, S. (1906). *The Structure and Connexions of Neurons.* Available at: http://www.nobelprize.org/nobel_prizes/medicine/laureates/1906/cajal-lecture.pdf

Riazanski, V., Deriy, L. V., Shevchenko, P. D., Le, B., Gomez, E. A., and Nelson, D. J. (2011). Presynaptic CLC-3 determines quantal size of inhibitory transmission in the hippocampus. *Nat. Neurosci.* 14, 487–494. doi: 10.1038/nn.2775

Ribak, C. E., Tong, W. M., and Brecha, N. C. (1996). GABA plasma membrane transporters, GAT-1 and GAT-3, display different distributions in the rat hippocampus. *J. Comp. Neurol.* 367, 595–606. doi: 10.1002/(SICI)1096-9861(19960415)367:4<595::AID-CNE9>3.0.CO;2-#

Rollenhagen, A., and Lübke, J. H. R. (2010). The mossy fiber bouton: the "common" or the "unique" synapse? *Front. Synaptic Neurosci.* 2:2. doi: 10.3389/fnsyn.2010.00002

Romo-Parra, H., Treviño, M., Heinemann, U., and Gutiérrez, R. (2008). GABA actions in hippocampal area CA3 during postnatal development: differential shift from depolarizing to hyperpolarizing in somatic and dendritic compartments. *J. Neurophysiol.* 99, 1523–1534. doi: 10.1152/jn.01074.2007

Romo-Parra, H., Vivar, C., Maqueda, J., Morales, M. A., and Gutiérrez, R. (2003). Activity-dependent induction of multitransmitter signaling onto pyramidal cells and interneurons of area CA3 of the rat hippocampus. *J. Neurophysiol.* 89, 3155–3167. doi: 10.1152/jn.00985.2002

Rost, B. R., Breustedt, J., Schoenherr, A., Grosse, G., Ahnert-Hilger, G., and Schmitz, D. (2010). Autaptic cultures of single hippocampal granule cells of mice and rats. *Eur. J. Neurosci.* 32, 939–947. doi: 10.1111/j.1460-9568.2010.07387.x

Rothe, F., Brosz, M., and Storm-Mathisen, J. (1995). Quantitative ultrastructural localization of glutamate dehydrogenase in the rat cerebellar cortex. *Neuroscience* 64, iii–xvi. doi: 10.1016/0306-4522(94)E0200-N

Rothstein, J. D., Dykes-Hoberg, M., Pardo, C. A., Bristol, L. A., Jin, L., Kuncl, R. W., et al. (1996). Knockout of glutamate transporters reveals a major role for astroglial transport in excitotoxicity and clearance of glutamate. *Neuron* 16, 675–686. doi: 10.1016/S0896-6273(00)80086-0

Rothstein, J. D., Martin, L., Levey, A. I., Dykes-Hoberg, M., Jin, L., Wu, D., et al. (1994). Localization of neuronal and glial glutamate transporters. *Neuron* 13, 713–725. doi: 10.1016/0896-6273(94)90038-8

Ruiz, A., Campanac, E., Scott, R. S., Rusakov, D. A., and Kullmann, D. M. (2010). Presynaptic GABAA receptors enhance transmission and LTP induction at hippocampal mossy fiber synapses. *Nat. Neurosci.* 13, 431–438. doi: 10.1038/nn.2512

Ruiz, A., Fabian-Fine, R., Scott, R., Walker, M. C., Rusakov, D. A., and Kullmann, D. M. (2003). GABAA receptors at hippocampal mossy fibers. *Neuron* 39, 961–973. doi: 10.1016/S0896-6273(03)00559-2

Ruiz, A. J., and Kullmann, D. M. (2013). Ionotropic receptors at hippocampal mossy fibers: roles in axonal excitability, synaptic transmission, and plasticity. *Front. Neural Circuits* 6:112. doi: 10.3389/fncir.2012.00112

Safiulina, V. F., Caiati, M. D., Sivakumaran, S., Bisson, G., Migliore, M., and Cherubini, E. (2010). Control of GABA release at mossy fiber-CA3 connections in the developing hippocampus. *Front. Synaptic Neurosci.* 2:1. doi: 10.3389/neuro.19.001.2010

Safiulina, V. F., and Cherubini, E. (2009). At immature mossy fibers-CA3 connections, activation of presynaptic GABA(B) receptors by endogenously released GABA contributes to synapses silencing. *Front. Cell Neurosci.* 3:1. doi: 10.3389/neuro.03.001.2009

Safiulina, V. F., Fattorini, G., Conti, F., and Cherubini, E. (2006). GABAergic signaling at mossy fiber synapses in neonatal rat hippocampus. *J. Neurosci.* 26, 597–608. doi: 10.1523/JNEUROSCI.4493-05.2006

Sagne, C., El Mestikawy, S., Isambert, M. F., Hamon, M., Henry, J. P., Giros, B., et al. (1997). Cloning of a functional vesicular GABA and glycine transporter by screening of genome databases. *FEBS Lett.* 417, 177–183. doi: 10.1016/S0014-5793(97)01279-9

Sandler, R., and Smith, A. D. (1991). Coexistence of GABA and glutamate in mossy fiber terminals of the primate hippocampus: an ultrastructural study. *J. Comp. Neurol.* 303, 177–192. doi: 10.1002/cne.903030202

Sarup, A., Larsson, O. M., and Schousboe, A. (2003). GABA transporters and GABA-transaminase as drug targets. *Curr. Drug Targets CNS Neurol. Disord.* 2, 269–277. doi: 10.2174/1568007033482788

Schmidt-Hieber, C., Jonas, P., and Bischofberger, J. (2004). Enhanced synaptic plasticity in newly generated granule cells of the adult hippocampus. *Nature* 429, 184–187. doi: 10.1038/nature02553

Schmitt, A., and Kugler, P. (1999). Cellular and regional expression of glutamate dehydrogenase in the rat nervous system: non-radioactive in situ hybridization and comparative immunocytochemistry. *Neuroscience* 92, 293–308. doi: 10.1016/S0306-4522(98)00740-4

Schmitz, D., Schuchmann, S., Fisahn, A., Draguhn, A., Buhl, E. H., Petrasch-Parwez, E., et al. (2001). Axo-axonal coupling. A novel mechanism for ultrafast neuronal communication. *Neuron* 31, 831–840. doi: 10.1016/S0896-6273(01)00410-X

Schwarzer, C., and Sperk, G. (1995). Hippocampal granule cells express glutamic acid decarboxylase-67 after limbic seizures in the rat. *Neuroscience* 69, 705–779. doi: 10.1016/0306-4522(95)00348-M

Seress, L., and Frotscher, M. (1990). Morphological variability is a characteristic feature of granule cells in the primate fascia dentata: a combined golgi/electron microscope study. *J. Comp. Neurol.* 293, 253–267. doi: 10.1002/cne.902930208

Shashidharan, P., and Plaitakis, A. (1993). Cloning and characterization of a glutamate transporter cDNA from human cerebellum. *Biochim. Biophys. Acta* 1216, 161–164. doi: 10.1016/0167-4781(93)90057-K

Sirvanci, S., Meshul, C. K., Onat, F., and San, T. (2005). Glutamate and GABA immunocytochemical electron microscopy in the hippocampal dentate gyrus of normal and genetic absence epilepsy rats. *Brain Res.* 1053, 108–115. doi: 10.1016/j.brainres.2005.06.024

Sloviter, R. S., Dichter, M. A., Rachinsky, T., Dean, E., Goodman, J. H., Sollas, A. L., et al. (1996). Basal expression and induction of glutamate decarboxylase and GABA in excitatory granule cells of the rat and monkey hippocampal dentate gyrus. *J. Comp. Neurol.* 373, 593–618. doi: 10.1002/(SICI)1096-9861(19960930)373:4<593::AID-CNE8>3.0.CO;2-X

Söhl, G., Maxeiner, S., and Willecke, K. (2005). Expression and functions of neuronal gap junctions. *Nat. Rev. Neurosci.* 6, 191–200. doi: 10.1038/nrn1627

Söllner, T., and Rothman, J. E. (1994). Neurotransmission: harnessing fusion machinery at the synapse. *Trends Neurosci.* 17, 344–348. doi: 10.1016/0166-2236(94)90178-3

Sperk, G., Schwarzer, C., Heilman, J., Furtinger, S., Reimer, R. J., Edwards, R. H., et al. (2003). Expression of plasma membrane GABA transporters but not of the vesicular GABA transporter in dentate granule cells after kainic acid seizures. *Hippocampus* 13, 806–815. doi: 10.1002/hipo.10133

Sperk, G., Wieselthaler-Hölzl, A., Pirker, S., Tasan, R., Strasser, S. S., Drexel, M., et al. (2012). Glutamate decarboxylase 67 is expressed in hippocampal mossy fibers of temporal lobe epilepsy patients. *Hippocampus* 22, 590–603. doi: 10.1002/hipo.20923

Steward, O., and Scoville, S. A. (1976). Cells of origin of entorhinal cortical afferents to the hippocampus and fascia dentata of the rat. *J. Comp. Neurol.* 169, 347–370. doi: 10.1002/cne.901690306

Storm-Mathisen, J. (1977). Localization of transmitter candidates in the brain: the hippocampal formation as a model. *Prog. Neurobiol.* 8, 119–181. doi: 10.1016/0301-0082(77)90013-2

Storm-Mathisen, J. (1981). Glutamate in hippocampal pathways. *Adv. Biochem. Psychopharmacol.* 27, 43–55.

Storm-Mathisen, J., Leknes, A. K., Bore, A. T., Vaaland, J. L., Edminson, P., Hauq, F. M., et al. (1983). First visualization of glutamate and GABA in neurones by immunocytochemistry. *Nature* 301, 517–520. doi: 10.1038/301517a0

Südhof, T. C., Petrenko, A. G., Whittake, V. P., and Jahn, R. (1993). Molecular approaches to synaptic vesicle exocytosis. *Prog. Brain Res.* 98, 235–240. doi: 10.1016/S0079-6123(08)62404-8

Takamori, S., Rhee, J. S., Rosenmund, C., and Jahn, R. (2000). Identification of a vesicular glutamate transporter that defines a glutamatergic phenotype in neurons. *Nature* 407, 189–194. doi: 10.1038/35025070

Tanaka, K., Watase, K., Manabe, T., Yamada, K., Watanabe, M., Takahashi, K., et al. (1997). Epilepsy and exacerbation of brain injury in mice lacking the glutamate transporter GLT-1. *Science* 276, 1699–1702. doi: 10.1126/science.276.5319.1699

Toni, N., Laplagne, D. A., Zhao, C., Lombardi, G., Ribak, C. E., Gage, F. H., et al. (2008). Neurons born in the adult dentate gyrus form functional synapses with target cells. *Nat. Neurosci.* 11, 901–907. doi: 10.1038/nn.2156

Treviño, M., and Gutiérrez, R. (2005). The GABAergic projection of the dentate gyrus to hippocampal area CA3 of the rat: pre- and postsynaptic actions after seizures. *J. Physiol.* 567, 939–949. doi: 10.1113/jphysiol.2005.092064

Treviño, M., Vivar, C., and Gutiérrez, R. (2007). Oscillatory activity in the CA3 hippocampal area is depressed by aberrant GABAergic transmission from the dentate gyrus after seizures. *J. Neurosci.* 27, 251–259. doi: 10.1523/JNEUROSCI.3815-06.2007

Treviño, M., Vivar, C., and Gutiérrez, R. (2011). Excitation-inhibition balance in the CA3 network – neuronal speicificity and activity-dependent plasticity. *Eur. J. Neurosci.* 33, 1771–1785. doi: 10.1111/j.1460-9568.2011.07670.x

Uchigashima, M., Fukaya, M., Watanabe, M., and Kamiya, H. (2007). Evidence against GABA release from glutamatergic mossy fiber terminals in the developing hippocampus. *J. Neurosci.* 27, 8088–8100. doi: 10.1523/JNEUROSCI.0702-07.2007

Urban, N. N., Henze, D. A., and Barrionuevo, G. (2001). Revisiting the role of the hippocampal mossy fiber synapse. *Hippocampus* 11, 408–417. doi: 10.1002/hipo.1055

Varoqui, H., Schäfer, M. K., Zhu, H., Weihe, E., and Erickson, J. D. (2002). Identification of the differentiation-associated Na+/PI transporter as a novel vesicular glutamate transporter expressed in a distinct set of glutamatergic synapses. *J. Neurosci.* 22, 142–155.

Vida, I., and Frotscher, M. (2000). A hippocampal interneuron associated with the mossy fiber system. *Proc. Natl. Acad. Sci. U.S.A.* 97, 1275–1280. doi: 10.1073/pnas.97.3.1275

Vivar, C., and Gutiérrez, R. (2005). Blockade of the membranal GABA transporter potentiates GABAergic responses evoked in pyramidal cells by mossy fiber activation after seizures. *Hippocampus* 15, 281–284. doi: 10.1002/hipo.20063

Vivar, C., Traub, R. D., and Gutiérrez, R. (2012). Mixed electrical–chemical transmission between hippocampal mossy fibers and pyramidal cells. *Eur. J. Neurosci.* 35, 76–82. doi: 10.1111/j.1460-9568.2011.07930.x

Walker, M. C., Ruiz, A., and Kullmann, D. M. (2001). Monosynaptic GABAergic signaling from dentate to CA3 with a pharmacological and physiological profile typical of mossy fiber synapses. *Neuron* 29, 703–715. doi: 10.1016/S0896-6273(01)00245-8

Wojcik, S. M., Katsurabayashi, S., Guillemin, I., Friauf, E., Rosenmund, C., Brose, N., et al. (2006). A shared vesicular carrier allows synaptic corelease of GABA and glycine. *Neuron* 50, 575–587. doi: 10.1016/j.neuron.2006.04.016

Zander, J. F., Münster-Wandowski, A., Brunk, I., Pahner, I., Gómez-Lira, G., Heinemann, U., et al. (2010). Synaptic and vesicular coexistence of VGLUT and VGAT in selected excitatory and inhibitory synapses. *J. Neurosci.* 30, 7634–7645. doi: 10.1523/JNEUROSCI.0141-10.2010

Conflict of Interest Statement: The authors declare that the research was conducted in the absence of any commercial or financial relationships that could be construed as a potential conflict of interest.

Received: 29 August 2013; accepted: 23 October 2013; published online: 22 November 2013.

Citation: Münster-Wandowski A, Gómez-Lira G and Gutiérrez R (2013) Mixed neurotransmission in the hippocampal mossy fibers. Front. Cell. Neurosci. ***7****:210. doi: 10.3389/fncel.2013.00210*

This article was submitted to the journal Frontiers in Cellular Neuroscience.

frontiers in
CELLULAR NEUROSCIENCE

ORIGINAL RESEARCH ARTICLE
published: 14 February 2014
doi: 10.3389/fncel.2014.00044

Electrophysiological characterization of granule cells in the dentate gyrus immediately after birth

Andrea Pedroni[1], Do Duc Minh[1], Antonello Mallamaci[1] and Enrico Cherubini[1,2]*

[1] *Department of Neuroscience, Scuola Internazionale Superiore di Studi Avanzati, Trieste, Italy*
[2] *European Brain Research Institute, Rome, Italy*

Edited by:
Richard Miles, Institut pour le Cerveau et la Moëlle Epinière, France

Reviewed by:
Claudia Lodovichi, Venetian Institute of Molecular Medicine, Italy
Carolina Hoyo-Becerra, Clinic Hospital Essen, Germany

***Correspondence:**
Enrico Cherubini, Department of Neuroscience, Scuola Internazionale Superiore di Studi Avanzati, Via Bonomea 265, 34136 Trieste, Italy
e-mail: cher@sissa.it

Granule cells (GCs) in the dentate gyrus are generated mainly postnatally. Between embryonic day 10 and 14, neural precursors migrate from the primary dentate matrix to the dentate gyrus where they differentiate into neurons. Neurogenesis reaches a peak at the end of the first postnatal week and it is completed at the end of the first postnatal month. This process continues at a reduced rate throughout life. Interestingly, immediately after birth, GCs exhibit a clear GABAergic phenotype. Only later they integrate the classical glutamatergic trisynaptic hippocampal circuit. Here, whole cell patch clamp recordings, in current clamp mode, were performed from immature GCs, intracellularly loaded with biocytin (in hippocampal slices from P0 to P3 old rats) in order to compare their morphological characteristics with their electrophysiological properties. The vast majority of GCs were very immature with small somata, few dendritic branches terminating with small varicosities and growth cones. In spite of their immaturity their axons reached often the cornu ammonis 3 area. Immature GCs generated, upon membrane depolarization, either rudimentary sodium spikes or more clear overshooting action potentials that fired repetitively. They exhibited also low threshold calcium spikes. In addition, most spiking neurons showed spontaneous synchronized network activity, reminiscent of giant depolarizing potentials (GDPs) generated in the hippocampus by the synergistic action of glutamate and GABA, both depolarizing and excitatory. This early synchronized activity, absent during adult neurogenesis, may play a crucial role in the refinement of local neuronal circuits within the developing dentate gyrus.

Keywords: dentate gyrus granule cells, immature hippocampus, postnatal development, sodium spikes, low threshold calcium spikes, synchronized network activity, neurogenesis, giant depolarizing potentials

INTRODUCTION

Granule cells (GCs) in the dentate gyrus are crucial for transferring information from the entorhinal cortex to the hippocampus proper where they integrate the classical excitatory trisynaptic circuit (McBain, 2008). Although primarily glutamatergic, the axons of GCs, the mossy fibers (MFs), contain GABA, its synthesizing enzyme glutamic acid decarboxylase (Schwarzer and Sperk, 1995; Sloviter et al., 1996) and the vesicular GABA transporter VIAAT (Zander et al., 2010). In addition, immunogold experiments have demonstrated the presence of both AMPA and $GABA_A$ receptors, co-localized on MF terminals in close spatial relation with synaptic vesicles (Bergersen et al., 2003). All these pieces of evidence suggest that MF-cornu ammon (CA3) synapses can use GABA as a neurotransmitter since they posses all the machinery for synthesizing, storing, releasing, and sensing it.

Indeed, electrophysiological experiments from juvenile animals have revealed the presence of mixed GABAergic and glutamatergic monosynaptic currents in CA3 principal cells upon stimulation of GCs in the dentate gyrus (Walker et al., 2001; Gutierrez et al., 2003). Furthermore, in line with the sequential formation of GABAergic and glutamatergic synapses in the immature hippocampus (Hennou et al., 2002), GABA appears to be the only neurotransmitter released from MF terminals during the first few days of postnatal life (Kasyanov et al., 2004; Safiulina et al., 2006, 2010; Sivakumaran et al., 2009) while AMPA/kainate receptor mediated synaptic currents start appearing only after postnatal (P) day 3 (Marchal and Mulle, 2004).

Granule cells are characterized by their peculiar delayed and heterogeneous maturation. Most of them (85%) are generated postnatally. From the primary dentate matrix, neural precursors migrate to the dentate gyrus between embryonic day 10 and 14 where they differentiate into neurons (Altman and Bayer, 1990a,b). Neurogenesis reaches a peak at the end of the first postnatal week and is largely completed toward the end of the first postnatal month (Schlessinger et al., 1975). Interestingly, the dentate gyrus retains the capability to give rise to new neurons throughout life, although at a reduced rate (Duan et al., 2008). In adulthood, after being generated in the subgranular zone, immature GCs are incorporated into pre-existing circuits, thus contributing to improve several brain functions including learning and memory processes (Deng et al., 2010).

The maturation of GCs during postnatal development has been extensively investigated (Liu et al., 1996; Liu et al., 2000; Ye et al., 2000; Ambrogini et al., 2004; Overstreet et al., 2004; Espósito et al., 2005; Overstreet-Wadiche and Westbrook, 2006; Overstreet-Wadiche et al., 2006). However, only few studies, have

tried to compare the morphological characteristics of immature GCs with their functional properties before P7, when neurogenesis in the dentate gyrus is very active and GCs exhibit immature-like features (Liu et al., 1996, 2000; Ambrogini et al., 2004).

Therefore, in the present study, whole-cell patch clamp recordings were performed from biocytin-labeled GCs in the immediate postnatal period, between P0 and P3, when GCs convey exclusively monosynaptic GABAergic signals to CA3 pyramidal cells (Safiulina et al., 2006).

MATERIALS AND METHODS

ETHICAL APPROVAL

All experiments were performed in accordance with the European Community Council Directive of November 24, 1986 (86/609EEC) and were approved by the local authority veterinary service and by SISSA ethical committee. All efforts were made to minimize animal suffering and to reduce the number of animals used.

HIPPOCAMPAL SLICES PREPARATION

Wistar rats of both sexes were decapitated after being anesthetized with CO_2. Hippocampal slices were obtained from neonatal animals at postnatal (P) days P0–P3 (the day 0 was considered as the day of birth) as previously described (Caiati et al., 2010). Briefly, the brain was quickly removed from the skull and placed in ice-cold ACSF containing (in mM): NaCl 130, KCl 3.5, NaH_2PO_4 1.2, $MgCl_2$ 1.3, $CaCl_2$ 2, Glucose 24, $NaHCO_3$ 27 (pH 7.3), saturated with 95% O_2 and 5% CO_2 (pH 7.3–7.4)

Transverse hippocampal slices (400 μm thick) were cut with a vibratome and stored at room temperature (20–24°C) in a holding bath containing the same solution as above. After a recovery period of at least 1 h, an individual slice was transferred to the recording chamber where it was continuously superfused with oxygenated ACSF at 31–33°C at the rate of 3–4 ml min^{-1}.

ELECTROPHYSIOLOGICAL RECORDINGS

Whole-cell patch clamp recordings (mainly in current clamp mode) were obtained from visually identified GCs in the dentate gyrus, using the Multiclamp 700A amplifier (Axon Instrument, USA).

Patched electrodes were pulled from borosilicate glass capillaries (Hingelberg, Malsfeld, Germany). They had a resistance of 5–8 MΩ when filled with an intracellular solution containing (in mM): KCl 140, $MgCl_2$ 1, EGTA 0.5, HEPES 10, Mg ATP 4 (pH 7.3; the osmolarity was adjusted to 280 mOsmol).

The stability of the patch was checked by repetitively monitoring the input and series resistance during the experiment. Cells exhibiting > 15 changes in series resistance were excluded from the analysis. The series resistance was <20 MΩ and was not compensated.

Spontaneously occurring giant depolarizing potentials (GDPs) were routinely recorded from a holding potential of −70 mV.

DRUGS

Drugs used were: tetrodotoxin (TTX, purchased from Latoxan, Valence, France), 6,7-dinitroquinoxaline-2,3-dione (DNQX), bicuculline methiodide (purchased from Tocris Cookson Inc., UK), and biocytin (purchased from Sigma-Aldrich Milano, Italy). All drugs were dissolved in ACSF except DNQX that was dissolved in DMSO. The final concentration of DMSO in the bathing solution was 0.1%. At this concentration, DMSO alone did not modify the shape or the kinetics of synaptic currents. Drugs were applied in the bath via a three-way tap system, by changing the superfusion solution to one differing only in its drug(s) content. The ratio of flow rate to bath volume ensured complete exchange within 2 min.

DATA ACQUISITION AND ANALYSIS

Data were acquired and digitized with an A/D converter (Digidata 1200, Molecular Devices) and stored on a computer hard disk. Acquisition and analysis were performed with Clampfit 9 (Axon Instruments, USA). Data were sampled at 20 kHz and filtered with a cut off frequency of 2 kHz. The resting membrane potential (RMP) was measured immediately after break-in and establishing whole-cell recording. The input resistance (R_{in}) was calculated by the slope of the linear portion of the I/V relationship obtained by measuring the steady-state potential changes in response to hyperpolarizing current steps of increasing intensity (from −60 to +120 pA, 20 pA increments, 500 ms duration) using the Clampfit program (pClamp 9.0 software, Axon Instrument, USA). The membrane surface was estimated in voltage clamp mode by integrating the area under the average of four uncompensated and unfiltered charging transients in response to hyperpolarizing steps from a holding potential of −60 mV.

Action potentials were evoked in current clamp mode from a holding potential of −60 mV by 500 ms depolarizing current pulses. Spike width was measured at the base of action potentials and spike amplitude from the baseline to the peak. Spike threshold was determined at the beginning of the fast up rise of an action potential. Possible sag in electrotonic potentials were identified by injecting hyperpolarizing current pulses of different intensities through the recording pipette.

Unless otherwise stated, data are presented as mean ± SEM. Quantitative comparisons were based on students paired or unpaired *t*-test, as required and a p value < 0.05 was considered as significant.

CELL STAINING

Post hoc identification of recorded cells was achieved by injecting biocytin (1–2%, from Sigma Aldrich, Milano, Italy, dissolved in the internal solution) throughout the recording electrode for at least 40–60 min. After electrode removal slices were kept in the recording chamber, continuously superfused for at least 15–20 min. to optimize the complete diffusion of biocytin. Slices were then removed from recording chamber, thoroughly washed with phosphate buffered saline (PBS) 1X and fixed with parafolmaldehyde 4% for 20 min. at room temperature and stored at 4°C. Slices were incubated with Alexa Flour 647-labeled streptavidin, 1:500 for 1 h at room temperature, sheltered from the light. They were washed, thoroughly rinsed with 1x PBS, mounted onto slides, embedded with Vectashield (Vector Laboratories), and coverslipped. Individual pictures of biocytin-filled cells were acquired with a Nikon microscope (Eclipse Series TiE, equipped with a C1 confocal system) along progressive focal planes to fully cover their volume (including their dendritic and axonal projections).

IMMUNOCYTOCHEMISTRY

Free-floating recorded slices were rinsed several times with 1x PBS and incubated in a blocking solution containing 5% FBS (fetal bovine serum) and 0.3% Triton X-100 in PBS, for 30 min. Primary antibodies (anti-Prox1, ab37128, rabbit polyclonal, Abcam, Cambridge, MA, USA 1:500; anti-NeuN, MAB377, mouse monoclonal, Millipore, Billerica, MA, USA, 1:500), diluted in 95% PBS-5% FBS solution, were applied and incubated at room temperature for 2 h. Then, slices were washed several times with 1x PBS and incubated with secondary antibody (Alexa 488-conjugated goat anti-mouse immunoglobulin G [IgG], 1:500, 594-conjugated goat anti-rabbit IgG, 1:500, Alexa Flour 647-labeled streptavidin, 1:500 and 4,6′-diamidino-2-phenylindole [DAPI], 1:1000) for 1 h at room temperature, sheltered from the light. Finally, slices were washed, thoroughly rinsed with 1x PBS, mounted onto slides, embedded with Vectashield (Vector Laboratories), and coverslipped.

RESULTS

IDENTIFICATION OF GRANULE CELLS

Granule cells were identified thanks to their immunoreactivity for Prox1. This is a homeoprotein expressed in several brain regions including the dentate gyrus, where it is present throughout development and in adulthood (Lavado and Oliver, 2007). Mature GCs were further distinguished as immunoreactive for NeuN. This is a nuclear antigen expressed in most neuronal cell types throughout the adult nervous system (Mullen et al., 1992), which is specifically activated in GCs by the end of their maturation (Ming and Song, 2011; Hsieh, 2012; Iwano et al., 2012). The spatio-temporal distribution of immature GCs in the dentate area was investigated at three postnatal stages: P2, P6, and P28. As shown in **Figure 1**, at P2, NeuN-positive cells were mainly clustered in the pyramidal layer of the CA3 region and scattered throughout the hilus. At this age, only a few NeuN-positive cells where found in the coalescing Prox1-positive dentate gyrus, where NeuN co-localized with Prox1. At P6, comparable numbers of Prox1-positive/NeuN-negative and Prox1-positive /NeuN-positive cells were detectable within the inner layer and the outer layer of the granule cell layer (GCL), respectively, Finally, at P28, almost all Prox1-positive neurons expressed NeuN, except a few NeuN- elements close to the subgranular zone. In a few words, immature GCs, largely prominent at P2, coexist with similar numbers of mature elements at P6 and become a minority by P28.

BIOCYTIN-LABELED GCs EXHIBIT AN IMMATURE PHENOTYPE

Immunocytochemical data have clearly demonstrated that at P2 GCs exhibit a typical immature phenotype. To fully characterize the functional properties of these cells, stable whole-cell recordings (mainly in current clamp configuration), lasting more than 30 min, were obtained from 63 putative GCs in slices obtained from P0 to P3 old rats. Some of these cells (11/63), were intracellularly labeled with biocytin. Cells were identified as GCs on the basis of their cell bodies localized in the GC layer and dendrites oriented toward the molecular layer. The vast majority of labeled cells exhibited small bodies and few short dendrites emerging mainly from the top or sides of cell bodies, oriented toward the molecular layer or running tangentially to the GC layer (**Figure 2**). In comparison with more mature GCs (see Liu et al., 2000; Overstreet et al., 2004; Markwardt et al., 2009) dendrites never penetrated deeply into the molecular layer or reached the top (**Figures 2A–C**). They were short, thick and spineless with limited branching. They often displayed small varicosities, filopodia and growth cones (**Figures 2A–C,E**). Presumed GC axons with initial extension toward the hilus could be visualized. In four cases, these could be followed up to stratum

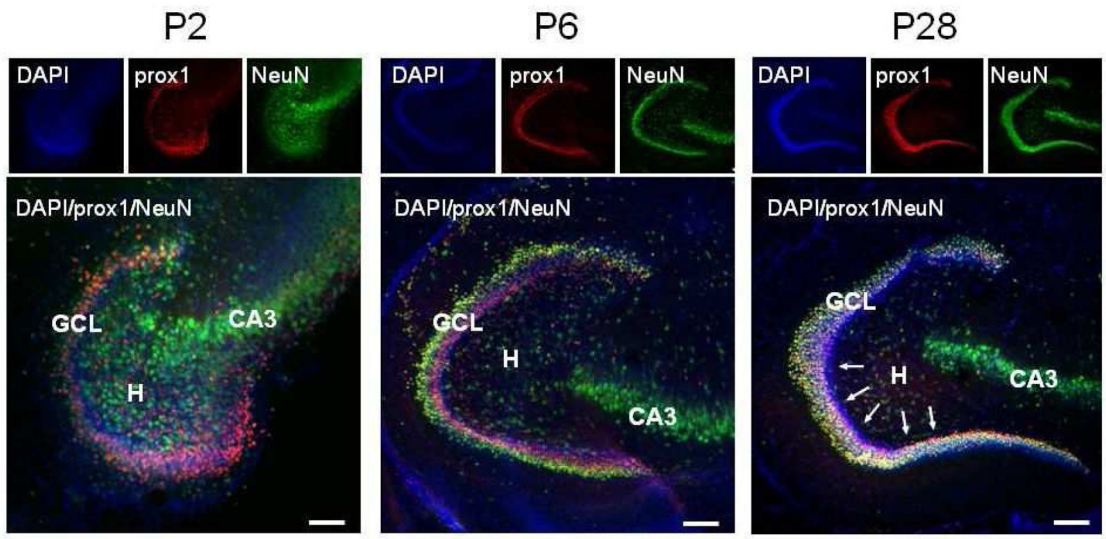

FIGURE 1 | Representative confocal images of immunostained P2, P6, and P28 horizontal sections of the hippocampus. DAPI staining, Prox1 and NeuN immunoreactivity are in blue, red, and green, respectively. Pink (DAPI+, Prox1+, NeuN−), immature granule cells predominate in the coalescing P2 GCL, they occupy the inner half of the P6 GCL and are rare in the P28 GCL, where they are confined to a row close to the subgranular zone (arrows). GCL, granule cell layer; H, hilus; CA3, cornu ammonis 3 field.

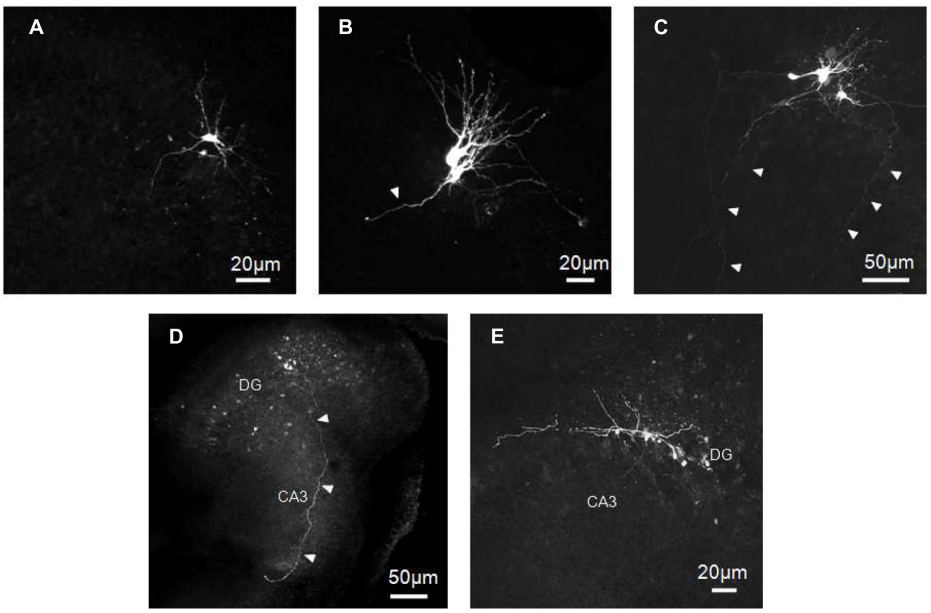

FIGURE 2 | Biocytin-labeled GCs at P0–P2. GCs exhibit small cell bodies with few short and tick dendrites oriented toward the molecular layer **(A–C)** and/or running tangentially to the GC layer **(C,E)**. Dendrites often display small varicosities, filopodia and growth cones **(B,C,E)**. Presumed GC axons projecting through the hilus toward stratum lucidum can be seen in **C,D**. Arrowheads indicate presumable axons.

lucidum in the CA3 subfield (**Figures 2C,D**). The axons expressed varicosities but lacked mature MF boutons and often gave rise to collateral branches that terminated with growth cones. Although care was used to pull out the patch pipette from the recorded neuron at the end of the experiments, more than one GC was often labeled, suggesting dye-coupling (**Figures 2** and **7A**). However, due to their small diameter, we failed to patch two adjacent neurons to verify whether dye-coupled cells were also electrically coupled.

ELECTROPHYSIOLOGICAL CHARACTERISTICS OF IMMATURE GCs

Immature GCs were identified as neurons by their capacity to generate action potentials. We examined firstly the passive membrane properties ($n = 63$). On average, the RMP was -39 ± 1 mV (ranging from -58 to -23 mV); the input resistance (R_{in}) 1.2 ± 0.1 GΩ (ranging from 0.3 to 2.9 GΩ), the membrane capacitance (C) 15.4 ± 0.7 pF (ranging from 8 to 31 pF) and the membrane time constant (τ) 285 ± 17 ms.

A large variability of individual RMP, C, and R_{in} values occurred between P0 and P3 (**Figure 3**). A large variability was also observed within the same postnatal group and between different cells recorded from the same slice. In spite of similar values of RMP, R_{in}, capacitance and membrane time constant, immature GCs exhibited marked changes in their excitability as assessed by the large variability in spike detection. Four cells, exhibiting relatively low R_{in} (0.8 ± 1 MΩ), more depolarized RMP (-35 ± 1 mV) and low capacitance values (8 ± 1 pF) were unable to generate action potentials in response to depolarizing currents pulses (non-spiking cells). These cells could be non-differentiated progenitors, astrocytes, oligodendrocytes and/or very immature neurons. Therefore, they were excluded from the present analysis.

Spiking neurons were divided in two groups on the basis of their ability to generate over-shooting action potentials or not (**Table 1**).

The first group ($n = 36$) comprised more immature cells with rudimentary short and wide TTX-sensitive sodium spikes. Often in the presence of TTX, low threshold calcium spikes appeared and these were blocked by low concentrations of nickel (100 μM; **Figure 4**). The second group of cells ($n = 27$) was characterized by clear overshooting action potentials, which in some cases fired repetitively (**Figure 5**).

In comparison with more immature cells, these exhibited a lower threshold for action potential generation, and a reduced spike half-width value (**Table 1**).

In the presence of TTX, low threshold calcium spike could be sometimes evoked from a more hyperpolarized holding potential (-80 mV; **Figure 4**).

Both groups exhibited electrotonic potentials that strongly rectified in the depolarizing direction, probably due to the activation of voltage-gated potassium conductances. In 23 GCs exhibiting both rudimentary and more mature spikes, a prominent time-dependent sag in the electrotonic potentials could be elicited by hyperpolarizing current steps. The sag accounted for most of the rectification in the hyperpolarizing range and had the characteristics of the time-dependent inward rectifier cationic current I_Q, described in the hippocampus (Halliwell and Adams, 1982; data not shown).

CORRELATED NETWORK ACTIVITY

Most (58/63) spiking neurons, recorded from P0 to P3, exhibited patterns of coherent activity reminiscent of that found in the developing Ammon's horn (Ben-Ari et al., 1989) and described as GDPs. As in the CA1 and CA3 hippocampal regions, GDPs

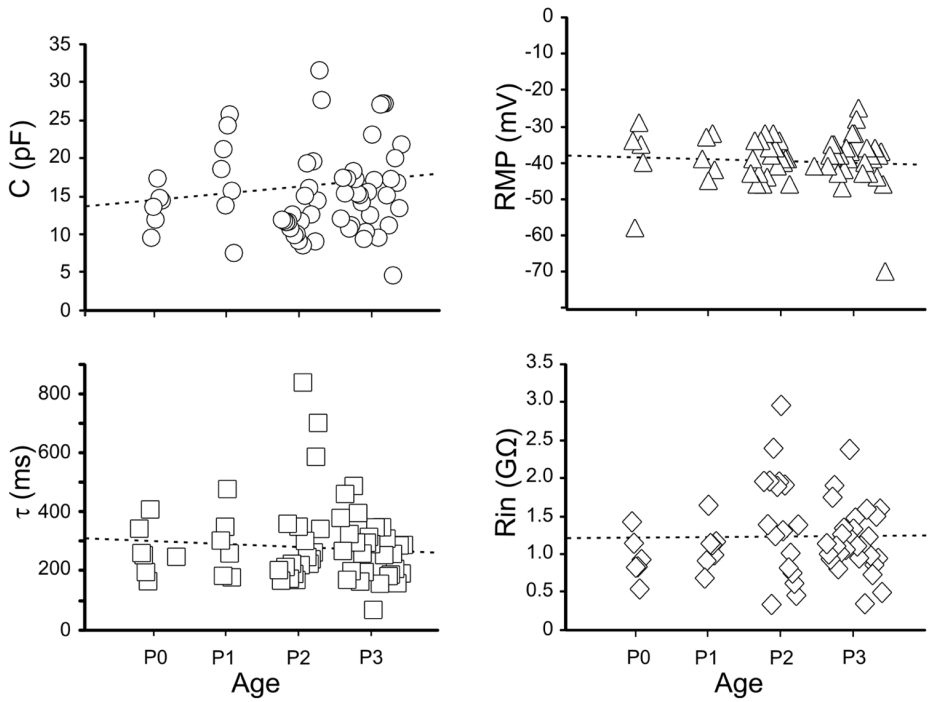

FIGURE 3 | Passive membrane properties of immature granule cells. Individual values of capacitance (C, open circles), resting membrane potential (RMP, open triangles), decay time constant (τ, open squares) and membrane input resistance (R_{in}, open diamonds), detected between P0 and P3.

were either grouped in clusters of 2–5 (**Figure 6B**) or occurred at more or less regular intervals (**Figure 6C**) at the frequency of 0.1 ± 0.3 Hz, often preceded by a barrage of synaptic events. Few spiking neurons did not exhibit GDPs but only spontaneous activity either isolated or in bursts that often reached the threshold for action potential generation (**Figure 6A**).

Giant depolarizing potentials were characterized by long-lasting recurrent membrane depolarizations (up to 30 mV in amplitude) giving rise to action potentials often grouped in bursts and separated by silent periods. GDPs were network-driven events since their frequency, but not their amplitude, was unaffected by changing the membrane potential to more depolarized or hyperpolarized values.

Although reduced in frequency, GDPs were still present in DNQX (20 μM; **Figure 7**) suggesting that, in the absence of a glutamatergic drive, the depolarizing action of GABA was still able to exert an excitatory action at the network level. In two cases, in the presence of DNQX long-lasting (13 and 19 s duration) plateau potentials could be unveiled.

These were probably generated by the activation of intrinsic membrane conductances, known to involve small groups of neurons coupled by gap-junctions (**Figure 7**; Crépel et al., 2007). However, the rare occurrence of these events did not allow testing whether they were sensitive to gap junction uncouplers or could be blocked by hyperpolarizing the membrane toward more negative values. GDPs were completely abolished by DNQX plus bicuculline (20 μM), indicating that they were triggered by the synergistic action of both glutamate and GABA. As in immature CA3 principal cells (Ben-Ari et al., 1989), synchronized activity was blocked by TTX (1 μM) further supporting their network origin (data not shown).

Table 1 | Passive and active membrane properties of granule cells at P0–P3 (*$p < 0.05$; **$p < 0.01$).

	Immature neurons with rudimentary spikes	More mature neurons with overshooting action potentials and repetitive firing
n	36	27
C (pF)	14 ± 1	17 ± 1*
RMP (mV)	−38 ± 1	−40 ± 1
R_{in} (GΩ)	1.4 ± 0.1	1 ± 0.1**
τ (ms)	283 ± 23	285 ± 25
Spike threshold (mV)	−26 ± 1	−34 ± 1**
Spike amplitude (mV)	13 ± 1	22 ± 2**
Spike half-width (ms)	6.1 ± 0.6	3.8 ± 0.2**

DISCUSSION

The present data clearly show that, immediately after birth, GCs in the dentate gyrus exhibit different degrees of immaturity as revealed by immunocytochemical experiments and *post hoc* morphological reconstruction of biocytin-labeled cells.

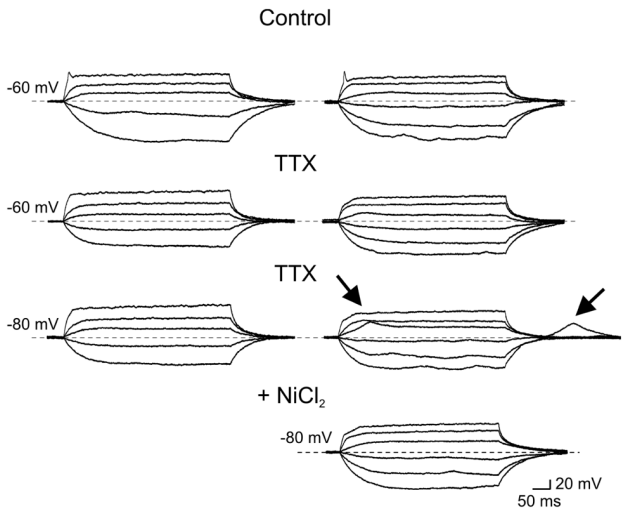

FIGURE 4 | Immature granule cells exhibit rudimentary sodium spikes and low threshold calcium spikes. Voltage responses obtained in two GCs (at P2) exhibiting sodium (right and left columns) and low threshold calcium currents (right). In control, both GCs exhibited small amplitude rudimentary spikes (at −60 mV, upper traces) that were blocked by TTX (1 μM). In the presence of TTX, depolarizing current pulses from −80 mV evoked only in the cell to the right a low threshold calcium spike. This was also present upon membrane re-polarization following an hyperpolarizing current step. Low threshold calcium spikes (marked by arrows) were blocked by nickel (100 μM, lower trace on the right).

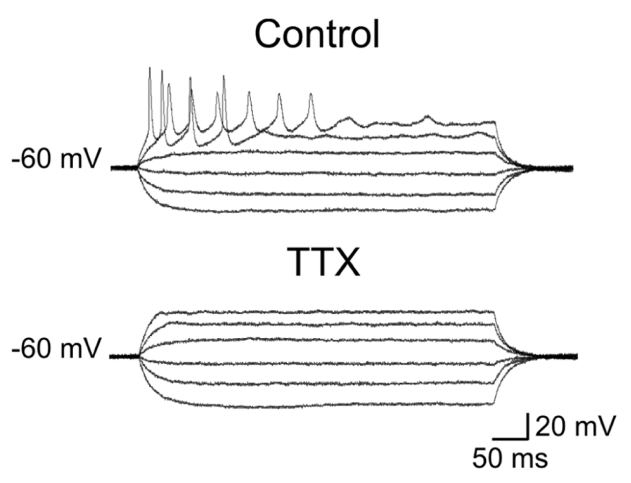

FIGURE 5 | Repetitive firing evoked in more mature granule cells. Voltage responses to depolarizing and hyperpolarizing currents steps of increasing intensity. Note clear overshooting spikes firing repetitively during depolarizing current pulses. Action potentials were readily blocked by TTX.

Thus, at P2, only a small percentage of Prox1-positive GCs were labeled with NeuN, which is specifically activated near the end of their differentiation process (Ming and Song, 2011). In keeping with a mixed GABAergic and glutamatergic neurotransmission of immature MF (Münster-Wandowski et al., 2013), a recent study has unveiled that Prox1-positive GCs transiently express the GABA synthesizing enzyme GAD67, thus supporting

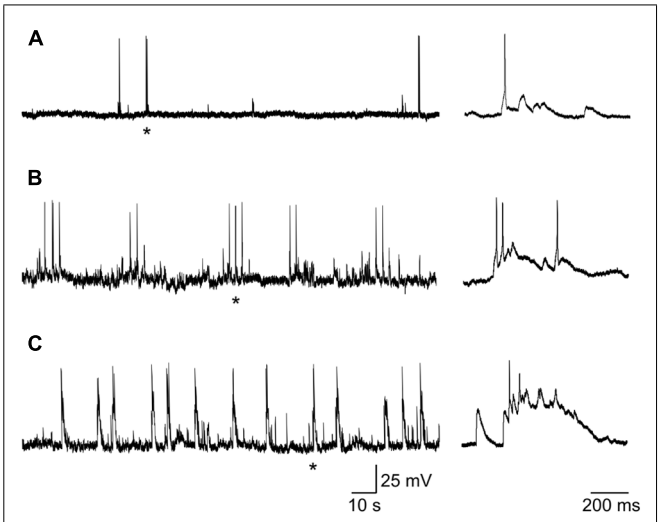

FIGURE 6 | Different patterns of coherent activities in neonatal GCs. **(A)** neuron (at P1) exhibiting sporadic depolarizing synaptic potentials that in few cases reached the threshold for action potential generation. **(B)** GDPs occurring in clusters of 2–3. **(C)** GDPs occurring at more regular intervals. Single action potentials or GDPs marked with * are shown on the right on an expanded time scale.

the view that, immediately after birth, GCs are able to synthesize GABA in addition to glutamate (Cabezas et al., 2013). GABA released from MF terminals may activate pre (Cabezas et al., 2012) and/or postsynaptic $GABA_A$ receptors (Safiulina et al., 2006, 2010) to modulate MF excitability and to generate $GABA_A$ mediated postsynaptic currents in targeted neurons, respectively.

Biocytin-labeled GCs express different degrees of immaturity. In general, they revealed few dendritic branches with short dendrites barely penetrating into the molecular layer and exhibiting varicosities and filopodia. In contrast with their dendritic arborization the axons of immature GCs, the MF, were able to reach the CA3 pyramidal layer already at P1. Although we don't know whether GCs axons made synaptic contacts with principal cells, it is likely that, similarly to the visual system (Kasper et al., 1994), the maturation of the dendritic tree takes place after GC axons have reached the CA3 subfield, supporting the view that this process is influenced by retrograde signals (Jones et al., 2003). Previous studies have shown that mature adult-like GCs, characterized by elongated dendrites (with spines) penetrating into the molecular layer, start appearing toward the end of the first postnatal week (Jones et al., 2003).

Our electrophysiological data obtained from P0 to P3 old rats unveiled passive membrane properties similar to those obtained from older rats at P5–P8 (Liu et al., 1996; Liu et al., 2000; Ye et al., 2000; Ambrogini et al., 2004), indicating that a certain degree of immaturity persists at late developmental stages. Usually, maturity is characterized by progressive more hyperpolarized values of RMP, decrease in membrane time constant, in R_{in} and increase in membrane capacitance (Spigelman et al., 1992). However, in the present case, these values were rather scattered and no significant differences were observed between GCs recorded at P0

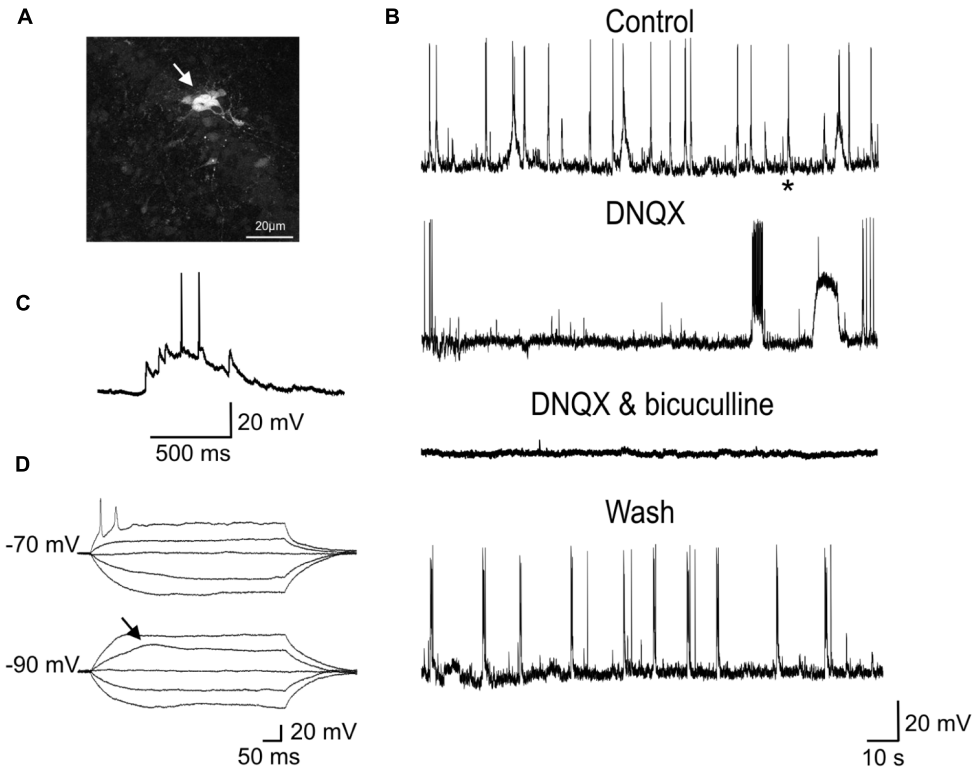

FIGURE 7 | Network-driven GDPs were reduced in frequency by DNQX and blocked by DNQX plus bicuculline. (A) Whole-cell recording of a P2 GC with biocytin revealed a cluster of several dye-coupled neurons. **(B)** Sample traces of spontaneous activity (GDPs) recorded from the same neuron in control conditions, in DNQX (20 μM), in DNQX and bicuculline (20 μM) and after wash. In the presence of DNQX, GDPs occurred at lower frequency. In DNQX it is visible also a plateau potential. **(C)** The GDP marked with an asterisk in the control trace is shown on an expanded time scale. **(D)** Voltage responses to depolarizing and hyperpolarizing currents steps of increasing intensity obtained from the same neuron. Note sodium and low threshold calcium spikes.

and P3. All patched cells exhibited high values of R_{in}. However, respect to more mature cells, immature neurons with rudimentary spikes displayed higher R_{in} values associated with lower capacitance. These factors, combined with the compact size of immature GCs, likely contribute to their high degree of excitability, such that even small fluctuations in membrane conductance may produce large voltage responses. This can be attributed to changes in the expression of intracellular anions and potassium efflux. Moreover, a developmentally regulated expression of voltage-gated sodium, calcium and potassium channels (Spigelman et al., 1992) may account for differences in active membrane properties such as spike amplitude and duration. The fact that rudimentary spikes were blocked by TTX suggests that voltage-dependent sodium channels are responsible for spike genesis. Interestingly, rudimentary sodium spikes were accompanied with low threshold calcium spikes. T-type Ca^{2+} currents underling low threshold calcium spikes have been originally described in sensory neurons where they are developmentally regulated since they disappear during the first few weeks of postnatal life, suggesting a major role in the generation of oscillatory activities (Huguenard, 1996). In the cerebellum, the developmental expression of low threshold calcium spikes parallels that of the dendritic tree, indicating a possible dendritic localization of this conductance (Gruol et al., 1992). In the present experiments we cannot exclude the involvement of calcium conductances localized on dendrites. However, this hypothesis seems unlikely since maturation of GC dendrites is usually associated with the loss of low threshold calcium spikes. Although the functional role of low threshold calcium channels in immature GCs is still unclear, these may boost calcium entry *via* high threshold calcium channels and/or NMDA receptors following the depolarizing action of GABA thus contributing to GDPs generation. The transient elevation in intracellular calcium level during GDPs activates signaling pathways known to control several developmental processes, including DNA synthesis, neuronal migration, differentiation, and synaptogenesis (Cherubini et al., 2011). It is worth mentioning that in adult-born GCs low threshold calcium currents were present only in cells with synaptic inputs, suggesting that T-type of channels may play a crucial role in cell differentiation and in synaptic plasticity processes (Ambrogini et al., 2004; Schmidt-Hieber et al., 2004).

Although the present experiments clearly show that immature GCs are in several aspects similar to adult-born neurons in the inner GC layer (Laplagne et al., 2006, 2007; Overstreet-Wadiche and Westbrook, 2006; Overstreet-Wadiche et al., 2006; Zhao et al., 2010), they are functionally different since, unlike adult-born GCs, immature GCs display network-driven GDPs. This can be

attributed to the depolarizing and excitatory action of GABA that, compared with the adult hippocampus, early in postnatal life is very pronounced. GABA-induced membrane depolarization may act in synergy with glutamate to synchronize neuronal networks. GDPs have been already described in the fascia dentata of immature rabbits (Menendez de la Prida et al., 1998) and rats (Hollrigel et al., 1998). In rabbits GDPs persisted when the dentate gyrus was isolated from the Ammon's horn indicating that the entire hippocampal network possesses the capacity to generate them.

Here, the observation that GDPs persisted at lower frequency in the presence of the AMPA/kainate receptor antagonist DNQX strongly suggests the depolarizing and excitatory action of GABA is crucial for network synchronization. In addition, in immature GCs, oscillatory activity can be facilitated by the slow kinetics of $GABA_A$-mediated synaptic currents that may contribute to integrate incoming excitatory inputs (both GABAergic and glutamatergic) over a large time window (Draguhn and Heinemann, 1996; Hollrigel and Soltesz, 1997). In analogy with the synchronized activity generated in the disinhibited hippocampus (de la Prida et al., 2006), GDPs emerge when a sufficient number of cells fire and the excitability of the network attains a certain threshold within a restricted time window. Dye-coupling between immature GCs would facilitate this task.

Although neonatal and adult neurogenesis in the dentate gyrus seem to follow similar steps, the possibility that early synchronized activity early in postnatal development may play a role in synaptic wiring, thus contributing to refine local neuronal circuits according to aphorism "neurons that fire together wire together," cannot be excluded. Therefore, it is likely that changes in the environmental factors such as activity may determine the different phenotype of neonatal or adult GCs progenitors.

AUTHOR CONTRIBUTIONS

Andrea Pedroni, Antonello Mallamaci and Enrico Cherubini conceived and designed the experiments. Andrea Pedroni performed most of the electrophysiological and immunocytochemical experiments and analyzed the data. Do Duc Minh performed some immunocytochemical experiments. Enrico Cherubini wrote the paper with the approval of all the authors.

ACKNOWLEDGMENTS

The authors are particularly grateful to Drs R. Rauti and L. Ballerini for advice on biocytin morphological reconstruction; to Drs. R. Antonelli and F. Ruggeri for helpful comments and suggestions. This study was partially supported by a grant from Ministero dell'Istruzione, dell'Universita' e della Ricerca (PRIN 2011) to Enrico Cherubini.

REFERENCES

Altman, J., and Bayer, S. A. (1990a). Migration and distribution of two populations of hippocampal granule cell precursors during the perinatal and postnatal periods. *J. Comp. Neurol.* 301, 365–381. doi: 10.1002/cne.903010304

Altman, J., and Bayer, S. A. (1990b). Mosaic organization of the hippocampal neuroepithelium and the multiple germinal sources of dentate granule cells. *J. Comp. Neurol.* 301, 325–342. doi: 10.1002/cne.903010302

Ambrogini, P., Lattanzi, D., Ciuffoli, S., Agostini, D., Bertini, L., Stocchi, V., et al. (2004). Morpho-functional characterization of neuronal cells at different stages of maturation in granule cell layer of adult rat dentate gyrus. *Brain Res.* 1017, 21–31. doi: 10.1016/j.brainres.2004.05.039

Ben-Ari, Y., Cherubini, E., Corradetti, R., and Gaiarsa, J. L. (1989). Giant synaptic potentials in immature rat CA3 hippocampal neurones. *J. Physiol.* 416, 303–325.

Bergersen, L., Ruiz, A., Bjaalie, J. G., Kullmann, D. M., and Gundersen, V. (2003). GABA and GABAA receptors at hippocampal mossy fibre synapses. *Eur. J. Neurosci.* 18, 931–941. doi: 10.1046/j.1460-9568.2003.02828.x

Cabezas, C., Irinopoulou, T., Cauli, B., and Poncer, J. C. (2013). Molecular and functional characterization of GAD67-expressing, newborn granule cells in mouse dentate gyrus. *Front. Neural Circuits* 7:60. doi: 10.3389/fncir.2013.00060

Cabezas, C., Irinopoulou, T., Gauvain, G., and Poncer, J. C. (2012). Presynaptic but not postsynaptic GABA signaling at unitary mossy fiber synapses. *J. Neurosci.* 32, 11835–11840. doi: 10.1523/JNEUROSCI.5543-11.2012

Caiati, M. D., Sivakumaran, S., and Cherubini, E. (2010). In the developing rat hippocampus, endogenous activation of presynaptic kainate receptors reduces GABA release from mossy fiber terminals. *J. Neurosci.* 30, 1750–1759. doi: 10.1523/JNEUROSCI.4566-09.2010

Cherubini, E., Griguoli, M., Safiulina, V., and Lagostena, L. (2011). The depolarizing action of GABA controls early network activity in the developing hippocampus. *Mol. Neurobiol.* 43, 97–106 doi: 10.1007/s12035-010-8147-z

Crépel, V., Aronov, D., Jorquera, I., Represa, A., Ben-Ari, Y., and Cossart, R. (2007). A parturition-associated nonsynaptic coherent activity pattern in the developing hippocampus. *Neuron* 54, 105–120. doi: 10.1016/j.neuron.2007.03.007

de la Prida, L. M., Huberfeld, G., Cohen, I., and Miles, R. (2006). Threshold behavior in the initiation of hippocampal population bursts. *Neuron* 49, 131–142. doi: 10.1016/j.neuron.2005.10.034

Deng, W., Aimone, J. B., and Gage, F. H. (2010). New neurons and new memories: how does adult hippocampal neurogenesis affect learning and memory? *Nat. Rev. Neurosci.* 11, 339–350. doi: 10.1038/nrn2822

Draguhn, A., and Heinemann, U. (1996). Different mechanisms regulate IPSC kinetics in early postnatal and juvenile hippocampal granule cells. *J. Neurophysiol.* 76, 3983–3993.

Duan, X., Kang, E., Liu, C. Y., Ming, G. L., and Song, H. (2008). Development of neural stem cell in the adult brain. *Curr. Opin. Neurobiol.* 18, 108–115. doi: 10.1016/j.conb.2008.04.001

Espósito, M. S., Piatti, V. C., Laplagne, D. A., Morgenstern, N. A., Ferrari, C. C., Pitossi, F. J., et al. (2005). Neuronal differentiation in the adult hippocampus recapitulates embryonic development. *J. Neurosci.* 25, 10074–10086. doi: 10.1523/JNEUROSCI.3114-05.2005

Gruol, D. L., Deal, C. R., and Yool, A. J. (1992). Developmental changes in calcium conductances contribute to the physiological maturation of cerebellar Purkinje neurons in culture. *J. Neurosci.* 12, 2838–2848.

Gutierrez, R., Romo-Parra, H., Maqueda, J., Vivar, C., Ramìrez, M., Morales, M. A., et al. (2003). Plasticity of the GABAergic phenotype of the "glutamatergic" granule cells of the rat dentate gyrus. *J. Neurosci.* 23, 5594–5598.

Halliwell, J. V., and Adams, P. R. (1982). Voltage-clamp analysis of muscarinic excitation in hippocampal neurons. *Brain Res.* 250, 71–92. doi: 10.1016/0006-8993(82)90954-4

Hennou, S., Khalilov, I., Diabira, D., Ben-Ari, Y., and Gozlan, H. (2002). Early sequential formation of functional $GABA_A$ and glutamatergic synapses on CA1 interneurons of the rat foetal hippocampus. *Eur. J. Neurosci.* 16, 197–208. doi: 10.1046/j.1460-9568.2002.02073.x

Hollrigel, G. S., Ross, S. T., and Soltesz, I. (1998). Temporal patterns and depolarizing actions of spontaneous GABAA receptor activation in granule cells of the early postnatal dentate gyrus. *J. Neurophysiol.* 80, 2340–2351.

Hollrigel, G. S., and Soltesz, I. (1997). Slow kinetics of miniature IPSCs during early postnatal development in granule cells of the dentate gyrus. *J. Neurosci.* 17, 5119–5128.

Hsieh, J. (2012). Orchestrating transcriptional control of adult neurogenesis. *Genes Dev.* 26, 1010–1021. doi: 10.1101/gad.187336.112

Huguenard, J. R. (1996). Low-threshold calcium currents in central nervous system neurons. *Annu. Rev. Physiol.* 58, 329–348. doi: 10.1146/annurev.ph.58.030196.001553

Iwano, T., Masuda, A., Kiyonari, H., Enomoto, H., and Matsuzaki, F. (2012). Prox1 postmitotically defines dentate gyrus cells by specifying granule cell identity over CA3 pyramidal cell fate in the hippocampus. *Development* 139, 3051–3062. doi: 10.1242/dev.080002

Jones, S. P., Rahimi, O., O'Boyle, M. P., Diaz, D. L., and Claiborne, B. J. (2003). Maturation of granule cell dendrites after mossy fiber arrival in hippocampal field CA3. *Hippocampus* 13, 413–427. doi: 10.1002/hipo.10121

Kasper, E. M., Lübke, J., Larkman, A. U., and Blakemore, C. (1994). Pyramidal neurons in layer 5 of the rat visual cortex. III. Differential maturation of axon targeting, dendritic morphology, and electrophysiological properties. *J. Comp. Neurol.* 339, 495–518. doi: 10.1002/cne.903390404

Kasyanov, A. M., Safiulina, V. F., Voronin, L. L., and Cherubini, E. (2004). GABA-mediated giant depolarizing potentials as coincidence detectors for enhancing synaptic efficacy in the developing hippocampus. *Proc. Natl. Acad. Sci. U.S.A.* 101, 3967–3972. doi: 10.1073/pnas.0305974101

Laplagne, D. A., Espósito, M. S., Piatti, V. C., Morgenstern, N. A., Zhao, C., van Praag, H., et al. (2006). Functional convergence of neurons generated in the developing and adult hippocampus. *PLoS Biol.* 4:e409. doi: 10.1371/journal.pbio.0040409

Laplagne, D. A., Kamienkowski, J. E., Espósito, M. S., Piatti, V. C., Zhao, C., Gage, F. H., et al. (2007). Similar GABAergic inputs in dentate granule cells born during embryonic and adult neurogenesis. *Eur. J. Neurosci.* 25, 2973–2981. doi: 10.1111/j.1460-9568.2007.05549.x

Lavado, A., and Oliver, G. (2007). Prox1 expression patterns in the developing and adult murine brain. *Dev. Dyn.* 236, 518–524. doi: 10.1002/dvdy.21024

Liu, X., Tilwalli, S., Ye, G., Lio, P. A., Pasternak, J. F., and Trommer, B. L. (2000). Morphologic and electrophysiologic maturation in developing dentate gyrus granule cells. *Brain Res.* 856, 202–212. doi: 10.1016/S0006-8993(99)02421-X

Liu, Y. B., Lio, P. A., Pasternak, J. F., and Trommer, B. L. (1996). Developmental changes in membrane properties and postsynaptic currents of granule cells in rat dentate gyrus. *J. Neurophysiol.* 76, 1074–1088.

Marchal, C., and Mulle, C. (2004). Postnatal maturation of mossy fibre excitatory transmission in mouse CA3 pyramidal cells: a potential role for kainate receptors. *J. Physiol.* 561, 27–37. doi: 10.1113/jphysiol.2004.069922

Markwardt, S. J., Wadiche, J. I., and Overstreet-Wadiche, L. S. (2009). Input-specific GABAergic signaling to newborn neurons in adult dentate gyrus. *J. Neurosci.* 29, 15063–15072. doi: 10.1523/JNEUROSCI.2727-09.2009

McBain, C. J. (2008). Differential mechanisms of transmission and plasticity at mossy fiber synapses. *Prog. Brain Res.* 169, 225–240. doi: 10.1016/S0079-6123(07)00013-1

Menendez de la Prida, L., Bolea, S., and Sanchez-Andres, J. V. (1998). Origin of the synchronized network activity in the rabbit developing hippocampus. *Eur. J. Neurosci.* 10, 899–906. doi: 10.1046/j.1460-9568.1998.00097.x

Ming, G. L., and Song, H. (2011). Adult neurogenesis in the mammalian brain: significant answers and significant questions. *Neuron* 70, 687–702. doi: 10.1016/j.neuron.2011.05.001

Mullen, R. J., Buck, C. R., and Smith, A. M. (1992). NeuN, a neuronal specific nuclear protein in vertebrates. *Development* 116, 201–211.

Münster-Wandowski, A., Gómez-Lira, G., and Gutiérrez, R. (2013). Mixed neurotransmission in the hippocampal mossy fibers. *Front. Cell. Neurosci.* 7:210. doi: 10.3389/fncel.2013.00210

Overstreet, L. S., Hentges, S. T., Bumaschny, V. F., de Souza, F. S., Smart, J. L., Santangelo, A. M., et al. (2004). A transgenic marker for newly born granule cells in dentate gyrus. *J. Neurosci.* 24, 3251–3259. doi: 10.1523/JNEUROSCI.5173-03.2004

Overstreet-Wadiche, L. S., Bensen, A. L., and Westbrook, G. L. (2006). Delayed development of adult-generated granule cells in dentate gyrus. *J. Neurosci.* 26, 2326–2334. doi: 10.1523/JNEUROSCI.4111-05.2006

Overstreet-Wadiche, L. S., and Westbrook, G. L. (2006). Functional maturation of adult-generated granule cells. *Hippocampus* 16, 208–215. doi: 10.1002/hipo.20152

Safiulina, V. F., Caiati, M. D., Sivakumaran, S., Bisson, G., Migliore, M., and Cherubini, E. (2010). Control of GABA release at single mossy fiber-CA3 connections in the developing hippocampus. *Front. Syn. Neurosci.* 2:1. doi: 10.3389/neuro.19.001.2010

Safiulina, V. F., Fattorini, G., Conti, F., and Cherubini, E. (2006). GABAergic signaling at mossy fiber synapses in neonatal rat hippocampus. *J. Neurosci.* 26, 597–608. doi: 10.1523/JNEUROSCI.4493-05.2006

Schlessinger, A. R., Cowan, W. M., and Gottlieb, D. I. (1975). An autoradiographic study of the time of origin and the pattern of granule cell migration in the dentate gyrus of the rat. *J. Comp. Neurol.* 159, 149–175. doi: 10.1002/cne.901590202

Schmidt-Hieber, C., Jonas, P., and Bischofberger, J. (2004). Enhanced synaptic plasticity in newly generated granule cells of the adult hippocampus. *Nature* 429, 184–187. doi: 10.1038/nature02553

Schwarzer, C., and Sperk, G. (1995). Hippocampal granule cells express glutamic aci decarboxylase-67 after limbic seizures in the rat. *Neuroscience* 69, 705–709. doi: 10.1016/0306-4522(95)00348-M

Sivakumaran, S., Mohajerani, M. H., and Cherubini, E. (2009). At immature mossy-fiber-CA3 synapses, correlated presynaptic and postsynaptic activity persistently enhances GABA release and network excitability via BDNF and cAMP-dependent PKA. *J. Neurosci.* 29, 2637–2647. doi: 10.1523/JNEUROSCI.5019-08.2009

Sloviter, R. S., Dichter, M. A., and Rachinsky, T. L. (1996). Basal expression and induction of glutamate decarboxylase and GABA in excitatory granule cells of the rat and monkey hippocampal dentate gyrus. *J. Comp. Neurol.* 373, 593–618. doi: 10.1002/(SICI)1096-9861(19960930)373:4<593::AID-CNE8>3.0.CO;2-X

Spigelman, I., Zhang, L., and Carlen, P. L. (1992). Patch-clamp study of postnatal development of CA1 neurons in rat hippocampal slices: membrane excitability and K+ currents. *J. Neurophysiol.* 68, 55–69.

Walker, M. C., Ruiz, A., and Kullmann, D. M. (2001). Monosynaptic GABAergic signaling from dentate to CA3 with a pharmacological and physiological profile typical of mossy fiber synapses. *Neuron* 29, 703–715. doi: 10.1016/S0896-6273(01)00245-8

Ye, G. L., Song Liu, X., Pasternak, J. F., and Trommer, B. L. (2000). Maturation of glutamatergic neurotransmission in dentate gyrus granule cells. *Brain Res. Dev. Brain Res.* 124, 33–42. doi: 10.1016/S0165-3806(00)00103-6

Zander, J.-F., Munster-Wandowski, A., Brunk, I., Pahner, I., Gómez-Lira, G., Heinemann, U., et al. (2010). Synaptic and vesicular coexistence of VGLUT and VGAT in selected excitatory and inhibitory synapses. *J. Neurosci.* 30, 7634–7645. doi: 10.1523/JNEUROSCI.0141-10.2010

Zhao, S., Zhou, Y., Gross, J., Miao, P., Qiu, L., Wang, D., et al. (2010). Fluorescent labeling of newborn dentate granule cells in GAD67-GFP transgenic mice: a genetic tool for the study of adult neurogenesis. *PLoS ONE* 5:e12506. doi: 10.1371/journal.pone.0012506

Conflict of Interest Statement: The authors declare that the research was conducted in the absence of any commercial or financial relationships that could be construed as a potential conflict of interest.

Received: 20 December 2013; accepted: 30 January 2014; published online: 14 February 2014.

Citation: Pedroni A, Minh DD, Mallamaci A and Cherubini E (2014) Electrophysiological characterization of granule cells in the dentate gyrus immediately after birth. Front. Cell. Neurosci. ***8****:44. doi: 10.3389/fncel.2014.00044*

This article was submitted to the journal Frontiers in Cellular Neuroscience.

frontiers in
CELLULAR NEUROSCIENCE

REVIEW ARTICLE
published: 04 March 2014
doi: 10.3389/fncel.2014.00063

Neuronal migration and its disorders affecting the CA3 region

Richard Belvindrah*[1,2,3]*, Marika Nosten-Bertrand*[1,2,3] ***and Fiona Francis*[1,2,3]****

[1] *INSERM UMR-S 839, Paris, France*
[2] *Sorbonne Universités, Université Pierre et Marie Curie, Univ Paris 06, Paris, France*
[3] *Institut du Fer à Moulin, Paris, France*

Edited by:
Richard Miles, Institut pour le Cerveau et la Moëlle Epinière, France

Reviewed by:
Alfonso Represa, INMED, France
Michael Frotscher, University Medical Center Hamburg-Eppendorf, Germany
Scott C. Baraban, University of California, San Francisco, USA

****Correspondence:***
Fiona Francis, Institut du Fer à Moulin, INSERM UMR-S 839, 17 Rue du Fer à Moulin, 75005 Paris, France
e-mail: fiona.francis@inserm.fr

In this review, we focus on CA3 neuronal migration disorders in the rodent. We begin by introducing the main steps of hippocampal development, and we summarize characteristic hippocampal malformations in human. We then describe various mouse mutants showing structural hippocampal defects. Notably, genes identified in human cortical neuronal migration disorders consistently give rise to a CA3 phenotype when mutated in the mouse. We successively describe their molecular, physiological and behavioral phenotypes that together contribute to a better understanding of CA3-dependent functions. We finally discuss potential factors underlying the CA3 vulnerability revealed by these mouse mutants and that may also contribute to other human neurological and psychiatric disorders.

Keywords: neurodevelopment, mouse mutant, epilepsy, lamination, hippocampus

BASIC STEPS OF HIPPOCAMPAL DEVELOPMENT

The development of the rodent hippocampus in the medial telencephalon starts in mid-embryogenesis, as factors are secreted from the cortical hem to induce, specify and amplify the adjacent neuroepithelium to produce cortical tissue (Hoch et al., 2009; Pierani and Wassef, 2009; Subramanian and Tole, 2009; Subramanian et al., 2009). Hippocampal Cajal Retzius cells are also derived from the cortical hem and required for correct hippocampal organization (Bielle et al., 2005; Chizhikov et al., 2010; reviewed in Khalaf-Nazzal and Francis, 2013). The hippocampus shares a neuroepithelium which extends dorsally to ventrally through neocortical, subicular, hippocampal and septal regions. During hippocampal pyramidal cell neurogenesis, progenitor cells in these neuroepithelial ventricular zones (VZs) divide to produce neurons, which migrate radially toward the pial surface. Specialized progenitors are radial glial cells which have their somata in the VZ, a short apical process descending to the ventricular lining and a long basal process extending up to the pial surface (Nowakowski and Rakic, 1979; Seri et al., 2001). Cajal-Retzius cells in the marginal zone (MZ) play a critical role during development, initially secreting factors, which help maintain radial glial cell morphology and attachment to the pial surface (Zhao et al., 2004).

As shown extensively in the neocortex, radial glial cells can divide either symmetrically or asymmetrically, producing other progenitor cells (basal progenitors) and neurons (reviewed by Götz and Huttner, 2005; Kriegstein et al., 2006). In earlier stages of development, neurons may migrate by somal translocation, moving their nuclei within a long basal process attached to the pial surface (Nadarajah and Parnavelas, 2002). As shown firstly by classical neuroanatomical methods and later by videomicroscopy, radial glial cell processes later serve as guides for migrating neurons (radial glial guided locomotion). A variety of molecules, both intracellular and extracellular, have been shown to influence this mode of migration (see section Mouse Mutants and Molecular Mechanisms Important for Migration and Lamination). Neurons detach from these guides to settle in the cortical plate in a characteristic inside-out lamination pattern (reviewed by Gupta et al., 2002). Somal translocation may also play a role at these end stages of migration. Different waves of migration correspond to neurons born at different timepoints of neurogenesis. Earlier-born neurons settle in the deeper neocortical layers, whilst later born neurons cross through these layers to reach more superficial regions. The exact mechanisms regulating pyramidal neuron detachment from radial glial processes are unclear, although the reelin protein (see section Mouse Mutants and Molecular Mechanisms Important for Migration and Lamination), secreted by Cajal-Retzius cells, may play an instrumental role (Franco et al., 2011). Detached neurons then continue to differentiate, growing their apical and basal dendrites, and long axons.

Development occurs similarly in the hippocampus. As characterized in detail by Altman and Bayer in the rat dorsal hippocampus (Altman and Bayer, 1990a), using radioactive thymidine to label cells at different ages, radial glial progenitor cells in the convex-shaped ammonic neuroepithelium show a high level of proliferative activity and cycle their nuclei spatially within the VZ in a process termed interkinetic nuclear migration. Waves of migrating cells born at different time-points have also been characterized, however distinct inside-out lamination in the compact hippocampal plate is less well recognized (Altman and Bayer, 1990a; Fleck et al., 2000; Tole and Grove, 2001; Nakahira and Yuasa, 2005). A majority of pyramidal neurons are generated

between E16 and E20 in the rat hippocampus. By E20/E21 there are many fewer cells proliferating in the ammonic neuroepithelium. Migrating neurons in the hippocampal intermediate zone (IZ) were recognized as scattered spindle-shaped cells distinguishable from periventricular mitotic cells. In a second paper by the same authors (Altman and Bayer, 1990b), migrating cells were found to organize in bands, one more compact closer to the neuroepithelium and one more diffuse closer to the forming pyramidal cell layer. Cells were found to settle in the pyramidal cell layer (or hippocampal plate) 3–5 days after leaving the neuroepithelium (**Figure 1**), after a pause period, which the authors termed "sojourning." Sojourning has been proposed to allow pyramidal neurons to begin to polarize and to initiate axon growth which may occur far from the hippocampal plate (Altman and Bayer, 1990b). As post-mitotic neurons leave the VZs, they first take on a transient "multipolar" morphology, moving small distances laterally in the sub-VZ, whilst potentially waiting for appropriate signals which will induce them to acquire a bi-polar morphology with a leading and trailing process, perpendicularly oriented with respect to the ventricular lining. These morphological changes have been nicely characterized using the technique of *in utero* electroporation to label isolated cells focally with a fluorescent marker (Nakahira and Yuasa, 2005; Navarro-Quiroga et al., 2007).

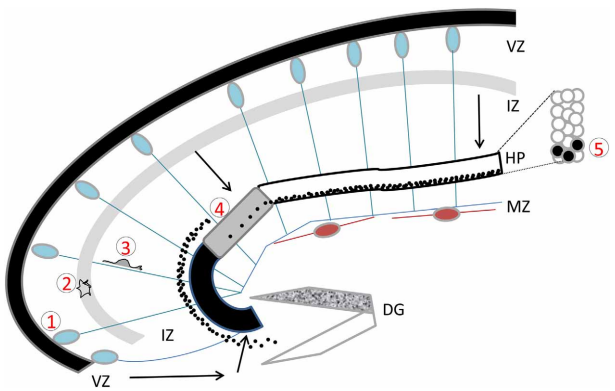

FIGURE 1 | The developing hippocampus. Radial glial cells are represented with their somata in the ventricular zone (VZ) and long basal processes extending up to the marginal zone (MZ). These processes serve as guides for migration. Cajal Retzius cells are schematized in brown. Migration pathways across the intermediate zone (IZ) are indicated by arrows. The hippocampal plate (HP) is shown in white, gray, and black to indicate the CA1, CA2, and CA3 fields respectively. The dentate gyrus (DG) is indicated as a V-shaped structure, at this stage the inferior blade (shown in white) is not completely formed, whereas the superior blade (shown in mottled gray) is taking shape. A BrdU injection at E18 in the rat, with sacrifice 4 days later reveals BrdU-labeled cells as schematized by the black dots: cells born at E18 have already reached the CA1 developing pyramidal cell layer, whereas CA3 cells are still found in the IZ, requiring another full day to cross the CA3 pyramidal cell layer. An inset shows the organization of somata in the pyramidal cell layer. Five successive steps of development are indicated, (1) cell proliferation and neurogenesis in the VZ; (2) a multipolar phase above the VZ; (3) a bipolar phase of migration through the IZ; (4) insertion in the hippocampal plate; (5) settling in the appropriate layer. Schema based on data shown in Altman and Bayer (1990b), Figure 3.

Nowakowski and Rakic (1979), studying migration in the fetal monkey hippocampus, also extensively characterized this radial-glial guided migration, but no mention was made of other migration modes. Even concerning the end stages of migration, as cells reached the hippocampal plate, although these authors recognized less dependence on radial glial cells and more complex multipolar morphologies, no mention was made of somal translocation. This is also true for the more recent studies in the rodent using immunofluorescence to reveal cell morphologies (Manent et al., 2005; Nakahira and Yuasa, 2005; Navarro-Quiroga et al., 2007). Nowakowski and Rakic do cite Morest (1970), studying the opossum brain, who identified an outer process extending through the hippocampal plate from the time the cell somata leave the VZ until they attain their final position. It is unclear if this data refers to somally translocating cells, or radial glial cell guided migration. From these studies, it is hence not yet possible to conclude if somal translocation is used in the hippocampus. Instead, another mode of migration, the "climbing mode" has recently been characterized. This occurs at late stages of cellular integration in the pyramidal cell layer, when migrating neurons are observed to exhibit multiple highly branched neuronal processes which interact with a number of radial fibers. Neurons are seen to switch radial fibers regularly, advancing in a zigzag manner through the hippocampal plate (Kitazawa et al., 2014). This mode of migration has never been characterized in the neocortex, may be specific to the hippocampus and may contribute to its less distinct lamination.

The pyramidal cell layer grows progressively from the subiculum to the dentate gyrus (DG), with the CA1 formed before the CA3 region. Studies in the rodent show that the migration time was shorter for CA1 pyramidal cells (4 days) than CA3 (5 days), although migration to both these regions is slower than cortical neurons migrating in the neocortex (Altman and Bayer, 1990b; Nakahira and Yuasa, 2005). Thus the CA1 layer becomes visible before the CA3, although its peak of neurogenesis (E18 in the rat) is a day later than the CA3 region (E17 in the rat). In the gradient of neurogenesis from the subiculum to the DG, CA1 neurogenesis is noticeably retarded and this has been associated with the requirement for thalamic inputs (Bayer, 1980). Alternatively, there is cumulative evidence for coordinated development and connectivity of different neuronal types within and outside the hippocampus (Bayer, 1980; Altman and Bayer, 1990b; Manent et al., 2005, 2006; Deguchi et al., 2011) which might help explain the comparatively longer "sojourning" time for CA3 pyramidal cells, which need to coordinate with DG granule cells. The curvature of the CA3 region and complexity of the migration path are also likely to contribute to this phenomenon. Indeed, unlike the CA1 region, CA3 cells not only have to migrate further, but they form a pyramidal cell layer which curves away from the neuroepithelium toward the DG. There is also a gradient of production of cells within the CA3 region itself, the regions closer to the CA1 region (CA3a and b subdivisions) forming before the region closest to the DG, and dorsal CA3 forming before ventral (Bayer, 1980). Indeed, CA3 cells destined for the hilar region (CA3c subdivision) have the furthest to travel, and they are eventually framed by the DG blades. Particular characteristics of radial glial cells at this stage of development are likely to be instrumental,

playing a role as a substrate to guide CA3 cells to this destination. DG cells may use the same migratory path as they migrate tangentially from the dentate neuroepithelium to the DG region (Altman and Bayer, 1990a,b; Nakahira and Yuasa, 2005; Danglot et al., 2006; Barry et al., 2008; Khalaf-Nazzal and Francis, 2013). Barry et al. (2008) have shown that RG cells progressively express different markers, and the formation of the DG (and most probably the hilar CA3) region is particularly dependent on a radial glial subtype present at later stages of development, extending from the neuroepithelium to the DG region. This represents a difference compared to the CA1 region, which can still form in the presence of "earlier" RG cells. There is also a less distinct deep to superficial lamination in regions of the CA3c layer, with these cells, although grouped together, showing a certain amount of spreading compared to other CA regions (Bayer, 1980). All in all, and despite the shorter migration distances, the pattern of development and morphogenesis of the hippocampus seems relatively more complicated than the formation of the neocortex, related to its fields of different shapes and compositions, with the CA3 pyramidal cell layer being more complex than the CA1 in this respect. Cell heterogeneity within each of the CA1 and CA3 regions is also now a well-recognized phenomenon (Thompson et al., 2008; Dong et al., 2009; Christian et al., 2011; Slomianka et al., 2011; Graves et al., 2012; Nielsen et al., 2013). Time of birth, migration pathways, as well as extracellular factors all contribute to different cell identities in the adult.

Elizabeth Grove and colleagues characterized genetic markers distinguishing CA1 and CA3 fields, appearing during development (Tole et al., 1997). Many markers are now known in the adult, related to large-scale *in situ* hybridization data in the mouse (Thompson et al., 2008) which have revealed nine different subfields for the CA3 region, showing a remarkable relationship with different functional connectivity boundaries. Laser microdissection transcriptome studies are also adding to the identification of CA3-specific markers (Datson et al., 2004, 2009; Greene et al., 2009; Deguchi et al., 2011), which may in the future reveal novel developmental gene networks playing key roles specifically in CA3 migration and differentiation.

While the settling of pyramidal neurons in the CA regions occurs through local migration from the ammonic neuroepithelium, hippocampal interneurons have to migrate very long distances from their places of origin to their final destination in the hippocampus (reviewed by Danglot et al., 2006). Hippocampal interneurons destined for the CA region are produced in the ventral telencephalon of the mouse from E12 onwards (Soriano et al., 1986, 1989; Pleasure et al., 2000; Manent et al., 2006). When the transcription factor genes *Dlx*1 and 2 are inactivated, the migration of interneuron precursors is completely arrested in the subpallium, related to an upregulation of a cytoskeleton regulator, p21-activated serine/threonine kinase, PAK3 (Anderson et al., 1997; Cobos et al., 2007). Interneurons are indeed derived from the medial (MGE) and the caudal ganglionic eminences (CGE), which generate interneurons sequentially in two waves at E9–E12 and E12–E16, respectively (Anderson et al., 1997; Marin et al., 2001; Danglot et al., 2006). The first interneurons arrive in the hippocampus from E14 onwards. Interneurons use a tangential mode of migration to reach the pallium, migrating in streams, and progressively invading the hippocampus through the MZ and the IZ/subventricular zone (SVZ), with the MZ contributing the vast majority of interneurons (Manent et al., 2006). They terminate migration locally, with MGE interneurons reaching the *strata pyramidale* and *oriens*, and CGE interneurons arriving in the superficial *strata lacunosum moleculare* and *radiatum* (Tricoire et al., 2011). Although the routes of migration are clearly defined, the substrate of migration of interneuron precursors is not. It has been suggested that corticofugal axons might serve as a scaffold for interneuron migration by recruiting the adhesion molecule TAG-1 (Denaxa et al., 2001), but this remains controversial and needs to be further clarified (Denaxa et al., 2005). Similarly, while it has been proposed that radial glia could also constitute guides for interneuron migration final positioning (Polleux et al., 2002; Poluch and Juliano, 2007), these observations lack molecular evidence and still need to be explored. Because of the important diversity of interneurons in the CA fields (Fishell and Rudy, 2011), different approaches of genetic fate mapping have successfully correlated the precise location of neurogenesis in the subpallium with the generated subtype. Mice carrying a GFP transgene either under the control of the *Gad*65 or *Nkx*2-1 promoters, allowed a specific tracking of the fate of interneuron precursors from the CGE or MGE respectively (Tricoire et al., 2011). There exists a striking association between the origin of interneurons, their respective markers and their electrophysiological properties. For instance, precursors originating from the MGE generate parvalbumin$^+$, somatostatin$^+$, and nNOS$^+$ interneurons with specific individual electrophysiological signatures, while the CGE-generated interneurons are cholecystokinin$^+$, calretinin$^+$, vasoactive intestinal peptide (VIP)$^+$ and reelin$^+$, each with distinct properties (Tricoire et al., 2011). These markers appear relatively homogenously distributed in the different strata constituting each of the CA fields, although subtle differences in number, morphology and layer distribution are recognized (Freund and Buzsaki, 1996; Matyas et al., 2004). For instance, while parvalbumin$^+$, calretinin$^+$, and neuropeptide Y$^+$ interneurons are mainly located in the *stratum pyramidale* in the CA1 region, they are distributed throughout all strata of the CA3 region. Also, VIP$^+$ interneurons seem to be more abundant in CA1 than in CA3 (Freund and Buzsaki, 1996; Matyas et al., 2004). The impact of these and other differences on CA1 vs. CA3 pyramidal cell functions remains to be completely explored.

All in all each of these steps of hippocampal development are instrumental to create the specific identities of the fields. Fundamental molecular, anatomical, and structural network differences between CA1 and CA3 regions suggest that these pyramidal cells have distinct functions. For instance, the recurrent network related to CA3 pyramidal cells differs greatly from the feed-forward network of the CA1 region. Functional intrinsic properties however, that might distinguish these pyramidal cell populations have not however been easily identified between CA1 and CA3 pyramidal cells (for example, Paz-Villagrán et al., 2004). It is possible that such differences at the single cell level could be very small. It has hence not been possible to ascertain the impact of potentially specific intrinsic properties compared to network effects on their functions. However, recently *in vivo* recordings from large sets of CA1 and CA3 pyramidal cells under various

brain states and in different environments, clearly demonstrated significant differences in firing rates, spike burst propensity, spike entrainment by theta rhythm, and other spiking dynamics in a brain state-dependent manner (Mizuseki et al., 2012). Studies such as this are hence revealing functional measures to distinguish the two cell populations. Thus, CA1 and CA3 pyramidal cells seem to exhibit specific activity dynamics that may support their distinct computational roles.

HUMAN HIPPOCAMPAL DEVELOPMENT AND DISORDERS

As mentioned above, radial glial guided migration has been characterized in the fetal monkey hippocampus, suggesting that in primate, hippocampal development occurs in a similar fashion to rodent (Nowakowski and Rakic, 1979). The different steps of human hippocampal development have been characterized (Arnold and Trojanowski, 1996; Abraham et al., 2004) by immunohistochemistry experiments using fetal tissue. At 10 gestational weeks (GW), Abraham et al. described that the compact ammonic plate was not yet visible, but many proliferating cells were observed in the ammonic VZ. Cajal-Retzius cells were also observed in the MZ at this stage. Between 11 and 16 GW, the CA and DG fields became obvious and vimentin staining revealed radial glial like cells in the neuroepithelia, extending from the VZ to the pial surface (Abraham et al., 2004). In this same study, reelin positive interneurons were also identified in the MZ above the hippocampal plate from 14 GW onwards. Proliferating cells become obvious in the dentate matrix from 14 GW onwards and had receded by 21 GW, when a tertiary matrix had formed in the hilar region. These cells had distributed to the DG region by 16 GW. Quantitative Golgi studies have also revealed that dendritic arborization, spine development and synaptogenesis of pyramidal neurons (CA3) occur during the second and third trimesters, and may continue throughout childhood (Lu et al., 2013). By 32–34 GW, it was described that neurons in CA2 and CA3 had undergone rapid enlargement and morphologic maturation, surpassing CA1, which still contained some immature neurons (Arnold and Trojanowski, 1996). Histological data has also been compared to 7-Tesla magnetic resonance imaging (MRI) data, which allowed a high resolution visualization of the different hippocampal fields in post-mortem fetal tissue (Milesi et al., 2014). These results are useful as a reference for the identification of human hippocampal abnormalities.

Hippocampal abnormalities have been found in association with a number of brain malformations, including agenesis of the corpus callosum, lissencephaly, holoprosencephaly, Fukuyama muscular dystrophy, polymicrogyria, heterotopia, focal cortical dysplasia, tuberous sclerosis, and schizencephaly (Sato et al., 2001; Porter et al., 2003; Montenegro et al., 2006; Kappeler et al., 2007; Fallet-Bianco et al., 2008; Donmez et al., 2009; Kuchukhidze et al., 2010). Such hippocampal defects in the past may have often been overshadowed by severe neocortical defects and not well-detailed due to the resolution of the MRI. It has more recently been shown in large cohorts that 30–55% of patients with cortical defects show hippocampal abnormalities (Donmez et al., 2009; Kuchukhidze et al., 2010). In these studies, bilateral and diffuse malformations were most often associated with such hippocampal abnormalities. Defects vary from small hippocampi and hypoplasia, enlarged hippocampi, to abnormally oriented hippocampi, related to abnormal gyration or infolding (Sato et al., 2001). Abnormal atrophy and severe neuronal loss can also be observed. Similar abnormalities are sometimes observed in febrile seizure, partial and refractory epilepsy patients, with no other obvious cortical abnormalities (Porter et al., 2003). Among cortical development disorders, those related to neuronal migration are the most highly associated with hippocampal abnormalities, as reported for lissencephaly (78%) (Donmez et al., 2009). In two neuropathological studies of type 1 lissencephaly cases, the pyramidal cell layers were found to be diffuse, in some cases the CA and DG fields were difficult to distinguish, and a general hypoplasia was observed (Kappeler et al., 2007; Fallet-Bianco et al., 2008). As mentioned below, hippocampal defects are a signature of mice which are mutant for these type I lissencephaly genes (Khalaf-Nazzal and Francis, 2013). This suggests that some genes play conserved functions during hippocampal neuron migration in rodent and primate.

MOUSE MUTANTS AND MOLECULAR MECHANISMS IMPORTANT FOR MIGRATION AND LAMINATION

The pyramidal cell layer is crudely laminated along the radial axis, with deep to superficial, molecular, morphological and connectivity specificities (Altman and Bayer, 1990a,b,c; Thompson et al., 2008; Deguchi et al., 2011; Slomianka et al., 2011). Thus pyramidal cells are heterogeneous, their birth-date determines their final position, and both the timing of neurogenesis and external factors contribute to their identity. Concerning cell positioning, migratory mechanisms are finely tuned in different cell autonomous and non-cell-autonomous ways and play a key role for the appropriate development and lamination of the CA3 region. At the level of the individual cell, settled in the pyramidal cell layer, it is also sequentially connected by afferent fibers, which also follow a strict temporal and spatial order (Bayer, 1980; reviewed by Förster et al., 2006). Lamination, at both the somal and connectivity levels, may hence be critical for function.

CELL AUTONOMOUS MECHANISMS

The main cell intrinsic actors known to regulate the migratory activity of pyramidal cell precursors are major components of microtubule (MT) structures, or proteins linked to MTs, such as Microtubule Associated Proteins (MAPs) or MT motors. They regulate different aspects of saltatory cellular migration movements such as the elongation of the leading process or nuclear translocation. Some of these regulators, which are part of a generic program that commonly regulates neuronal migration in different cerebral regions such as the cortex, the cerebellum or the hippocampus, are also tightly regulated by region-specific cell to cell signaling.

Several mouse mutant lines for either tubulin or MT associated components present severe defects in the CA3 region. The ENU-induced mouse mutant showing a mutation in *tubulin-alpha1a* (*Tuba1a*) presents a severe fragmentation of the CA layers, including the CA3 region (Keays et al., 2007, see **Figure 2** for schemas). The S140G mutation in Tuba1a might generate a haploinsufficiency phenotype with a defect in the incorporation of this mutant tubulin in MTs, which in turn is likely to perturb

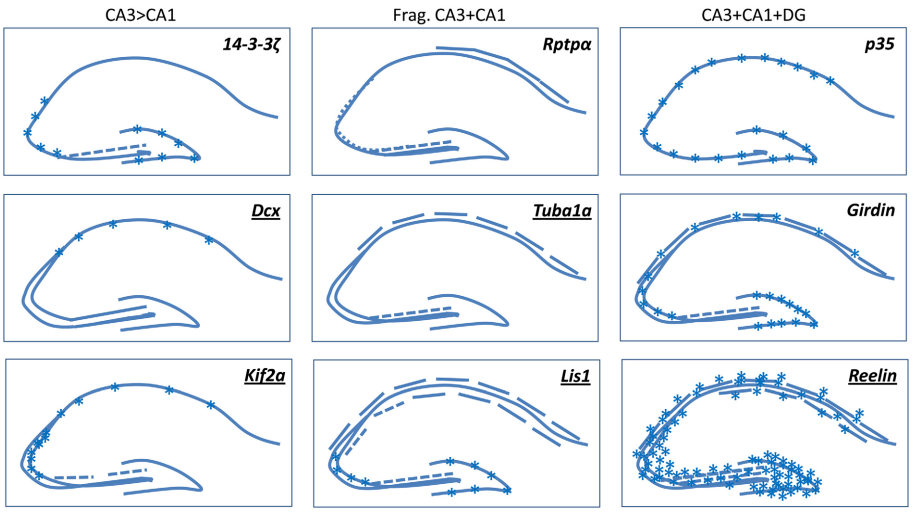

FIGURE 2 | A selection of mouse mutants showing somal lamination defects in the hippocampus. Underlined genes are known to be involved in cortical malformations in human. Frag, Fragmented. Broken lines indicate degrees of fragmentation. Asterisks indicate either heterotopic cells or diffusely packed cells. Schemas based on images presented in the following papers: (Del Río et al., 1997; Fleck et al., 2000; Wenzel et al., 2001; Corbo et al., 2002; Homma et al., 2003; Petrone et al., 2003; Kappeler et al., 2007; Keays et al., 2007; Enomoto et al., 2009; Cheah et al., 2012). *Kif*2a mutants die at birth, the P0 images shown in Homma et al. (2003) are similar to *Dcx*-KO brains, we have hence extrapolated these data in our schema depicting adult brains.

MT growth rate and consequently migration. Following the identification of this mutant gene in the mouse, mutations were identified in *TUBA1A* in type 1 lissencephaly in human (Keays et al., 2007). Despite the importance of structural homology with several other existing tubulin isotypes in migrating neurons, these results reveal the unique properties of some individual tubulins.

When the expression of certain MAPs is perturbed in mice, similar phenotypes have been observed. Among them, the Doublecortin (Dcx) MAP (Francis et al., 1999; Gleeson et al., 1999), also involved in type 1 lissencephaly, when inactivated in mouse generates a striking anatomical defect, mainly restricted in the CA3 region, with an abnormal double layer of pyramidal neurons. Interestingly, partners of Dcx, spinophilin and Usp9x, when inactivated in the mouse give a similar phenotype (Friocourt et al., 2005; Bielas et al., 2007; Stegeman et al., 2013). The origin of the defects is likely an altered migration although the exact perturbed mechanisms have yet to be fully characterized (Corbo et al., 2002; Kappeler et al., 2007; Nosten-Bertrand et al., 2008; Bazelot et al., 2012). Comparing with what is known for cortical pyramidal neurons and during interneuron migration, Dcx is likely to control neuronal migration by regulating branching and elongation of the leading process, and nuclear translocation, by stabilizing MT structures (Bai et al., 2003; Kappeler et al., 2006; Koizumi et al., 2006a; Belvindrah et al., 2011). The mouse model in particular has been extensively queried for CA3 functions (see "Electrophysiological, Behavioral, and Cognitive Phenotypes" section). Other members of the Dcx family also contribute to radial neuronal migration. *Doublecortin-like kinase* 1 (*Dclk*1) mutants show no obvious hippocampal abnormalities (Deuel et al., 2006; Koizumi et al., 2006b), however, double knockouts for Dcx and Dclk1, show both neocortical and hippocampal defects, conserving a severe fragmentation of the CA3 layer (Deuel et al., 2006). Mice deficient for both *Dcx* and *Dclk*2 show CA1 and CA3 lamination defects, without neocortical defects, and a reduced packing density of cells in the DG, as well as spontaneous seizures (Kerjan et al., 2009). Thus Dclk1 and 2 contribute to neuronal migration in other regions, although Dcx itself seems to have a primary importance in the CA3 region.

Another important MT regulator is the lissencephaly protein Lis1 that interacts within a multiple protein complex formed by dynactin/dynein and Ndel1. *Lis*1 mouse mutants (Hirotsune et al., 1998) present severe defects in hippocampal development such as the presence of heterotopic pyramidal cells in both CA1 and CA3 regions, forming multiple distinct fragmented cell layers (Fleck et al., 2000), as well as granule cell dispersion and aberrant neurogenesis in the DG (Wang and Baraban, 2007, 2008; Hunt et al., 2012). Lis1 by interacting with Ndel1 and dynein participates in a dose-dependent manner to the coupling of the centrosome with the nucleus, an essential step that synchronizes the nuclear movement with the elongation of the leading process (Hirotsune et al., 1998; Shu et al., 2004). Lis1 also contributes to neuronal process stabilization *per se* during migration by interacting with MT motors (Sasaki et al., 2000; Smith et al., 2000). Lis1 and Dcx may act synergistically by regulating dynein function to mediate the coupling of the centrosome to the nucleus (Tanaka et al., 2004a) or by influencing MT stabilization and bundling (Sapir et al., 1997; Francis et al., 1999; Gleeson et al., 1999). Perhaps related to this partial functional overlap, *Lis*1 and *Dcx* mutants present similarities in their respective pyramidal cell phenotypes but, interestingly, also noteworthy differences. While pyramidal cell somata are heterotopic and are less densely packed in both CA1 and CA3 in *Lis*1 mutant mice (Fleck et al., 2000), *Dcx* mutants present mainly defects in the CA3 region, evoking once

again possible divergent redundancies at least for the CA3 region, between these molecules.

The MT motor Kif2a is a further example of a protein with a MT function, which is required for hippocampal pyramidal cell organization in the mouse (Homma et al., 2003) and neocortical development in human (Poirier et al., 2013). This protein regulates MT dynamics by depolymerizing MTs. Mutant mice show a hippocampal phenotype, which is similar to *Dcx* mutants, the CA3 region is divided into two layers, and a thin heterotopic band is also seen during development in the CA1 region (Homma et al., 2003). The morphology of cells after settling in the CA1 pyramidal layer was analyzed in these mutants revealing an excess of axon collateral branching. This protein is likely to have pleiotropic functions, and an excess of branching may similarly perturb neuronal migration, as has been observed in *Dcx* mutant cells (Kappeler et al., 2006; Koizumi et al., 2006a; Belvindrah et al., 2011). A fragmented CA3 region is also seen in *14-3-3ζ* mutant mice, once again resembling *Dcx* and *Kif2a* mutants (Cheah et al., 2012). It will be interesting to search for physical interactions between these intracellular proteins, likely to act in the same pathways in CA3 cells.

An important regulator of cytoskeletal proteins is Cyclin Dependent Kinase-5 (Cdk5). Cdk5 mediates phosphorylation of Neurofilament proteins, Map1b, Map2 as well as the MAP Tau. Genetic alteration of its expression (or its activator p35) revealed its important function in neuronal migration since the mutation generates a lack of a confined layer of pyramidal neurons in CA regions (Ohshima et al., 1996; Wenzel et al., 2001; Ohshima et al., 2007). Pyramidal neurons in both CA1 and CA3 are less densely packed and interrupted in places (Chae et al., 1997). Among other Cdk5 substrates are Nudel, a Lis1 interacting protein (Niethammer et al., 2000), Dcx (Tanaka et al., 2004b), Fak (Xie et al., 2003) and Disc-1, a protein associated with the centrosome and MTs (Ishizuka et al., 2011). Thus, Cdk5 fulfills a range of functions extending from nuclear translocation to remodeling of the cytoskeleton by regulating MT dynamics, and its function is critical for neocortical and hippocampal development.

Most of the cytoskeletal components shown to be important for neuronal migration are either intrinsic to MTs or are related to proteins associated with MTs. MT structures are thus required for the dynamics of the anterior part of the leading process, the elongation of the leading process *per se* and the remodeling of the perinuclear cage structure. How the different actin regulators also participate during neuronal migration, in synergy with the MT components, is not completely understood, even for the well studied migration of excitatory neurons in the neocortex. However, the function of the actin cytoskeleton has been revealed at the leading edge of the growth cone, where actin polymerization is finely tuned by Rho-GTPases, such as RhoA (likely regulated by p27Kip1, Kawauchi et al., 2006; Nguyen et al., 2006) and Rac1 (Kholmanskikh et al., 2003). The actin cytoskeleton is also important at different focal contacts initiated in part by N-cadherins (Franco et al., 2011), where adhesions are formed, stabilized or removed. Moreover, the Rho effectors such as mDia and ROCK, interacting with the actin filaments located at the rear of the nucleus promote the actomyosin bundles required for nuclear translocation (Shinohara et al., 2012). There is also molecular evidence of cross interactions between the MT and actin cytoskeletons, and of interest here, certain mouse mutants show hippocampal malformations. Among them, we can identify the Lis1/Cdc42/Iqgap1 complex where Lis1 could increase active Cdc42 and connect the plus-end MT to cortical actin required for neuronal motility (Kholmanskikh et al., 2006). Girdin is also an actin-binding protein which interacts with Disc-1, itself interacting with the MT cytoskeleton (Enomoto et al., 2009). Girdin mouse mutants show hippocampal defects (see below). More recently, a conditional mouse mutant for the MT-actin crosslinking factor 1a (Macf1), that is part of the plakin family and is supposed to bridge MTs with the actin meshwork, also revealed the importance of these regulatory cross-talks, since the mutants present single-band heterotopias in the CA1-CA3 regions (Goryunov et al., 2010). Thus correct functioning of the actin cytoskeleton seems clearly also critical for hippocampal cell migration.

One further similar mouse mutant, *hippocampal lamination defect* (*Hld*, Nowakowski and Davis, 1985), which arose spontaneously on the BALBc background, has also been described although to our knowledge the mutant gene (autosomal) is still unknown. In this mutant, the CA3c region was shown to be inverted, with later-generated neurons found in the deeper instead of superficial layers. This situation could also be true for certain of the above-mentioned mutants and the consequences of such an inversion on function are still unknown.

NON-CELL-AUTONOMOUS MECHANISMS

Cell autonomous processes are also entry points for specific modulation of neuronal migration by environmental cues provided by neighboring cells that could be Cajal-Retzius cells, radial glial cells, migrating interneurons or the migrating pyramidal cells themselves, as well as incoming mossy fibers for CA3 cells. Thus, despite the existence of an intrinsic program that defines subtype specificity according to the timing of neurogenesis (Deguchi et al., 2011), the overall architecture of a layered CA3 region is also determined by the cellular integration of complex environmental cues.

As mentioned previously, maintenance of radial glial scaffold integrity is crucial for appropriate glial-guided locomotion of pyramidal neurons. Different mouse mutant models present severe defects in neuronal migration in the CA regions when these glial fibers are disorganized. As in the neocortex, when these fibers lose their apical attachment or their parallel orientation, neuronal migration is strongly compromised. Components of the extracellular matrix are known to regulate neuronal migration during CA3 development. The 385 kDa protein reelin, a major protein secreted by Cajal Retzius cells and shown to control cell positioning in the neocortex, is also implicated in the migratory mechanism of CA1 and CA3 pyramidal neurons. Reelin interacts with its receptors ApoER2/VLDLR to regulate intracellular effectors such as Dab1 (Hiesberger et al., 1999). Mutants for *reelin* (Stanfield and Cowan, 1979b; Niu et al., 2004) and *ApoEr2*/*Vldlr* (Trommsdorff et al., 1999) or their cytoplasmic effector *Dab*1 (Rice et al., 1998), present severe hippocampal development defects, among them, an absence of formation of a tight layer of pyramidal neurons, with cells only loosely organized.

Since the radial glial scaffold is also severely perturbed in these *reelin* signaling hippocampal mutants (Forster et al., 2002; Weiss et al., 2003), the contribution of this signaling pathway to different aspects of neuronal migration is certainly multiple, and this is very likely to be a convergence point between non-cell-autonomous and cell-autonomous regulators. For example, secreted reelin can control radial glial scaffold development, however it can also influence interaction of phosphorylated Dab1 with Lis1 within migrating neurons (Assadi et al., 2003; Zhang et al., 2007). The severe phenotype observed in Lis1 mutants could also be the consequence of a deregulation of the reelin signaling pathway within these neurons themselves. The other cell intrinsic regulator of neuronal migration, Cdk5, also converges with Reelin signaling (Ohshima et al., 2001; Beffert et al., 2004).

Another important regulator of cell migration in the CA3 region is the Receptor Protein Tyrosine Phosphatase, Rptp-α (gene name *Ptpra*). While *Rptp-α* mouse mutants present neuronal migration defects in CA regions, the primary cause of these defects is still unclear. Rptp-α has been shown to be important in the formation of apical dendrites (Ye et al., 2011). The Rptp-α signaling pathway that activates Fyn and Src kinases might also contribute to the proper development of the radial glial scaffold for promoting appropriate neuronal migration, but in this case, this would be through a mechanism independent of reelin signaling (Petrone et al., 2003). More recently, mutants for *Nuclear Factor Ib* (*Nfib*) have also confirmed the importance of the integrity of the glial scaffold to provide the appropriate substrate for neuronal migration. Indeed, in these mutants the glial fibers originating in the ammonic neuroepithelium may fail to mature, compromising severely the development of the hippocampal structure, especially in the DG, and potentially also CA3 subregions (Barry et al., 2008).

The proper migration stimulatory cues for pyramidal neurons in the CA3 region are also provided by migratory interneurons through non-vesicular release of GABA and likely by the migratory pyramidal cells themselves, with glutamate release stimulating the migration through the activation of NMDA receptors (Manent et al., 2005). Thus multiple factors and multiple membrane proteins are likely to influence migration. The sensitivity of migrating neurons to extracellular cues can also be modulated by the turn-over of membrane receptors at the level of the neuronal growth cone. Intracellular factors such as MTs and MAPs are also likely to play a role in this process, adjusting the sensitivity to such extrinsic parameters by modulating the levels of proteins on the surface of the cell by endocytosis and recycling, as has been suggested for Dcx (Friocourt et al., 2001; Kizhatil et al., 2002; Yap et al., 2012).

NON-GENETIC MECHANISMS PERTURBING CA MIGRATION

Up till now we have mentioned genetic factors leading to perturbed CA cell migration. Other factors can lead to this phenotype including injection of methylazoxymethanol (MAM) a DNA alkylating agent (Cattabeni and Di Luca, 1997; Colacitti et al., 1999; Battaglia et al., 2003). This agent when injected in pregnant female rats or mice leads to brain malformations in the embryos, associated with perturbed hippocampal development and susceptibility to seizures (Chevassus-Au-Louis et al., 1998a,b; Colacitti et al., 1999; Baraban et al., 2000). Focal heterotopias are related to a perturbation of radial glial cells during development (Paredes et al., 2006). Developmental mechanisms appear different though from mouse models mentioned above, CA1 heterotopic hippocampal neurons were characterized as being derived from the neocortex and integrated in both neocortical and hippocampal circuitry (Chevassus-Au-Louis et al., 1998b,a; Paredes et al., 2006). Hippocampal cells have been shown to have altered glutamate receptor subunit and transporter expression and the affected animals to suffer from epilepsy (Harrington et al., 2007). This model may be useful for further studying structural and functional defects related to CA migration disorders.

TEMPORAL ASPECTS OF CA3 CELL MIGRATION AND THE INFLUENCE OF MOSSY FIBERS—AN ANALYSIS OF FURTHER MUTANTS

The migration process follows a temporal sequence that is likely to impact cell connectivity (Stanfield and Cowan, 1979a; Bayer, 1980; Deguchi et al., 2011). While pyramidal neurons migrate uniformly and synchronously through the cortical wall along glial fibers, it has been proposed that the long pausing of CA3 cells in the IZ may be due to a necessary synchronization with the development of mossy fibers (largely starting at E17–E18). Initial observations showed that a major proportion of DG granule cells are born later than CA3 cells, and the DG blades are established in early postnatal stages (Altman and Bayer, 1990a; reviewed in Danglot et al., 2006). On the other hand, Deguchi et al. (2011) using sparse Thy1-mGFP reporter lines, were also able to show that some DG cells are born as early as E12 in the mouse hippocampus and that there is selective connectivity (neuronal specification and synaptogenesis) between CA3 and DG cells, and CA3 and CA1 cells, born at the same times. These latter data suggest that synchronization of the production of different cell types occurs and that microcircuits may be important in the hippocampus.

Although the production of connecting granule cells may therefore be temporally correlated with CA3 cell partners (Deguchi et al., 2011), it is possible that the CA3 pyramidal layer can assemble correctly even if DG formation is perturbed. However, as mentioned above, there do exist mouse mutants where both the DG and CA pyramidal layers are disorganized, for example, *reelin* (Del Río et al., 1997; Lambert de Rouvroit and Goffinet, 1998) and *Lis*1 mutants (Fleck et al., 2000; Wang and Baraban, 2007, 2008). The *Girdin* mutant also, related to the Disc1 pathway, and *Grik2* "*weaver*" mutants show abnormal pathfinding of MFs and also some abnormal CA lamination or clusters of heterotopic cells (Sekiguchi et al., 1995; Enomoto et al., 2009). Differing from this, in the case of the *Cxcr*4 or *Disc*1 mouse mutants, granule cells are not guided properly to the DG region and remain accumulated in the migration path (Lu et al., 2002; Meyer and Morris, 2009; Kvajo et al., 2011), but in each case the pyramidal cell layer appears to form correctly, despite the granule cell abnormalities. It still remains possible on the other hand, that mossy fiber outgrowth occurs correctly in these mutants, despite abnormal granule cell position, hence still allowing for an effect of mossy fibers on CA3 cell migration. Conditional mutants are

required to inactivate genes specifically in mossy fibers in order to verify pre-synaptic consequences on CA cell lamination.

A further set of mutants, with apparently correctly formed CA3 pyramidal and DG layers but more subtle perturbed mossy fiber targeting or pruning, are related to several axon guidance or adhesion molecules. For example inactivation of the semaphorin 3 receptors, *plexin* A3 and *neuropilin* 2 (Chen et al., 2000; Giger et al., 2000; Bagri et al., 2003), the guidance receptor *ephrin* B3 (Xu and Henkemeyer, 2009), and the adhesion molecule *nectin* (Honda et al., 2006), show mossy fibers which target infrapyramidal, as well as suprapyramidal regions, most probably due to abnormal fasciculation, targeting and pruning. Also, mouse mutants for *serum response factor* (Knöll et al., 2006), and adhesion molecules *Chl*1 (Montag-Sallaz et al., 2002), *Ncam*-180 (Seki and Rutishauser, 1998) and *cadherin* (Bekirov et al., 2008; Williams et al., 2011), have mossy fibers which aberrantly synapse on CA3 somata within the pyramidal cell layer instead of apical dendrites in the suprapyramidal regions. Furthermore, in mutants for semaphorin 6 receptors *plexin* A2 and A4, the mossy fibers also continue to project either to the infra- and/or intrapyramidal regions (Suto et al., 2007; Tawarayama et al., 2010). In some of these cases of aberrant intrapyramidal connections, the CA3c region appears thickened, but this may be due to the presence of excess neuropil within the layer, more so than abnormal migration, although this remains to be formally demonstrated. A different problem was revealed by mutation of the *grik2* gene, associated with autism spectrum disorder and intellectual disability, which slowed the structural and functional maturation of the hippocampal mossy fiber to CA3 pyramidal cell synapses (Lanore et al., 2012). These problems affecting mossy fiber fasciculation, targeting, synaptogenesis, and refinement do not hence answer the question if correct mossy fiber outgrowth and contact are strictly required for the final stages of CA3 cell migration and lamination, although this data seems to suggest that the migration of CA3 pyramidal neurons can occur relatively correctly, independently of mossy fibers. Specific bi-directional, trans-synaptic, interactions between DG and CA3 neurons remain however, critical to drive synapse formation.

ELECTROPHYSIOLOGICAL, BEHAVIORAL, AND COGNITIVE PHENOTYPES

In all mouse mutants for genes associated with type I lissencephaly, or other similar cortical malformations (*Dcx*, *Kif2a*, *Tuba1a*, *Lis*1, *reelin*), a gradient of severity is observed at the functional and behavioral levels that parallels the gradient of severity that is observed at the cellular level. Consistent with an extensive neuronal disorganization in both the neocortex and hippocampus, *reeler* mice exhibit severe motor, behavioral, and emotional impairments (Falconer, 1951; Tueting et al., 1999, 2006; Gebhardt et al., 2002; Salinger et al., 2003). In the *Lis*1 model, the neuronal migration defects are associated with morphological and functional alterations of the Schaffer collateral–CA1 synapse and enhanced excitability in pyramidal neurons (Fleck et al., 2000; Jones and Baraban, 2007, 2009; Valdés-Sánchez et al., 2007; Greenwood et al., 2009). DG granule cells are also affected (Hunt et al., 2012). These mice exhibit spontaneous seizures (Hirotsune et al., 1998; Fleck et al., 2000; Jones and Baraban, 2009), as well as limited, albeit severe, cognitive deficits (Hirotsune et al., 1998; Lambert de Rouvroit and Goffinet, 1998; Paylor et al., 1999). Most studies which have been performed in *Lis*1 mutant mice have been focused on the CA1 region. Firstly, it was shown that CA1 heterotopic cells are more excitable compared to WT when hippocampal slices were subjected to increasingly elevated concentrations of potassium (Fleck et al., 2000). Single cell studies after stimulation of the Schaffer collaterals, further showed increased excitatory post-synaptic events (EPSPs) in mutant CA1 cells compared to WT. A laminar analysis of evoked EPSPs (with the recording electrode placed at different positions), showed that abnormally positioned heterotopic CA1 cells are also functionally innervated. Migration defects, EPSP abnormalities and some behavioral phenotypes were rescued by calpain inhibitors, which increase the quantities of Lis1 (Yamada et al., 2009; Sebe et al., 2013). Inhibitory post-synaptic currents (IPSCs) were recorded in CA1 cells and also found to be increased (Valdés-Sánchez et al., 2007). Furthermore, interneuron distribution and firing was abnormal in this model (Jones and Baraban, 2007, 2009). These combined data hence illustrate the multiple consequences on hippocampal circuits due to perturbed hippocampal development.

Unlike *Lis*1 mutants, *Dcx*-KO mice with cellular lamination defects largely restricted to the CA3 region, have provided a unique model to explore hippocampus-and CA3-dependent functions. At the clinical level, these mice exhibit spontaneous convulsive seizures and are more prone to seizures induced by chemoconvulsants than their WT littermates (Nosten-Bertrand et al., 2008). The precise anatomical characterization of the CA3 region revealed three distinct patterns of lamination in *Dcx*-KO mice along the rostro-caudal axis, with CA3b and c subregions exhibiting both double and dispersed layers of pyramidal cell somata, while the CA3a region was mostly a single layer (Bazelot et al., 2012; Germain et al., 2013). The density and distribution of parvalbumin-containing interneurons were not affected in *Dcx*-KO mice, and they were found to innervate pyramidal cell somata of both single and double (internal and external), layers. In addition, intracellular recordings, biocytin filling, as well as multi-electrode recordings showed that both layers of CA3 KO pyramidal cells exhibited an altered dendritic form and were more excitable than their WT counterparts (Bazelot et al., 2012). However, the bi-layer seems to have dramatic effects on pyramidal cell form, with the internal layer showing reduced basal dendrites, whereas the external layer showed reduced apical dendrites (**Figure 3**). Mossy fiber connections were also altered, related to the bi-layer, with some connections abnormally retained on the basal dendrites of the internal layer, whereas connections were interrupted on the apical dendrites of cells in the external layer, as they passed through the internal layer. The threshold current required to initiate an action potential was reduced in *Dcx*-KO cells, and mean firing rates were increased. Thus, the absence of Dcx affects synaptic connectivity and results in enhanced pyramidal cell excitability.

At the behavioral level, *Dcx*-KO mice were shown to be hyperactive in novel environments, less aggressive, and more ambidextrous than their WT littermates (Germain et al., 2013). Given its central position within the trisynaptic hippocampal pathway, the

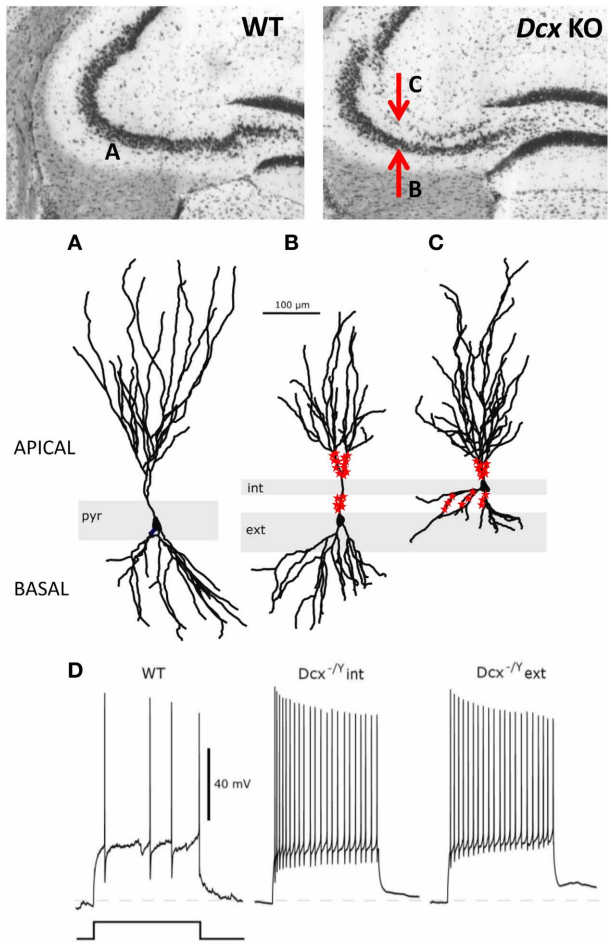

FIGURE 3 | Morphological and functional abnormalities in the *Dcx*-KO hippocampus. Upper images show coronal slices of the adult *Dcx*-KO hippocampus (right) compared to wild-type (WT, left). Red arrows in the KO image point to the internal (upper) and external (lower) CA3 layers. Whole cell recordings and biocytin fills were performed to characterize internal (int) and external (ext) pyramidal cells. **(A)** WT cell; **(B)** KO external cell; **(C)** KO internal cell (taken and modified from Bazelot et al., 2012 Figure 5, published by John Wiley & Sons Ltd). Analyses of cell morphologies revealed reduced lengths of apical dendrites for external layer cells and reduced lengths of basal dendrites for internal layer cells (Bazelot et al., 2012). Red labeling on dendrites schematizes mossy fiber innervation in the form of post-synaptic thorny excrescence-like spines. Note non-continuous innervation on apical dendrites of external layer cells, and basal as well as apical innervation on internal layer cells (schematizing data presented in Bazelot et al., 2012, Figure 4). **(D)** Whole cell recordings taken from Bazelot et al. (2012) Figure 6 (published by John Wiley & Sons Ltd) revealed that KO cells are more excitable than their WT counterparts. In response to identical depolarizing current injection, KO cells fired at higher frequencies.

CA3 region may contribute to the prominent role of the hippocampus in episodic memory and spatial representation of the environment (Eichenbaum et al., 2012). However, interestingly, we have shown that *Dcx*-KO mice exhibit normal spatial learning and contextual or cued memory as tested in the Barnes or water mazes, and in the fear-conditioning paradigms. *Dcx*-KO mice also exhibited spared CA3-dependent cognitive functions such as rapid contextual representation, novelty detection, and one-trial short-term memory, tested with a large battery of tests such as fear conditioning, paired associate learning and object recognition (Germain et al., 2013). Strikingly, in another mouse model, the *Dcx* mutation was associated with lethality in hemizygous male mice, probably due to the different genetic backgrounds (Corbo et al., 2002). Interestingly however, both *Dcx* models are largely identical anatomically, with identical lamination defects largely restricted to the CA3 region. In addition, this study showed very mild behavioral deficits in *Dcx* heterozygous females, including reduced freezing in both cued and contextual fear conditioning tests, similarly identified in Germain et al. (2013), that could be indicative of an anxiety-related phenotype.

Thus, in *Dcx* mutants, the CA3 heterotopia is responsible for hyperexcitability and seizures, whereas hippocampal-dependent cognitive circuits may have at least partially adapted to the CA3 bi-layer. This differs from the situation in *Lis*1 mice and other mutants, with a more severely malformed hippocampus, hyperexcitability and perturbed cognitive functions. Although, a genetic redundancy underlying functional compensatory mechanisms between Dcx and its closest homologs Dclk1 and Dclk2 has been specifically addressed and demonstrated to be important in the neocortex and CA1 region of murine *Dcx* models (Deuel et al., 2006; Koizumi et al., 2006b; Kerjan et al., 2009), the CA3 anatomical defects are present in single *Dcx* knockouts. These observations again suggest more complex and specific features of cell migration in the CA3 region. The presence of Dclk1 and 2, and other potential compensatory proteins, in the developing CA3 region is not sufficient to allow correct neuronal migration and excitability, however the KO hippocampus still correctly performs hippocampus-dependent cognitive functions.

Two further mouse mutants showed mainly CA3 disorganization in the hippocampus, *Kif*2a and *14-3-3ζ* (Homma et al., 2003; Cheah et al., 2012) and it would hence be interesting to compare their behavioral phenotypes. Constitutive *Kif*2a mutants, have multiple brain abnormalities and die within a day of birth (Homma et al., 2003), however, *14-3-3ζ* mutants survive and exhibit striking behavioral deficits including hyperactivity, disrupted sensorimotor gating, and impaired learning and memory (Cheah et al., 2012). Some of these abnormalities are likely to be related to the hippocampal abnormalities. Notably though these mice also have developmental DG abnormalities, as well as severer abnormal mossy fiber targeting, differing hence from *Dcx*-KO mice.

WHAT HAVE WE LEARNT FROM STUDYING THE CA3 REGION IN NEURONAL MIGRATION MUTANTS?

1. The most striking observation from the murine models for genes involved in human neuronal migration disorders is that the CA3 region seems the most sensitive and consistently affected brain region. Indeed, all the mouse mutants for genes associated with type 1 lissencephaly, or other similar cortical malformations (*Lis1*, *Dcx*, *Tuba1a*, *reelin*, *Kif2a*), have a CA3 lamination defect as a common, and the most obvious, feature (**Figure 2**, Hirotsune et al., 1998; Lambert de Rouvroit and Goffinet, 1998; Fleck et al., 2000; Corbo et al., 2002; Homma et al., 2003; Kappeler et al., 2007; Keays et al.,

2007; Poirier et al., 2013). Human patients also have severe hippocampal abnormalities, however, these are not restricted to the CA3 region. The mouse CA3 phenotype is also often associated with other variable defects. CA3 lamination defects also seem to cluster in some mouse mutants of genes associated with neuropsychiatric disorders (Enomoto et al., 2009; Petrone et al., 2003). Thus CA3 lamination abnormalities in the mouse are correlated with neurodevelopmental cortical problems in human, and models derived from large-scale ENU mutagenesis projects may be tested to search for CA3 migration defects in order to easily select interesting models for further exploration (Keays et al., 2007; Furuse et al., 2012).

From a developmental point of view (section—Basic Steps of Hippocampal Development), it seems clear that CA3 cell migration is more complex than CA1. CA3 cells, especially in CA3b and c regions, have to migrate curved routes, which might involve several modes of migration, and particular features of radial glial cells that provide a cellular substrate. CA3 cell migration could hence require extra molecular and cellular pathways compared to CA1. The genes we mention in this review such as *Dcx*, are strictly necessary to achieve CA3 cell migration correctly and even close homologs cannot compensate their function. In genetic terms, there seems hence to be lower redundancy in the CA3 region. Further study of CA3 mutants will help to reveal the very particular aspects of CA3 development, compared to CA1. Some of these mechanisms may also be required for human neocortical development.

It also remains possible that the CA3 region shows other susceptibilities. In the adult, CA3 cells are known to have a higher metabolic rate than CA1 cells, and to be more vulnerable to chronic stress and seizure-induced damages (Greene et al., 2009; Christian et al., 2011). Indeed, the CA3 is the most vulnerable subregion of the hippocampus in response to chronic stress and exhibits the most severe neuronal changes such as decrease in complexity and retraction of dendrites as compared to the CA1 subregion (Woolley et al., 1990; Watanabe et al., 1992). On the other hand, CA1 cells may be more susceptible to ischemia than CA3 pyramidal cells (Pulsinelli and Brierley, 1979; Zola-Morgan et al., 1986). CA3 cell organelle defects and increased cell death have also been identified in the *Dcx*-KO postnatal hippocampus (Khalaf-Nazzal et al., 2013). It is too early to tell if this may be a consequence of the aberrant migration, related to cell stress, or alternatively a consequence of the intrinsic function of Dcx, associated with MTs, which may affect organelle trafficking and subsequently migration. We cannot rule out however, that early metabolic or other differences during development also contribute to CA3 vs. CA1 migration susceptibilities.

2. Slowed and arrested migration in CA3 mutants clearly leads to a situation resembling heterotopia, with a small distance along the radial axis between different layers of cell somata. In this respect, it is interesting to recall, that phylogenetic differences in lamination have arisen, such that a bi-laminar CA1 region exists naturally in various mammalian species (Slomianka et al., 2011). Bi-lamination of hippocampal pyramidal cells *per se*, therefore is not necessarily expected to lead to aberrant functional consequences. It does however seem detrimental in CA3 mouse mutants, at least at the level of morphology, mossy fiber connectivity and potentially hyperexcitability (Kerjan et al., 2009; Bazelot et al., 2012; Cheah et al., 2012). Mossy fiber connectivity abnormalities seem to go together with abnormal lamination, even if the inverse is not always true (see discussion in section Temporal Aspects of CA3 Cell Migration and the Influence of Mossy Fibers—An Analysis of Further Mutants).
3. Further connectivity and functional studies still need to be performed, especially taking into account different interneuron populations, because interneuron migration abnormalities have also been identified in some mutants (*Lis*1, *Dcx*, *Dcx*/*Dclk*2, McManus et al., 2004; Kappeler et al., 2006; Kerjan et al., 2009). It is too early to tell if perturbed lamination contributes to abnormal positioning of hippocampal interneurons, even if the two processes may be coordinated (Manent et al., 2005; Lodato et al., 2011; Ciceri et al., 2013). During development, we and others have observed some interneuron and oligodendrocyte precursor cell disorganization within the developing CA3 layers (Kerjan et al., 2009; Khalaf-Nazzal et al., 2013). This may be related to a more diffuse organization of pyramidal cells (Khalaf-Nazzal et al., 2013).

   In the *Lis*1 model, as well as abnormal interneuron distribution, cell attached recordings showed that synaptic excitation of interneurons (EPSCs) was increased. IPSCs recorded in CA1 cells were also found to be increased (Jones and Baraban, 2007). The authors concluded that since precisely coordinated GABAergic activity is vital for the generation of oscillatory activity and place field precision in the hippocampus, these alterations in synaptic inhibition are likely to contribute to the seizures and the altered cognitive function observed. Loss of certain subpopulations is known to have a strong impact on susceptibility to epilepsy in other models (Cobos et al., 2005). Interneuron number and distribution can also change after seizures (Nosten-Bertrand et al., 2008; Kerjan et al., 2009). Interneuron function hence needs to be more closely examined in relation with CA3 phenotypes.
4. Concerning CA3-dependant cognitive function, it seems that it may be remarkably preserved in the *Dcx*-KO despite a bi-lamination of the CA3 pyramidal layer. However in this model, the synaptic excitatory and inhibitory input seem to be preserved in both CA3 layers (Bazelot et al., 2012), suggesting that despite the enhanced pyramidal cell excitability, synaptic transmission and plasticity could still be retained to an extent compatible with normal CA3-dependent function. Some previous studies have clearly shown intact spatial navigation despite focal CA3 impairment (Nakazawa et al., 2003; Nakashiba et al., 2008). In addition, several alternative systems may also adapt and compensate to maintain hippocampal function. Of interest, impaired CA3- and hippocampal cognitive function are reported when migration defects expand to other hippocampal subregions, such as the DG (*14-3-3*ζ mutants) or CA1 (*Lis*1 mutants).
5. CA3 deficits may be correlated with hyperexcitability and epilepsy, e.g., *Dcx* and *Lis*1 mutants, although defects in other cell types (e.g., interneurons), and in different hippocampal (e.g., CA1) and/or other brain regions (e.g., the neocortex) are

very likely to also contribute to such a phenotype. Identifying the origins of hyperexcitability remains a complex subject, as does distinguishing between causative and neuroprotective mechanisms. Cataloguing the different mutants available for study and focusing on the most restricted phenotypes may help dissect out these pathogenic and pathophysiological mechanisms.

FINAL CONCLUSIONS

These fundamental studies concerning rodent models thus contribute to deepen our understanding of basic genetic and cellular mechanisms underlying lissencephaly and related disorders. They also shed light on specific CA3 molecular and cellular features, including more complex curved routes and longer pausing steps during cell migration, as well as a reduced potential of genetic and functional redundancy, that may all contribute to a higher vulnerability of this region. This may indeed extend to other human neurological and psychiatric disorders, for example different types of epilepsy and schizophrenia. In the past decade, thanks to rodent studies, the identification of cellular mechanisms underlying CA3 hyperactivity, including increased glutamatergic input from the amygdala, leading to CA3 interneuron loss, has significantly contributed to our understanding of psychotic-related symptoms such as social phobia and hallucinations (Liddle et al., 2000; Olypher et al., 2006; Lodge and Grace, 2007; Behrendt, 2010). Characterizing further these vulnerabilities will contribute to an improved pharmacological treatment of these morbid disorders in the future.

AUTHOR CONTRIBUTIONS

Richard Belvindrah, Marika Nosten-Bertrand, and Fiona Francis wrote the review.

ACKNOWLEDGMENTS

We thank Michael Bazelot, Richard Miles and other members of his lab for their contribution to *Dcx* KO data and discussions. We thank Jean-Christophe Poncer for his opinion on certain aspects of this review. We are grateful for financial support from the Agence National de la Recherche (ANR- 08-MNP-013), as well as from INSERM, including the Avenir program, the CNRS and UPMC, the Fondation Bettencourt Schueller, the Région Ile-de-France, and the Fondation Jérôme Lejeune. Authors are associated with the BioPsy Labex project and the Ecole des Neurosciences de Paris Ile-de-France network.

REFERENCES

Abraham, H., Pérez-García, C. G., and Meyer, G. (2004). p73 and reelin in Cajal-Retzius cells of the developing human hippocampal formation. *Cereb. Cortex* 14, 484–495. doi: 10.1093/cercor/bhh010

Altman, J., and Bayer, S. A. (1990a). Mosaic organization of the hippocampal neuroepithelium and the multiple germinal sources of dentate granule cells. *J. Comp. Neurol.* 301, 325–342. doi: 10.1002/cne.903010302

Altman, J., and Bayer, S. A. (1990b). Prolonged sojourn of developing pyramidal cells in the intermediate zone of the hippocampus and their settling in the stratum pyramidale. *J. Comp. Neurol.* 301, 343–364. doi: 10.1002/cne.903010303

Altman, J., and Bayer, S. A. (1990c). Migration and distribution of two populations of hippocampal granule cell precursors during the perinatal and postnatal periods. *J. Comp. Neurol.* 301, 365–381. doi: 10.1002/cne.903010304

Anderson, S. A., Eisenstat, D. D., Shi, L., and Rubenstein, J. L. (1997). Interneuron migration from basal forebrain to neocortex: dependence on Dlx genes. *Science* 278, 474–476. doi: 10.1126/science.278.5337.474

Arnold, S. E., and Trojanowski, J. Q. (1996). Human fetal hippocampal development: I. Cytoarchitecture, myeloarchitecture, and neuronal morphologic features. *J. Comp. Neurol.* 367, 274–292. doi: 10.1002/(SICI)1096-9861(19960401)367:2<274::AID-CNE9>3.0.CO;2-2

Assadi, A. H., Zhang, G., Beffert, U., McNeil, R. S., Renfro, A. L., Niu, S., et al. (2003). Interaction of reelin signaling and Lis1 in brain development. *Nat. Genet.* 35, 270–276. doi: 10.1038/ng1257

Bagri, A., Cheng, H. J., Yaron, A., Pleasure, S. J., and Tessier-Lavigne, M. (2003). Stereotyped pruning of long hippocampal axon branches triggered by retraction inducers of the semaphorin family. *Cell* 113, 285–299. doi: 10.1016/S0092-8674(03)00267-8

Bai, J., Ramos, R. L., Ackman, J. B., Thomas, A. M., Lee, R. V., and LoTurco, J. J. (2003). RNAi reveals doublecortin is required for radial migration in rat neocortex. *Nat. Neurosci.* 6, 1277–1283. doi: 10.1038/nn1153

Baraban, S. C., Wenzel, H. J., Hochman, D. W., and Schwartzkroin, P. A. (2000). Characterization of heterotopic cell clusters in the hippocampus of rats exposed to methylazoxymethanol *in utero*. *Epilepsy Res.* 39, 87–102. doi: 10.1016/S0920-1211(99)00104-7

Barry, G., Piper, M., Lindwall, C., Moldrich, R., Mason, S., Little, E., et al. (2008). Specific glial populations regulate hippocampal morphogenesis. *J. Neurosci.* 28, 2328–12340. doi: 10.1523/JNEUROSCI.4000-08.2008

Battaglia, G., Bassanini, S., Granata, T., Setola, V., Giavazzi, A., and Pagliardini, S. (2003). The genesis of epileptogenic cerebral heterotopia: clues from experimental models. *Epileptic Disord.* 5, S51–S58.

Bayer, S. A. (1980). Development of the hippocampal region in the rat 1. Neurogenesis examined with 3H-thymidine autoradiography. *J. Comp. Neurol.* 190, 87–114. doi: 10.1002/cne.901900107

Bazelot, M., Simonnet, J., Dinocourt, C., Bruel-Jungerman, E., Miles, R., Fricker, D., et al. (2012). Cellular anatomy, physiology and epileptiform activity in the CA3 region of Dcx knockout mice: a neuronal lamination defect and its consequences. *Eur. J. Neurosci.* 35, 244–256. doi: 10.1111/j.1460-9568.2011.07962.x

Beffert, U., Weeber, E. J., Morfini, G., Ko, J., Brady, S. T., Tsai, L. H., et al. (2004). Reelin and cyclin-dependent kinase 5-dependent signals cooperate in regulating neuronal migration and synaptic transmission. *J. Neurosci.* 24, 1897–1906. doi: 10.1523/JNEUROSCI.4084-03.2004

Behrendt, R. P. (2010). Contribution of hippocampal region CA3 to consciousness and schizophrenic hallucinations. *Neurosci. Biobehav. Rev.* 34, 1121–1136. doi: 10.1016/j.neubiorev.2009.12.009

Bekirov, I. H., Nagy, V., Svoronos, A., Huntley, G. W., and Benson, D. L. (2008). Cadherin-8 and N-cadherin differentially regulate pre- and postsynaptic development of the hippocampal mossy fiber pathway. *Hippocampus* 18, 349–363. doi: 10.1002/hipo.20395

Belvindrah, R., Nissant, A., and Lledo. P. M. (2011). Abnormal neuronal migration changes the fate of developing neurons in the postnatal olfactory bulb. *J. Neurosci.* 31, 7551–7562. doi: 10.1523/JNEUROSCI.6716-10.2011

Bielas, S. L., Serneo, F. F., Chechlacz, M., Deerinck, T. J., Perkins, G. A., Allen, P. B., et al. (2007). Spinophilin facilitates dephosphorylation of doublecortin by PP1 to mediate microtubule bundling at the axonal wrist. *Cell* 129, 579–591. doi: 10.1016/j.cell.2007.03.023

Bielle, F., Griveau, A., Narboux-Nême, N., Vigneau, S., Sigrist, M., Arber, S., et al. (2005). Multiple origins of Cajal-Retzius cells at the borders of the developing pallium. *Nat. Neurosci.* 8, 1002–1012. doi: 10.1038/nn1511

Cattabeni, F., and Di Luca, M. (1997). Developmental models of brain dysfunctions induced by targeted cellular ablations with methylazoxymethanol. *Physiol. Rev.* 77, 199–215.

Chae, T., Kwon, Y. T., Bronson, R., Dikkes, P., Li, E., and Tsai, L. H. (1997). Mice lacking p35, a neuronal specific activator of Cdk5, display cortical lamination defects, seizures, and adult lethality. *Neuron* 18, 29–42. doi: 10.1016/S0896-6273(01)80044-1

Cheah, P.-S., Ramshaw, H. S., Thomas, P. Q., Toyo-oka, K., Xu, X., Martin, S., et al. (2012). Neurodevelopmental and neuropsychiatric behaviour defects arise from 14-3-3ζ deficiency. *Mol. Psychiatry* 17, 451–466. doi: 10.1038/mp.2011.158

Chen, H., Bagri, A., Zupicich, J. A., Zou, Y., Stoeckli, E., Pleasure, S. J., et al. (2000). Neuropilin-2 regulates the development of selective cranial and sensory nerves and hippocampal mossy fiber projections. *Neuron* 25, 43–56. doi: 10.1016/S0896-6273(00)80870-3

Chevassus-Au-Louis, N., Congar, P., Represa, A., Ben-Ari, Y., and Gaïarsa, J. L. (1998b). Neuronal migration disorders: heterotopic neocortical neurons in CA1 provide a bridge between the hippocampus and the neocortex. *Proc. Natl. Acad. Sci. U.S.A.* 95, 10263–10268. doi: 10.1073/pnas.95.17.10263

Chevassus-Au-Louis, N., Rafiki, A., Jorquera, I., Ben-Ari, Y., and Represa, A. (1998a). Neocortex in the hippocampus: an anatomical and functional study of CA1 heterotopias after prenatal treatment with methylazoxymethanol in rats. *J. Comp. Neurol.* 394, 520–536. doi: 10.1002/(SICI)1096-9861(19980518)394:4<520::AID-CNE9>3.0.CO;2-3

Chizhikov, V. V., Lindgren, A. G., Mishima, Y., Roberts, R. W., Aldinger, K. A., Miesegaes, G. R., et al. (2010). Lmx1a regulates fates and location of cells originating from the cerebellar rhombic lip and telencephalic cortical hem. *Proc. Natl. Acad. Sci. U.S.A.* 107, 10725–10730. doi: 10.1073/pnas.0910786107

Christian, K. M., Miracle, A. D., Wellman, C. L., and Nakazawa, K. (2011). Chronic stress-induced hippocampal dendritic retraction requires CA3 NMDA receptors. *Neuroscience* 174, 26–36. doi: 10.1016/j.neuroscience.2010.11.033

Ciceri, G., Dehorter, N., Sols, I., Huang, Z. J., Maravall, M., and Marín, O. (2013). Lineage-specific laminar organization of cortical GABAergic interneurons. *Nat. Neurosci.* 16, 1199–1210. doi: 10.1038/nn.3485

Cobos, I., Borello, U., and Rubenstein, J. L. (2007). Dlx transcription factors promote migration through repression of axon and dendrite growth. *Neuron* 54, 873–888. doi: 10.1016/j.neuron.2007.05.024

Cobos, I., Calcagnotto, M. E., Vilaythong, A. J., Thwin, M. T., Noebels, J. L., Baraban, S. C., et al. (2005). Mice lacking Dlx1 show subtype-specific loss of interneurons, reduced inhibition and epilepsy. *Nat. Neurosci.* 8, 1059–1068. doi: 10.1038/nn1499

Colacitti, C., Sancini, G., DeBiasi, S., Franceschetti, S., Caputi, A., Frassoni, C., et al. (1999). Prenatal methylazoxymethanol treatment in rats produces brain abnormalities with morphological similarities to human developmental brain dysgeneses. *J. Neuropathol. Exp. Neurol.* 58, 92–106. doi: 10.1097/00005072-199901000-00010

Corbo, J. C., Deuel, T. A., Long, J. M., LaPorte, P., Tsai, E., Wynshaw-Boris, A., et al. (2002). Doublecortin is required in mice for lamination of the hippocampus but not the neocortex. *J. Neurosci.* 22, 7548–7557.

Danglot, L., Triller, A., and Marty, S. (2006). The development of hippocampal interneurons in rodents. *Hippocampus* 16, 1032–1060. doi: 10.1002/hipo.20225

Datson, N. A., Meijer, L., Steenbergen, P. J., Morsink, M. C., van der Laan, S., Meijer, O. C., et al. (2004). Expression profiling in laser-microdissected hippocampal subregions in rat brain reveals large subregion-specific differences in expression. *Eur. J. Neurosci.* 20, 2541–2554. doi: 10.1111/j.1460-9568.2004.03738.x

Datson, N. A., Morsink, M. C., Steenbergen, P. J., Aubert, Y., Schlumbohm, C., Fuchs, E., et al. (2009). A molecular blueprint of gene expression in hippocampal subregions CA1, CA3, and DG is conserved in the brain of the common marmoset. *Hippocampus* 19, 739–752. doi: 10.1002/hipo.20555

Deguchi, Y., Donato, F., Galimberti, I., Cabuy, E., and Caroni, P. (2011). Temporally matched subpopulations of selectively interconnected principal neurons in the hippocampus. *Nat. Neurosci.* 14, 495–504. doi: 10.1038/nn.2768

Del Río, J. A., Heimrich, B., Borrell, V., Förster, E., Drakew, A., Alcántara, S., et al. (1997). A role for Cajal-Retzius cells and reelin in the development of hippocampal connections. *Nature* 385, 70–74. doi: 10.1038/385070a0

Denaxa, M., Chan, C. H., Schachner, M., Parnavelas, J. G., and Karagogeos, D. (2001). The adhesion molecule TAG-1 mediates the migration of cortical interneurons from the ganglionic eminence along the corticofugal fiber system. *Development* 128, 4635–4644.

Denaxa, M., Kyriakopoulou, K., Theodorakis, K., Trichas, G., Vidaki, M., Takeda, Y., et al. (2005). The adhesion molecule TAG-1 is required for proper migration of the superficial migratory stream in the medulla but not of cortical interneurons. *Dev. Biol.* 288, 87–99. doi: 10.1016/j.ydbio.2005.09.021

Deuel, T. A., Liu, J. S., Corbo, J. C., Yoo, S. Y., Rorke-Adams, L. B., and Walsh, C. A. (2006). Genetic interactions between doublecortin and doublecortin-like kinase in neuronal migration and axon outgrowth. *Neuron* 49, 41–53. doi: 10.1016/j.neuron.2005.10.038

Dong, H.-W., Swanson, L. W., Chen, L., Fanselow, M. S., and Toga, A. W. (2009). Genomic-anatomic evidence for distinct functional domains in hippocampal field CA1. *Proc. Natl. Acad. Sci. U.S.A.* 106, 11794–11799. doi: 10.1073/pnas.0812608106

Donmez, F. Y., Yildirim, M., Erkek, N., Demir Karacan, C., and Coskun, M. (2009). Hippocampal abnormalities associated with various congenital malformations. *Childs Nerv. Syst.* 25, 933–939. doi: 10.1007/s00381-009-0823-9

Eichenbaum, H., Sauvage, M., Fortin, N., Komorowski, R., and Lipton, P. (2012). Towards a functional organization of episodic memory in the medial temporal lobe. *Neurosci. Biobehav. Rev.* 36, 1597–1608. doi: 10.1016/j.neubiorev.2011.07.006

Enomoto, A., Asai, N., Namba, T., Wang, Y., Kato, T., Tanaka, M., et al. (2009). Roles of disrupted-in-schizophrenia 1-interacting protein girdin in postnatal development of the dentate gyrus. *Neuron* 63, 774–787. doi: 10.1016/j.neuron.2009.08.015

Falconer, D. S. (1951). Two new mutants, 'trembler' and 'reeler,' with neurological actions in the house mouse (Mus musculus L.). *J. Genet.* 50, 192–200. doi: 10.1007/BF02996215

Fallet-Bianco, C., Loeuillet, L., Poirier, K., Loget, P., Chapon, F., Pasquier, L., et al. (2008). Neuropathological phenotype of a distinct form of lissencephaly associated with mutations in TUBA1A. *Brain* 131(Pt 9), 2304–2320. doi: 10.1093/brain/awn155

Fishell, G., and Rudy, B. (2011). Mechanisms of inhibition within the telencephalon: "where the wild things are." *Annu. Rev. Neurosci.* 34, 535–567. doi: 10.1146/annurev-neuro-061010-113717

Fleck, M. W., Hirotsune, S., Gambello, M. J., Phillips-Tansey, E., Suares, G., Mervis, R. F., et al. (2000). Hippocampal abnormalities and enhanced excitability in a murine model of human lissencephaly. *J. Neurosci.* 20, 2439–2450.

Forster, E., Tielsch, A., Saum, B., Weiss, K. H., Johanssen, C., Graus-Porta, D., et al. (2002). Reelin, disabled 1, and beta 1 integrins are required for the formation of the radial glial scaffold in the hippocampus. *Proc. Natl. Acad. Sci. U.S.A.* 99, 13178–13183. doi: 10.1073/pnas.202035899

Förster, E., Zhao, S., and Frotscher, M. (2006). Laminating the hippocampus. *Nat. Rev. Neurosci.* 7, 259–267. doi: 10.1038/nrn1882

Francis, F., Koulakoff, A., Boucher, D., Chafey, P., Schaar, B., Vinet, M. C., et al. (1999). Doublecortin is a developmentally regulated, microtubule-associated protein expressed in migrating and differentiating neurons. *Neuron* 23, 247–256. doi: 10.1016/S0896-6273(00)80777-1

Franco, S. J., Martinez-Garay, I., Gil-Sanz, C., Harkins-Perry, S. R., and Muller, U. (2011). Reelin regulates cadherin function via Dab1/Rap1 to control neuronal migration and lamination in the neocortex. *Neuron* 69, 482–497. doi: 10.1016/j.neuron.2011.01.003

Freund, T. F., and Buzsaki, G. (1996). Interneurons of the hippocampus. *Hippocampus* 6, 347–470. doi: 10.1002/(SICI)1098-1063(1996)6:4<347::AID-HIPO1>3.0.CO;2-I

Friocourt, G., Chafey, P., Billuart, P., Koulakoff, A., Vinet, M. C., Schaar, B. T., et al. (2001). Doublecortin interacts with mu subunits of clathrin adaptor complexes in the developing nervous system. *Mol. Cell. Neurosci.* 18, 307–319. doi: 10.1006/mcne.2001.1022

Friocourt, G., Kappeler, C., Saillour, Y., Fauchereau, F., Rodriguez, M. S., Bahi, N., et al. (2005). Doublecortin interacts with the ubiquitin protease DFFRX, which associates with microtubules in neuronal processes. *Mol. Cell. Neurosci.* 28, 153–164. doi: 10.1016/j.mcn.2004.09.005

Furuse, T., Yamada, I., Kushida, T., Masuya, H., Miura, I., Kaneda, H., et al. (2012). Behavioral and neuromorphological characterization of a novel Tuba1 mutant mouse. *Behav. Brain Res.* 227, 167–174. doi: 10.1016/j.bbr.2011.11.002

Gebhardt, C., Del Turco, D., Drakew, A., Tielsch, A., Herz, J., Frotscher, M., et al. (2002). Abnormal positioning of granule cells alters afferent fiber distribution in the mouse fascia dentata: morphologic evidence from reeler, apolipoprotein E receptor 2-, and very low density lipoprotein receptor knockout mice. *J. Comp. Neurol.* 445, 278–292. doi: 10.1002/cne.10172

Germain, J., Bruel-Jungerman, E., Grannec, G., Denis, C., Lepousez, G., Giros, B., et al. (2013). Doublecortin knockout mice show normal hippocampal-dependent memory despite CA3 lamination defects. *PLoS ONE* 8:e74992. doi: 10.1371/journal.pone.0074992

Giger, R. J., Cloutier, J. F., Sahay, A., Prinjha, R. K., Levengood, D. V., Moore, S. E., et al. (2000). Neuropilin-2 is required *in vivo* for selective axon guidance responses to secreted semaphorins. *Neuron* 25, 29–41. doi: 10.1016/S0896-6273(00)80869-7

Gleeson, J. G., Lin, P. T., Flanagan, L. A., and Walsh. C. A. (1999). Doublecortin is a microtubule-associated protein and is expressed widely by migrating neurons. *Neuron* 23, 257–271. doi: 10.1016/S0896-6273(00)80778-3

Goryunov, D., He, C. Z., Lin, C. S., Leung, C. L., and Liem. R. K. (2010). Nervous-tissue-specific elimination of microtubule-actin crosslinking factor 1a results in multiple developmental defects in the mouse brain. *Mol. Cell. Neurosci.* 44, 1–14 doi: 10.1016/j.mcn.2010.01.010

Götz, M., and Huttner, W. B. (2005). The cell biology of neurogenesis. *Nat. Rev. Mol. Cell Biol.* 6, 777–788. doi: 10.1038/nrm1739

Graves, A. R., Moore, S. J., Bloss, E. B., Mensh, B. D., Kath, W. L., and Spruston, N. (2012). Hippocampal pyramidal neurons comprise two distinct cell types that are countermodulated by metabotropic receptors. *Neuron* 76, 776–789. doi: 10.1016/j.neuron.2012.09.036

Greene, J. G., Borges, K., and Dingledine, R. (2009). Quantitative transcriptional neuroanatomy of the rat hippocampus: evidence for wide-ranging, pathway-specific heterogeneity among three principal cell layers. *Hippocampus* 19, 253–264. doi: 10.1002/hipo.20502

Greenwood, J. S., Wang, Y., Estrada, R. C., Ackerman, L., Ohara, P. T., and Baraban, S. C. (2009). Seizures, enhanced excitation, and increased vesicle number in Lis1 mutant mice. *Ann. Neurol.* 66, 644–653. doi: 10.1002/ana.21775

Gupta, A., Tsai, L. H., and Wynshaw-Boris, A. (2002). Life is a journey: a genetic look at neocortical development. *Nat. Rev. Genet.* 3, 342–355. doi: 10.1038/nrg799

Harrington, E. P., Möddel, G., Najm, I. M., and Baraban, S. C. (2007). Altered glutamate receptor - transporter expression and spontaneous seizures in rats exposed to methylazoxymethanol *in utero*. *Epilepsia* 48, 158–168. doi: 10.1111/j.1528-1167.2006.00838.x

Hiesberger, T., Trommsdorff, M., Howell, B. W., Goffinet, A., Mumby, M. C., Cooper, J. A., et al. (1999). Direct binding of reelin to VLDL receptor and ApoE receptor 2 induces tyrosine phosphorylation of disabled-1 and modulates tau phosphorylation. *Neuron* 24, 481–489. doi: 10.1016/S0896-6273(00)80861-2

Hirotsune, S., Fleck, M. W., Gambello, M. J., Bix, G. J., Chen, A., Clark, G. D., et al. (1998). Graded reduction of Pafah1b1 (Lis1) activity results in neuronal migration defects and early embryonic lethality. *Nat. Genet.* 19, 333–339. doi: 10.1038/1221

Hoch, R. V., Rubenstein, J. L. R., and Pleasure, S. (2009). Genes and signaling events that establish regional patterning of the mammalian forebrain. *Semin. Cell Dev. Biol.* 20, 378–386. doi: 10.1016/j.semcdb.2009.02.005

Homma, N., Takei, Y., Tanaka, Y., Nakata, T., Terada, S., Kikkawa, M., et al. (2003). Kinesin superfamily protein 2A (KIF2A) functions in suppression of collateral branch extension. *Cell* 114, 229–239. doi: 10.1016/S0092-8674(03)00522-1

Honda, T., Sakisaka, T., Yamada, T., Kumazawa, N., Hoshino, T., Kajita, M., et al. (2006). Involvement of nectins in the formation of puncta adherentia junctions and the mossy fiber trajectory in the mouse hippocampus. *Mol. Cell. Neurosci.* 31, 315–325. doi: 10.1016/j.mcn.2005.10.002

Hunt, R. F., Dinday, M. T., Hindle-Katel, W., and Baraban, S. C. (2012). LIS1 deficiency promotes dysfunctional synaptic integration of granule cells generated in the developing and adult dentate gyrus. *J. Neurosci.* 32, 12862–12875. doi: 10.1523/JNEUROSCI.1286-12.2012

Ishizuka, K., Kamiya, A., Oh, E. C., Kanki, H., Seshadri, S., Robinson, J. F., et al. (2011). DISC1-dependent switch from progenitor proliferation to migration in the developing cortex. *Nature* 473, 92–96. doi: 10.1038/nature09859

Jones, D. L., and Baraban, S. C. (2007). Characterization of inhibitory circuits in the malformed hippocampus of Lis1 mutant mice. *J. Neurophysiol.* 98, 2737–2746. doi: 10.1152/jn.00938.2007

Jones, D. L., and Baraban, S. C. (2009). Inhibitory inputs to hippocampal interneurons are reorganized in Lis1 mutant mice. *J. Neurophysiol.* 102, 648–658. doi: 10.1152/jn.00392.2009

Kappeler, C., Dhenain, M., Phan Dinh Tuy, F., Saillour, Y., Marty, S., Fallet-Bianco, C., et al. (2007). Magnetic resonance imaging and histological studies of corpus callosal and hippocampal abnormalities linked to doublecortin deficiency. *J. Comp. Neurol.* 500, 239–254. doi: 10.1002/cne.21170

Kappeler, C., Saillour, Y., Baudoin, J. P., Tuy, F. P., Alvarez, C., Houbron, C., et al. (2006). Branching and nucleokinesis defects in migrating interneurons derived from doublecortin knockout mice. *Hum. Mol. Genet.* 15, 1387–1400. doi: 10.1093/hmg/ddl062

Kawauchi, T., Chihama, K., Nabeshima, Y., and Hoshino, M. (2006). Cdk5 phosphorylates and stabilizes p27kip1 contributing to actin organization and cortical neuronal migration. *Nat. Cell Biol.* 8, 17–26. doi: 10.1038/ncb1338

Keays, D. A., Tian, G., Poirier, K., Huang, G. J., Siebold, C., Cleak, J., et al. (2007). Mutations in alpha-tubulin cause abnormal neuronal migration in mice and lissencephaly in humans. *Cell* 128, 45–57. doi: 10.1016/j.cell.2006.12.017

Kerjan, G., Koizumi, H., Han, E. B., Dubé, C. M., Djakovic, S. N., Patrick, G. N., et al. (2009). Mice lacking doublecortin and doublecortin-like kinase 2 display altered hippocampal neuronal maturation and spontaneous seizures. *Proc. Natl. Acad. Sci. U.S.A.* 106, 6766–6771. doi: 10.1073/pnas.0812687106

Khalaf-Nazzal, R., Bruel-Jungerman, E., Rio, J.-P., Bureau, J., Irinopoulou, T., Sumia, I., et al. (2013). Organelle and cellular abnormalities associated with hippocampal heterotopia in neonatal doublecortin knockout mice. *PLoS ONE* 8:e72622. doi: 10.1371/journal.pone.0072622

Khalaf-Nazzal, R., and Francis, F. (2013). Hippocampal development - Old and new findings. *Neuroscience* 248C, 225–242. doi: 10.1016/j.neuroscience.2013.05.061

Kholmanskikh, S. S., Dobrin, J. S., Wynshaw-Boris, A., Letourneau, P. C., and Ross, M. E. (2003). Disregulated RhoGTPases and actin cytoskeleton contribute to the migration defect in Lis1-deficient neurons. *J. Neurosci.* 23, 8673–8681.

Kholmanskikh, S. S., Koeller, H. B., Wynshaw-Boris, A., Gomez, T., Letourneau, P. C., and Ross, M. E. (2006). Calcium-dependent interaction of Lis1 with IQGAP1 and Cdc42 promotes neuronal motility. *Nat. Neurosci.* 9, 50–57. doi: 10.1038/nn1619

Kitazawa, A., Kubo, K., Hayashi, K., Matsunaga, Y., Ishii, K., and Nakajima, K. (2014). Hippocampal pyramidal neurons switch from a multipolar migration mode to a novel "Climbing" migration mode during development. *J. Neurosci.* 34, 1115–1126. doi: 10.1523/JNEUROSCI.2254-13.2014

Kizhatil, K., Wu, Y. X., Sen, A., and Bennett, V. (2002). A new activity of doublecortin in recognition of the phospho-FIGQY tyrosine in the cytoplasmic domain of neurofascin. *J. Neurosci.* 22, 7948–7958.

Knöll, B., Kretz, O., Fiedler, C., Alberti, S., Schütz, G., Frotscher, M., et al. (2006). Serum response factor controls neuronal circuit assembly in the hippocampus. *Nat. Neurosci.* 9, 195–204. doi: 10.1038/nn1627

Koizumi, H., Higginbotham, H., Poon, T., Tanaka, T., Brinkman, B. C., and Gleeson, J. G. (2006a). Doublecortin maintains bipolar shape and nuclear translocation during migration in the adult forebrain. *Nat. Neurosci.* 9, 779–786. doi: 10.1038/nn1704

Koizumi, H., Tanaka, T., and Gleeson, J. G. (2006b). Doublecortin-like kinase functions with doublecortin to mediate fiber tract decussation and neuronal migration. *Neuron* 49, 55–66. doi: 10.1016/j.neuron.2005.10.040

Kriegstein, A., Noctor, S., and Martínez-Cerdeño, V. (2006). Patterns of neural stem and progenitor cell division may underlie evolutionary cortical expansion. *Nat. Rev. Neurosci.* 7, 883–890. doi: 10.1038/nrn2008

Kuchukhidze, G., Koppelstaetter, F., Unterberger, I., Dobesberger, J., Walser, G., Zamarian, L., et al. (2010). Hippocampal abnormalities in malformations of cortical development: MRI study. *Neurology* 74, 1575–1582. doi: 10.1212/WNL.0b013e3181df09b6

Kvajo, M., McKellar, H., Drew, L. J., Lepagnol-Bestel, A. M., Xiao, L., Levy, R. J., et al. (2011). Altered axonal targeting and short-term plasticity in the hippocampus of Disc1 mutant mice. *Proc. Natl. Acad. Sci. U.S.A.* 108, E1349–E1358. doi: 10.1073/pnas.1114113108

Lambert de Rouvroit, C., and Goffinet, A. M. (1998). The reeler mouse as a model of brain development. *Adv. Anat. Embryol. Cell Biol.* 150, 1–106. doi: 10.1007/978-3-642-72257-8_1

Lanore, F., Labrousse, V. F., Szabo, Z., Normand, E., Blanchet, C., and Mulle, C. (2012). Deficits in morphofunctional maturation of hippocampal mossy fiber synapses in a mouse model of intellectual disability. *J. Neurosci.* 32, 17882–17893. doi: 10.1523/JNEUROSCI.2049-12.2012

Liddle, P. F., Lane, C. J., and Ngan, E. T. (2000). Immediate effects of risperidone on cortico-striato-thalamic loops and the hippocampus. *Br. J. Psychiatry* 177, 402–407. doi: 10.1192/bjp.177.5.402

Lodato, S., Rouaux, C., Quast, K. B., Jantrachotechatchawan, C., Studer, M., Hensch, T. K., et al. (2011). Excitatory projection neuron subtypes control the distribution of local inhibitory interneurons in the cerebral cortex. *Neuron* 69, 763–779. doi: 10.1016/j.neuron.2011.01.015

Lodge, D. J., and Grace, A. A. (2007). Aberrant hippocampal activity underlies the dopamine dysregulation in an animal model of schizophrenia. *J. Neurosci.* 27, 11424–11430. doi: 10.1523/JNEUROSCI.2847-07.2007

Lu, D., He, L., Xiang, W., Ai, W. M., Cao, Y., Wang, X. S., et al. (2013). Somal and dendritic development of human CA3 pyramidal neurons from midgestation to middle childhood: a quantitative Golgi study. *Anat. Rec. (Hoboken)*. 296, 123–132. doi: 10.1002/ar.22616

Lu, M., Grove, E. A., and Miller, R. J. (2002). Abnormal development of the hippocampal dentate gyrus in mice lacking the CXCR4 chemokine receptor. *Proc. Natl. Acad. Sci. U.S.A.* 99, 7090–7095. doi: 10.1073/pnas.092013799

Manent, J. B., Demarque, M., Jorquera, I., Pellegrino, C., Ben-Ari, Y., Aniksztejn, L., et al. (2005). A noncanonical release of GABA and glutamate modulates neuronal migration. *J. Neurosci.* 25, 4755–4765. doi: 10.1523/JNEUROSCI.0553-05.2005

Manent, J.-B., Jorquera, I., Ben-Ari, Y., Aniksztejn, L., and Represa, A. (2006). Glutamate acting on AMPA but not NMDA receptors modulates the migration of hippocampal interneurons. *J. Neurosci.* 26, 5901–5909. doi: 10.1523/JNEUROSCI.1033-06.2006

Marin, O., Yaron, A., Bagri, A., Tessier-Lavigne, M., and Rubenstein, J. L. (2001). Sorting of striatal and cortical interneurons regulated by semaphorin-neuropilin interactions. *Science* 293, 872–875. doi: 10.1126/science.1061891

Matyas, F., Freund, T. F., and Gulyas, A. I. (2004). Immunocytochemically defined interneuron populations in the hippocampus of mouse strains used in transgenic technology. *Hippocampus* 14, 460–481. doi: 10.1002/hipo.10191

McManus, M. F., Nasrallah, I. M., Pancoast, M. M., Wynshaw-Boris, A., and Golden, J. A. (2004). Lis1 is necessary for normal non-radial migration of inhibitory interneurons. *Am. J. Pathol.* 165, 775–784. doi: 10.1016/S0002-9440(10)63340-8

Meyer, K. D., and Morris, J. A. (2009). Disc1 regulates granule cell migration in the developing hippocampus. *Hum. Mol. Genet.* 18, 3286–3297. doi: 10.1093/hmg/ddp266

Milesi, G., Garbelli, R., Zucca, I., Aronica, E., Spreafico, R., and Frassoni, C. (2014). Assessment of human hippocampal developmental neuroanatomy by means of *ex-vivo* 7T magnetic resonance imaging. *Int. J. Dev. Neurosci.* 34, 33–41. doi: 10.1016/j.ijdevneu.2014.01.002

Mizuseki, K., Royer, S., Diba, K., and Buzsáki, G. (2012). Activity dynamics and behavioral correlates of CA3 and CA1 hippocampal pyramidal neurons. *Hippocampus* 22, 1659–1680. doi: 10.1002/hipo.22002

Montag-Sallaz, M., Schachner, M., and Montag, D. (2002). Misguided axonal projections, neural cell adhesion molecule 180 mRNA upregulation, and altered behavior in mice deficient for the close homolog of L1. *Mol. Cell. Biol.* 22, 7967–7981. doi: 10.1128/MCB.22.22.7967-7981.2002

Montenegro, M. A., Kinay, D., Cendes, F., Bernasconi, A., Bernasconi, N., Coan, A. C., et al. (2006). Patterns of hippocampal abnormalities in malformations of cortical development. *J. Neurol. Neurosurg. Psychiatry* 77, 367–371. doi: 10.1136/jnnp.2005.070417

Morest, D. K. (1970). A study of neurogenesis in the forebrain of opossum pouch young. *Z. Anat. Entwicklungsgesch.* 130, 265–305. doi: 10.1007/BF00520999

Nadarajah, B., and Parnavelas, J. G. (2002). Modes of neuronal migration in the developing cerebral cortex. *Nat. Rev. Neurosci.* 3, 423–432. doi: 10.1038/nrn845

Nakahira, E., and Yuasa, S. (2005). Neuronal generation, migration, and differentiation in the mouse hippocampal primoridium as revealed by enhanced green fluorescent protein gene transfer by means of *in utero* electroporation. *J. Comp. Neurol.* 483, 329–340. doi: 10.1002/cne.20441

Nakashiba, T., Young, J. Z., McHugh, T. J., Buhl, D. L., and Tonegawa, S. (2008). Transgenic inhibition of synaptic transmission reveals role of CA3 output in hippocampal learning. *Science* 319, 1260–1264. doi: 10.1126/science.1151120

Nakazawa, K., Sun, L. D., Quirk, M. C., Rondi-Reig, L., Wilson, M. A., and Tonegawa, S. (2003). Hippocampal CA3 NMDA receptors are crucial for memory acquisition of one-time experience. *Neuron* 38, 305–315. doi: 10.1016/S0896-6273(03)00165-X

Navarro-Quiroga, I., Chittajallu, R., Gallo, V., and Haydar, T. F. (2007). Long-term, selective gene expression in developing and adult hippocampal pyramidal neurons using focal *in utero* electroporation. *J. Neurosci.* 27, 5007–5011. doi: 10.1523/JNEUROSCI.0867-07.2007

Nguyen, L., Besson, A., Heng, J. I., Schuurmans, C., Teboul, L., Parras, C., et al. (2006). p27kip1 independently promotes neuronal differentiation and migration in the cerebral cortex. *Genes Dev.* 20, 1511–1524. doi: 10.1101/gad.377106

Nielsen, J. V., Thomassen, M., Møllgård, K., Noraberg, J., and Jensen, N. A. (2013). Zbtb20 defines a hippocampal neuronal identity through direct repression of genes that control projection neuron development in the isocortex. *Cereb. Cortex*. doi: 10.1093/cercor/bhs400. [Epub ahead of print].

Niethammer, M., Smith, D. S., Ayala, R., Peng, J., Ko, J., Lee, M. S., et al. (2000). NUDEL is a novel Cdk5 substrate that associates with LIS1 and cytoplasmic dynein. *Neuron* 28, 697–711. doi: 10.1016/S0896-6273(00)00147-1

Niu, S., Renfro, A., Quattrocchi, C. C., Sheldon, M., and D'Arcangelo, G. (2004). Reelin promotes hippocampal dendrite development through the VLDLR/ApoER2-Dab1 pathway. *Neuron* 41, 71–84. doi: 10.1016/S0896-6273(03)00819-5

Nosten-Bertrand, M., Kappeler, C., Dinocourt, C., Denis, C., Germain, J., Phan Dinh Tuy, F., et al. (2008). Epilepsy in Dcx knockout mice associated with discrete lamination defects and enhanced excitability in the hippocampus. *PLoS ONE* 3:e2473. doi: 10.1371/journal.pone.0002473

Nowakowski, R. S., and Davis, T. L. (1985). Dendritic arbors and dendritic excrescences of abnormally positioned neurons in area CA3c of mice carrying the mutation "hippocampal lamination defect." *J. Comp. Neurol.* 239, 267–275. doi: 10.1002/cne.902390303

Nowakowski, R. S., and Rakic, P. (1979). The mode of migration of neurons to the hippocampus: a golgi and electron microscopic analysis in foetal rhesus monkey. *J. Neurocytol.* 8, 697–718. doi: 10.1007/BF01206671

Ohshima, T., Hirasawa, M., Tabata, H., Mutoh, T., Adachi, T., Suzuki, H., et al. (2007). Cdk5 is required for multipolar-to-bipolar transition during radial neuronal migration and proper dendrite development of pyramidal neurons in the cerebral cortex. *Development* 134, 2273–2282. doi: 10.1242/dev.02854

Ohshima, T., Ogawa, M., Veeranna, Hirasawa, M., Longenecker, G., Ishiguro, K., et al. (2001). Synergistic contributions of cyclin-dependant kinase 5/p35 and Reelin/Dab1 to the positioning of cortical neurons in the developing mouse brain. *Proc. Natl. Acad. Sci. U.S.A.* 98, 2764–2769. doi: 10.1073/pnas.051628498

Ohshima, T., Ward, J. M., Huh, C. G., Longenecker, G., Veeranna, Pant, H. C., et al. (1996). Targeted disruption of the cyclin-dependent kinase 5 gene results in abnormal corticogenesis, neuronal pathology and perinatal death. *Proc. Natl. Acad. Sci. U.S.A.* 93, 11173–11178. doi: 10.1073/pnas.93.20.11173

Olypher, A. V., Klement, D., and Fenton, A. A. (2006). Cognitive disorganization in hippocampus: a physiological model of the disorganization in psychosis. *J. Neurosci.* 26, 158–168. doi: 10.1523/JNEUROSCI.2064-05.2006

Paredes, M., Pleasure, S. J., and Baraban, S. C. (2006). Embryonic and early postnatal abnormalities contributing to the development of hippocampal malformations in a rodent model of dysplasia. *J. Comp. Neurol.* 495, 133–148. doi: 10.1002/cne.20871

Paylor, R., Hirotsune, S., Gambello, M. J., Yuva-Paylor, L., Crawley, J. N., and Wynshaw-Boris, A. (1999). Impaired learning and motor behavior in heterozygous Pafah1b1 (Lis1) mutant mice. *Learn. Mem.* 6, 521–537. doi: 10.1101/lm.6.5.521

Paz-Villagrán, V., Save, E., and Poucet, B. (2004). Independent coding of connected environments by place cells. *Eur. J. Neurosci.* 20, 1379–1390. doi: 10.1111/j.1460-9568.2004.03570.x

Petrone, A., Battaglia, F., Wang, C., Dusa, A., Su, J., Zagzag, D., et al. (2003). Receptor protein tyrosine phosphatase alpha is essential for hippocampal neuronal migration and long-term potentiation. *EMBO J.* 22, 4121–4131. doi: 10.1093/emboj/cdg399

Pierani, A., and Wassef, M. (2009). Cerebral cortex development: from progenitors patterning to neocortical size during evolution. *Dev. Growth Differ.* 51, 325–342. doi: 10.1111/j.1440-169X.2009.01095.x

Pleasure, S. J., Anderson, S., Hevner, R., Bagri, A., Marin, O., Lowenstein, D. H., et al. (2000). Cell migration from the ganglionic eminences is required for the development of hippocampal GABAergic interneurons. *Neuron* 28, 727–740. doi: 10.1016/S0896-6273(00)00149-5

Poirier, K., Lebrun, N., Broix, L., Tian, G., Saillour, Y., Boscheron, C., et al. (2013). Mutations in TUBG1, DYNC1H1, KIF5C and KIF2A cause malformations of cortical development and microcephaly. *Nat. Genet.* 45, 639–647. doi: 10.1038/ng.2613

Polleux, F., Whitford, K. L., Dijkhuizen, P. A., Vitalis, T., and Ghosh, A. (2002). Control of cortical interneuron migration by neurotrophins and PI3-kinase signaling. *Development* 129, 3147–3160.

Poluch, S., and Juliano, S. L. (2007). A normal radial glial scaffold is necessary for migration of interneurons during neocortical development. *Glia* 55, 822–830. doi: 10.1002/glia.20488

Porter, B. E., Judkins, A. R., Clancy, R. R., Duhaime, A., Dlugos, D. J., and Golden, J. A. (2003). Dysplasia: a common finding in intractable pediatric temporal lobe epilepsy. *Neurology* 61, 365–368. doi: 10.1212/01.WNL.0000076487.28227.6E

Pulsinelli, W. A., and Brierley, J. B. (1979). A new model of bilateral hemispheric ischemia in the unanesthetized rat. *Stroke* 10, 267–272. doi: 10.1161/01.STR.10.3.267

Rice, D. S., Sheldon, M., D'Arcangelo, G., Nakajima, K., Goldowitz, D., and Curran, T. (1998). Disabled-1 acts downstream of reelin in a signaling pathway that controls laminar organization in the mammalian brain. *Development* 125, 3719–3729.

Salinger, W. L., Ladrow, P., and Wheeler, C. (2003). Behavioral phenotype of the reeler mutant mouse: effects of RELN gene dosage and social isolation. *Behav. Neurosci.* 117, 1257–1275. doi: 10.1037/0735-7044.117.6.1257

Sapir, T., Elbaum, M., and Reiner, O. (1997). Reduction of microtubule catastrophe events by LIS1, platelet-activating factor acetylhydrolase subunit. *EMBO J.* 16, 6977–6984. doi: 10.1093/emboj/16.23.6977

Sasaki, S., Shionoya, A., Ishida, M., Gambello, M. J., Yingling, J., Wynshaw-Boris, A., et al. (2000). A LIS1/NUDEL/cytoplasmic dynein heavy chain complex in the developing and adult nervous system. *Neuron* 28, 681–696. doi: 10.1016/S0896-6273(00)00146-X

Sato, N., Hatakeyama, S., Shimizu, N., Hikima, A., Aoki, J., and Endo, K. (2001). MR evaluation of the hippocampus in patients with congenital malformations of the brain. *AJNR Am. J. Neuroradiol.* 22, 389–393.

Sebe, J. Y., Bershteyn, M., Hirotsune, S., Wynshaw-Boris, A., and Baraban, S. C. (2013). ALLN rescues an *in vitro* excitatory synaptic transmission deficit in Lis1 mutant mice. *J. Neurophysiol.* 109, 429–436. doi: 10.1152/jn.00431.2012

Seki, T., and Rutishauser, U. (1998). Removal of polysialic acid-neural cell adhesion molecule induces aberrant mossy fiber innervation and ectopic synaptogenesis in the hippocampus. *J. Neurosci.* 18, 3757–3766.

Sekiguchi, M., Nowakowski, R. S., Nagato, Y., Tanaka, O., Guo, H., Madoka, M., et al. (1995). Morphological abnormalities in the hippocampus of the weaver mutant mouse. *Brain Res.* 696, 262–267. doi: 10.1016/0006-8993(95)00974-U

Seri, B., García-Verdugo, J. M., McEwen, B. S., and Alvarez-Buylla, A. (2001). Astrocytes give rise to new neurons in the adult mammalian hippocampus. *J. Neurosci.* 21, 7153–7160.

Shinohara, R., Thumkeo, D., Kamijo, H., Kaneko, N., Sawamoto, K., Watanabe, K., et al. (2012). A role for mDia, a Rho-regulated actin nucleator, in tangential migration of interneuron precursors. *Nat. Neurosci.* 15, 373–380, S1–S2. doi: 10.1038/nn.3020

Shu, T., Ayala, R., Nguyen, M. D., Xie, Z., Gleeson, J. G., and Tsai, L. H. (2004). Ndel1 operates in a common pathway with LIS1 and cytoplasmic dynein to regulate cortical neuronal positioning. *Neuron* 44, 263–277. doi: 10.1016/j.neuron.2004.09.030

Slomianka, L., Amrein, I., Knuesel, I., Sørensen, J. C., and Wolfer, D. P. (2011). Hippocampal pyramidal cells: the reemergence of cortical lamination. *Brain Struct. Funct.* 216, 301–317. doi: 10.1007/s00429-011-0322-0

Smith, D. S., Niethammer, M., Ayala, R., Zhou, Y., Gambello, M. J., Wynshaw-Boris, A., et al. (2000). Regulation of cytoplasmic dynein behaviour and microtubule organization by mammalian Lis1. *Nat. Cell Biol.* 2, 767–775. doi: 10.1038/35041000

Soriano, E., Cobas, A., and Fairén, A. (1986). Asynchronism in the neurogenesis of GABAergic and non-GABAergic neurons in the mouse hippocampus. *Brain Res.* 395, 88–92. doi: 10.1016/0165-3806(86)90134-3

Soriano, E., Cobas, A., and Fairén, A. (1989). Neurogenesis of glutamic acid decarboxylase immunoreactive cells in the hippocampus of the mouse. I: regio superior and regio inferior. *J. Comp. Neurol.* 281, 586–602. doi: 10.1002/cne.902810408

Stanfield, B. B., and Cowan, W. M. (1979a). The development of the hippocampus and dentate gyrus in normal and reeler mice. *J. Comp. Neurol.* 185, 423–459. doi: 10.1002/cne.901850303

Stanfield, B. B., and Cowan, W. M. (1979b). The morphology of the hippocampus and dentate gyrus in normal and reeler mice. *J. Comp. Neurol.* 185, 393–422. doi: 10.1002/cne.901850302

Stegeman, S., Jolly, L. A., Premarathne, S., Gecz, J., Richards, L. J., Mackay-Sim, A., et al. (2013). Loss of Usp9x disrupts cortical architecture, hippocampal development and TGFβ-mediated axonogenesis. *PLoS ONE* 8:e68287. doi: 10.1371/journal.pone.0068287

Subramanian, L., Remedios, R., Shetty, A., and Tole, S. (2009). Signals from the edges: the cortical hem and antihem in telencephalic development. *Semin. Cell Dev. Biol.* 20, 712–718. doi: 10.1016/j.semcdb.2009.04.001

Subramanian, L., and Tole, S. (2009). Mechanisms underlying the specification, positional regulation, and function of the cortical hem. *Cereb. Cortex* 19 (Suppl. 1), i90–i95. doi: 10.1093/cercor/bhp031

Suto, F., Tsuboi, M., Kamiya, H., Mizuno, H., Kiyama, Y., Komai, S., et al. (2007). Interactions between plexin-A2, plexin-A4, and semaphorin 6A control lamina-restricted projection of hippocampal mossy fibers. *Neuron* 53, 535–547. doi: 10.1016/j.neuron.2007.01.028

Tanaka, T., Serneo, F. F., Higgins, C., Gambello, M. J., Wynshaw-Boris, A., and Gleeson, J. G. (2004a). Lis1 and doublecortin function with dynein to mediate coupling of the nucleus to the centrosome in neuronal migration. *J. Cell Biol.* 165, 709–721. doi: 10.1083/jcb.200309025

Tanaka, T., Serneo, F. F., Tseng, H. C., Kulkarni, A. B., Tsai, L. H., and Gleeson, J. G. (2004b). Cdk5 phosphorylation of doublecortin ser297 regulates its effect on neuronal migration. *Neuron* 41, 215–227. doi: 10.1016/S0896-6273(03)00852-3

Tawarayama, H., Yoshida, Y., Suto, F., Mitchell, K. J., and Fujisawa, H. (2010). Roles of semaphorin-6B and plexin-A2 in lamina-restricted projection of hippocampal mossy fibers. *J. Neurosci.* 30, 7049–7060. doi: 10.1523/JNEUROSCI.0073-10.2010

Thompson, C. L., Pathak, S. D., Jeromin, A., Ng, L. L., MacPherson, C. R., Mortrud, M. T., et al. (2008). Genomic anatomy of the hippocampus. *Neuron* 60, 1010–1021. doi: 10.1016/j.neuron.2008.12.008

Tole, S., Christian, C., and Grove, E. A. (1997). Early specification and autonomous development of cortical fields in the mouse hippocampus. *Development* 124, 4959–4970.

Tole, S., and Grove, E. A. (2001). Detailed field pattern is intrinsic to the embryonic mouse hippocampus early in neurogenesis. *J. Neurosci.* 21, 1580–1589.

Tricoire, L., Pelkey, K. A., Erkkila, B. E., Jeffries, B. W., Yuan, X., and McBain, C. J. (2011). A blueprint for the spatiotemporal origins of mouse hippocampal interneuron diversity. *J. Neurosci.* 31, 10948–10970. doi: 10.1523/JNEUROSCI.0323-11.2011

Trommsdorff, M., Gotthardt, M., Hiesberger, T., Shelton, J., Stockinger, W., Nimpf, J., et al. (1999). Reeler/Disabled-like disruption of neuronal migration in knockout mice lacking the VLDL receptor and ApoE receptor 2. *Cell* 97, 689–701. doi: 10.1016/S0092-8674(00)80782-5

Tueting, P., Costa, E., Dwivedi, Y., Guidotti, A., Impagnatiello, F., Manev, R., et al. (1999). The phenotypic characteristics of heterozygous reeler mouse. *Neuroreport* 10, 1329–1334. doi: 10.1097/00001756-199904260-00032

Tueting, P., Doueiri, M. S., Guidotti, A., Davis, J. M., and Costa, E. (2006). Reelin down-regulation in mice and psychosis endophenotypes. *Neurosci. Biobehav. Rev.* 30, 1065–1077. doi: 10.1016/j.neubiorev.2006.04.001

Valdés-Sánchez, L., Escámez, T., Echevarria, D., Ballesta, J. J., Tabarés-Seisdedos, R., Reiner, O., et al. (2007). Postnatal alterations of the inhibitory synaptic responses recorded from cortical pyramidal neurons in the Lis1/sLis1 mutant mouse. *Mol. Cell. Neurosci.* 35, 220–229. doi: 10.1016/j.mcn.2007.02.017

Wang, Y., and Baraban, S. C. (2007). Granule cell dispersion and aberrant neurogenesis in the adult hippocampus of an LIS1 mutant mouse. *Dev. Neurosci.* 29, 91–98. doi: 10.1159/000096214

Wang, Y., and Baraban, S. C. (2008). Aberrant dentate gyrus cytoarchitecture and fiber lamination in Lis1 mutant mice. *Hippocampus* 18, 758–765. doi: 10.1002/hipo.20434

Watanabe, Y., Gould, E., and McEwen, B. S. (1992). Stress induces atrophy of apical dendrites of hippocampal CA3 pyramidal neurons. *Brain Res.* 588, 341–345. doi: 10.1016/0006-8993(92)91597-8

Weiss, K. H., Johanssen, C., Tielsch, A., Herz, J., Deller, T., Frotscher, M., et al. (2003). Malformation of the radial glial scaffold in the dentate gyrus of reeler mice, scrambler mice, and ApoER2/VLDLR-deficient mice. *J. Comp. Neurol.* 460, 56–65. doi: 10.1002/cne.10644

Wenzel, H. J., Robbins, C. A., Tsai, L. H., and Schwartzkroin, P. A. (2001). Abnormal morphological and functional organization of the hippocampus in a p35 mutant model of cortical dysplasia associated with spontaneous seizures. *J. Neurosci.* 21, 983–998.

Williams, M. E., Wilke, S. A., Daggett, A., Davis, E., Otto, S., Ravi, D., et al. (2011). Cadherin-9 regulates synapse-specific differentiation in the developing hippocampus. *Neuron* 71, 640–655. doi: 10.1016/j.neuron.2011.06.019

Woolley, C. S., Gould, E., and McEwen, B. S. (1990). Exposure to excess glucocorticoids alters dendritic morphology of adult hippocampal pyramidal neurons. *Brain Res.* 531, 225–231. doi: 10.1016/0006-8993(90)90778-A

Xie, Z., Sanada, K., Samuels, B. A., Shih, H., and Tsai, L. H. (2003). Serine 732 phosphorylation of FAK by Cdk5 is important for microtubule organization, nuclear movement, and neuronal migration. *Cell* 114, 469–482. doi: 10.1016/S0092-8674(03)00605-6

Xu, N. J., and Henkemeyer, M. (2009). Ephrin-B3 reverse signaling through Grb4 and cytoskeletal regulators mediates axon pruning. *Nat. Neurosci.* 12, 268–276. doi: 10.1038/nn.2254

Yamada, M., Yoshida, Y., Mori, D., Takitoh, T., Kengaku, M., Umeshima, H., et al. (2009). Inhibition of calpain increases LIS1 expression and partially rescues *in vivo* phenotypes in a mouse model of lissencephaly. *Nat. Med.* 15, 1202–1207. doi: 10.1038/nm.2023

Yap, C. C., Vakulenko, M., Kruczek, K., Motamedi, B., Digilio, L., Liu, J. S., et al. (2012). Doublecortin (DCX) mediates endocytosis of neurofascin independently of microtubule binding. *J. Neurosci.* 32, 7439–7453. doi: 10.1523/JNEUROSCI.5318-11.2012

Ye, H., Zhao, T., Tan, Y. L., Liu, J., Pallen, C. J., and Xiao, Z. C. (2011). Receptor-like protein-tyrosine phosphatase α enhances cell surface expression of neural adhesion molecule NB-3. *J. Biol. Chem.* 286, 26071–26080. doi: 10.1074/jbc.M110.214080

Zhang, G., Assadi, A. H., McNeil, R. S., Beffert, U., Wynshaw-Boris, A., Herz, J., et al. (2007). The Pafah1b complex interacts with the reelin receptor VLDLR. *PLoS ONE* 2:e252. doi: 10.1371/journal.pone.0000252

Zhao, S., Chai, X., Förster, E., and Frotscher, M. (2004). Reelin is a positional signal for the lamination of dentate granule cells. *Development* 131, 5117–5125. doi: 10.1242/dev.01387

Zola-Morgan, S., Squire, L. R., and Amaral, D. G. (1986). Human amnesia and the medial temporal region: enduring memory impairment following a bilateral lesion limited to field CA1 of the hippocampus. *J. Neurosci.* 6, 2950–2967.

Conflict of Interest Statement: The authors declare that the research was conducted in the absence of any commercial or financial relationships that could be construed as a potential conflict of interest.

Received: 22 November 2013; accepted: 13 February 2014; published online: 04 March 2014.

*Citation: Belvindrah R, Nosten-Bertrand M and Francis F (2014) Neuronal migration and its disorders affecting the CA3 region. Front. Cell. Neurosci. **8**:63. doi: 10.3389/fncel.2014.00063*

This article was submitted to the journal Frontiers in Cellular Neuroscience.

frontiers in
CELLULAR NEUROSCIENCE

REVIEW ARTICLE
published: 04 February 2014
doi: 10.3389/fncel.2014.00028

Information processing and synaptic plasticity at hippocampal mossy fiber terminals

Alesya Evstratova and Katalin Tóth*

Faculty of Medicine, Department of Psychiatry and Neuroscience, Quebec Mental Health Institute, Université Laval, Quebec City, QC, Canada

Edited by:
Richard Miles, Institut pour le Cerveau et la Moëlle Epinière, France

Reviewed by:
Enrico Cherubini, International School for Advanced Studies, Italy
Oscar Herreras, Consejo Superior de Investigaciones Científicas (CSIC), Spain

***Correspondence:**
Katalin Tóth, Faculty of Medicine, Department of Psychiatry and Neuroscience, Quebec Mental Health Institute, Université Laval, 2601 chemin de la Canardière, Quebec City, QC, G1J 2G3 Canada
e-mail: toth.katalin@crulrg.ulaval.ca

Granule cells of the dentate gyrus receive cortical information and they transform and transmit this code to the CA3 area via their axons, the mossy fibers (MFs). Structural and functional complexity of this network has been extensively studied at various organizational levels. This review is focused on the anatomical and physiological properties of the MF system. We will discuss the mechanism by which dentate granule cells process signals from single action potentials (APs), short bursts and longer stimuli. Various parameters of synaptic interactions at different target cells such as quantal transmission, short- and long-term plasticity (LTP) will be summarized. Different types of synaptic contacts formed by MFs have unique sets of rules for information processing during different rates of granule cell activity. We will investigate the complex interactions between key determinants of information transfer between the dentate gyrus and the CA3 area of the hippocampus.

Keywords: mossy fiber, synaptic plasticity, CA3 region, hippocampal, interneurons, information transfer

INTRODUCTION

One of the most studied synapses in the central nervous system (CNS) is the dentate mossy fiber (MF) input onto hippocampal CA3 pyramidal cells. Nevertheless, in spite of the large amount of information about the organization and function of this synapse, we are far from the complete understanding of this complex structure. MFs play a unique role in the transformation of incoming cortical signals and ensure the faithful transfer of the resulting code to the CA3 area. The dentate gyrus is the first relay in the cortico-hippocampal loop, it is involved in the translation of densely coded cortical signals to sparse and specific hippocampal code, which is essential for hippocampal memory formation (Acsady and Kali, 2007). The high-pass filter nature of the dentate–CA3 circuit allows the conversion of multiple place fields of dentate place cells into a single receptive field observed in CA3 place cells. This process critically relies on the exact firing pattern of dentate granule cells and results in more orthogonalized stimulus representation in the CA3 area (Leutgeb et al., 2007). Likewise, in case of repetitive stimulus presentation or autonomous memory trace replay, presynaptic MF long-term plasticity (LTP) may help the orthogonalization process, creating an opportunity for the faithful reactivation of the same cornu ammonis region 3 (CA3) circuit pattern.

The aim of this review is to provide an overview about the cellular processes responsible for the transformation of entorhinal inputs into hippocampal codes by granule cells of the dentate gyrus. We will review how single granule cell action potential (AP) influence postsynaptic CA3 pyramidal cells and interneurons, we will discuss the unique morphological and physiological properties of the presynaptic specializations of these cells and how these features contribute to postsynaptic signaling. Next, we will discuss how communication between the dentate gyrus and the CA3 area is influenced by changes in presynaptic firing frequencies. Finally, the complex and diverse synaptic plastic properties of MF synapses will be summarized and discussed.

STRUCTURAL PROPERTIES OF HIPPOCAMPAL MOSSY FIBERS

MFs are nonmyelinated axons of granule cells, located in the dentate gyrus. These axons are projecting primarily to the proximal parts of CA3 pyramidal cell dendrites and distal dendrites of interneurons (Acsady et al., 1998). Axonal tracing revealed that during its passage through the hilus, each MF gives rise to a number of branching collaterals, contacting various hilar neurons, while the main axons continues toward the pyramidal cell layer of the hippocampal CA3 area. MFs do not form collaterals within the CA3 area, they are organized in a laminar fashion along the pyramidal cell layer, their projection is restricted to the stratum lucidum.

Each MF forms several, sparsely located large boutons (3–10 μm diameter), which envelop postsynaptic thorny excrescences emerging from CA3 pyramidal cell apical dendrites, while 2–4 tiny filopodial extensions stemming from these large boutons innervate dendrites of inhibitory interneurons (**Figure 1A**). In average, one MF fiber makes four different types of excitatory synapses: 7–12 large terminals contacting hilar mossy cells; 11–18 large terminals innervating CA3 pyramidal cells; 120–150 small terminals forming synapses on hilar interneurons and 40–50

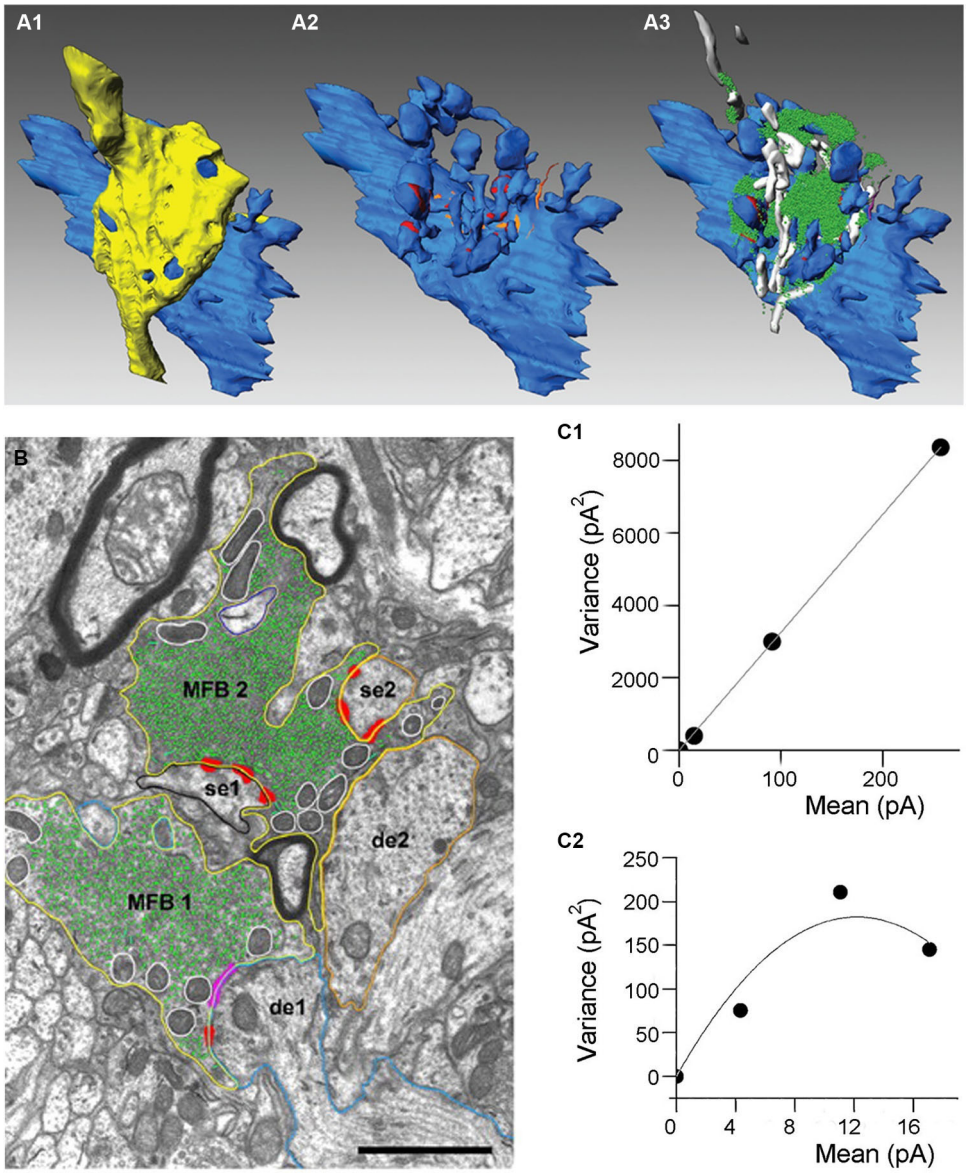

FIGURE 1 | Anatomical organization and quantal parameters of MF synapses. **(A)** Three-dimensional reconstructions of an adult MF bouton and its postsynaptic target dendrite. **(A1)** Volume reconstructions of bouton (yellow) and its postsynaptic target dendrite (blue). **(A2)** Distribution of the two membrane specializations, active zones (in red) and puncta adherentia (in orange) on the postsynaptic target dendrite. Note, that active zones were mainly located on the spiny excrescences, whereas puncta adherentia were exclusively found at the dendritic shaft. **(A3)** Organization of the pool of synaptic vesicles (green dots) and mitochondria (in white) at an individual MF bouton. Adapted from Rollenhagen and Lübke (2010). **(B)** Electron microscopic image of two adjacent MF boutons (MFB1, MFB2). Both boutons outlined in yellow terminate on different dendritic segments (de1, blue contour; de2, orange contour), but preferentially on spiny excrescences (se1, black contour; se2, orange contour). Active zones (red), puncta adherentia (magenta), mitochondria (white contours), and individual synaptic vesicles (green). Scale bar corresponds to 1 μm, adapted from Rollenhagen and Lübke (2007). **(C)** Variance-mean analysis of mossy fiber-CA3 pyramidal cell **(C1)** and mossy fiber-interneurone **(C2)** synapses. Data obtained at three different calcium conditions (1 mM, 2.5 mM and 3.8 mM of $CaCl_2$). Solid lines correspond to either liner **(C1)** or parabolic fit **(C2)**. Adapted from Lawrence and McBain (2003).

filopodial extensions terminating on CA3 interneurons (Acsady et al., 1998). MF boutons contact multiple dendritic segments of the same or different pyramidal neurons (Chicurel and Harris, 1992; Galimberti et al., 2006). The number of granule cells converging on CA3 pyramidal cell is remarkably high, an apical dendrite of a single pyramidal cell is contacted by ∼50 MF boutons each originating from different granule cells (Amaral et al., 1990).

Three different types of vesicles have been described within the giant MF boutons: majority of them are small clear vesicles (∼40 nm) containing glutamate, there are also large dense-core vesicles filled with various neuropeptides (dynorphin,

enkephalin, cholecystokinin, neuropeptide Y and neurokinin-β) and large clear vesicles (∼200 nm). MF boutons also contain the neuromodulator ATP/adenosine and Zn^{2+}, which is co-localised in the same vesicles as glutamate. Large MF boutons forming excitatory inputs on CA3 pyramidal cells exhibit several unique properties shaping neurotransmission at these synapses. MF boutons have multiple release sites, which were initially observed using electron microscopy of reconstructed terminals (Chicurel and Harris, 1992; Rollenhagen et al., 2007; Rollenhagen and Lubke, 2010). According to these reconstructions the number of release sites varies between 18–45 with a mean surface area of 0.1 μm^2 and a short distance of 0.45 μm between individual sites, **Figure 1B** (Rollenhagen et al., 2007). The short distance between release sites indicates that crosstalk may occur either presynaptically via Ca^{2+} diffusion or postsynaptically via glutamate spillover from neighboring release sites. MF terminals contain very large number of synaptic vesicles, ∼25,000 vesicles are observed in young rats, approximately 75% of these vesicles corresponds to the reserve pool (Rollenhagen et al., 2007). The putative releasable pool of ∼5700 vesicles was estimated from 3D-reconstructions of MF boutons (Rollenhagen et al., 2007). In contrast, direct capacitance measurement from MF boutons suggests that ∼1400 vesicles comprise the readily releasable pool (RRP; Hallermann et al., 2003). Moreover, the number of vesicles at individual release sites is also very high, which might be important for the support of reliable neurotransmission during high-frequency activity.

NEUROTRANSMITTER RELEASE TRIGGERED BY SINGLE ACTION POTENTIALS

Synaptic transmission is primarily based on the regulated release of neurotransmitter from synaptic vesicles. When an AP arrives at the presynaptic axonal terminal, depolarization opens voltage-gated Ca^{2+} channels (VGCCs) and Ca^{2+} influx triggers the fusion of synaptic vesicles docked and primed at the active zone of the presynaptic plasma membrane. Subsequently, neurotransmitter is released into the synaptic cleft and diffuses to the postsynaptic membrane to activate neurotransmitter receptors. Finally, synaptic vesicles are retrieved via endocytosis in order to restore the releasable vesicle pool (Littleton, 2006; Ryan, 2006). Thus, synaptic transmission depends not only on the number of active zones and vesicles available for release, but also on the properties of the release machinery and composition of pre and postsynaptic receptors and signaling cascades.

MOSSY FIBER BOUTONS

An important parameter of neurotransmission is the quantal size (Q), the amplitude of a synaptic response evoked by glutamate release from a single vesicle. This parameter characterizes the amount of glutamate packed into the vesicle and was calculated for this synaptic connection using stationary variance-mean analysis at different Ca^{2+} concentrations, Q = 29 pA, **Figure 1D** (Lawrence et al., 2004). MF-pyramidal cell synapses exhibit very low release probability (p = 0.2–0.28), (von Kitzing et al., 1994), but due to the large number of release sites unitary excitatory postsynaptic currents (EPSCs) and excitatory postsynaptic potentials (EPSPs) can reach unusually high amplitude (1 nA and 10 mV, respectively) (Bischofberger et al., 2006).

The properties of APs recorded from boutons are different from the APs observed in the soma of granule cells. In particular, they are almost twice faster (half-duration 379 ± 8 μs compared to 678 ± 45 μs at the some) and have less pronounced afterdepolarization (Geiger and Jonas, 2000). These properties are mediated by the dendrotoxin (DTX)-sensitive K^+ channels (presumably composed of Kv1.1α/1.4α or Kv1.1α/β subunits; Coghlan et al., 2001). The combination of low activation and deactivation thresholds (∼60 mV) provides rapid and complete reset of the membrane potential after AP generation (Geiger and Jonas, 2000). While the properties of K^+ channels shape the repolarizating phase of AP, its rising phase depends mainly on the activation of Na^+ channels. In contrast to many other axonal terminals, MF boutons have active properties and express a large number of Na^+ channels (∼2000 per bouton; Engel and Jonas, 2005). Moreover, these channels have faster inactivation kinetic and serve to boost presynaptic APs and enhance calcium influx, rather than to ensure AP propagation.

Interestingly, not only APs, but also subthreshold dendritic synaptic inputs participate in information processing at this synapse. Excitatory presynaptic potentials evoked by such inputs can propagate along the granule cell axon and modulate glutamate release evoked by APs (Alle and Geiger, 2006). A single presynaptic subthreshold potential combined with APs resulted in a significantly larger postsynaptic response; this effect was dependent on calcium signaling and direct voltage modulation of vesicle release.

Presynaptic calcium currents at MF boutons are primarily mediated by P/Q-type Ca^{2+} channels (Castillo et al., 1994; Breustedt et al., 2003; Miyazaki et al., 2005). Whole-bouton recordings were used to investigate directly the kinetic properties of these channels. MF boutons have large high-voltage-activated calcium currents, with fast activation and deactivation (Bischofberger et al., 2002). Furthermore, computational modeling of these calcium currents indicated that the gating kinetics of the Ca^{2+} channels and sharp, pulse-like shape of the presynaptic AP act together to maximize calcium influx. The presence of Na^+ channels in the bouton leads to additional ∼40 mV increase in the depolarization and therefore can amplify calcium currents by two fold (Engel and Jonas, 2005). Based on the large amplitude of Ca^{2+} currents evoked by single APs (Bischofberger et al., 2002) and assuming a single channel current of ∼0.2 pA (Gollasch et al., 1992; Brandt et al., 2005), it has been proposed that approximately 850 Ca^{2+} channels contribute to the peak amplitude of calcium signals, which corresponds to ∼23 opened Ca^{2+} channels per release site.

Glutamate released from MF boutons mediates fast ionotropic responses at the postsynaptic membrane mainly by activating α-amino-3-hydroxy-5-methyl-4- isoxazolepropionic acid (AMPA)-type receptors (Lanthorn et al., 1984; Neuman et al., 1988; Ito and Sugiyama, 1991; Jonas et al., 1993). Ca^{2+}-impermeable AMPARs prevail at mature MF-CA3 pyramidal neuron synapses, while Ca^{2+}-permeable AMPARs undergo developmental regulation (Ho et al., 2007). In contrast to other hippocampal synapses, thorny excrescences of CA3 pyramidal neurons express low density of N-Methyl-D-aspartic acid receptors (NMDARs), which nevertheless provide a small, but measurable, NMDAR-mediated

current upon glutamate release from MFs (Jonas et al., 1993; Weisskopf and Nicoll, 1995).

MOSSY FIBER FILOPODIAL EXTENSIONS

In contrast to large boutons, tiny filopodial extensions selectively contacting CA3 interneurons have only 1–2 release sites, which was initially observed using electron microscopy (Acsady et al., 1998) and later confirmed using several electrophysiological approaches, including variance-mean analysis (Lawrence et al., 2004). From the same set of experiments quantal size was estimated to be ∼27 pA, which is similar to the quantal size at synapse between large MF boutons and CA3 pyramidal cells (**Figure 1C**). Interestingly, the probability of release at filopodial extensions varied between 0.34 and 0.51 during normal calcium concentration (2.5 mM) and increased up to 0.44–0.78 at high calcium concentration (3.8 mM), which is several folds higher than at MF-CA3 pyramidal cell synapses (Lawrence et al., 2004). The high probability of release could be explained by active properties of filopodial extensions, where activation of Na^+ channels may lead to more prominent increase in local AP amplitude than in the main bouton (Engel and Jonas, 2005).

The total number of vesicles within filopodial extensions is two orders of magnitude smaller than in the large boutons (200–700 vesicles; Rollenhagen et al., 2007). The number of releasable vesicle has not been quantitatively assessed in filopodia. However, given that size of the RRP at large mossy boutons is ∼5% of the total number of vesicles, the putative RRP at filopodial extensions could contain 10–40 vesicles.

The filopodial extensions are too small for direct electrophysiological recordings; however it's possible to fill individual MF terminals with a membrane-permeable calcium indicator and perform simultaneous calcium imaging at the large bouton and the filopodia (Pelkey et al., 2006). Similarly to the main bouton, calcium currents in small filopodia are primarily mediated by the activation of P/Q-type Ca^{2+} channels, with small contribution from N-type channels (Pelkey et al., 2006). In spite of this similarity, different signaling cascades control the activation of Ca^{2+} channels during repetitive stimulation, this mechanism will be described in more details below.

CA3 interneurons located in the stratum lucidum receive synapses from MFs or local CA3 pyramidal cell collaterals. MF inputs could activate either synapses containing postsynaptic calcium-permeable AMPARs sensitive to philanthotoxin (Toth and Mcbain, 1998) or synapses expressing calcium-impermeable AMPARs (Toth et al., 2000), while inputs from CA3 pyramidal cells only contact synapses expressing only calcium-impermeable AMPARs. Biocytin filling and subsequent visualization of recorded interneurons did not reveal any preferential localization of calcium-permeable and -impermeable AMPARs on specific subtypes of the stratum lucidum interneurons (Lei and Mcbain, 2002). However, an important correlation between calcium permeability of AMPA receptors and the presence of NMDA receptors in a given synapse was unveiled. At MF-interneuron synapses where AMPARs are calcium permeable only a small fraction of evoked EPSPs are mediated by NMDARs (Lei and Mcbain, 2002). Therefore, inhibition provided onto CA3 pyramidal cells is shaped largely by fast AMPAR currents which controls the precise timing of APs. In contrast, MF-interneuron synapses containing calcium-impermeable AMPARs exhibit a prominent NMDAR component. Here, activation of NMDARs leads to substantially slower EPSP decays and thus a much longer time window for synaptic integration (Maccaferri and Dingledine, 2002), this, in turn, can be translated to a wider temporal window for spike integration in CA3 pyramidal cells. Thus, two different modes of inhibition could be triggered by the activation of MF inputs at synapses composed of distinct sets of postsynaptic glutamate receptors.

INFORMATION PROCESSING DURING BURST FIRING

The average firing rate of granule cells recorded *in vivo* is very low, approximately 0.01–0.1 Hz (Jung and Mcnaughton, 1993). However, spiking activity increase considerably when granule cells participate in information transfer. For instance, the firing frequency of dentate gyrus granule cells can increase up to 10–50 Hz during place cell activity, with the individual bursts reaching 100–300 Hz (Jung and Mcnaughton, 1993; Skaggs et al., 1996; Gundlfinger et al., 2010). These bursts participate in spatial information coding. Therefore, the mechanism by which granule cell burst firing is transmitted at the MF synapses is a key element of information transfer from the dentate gyrus to the CA3 area of the hippocampus. Short-term plasticity plays a significant role in this process, it is primarily expressed presynaptically and it plays a substantial role in the regulation of the balance between excitation and inhibition and the resultant network activity.

MOSSY FIBER BOUTONS

One of the remarkable properties of the MF-CA3 pyramidal cell synapse is their unusually high degree of facilitation during repetitive stimulation (**Figure 2**). For example, a 15 stimuli train delivered at 4 Hz can increase EPSC amplitude more than 10 times (Toth et al., 2000). Moreover, natural stimulation patterns including place cell burst firing, can efficiently lead to short term facilitation increasing postsynaptic responses by 400–500% (Gundlfinger et al., 2010). The large degree of facilitation is associated with low initial release probability, which is significantly augmented during repetitive stimulation. Short-term facilitation is supported by a large RRP providing constant and reliable supply of vesicles during long high-frequency stimuli.

The exact molecular mechanism of synaptic facilitation at MF-CA3 pyramidal cell synapses have been extensively studied, while several key components are well defined, some aspects remain controversial. One of the key players in short-term facilitation is the prominent increase in intra-bouton calcium concentration during repeated stimuli. This, in turn, is directly linked to enhanced glutamate release due to calcium-dependent regulation of synaptic vesicle exocytosis. Fast APs recorded in MF boutons undergo activity-dependent broadening during repetitive stimulation which results in substantially increased presynaptic calcium influx, **Figure 2.** (Geiger and Jonas, 2000). Interestingly, although AP broadening decreases the peak amplitude of calcium currents, it increases the total calcium influx per spike and leads to augmented glutamate release. This suggests that integral calcium current, rather than its peak amplitude determines release probability.

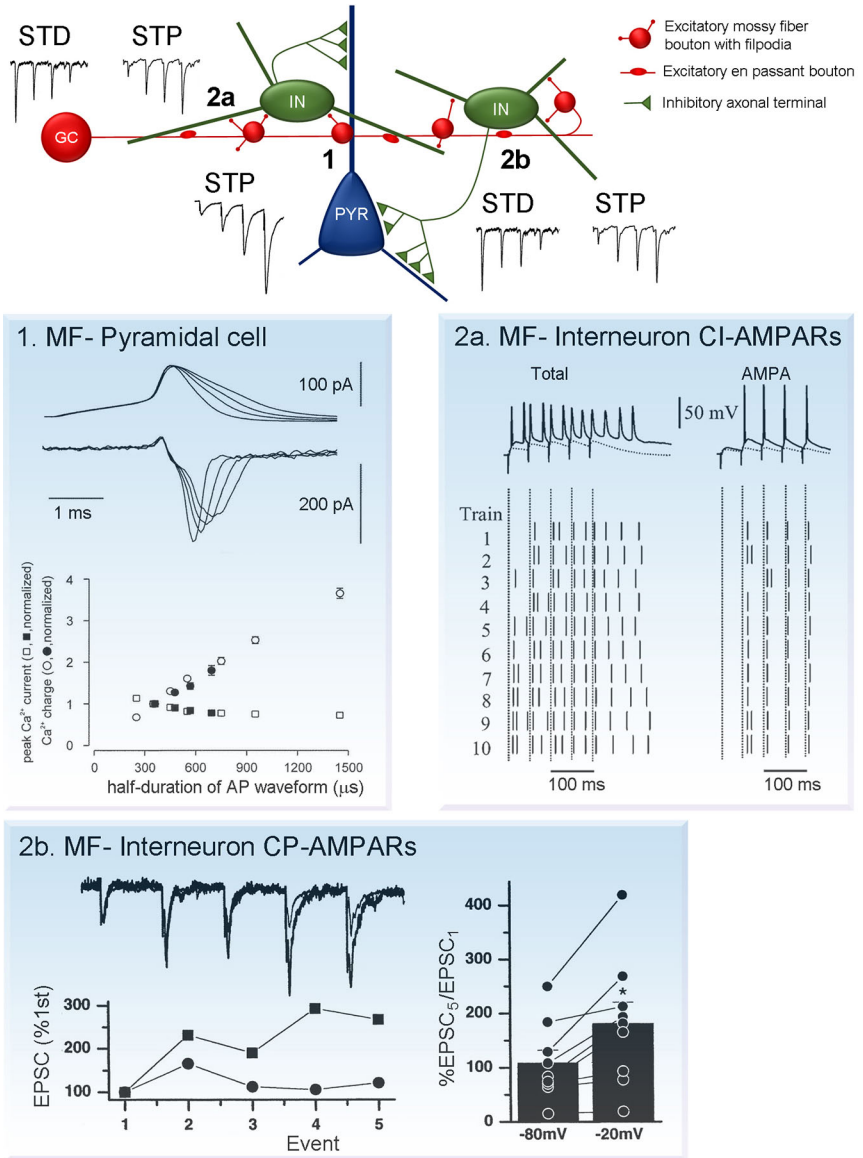

FIGURE 2 | Short-term plasticity at synapses formed by MF boutons on CA3 neurons. (Center) Schematic diagram showing connection formed by individual granule cells with CA3 pyramidal cells and interneurons. Note that the number of contacts with interneurons is large, compared to pyramidal cells. Moreover, each interneuron forms multiple inhibitory contacts on pyramidal cells. This network organization leads to the prevalence of inhibition on CA3 pyramidal cells during low granule cell activity. However, during granule cell burst firing MF synapses on pyramidal cells undergo robust facilitation short-term potentiation (STP, synapse **1**), while synapses on interneurons either depress or exhibit mild facilitation short-term depression (STD/STP, synapses **2a** and **2b**). As a result, MF neurotransmission leads to reliable AP generation at postsynaptic CA3 pyramidal neurons. Plasticity traces adapted from Toth and Mcbain (2000). Examples of mechanism underlying short-term plasticity at each type of the synapses are shown on panels **1**, **2a** and **2b**. **(1)** MF-pyramidal cell synapses: AP broadening increases presynaptic calcium influx. Top (upper traces), current-clamp recordings of APs and top (lower traces), corresponding calcium currents. Bottom, peak current amplitude (squares) and integral (circles; determined in a 5 ms time window), plotted against half-duration of the voltage-clamp command. Open symbols indicate values for mock APs, filled symbols represent realistic APs. Adapted from Geiger and Jonas (2000). **(2a)** MF-interneuron synapses expressing calcium-impermeable AMPARs (CI-AMPARs): contributions of NMDARs and AMPARs to AP transmission. EPSP/AP sequences elicited by trains of stimuli (5 stimuli, 20 Hz) in the absence (left column) or presence (right column) of (2R)-amino-5-phosphonovaleric acid (APV). Upper trace shows a single representative example of response evoked by stimulation. Lower panel shows the raster plot of spikes induced by each of the 5 stimuli in the 10 trials. Each short vertical line represents a single AP, dashed lines represent the timing of the stimulus artifact. Adapted from Lei and Mcbain (2002). **(2b)** MF-interneuron synapses expressing calcium-permeable AMPARs (CP-AMPARs): voltage-dependent relief from polyamine block enhances facilitation at depolarized potentials. Top, trains of five MF EPSCs evoked by 20 Hz stimulation at two holding potentials (−80 and −20 mV). Bottom, normalizing the first EPSCs in the trains reveals a greater degree of facilitation at −20 mV. Right, Summary histogram shows that the $EPSC_5/EPSC_1$ ratio always larger at −20 mV, polyamine block is relieved. (Toth and Mcbain, 2000).

Application of the membrane permeable, slow calcium chelator ethylene glycol tetraacetic acid, tetra (acetoxymethyl ester) (EGTA-AM) significantly reduces the degree of facilitation (Regehr et al., 1994; Salin et al., 1996; Tzounopoulos et al., 1998), indicating that accumulation of residual calcium during stimulation trains is essential. Calcium release from ryanodine sensitive stores might also be involved in short-term facilitation, as the blockade of calcium release from stores with ryanodine significantly reduces paired pulse facilitation (Scott and Rusakov, 2006; Scott et al., 2008). Interestingly, in other systems, ryanodine failed to have similar effect on synaptic facilitation (Carter et al., 2002; Shimizu et al., 2008). It is yet to be determined whether calcium release from stores plays a significant role in synaptic signal integration during longer, natural-like stimulations patterns.

Presynaptic glutamate receptors can play a crucial role in short-term facilitation as their activation can alter the amplitude of subsequent postsynaptic signals. Activation of presynaptic metabotropic glutamate receptors (mGluRs) leads to the suppression of glutamate release most likely via the inhibition of VGCCs (Castillo et al., 1994; Min et al., 1998; Kamiya and Ozawa, 1999; Toth et al., 2000; Pelkey et al., 2006). Endogenous glutamate can also activate presynaptic kainate receptors (KARs), leading to the enhancement of AP evoked calcium influx in the terminal, and therefore increased facilitation (Lauri et al., 2001; Schmitz et al., 2001; Scott et al., 2008; Dargan and Amici, 2009). Interestingly, there are also data suggesting that during short stimulation bursts (0.5–25 Hz) depression of glutamate release induced via mGluRs predominantly shapes the evoked responses while the effect of KARs activation is very small (Kwon and Castillo, 2008b). These findings indicate that glutamate release from MFs during repetitive stimulation acts not only postsynaptically, but also activates several types of presynaptic autoreceptors triggering distinct molecular cascades which modulate calcium signaling and neurotransmitter release.

At the postsynaptic site glutamate receptor activation can also undergo short-term changes during bursts. In particular, activation of postsynaptic KARs can generate slow depolarizing synaptic currents, which contribute minimally to postsynaptic potentials during low-frequency stimulation (Castillo et al., 1997; Vignes and Collingridge, 1997). However, these currents start to play a significant role in postsynaptic AP generation during repetitive high-frequency MF firing (Kwon and Castillo, 2008b; Sachidhanandam et al., 2009) and express short-term depression (STD) mediated by NMDARs (Rebola et al., 2007).

MOSSY FIBER FILOPODIAL EXTENSIONS

MF synapses established between filopodial extensions and interneurons can exhibit both short-term potentiation (STP) and depression during repetitive stimulation, **Figure 2** (Toth et al., 2000; McBain, 2008). Interestingly, the direction of plasticity is independent of the presence of calcium-permeable AMPARs and it is rather determined by the initial release probability. In general, potentiation at MF-interneuron synapses is remarkably small compared to that observed at synapses terminating on pyramidal cells (4X increase vs. 10X increase, at 4 Hz). Moreover, while at synapses terminating pyramidal cells significant facilitation could be observed as low as 0.1 Hz stimulation frequency, at synapses impinging on interneurons facilitation only occurs at stimulation frequencies higher than 1–2 Hz (Toth et al., 2000). The magnitude of synaptic response evoked by MF inputs in interneurons and pyramidal cells largely depends on the frequency of granule cell firing. In fact, it's believed that short-term plasticity at both types of synapses is crucial for hippocampal information processing and regulates network activity.

A unique form of short-term plasticity exists at synapses expressing calcium-permeable AMPARs. In contrast to conventional forms of short-term plasticity it is induced postsynaptically. Calcium-permeable AMPARs under resting conditions are tonically blocked with intracellular ployamines, such as spermine and spermidine (Kamboj et al., 1995; Koh et al., 1995), this blockade is use-and voltage-dependent and requires multiple receptor activations (i.e., repetitive stimulation) to remove polyamine from the channel pore (Bowie and Mayer, 1995). Thus, due to the use-dependence of polyamine block, current flowing through calcium-permeable AMPARs increases during presynaptic bursts. However, as polyamine block and the resulting facilitation are voltage-dependent this form of STP is almost absent at resting membrane potentials and becomes prominent only when neurons are depolarized (Toth et al., 2000). Due to these unique properties, under physiological conditions, calcium-permeable AMPARs may play a role of coincidence detectors.

Synapses expressing calcium-impermeable AMPARs also contain N-methyl D-aspartate receptor subtype 2B (NR2B)-lacking NMDARs. The NMDA component significantly influences temporal summation and increases the number of evoked postsynaptic APs, **Figure 2a** (Lei and Mcbain, 2002). In contrast, synapses with calcium-permeable AMPARs co-express NR2B-containing NMDARs (Bischofberger et al., 2002; Lei and Mcbain, 2002). At this type of synapse repetitive stimulation results in rapid and brief EPSPs and APs with little jitter, **Figure 2b** (Lei and Mcbain, 2002; Walker et al., 2002). Thus, these two types of MF synapses are designed for two different modes of neurotransmission: calcium permeable AMPAR expressing synapses for precise and rapid synaptic transmission; synapses containing calcium-impermeable APMARs for large depolarization and multiple APs without accurate timing (Lawrence and McBain, 2003; Jonas et al., 2004).

Similarly to MF-CA3 pyramidal cell synapses, activation of presynaptic mGluRs during repetitive stimulation decreases the amplitude of facilitation at synapses terminating on interneurons (Toth et al., 2000; Cosgrove et al., 2011), however this effect is less pronounced (Kamiya and Ozawa, 1999). In contrast, the enhancement of synaptic transmission by kainate autoreceptors is specific to MF-pyramidal cell synapses. Inhibition of KARs does not alter synaptic currents and presynaptic calcium influx at synapse formed onto inhibitory interneurons (Scott et al., 2008).

ACTIVITY-DEPENDENT NETWORK OUTPUT

The combined effect of the aforementioned diverse postsynaptic responses observed in MF targets in response to presynaptic bursts will largely depend on the particular pattern of the stimuli. Frequency-dependent alteration of direct excitatory and indirect feed-forward inhibitory responses will determine network output. This combined output is influenced by the connectivity pattern

of MFs and its targets and the temporal summation of synaptic inputs.

Anatomical data indicate that MFs form larger number of synaptic contacts on interneurons than on CA3 pyramidal cells. Since inhibitory neurons receiving MF inputs contact several hundreds of CA3 pyramidal cells, granule cell firing also triggers powerful disynaptic feed-forward inhibition. While MF-principal cell synapses have low release probability, they also exhibit very large facilitation during repetitive stimulation. In contrast, similar stimulation at the MF-interneuron synapse leads to synaptic depression or mild potentiation.

The balance between excitation and inhibition is a key determinant of network output and it is developmentally regulated. In young animals, polysynaptic feed-forward inhibition of CA3 pyramidal cells facilitates during burst activity, while in adults both facilitation and depression can occur (Torborg et al., 2010). The temporal precision of postsynaptic APs is not influenced by feed-forward inhibition, but it is rather determined by the amplitude and kinetic properties of excitatory inputs. However, feed-forward inhibition plays a key role in the regulation of CA3 pyramidal cell excitability and prevents the development of excitatory plateaus and repetitive postsynaptic cell firing. In adults, a shift between the facilitation and depression of network inhibition may act as a switch between tonic and burst firing modes (Torborg et al., 2010).

Frequency-dependent facilitation of MF neurotransmission has been demonstrated *in vivo*, using recordings from monosynaptically connected granule cell-pyramidal cells (Henze et al., 2002). The probability of postsynaptic AP firing rose rapidly with increased granule cell firing frequency. Four-five presynaptic APs were sufficient to reach maximum AP probability in CA3 pyramidal neurons. In contrast, at granule cell–interneuron synapses, increase in the number of the presynaptic spikes delivered at 100 Hz did not enhance the probability of postsynaptic APs. These data indicate that various forms of short-term plasticity at different postsynaptic targets lead to frequency-dependent alterations in the net postsynaptic response.

Anatomical data demonstrating that the number of inhibitory postsynaptic targets of MFs is several times bigger than the number of innervated pyramidal cells (Acsady et al., 1998), and physiological data depicting the mechanism by which the balance between excitation and inhibition can be shifted when granule cell firing rate is altered (Henze et al., 2002) suggest that the combined effect of granule cell activity in a behaving animal is inhibitory rather than excitatory. This idea is supported by *in vivo* data demonstrating that during cortical UP states activity in entorhinal cortex, dentate gyrus and most CA1 neurons increased, in contrast neurons in the CA3 are not active (Isomura et al., 2006). Similarly, dentate spikes resulting from the synchronous excitation of dentate granule cells by entorhinal stellate cells, decreased multiunit activity recorded in the CA3 area (Bragin et al., 1995). The general inhibitory effect of granule cell activity is also supported by the simultaneous and opposite effects of sensory stimulation on population activity in the CA1 area and the dentate gyrus; perforant pathway responses in granule cells are facilitated by sensory stimulation while CA1 population spikes are reduced (Herreras et al., 1988).

SYNAPTIC PLASTICITY

Synaptic efficacy at MF synapses, similarly to other synapses in the CNS, can persistently be altered. Remarkably, synapses formed by MFs on both pyramidal cells and interneurons show unusual forms of LTP, and almost all elements including the direction of plasticity, induction and expression sites manifest in a target cell-dependent manner.

LONG-TERM PLASTICITY AT MOSSY FIBER-PYRAMIDAL CELL SYNAPSES

LTP of MF inputs on CA3 pyramidal neurons can be evoked by various high frequency stimulation protocols (Yamamoto et al., 1980; Zalutsky and Nicoll, 1990; Castillo et al., 1994; Nicoll and Schmitz, 2005), and with natural granule cell firing patterns (Mistry et al., 2011). Interestingly, only firing patterns containing high frequency bursts with low average firing rate were efficient to induce LTP, such patterns are characteristic of granule cell firing during memory tasks (Mistry et al., 2011).

It is widely accepted that MF LTP induction is independent of the activation of postsynaptic NMDARs (Harris and Cotman, 1986); reviewed by Nicoll and Schmitz (2005). In fact, evidence point to exclusive contribution of presynaptic mechanisms, including increase in presynaptic calcium currents and the activation of adenylyl cyclase-cAMP cascade, **Figure 3** (Zalutsky and Nicoll, 1992; Weisskopf et al., 1994; Villacres et al., 1998). There are also data suggesting, that activation of presynaptic KARs and calcium release from internal stores might be involved (Contractor et al., 2001; Lauri et al., 2001, 2003; Bortolotto et al., 2003). However, several studies shed light on the importance of postsynaptic calcium signaling associated with VGCCs and mGluRs in MF LTP (Kapur et al., 1998, 2001; Yeckel et al., 1999; Wang et al., 2004). Pre and postsynaptic mechanism were suggested to be recruited based on the particular stimulus conditions used (Urban and Barrionuevo, 1996). While multiple evidence show that presynaptic enhancement of glutamate release is a key element in the development of MF LTP (Yamamoto et al., 1992; Zalutsky and Nicoll, 1992; Yeckel et al., 1999; Reid et al., 2004), postsynaptic regulation of MF LTP by retrograde ephrin signaling has also been proposed (Contractor et al., 2002; Armstrong et al., 2006).

Induction of LTD by low frequency stimulation is NMDAR independent, similarly to LTP (Kobayashi et al., 1996), and relies on the activation of presynaptic group II mGluRs, **Figure 3** (Manzoni et al., 1995; Yoshino et al., 1996). Activation of mGluRs leads to decreased cAMP levels and subsequent PKA activation (Tzounopoulos et al., 1998), which in turn, down-regulates the vesicle release machinery and leads to synaptic depression. Thus, both LTD and LTP at MF-CA3 pyramidal cell synapses are expressed presynaptically and depend on cAMP production. LTD evoked with short depolarization (DiLTD) can only be observed at this synapse during the first 2–3 postnatal weeks. This form of plasticity is mediated by the transient presence of CP-AMPA receptors at MF-pyramidal cells synapse in these young animals (Ho et al., 2007).

This synapse also expresses a very unique form of plasticity, NMDARs mediated responses can be selectively potentiated, while the AMPAR component remains unaffected (Kwon and

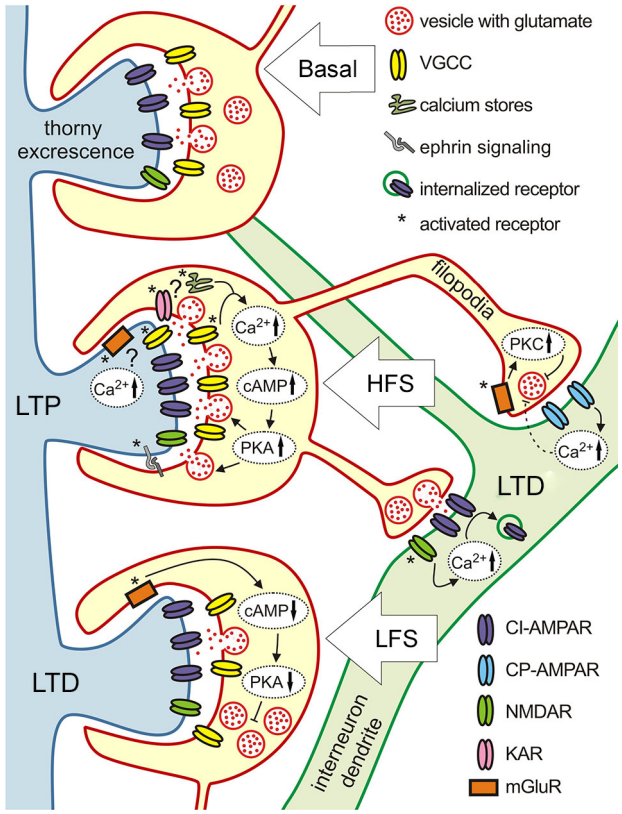

FIGURE 3 | Target-specific plasticity at three different types of MF synapses. Schematics illustration of the various molecular mechanisms underlying different forms of plasticity at MF synapses terminating on pyramidal cells (blue dendrite with thorny excrescencies) and inhibitory interneurons (green dendrite). High frequency stimulation induces LTP at pyramidal cell synapses that is NMDAR-independent and expressed presynaptically. Mechanisms involved are: increase in presynaptic calcium, adenylyl cyclase 1 (AC1), cAMP, protein kinase A (PKA), and ephrin signaling which up-regulate release machinery. At the presynaptic cite KARs and calcium release from stores might be involved, postsynaptic calcium increase due to the activation of mGluRs and VGCCs also might play a role. Same type of intense stimulation evokes LTD at filopodial synapses onto interneurons. At synapses expressing calcium-impermeable AMPARs (CI-AMPARs) LTD has a postsynaptic locus of induction and expression. It depends on calcium influx through NMDARs, and involves the endocytosis of surface AMPARs. LTD at synapses containing calcium-permeable AMPARs (CP-AMPARs) requires postsynaptic calcium increase, but is expressed presynaptically through activation of presynaptic mGluR7 and downstream Protein kinase C (PKC)-dependent cascades reducing neurotransmitter release probability. Low frequency stimulation evokes LTD at MF-pyramidal cell synapses. This form of LTD involves activation of presynaptic mGluR2, which in turn reduces cAMP level and subsequent decrease of PKA activity lowers the release probability.

Castillo, 2008a; Rebola et al., 2008). This form of plasticity is mediated by the PKC-dependent recruitment of NMDARs. Interestingly, NMDAR-LTP participates in several metaplastic changes including: induction of NMDA-dependent LTP of AMPARs (Rebola et al., 2011) and a recently described heterosynaptic metaplasticity between MF and associational-commissural synapses (Hunt et al., 2013). Moreover, paired burst stimulation of presynaptic MFs and postsynaptic pyramidal cells, mimicking *in vivo* activity, efficiently induced bidirectional changes in the NMDAR-mediated currents. The direction of LTP was dependent on the timing of pre and postsynaptic bursts similarly to conventional spike-timing-dependent plasticity (Hunt et al., 2013). Bidirectional, long-term changes in NMDAR mediated responses provide higher degree of flexibility in information processing at this synapses.

LONG-TERM PLASTICITY OF AT MOSSY FIBER-INTERNEURON SYNAPSES

Unlike in pyramidal cells, high frequency stimulation leads to LTD at synapses formed on interneurons (Maccaferri et al., 1998; Lei and Mcbain, 2004; Pelkey et al., 2005; Galvan et al., 2011). Furthermore, although this LTD could be equally evoked at synapses expressing calcium-permeable and calcium-impermeable AMPARs, both depending on postsynaptic calcium elevation, there is a drastic difference in the molecular mechanisms of LTD induction and expression at these two different types of synapses (**Figure 3**). At synapses expressing calcium impermeable AMPA receptors, LTD is expressed postsynaptically and it is NMDAR-dependent. Calcium entry through NMDAR triggers AP-2 dependent AMPAR internalization, by a mechanism similar to that at other synapses expressing NMDAR-dependent LTD (Lei and Mcbain, 2004). The fact that at this type of MF-interneuron synapse LTD seems to rely on a conventional molecular pathway is striking, given that this particular type of LTD could only be evoked with high and not low frequency stimulation which is commonly associated with LTD induction (Luthi et al., 1999; Lee et al., 2002).

At calcium-permeable AMPAR synapses LTD is NMDAR-independent, it requires calcium influx through AMPAR, but is expressed presynaptically via decreased glutamate release (Lei and Mcbain, 2004). The activation of mGluR7 which is selectively expressed on filopodia, but not the main MF bouton (Shigemoto et al., 1997), is required for this type of plasticity (Pelkey et al., 2005). This form of LTD involves the inhibition of calcium influx to the terminal through P/Q-type VGCCs (Pelkey et al., 2005). Since activation of presynaptic mGluR7s and postsynaptic calcium influx through AMPARs are necessary, this form of LTD most likely involves retrograde signaling, however its nature remains unknown (Pelkey et al., 2005). Interestingly, in synapses that contain a mixture of calcium-permeable and -impermeable AMPARs, LTD relies on presynaptic mechanisms (Lei and Mcbain, 2004).

Early studies did not reveal LTP at mossy fiber synapses formed on interneurons. However, subsequently it was discovered not only in dentate basket cells (Alle et al., 2001), but also in two types of CA3 inhibitory cells: stratum lucidum and stratum lacunosum-moleculare interneurons. Presynaptic form of LTP could be induced at calcium-permeable AMPAR containing MF synapses on stratum lucidum interneurons after prolonged application of mGluR7 agonist followed by high frequency stimulation. The initial LTD induced by the activation of mGluR7 was transformed into LTP after tetanus stimulation. This switch in the direction of plasticity occurred due to the internalization of surface mGluR7 receptors induced by L-(+)-2-Amino-4-phosphonobutyric acid (L-AP4) application (Pelkey et al., 2005). Receptor internalization

is a key element of this phenomenon, as pharmacological blockade of mGluRs was not sufficient to unmask LTP at this synapse. Internalization of mGluR7 changes the direction of plasticity by turning on release sensitivity to cAMP. At naive mGluR7 expressing synapses cAMP elevation does not have any effect, while at synapses with internalized mGluR7 it leads to strong potentiation (Pelkey et al., 2008). Moreover, the molecular cascaded involves adenylate cyclase and PKA activation, as well as an active zone protein replication in mitochondria 1a (RIM1a). Therefore, this synapses shows bidirectional LTP, dependent on the presence of mGluR7, which adds an additional layer of complexity to the interaction between different forms of plasticity at the same synapse.

In stratum lacunosum-moleculare interneurons classic, high frequency stimulation of MFs triggered LTP. This form of LTP is expressed postsynaptically at synapses containing calcium-impermeable AMPARs, but in contrast to the plasticity at calcium-impermeable AMPAR synapses on stratum lucidum interneurons, it does not depend on the activation of NMDARs (Galvan et al., 2008). It involves activation of mGluR1 and could be mimicked by either application of forskolin, indicating the involvement of the cAMP/PKA signaling cascade, or by PKC activation. Downstream of mGluR1 activation, postsynaptic calcium signaling, including calcium release from internal stores and influx through L-type VGCCs is necessary for this form of plasticity. When calcium signaling is blocked, the direction of plasticity is reversed and high frequency stimulation leads to LTD (Galvan et al., 2008).

CONCLUSION

MF projection to the CA3 area is a remarkably complex system both anatomically and functionally. Synaptic communication between MFs and their target cells is regulated in an activity- and target cell-dependent manner. We are only at the beginning of understanding the mechanism by which these diverse synaptic responses combine to determine how dentate granule cells translate cortical information to hippocampal code. While intricate details of synaptic interaction between granule cells and their postsynaptic targets are well known, the major outstanding question is how *in vivo* activity patterns of several presynaptic cells combine at single cell and population level. In order to properly investigate this question, simultaneous detection of *in vivo* activity patterns of pre and postsynaptic cells and their exact connectivity patterns needs to be defined. Recent advances in imaging techniques using voltage-sensitive and calcium dyes and viral technologies allowing the visualization of certain subset of neurons and their projections could help to attain this aim.

ACKNOWLEDGMENTS

This work was supported by CIHR operating grant to Katalin Tóth and Alesya Evstratova was supported by CTRN.

REFERENCES

Acsady, L., and Kali, S. (2007). Models, structure, function: the transformation of cortical signals in the dentate gyrus. *Prog. Brain Res.* 163, 577–599. doi: 10.1016/s0079-6123(07)63031-3

Acsady, L., Kamondi, A., Sik, A., Freund, T., and Buzsaki, G. (1998). GABAergic cells are the major postsynaptic targets of mossy fibers in the rat hippocampus. *J. Neurosci.* 18, 3386–3403.

Alle, H., and Geiger, J. R. (2006). Combined analog and action potential coding in hippocampal mossy fibers. *Science* 311, 1290–1293. doi: 10.1126/science.1119055

Alle, H., Jonas, P., and Geiger, J. R. (2001). PTP and LTP at a hippocampal mossy fiber-interneuron synapse. *Proc. Natl. Acad. Sci. U S A* 98, 14708–14713. doi: 10.1073/pnas.251610898

Amaral, D. G., Ishizuka, N., and Claiborne, B. (1990). Neurons, numbers and the hippocampal network. *Prog. Brain Res.* 83, 1–11. doi: 10.1016/s0079-6123(08)61237-6

Armstrong, J. N., Saganich, M. J., Xu, N. J., Henkemeyer, M., Heinemann, S. F., and Contractor, A. (2006). B-ephrin reverse signaling is required for NMDA-independent long-term potentiation of mossy fibers in the hippocampus. *J. Neurosci.* 26, 3474–3481. doi: 10.1523/jneurosci.4338-05.2006

Bischofberger, J., Engel, D., Li, L., Geiger, J. R., and Jonas, P. (2006). Patch-clamp recording from mossy fiber terminals in hippocampal slices. *Nat. Protoc.* 1, 2075–2081. doi: 10.1038/nprot.2006.312

Bischofberger, J., Geiger, J. R., and Jonas, P. (2002). Timing and efficacy of Ca2+ channel activation in hippocampal mossy fiber boutons. *J. Neurosci.* 22, 10593–10602.

Bortolotto, Z. A., Lauri, S., Isaac, J. T., and Collingridge, G. L. (2003). Kainate receptors and the induction of mossy fibre long-term potentiation. *Philos. Trans. R. Soc. Lond. B Biol. Sci.* 358, 657–666. doi: 10.1098/rstb.2002.1216

Bowie, D., and Mayer, M. L. (1995). Inward rectification of both AMPA and kainate subtype glutamate receptors generated by polyamine-mediated ion channel block. *Neuron* 15, 453–462. doi: 10.1016/0896-6273(95)90049-7

Bragin, A., Jando, G., Nadasdy, Z., Van Landeghem, M., and Buzsaki, G. (1995). Dentate EEG spikes and associated interneuronal population bursts in the hippocampal hilar region of the rat. *J. Neurophysiol.* 73, 1691–1705.

Brandt, A., Khimich, D., and Moser, T. (2005). Few CaV1.3 channels regulate the exocytosis of a synaptic vesicle at the hair cell ribbon synapse. *J. Neurosci.* 25, 11577–11585. doi: 10.1523/jneurosci.3411-05.2005

Breustedt, J., Vogt, K. E., Miller, R. J., Nicoll, R. A., and Schmitz, D. (2003). Alpha1E-containing Ca2+ channels are involved in synaptic plasticity. *Proc. Natl. Acad. Sci. U S A* 100, 12450–12455. doi: 10.1073/pnas.2035117100

Carter, A. G., Vogt, K. E., Foster, K. A., and Regehr, W. G. (2002). Assessing the role of calcium-induced calcium release in short-term presynaptic plasticity at excitatory central synapses. *J. Neurosci.* 22, 21–28.

Castillo, P. E., Malenka, R. C., and Nicoll, R. A. (1997). Kainate receptors mediate a slow postsynaptic current in hippocampal CA3 neurons. *Nature* 388, 182–186. doi: 10.1038/40645

Castillo, P. E., Weisskopf, M. G., and Nicoll, R. A. (1994). The role of Ca2+ channels in hippocampal mossy fiber synaptic transmission and long-term potentiation. *Neuron* 12, 261–269. doi: 10.1016/0896-6273(94)90269-0

Chicurel, M. E., and Harris, K. M. (1992). Three-dimensional analysis of the structure and composition of CA3 branched dendritic spines and their synaptic relationships with mossy fiber boutons in the rat hippocampus. *J. Comp. Neurol.* 325, 169–182. doi: 10.1002/cne.903250204

Coghlan, M. J., Carroll, W. A., and Gopalakrishnan, M. (2001). Recent developments in the biology and medicinal chemistry of potassium channel modulators: update from a decade of progress. *J. Med. Chem.* 44, 1627–1653. doi: 10.1021/jm000484+

Contractor, A., Rogers, C., Maron, C., Henkemeyer, M., Swanson, G. T., and Heinemann, S. F. (2002). Trans-synaptic Eph receptor-ephrin signaling in hippocampal mossy fiber LTP. *Science* 296, 1864–1869. doi: 10.1126/science.1069081

Contractor, A., Swanson, G., and Heinemann, S. F. (2001). Kainate receptors are involved in short- and long-term plasticity at mossy fiber synapses in the hippocampus. *Neuron* 29, 209–216. doi: 10.1016/s0896-6273(01)00191-x

Cosgrove, K. E., Meriney, S. D., and Barrionuevo, G. (2011). High affinity group III mGluRs regulate mossy fiber input to CA3 interneurons. *Hippocampus* 21, 1302–1317. doi: 10.1002/hipo.20842

Dargan, S. L., and Amici, M. (2009). Role of kainate autoreceptors in short-term plasticity at hippocampal mossy fiber synapses. *J. Neurosci.* 29, 5713–5715. doi: 10.1523/JNEUROSCI.0549-09.2009

Engel, D., and Jonas, P. (2005). Presynaptic action potential amplification by voltage-gated Na+ channels in hippocampal mossy fiber boutons. *Neuron* 45, 405–417. doi: 10.1016/j.neuron.2004.12.048

Galimberti, I., Gogolla, N., Alberi, S., Santos, A. F., Muller, D., and Caroni, P. (2006). Long-term rearrangements of hippocampal mossy fiber terminal connectivity in the adult regulated by experience. *Neuron* 50, 749–763. doi: 10.1016/j.neuron.2006.04.026

Galvan, E. J., Calixto, E., and Barrionuevo, G. (2008). Bidirectional Hebbian plasticity at hippocampal mossy fiber synapses on CA3 interneurons. *J. Neurosci.* 28, 14042–14055. doi: 10.1523/JNEUROSCI.4848-08.2008

Galvan, E. J., Cosgrove, K. E., and Barrionuevo, G. (2011). Multiple forms of long-term synaptic plasticity at hippocampal mossy fiber synapses on interneurons. *Neuropharmacology* 60, 740–747. doi: 10.1016/j.neuropharm.2010.11.008

Geiger, J. R., and Jonas, P. (2000). Dynamic control of presynaptic Ca(2+) inflow by fast-inactivating K(+) channels in hippocampal mossy fiber boutons. *Neuron* 28, 927–939. doi: 10.1016/s0896-6273(00)00164-1

Gollasch, M., Hescheler, J., Quayle, J. M., Patlak, J. B., and Nelson, M. T. (1992). Single calcium channel currents of arterial smooth muscle at physiological calcium concentrations. *Am. J. Physiol.* 263, C948–C952.

Gundlfinger, A., Breustedt, J., Sullivan, D., and Schmitz, D. (2010). Natural spike trains trigger short- and long-lasting dynamics at hippocampal mossy fiber synapses in rodents. *PLoS One* 5:e9961. doi: 10.1371/journal.pone.0009961

Hallermann, S., Pawlu, C., Jonas, P., and Heckmann, M. (2003). A large pool of releasable vesicles in a cortical glutamatergic synapse. *Proc. Natl. Acad. Sci. U S A* 100, 8975–8980. doi: 10.1073/pnas.1432836100

Harris, E. W., and Cotman, C. W. (1986). Long-term potentiation of guinea pig mossy fiber responses is not blocked by N-methyl D-aspartate antagonists. *Neurosci. Lett.* 70, 132–137. doi: 10.1016/0304-3940(86)90451-9

Henze, D. A., Wittner, L., and Buzsaki, G. (2002). Single granule cells reliably discharge targets in the hippocampal CA3 network in vivo. *Nat. Neurosci.* 5, 790–795. doi: 10.1038/nn887

Herreras, O., Solis, J. M., Munoz, M. D., Martin Del Rio, R., and Lerma, J. (1988). Sensory modulation of hippocampal transmission. I. Opposite effects on CA1 and dentate gyrus synapsis. *Brain Res.* 461, 290–302. doi: 10.1016/0006-8993(88)90259-4

Ho, M. T., Pelkey, K. A., Topolnik, L., Petralia, R. S., Takamiya, K., Xia, J., et al. (2007). Developmental expression of Ca2+-permeable AMPA receptors underlies depolarization-induced long-term depression at mossy fiber CA3 pyramid synapses. *J. Neurosci.* 27, 11651–11662. doi: 10.1523/jneurosci.2671-07.2007

Hunt, D. L., Puente, N., Grandes, P., and Castillo, P. E. (2013). Bidirectional NMDA receptor plasticity controls CA3 output and heterosynaptic metaplasticity. *Nat. Neurosci.* 16, 1049–1059. doi: 10.1038/nn.3461

Isomura, Y., Sirota, A., Ozen, S., Montgomery, S., Mizuseki, K., Henze, D. A., et al. (2006). Integration and segregation of activity in entorhinal-hippocampal subregions by neocortical slow oscillations. *Neuron* 52, 871–882. doi: 10.1016/j.neuron.2006.10.023

Ito, I., and Sugiyama, H. (1991). Roles of glutamate receptors in long-term potentiation at hippocampal mossy fiber synapses. *Neuroreport* 2, 333–336. doi: 10.1097/00001756-199106000-00008

Jonas, P., Bischofberger, J., Fricker, D., and Miles, R. (2004). Interneuron Diversity series: fast in, fast out–temporal and spatial signal processing in hippocampal interneurons. *Trends Neurosci.* 27, 30–40. doi: 10.1016/j.tins.2003.10.010

Jonas, P., Major, G., and Sakmann, B. (1993). Quantal components of unitary EPSCs at the mossy fibre synapse on CA3 pyramidal cells of rat hippocampus. *J. Physiol.* 472, 615–663.

Jung, M. W., and Mcnaughton, B. L. (1993). Spatial selectivity of unit activity in the hippocampal granular layer. *Hippocampus* 3, 165–182. doi: 10.1002/hipo.450030209

Kamboj, S. K., Swanson, G. T., and Cull-Candy, S. G. (1995). Intracellular spermine confers rectification on rat calcium-permeable AMPA and kainate receptors. *J. Physiol.* 486(Pt. 2), 297–303.

Kamiya, H., and Ozawa, S. (1999). Dual mechanism for presynaptic modulation by axonal metabotropic glutamate receptor at the mouse mossy fibre-CA3 synapse. *J. Physiol.* 518(Pt. 2), 497–506. doi: 10.1111/j.1469-7793.1999.0497p.x

Kapur, A., Yeckel, M. F., Gray, R., and Johnston, D. (1998). L-Type calcium channels are required for one form of hippocampal mossy fiber LTP. *J. Neurophysiol.* 79, 2181–2190.

Kapur, A., Yeckel, M., and Johnston, D. (2001). Hippocampal mossy fiber activity evokes Ca2+ release in CA3 pyramidal neurons via a metabotropic glutamate receptor pathway. *Neuroscience* 107, 59–69. doi: 10.1016/s0306-4522(01)00293-7

Kobayashi, K., Manabe, T., and Takahashi, T. (1996). Presynaptic long-term depression at the hippocampal mossy fiber-CA3 synapse. *Science* 273, 648–650. doi: 10.1126/science.273.5275.648

Koh, D. S., Burnashev, N., and Jonas, P. (1995). Block of native Ca(2+)-permeable AMPA receptors in rat brain by intracellular polyamines generates double rectification. *J. Physiol.* 486(Pt. 2), 305–312.

Kwon, H. B., and Castillo, P. E. (2008a). Long-term potentiation selectively expressed by NMDA receptors at hippocampal mossy fiber synapses. *Neuron* 57, 108–120. doi: 10.1016/j.neuron.2007.11.024

Kwon, H. B., and Castillo, P. E. (2008b). Role of glutamate autoreceptors at hippocampal mossy fiber synapses. *Neuron* 60, 1082–1094. doi: 10.1016/j.neuron.2008.10.045

Lanthorn, T. H., Ganong, A. H., and Cotman, C. W. (1984). 2-Amino-4-phosphonobutyrate selectively blocks mossy fiber-CA3 responses in guinea pig but not rat hippocampus. *Brain Res.* 290, 174–178. doi: 10.1016/0006-8993(84)90750-9

Lauri, S. E., Bortolotto, Z. A., Bleakman, D., Ornstein, P. L., Lodge, D., Isaac, J. T., et al. (2001). A critical role of a facilitatory presynaptic kainate receptor in mossy fiber LTP. *Neuron* 32, 697–709. doi: 10.1016/s0896-6273(01)00511-6

Lauri, S. E., Bortolotto, Z. A., Nistico, R., Bleakman, D., Ornstein, P. L., Lodge, D., et al. (2003). A role for Ca2+ stores in kainate receptor-dependent synaptic facilitation and LTP at mossy fiber synapses in the hippocampus. *Neuron* 39, 327–341. doi: 10.1016/s0896-6273(03)00369-6

Lawrence, J. J., and McBain, C. J. (2003). Interneuron diversity series: containing the detonation–feedforward inhibition in the CA3 hippocampus. *Trends Neurosci.* 26, 631–640. doi: 10.1016/j.tins.2003.09.007

Lawrence, J. J., Grinspan, Z. M., and Mcbain, C. J. (2004). Quantal transmission at mossy fibre targets in the CA3 region of the rat hippocampus. *J. Physiol.* 554, 175–193. doi: 10.1113/jphysiol.2003.049551

Lee, N., Jansen, J., Aspegren, H., Henze, M., Nielsen, P. H., and Wagner, M. (2002). Population dynamics in wastewater treatment plants with enhanced biological phosphorus removal operated with and without nitrogen removal. *Water Sci. Technol.* 46, 163–170.

Lei, S., and Mcbain, C. J. (2002). Distinct NMDA receptors provide differential modes of transmission at mossy fiber-interneuron synapses. *Neuron* 33, 921–933. doi: 10.1016/s0896-6273(02)00608-6

Lei, S., and Mcbain, C. J. (2004). Two Loci of expression for long-term depression at hippocampal mossy fiber-interneuron synapses. *J. Neurosci.* 24, 2112–2121. doi: 10.1523/jneurosci.4645-03.2004

Littleton, J. T. (2006). Mixing and matching during synaptic vesicle endocytosis. *Neuron* 51, 149–151. doi: 10.1016/j.neuron.2006.07.002

Leutgeb, J. K., Leutgeb, S., Moser, M. B., and Moser, E. I. (2007). Pattern separation in the dentate gyrus and CA3 of the hippocampus. *Science* 315, 961–966. doi: 10.1126/science.1135801

Luthi, A., Chittajallu, R., Duprat, F., Palmer, M. J., Benke, T. A., Kidd, F. L., et al. (1999). Hippocampal LTD expression involves a pool of AMPARs regulated by the NSF-GluR2 interaction. *Neuron* 24, 389–399. doi: 10.1016/s0896-6273(00)80852-1

Maccaferri, G., and Dingledine, R. (2002). Control of feedforward dendritic inhibition by NMDA receptor-dependent spike timing in hippocampal interneurons. *J. Neurosci.* 22, 5462–5472.

Maccaferri, G., Toth, K., and Mcbain, C. J. (1998). Target-specific expression of presynaptic mossy fiber plasticity. *Science* 279, 1368–1370. doi: 10.1126/science.279.5355.1368

Manzoni, O. J., Castillo, P. E., and Nicoll, R. A. (1995). Pharmacology of metabotropic glutamate receptors at the mossy fiber synapses of the guinea pig hippocampus. *Neuropharmacology* 34, 965–971. doi: 10.1016/0028-3908(95)00060-j

McBain, C. J. (2008). Differential mechanisms of transmission and plasticity at mossy fiber synapses. *Prog. Brain Res.* 169, 225–240. doi: 10.1016/s0079-6123(07)00013-1

Min, M. Y., Rusakov, D. A., and Kullmann, D. M. (1998). Activation of AMPA, kainate and metabotropic receptors at hippocampal mossy fiber synapses: role of glutamate diffusion. *Neuron* 21, 561–570. doi: 10.1016/s0896-6273(00)80566-8

Mistry, R., Dennis, S., Frerking, M., and Mellor, J. R. (2011). Dentate gyrus granule cell firing patterns can induce mossy fiber long-term potentiation in vitro. *Hippocampus* 21, 1157–1168. doi: 10.1002/hipo.20815

Miyazaki, K., Ishizuka, T., and Yawo, H. (2005). Synapse-to-synapse variation of calcium channel subtype contributions in large mossy fiber terminals of mouse hippocampus. *Neuroscience* 136, 1003–1014. doi: 10.1016/j.neuroscience.2005.08.049

Neuman, R. S., Ben-Ari, Y., Gho, M., and Cherubini, E. (1988). Blockade of excitatory synaptic transmission by 6-cyano-7-nitroquinoxaline-2,3-dione (CNQX) in the hippocampus in vitro. *Neurosci. Lett.* 92, 64–68. doi: 10.1016/0304-3940(88)90743-4

Nicoll, R. A., and Schmitz, D. (2005). Synaptic plasticity at hippocampal mossy fibre synapses. *Nat. Rev. Neurosci.* 6, 863–876. doi: 10.1038/nrn1786

Pelkey, K. A., Lavezzari, G., Racca, C., Roche, K. W., and Mcbain, C. J. (2005). mGluR7 is a metaplastic switch controlling bidirectional plasticity of feedforward inhibition. *Neuron* 46, 89–102. doi: 10.1016/j.neuron.2005.02.011

Pelkey, K. A., Topolnik, L., Lacaille, J. C., and Mcbain, C. J. (2006). Compartmentalized Ca(2+) channel regulation at divergent mossy-fiber release sites underlies target cell-dependent plasticity. *Neuron* 52, 497–510. doi: 10.1016/j.neuron.2006.08.032

Pelkey, K. A., Topolnik, L., Yuan, X. Q., Lacaille, J. C., and Mcbain, C. J. (2008). State-dependent cAMP sensitivity of presynaptic function underlies metaplasticity in a hippocampal feedforward inhibitory circuit. *Neuron* 60, 980–987. doi: 10.1016/j.neuron.2008.11.018

Rebola, N., Carta, M., Lanore, F., Blanchet, C., and Mulle, C. (2011). NMDA receptor-dependent metaplasticity at hippocampal mossy fiber synapses. *Nat. Neurosci.* 14, 691–693. doi: 10.1038/nn.2809

Rebola, N., Lujan, R., Cunha, R. A., and Mulle, C. (2008). Adenosine A2A receptors are essential for long-term potentiation of NMDA-EPSCs at hippocampal mossy fiber synapses. *Neuron* 57, 121–134. doi: 10.1016/j.neuron.2007.11.023

Rebola, N., Sachidhanandam, S., Perrais, D., Cunha, R. A., and Mulle, C. (2007). Short-term plasticity of kainate receptor-mediated EPSCs induced by NMDA receptors at hippocampal mossy fiber synapses. *J. Neurosci.* 27, 3987–3993. doi: 10.1523/jneurosci.5182-06.2007

Regehr, W. G., Delaney, K. R., and Tank, D. W. (1994). The role of presynaptic calcium in short-term enhancement at the hippocampal mossy fiber synapse. *J. Neurosci.* 14, 523–537.

Reid, C. A., Dixon, D. B., Takahashi, M., Bliss, T. V., and Fine, A. (2004). Optical quantal analysis indicates that long-term potentiation at single hippocampal mossy fiber synapses is expressed through increased release probability, recruitment of new release sites and activation of silent synapses. *J. Neurosci.* 24, 3618–3626. doi: 10.1523/jneurosci.3567-03.2004

Rollenhagen, A., and Lubke, J. H. (2010). The mossy fiber bouton: the "common" or the "unique" synapse? *Front. Synaptic Neurosci.* 2:2. doi: 10.3389/fnsyn.2010.00002

Rollenhagen, A., Satzler, K., Rodriguez, E. P., Jonas, P., Frotscher, M., and Lubke, J. H. (2007). Structural determinants of transmission at large hippocampal mossy fiber synapses. *J. Neurosci.* 27, 10434–10444. doi: 10.1523/jneurosci.1946-07.2007

Ryan, T. A. (2006). A pre-synaptic to-do list for coupling exocytosis to endocytosis. *Curr. Opin. Cell Biol.* 18, 416–421. doi: 10.1016/j.ceb.2006.06.013

Sachidhanandam, S., Blanchet, C., Jeantet, Y., Cho, Y. H., and Mulle, C. (2009). Kainate receptors act as conditional amplifiers of spike transmission at hippocampal mossy fiber synapses. *J. Neurosci.* 29, 5000–5008. doi: 10.1523/JNEUROSCI.5807-08.2009

Salin, P. A., Scanziani, M., Malenka, R. C., and Nicoll, R. A. (1996). Distinct short-term plasticity at two excitatory synapses in the hippocampus. *Proc. Natl. Acad. Sci. U S A* 93, 13304–13309. doi: 10.1073/pnas.93.23.13304

Schmitz, D., Mellor, J., and Nicoll, R. A. (2001). Presynaptic kainate receptor mediation of frequency facilitation at hippocampal mossy fiber synapses. *Science* 291, 1972–1976. doi: 10.1126/science.1057105

Scott, R., and Rusakov, D. A. (2006). Main determinants of presynaptic Ca2+ dynamics at individual mossy fiber-CA3 pyramidal cell synapses. *J. Neurosci.* 26, 7071–7081. doi: 10.1523/jneurosci.0946-06.2006

Scott, R., Lalic, T., Kullmann, D. M., Capogna, M., and Rusakov, D. A. (2008). Target-cell specificity of kainate autoreceptor and Ca2+-store-dependent short-term plasticity at hippocampal mossy fiber synapses. *J. Neurosci.* 28, 13139–13149. doi: 10.1523/JNEUROSCI.2932-08.2008

Shigemoto, R., Kinoshita, A., Wada, E., Nomura, S., Ohishi, H., Takada, M., et al. (1997). Differential presynaptic localization of metabotropic glutamate receptor subtypes in the rat hippocampus. *J. Neurosci.* 17, 7503–7522.

Shimizu, H., Fukaya, M., Yamasaki, M., Watanabe, M., Manabe, T., and Kamiya, H. (2008). Use-dependent amplification of presynaptic Ca2+ signaling by axonal ryanodine receptors at the hippocampal mossy fiber synapse. *Proc. Natl. Acad. Sci. U S A* 105, 11998–12003. doi: 10.1073/pnas.0802175105

Skaggs, W. E., Mcnaughton, B. L., Wilson, M. A., and Barnes, C. A. (1996). Theta phase precession in hippocampal neuronal populations and the compression of temporal sequences. *Hippocampus* 6, 149–172. doi: 10.1002/(sici)1098-1063(1996)6:2<149::aid-hipo6>3.0.co;2-k

Torborg, C. L., Nakashiba, T., Tonegawa, S., and Mcbain, C. J. (2010). Control of CA3 output by feedforward inhibition despite developmental changes in the excitation-inhibition balance. *J. Neurosci.* 30, 15628–15637. doi: 10.1523/JNEUROSCI.3099-10.2010

Toth, K., and Mcbain, C. J. (1998). Afferent-specific innervation of two distinct AMPA receptor subtypes on single hippocampal interneurons. *Nat. Neurosci.* 1, 572–578. doi: 10.1038/2807

Toth, K., and Mcbain, C. J. (2000). Target-specific expression of pre- and postsynaptic mechanisms. *J Physiol.* 525(Pt. 1), 41–51. doi: 10.1111/j.1469-7793.2000.00041.x

Toth, K., Suares, G., Lawrence, J. J., Philips-Tansey, E., and Mcbain, C. J. (2000). Differential mechanisms of transmission at three types of mossy fiber synapse. *J. Neurosci.* 20, 8279–8289.

Tzounopoulos, T., Janz, R., Sudhof, T. C., Nicoll, R. A., and Malenka, R. C. (1998). A role for cAMP in long-term depression at hippocampal mossy fiber synapses. *Neuron* 21, 837–845. doi: 10.1016/s0896-6273(00)80599-1

Urban, N. N., and Barrionuevo, G. (1996). Induction of hebbian and non-hebbian mossy fiber long-term potentiation by distinct patterns of high-frequency stimulation. *J. Neurosci.* 16, 4293–4299.

Vignes, M., and Collingridge, G. L. (1997). The synaptic activation of kainate receptors. *Nature* 388, 179–182. doi: 10.1038/40639

Villacres, E. C., Wong, S. T., Chavkin, C., and Storm, D. R. (1998). Type I adenylyl cyclase mutant mice have impaired mossy fiber long-term potentiation. *J. Neurosci.* 18, 3186–3194.

von Kitzing, E., Jonas, P., and Sakmann, B. (1994). Quantal analysis of excitatory postsynaptic currents at the hippocampal mossy fiber-CA3 pyramidal cell synapse. *Adv. Second Messenger Phosphoprotein Res.* 29, 235–260. doi: 10.1016/s1040-7952(06)80019-4

Walker, H. C., Lawrence, J. J., and Mcbain, C. J. (2002). Activation of kinetically distinct synaptic conductances on inhibitory interneurons by electrotonically overlapping afferents. *Neuron* 35, 161–171. doi: 10.1016/s0896-6273(02)00734-1

Wang, J., Yeckel, M. F., Johnston, D., and Zucker, R. S. (2004). Photolysis of postsynaptic caged Ca2+ can potentiate and depress mossy fiber synaptic responses in rat hippocampal CA3 pyramidal neurons. *J. Neurophysiol.* 91, 1596–1607. doi: 10.1152/jn.01073.2003

Weisskopf, M. G., and Nicoll, R. A. (1995). Presynaptic changes during mossy fibre LTP revealed by NMDA receptor-mediated synaptic responses. *Nature* 376, 256–259. doi: 10.1038/376256a0

Weisskopf, M. G., Castillo, P. E., Zalutsky, R. A., and Nicoll, R. A. (1994). Mediation of hippocampal mossy fiber long-term potentiation by cyclic AMP. *Science* 265, 1878–1882. doi: 10.1126/science.7916482

Yamamoto, C., Matsumoto, K., and Takagi, M. (1980). Potentiation of excitatory postsynaptic potentials during and after repetitive stimulation in thin hippocampal sections. *Exp. Brain Res.* 38, 469–477. doi: 10.1007/bf00237528

Yamamoto, C., Sawada, S., and Kamiya, H. (1992). Enhancement of postsynaptic responsiveness during long-term potentiation of mossy fiber synapses in guinea pig hippocampus. *Neurosci. Lett.* 138, 111–114. doi: 10.1016/0304-3940(92)90484-o

Yeckel, M. F., Kapur, A., and Johnston, D. (1999). Multiple forms of LTP in hippocampal CA3 neurons use a common postsynaptic mechanism. *Nat. Neurosci.* 2, 625–633. doi: 10.1038/10180

Yoshino, M., Sawada, S., Yamamoto, C., and Kamiya, H. (1996). A metabotropic glutamate receptor agonist DCG-IV suppresses synaptic transmission at mossy

fiber pathway of the guinea pig hippocampus. *Neurosci. Lett.* 207, 70–72. doi: 10.1016/0304-3940(96)12486-1

Zalutsky, R. A., and Nicoll, R. A. (1990). Comparison of two forms of long-term potentiation in single hippocampal neurons. *Science* 248, 1619–1624. doi: 10.1126/science.2114039

Zalutsky, R. A., and Nicoll, R. A. (1992). Mossy fiber long-term potentiation shows specificity but no apparent cooperativity. *Neurosci. Lett.* 138, 193–197. doi: 10.1016/0304-3940(92)90503-y

Conflict of Interest Statement: The authors declare that the research was conducted in the absence of any commercial or financial relationships that could be construed as a potential conflict of interest.

Received: 14 November 2013; accepted: 20 January 2014; published online: 04 February 2014.

Citation: Evstratova A and Tóth K (2014) Information processing and synaptic plasticity at hippocampal mossy fiber terminals. Front. Cell. Neurosci. ***8****:28. doi: 10.3389/fncel.2014.00028*

This article was submitted to the journal Frontiers in Cellular Neuroscience.

frontiers in
CELLULAR NEUROSCIENCE

REVIEW ARTICLE
published: 08 January 2014
doi: 10.3389/fncel.2013.00262

Recurrent synapses and circuits in the CA3 region of the hippocampus: an associative network

Caroline Le Duigou, Jean Simonnet, Maria T. Teleñczuk, Desdemona Fricker and Richard Miles*

Centre de Recherche de l'Institut du Cerveau et de la Moelle, INSERM U975, CHU Pitié-Salpêtrière, Université Pierre et Marie Curie, Paris, France

Edited by:
Enrico Cherubini, International School for Advanced Studies, Italy

Reviewed by:
Dominique Debanne, Aix-Marseille, France
Katalin Toth, Universite Laval, Canada

****Correspondence:***
Richard Miles, Centre de Recherche de l'Institut du Cerveau et de la Moelle, INSERM U975, CHU Pitié-Salpêtrière, Université Pierre et Marie Curie, 47 Boulevard de l'Hôpital, Paris 75013, France
e-mail: richard.miles@upmc.fr

In the CA3 region of the hippocampus, pyramidal cells excite other pyramidal cells and interneurons. The axons of CA3 pyramidal cells spread throughout most of the region to form an associative network. These connections were first drawn by Cajal and Lorente de No. Their physiological properties were explored to understand epileptiform discharges generated in the region. Synapses between pairs of pyramidal cells involve one or few release sites and are weaker than connections made by mossy fibers on CA3 pyramidal cells. Synapses with interneurons are rather effective, as needed to control unchecked excitation. We examine contributions of recurrent synapses to epileptiform synchrony, to the genesis of sharp waves in the CA3 region and to population oscillations at theta and gamma frequencies. Recurrent connections in CA3, as other associative cortices, have a lower connectivity spread over a larger area than in primary sensory cortices. This sparse, but wide-ranging connectivity serves the functions of an associative network, including acquisition of neuronal representations as activity in groups of CA3 cells and completion involving the recall from partial cues of these ensemble firing patterns.

Keywords: CA3, recurrent, synapse, circuit, hippocampus, associative

RECURRENT EXCITATORY SYNAPSES BETWEEN CA3 CELLS: EMERGENCE

Recurrent connections between CA3 cells in the hippocampus can be seen in early drawings of Golgi stained neurons. Schaffer (1892) and Ramón y Cajal (1899) drew pyramidal cell processes that ramify extensively in the CA3 region as well as projecting into CA1. Later, but still before cellular physiology, Lorente de Nó (1934) drew axonal terminals of a CA3 cell contacting mid-apical dendrites of a nearby pyramidal cell and a basket cell (**Figure 1**). So a basis for recurrent excitation existed before synaptic operations were fully accepted. The absence of this detail did not impede speculation. Recurrent connections between cells of the same region were linked to feedback in chains of connected neurons. Lorente de No (1938) and later Hebb (1949) proposed they might generate reverberating neuronal discharges as an immediate electrical memory.

Intracellular electrophysiology began for the hippocampus with the work of Spencer and Kandel. Initial results dampened the excitation somewhat. They showed that stimulating CA3 cell axons induced dominant inhibitory actions mediated by pyramidal cell excitation of interneurons (Spencer and Kandel, 1961). However recurrent actions were soon linked to reverberation and epileptic synchrony (Kandel and Spencer, 1961). This link was later strengthened by work on epileptiform synchrony induced by penicillin an early antagonist of inhibitory synaptic actions (Lebovitz et al., 1971). Explicitly combining computer simulations and *in vitro* physiology, Traub and Wong (1982) and Wong and Traub (1983) showed how recurrent excitatory synapses might underly delayed all-or-nothing population bursts induced by disinhibition. Physiological support for recurrent synaptic actions came from records of synaptic interactions between CA3 pyramidal cells in slices (Miles and Wong, 1986). Recurrent synapses together with the modeling work could explain the unexpected finding that stimulating a single cell could initiate interictal-like bursts of much larger neuronal populations (Miles and Wong, 1983).

AXONAL DISTRIBUTIONS OF CA3 PYRAMIDAL CELLS

Axons of single CA3 pyramidal cells of the rat (**Figure 1**) and guinea-pig have been traced from neurons filled with biocytin or horseradish peroxidase (Ishizuka et al., 1990; Sik et al., 1993; Li et al., 1994; Wittner et al., 2006a; Wittner and Miles, 2007). Before projecting out of the region, axons ramify in stratum oriens and radiatum of CA3 contacting apical and basilar dendrites of other pyramidal cells as well as interneurons. Typically they divide into 5–10 collaterals projecting in different directions but rarely returning towards their parent neuron. Longitudinal projections of single axons (Lorente de Nó, 1934) can extend for ∼70% of the dorso-ventral extent of rodent hippocampus (Sik et al., 1993; Li et al., 1994). A significant proportion of synapses made by a CA3 pyramidal cell may contact other CA3 cells. The Li et al. (1994) estimated 30–70%. Other connections are made onto CA1 neurons, while there is also a strong commissural projection.

The total axonal length of well-filled CA3 pyramidal cell arbors is estimated as 150–300 mm in the rat with about 30% of the ramification within CA3 (Ishizuka et al., 1990; Li et al., 1994). Terminals are present along all of this distance and a single pyramidal cell is estimated to form 30,000 to 60,000 terminals. Terminals have been thought to target pyramidal cells and interneurons with a frequency similar to the presence of these neuronal types. Recent data suggest some interneuron subtypes may be selectively innervated (Wittner et al., 2006b).

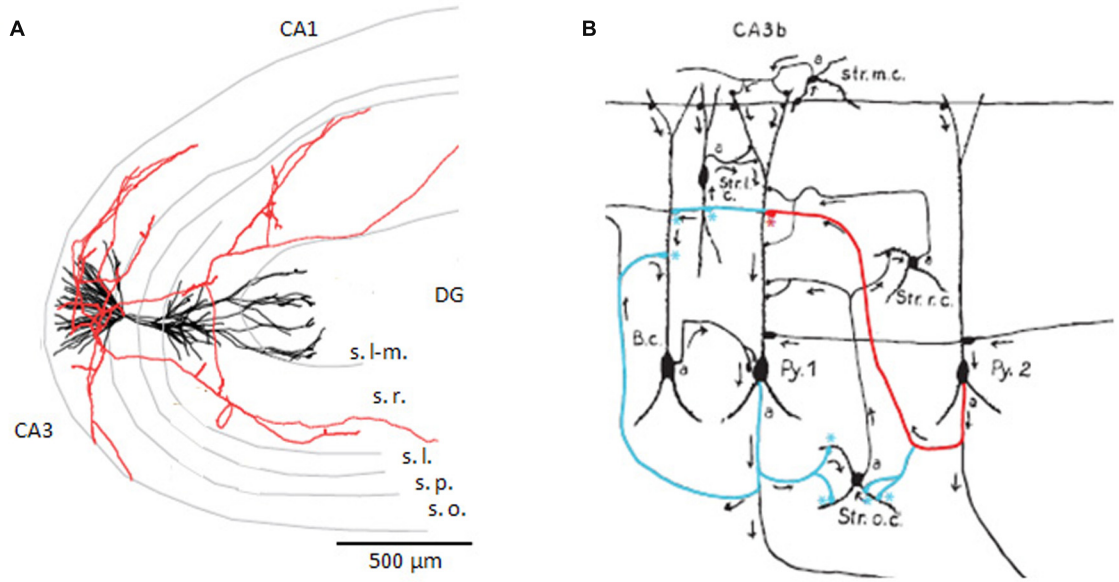

FIGURE 1 | CA3 pyramidal cell axon and targets. (A) Reconstruction of a CA3 pyramidal cell dendrites, in black, and partial reconstruction of the axon, in red. Adapted from a cell filled by Ishizuka et al. (1995; published as cell c12866 on neuromorpho.org). The CA3, CA1, and dentate gyrus (DG) regions are indicated as are the layers lacunosum-moleculare (s. l-m.), radiatum (s. r.), lucidum (s.l.), pyramidale (s.p.), and oriens (s.o.). **(B)** Drawing of putative axo-dendritic connexions between pyramidal cells (Py. 1 and 2) and interneurons with somata in different layers (B.c., Str. o.c., Str. r.c., Str. l.c., Str. m.c.). The axon of Py. 2 may contact the dendrites of Py. 1, in red, and the interneuron of stratum oriens, in blue. The axon of Py. 1 is drawn contacting the basket cell, in blue (drawing adapted from Lorente de Nó, 1934).

Intra-regional differences exist: CA3b pyramidal cells tend to innervate targets in stratum oriens and radiatum about equally, while CA3a pyramidal cell axons target stratum oriens targets more than those in stratum radiatum (Wittner and Miles, 2007).

CA3 PYRAMIDAL CELL AXON PHYSIOLOGY

Axon collaterals of CA3 pyramidal cells are un-myelinated. They include Schaffer collaterals that project to CA1 as well as those that ramify within the CA3 region. Action potentials are initiated at ∼30–40 µm from the soma, where sodium (Na) channel density reaches a peak according to physiology and immunostaining (Meeks and Mennerick, 2007). In regions beyond the action potential initiation site, recurrent axons of CA3 pyramidal cells conduct at velocities of 0.2–0.4 mm/ms (Soleng et al., 2003b; Meeks and Mennerick, 2007).

The Na channels expressed by CA3 recurrent collaterals seem likely to be Nav1.2 and Nav1.6 (Royeck et al., 2008; Debanne et al., 2011). These axons express multiple voltage-gated potassium (K) channels including Kv1.1, Kv1.2, and Kv1.4 (Lorincz and Nusser, 2008), ID (Saviane et al., 2003) the M-channel (Kv7/KCNQ Vervaeke et al., 2006), and the hyperpolarization activated h-current (Soleng et al., 2003a). This diversity of channel expression provides multiple means to modulate action potential shape and so control transmitter release (Bischofberger et al., 2006). Action potential modulation by axonal K-channels may become a total suppression of transmission when an IA-like K-current is fully activated (Debanne et al., 1997; Kopysova and Debanne, 1998).

CA3 PYRAMIDAL CELL TERMINALS: NUMBERS, FORM, CONTENTS, CHANNELS AND RELEASE

Varicosities are formed at distances of 2–5 µm all along CA3 recurrent axons. They often have an ovoid form of diameter ∼0.4 µm compared to an axonal diameter of ∼0.2 µm (Sik et al., 1993; Li et al., 1994; Wittner and Miles, 2007). Electron microscopy (EM; **Figure 2**) indicates they possess attributes of pre-synaptic boutons with active zones and synaptic vesicles and they face densities at post-synaptic sites (Schikorski and Stevens, 1997; Shepherd and Harris, 1998; Holderith et al., 2012). While varicosities may contain up to three to four active sites, typically they have just one. Synaptic vesicles in recurrent terminals have diameters of 20–40 nm. A terminal may contain up to 800 vesicles with a mean number of 150–270 vesicles.

A small proportion of vesicles are so close (∼5 nm) to pre-synaptic membrane that they are considered to be "docked" or available for release. The number of docked vesicles is estimated at 1–15 per terminal (Schikorski and Stevens, 1997; Shepherd and Harris, 1998; Holderith et al., 2012). Vesicles in terminals of CA3 pyramidal cell axons express the transporters, VGLUT1 and 2, and so presumably contain glutamate (Herzog et al., 2006). EM studies on CA3 axon terminals have not revealed a distinct population of large dense-core vesicles, which might contain peptides or other co-transmitters. About half of recurrent terminals contain one mitochondrion (Shepherd and Harris, 1998) and smooth endoplasmic reticulum is typically present: both organelles contribute to calcium (Ca) homeostasis (Sheng and Cai, 2012).

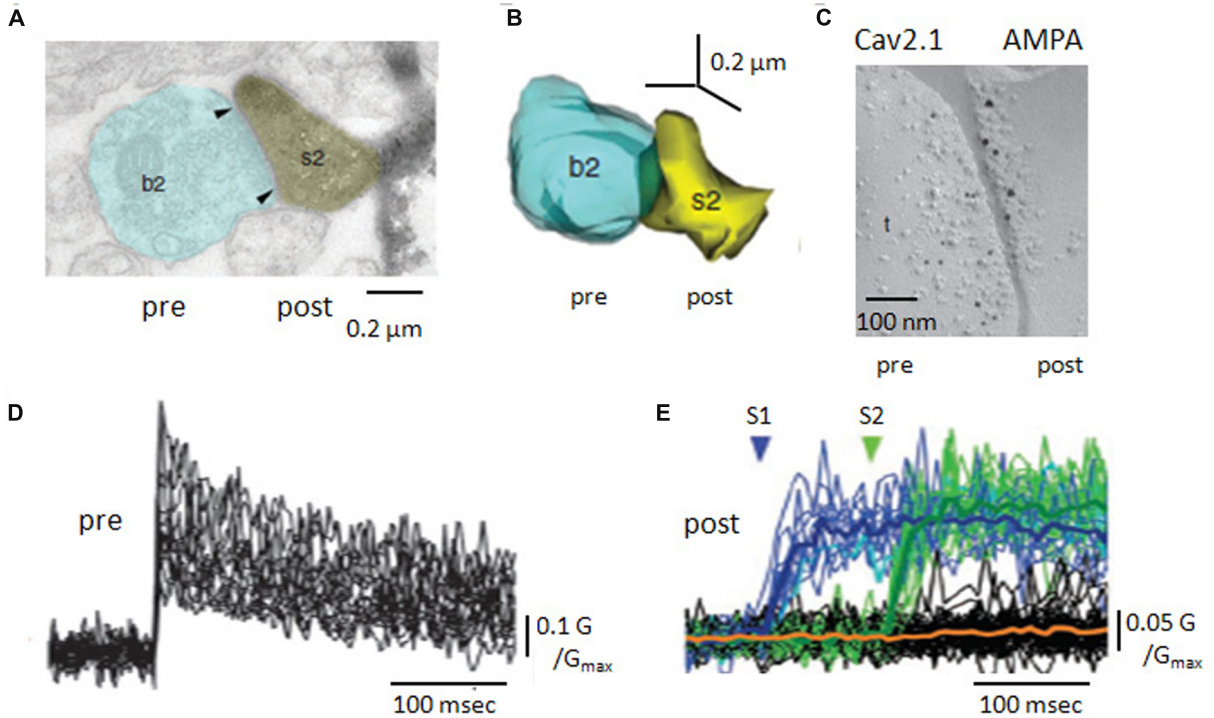

FIGURE 2 | Anatomy and Ca handling at recurrent synapses between CA3 pyramidal cells. (A) Electron microscopy of a recurrent terminal, b2, apposed to a CA3 pyramidal cell dendritic spine, s2. **(B)** Three-dimensional reconstruction of the contact. The area of the active zone [arrows in **(A)**] was 0.10 μm^2. **(C)** Double immuno-staining of SDS-digested freeze fracture replica of a recurrent synapse. The smaller gold particles label Cav2.1 molecules (pre) and the larger gold particles recognize a pan-AMPA antibody (post). **(D)** Pre-synaptic Ca transients, measured as changes in fluorescent intensity, for 25 axon terminals of a CA3 pyramidal cell. **(E)** Post-synaptic Ca transients, in response to two pre-synaptic stimuli. Note the occurrence of failures in both post-synaptic responses but their absence from pre-synaptic signals (adapted with permission from Holderith et al., 2012).

Ca entry into presynaptic terminals triggers transmitter release. CA3 axonal terminals express multiple Ca channel subtypes including Cav2.1, Cav2.2, Cav2.3 (Holderith et al., 2012), as do the mossy fiber terminals that also terminate on CA3 pyramidal cells (Li et al., 2007). Freeze-fracture replica gold immuno-labeling (**Figure 2**) suggests a single terminal expresses several tens of Cav2.1 channels (Holderith et al., 2012). This is more, but not many more, than estimates of the number of Ca-channels needed to trigger release from hippocampal inhibitory terminals (Bucurenciu et al., 2010). Possibly, an elevated Na channel density in terminals enhances Ca entry by boosting depolarization due to axonal spikes (Engel and Jonas, 2005). Certainly, recurrent terminals express various types of K channel which control transmitter release by limiting terminal depolarization. They may include the delayed rectifier type channels Kv1.1 and Kv1.2, the fast-inactivating A-type channel Kv1.4 (Debanne et al., 1997; Kopysova and Debanne, 1998; Lorincz and Nusser, 2008; Palani et al., 2010) as well as K-channels sensitive to both Ca and voltage (Saviane et al., 2003; Raffaelli et al., 2004) and the muscarine sensitive M-channel Kv7/KCNQ (Vervaeke et al., 2006).

Ca changes induced in local recurrent terminals by pyramidal cell firing have been resolved by imaging (Holderith et al., 2012; Sasaki et al., 2012). A single action potential induces a Ca signal of rise time less than 1 ms that decays over several 10 s of ms (**Figure 2**). Ca entry occurs without failure even if it varies between trials at the same terminal and Ca elevations at neighboring terminals are poorly correlated. For a given terminal, the mean amplitude of Ca-signals is better correlated with the area of the active zone than terminal volume (Holderith et al., 2012).

CA3 axon terminals express receptors for transmitters which modulate Ca entry or later steps in release processes (**Figure 2**). Receptors for the metabotropic glutamate receptor, mGluR7, expressed at active zones facing interneurons but not principal cells (Shigemoto et al., 1996) specifically control the excitation of inhibitory cells (Scanziani et al., 1998). The kainate receptor GluK1, reduces release by effects on both Ca entry and on G-protein mediated stages in transmitter release (Salmen et al., 2012). In contrast, presynaptic NMDA receptors enhance Ca entry and facilitate release at some synapses made by CA3 collaterals(McGuinness L et al., 2010).

PRE- MEETS POST: SYNAPSES MADE BY CA3 PYRAMIDAL CELLS WITH OTHER CA3 CELLS

When a single spike induces Ca entry into a CA3 axon terminal, one, or none, or several vesicles of the excitatory transmitter glutamate are liberated. Release fails, when Ca enters a terminal but no transmitter is liberated, as shown by imaging Ca-entry (**Figure 2**) via post-synaptic glutamate receptors (Koester

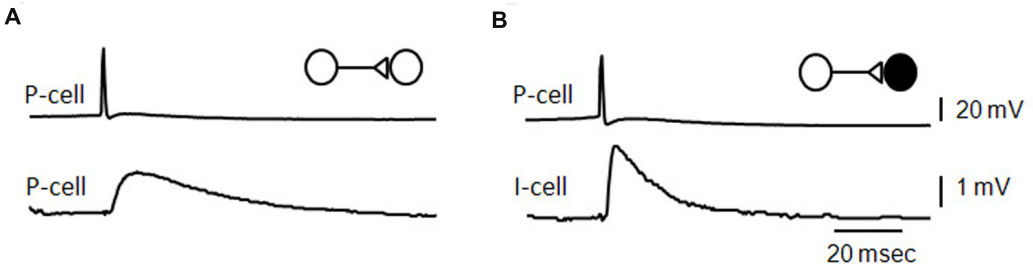

FIGURE 3 | Unitary effects of recurrent excitatory synapses. **(A)** Average of EPSPs initiated in a CA3 pyramidal cell by single action potentials in a pre-synaptic pyramidal cell **(B)**, average of EPSPs elicited in a fast-spiking CA3 interneuron by action potentials in a pyramidal cell [an unpublished data Miles and Wong **(B)** adapted from Miles, 1990].

and Johnston, 2005; Holderith et al., 2012). Multi-vesicular release following a single action potential is most convincingly demonstrated when two distinct post-synaptic events can be resolved in time, as at some inhibitory synapses in the cerebellum (Auger et al., 1998). Analysis of variations in synaptic events over a range of liberation probabilities supports multi-vesicular liberation (Conti and Lisman, 2003; Christie and Jahr, 2006).

Glutamate, released from a pre-synaptic terminal, binds to post-synaptic receptors. The number of receptors per site has been estimated with physiological, imaging, and anatomical techniques. Post-synaptic sites facing terminals of CA3 pyramidal cell axons in young animals, all express NMDA (*N*-methyl-D-aspartate) receptors (Takumi et al., 1999). Glutamate uncaging onto post-synaptic sites activates 3–10 NMDA receptors (Nimchinsky et al., 2004). Semi-quantitative immunostaining studies and imaging agree that about 30% of post-synaptic sites possess no AMPA (α-amino-3-hydroxy-5-methyl-4-isoxazolepropionic acid) receptors (Nusser et al., 1998; Takumi et al., 1999; Nimchinsky et al., 2004). At synapses where AMPA receptors are expressed, about 10 of them (**Figure 2**) are estimated to be activated after a single pre-synaptic spike in acute slices (Nimchinsky et al., 2004), 40–150 in culture (Matsuzaki et al., 2001). AMPA receptors are present at recurrent synapses with most types of interneuron (Nusser et al., 1998). NMDA receptors are less frequently expressed at synapses with interneurons and may be absent at contacts with fast-spiking, parvalbumin containing cells (Nyiri et al., 2003).

There are two other important differences between synapses made with interneurons and with pyramidal cells. First, recurrent contacts tend to innervate pyramidal cell spines, while those with most types of inhibitory cell innervate dendritic shafts (Gulyas et al., 1993; Freund and Buzsáki, 1996). Second, the AMPA receptor isoforms involved are different. AMPA receptor complexes at synapses formed with interneurons do not include the GluR2 subunit (Bochet et al., 1994; Geiger et al., 1995), resulting in faster kinetics (Miles, 1990), Ca-permeability, and a block by endogenous intraneuronal polyamines (Isaac, 2007).

PRE- MEETS POST IN DUAL RECORDS

Double records from pre- and post-synaptic neurones at recurrent synapses between CA3 cells were first made to prove their existence directly. They remain the most persuasive means to examine how one neuron influences another. They have permitted definition of the number of synaptic contacts involved in a unitary connection and assessment of variability and changes in synaptic efficacy (Debanne et al., 2008).

Records from pairs of CA3 pyramidal cells in acute slices (**Figure 3**) suggest one pyramidal cell excites 2–3% of possible pyramidal cell targets in a slice (Miles and Wong, 1986; Miles and Wong, 1987b). Odds are more favorable in organotypic slices. Connectivities are 30–60% (Debanne et al., 1995; Pavlidis and Madison, 1999). The number of release sites involved in a connection may also be higher in organotypic cultures. One to three contacts have been validated by EM for synapses between pyramidal cells and interneurons recorded and filled with biocytin in slices. In contrast, light microscopy suggests 14–19 putative contacts may be involved in connections between CA3 pyramidal cells in organotypic culture (Pavlidis and Madison, 1999).

The mean amplitude of synaptic potentials is about 1 mV at connections between pyramidal cells in acute slices (Miles and Wong, 1986) and in culture (Debanne et al., 1995). EPSPs induced in fast-spiking interneurons (**Figure 3**) are larger and faster than those initiated in pyramidal cells. Unitary synaptic current amplitude at connections made in culture can vary in the range 10–200 pA with an average near 30 pA (Pavlidis and Madison, 1999; Sasaki et al., 2012). In records from both acute slices and culture, events initiated successively at the same connection vary in amplitude. Transmission can fail, more often at connections with smaller averaged events. However pre-synaptic Ca entry never fails, even though it varies between successive action potentials (Holderith et al., 2012; Sasaki et al., 2012) and Ca signals are higher at terminals with a higher release probability (Koester and Johnston, 2005).

Synaptic events initiated sequentially at the same site vary in amplitude. This variability may have both pre- and post-synaptic components (Silver et al., 2003; Biró et al., 2005). Clear data on post-synaptic variability, is facilitated at connections with a single identified release site. At such a synapse, the variability in size of post-synaptic events was estimated at 20–50% (Gulyas et al., 1993). This variability might emerge from differences in the number of transmitter molecules released or in the activation of post-synaptic receptors.

The properties of recurrent synapses differ quite markedly from those of mossy fiber inputs, the other major source of excitation of CA3 pyramidal cells. A mossy fiber may make 10–20 connections with different CA3 pyramidal cells (Claiborne et al., 1986). A recurrent collateral makes several thousand contacts with a much larger target population. Mossy fiber boutons contact proximal apical dendrites of CA3 pyramidal cells and have a diameter of 4–8 μm. Each bouton may include 20–30 active zones, whereas a recurrent synapse may make one to three terminals on a post-synaptic cell. Finally mossy fibers contact apical dendrites near the CA3 soma, while recurrent synapses terminate at more distant dendritic sites resulting in smaller, slower somatic synaptic events. A mossy fiber input from one dentate granule cell can induce CA3 pyramidal cell firing and can so be termed a "detonator" synapse (Henze et al., 2002), whereas multiple spikes are needed to induce firing at recurrent synapses (Miles and Wong, 1987a).

SHORT-TERM AND LONG-TERM SYNAPTIC PLASTICITY IN DOUBLE RECORDINGS

Records from pre- and post-synaptic cells at recurrent synapses have offered novel insights into activity dependent changes in synaptic strength over times lasting from milliseconds to hours.

Short-term plasticity (milliseconds to seconds) results from at least two functionally opposing processes. First, a single spike may facilitate transmission when the same synapse is activated again (Ddel Castillo and Katz, 1954). An enhanced release probability over several tens of milliseconds is ascribed to a residual elevation of intra-terminal Ca (Holderith et al., 2012; Sasaki et al., 2012). Second, and inversely, depression may result if few vesicles are available for release (Schikorski and Stevens, 1997; Shepherd and Harris, 1998). If they are replaced slowly (Stevens and Tsujimoto, 1995; Staley et al., 1998) the probability of a second release may be reduced by depletion. Both processes occur at connections between CA3 pyramidal cells (Debanne et al., 1996; Pavlidis and Madison, 1999). When a first spike induces a large event, a second synaptic response tends to be smaller due to depletion. Inversely a second EPSP tends to be larger after a small first event due to the residual Ca enhancement of release probability. Reflecting the underlying mechanisms, facilitation is maximal at 20–70 ms and terminates at about 500 ms, while depression can take several seconds to recover completely.

Long-term plasticity (minutes to hours) at different synapses varies in mechanisms of induction and expression. One of the most studied forms, long-term synaptic potentiation at Schaffer collateral synapses made by CA3 pyramidal cells with CA1 cells, is induced via the activation of NMDA receptors and expressed as the post-synaptic recruitment of AMPA receptors (Kerchner and Nicoll, 2008). Long-term changes in synaptic efficacy seem to depend on similar mechanisms at recurrent synapses between CA3 pyramidal cells. Paired records from coupled CA3 cells have revealed some unitary details of this synaptic plasticity. The same connection can be potentiated or depotentiated (Debanne et al., 1998) by different temporal patterns of paired pre- and post-synaptic firing. About 20% of unitary interactions depend exclusively on NMDA receptors before potentiation (Montgomery et al., 2001), while both AMPA and NMDA receptors are activated after potentiation. Weak connections potentiate to a larger degree than initially strong connections (Debanne et al., 1999; Montgomery et al., 2001). Finally some connections between CA3 pyramidal cells do not seem to potentiate at all (Debanne et al., 1999; Montgomery and Madison, 2002).

TRANSMISSION OF RECURRENT EXCITATORY SIGNALS ON THE MEMBRANE OF A POST-SYNAPTIC CELL

Activation of membrane currents intrinsic to a post-synaptic cell by recurrent EPSPs affects how they sum, spread and eventually initiate firing. Initial evidence came from a prolongation of the decay of unitary EPSPs induced by pyramidal cell depolarization at subthreshold membrane potentials (Miles and Wong, 1986). In contrast unitary EPSPs initiated in fast-spiking inhibitory cells were not prolonged at depolarised subthreshold potentials (Miles, 1990). Work combining somatic records and synaptic stimuli with cell-attached records from dendrites, showed the activation of both inward currents, probably persistent Na channels, low-threshold Ca channels (Magee and Johnston, 1995), and outward currents, both inactivating and persistent (Hoffman et al., 1997). These currents have been more precisely described for EPSPs initiated by Schaffer collaterals (Lipowsky et al., 1996; Andreasen and Lambert, 1999; Perez-Rosello et al., 2011), as has evidence for a dendritic expression of the *I–h* current (Magee, 1999).

Distinct currents have been associated with specific effects on EPSP shape, summation, and spread. Na-channel activation near the peak of an EPSP tends to increase amplitude, while Ca-channels activated during the decay phase act to prolong EPSPs. The striking increase in dendritic expression of the *I–h* channel with distance from the soma (Lörincz et al., 2002) tends to equalize EPSPs impinging at proximal and distal sites (Magee, 1999). Dendritically expressed inactivating K-channels have been linked to less-than-linear summation of paired EPSPs impinging on different dendrites (Urban and Barrionuevo, 1998). Dual records from the soma and apical dendrites of CA3 pyramidal cells disclose two distinct regions of dendritic excitability (Kim et al., 2012). Fast Na-spikes are more easily initiated at distant sites corresponding to zones of recurrent synaptic inputs, while excitability of more proximal dendritic sites is lower.

The role of intrinsic currents in shaping interneuron EPSPs may be quite different to that in pyramidal cells. Simulated EPSPs induce purely inward currents in pyramidal cells but rather induce inward-outward current sequences in interneurons (Fricker and Miles, 2000). So, while, EPSPs in pyramidal cells are prolonged, EPSPs in interneurons may decay more rapidly due to the activation of an outward current at subthreshold potentials.

Synaptic inputs to a neuron are significant to surrounding cells when they initiate firing. Summed EPSPs initiated by repetitive firing of a single CA3 pyramidal cell sometimes induce cause a post-synaptic pyramidal cell to fire (Miles and Wong, 1986). Spike-to-spike latencies are 10–15 ms, consistent with a role for recurrent excitatory synapses in the genesis of delayed (50–100 ms) population bursts (Traub and Wong, 1982; de la Prida et al., 2006). Recent work suggests spike-to-spike transmission

may be limited to a few strong connections (Ikegaya et al., 2013).

Pyramidal cells induce interneuron firing more effectively and at shorter latencies of 1–3 ms (Miles, 1990; Csicsvari et al., 1998; Cohen and Miles, 2000). Interneuron EPSPs are larger and faster than recurrent EPSPs in pyramidal cells, and interneuron firing threshold is lower (**Figure 4**). When interneurons are excited to fire, pyramidal cells may trigger di-synaptic IPSPs (**Figure 4**) with high probability and considerable divergence (Miles, 1990; Csicsvari et al., 1998; Bazelot et al., 2010). While EPSP boosting mechanisms in interneuron dendrites are not clear, it is surprising that EPSPs induced from a single site (Gulyas et al., 1993) can induce firing. Even so, EPSP-spike coupling at single release site excitatory synapses with some cerebellar interneurons (Carter and Regehr, 2002) is also sufficiently strong that EPSPs control the timing of interneuron firing.

RECURRENT EXCITATORY CONTRIBUTIONS TO POPULATION ACTIVITIES IN THE CA3 REGION

Recurrent synapses transmit excitation from CA3 pyramidal cells to other pyramidal cells and to interneurons. They play a key role in operations and functions of the CA3 region, including the generation of physiological and pathological synchronous population activities.

INTERICTAL EPILEPTIFORM RHYTHM

A key finding linking recurrent excitation to epileptiform activity was that stimulating any afferent pathway induced epileptiform firing in CA3 (Ayala et al., 1973). Population bursts occurred with a variable delay of 20–100 ms after the afferent response. Traub and Wong (1982) suggested that during the delay recurrent synaptic interactions within the CA3 population generate a population synchrony. Synchrony induced in disinhibited slices is complete in that all neurons tend to fire together with a field potential decorated

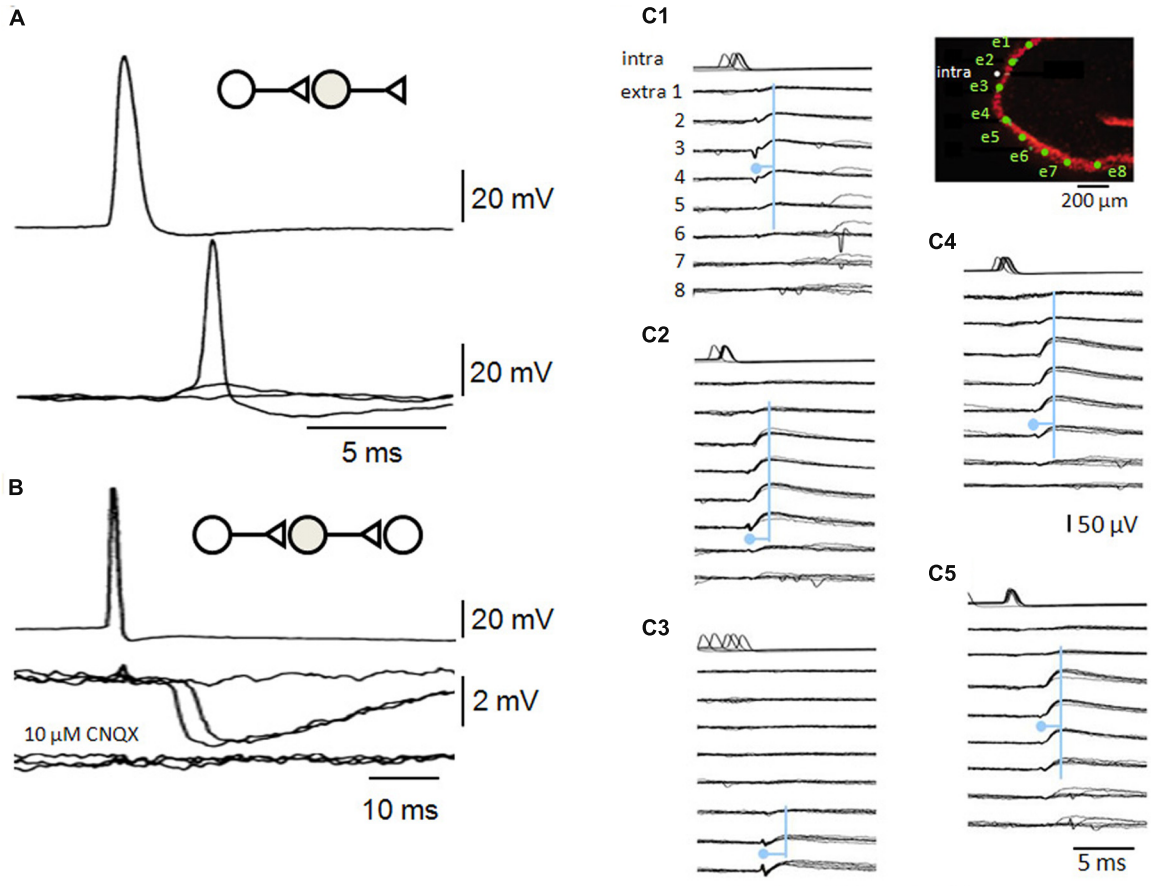

FIGURE 4 | Recurrent inhibitory circuits in the CA3 region. (A) Post-synaptic responses of a fast-spiking interneuron to single pre-synaptic action potentials in a CA3 pyramidal cell. Responses include a failure of transmission, an EPSP and an EPSP that initiates interneuron firing. **(B)** Di-synaptic inhibitory interactions between two CA3 pyramidal cells. Single action potentials in one cell induce IPSPs at variable latencies consistent with that of firing in **(A)**, as well as some failures. Di-synaptic IPSPs were suppressed by the glutamate receptor blocker CNQX. **(C)** A single pyramidal cell can initiate multiple di-synaptic IPSPs via firing in distinct interneurons. Records from a pyramidal cell (intra) and extracellular records from eight sites in st. pyramidale (extra 1–8, the diagram shows st. pyramidale in red and electrode sites in green). Field IPSPs were detected on electrodes 1–6 **(C1)**, 2–7 **(C2)**, 6–8 **(C3)**, 1–7 **(C4)**, and 2–6 **(C5)** repeatably following single action potentials (traces are aligned on six overlapping field IPSPs for each trace). Field IPSPs are preceded by extracellular action potentials of short duration on electrodes 2–3 **(C1)**, 6 **(C2)**, 7–8 **(C3)**, 6–7 **(C4)**, and 5–6 **(C5)**. The pyramidal cell may have initiated five distinct di-synaptic inhibitory interactions in these slice records (see Bazelot et al., 2010).

with high frequency oscillations (Jefferys et al., 2012). Traub and Wong suggested recurrent circuits should possess two properties to generate such an event. Recurrent contacts should be divergent and one cell could cause more than one target neuron to fire. These points were verified with the demonstration that some single pyramidal cells could induce or entrain inter-ictal-like events (Miles and Wong, 1983, 1986, 1987a; de la Prida et al., 2006). Disynaptic feedback inhibition via CA3 pyramidal cell excitation of feedback interneurons, was shown to prevent the spread of firing by recurrent excitatory pathways (Miles and Wong, 1986, 1987a,b).

Recurrent synaptic function controls several features of the epileptiform activity induced by disinhibition. The duration of the population burst (20–80 ms) has been shown to result from transmitter depletion (Staley et al., 1998). The delay from one burst to the next (1–10 s) depends on the time for docked vesicles to be replenished (Staley et al., 1998; Staley et al., 2001). Procedures that induce persistent synaptic changes have persistent effects on the strength and frequency of network burst firing (Bains et al., 1999; Behrens et al., 2005).

Cellular properties also affect disinhibition induced synchrony by controlling transmission in chains of connected neurons. In slices, population bursts tend to be initiated in the CA3a region, where cellular excitability and recurrent connectivity are high (Wittner and Miles, 2007). In CA3a, spontaneous events are preceded by a field potential of duration about 50 ms (Wittner and Miles, 2007) during which excitatory synaptic events occur with increasing frequency. This delay is similar to that between single cell firing and a population event (Miles and Wong, 1983; de la Prida et al., 2006). Modeling work suggested that during this time activity in the pyramidal cell population increases in non-linear fashion (Traub and Wong, 1982). An epileptiform burst occurs when population activity exceeds a threshold frequency (de la Prida et al., 2006).

SHARP-WAVE RHYTHM

Sharp waves (O'Keefe and Nadel, 1978; Buzsáki et al., 1992) are field potentials of duration 100–150 ms, corresponding to a partial neuronal synchrony during behaviors including immobility and slow wave sleep. They are initiated in the CA3 region (Csicsvari et al., 2000) and have been associated with the consolidation of acquired events (Girardeau et al., 2009; Jadhav et al., 2012) represented as firing in specific groups of neurons.

Both recurrent excitatory interactions and the actions of specific interneurons have been implicated in the genesis of sharp waves (Buzsáki et al., 1992; Csicsvari et al., 2000). Sharp wave fields are enhanced by inducing long-term changes at recurrent synapses (Behrens et al., 2005). And yet, sharp waves are not identical with epileptiform events and do not depend on recurrent excitation alone (Liotta et al., 2011). Repetitive firing of perisomatic interneurons may be a crucial element in sharp wave generation (Buzsáki et al., 1992; Klausberger et al., 2003). Gap-junctions have also been associated with sharp-waves, with the observation of "spikelets" in pyramidal cells and a blockade by gap-junction antagonists (Draguhn et al., 1998). However sharp waves persist, at reduced strength, in animals where the gap junction protein connexin 36 is genetically deleted (Pais et al., 2003). Possibly then, recurrent excitation of both pyramidal cells and interneurons (Hájos et al., 2013) may suffice to generate sharp waves.

THETA AND GAMMA RHYTHMS

In contrast to sharp waves, theta fields (4–12 Hz) are generated when spatial memory representations are first acquired during movements (Vanderwolf, 1969; O'Keefe and Nadel, 1978). Place-cells fire with theta oscillations and theta waves are also detected in rapid eye movement sleep.

Theta oscillations probably depend on signals generated outside the CA3 region. Signals from the septum may provide a sustained cholinergic excitation as well as glutamatergic (Huh et al., 2010) and inhibitory signals which selectively targeting hippocampal interneurons to disinhibit pyramidal cells (Freund and Antal, 1988; Tóth et al., 1997; King et al., 1998). Synaptic connections within the CA3 region probably reinforce the rhythm via reciprocal interactions between pyramidal cells and some, probably peri-somatic, interneurons (Soltesz and Deschênes, 1993).

Gamma oscillations at 30–70 Hz may be superimposed on theta rhythmicity (Bragin et al., 1995; Csicsvari et al., 2003; Hasselmo, 2005). They are suggested to bind, or coordinate, activity of spatially dispersed neurons due to a single stimulus (Gray et al., 1989). In contrast to theta, gamma oscillations are generated within the CA3 region. Reciprocal synaptic interactions between perisomatic inhibitory cells and CA3 pyramidal cells via recurrent synapses are suggested to contribute both *in vivo* (Csicsvari et al., 2003) and in slice models of gamma induced by cholinergic agonists (Oren et al., 2006) or kainate (Fisahn, 2005). Gap junctions that transmit excitation between CA3 pyramidal cell axons may be another crucial factor in gamma generation (Traub and Bibbig, 2000; Traub et al., 2003).

COMPARISON OF RECURRENT CONNECTIVITY IN CA3 AND OTHER CORTICAL REGIONS

The hippocampal treatment of events, memories or representations may depend in part on the associative nature of the recurrent excitatory network between CA3 pyramidal cells. How do recurrent circuits in CA3 compare to those in other associative or sensory cortical regions?

The spatial extent of excitatory terminals seems to differ for recurrent synapses in associative, allocortical regions, such as CA3 and the olfactory cortex, and in six-layered primary sensory neocortex. CA3 pyramidal cell axons project longitudinally through most of the hippocampus (Lorente de Nó, 1934; Li et al., 1994). Local axons diffusely cover most of the olfactory cortex (Haberly, 2001; Franks et al., 2011; Poo and Isaacson, 2011). Connectivity within a six-layered cortex is certainly more complex, but overall may be more restrained in space. For instance, axons of layer IV pyramidal cells from sensory cortices tend to ramify locally within modules such as a single somatosensory barrel (Petersen and Sakmann, 2000; Feldmeyer, 2012). Superficial or deep layer pyramidal cells of primary visual or somatosensory cortex make longer range but often patchy projections terminating in regions occupied by cell groups of similar function

(Gilbert and Wiesel, 1989; Holmgren et al., 2003; Ko et al., 2011; cf Feldmeyer, 2012)

The density of excitatory connections between pyramidal cells may be somewhat higher in sensory cortical modules than in associative allocortex such as CA3 or piriform cortex. Paired records from acute slices gave a value of 0.02–0.03 for the probability of a connection between two CA3 pyramidal cells (Miles and Wong, 1986) and recurrent connectivity in piriform cortex is estimated at 0.002–0.01 (Franks et al., 2011; Hagiwara et al., 2012). Estimates of connectivity are somewhat higher from paired records in slices of sensory cortex. The probability of connection between cells in different cortical layers ranges from 0.1 to 0.3 (0.2–0.3 in layer 4 of barrel cortex, Lefort et al., 2009; Feldmeyer, 2012; 0.1 in layer 2/3 of neocortex, Holmgren et al., 2003; 0.1 in layer 5 neocortex, Markram et al., 1997).

An alternative way to define connectivity could be to measure the spatial distribution of terminals formed by the axon of a single cell. Terminals of some pyramidal cells in sensory cortex (Petersen and Sakmann, 2000) seem likely to show a more focal topology than those of the CA3 region (Ishizuka et al., 1990; Li et al., 1994). Data from paired records in slices indicates a lower local connectivity in CA3 than in sensory cortex. Lower values for recurrent connectivity may be a design feature to ensure sparse representations in an associative region.

Recurrent excitatory synapses may contact cortical interneurons selectively in both associative and sensory cortices. Paired records suggest connectivity from pyramidal cells to fast-spiking interneurons is higher than onto pyramidal cells (0.5–0.7 in neocortex layer 2, Holmgren et al., 2003; in barrel cortex layer 2 ~0.6, Avermann et al., 2012; 0.2 in piriform cortex layer 3, Stokes and Isaacson, 2010). A higher connectivity as well as stronger signaling at single connections with GABAergic interneurons (Helmstaedter et al., 2008) protects against excessive synchrony, maintains stable population firing and sharpens signaling by imposing a sparse coding.

The strength of afferent and recurrent synapses may differ in both associative and sensory cortices. Mossy fiber synapses with CA3 pyramidal cells have more release sites (Claiborne et al., 1986) and stronger actions (Henze et al., 2002). Synapses from olfactory bulb onto piriform cortex cells are both stronger and less numerous that recurrent synapses (Franks et al., 2011; Poo and Isaacson, 2011). In barrel cortex however, recurrent connections between layer 4 pyramidal cells seem to be stronger (Feldmeyer et al., 1999; Feldmeyer, 2012) than thalamic synapses which excite the same cells (Bruno and Sakmann, 2006).

Thus recurrent networks of associative cortical regions have a wider spatial extent and a lower probability of connection between pyramidal cells than those in sensory cortices.

THE CA3 RECURRENT SYSTEM AS AN ASSOCIATIVE NETWORK

Associative synaptic networks have been linked to the processes of completion and recall of stored information (**Figure 5**). McNaughton and Morris (1987) noted that similar hypotheses have often been discovered. What do they assume? And how might they be tested?

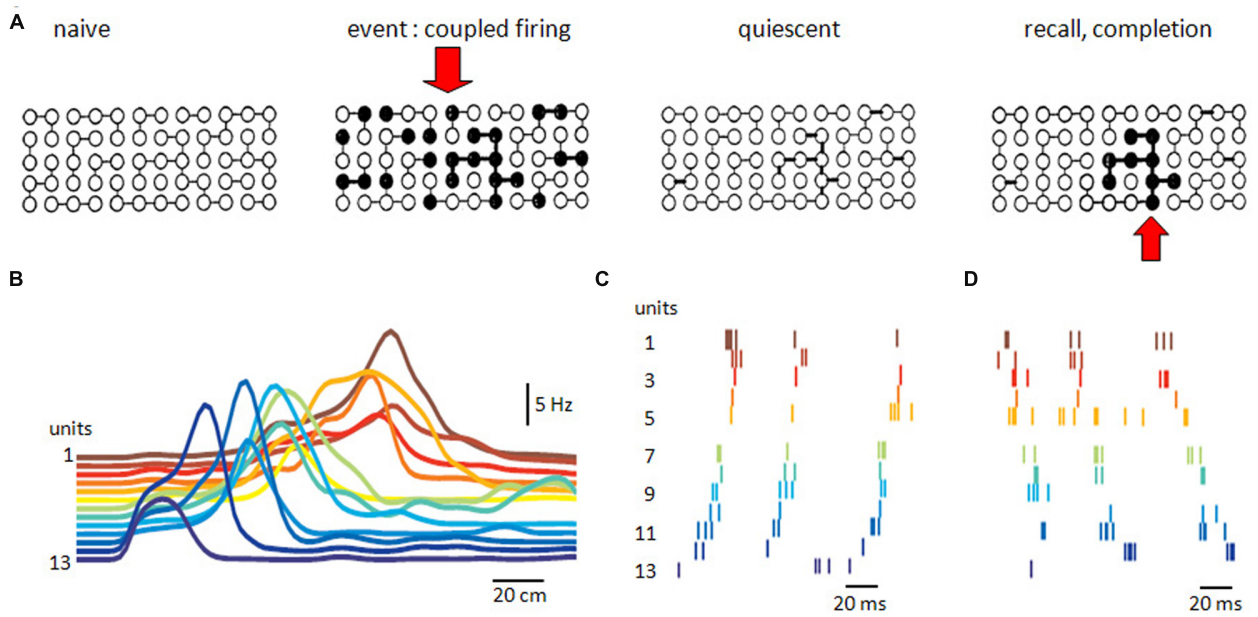

FIGURE 5 | Recurrent excitatory networks. (A) Possible schema of connectivity and operations in a recurrent neuronal network. Some neurons are connected in the naïve network. Coupled firing in a subset of neurons during an event reinforces synapses between them. Reinforcement persists during quiescence, until partial activation recalls or completes firing of the neuronal subset associated with the original event. **(B)** Sequential firing of 13 pyramidal place cells as an animal passes through a space (horizontal axis is distance). Reactivation of sequential firing of these cells as **(C)** forward replay or **(D)** backward replay (adapted with permission from Diba and Buzsáki, 2007).

Such hypotheses suppose that information, or a representation, or an event, or a memory, has a distributed existence as the correlated, or synchronous, discharge of a group of neurons (Hebb, 1949; Marr, 1971). Different informations presumably involve different groups, raising the question of how representations are constrained to be neuronally orthogonal (Marr, 1971; Rolls and Treves, 1998). They suppose that a way exists to associate or strengthen synaptic relations within such a group or ensemble of synchronously active neurons. It might correspond to the persistent synaptic potentiation which occurs when pre- and post-synaptic cells fire together (Hebb, 1949; Bliss and Lomo, 1973). They suppose that a full representation of an event can be recalled from some of its elements (Gardner-Medwin, 1976; McNaughton and Morris, 1987). The CA3 recurrent network where activity in some single cells can trigger population activities (Miles and Wong, 1983; Fujisawa et al., 2006) might be capable of operations similar to a cued recall (**Figure 5**). The spatially widespread but lower connectivity of associative recurrent networks may favor this form of information storage.

Improved techniques to record and manipulate activity in large groups of neurons begin to suggest distributed ensembles may contribute to storage and recall. Using tetrodes to separate firing in 50–100 single units, Wilson and McNaughton (1994) showed that CA1 place-sensitive neurons that fired together during a spatial behavior, discharged synchronously again during the following episode of sleep. Correlated firing in cell pairs was increased as animals learned a task and maintained during replay. A specific role for recurrent synapses was established by genetically deleting NMDA receptor expression at recurrent synapses of CA3 pyramidal cells (Nakazawa et al., 2002, 2003). With the basis for persistent changes abolished, recall of spatial memories from partial cues was suppressed. Optical stimulation has recently been used to re-activate neurons associated with a representation (Liu et al., 2012). An ensemble of granule cells active during fear conditioning was labeled with a construction including c-fos which also induced expression of a light-sensitive opsin. Re-activating the sparse granule cell ensemble optically later, induced a fear response in a different context.

These data point to distinct neuronal operations associated with acquisition and recall. A two-stage memory system has often been postulated (James, 1890; Buzsáki, 1989). The two stages may occur during distinct brain and behavioral states. External representations, especially those associated with space (O'Keefe and Nadel, 1978) and possibly also time (Huxter et al., 2003; Kraus et al., 2013) are acquired during theta activity. In contrast, recall or consolidation is linked with sharp-waves generated in CA3 (Buzsáki, 1989). Switching between these opposing behaviors might be achieved with distinct modulatory transmitters (Hasselmo et al., 1995) or, perhaps more economically, by external control of specific interneurons (Viney et al., 2013).

Acquisition and replay of ensemble activity were first described during theta and sharp waves respectively (Wilson and McNaughton, 1994). Several variants of the exact replay of neuronal firing sequences have now been distinguished most often in CA1 during sleep (Lee and Wilson, 2002; cf Matsumoto et al., 2013) and the awake state (Foster and Wilson, 2006; Diba and Buzsáki, 2007). Firing replay during sharp waves is increasingly linked to the consolidation of a memory or representation by transfer from the hippocampus to a more permanent storage in cortex (Rasch and Born, 2007; Nakashiba et al., 2009; O'Neill et al., 2010). During sharp waves of slow-wave sleep, similar firing sequences are detected in hippocampus and cortex (Ji and Wilson, 2007) and suppressing sharp waves during sleep interferes with consolidation (Girardeau et al., 2009).

The data on these forms of replay raises questions for future work. It needs to be re-examined in CA3. Many, but not all (Diba and Buzsáki, 2007), papers report data from CA1 with the caveat that the activity is likely to have originated in CA3. How is the apparent precision in firing maintained during the translation from CA3 to CA1? How is an appropriate sequence initiated in CA3? What neuronal and synaptic mechanisms can explain how a specific sharp wave is chosen, define the inhibitory and pyramidal cells that fire during it, and permit reversal of this sequence? Better techniques to define cellular and synaptic physiology in context of data on the activity of large numbers of neurons (Matsumoto et al., 2013) will be needed for the next steps to uncover the role of recurrent synapses and the functions of the CA3 region.

ACKNOWLEDGMENTS

We would like to thank Gyuri Buzsaki, Attila Gulyas, Kai Kaila, and Liset Menendez de la Prida for comments. This work was supported by ERC-senior award 322721 and ERA-net to R. Miles.

REFERENCES

Andreasen, M., and Lambert, J. D. C. (1999). Somatic amplification of distally generated subthreshold EPSPs in rat hippocampal pyramidal neurones. *J. Physiol.* 519, 85–100. doi: 10.1111/j.1469-7793.1999.0085o.x

Auger, C., Kondo, S., and Marty, A. (1998). Multivesicular release at single functional synaptic sites in cerebellar stellate and basket cells. *J. Neurosci.* 18, 4532–4547.

Avermann, M., Tomm, C., Mateo, C., Gerstner, W., and Petersen, C. C. (2012). Microcircuits of excitatory and inhibitory neurons in layer 2/3 of mouse barrel cortex. *J. Neurophysiol.* 107, 3116–3134. doi: 10.1152/jn.00917.2011

Ayala, G. F., Dichter, M., Gumnit, R. J., Matsumoto, H., and Spencer, W. A. (1973). Genesis of epileptic interictal spikes. New knowledge of cortical feedback systems suggests a neurophysiological explanation of brief paroxysms. *Brain Res.* 52, 1–17. doi: 10.1016/0006-8993(73)90647-1

Bains, J. S., Longacher, J. M., and Staley, K. J. (1999). Reciprocal interactions between CA3 network activity and strength of recurrent collateral synapses. *Nat. Neurosci.* 2, 720–726. doi: 10.1038/11184

Bazelot, M., Dinocourt, C., Cohen, I., and Miles, R. (2010). Unitary inhibitory field potentials in the CA3 region of rat hippocampus. *J. Physiol.* 588, 2077–2090. doi: 10.1113/jphysiol.2009.185918

Behrens, C. J., van den Boom, L. P., de Hoz, L., Friedman, A., and Heinemann, U. (2005). Induction of sharp wave-ripple complexes in vitro and reorganization of hippocampal networks. *Nat. Neurosci.* 8, 1560–1567. doi: 10.1038/nn1571

Biró, A. A., Holderith, N. B., and Nusser, Z. (2005). Quantal size is independent of the release probability at hippocampal excitatory synapses. *J. Neurosci.* 25, 223–232. doi: 10.1523/JNEUROSCI.3688-04.2005

Bischofberger, J., Engel, D., Frotscher, M., and Jonas, P. (2006). Timing and efficacy of transmitter release at mossy fiber synapses in the hippocampal network. *Pflugers. Arch.* 453, 361–372. doi: 10.1007/s00424-006-0093-2

Bliss, T. V., and Lomo, T. (1973). Long-lasting potentiation of synaptic transmission in the dentate area of the anaesthetized rabbit following stimulation of the perforant path. *J. Physiol.* 232, 331–356.

Bochet, P., Audinat, E., Lambolez, B., Crépel, F., Rossier, J, Iino, M., et al. (1994). Subunit composition at the single-cell level explains functional properties of a glutamate-gated channel. *Neuron* 12, 383–388. doi: 10.1016/0896-6273(94)90279-8

Bragin, A., Jandó, G., Nádasdy, Z., Hetke, J., Wise, K., and Buzsáki, G. (1995). Gamma (40-100 Hz) oscillation in the hippocampus of the behaving rat. *J. Neurosci.* 15, 47–60.

Bruno, R. M., and Sakmann, B. (2006). Cortex is driven by weak but synchronously active thalamocortical synapses. *Science* 312, 1622–1627. doi: 10.1126/science.1124593

Bucurenciu, I., Bischofberger, J., and Jonas, P. (2010). A small number of open Ca2++ channels trigger transmitter release at a central GABAergic synapse. *Nat. Neurosci.* 13, 19–21. doi: 10.1038/nn.2461

Buzsáki, G., Horváth, Z., Urioste, R., Hetke, J., and Wise, K. (1992). High-frequency network oscillation in the hippocampus. *Science* 256, 1025–1027. doi: 10.1126/science.1589772

Buzsáki, G. (1989). Two-stage model of memory trace formation: a role for "noisy" brain states. *Neuroscience* 31, 551–570. doi: 10.1016/0306-4522(89)90423-5

Carter, A. G., and Regehr, W. G. (2002). Quantal events shape cerebellar interneuron firing. *Nat. Neurosci.* 5, 1309–1318. doi: 10.1038/nn970

Christie, J. M., and Jahr, C. E. (2006). Multivesicular release at schaffer collateral – CA1 hippocampal synapses. *J. Neurosci.* 26, 210–216. doi: 10.1523/JNEUROSCI.4307-05.2006

Claiborne, B. J., Amaral, D. G., and Cowan, W. M. (1986). A light and electron microscopic analysis of the mossy fibers of the rat dentate gyrus. *J. Comp. Neurol.* 246, 435–458. doi: 10.1002/cne.902460403

Cohen, I., and Miles, R. (2000). Contributions of intrinsic and synaptic activities to the generation of neuronal discharges in in vitro hippocampus. *J. Physiol.* 524, 485–502. doi: 10.1111/j.1469-7793.2000.00485.x

Conti, R., and Lisman, J. (2003). The high variance of AMPA receptor- and NMDA receptor-mediated responses at single hippocampal synapses: evidence for multiquantal release. *Proc. Natl. Acad. Sci. U.S.A.* 100, 4885–4890. doi: 10.1073/pnas.0630290100

Csicsvari, J., Hirase, H., Czurko, A., and Buzsáki, G. (1998). Reliability and state dependence of pyramidal cell-interneuron synapses in the hippocampus: an ensemble approach in the behaving rat. *Neuron* 21, 179–189. doi: 10.1016/S0896-6273(00)80525-5

Csicsvari, J., Hirase, H., Mamiya, A., and Buzsáki, G. (2000). Ensemble patterns of hippocampal CA3-CA1 neurons during sharp wave-associated population events. *Neuron* 28, 585–594. doi: 10.1016/S0896-6273(00)00135-5

Csicsvari, J., Jamieson, B., Wise, K. D., and Buzsáki, G. (2003). Mechanisms of gamma oscillations in the hippocampus of the behaving rat. *Neuron* 37, 311–322. doi: 10.1016/S0896-6273(02)01169-8

de la Prida, L. M., Huberfeld, G., Cohen, I., and Miles, R. (2006). Threshold behavior in the initiation of hippocampal population bursts. *Neuron* 49, 131–142. doi: 10.1016/j.neuron.2005.10.034

Debanne, D., Boudkkazi, S., Campanac, E., Cudmore, R. H., Giraud, P., Fronzaroli-Molinieres, L., et al. (2008). Paired-recordings from synaptically coupled cortical and hippocampal neurons in acute and cultured brain slices. *Nat. Protoc.* 3, 1559–1568. doi: 10.1038/nprot.2008.147

Debanne, D., Campanac, E., Bialowas, A., Carlier, E., and Alcaraz, G. (2011). Axon physiology. *Physiol. Rev.* 91, 555–602. doi: 10.1152/physrev.00048.2009

Debanne, D., Gähwiler, B. H., and Thompson, S. M. (1998). Long-term synaptic plasticity between pairs of individual CA3 pyramidal cells in rat hippocampal slice cultures. *J. Physiol.* 507, 237–247. doi: 10.1111/j.1469-7793.1998.237bu.x

Debanne, D., Gähwiler, B. H., and Thompson, S. M. (1999). Heterogeneity of synaptic plasticity at unitary CA3-CA1 and CA3-CA3 connections in rat hippocampal slice cultures. *J. Neurosci.* 19, 10664–10671.

Debanne, D., Guérineau, N. C., Gähwiler, B. H., and Thompson, S. M. (1995). Physiology and pharmacology of unitary synaptic connections between pairs of cells in areas CA3 and CA1 of rat hippocampal slice cultures. *J. Neurophysiol.* 73, 1282–1294.

Debanne, D., Guérineau, N. C., Gähwiler, B. H., and Thompson, S. M. (1996). Paired-pulse facilitation and depression at unitary synapses in rat hippocampus: quantal fluctuation affects subsequent release. *J. Physiol.* 491, 163–176.

Debanne, D., Guérineau, N. C., Gähwiler, B. H., and Thompson, S. M. (1997). Action-potential propagation gated by an axonal I(A)-like K++ conductance in hippocampus. *Nature* 389, 286–289. doi: 10.1038/38502

Ddel Castillo, J., and Katz, B. (1954). Statistical factors involved in neuromuscular facilitation and depression. *J. Physiol.* 124, 574–585.

Diba, K. and Buzsáki, G. (2007). Forward and reverse hippocampal place-cell sequences during ripples. *Nat. Neurosci.* 10, 1241–1242. doi: 10.1038/nn1961

Draguhn, A., Traub, R. D., Schmitz, D., and Jefferys, J. G. (1998). Electrical coupling underlies high-frequency oscillations in the hippocampus in vitro. *Nature* 394, 189–192. doi: 10.1038/28184

Engel, D., and Jonas, P. (2005). Presynaptic action potential amplification by voltage-gated Na++ channels in hippocampal mossy fiber boutons. *Neuron* 45, 405–417. doi: 10.1016/j.neuron.2004.12.048

Feldmeyer, D., Egger, V., Lübke, J., and Sakmann, B. (1999). Reliable synaptic connections between pairs of excitatory layer 4 neurones within a single 'barrel' of developing rat somatosensory cortex. *J. Physiol.* 521, 169–190. doi: 10.1111/j.1469-7793.1999.00169.x

Feldmeyer, D. (2012). Excitatory neuronal connectivity in the barrel cortex. *Front. Neuroanat.* 6:24. doi: 10.3389/fnana.2012.00024

Fisahn, A. (2005). Kainate receptors and rhythmic activity in neuronal networks: hippocampal gamma oscillations as a tool. *J. Physiol.* 562, 65–72. doi: 10.1113/jphysiol.2004.077388

Foster, D. J., and Wilson, M. A. (2006). Reverse replay of behavioural sequences in hippocampal place cells during the awake state. *Nature* 440, 680–683. doi: 10.1038/nature04587

Franks, K. M., Russo, M. J., Sosulski, D. L., Mulligan, A. A., Siegelbaum, S. A., and Axel, R. (2011). Recurrent circuitry dynamically shapes the activation of piriform cortex. *Neuron* 72, 49–56. doi: 10.1016/j.neuron.2011.08.020

Freund, T. F., and Antal, M. (1988). GABA-containing neurons in the septum control inhibitory interneurons in the hippocampus. *Nature* 336, 170–173. doi: 10.1038/336170a0

Freund, T. F., and Buzsáki, G. (1996). Interneurons of the hippocampus. *Hippocampus* 6, 347–470.

Fricker, D., and Miles, R. (2000). EPSP amplification and the precision of spike timing in hippocampal neurons. *Neuron* 28, 559–569. doi: 10.1016/S0896-6273(00)00133-1

Fujisawa, S., Matsuki, N., and Ikegaya, Y. (2006). Single neurons can induce phase transitions of cortical recurrent networks with multiple internal states. *Cereb. Cortex* 16, 639–654. doi: 10.1093/cercor/bhj010

Gardner-Medwin, A. R. (1976). The recall of events through the learning of associations between their parts. *Proc. R. Soc. Lond. B Biol. Sci.* 194, 375–402. doi: 10.1098/rspb.1976.0084

Geiger, J. R., Melcher, T., Koh, D. S., Sakmann, B., Seeburg, P. H., Jonas, P., et al. (1995). Relative abundance of subunit mRNAs determines gating and Ca2++ permeability of AMPA receptors in principal neurons and interneurons in rat CNS. *Neuron* 15, 193–204. doi: 10.1016/0896-6273(95)90076-4

Gilbert, C. D., and Wiesel, T. N. (1989). Columnar specificity of intrinsic horizontal and corticocortical connections in cat visual cortex. *J. Neurosci.* 9, 2432–2442

Girardeau, G., Benchenane, K., Wiener, S. I., Buzsáki, G., and Zugaro, M. B. (2009). Selective suppression of hippocampal ripples impairs spatial memory. *Nat. Neurosci.* 12, 1222–1223. doi: 10.1038/nn.2384

Gray, C. M., König, P., Engel, A. K., and Singer, W. (1989). Oscillatory responses in cat visual cortex exhibit inter-columnar synchronization which reflects global stimulus properties. *Nature* 338, 334–337. doi: 10.1038/338334a0

Gulyas, A. I., Miles, R., Sik, A., Tamamaki, N., and Freund, T. F. (1993). Hippocampal pyramidal cells excite basket cells via a single release site. *Nature* 366, 683–687. doi: 10.1038/366683a0

Haberly, L. B. (2001). Parallel-distributed processing in olfactory cortex: new insights from morphological and physiological analysis of neuronal circuitry. *Chem. Senses* 26, 551–576. doi: 10.1093/chemse/26.5.551

Hagiwara, A., Pal, S. K., Sato, T. F., Wienisch, M., and Murthy, V. N. (2012). Optophysiological analysis of associational circuits in the olfactory cortex. *Front. Neural Circuits* 6:18. doi: 10.3389/fncir.2012.00018

Hájos, N., Karlócai, M. R., Németh, B., Ulbert, I., Monyer, H., Szabó, G., et al. (2013). Input-output features of anatomically identified CA3 neurons during hippocampal sharp wave/ripple oscillation in vitro. *J. Neurosci.* 33, 11677–11691. doi: 10.1523/JNEUROSCI.5729-12.2013

Hasselmo, M. E., Schnell, E., and Barkai, E. (1995). Dynamics of learning and recall at excitatory recurrent synapses and cholinergic modulation in rat hippocampal region CA3. *J. Neurosci.* 15, 5249–5262.

Hasselmo, M. E. (2005). What is the function of hippocampal theta rhythm – linking behavioral data to phasic properties of field potential and unit recording data. *Hippocampus* 15, 936–949. doi: 10.1002/hipo.20116

Hebb, D. O. (1949). *The Organization of Behaviour*. New York: John Wiley.

Helmstaedter, M., Staiger, J. F., Sakmann, B., and Feldmeyer, D. (2008). Efficient recruitment of layer 2/3 interneurons by layer 4 input in single columns of rat somatosensory cortex. *J. Neurosci.* 28, 8273–8284. doi: 10.1523/JNEUROSCI.5701-07.2008

Henze, D. A., Wittner, L., and Buzsáki, G. (2002). Single granule cells reliably discharge targets in the hippocampal CA3 network in vivo. *Nat. Neurosci.* 5, 790–795.

Herzog, E., Takamori, S., Jahn, R., Brose, N., and Wojcik, S. M. (2006). Synaptic and vesicular co-localization of the glutamate transporters VGLUT1 and VGLUT2 in the mouse hippocampus. *J. Neurochem.* 99, 1011–1018. doi: 10.1111/j.1471-4159.2006.04144.x

Hoffman, D., Magee, J. C., Colbert, C. M., and Johnston, D. (1997). Potassium channel regulation of signal propagation in dendrites of hippocampal pyramidal neurons. *Nature* 387, 869–875. doi: 10.1038/42571

Holderith, N., Lorincz, A., Katona, G., Rózsa, B., Kulik, A., Watanabe, M., et al. (2012). Release probability of hippocampal glutamatergic terminals scales with the size of the active zone. *Nat. Neurosci.* 15, 988–997. doi: 10.1038/nn.3137

Holmgren, C., Harkany, T., Svennenfors, B., and Zilberter, Y. (2003). Pyramidal cell communication within local networks in layer 2/3 of rat neocortex. *J. Physiol.* 551, 139–153. doi: 10.1113/jphysiol.2003.044784

Huh, C. Y., Goutagny, R., and Williams, S. (2010). Glutamatergic neurons of the mouse medial septum and diagonal band of Broca synaptically drive hippocampal pyramidal cells: relevance for hippocampal theta rhythm. *J. Neurosci.* 30, 15951–15961. doi: 10.1523/JNEUROSCI.3663-10.2010

Huxter, J., Burgess, N., and O'Keefe J. (2003). Independent rate and temporal coding in hippocampal pyramidal cells. *Nature* 425, 828–832. doi: 10.1038/nature02058

Ikegaya, Y., Sasaki, T., Ishikawa, D., Honma, N., Tao, K., Takahashi, N., et al. (2013). Interpyramid spike transmission stabilizes the sparseness of recurrent network activity. *Cereb. Cortex* 23, 293–304. doi: 10.1093/cercor/bhs006

Isaac, J. T., Ashby, M. C., and McBain CJ. (2007). The role of the GluR2 subunit in AMPA receptor function and synaptic plasticity. *Neuron* 54, 859–871. doi: 10.1016/j.neuron.2007.06.001

Ishizuka, N., Cowan, W. M., Amaral, D. G. (1995). A quantitative analysis of the dendritic organization of pyramidal cells in the rat hippocampus. *J. Comp. Neurol.* 362, 17–45. doi: 10.1002/cne.903620103

Ishizuka, N., Weber, J., and Amaral, D. G. (1990). Organization of intrahippocampal projections originating from CA3 pyramidal cells in the rat. *J. Comp. Neurol.* 295, 580–623. doi: 10.1002/cne.902950407

Jadhav, S. P., Kemere, C., German, P. W., and Frank, L. M. (2012). Awake hippocampal sharp-wave ripples support spatial memory. *Science* 336, 1454–1458. doi: 10.1126/science.1217230

James, W. (1890). "The principles of psychology," in *Memory* (New York: Henry Holt & Co.). Available at: http://psychclassics.yorku.ca/James/Principles/prin16.htm

Jefferys, J. G. R., Menendez de la Prida, L., Wendling, F., Bragin, A., Avoli, M., Timofeev, I., et al. (2012). Mechanisms of physiological and epileptic HFO generation. *Prog. Neurobiol.* 98, 250–264. doi: 10.1016/j.pneurobio.2012.02.005

Ji, D., and Wilson, M. A. (2007). Coordinated memory replay in the visual cortex and hippocampus during sleep. *Nat. Neurosci.* 10, 100–107. doi: 10.1038/nn1825

Kandel, E. R., and Spencer, W. A. (1961). Excitation and inhibition of single pyramidal cells during hippocampal seizure. *Exp. Neurol.* 4, 162–179. doi: 10.1016/0014-4886(61)90038-3

Kerchner, G. A., and Nicoll, R. A. (2008). Silent synapses and the emergence of a postsynaptic mechanism for LTP. *Nat. Rev. Neurosci.* 9, 813–825. doi: 10.1038/nrn2501

Kim, S., Guzman, S. J., Hu, H., and Jonas, P. (2012). Active dendrites support efficient initiation of dendritic spikes in hippocampal CA3 pyramidal neurons. *Nat. Neurosci.* 15, 600–606 doi: 10.1038/nn.3060

King, C., Recce, M., and O'Keefe J. (1998). The rhythmicity of cells of the medial septum/diagonal band of Broca in the awake freely moving rat: relationships with behaviour and hippocampal theta. *Eur. J. Neurosci.* 10, 464–477. doi: 10.1046/j.1460-9568.1998.00026.x

Klausberger, T., Magill, P. J., Márton, L. F., Roberts, J. D., Cobden, P. M., Buzsáki, G., et al. (2003). Brain-state- and cell-type-specific firing of hippocampal interneurons in vivo. *Nature* 421, 844–848. doi: 10.1038/nature01374

Ko, H., Hofer, S. B., Pichler, B., Buchanan, K. A., Sjöström, P. J., Mrsic-Flogel, T. D. (2011). Functional specificity of local synaptic connections in neocortical networks. *Nature* 473, 87–91. doi: 10.1038/nature09880

Koester, H. J., and Johnston, D. (2005). Target cell-dependent normalization of transmitter release at neocortical synapses. *Science* 308, 863–866. doi: 10.1126/science.1100815

Kopysova, I. L., and Debanne, D. (1998). Critical role of axonal A-type K++ channels and axonal geometry in the gating of action potential propagation along CA3 pyramidal cell axons: a simulation study. *J. Neurosci.* 18, 7436–7451.

Kraus, B. J., Robinson, R. J. II, White, J. A., Eichenbaum, H., and Hasselmo, M. E. (2013). Hippocampal "time cells": time versus path integration. *Neuron* 78, 1090–1101. doi: 10.1016/j.neuron.2013.04.015

Lebovitz, R. M., Dichter, M., and Spencer, W. A. (1971). Recurrent excitation in the CA3 region of cat hippocampus. *Int. J. Neurosci.* 2, 99–107. doi: 10.3109/00207457109146996

Lee, A. K., and Wilson, M. A. (2002). Memory of sequential experience in the hippocampus during slow wave sleep. *Neuron* 36, 1183–1194. doi: 10.1016/S0896-6273(02)01096-6

Lefort, S., Tomm, C., Floyd Sarria, J. C., and Petersen, C. C. (2009). The excitatory neuronal network of the C2 barrel column in mouse primary somatosensory cortex. *Neuron* 61, 301–316. doi: 10.1016/j.neuron.2008.12.020

Li, L., Bischofberger, J., and Jonas, P. (2007). Differential gating and recruitment of P/Q-, N-, and R-type Ca2++ channels in hippocampal mossy fiber boutons. *J. Neurosci.* 27, 13420–13429. doi: 10.1523/JNEUROSCI.1709-07.2007

Li, X. G., Somogyi, P., Ylinen, A., and Buzsáki, G. (1994). The hippocampal CA3 network – an in vivo intracellular labeling study. *J. Comp. Neurol.* 339, 181–208. doi: 10.1002/cne.903390204

Liotta, A., Caliskan, G., ul Haq, R., Hollnagel, J. O., Rösler, A., Heinemann, U., et al. (2011). Partial disinhibition is required for transition of stimulus-induced sharp wave-ripple complexes into recurrent epileptiform discharges in rat hippocampal slices. *J. Neurophysiol.* 105, 172–187. doi: 10.1152/jn.00186.2010

Lipowsky, R., Gillessen, T., and Alzheimer, C. (1996). Dendritic Na++ channels amplify EPSPs in hippocampal CA1 pyramidal cells. *J. Neurophysiol.* 76, 2181–2191.

Liu, X., Ramirez, S., Pang, P. T., Puryear, C. B., Govindarajan, A., Deisseroth, K., et al. (2012). Optogenetic stimulation of a hippocampal engram activates fear memory recall. *Nature* 484, 381–385. doi:10.1038/nature11028

Lorente de No, R. (1938) "Cerebral cortex: architecture, intracortical connections, motor projections," in *Physiology of the Nervous System*, ed. J. F. Fulton (London: Oxford University Press).

Lorente de Nó, R. (1934). Studies on the structure of the cerebral cortex. Continuation of the study of the ammonic system. *J. Psychol. Neurol.* 46, 113–177.

Lorincz, A., and Nusser, Z. (2008). Cell-type-dependent molecular composition of the axon initial segment. *J. Neurosci.* 28, 14329–14340. doi: 10.1523/JNEUROSCI.4833-08.2008

Lörincz, A., Notomi, T., Tamás, G., Shigemoto, R., and Nusser, Z. (2002). Polarized and compartment-dependent distribution of HCN1 in pyramidal cell dendrites. *Nat. Neurosci.* 5, 1185–1193. doi: 10.1038/nn962

Magee, J. C., and Johnston, D. (1995). Synaptic activation of voltage-gated channels in dendrites of hippocampal pyramidal neurons. *Science* 268, 301–304. doi: 10.1126/science.7716525

Magee, J. C. (1999). Dendritic lh normalizes temporal summation in hippocampal CA1 neurons. *Nat. Neurosci.* 2, 508–514. doi: 10.1038/9158

Markram, H., Lübke, J., Frotscher, M., Roth, A., and Sakmann, B. (1997). Physiology and anatomy of synaptic connections between thick tufted pyramidal neurones in the developing rat neocortex. *J. Physiol.* 500, 409–440.

Marr, D. (1971). Simple memory: a theory for archicortex. *Philos. Trans. R. Soc. Lond. B Biol. Sci.* 23–81. doi: 10.1098/rstb.1971.0078

Matsumoto, K., Ishikawa, T., Matsuki, N., and Ikegaya, Y. (2013). Multineuronal spike sequences repeat with millisecond precision. *Front. Neural Circuits* 7:112. doi: 10.3389/fncir.2013.00112

Matsuzaki, M., Ellis-Davies, G. C., Nemoto, T., Miyashita, Y., Iino, M., and Kasai, H. (2001). Dendritic spine geometry is critical for AMPA receptor expression in hippocampal CA1 pyramidal neurons. *Nat. Neurosci.* 4, 1086–1092. doi: 10.1038/nn736

McGuinness L, Taylor, C., Taylor, R. D., Yau, C., Langenhan, T., Hart, M. L., et al. (2010). Presynaptic, N. M.,DARs in the hippocampus facilitate transmitter release at theta frequency. *Neuron* 68, 1109–1127. doi: 10.1016/j.neuron.2010.11.023

McNaughton, B. L., and Morris, R. G. M. (1987). Hippocampal synaptic enhancement and information storage within a distributed memory system. *Trends Neurosci.* 10, 408–415. doi: 10.1016/0166-2236(87)90011-7

Meeks, J. P., and Mennerick, S. (2007). Action potential initiation and propagation in CA3 pyramidal axons. *J. Neurophysiol.* 97, 3460–3472. doi: 10.1152/jn.01288.2006

Miles, R. (1990). Excitation of inhibitory cells by single CA3 pyramidal cells in the guinea pig hippocampus in vitro. J. Physiol. 428, 61–77.

Miles, R., and Wong, R. K. S. (1983). Single neurones can initiate synchronized population discharge in the hippocampus. *Nature* 306, 371–373. doi: 10.1038/306371a0

Miles, R., and Wong, R. K. S. (1986). Excitatory synaptic interactions between CA3 neurones in the guinea-pig hippocampus. *J. Physiol.* 373, 397–418.

Miles, R., and Wong, R. K. S. (1987a). Inhibitory control of local excitatory circuits in the guinea-pig hippocampus. *J. Physiol.* 388, 611–629.

Miles, R., and Wong, R. K. S. (1987b). Latent synaptic pathways revealed after tetanic stimulation in the hippocampus. *Nature* 329, 724–726. doi: 10.1038/329724a0

Montgomery, J. M., and Madison, D. V. (2002). State-dependent heterogeneity in synaptic depression between pyramidal cell pairs. *Neuron* 33, 765–777. doi: 10.1016/S0896-6273(02)00606-2

Montgomery, J. M., and Pavlidis, P., and Madison, D. V. (2001). Pair recordings reveal all-silent synaptic connections and the postsynaptic expression of long-term potentiation. *Neuron* 29, 691–701. doi: 10.1016/S0896-6273(01)00244-6

Nakashiba, T., Buhl, D. L., McHugh, T. J., and Tonegawa, S. (2009). Hippocampal CA3 output is crucial for ripple-associated reactivation and consolidation of memory. *Neuron* 62, 781–787. doi: 10.1016/j.neuron.2009.05.013

Nakazawa, K., Quirk, M. C., Chitwood, R. A., Watanabe, M., Yeckel, M. F., Sun, L. D., et al. (2002). Requirement for hippocampal CA3 NMDA receptors in associative memory recall. *Science* 297, 211–218. doi: 10.1126/science.1071795

Nakazawa, K., Sun, L. D., Quirk, M. C., Rondi-Reig, L., Wilson, M. A., Tonegawa, S. (2003). Hippocampal CA3 NMDA receptors are crucial for memory acquisition of one-time experience. *Neuron* 38, 305–315. doi: 10.1016/S0896-6273(03)00165-X

Nimchinsky, E. A., Yasuda, R., Oertner, T. G., and Svoboda, K. (2004). The number of glutamate receptors opened by synaptic stimulation in single hippocampal spines. *J. Neurosci.* 24, 2054–2064. doi: 10.1523/JNEUROSCI.5066-03.2004

Nusser, Z., Lujan, R., Laube, G., Roberts, J. D., Molnar, E., and Somogyi, P. (1998). Cell type and pathway dependence of synaptic AMPA receptor number and variability in the hippocampus. *Neuron* 21, 545–559. doi: 10.1016/S0896-6273(00)80565-6

Nyiri, G., Stephenson, F. A., Freund, T. F., and Somogyi, P. (2003). Large variability in synaptic N-methyl-d-aspartate receptor density on interneurons and a comparison with pyramidal-cell spines in the rat hippocampus. *Neuroscience* 119, 347–363. doi: 10.1016/S0306-4522(03)00157-X

O'Keefe, J., and Nadel, L. (1978). *The Hippocampus as a Cognitive Map*. London: Oxford University Press.

O'Neill, J., Pleydell-Bouverie, B., Dupret, D., and Csicsvari, J. (2010). Play it again: reactivation of waking experience and memory. *Trends Neurosci.* 33, 220–229. doi: 10.1016/j.tins.2010.01.006

Oren, I., Mann, E. O., Paulsen, O., and Hájos, N. (2006). Synaptic currents in anatomically identified CA3 neurons during hippocampal gamma oscillations in vitro. *J. Neurosci.* 26, 9923–9934. doi: 10.1523/JNEUROSCI.1580-06.2006

Pais, I., Hormuzdi, S. G., Monyer, H., Traub, R. D., Wood, I. C., Buhl, E. H., et al. (2003). Sharp wave-like activity in the hippocampus in vitro in mice lacking the gap junction protein connexin 36. *J. Neurophysiol.* 89, 2046–2054. doi: 10.1152/jn.00549.2002

Palani, D., Baginskas, A., Raastad, M. (2010). Bursts and hyperexcitability in nonmyelinated axons of the rat hippocampus. *Neuroscience* 167, 1004–1013. doi: 10.1016/j.neuroscience.2010.03.021

Pavlidis, P., and Madison, DV. (1999). Synaptic transmission in pair recordings from CA3 pyramidal cells in organotypic culture. *J. Neurophysiol.* 81, 2787–2797

Perez-Rosello, T., Baker, J. L., Ferrante, M, Iyengar, S., Ascoli, G. A., and Barrionuevo, G. (2011). Passive and active shaping of unitary responses from associational/commissural and perforant path synapses in hippocampal CA3 pyramidal cells. *J. Comp. Neurosci.* 31, 159–182. doi: 10.1007/s10827-010-0303-y

Petersen, C. C., and Sakmann, B. (2000). The excitatory neuronal network of rat layer 4 barrel cortex. *J. Neurosci.* 20, 7579–7586.

Poo, C., and Isaacson, J. S. (2011). A major role for intracortical circuits in the strength and tuning of odor-evoked excitation in olfactorycortex. *Neuron* 72, 41–48. doi: 10.1016/j.neuron.2011.08.015

Raffaelli, G., Saviane, C., Mohajerani, M. H., Pedarzani, P., and Cherubini, E. (2004). BK potassium channels control transmitter release at CA3-CA3 synapses in the rat hippocampus. *J. Physiol.* 557, 147–157. doi: 10.1113/jphysiol.2004.062661

Ramón y Cajal, S. (1899). *Textura del Sistema Nervioso del Hombre y de los Vertebrados*. Madrid: Moya.

Rasch, B., and Born, J. (2007). Maintaining memories by reactivation. *Opin. Neurobiol.* 17, 698–703. doi: 10.1016/j.conb.2007.11.007

Rolls, E. T., and Treves, A. (1998). *Neural Networks and Brain Function*. London: Oxford University Press.

Royeck, M., Horstmann, M. T., Remy, S., Reitze, M., Yaari, Y., and Beck, H. (2008). Role of axonal NaV1.6 sodium channels in action potential initiation of CA1 pyramidal neurons. *J. Neurophysiol.* 100, 2361–2380. doi: 10.1152/jn.90332.2008

Salmen, B., Beed, P. S., Ozdogan, T., Maier, N., Johenning, F. W., Winterer, J., et al. (2012). GluK1 inhibits calcium dependent and independent transmitter release at associational/commissural synapses in area CA3 of the hippocampus. *Hippocampus* 22, 57–68. doi: 10.1002/hipo.20846

Sasaki, T., Matsuki, N., and Ikegaya, Y. (2012). Heterogeneity and independency of unitary synaptic outputs from hippocampal CA3 pyramidal cells. *J. Physiol.* 590, 4869–4880. doi: 10.1113/jphysiol.2012.237685

Saviane, C., Mohajerani, M. H., and Cherubini, E. (2003). An ID-like current that is downregulated by Ca2++ modulates information coding at CA3-CA3 synapses in the rat hippocampus. *J. Physiol.* 552, 513–524. doi: 10.1113/jphysiol.2003.051045

Scanziani, M., Gähwiler, B. H., and Charpak, S. (1998). Target cell-specific modulation of transmitter release at terrminals from a single axon. *Proc. Natl. Acad. Sci. U.S.A.* 95, 12004–12009. doi: 10.1073/pnas.95.20.12004

Schaffer, K. (1892). Beitrag zur histologie der ammonshornformation. *Arch. Mikroskop. Anat.* 39, 611–632. doi: 10.1007/BF02961541

Schikorski, T., and Stevens, C. F. (1997). Quantitative ultrastructural analysis of hippocampal excitatory synapses. *J. Neurosci.* 17, 5858–5867.

Sheng, Z. H., and Cai, Q. (2012). Mitochondrial transport in neurons: impact on synaptic homeostasis and neurodegeneration. *Nat. Rev. Neurosci.* 13, 77–93. doi:10.1038/nrn3156

Shepherd, G. M., and Harris, K. M. (1998). Three-dimensional structure and composition of CA3–CA1 axons in rat hippocampal slices: implications for connectivity and compartments. *J. Neurosci.* 18, 8300–8310.

Shigemoto, R., Kulik, A., Roberts, J. D., Ohishi, H., Nusser, Z., Kaneko, T., et al. (1996). Target-cell-specific concentration of a metabotropic glutamate receptor in the presynaptic active zone. *Nature* 381, 523–525. doi: 10.1038/381523a0

Sik, A., Tamamaki, N., and Freund, T. F. (1993). Complete axon arborization of a single CA3 pyramidal cell in the rat hippocampus and its relationship with postsynaptic parvalbumin containing interneurons. *Eur. J. Neurosci.* 5, 1719–1728. doi: 10.1111/j.1460-9568.1993.tb00239.x

Silver, R. A., Lubke, J., Sakmann, B., and Feldmeyer, D. (2003). High-probability uniquantal transmission at excitatory synapses in barrel cortex. *Science* 302, 1981–1984. doi: 10.1126/science.1087160

Soleng, A. F., Chiu, K., and Raastad, M. (2003a). Unmyelinated axons in the rat hippocampus hyperpolarize and activate an H current when spike frequency exceeds 1 Hz. *J. Physiol.* 552, 459–470. doi: 10.1113/jphysiol.2003.048058

Soleng, A. F., Raastad, M., and Andersen, P. (2003b). Conduction latency along CA3 hippocampal axons from rat. *Hippocampus* 13, 953–961. doi: 10.1002/hipo.10141

Soltesz, I., and Deschênes, M. (1993). Low- and high-frequency membrane potential oscillations during theta activity in CA1 and CA3 pyramidal neurons of the rat hippocampus under ketamine-xylazine anesthesia. *J. Neurophysiol.* 70, 97–116.

Spencer, W. A., and Kandel, E. R. (1961). Hippocampal neuron responses to selective activation of recurrent collaterals of hippocampofugal axons. *Exp. Neurol.* 4, 2149–2161. doi: 10.1016/0014-4886(61)90037-1

Staley, K. J., Bains, J. S., Yee, A., Hellier, J., and Longacher, J. M. (2001). Statistical model relates CA3 burst probability to recovery from burst-induced depression at recurrent collateral synapses. *J. Neurophysiol.* 86, 2736–2747.

Staley, K. J., Longacher, M., Bains, J. S., and Yee, A. (1998). Presynaptic modulation of CA3 network activity. *Nat. Neurosci.* 1, 201–209. doi: 10.1038/651

Stevens, C. F., and Tsujimoto, T. (1995). Estimates for the pool size of releasable quanta at a single central synapse and for the time required to refill the pool. *Proc. Natl. Acad. Sci. U.S.A.* 92, 846–849. doi: 10.1073/pnas.92.3.846

Stokes, C. C., and Isaacson, J. S. (2010). From dendrite to soma: dynamic routing of inhibition by complementary interneuron microcircuits in olfactory cortex. *Neuron* 67, 452–465. doi: 10.1016/j.neuron.2010.06.029

Takumi, Y., Ramirez-Leon, V., Laake, P., Rinvik, E., and Ottersen, O. P. (1999). Different modes of expression of AMPA and NMDA receptors in hippocampal synapses. *Nat. Neurosci.* 2, 618–624. doi: 10.1038/10172

Tóth, K., Freund, T. F., and Miles, R. (1997). Disinhibition of rat hippocampal pyramidal cells by GABAergic afferents from the septum. *J. Physiol.* 500, 463–474.

Traub, R. D., and Bibbig, A. (2000). A model of high-frequency ripples in the hippocampus based on synaptic coupling plus axon-axon gap junctions between pyramidal neurons. *J. Neurosci.* 20, 2086–2093.

Traub, R. D., and Wong, R. K. S. (1982). Cellular mechanism of neuronal synchronization in epilepsy. *Science* 216, 745–747. doi: 10.1126/science.7079735

Traub, R. D., Pais, I., Bibbig, A., LeBeau, F. E., Buhl, E. H., Hormuzdi, S. G., et al. (2003). Contrasting roles of axonal (pyramidal cell) and dendritic (interneuron) electrical coupling in the generation of neuronal network oscillations. *Proc. Natl. Acad. Sci. U.S.A.* 100, 1370–1374. doi: 10.1073/pnas.0337529100

Urban, N. N., and Barrionuevo, G. (1998). Active summation of excitatory postsynaptic potentials in hippocampal CA3 pyramidal neurons. *Proc. Natl. Acad. Sci. U.S.A.* 95, 11450–11455. doi: 10.1073/pnas.95.19.11450

Vanderwolf, C. H. (1969). Hippocampal electrical activity and voluntary movement in the rat. *Electroencephalogr. Clin. Neurophysiol.* 26, 407–418. doi: 10.1016/0013-4694(69)90092-3

Vervaeke, K., Gu, N., Agdestein, C., Hu, H., and Storm, J. F. (2006). Kv7/KCNQ/M-channels in rat glutamatergic hippocampal axons and their role in regulation of excitability and transmitter release. *J. Physiol.* 576, 235–256. doi: 10.1113/jphysiol.2006.111336

Viney, T. J., Lasztoczi, B., Katona, L., Crump, M. G., Tukker, J. J., Klausberger, T., et al. (2013). Network state-dependent inhibition of identified hippocampal CA3 axo-axonic cells in vivo. *Nat. Neurosci.* 16, 1802–1811. doi: 10.1038/nn.3550

Wilson, M. A., and McNaughton, B. L. (1994). Reactivation of hippocampal ensemble memories during sleep. *Science* 265, 676–679. doi: 10.1126/science.8036517

Wittner, L., and Miles, R. (2007). Factors defining a pacemaker region for synchrony in the hippocampus. *J. Physiol.* 584, 867–883. doi: 10.1113/jphysiol.2007.138131

Wittner, L., Henze, D. A., Záborszky, L., and Buzsáki, G. (2006a). Three-dimensional reconstruction of the axon arbor of a CA3 pyramidal cell recorded and filled in vivo. *Eur. J. Neurosci.* 24, 1286–1298. doi: 10.1111/j.1460-9568.2006.04992.x

Wittner, L., Henze, D. A., Záborszky, L., and Buzsáki, G. (2006b). Hippocampal, CA3 pyramidal cells selectively innervate aspiny interneurons. *Eur. J. Neurosci.* 24, 1286–1298. doi: 10.1111/j.1460-9568.2006.04992.x

Wong, R. K. S., and Traub, R. D. (1983) Synchronized burst discharge in disinhibited hippocampal slice. I. Initiation in CA2-CA3 region. *J. Neurophysiol.* 49, 442–458.

Conflict of Interest Statement: The authors declare that the research was conducted in the absence of any commercial or financial relationships that could be construed as a potential conflict of interest.

Received: 03 November 2013; accepted: 02 December 2013; published online: 08 January 2014.

*Citation: Le Duigou C, Simonnet J, Teleñczuk MT, Fricker D and Miles R (2014) Recurrent synapses and circuits in the CA3 region of the hippocampus: an associative network. Front. Cell. Neurosci. **7**:262. doi: 10.3389/fncel.2013.00262*

This article was submitted to the journal Frontiers in Cellular Neuroscience.

frontiers in
CELLULAR NEUROSCIENCE

GENERAL COMMENTARY
published: 20 February 2014
doi: 10.3389/fncel.2014.00048

Erratum: Recurrent synapses and circuits in the CA3 region of the hippocampus: an associative network

Caroline Le Duigou, Jean Simonnet, Maria T. Teleńczuk, Desdemona Fricker and Richard Miles*

Centre de Recherche de l'Institut du Cerveau et de la Moelle, INSERM U975, CHU Pitié-Salpêtrière, Université Pierre et Marie Curie, Paris, France
**Correspondence: richard.miles@upmc.fr*

Edited and reviewed by:
Enrico Cherubini, International School for Advanced Studies, Italy

Keywords: erratum

An erratum on

Recurrent synapses and circuits in the CA3 region of the hippocampus: an associative network
by Le Duigou, C., Simonnet, J., Teleńczuk, M. T., Fricker, D., and Miles, R. (2014). Front. Cell. Neurosci. 7:262. doi: 10.3389/fncel.2013.00262

1. We should like to correct the name for one of the authors. Maria T. Teleñczuk should be corrected to Maria T. Teleńczuk.

2. ACKNOWLEDGMENTS: Maria T. Teleńczuk would also like to acknowledge support from the Ecole des Neurosciences and the DIM Cerveau et Pensée (Paris, Ile de France).

Received: 24 January 2014; accepted: 03 February 2014; published online: 20 February 2014.
*Citation: Le Duigou C, Simonnet J, Teleńczuk MT, Fricker D and Miles R (2014) Erratum: Recurrent synapses and circuits in the CA3 region of the hippocampus: an associative network. Front. Cell. Neurosci. **8**:48. doi: 10.3389/fncel.2014.00048*
This article was submitted to the journal Frontiers in Cellular Neuroscience.

frontiers in
CELLULAR NEUROSCIENCE

REVIEW ARTICLE
published: 27 May 2013
doi: 10.3389/fncel.2013.00078

A process analysis of the CA3 subregion of the hippocampus

Raymond P. Kesner*

Department of Psychology, University of Utah, Salt Lake City, UT, USA

Edited by:
Enrico Cherubini, International School for Advanced Studies, Italy

Reviewed by:
Kazu Nakazawa, National Institute of Mental Health, USA
Ehren Lee Newman, Boston University, USA

****Correspondence:***
Raymond P. Kesner, Department of Psychology, University of Utah, 380 South 1530 East, Room 502, Salt Lake City, UT 84112, USA.
e-mail: rpkesner@behsci.utah.edu

From a behavioral perspective, the CA3a,b subregion of the hippocampus plays an important role in the encoding of new spatial information within short-term memory with a duration of seconds and minutes. This can easily be observed in tasks that require rapid encoding, novelty detection, one-trial short-term or working memory, and one-trial cued recall primarily for spatial information. These are tasks that have been assumed to reflect the operations of episodic memory and require interactions between CA3a,b and the dentate gyrus (DG) via mossy fiber inputs into the CA3a,b. The CA3a,b is also important for encoding of spatial information requiring the acquisition of arbitrary and relational associations. All these tasks are assumed to operate within an autoassociative network function of the CA3 region. The CA3a,b also supports retrieval of short-term memory information based on a spatial pattern completion process. Based on afferent inputs into CA3a,b from the DG via mossy fibers and afferents from the entorhinal cortex into CA3a,b as well as reciprocal connections with the septum, CA3a,b can bias the process of encoding utilizing the operation of spatial pattern separation and the process of retrieval utilizing the operation of pattern completion. The CA3a,b also supports sequential processing of information in cooperation with CA1 based on the Schaffer collateral output from CA3a,b to CA1. The CA3c function is in part based on modulation of the DG in supporting pattern separation processes.

Keywords: CA3, memory, pattern completion, rapid encoding, associative processes

INTRODUCTION

This review article emphasizes the importance of behavioral functions of the CA3 subregion of the hippocampus. After an anatomical description of the CA3a,b,c network, the influence of an autoassociative network function of the CA3 region in supporting mnemonic functions is presented. In general terms, the data suggest that CA3a,b mediates the acquisition and encoding of spatial information within short-term memory with a duration of seconds and minutes. In the context of short-term memory, the CA3a,b mediates rapid encoding of especially spatial information, novelty detection, and one-trial cued recall (all forms of episodic memory). Also, CA3a,b supports the acquisition of paired-associate associations as well as arbitrary associations. It should be noted that CA3a,b can also be involved in short-term memory retrieval as evidenced by support for a pattern completion process. Finally, CA3c function is in part based on modulation of the dentate gyrus (DG) in supporting pattern separation processes. Spatial information represents the critical attribute or domain that is processed in CA3. I will emphasize that the mnemonic functions of the autoassociative network of CA3 depend upon inputs into CA3 from other brain regions within the hippocampus (i.e., DG) and brain regions outside the hippocampus (i.e., medial and lateral entorhinal cortex) as well as outputs from CA3 to brain regions within the hippocampus (i.e., DG, CA1) and brain regions outside the hippocampus (i.e., medial and lateral septum). **Table 1** summarizes the functions of the CA3 region.

ANATOMY

The most prominent anatomical feature of the CA3 subregion is that there are extensive interconnections among the principal cells via a recurrent collateral fiber system (Amaral and Witter, 1995). CA3 also receives converging inputs from multiple input pathways; for example, perforant path inputs from the medial and lateral entorhinal cortex, mossy fiber inputs from the DG, and its own outputs fed back as inputs via the recurrent collaterals (Amaral and Witter, 1995). In addition to the projections originating in CA1, projections out of Ammon's horn originate in CA3. Many researchers have reported that CA3 projects to the lateral and medial septal nuclei as well as to the vertical limb of the diagonal band of Broca (Gaykema et al., 1991; Amaral and Witter, 1995; Risold and Swanson, 1997). The medial septum and vertical limb of the diagonal band of Broca, in turn, provides cholinergic and GABAergic inputs into the hippocampus (Amaral and Witter, 1995). It has been shown that the CA3 region can be divided into a CA3a, b, and c subareas (Lorente de Nó, 1934; Li et al., 1994). Based on the research of Li et al. (1994) and Buckmaster and Schwartzkroin (1994), it has been proposed that mossy cells receive excitatory inputs from granule cells and CA3c pyramidal cells and integrate the inputs from granule cells and CA3c pyramidal cells, which, in turn, via excitatory recurrent axonal projections activate many distal granule cells. Thus, CA3c may have a back-projection output that can influence the DG granule cells (Scharfman, 2007; Myers and Scharfman, 2011). It should also be noted that the CA3c regions do not have

Table 1 | Functions of the CA3 subregion of the hippocampus.

Function	CA3a	CA3b	CA3c
Rapid encoding of novel information	X	X	
Paired-associate learning	X	X	
Cued recall and arbitrary associations	X	X	
Pattern completion and retrieval	X	X	
Contribution to temporal processing via modulation of CA1	X	X	
Biasing information processing based on an interaction between pattern completion derived from the perforant path input into CA3 and pattern separation derived from the mossy fiber input into CA3	X	X	
Modulation of CA1 in temporal processing	X	X	
Modulation of CA1 in consolidation	X	X	
Spatial pattern separation in conjunction with the dentate gyrus			X

recurrent collaterals and it has a direct projection to CA1. Most of the synaptic connections embedded in those different pathways in CA3 are modifiable in their strength (Harris and Cotman, 1986; Marr, 1971; Zalutsky and Nicoll, 1990; Treves and Rolls, 1994; Debanne et al., 1998; Do et al., 2002; Nakazawa et al., 2002). These anatomical and physiological characteristics inspired many investigators to develop theoretical models to assign specific cognitive processes to CA3 (Marr, 1971; O'Reilly and McClelland, 1994; Treves and Rolls, 1994; Hasselmo et al., 1995, 2002a; Rolls, 1996; Hasselmo and Wyble, 1997; Samsonovich and McNaughton, 1997; Lisman, 1999; Mizumori et al., 1999; Kesner et al., 2004; Rolls and Kesner, 2006). The neural circuit that affects the operation of the CA3 subregion of the hippocampus is shown in **Figure 1**.

AUTOASSOCIATIVE NETWORK FUNCTIONS OF THE CA3 REGION

RAPID ENCODING OF NOVEL INFORMATION

One of the mnemonic processes suggested for CA3a,b within short-term memory is the rapid acquisition of novel information. Marr proposed that the hippocampus should be capable of a rapid formation of simple representations, based on modifiable synaptic recurrent collateral associative connections among its neurons. This idea was further developed by McNaughton and Morris (1987) and Rolls (1989b) who have suggested that, based on CA3 recurrent collateral associative connections, the CA3 system may operate as an attractor network which is useful for some types of working memory. Support for this idea comes from a variety of studies analyzed by Kesner and Rolls (2001) and Rolls and Kesner (2006), including a study by Lee and Kesner (2002), who manipulated the *N*-methyl-D-aspartate (NMDA) receptors in CA3a,b by injecting dl-2-amino-5-phosphonovaleric acid (AP5), a pharmacological blocker for the NMDA receptors, selectively into CA3a,b in a delayed non-matching-to-place (DNMP) task. During a study phase of the task, rats visited a randomly chosen arm in the eight-arm maze and came back to the center platform where a delay period (10 s) was imposed in a bucket. After the delay period, the rats faced two adjacent arms on the maze (including the arm that had been visited before the delay period) and the task was to choose the arm that had not been visited during the previous study phase. Rats injected with AP5 were not impaired in performing the DNMP task in the familiar environment in which they had been trained. However, they were initially impaired in performing the task normally when the same task was carried out in a novel environment (i.e., on a novel maze in a novel testing room). AP5 injected into adjacent hippocampal subregions (e.g., DG or CA1) did not produce such deficits in the novel environment. In the same task CA3a,b, but not CA1, lesions disrupt performance with 10 s delays (Lee and Kesner, 2003). Similar results were obtained with CA3-specific neurotoxic lesions (Lee and Kesner, 2003). Nakazawa et al. (2003) also reported similar findings with a mouse strain in which the function of CA3 NMDA receptors was disrupted. These mutant mice were impaired in learning a novel platform location in a modified water maze task, whereas they were normal in finding familiar platform locations. In sum, these results strongly suggest that rapid, plastic changes in the CA3 network are essential for encoding novel information quickly into the hippocampal memory system and NMDA receptor-mediated plasticity mechanisms appear to play a significant role in the process.

Additional experimental evidence supporting the role of CA3a,b in rapid acquisition of novel information comes from a contextual fear-conditioning experiment with subregion-specific lesions (Lee and Kesner, 2004a). In this experiment, rats with CA3a,b-specific neurotoxic lesions were placed in a contextual fear-conditioning chamber (placed in a room with multiple visual landmarks and distinctive odors as contextual cues). The animals were given a 10-s tone stimulus footshock which co-terminated with a 2-s footshock. When the freezing response was measured during the intertrial interval period during acquisition (when only contextual cues were available), normal animals exhibited freezing behavior from the beginning. However, rats with CA3a,b lesions displayed a delayed onset of freezing behavior, suggesting that rapid formation of memory for the novel contextual cues was disrupted in these animals. Comparable results were reported by Cravens et al. (2006). They showed that rats with CA3 deletion of NMDA receptors failed to acquire a one-trial context discrimination task when tested 3 h, but not 24 h after acquisition.

Using a paradigm developed by Poucet (1989), rats with direct infusions of AP5 (an NMDA antagonist) or naloxone (a μ opiate antagonist) into the CA3a,b, were tested for the detection of a novel spatial configuration of familiar objects and the detection of a novel visual object change The results indicated that naloxone or AP5 infusions into the CA3a,b disrupted both novelty detection of a spatial location and a visual object (Hunsaker et al., 2007c).

Rapid encoding for novel object–place associations has also been shown to be mediated by CA3a,b in that lesions of CA3a,b totally disrupt performance of object-cued recall or place-cued recall tasks (Kesner et al., 2008). More detail is provided in the Section "Cued Recall and Arbitrary Associations."

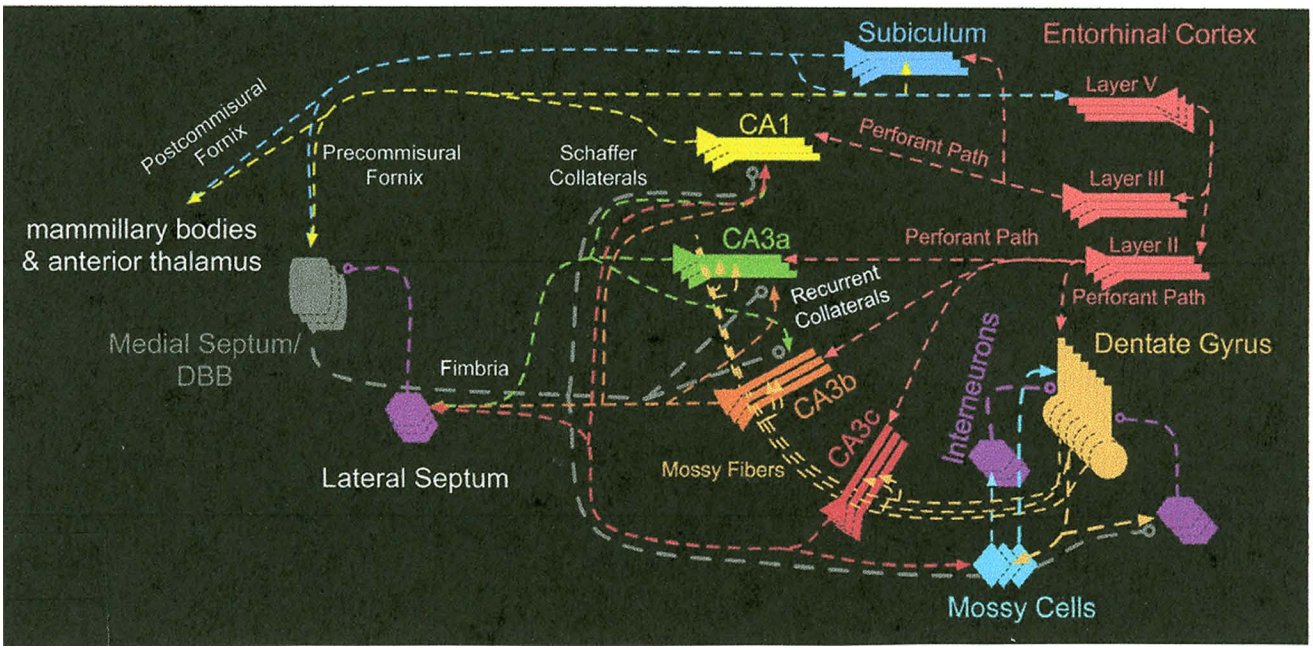

FIGURE 1 | The neural circuit that affects the operation of the CA3 subregion of the hippocampus.

Finally, the CA3 network also seems essential in supporting the retrieval of information from memory when a short-term delay (e.g., 10 s) is introduced (Kesner and Rolls, 2001; Rolls and Kesner, 2006; Kesner et al., 2008). As the information circulates through the recurrent network in CA3, buffering of information within the network is likely to occur. Due to such holding phenomenon for neural activities within the recurrent network, CA3 may play a key role in short-term memory tasks especially when the nature of the tasks entails encoding of novel information or pattern completion. Most experimental results previously described here support this short-term memory function of CA3, since a short-term delay period was imposed in those tasks before the animals made choices. When the delay is prolonged exceeding the short-term range (e.g., 5 min or 24 h), CA3a,b did not remain as a key player in retrieving memory, because after the increased delay CA1 became more important (Lee and Kesner, 2003).

Recently, Lee et al. (2004) showed physiologically that the plasticity mechanism in CA3a,b was activated only when animals encountered novel configurations of familiar cues for the first time. Specifically, rats were trained to circle clockwise on a ring track whose surface was composed of four different textural cues (local cues). The ring track was positioned in the center of a curtained area in which various visual landmarks were also available along the curtained walls. To produce a novel cue configuration in the environment, distal landmarks and local cues on the track were rotated in opposite directions (distal landmarks were rotated clockwise and local cues were rotated counterclockwise by equal amounts). It is well known that principal cells in the hippocampus fire when the animal occupies a certain location of space, known as the "place field" of the cell. Mehta et al. (1997) originally showed that the location of the CA1 place field (measured by the center of mass of the place field) changed over time (shifting backward opposite to the direction of rat's motion) in a familiar environment as the animal experienced the environment repeatedly. Such a prominent shift in the place field location appears to be associated with the NMDA receptor-dependent plasticity mechanism in the hippocampus (Ekstrom et al., 2001). When the rats encountered the changed cue configurations for the first time in the Lee et al. (2004) experiment, the CA3a,b place fields shifted their locations backward prominently compared to the place fields in CA1. However, such prominent shift was not observed in CA3a,b from day 2 onward (CA1 place fields started to exhibit a similar property from day 2). This double dissociation in the time course of plasticity between CA1 and CA3a,b place fields suggests that CA3a,b reacts rapidly to any changed components in the environment, presumably to incorporate the novel components into an existing system (or build a new representation of the environment if changes are significant).

Finally, single unit activity has been recorded in CA3 during the delay period in rats in a spatial position short-term memory task (Hampson et al., 2000) and in monkeys in an object–place and a location–scene association short-term memory task (Watanabe and Niki, 1985; Rolls, 1989a; Colombo et al., 1998; Wirth et al., 2003).

In sum, these results strongly suggest that rapid, plastic changes in the CA3a,b network are essential in encoding novel information involving associations between objects and places, odors and places, or between landmark visual cues and spatial locations, and that NMDA receptor-mediated plasticity mechanisms appear to play a significant role in the process.

PAIRED-ASSOCIATE LEARNING

It has been suggested that the hippocampus and its subregions support associative processes as observed in paired-associate learning tasks (Eichenbaum and Cohen, 2001). McNaughton and Morris (1987), Hasselmo and Wyble (1997), and Rolls (1996) have suggested that the hippocampus and specifically the CA3a,b auto associative network is responsible for the formation and storage of associations. For example, information from parietal cortex regarding the location of an object may be associated with information from temporal cortex regarding the identity of an object. These two kinds of information may be projected to the CA3 a,b region of the hippocampus via the medial and lateral perforant path to enable the organism to remember a particular object and its location. Support for this idea comes from the observation that under the influence of direct infusions into the CA3a,b of AP5 (an NMDA antagonist), which should block transmission of spatial information from the medial perforant path, or naloxone (a μ opiate antagonist), which should block transmission of object information from the lateral perforant path (Breindl et al., 1994), naloxone or AP5 infusions into the CA3a,b disrupted both novelty detection of a spatial location and a visual object (Hunsaker et al., 2007c).

In order to directly test the involvement of the CA3a,b subregion of the hippocampus in spatial paired-associate learning, rats were trained on a successive discrimination go/no-go task to examine object–place paired-associate learning. In this task, two paired-associates were reinforced which consisted of one particular object (A) in one particular location (1) and a different object (B) in a different location (2). Mispairs that were not reinforced included object (A) in location (2) and object (B) in location (1). Rats should learn that if an object was presented in its paired location then the rat should displace the object to receive a reward (Go). However, the rat should withhold displacing the object if it was not in its paired location (no-go). The results indicate that rats with CA3a,b lesions were impaired in learning object–place paired-associations relative to controls (Gilbert and Kesner, 2003).

In a second task, rats were trained on a successive discrimination go/no-go task to examine odor–place paired-associate learning. In this task, the same procedure was used, except that rats needed to learn that when an odor was presented in its paired location the rat should dig in sand mixed with the odor to receive a reward. The results indicated that rats with CA3a,b lesions were severely impaired relative to controls in learning odor–place paired-associations (Gilbert and Kesner, 2003). However, it should be noted that animals with DG or CA1 lesions learned the object–place or odor–place task as well as controls (Gilbert and Kesner, 2003). Similar impairments were obtained following deletion of CA3 NMDA receptors in mice in the acquisition of an odor–context paired-associate learning task (Rajji et al., 2006). These data support the hypothesis that CA3a,b, but not DG or CA1, support paired-associate learning when a stimulus must be associated with a spatial location. To test this idea further, rats were given CA1, CA3a,b, or control lesions prior to learning an object–trace–odor task. The task was run in a 115-cm linear box in which the rat was presented with an object for 10 s, after which it was removed, followed by a 10-s trace period and by the presentation of an odor 50 cm away. If the odor and the object were paired, the rat was to dig in the odor cup for a reward. If unpaired, the rat was to refrain from digging. Animals that had CA1 lesions were unable to make the association and never performed above chance, whereas animals that had CA3a,b lesions performed as well as controls (Kesner et al., 2005). These results support the idea that the CA1 is involved in forming associations that do not necessarily involve spatial information, as long as temporal processing is required. Thus, the CA1 appears to be critical for mediating associations with temporal components, whereas the CA3a,b is important for mediating associations that involve spatial components. In support of the above mentioned statement, it has been shown that both CA3a,b and CA1 lesions disrupt the acquisition of an object–trace–place paired-associate learning task, suggesting that the CA1 appears to be critical for mediating an association with a temporal component, whereas the CA3a,b is important for an association that involves a spatial component (Hunsaker et al., 2006).

Computationally, one hypothesis would be that the CA3 system could provide the working memory necessary for hippocampus-dependent associations across time, and that the CA3 then influences the CA1 for this function to be implemented. The actual learning could involve holding one item active in CA3 but continuing firing in an attractor state until the next item in the sequence arrives, when it could be associated with the preceding item by temporally asymmetric synaptic associativity (Rolls and Kesner, 2006). The computational suggestion thus is that associations across time could be implemented in the hippocampus by using the same functionality that may be used for sequence memory. This model can account for the CA3a,b and CA1 deficits in the object–trace–place paired-associate learning, but cannot account for the CA1, but not CA3a,b, deficit in the object–trace–odor paired-associate learning task. A different computational model to explain the role of the hippocampus in mediating arbitrary associations across time is the temporal context model described by Howard et al. (2005) and Howard and Natu (2005). They suggest that the hippocampus binds arbitrary associations supplied by the entorhinal cortex into a retrievable spatio-temporal context. If one assumes that this could occur via the CA3a,b network or via direct connections to CA1, then this model could account for a significant role of CA1 in mediating arbitrary associations across time, including object–trace–odor and object–trace–place associations. However, it should be noted that the temporal context model only addresses the function of the hippocampus as a whole and does not address the role of CA1 and its potential underlying network in mediating arbitrary associations across time.

CUED RECALL AND ARBITRARY ASSOCIATIONS

Even though the studies above measure the acquisition of paired-associate information, the tasks do not address whether the learning is based on arbitrary associations, in part because the stimuli in the object–place task are integral and cannot be separated from each other. Furthermore, since the tasks are bidirectional discrimination tasks, they are, according to O'Reilly and Rudy (2001) and Morris (2007), likely based on the learning of conjunctions of the cues associated with the task implying that that the cues cannot easily be separated from each other. In the standard model (Marr, 1971; McNaughton and Morris, 1987; Levy,

1996; Hasselmo and Wyble, 1997; Rolls and Treves, 1998; Rolls and Kesner, 2006), the CA3 system acts as an autoassociation system. This enables arbitrary (especially spatial in animals and likely language for humans as well) associations to be formed within the hippocampus. The CA3 recurrent collateral associative connections enable bidirectional associations to be formed between whatever stimuli are represented in the hippocampus, in that, for example, any place could be associated with any object, and in that the object could be recalled with a spatial recall cue, or the place with an object recall cue (Rolls and Treves, 1998).

In one ingenious experiment, Day et al. (2003) trained rats in a study phase to learn in one trial an association between two flavors of food and two spatial locations. During a recall test phase they were presented with a flavor which served as a cue for the selection of the correct location. They found that injections of an NMDA receptor antagonist (APV) or α-amino-3-hydroxy-5-methyl-4-isoxazolepropionic acid (AMPA) receptor antagonist (6-cyano-7-nitroquinoxaline-2,3-dione, CNQX) to the dorsal hippocampus prior to the study phase impaired encoding, but injections of APV prior to the test phase did not impair place recall, whereas injections of CNQX did impair place recall. The interpretation is that, in the hippocampus, NMDA receptors are necessary for forming one-trial flavor–place associations, and that recall can be performed without further involvement of NMDA receptors. The reverse order of cuing the location to recall the flavor has not been tested, so that one cannot be sure whether the hippocampus supports arbitrary associations based on this set of experiments.

Based on the Day et al. (2003) experiment, in the Kesner laboratory, a visual object recall for a spatial location task has been developed. In this task, after training to displace objects, rats in the study phase are placed in the start box and when the door in front of the start box is opened the rats are allowed to displace one object in one location, and then after returning to the start box, the door is opened again and the rats are allowed to displace a second object in another location. There are 50 possible objects and 48 locations. In the test phase, the rat is shown one object (first or second randomized) in the start box as a cue, and then, after a 10-s delay, the door is opened and the rats must go to the correct location (choosing and displacing one of two identical neutral objects). The rats receive a reward for selecting the correct location that was associated with the object cue. A spatial location-recall for a visual object task has also been developed. For the spatial recall for a visual object task, the study phase will be the same, but in this case in the test phase when the door is opened the rat is allowed to displace a neutral object in one location (first or second randomized) on the maze as a location cue, return to the start box, and then, after a 10-s delay, the door is opened and the rats must select the correct object (choosing and displacing one of two visual objects). The rats received a reward for selecting the correct visual object that was associated with the location cue. Rats learn both tasks with 75% or better accuracy. Results indicate that CA3a,b lesions produce chance performance on both the one-trial object–place recall and the place–object recall task (Kesner et al., 2008). The potential implications of such results are that indeed the CA3a,b supports arbitrary associations as well as episodic memory based on one-trial learning. A control fixed visual conditional to place task with the same delay was not impaired, showing that it is recall after one-trial (or rapid) learning that is impaired. Additional support comes from the finding that in a similar one-trial object–place learning followed by recall of the spatial position in which to respond when shown the object, Rolls et al. (2005) showed that some primate hippocampal (including especially CA3a,b) neurons respond with increased activity in the correct spatial location during and after the recall object cue. Thus, some hippocampal neurons appear to reflect spatial recall given an object recall cue. These data are consistent with the prediction of the standard computational model which emphasizes the importance of CA3a,b in mediating the development of arbitrary associations.

There is anatomical support for CA3a,b involvement in support of the mediation of associative processes including arbitrary associations. The perforant path from the entorhinal cortex can be divided into a medial and lateral component. It has been suggested that the medial component processes spatial information and that the lateral component processes non-spatial (e.g., objects, odors) information (Witter et al., 1989; Hargreaves et al., 2005). In one study, Ferbinteanu et al. (1999) showed that lesions of the medial perforant path disrupted water maze learning, whereas lateral perforant path lesions had no effect. In a more recent study based on the idea that the medial perforant path input into the CA3 mediates spatial information via activation of NMDA receptors and the lateral perforant path input into the CA3 mediates visual object information via activation of opioid receptors, the following experiment was conducted. Using a paradigm developed by Poucet (1989), rats were tested for the detection of a novel spatial change and the detection of a novel visual object change under the influence of direct infusions of AP5 (an NMDA antagonist) or naloxone (a μ opiate antagonist) into the CA3a,b. The results indicated that naloxone or AP5 infusions into the CA3a,b disrupted both novelty detection of a spatial location and a visual object (Hunsaker et al., 2007c). Based on electrophysiological data, there is associative long-term potentiation (LTP) between the medial or lateral perforant path and the intrinsic commissural/associational–CA3 synapses, demonstrated by the finding of an associative (cooperative) LTP between the medial and lateral perforant path inputs to the CA3 neurons (Martinez et al., 2002). This could provide a mechanism for object (via lateral perforant path)–place (via medial perforant path) associative learning, with either the object or the place during recall activating a CA3 neuron. Either place or object recall cues could thus be introduced by the associative medial and lateral perforant path connections to CA3 cells.

It should be noted that in contrast to the results obtained with a CA3a,b injection of naloxone or AP5, naloxone infusions into the DG disrupted both novelty detection of a spatial location and a visual object, whereas AP5 infusions into the DG disrupted only detection of a novel spatial location, but had no effect on detection of a novel object. Furthermore, infusions of AP5 into the CA1 region disrupts only the detection of a spatial location change, but not a visual object change, whereas naloxone into the CA1 region disrupts only the detection of a visual object change, but not a spatial location change (Krug et al., 2001; Hunsaker et al., 2007c). Thus, input pathways from medial and lateral perforant path have a different effect on each subregion in part based on the computational processes carried out by that specific subregion.

PATTERN COMPLETION

During retrieval of information, Marr (1971) suggested that the hippocampus recurrent collaterals should play a major role in the hippocampus in retrieving originally stored information patterns in the face of partial inputs to the hippocampus ("collateral effect" or pattern completion). McNaughton and Morris (1987) and Rolls and Treves (1998) suggested that an autoassociative network within CA3 should be able to support pattern completion. Experimental efforts to find evidence of pattern completion within the CA3 region have been successful in recent years. Support for the pattern completion process in CA3 can be found in lesion studies. In one study, Nakazawa et al. (2002) trained CA3 NMDA receptor-knockout mice in the standard water maze task. When the animals were required to perform the task in an environment where some of the familiar cues were removed, they were impaired in performing the task. The result suggests that the NMDA receptor-dependent synaptic plasticity mechanisms in CA3 are critical to perform the pattern completion process in the hippocampus. In a different study, Fellini et al. (2009) reported that with the use of the water maze, NMDA receptors were critical for long-term memory retrieval in pattern completion. In another study (Gold and Kesner, 2005), rats were tested on a cheese board with a black curtain with four extramaze cues surrounding the apparatus. (The cheese board is like a dry land water maze with 177 holes on a 119-cm diameter board.) A Plexiglas partition, 7 cm deep and 8 cm tall, with a 7-cm opening to permit the animal access to each individual food well was placed on the 10th row of the cheese board. Rats were trained to move a sample phase object covering a food well that could appear in one of five possible spatial locations. During the test phase of the task, following a 30-s delay, the animal needs to find the same food well in order to receive reinforcement with the object now removed. Without the Plexiglas partition, rats would adopt a strategy of leaving the goal box directly to the center of the maze and make a right or left turn across the line of potential locations of the reward. The Plexiglas partition discouraged rats from using this strategy and forced the animal to make a clear location choice on the test phase by entering the partition surrounding a particular food well. The rats could not see the food until they made a choice. After reaching stable performance in terms of accuracy to find the correct location, rats received lesions in of dorsal CA3a,b. During post-surgery testing, four extramaze cues were always available during the sample phase. However, during the test phase, zero, one, two, or three cues were removed in different combinations. The results indicate that controls performed well on the task regardless of the availability of one, two, three, or all cues, suggesting intact spatial pattern completion. Following the CA3a,b lesion, however, there was an impairment in accuracy compared to the controls especially when only one or two cues were available, suggesting impairment in spatial pattern completion in CA3a,b-lesioned rats (Gold and Kesner, 2005). A useful aspect of this task is that the test for the ability to remember a spatial location learned in one presentation can be tested with varying number of available cues, and many times in which the locations vary, to allow for accurate measurement of pattern completion ability when the information stored on the single presentation must be recalled. In a subsequent study, naloxone which blocks μ opioid receptors or AP5 which blocks glutamate NMDA receptors were injected into the CA3 a,b region resulted in a disruption visual–spatial pattern completion, whereas AP5 did not disrupt visual–spatial pattern completion, but instead inhibited short-term or working memory (Kesner and Warthen, 2010).

In a different study, Vazdarjanova and Guzowski (2004) placed rats in two different environments separated by ∼30 min. Different objects were located in two different environments. The authors were able to monitor the time course of activations of ensembles of neurons in both CA3 and CA1, using a new immediate-early gene-based brain-imaging method (Arc/H1a catFISH). When the two environments were only modestly different, CA3 neurons exhibited higher overlap in their activity between the two environments compared to CA1 neurons. In the early physiological studies, Robertson et al. (1998) and Rolls (1996) showed that some cells in CA3 respond when a monkey's view of a specific part of space is obscured by a curtain or darkness creating an absence of specific visual inputs. Similar findings have been reported in rats (Samsonovich and McNaughton, 1997). In a more recent study Lee et al. (2004) recorded from ensembles of neurons using multiple electrodes in both CA1 and CA3a,b in freely behaving animals. By altering cue configuration in a ring track, Lee et al. (2004) demonstrated that modestly altered cue configurations was less disruptive in the population spatial code in CA3a,b. However, the population representation of space in CA1 was more easily disrupted by such moderately altered cue configurations. This can be considered as a pattern completion process in CA3a,b, since the CA3a,b network maintained similar spatial representation of the environment (compared to the original spatial representation of the familiar cue configurations) even though the relationships among cues in the environment were altered.

In general, there is good agreement as to the functions of the CA3. Differences emerge in determining whether the CA3 stores long-term episodic information (Rolls and Treves, 1998) that would aid in the pattern completion process or that the neocortex stores long-term episodic information that is transmitted to the CA3 region via the entorhinal cortex and the perforant path (Hunsaker and Kesner, 2013). Most likely the CA3 would employ both sets of information in the process of supporting pattern completion. Two sets of data support the influence of the perforant path into CA3 in that naloxone which blocks μ opioid receptors injected into the CA3 disrupts pattern completion (Kesner and Warthen, 2010) and lesions of the perforant path input into CA3 disrupts retrieval of newly learned information based on previous day learning of the Hebb–Williams maze (Lee and Kesner, 2004b).

Does the dorsal CA3a,b region also play a role in completing a previously learned fixed sequence of spatial locations when the rats are placed in any start position other than the first position and thereby supporting temporal–spatial pattern completion? In one study, Olton et al. (1984) trained rats on fixed sequence in an eight-arm maze based on the magnitude of the reward available in each of four arms (18, 6, 1, or 0 sucrose pellets). After learning the sequence and with some experience of starts in a different arm of the sequence, the rats were given fimbria-fornix or control lesions. The control rats performed the sequence with no difficulty even when new start arms were used, demonstrating temporal–spatial pattern completion. The fimbria-fornix lesioned rats made errors

by always returning to the first position in the sequence regardless of which start position was used. This suggests that fimbria-fornix lesioned rats cannot remember the correct temporal–spatial context, but they do not have any difficulty remembering the serial order of the sequence.

In a more recent study, DeCoteau and Kesner (2000) trained rats in a sequential spatial location list learning paradigm using a correction procedure to visit the arms of an eight-arm maze in a particular sequence, with food obtained in each arm if a correct choice (made by orienting) was made. Even though lesions of the hippocampus impaired the acquisition of this task, there were no deficits when hippocampus lesions were made after reaching 90–100% correct performance (DeCoteau and Kesner, 2000). Thus, the hippocampus may be necessary for learning new spatial sequences, but once learned, the hippocampus lesioned rats can perform the sequence as long as the rats are started from the beginning of the sequence. To test for subregional specificity, control, dorsal CA3a,b, and dorsal CA1 lesioned rats were tested postoperatively for completion of the sequence when started in different positions in a previously learned list of spatial locations (Hoang and Kesner, 2008). The results indicate that control and dorsal DG lesioned rats had no difficulty completing the sequence, regardless of starting point. In contrast, when the dorsal CA3a,b lesioned rats were started in different positions within the sequence, they would invariably orient in front of the first position before making other response sequence errors. On a quantitative level when they made an orienting response to the wrong door (error) in the sequence, the average probability of making incorrect orienting responses for each position indicated that the dorsal CA3a,b rats made many incorrect orienting responses (errors). This suggests that CA3a,b lesioned rats cannot remember the correct temporal–spatial context implying difficulty in temporal–spatial pattern completion (Hoang and Kesner, 2008). These data are consistent with the observation that fimbria-fornix lesioned rats always returned to the beginning of the first position in the sequence regardless of which start position was used (Olton et al., 1984), even though it should be noted that in the Olton et al. (1984) study, the list length was shorter, the list sequence was influenced by magnitude of reinforcement, and the lesioned rats completed the sequence without making many errors. In the same study, when the dorsal CA1 lesioned rats were started in different positions within the sequence, they would orient in front of any of the forward located positions suggesting the use of random orienting responses (errors) across the completion of the sequence. On a quantitative level when they made an orienting response to the wrong door (error) in the sequence, the average probability of making incorrect orienting response indicated that CA1 lesioned rats made decreasing numbers of incorrect orienting responses as the starting position is increased. The errors made by CA1 lesioned rats appeared to be due to difficulty in temporal spatial pattern completion in that the decrease in errors was due to the observation that all the errors were made in the process of completing the spatio-temporal sequence, suggesting that CA1 lesioned rats have difficulty in remembering the serial order of the spatial sequence. These results suggest that the dorsal CA3a,b in conjunction with CA1 supports recall of a temporal sequence of spatial locations, requiring a completion process. Both CA3a,b and CA1 are likely involved because CA3a,b processes the spatial–temporal context and CA1 processes temporal information. From a computational point of view it has been suggested that temporally asymmetric associations between the successive pairs of items in a sequence are implemented in dorsal CA3 by some temporally asymmetric synaptic modifiability (Levy, 1996; Mehta et al., 2002; Howard et al., 2005; Jensen and Lisman, 2005) and the dorsal CA1 network in this situation could help to separate out the representation of the next item in the list from the currently processed item via a chunking process and thus providing for a temporal–spatial context suggesting that the dorsal CA1 can be thought of as performing temporal pattern completion for spatial locations (Kesner et al., 2004; Rolls and Kesner, 2006). These models are consistent with the evidence that rats with hippocampus lesions do not learn the fixed spatial sequence task (DeCoteau and Kesner, 2000). Alternatively, Lisman (1999), Lisman and Otmakhova (2001), and Lisman and Grace (2005) have suggested that the hippocampus operates a match–mismatch detector during the processing of novel changes within a sequence or start of a sequence. They suggest that the first spatial location can serve as a trigger for recall of the entire sequence within the dorsal CA3 region, which would be consistent with the errors made by CA3a,b lesioned rats which involved an error for the first position regardless of which start position was used. Because the readout is presumed to be time compressed, it reaches dorsal CA1 more quickly allowing the dorsal CA1 region to anticipate what will happen next based on previous experience. Based on the idea that the dorsal CA1 operates as a match–mismatch detector comparing predictions arriving from dorsal CA3a,b compared to direct entorhinal inputs into dorsal CA1 (Hasselmo and Schnell, 1994; Hasselmo and Wyble, 1997), the dorsal CA1 should play an important role in detection of changes in the sequence, which is consistent with the observation that lesions of the dorsal CA1 region results in errors that appeared to be random. Thus, the hippocampus and more specifically the dorsal CA1 and dorsal CA3a,b subregions contribute to the processing of previously learned sequence information for spatial locations and most likely contribute to the establishment of learned sequences.

A SPECIAL ROLE FOR CA3c

It has been suggested that CA3 might also play a role in spatial pattern separation, but in this case not for a metric spatial representation, but for spatial representation of the geometry of the environment. This idea is supported by the finding of Tanila (1999) who showed that CA3c place cells were able to maintain distinct representations of two visually identical environments, and selectively reactivate either one of the representation patterns depending on the experience of the rat. Also, Leutgeb et al. (2005, 2007) recently showed that when rats experienced a completely different environment, CA3c place cells developed orthogonal representations of those different environments by changing their firing rates between the two environments, whereas CA1 place cells maintained similar responses. One model described by Rolls and Kesner (2006) to account for these results proposes that the CA3 and DG may have similar representations of the environment. This may be consistent with the computational point of view that if dorsal CA3 is an autoassociator, the pattern representations in it

should be as orthogonal as possible to maximize memory capacity and minimize interference. The theory holds that the actual pattern separation may be performed as a result of the operation of the dentate granule cells as a competitive net, and the nature of the mossy fiber connections to dorsal CA3 cells. To test this idea an experiment was conducted to determine whether the DG or CA3 regions cooperate to perform spatial pattern separation operations for specific spatial locations as well as the spatial geometry of the environment or whether the DG performs spatial pattern separation on the basis of specific locations in space and the CA3 performs spatial pattern separation on the basis of the geometry of the environment. Rats with lesions of DG and CA3a,b were given the opportunity to explore a white or black circular or square box of the same size as reported by Leutgeb et al. (2007) and in addition in the box there were two objects spaced 68 cm apart. After habituation to the box and the objects, the rats received one of two transfer tests. In the first test, the objects were changed to a 38 cm distance, but the box shape (geometry of the environment) remained the same (Hunsaker et al., 2008a). In the second test, the box shape (geometric environment) was changed, but the distance between the objects remained the same. The efficacy of the transfer test in terms of re-exploration of the metric change is based on a comparison between the level of object exploration during the transfer session versus the level of object exploration during the last session of habituation. Similarly, the efficacy of the transfer test in terms of re-exploration of the geometry of the environment is based on the number of grid crossings (activity level) and rearings during the transfer session versus the number of grid crossings and rearings during the last session of habituation. The results indicate that lesions of the DG, but not CA3a,b, disrupt both the detection of metric changes in the spatial location of objects and changes in a geometrical environment. Thus far, these data are consistent with the prediction of the Rolls computational model that the DG is the critical substrate for spatial pattern separation. These data are not consistent with (Tanila, 1999; Leutgeb et al., 2005, 2007) findings of a pattern separation function for geometrical environments. It has been shown that the CA3 region can be divided into a CA3a, b, and c subareas (Lorente de Nó, 1934; Li et al., 1994). Most of the recording of cells that respond to different environments reported by Tanila (1999) and Leutgeb et al. (2005, 2007) were based on electrode placements in the CA3c area. The present lesion data are based on lesions within CA3a,b, but not CA3c. Based on the research of Li et al. (1994) and Buckmaster and Schwartzkroin (1994), it has been proposed that mossy cells receive excitatory inputs from granule cells and CA3c pyramidal cells and integrate the inputs from granule cells and CA3c pyramidal cells, which, in turn, via excitatory recurrent axonal projections activate many distal granule cells. Such a circuit could integrate spatial location information and form representations of geometrical environments. Additional experiments with CA3c lesions in contrast to the CA3a,b lesions revealed that dorsal CA3c is only involved in pattern separation processes when the animal is required to detect a metric change in object location. This was observed during the metric change in object location task (with both decreased object exploration and rearing; but at a smaller magnitude than the DG effect). There was no apparent effect of a CA3c lesion during the environmental change task. To explain these results, it may be that the DG selectively recruits CA3c to assist in the metric detection and not the detection of the overall environmental change. This interpretation is in agreement with the suggestions of Scharfman (2007), who suggests that CA3c cooperates with the DG to support efficient spatial memory formation and subsequent recall and is supported by Jinde et al. (2012) and Jinde et al. (2013), who demonstrated that hilar mossy cells, receiving CA3c inputs, play an overall inhibitory role in DG excitability. Also, it is possible that if CA3c forms a circuit with the DG that participates in sparse encoding of entorhinal inputs, the feedback circuit would be more critical for detection of discrete changes, such as after metric shifts in object locations. Since the change in overall environmental geometry is a very large and prominent change, the feedback circuit may not be as relevant due to the size of the change (i.e., the DG can easily orthogonalize the two environments with or without CA3c feedback modulation). The implication of this theory is that for small-scale or subtle changes, the dorsal DG and dorsal CA3c cooperate to orthogonalize the incoming visuo-spatial data with a fair degree of resolution. The CA3c projection to the hilar mossy cells would act to inhibit the granule cells, facilitating even sparser encoding than the DG would normally provide (i.e., a more orthogonal representation). For larger changes, such as for an overall environmental change, CA3c is not needed because the requirement for sparse encoding is not present (low spatial resolution is more than sufficient to distinguish a circle from a square environment). That is to say, it is easier for the animal to identify orthogonal charts than to process metric relationships between stimuli (Rolls and Kesner, 2006).

FUNCTIONAL ANALYSIS OF THE CA3 SCHAFFER COLLATERAL INPUTS INTO CA1

The CA3 has a direct output pathway into CA1, suggesting the possibility of CA3 modulation of CA1 functions. Rolls and Kesner (2006) have suggested that the CA1 has at least four major functions, including temporal processing of information (temporal order memory), associations across time, intermediate memory, and consolidation of new information. One of the mnemonic processes suggested for CA1 involves the mediation of temporal processing of information involving chunking and temporally separating information to endow spatial and/or non-spatial contexts with a temporal structure of the information to be remembered. This process would require extensive processing of information in CA1 and thus may influence intermediate-term rather than short-term memory representations. If one assumes that CA3 is important for associating, processing, and integrating sequential information, and perhaps for maintaining a short-term memory representation of sequentially associated information as a context, then this information might be sent via feed-forward connections to CA1. Computational models and physiological data (Skaggs et al., 1995; Rolls, 1996) have suggested that CA1 may play a role in compressing temporal sequences. Rolls and Kesner (2006) have suggested that CA1 recodes the information represented in the CA3 network by holding one item active in CA3, but continuing firing in an attractor state until the next item in the sequence arrives, when it can be associated with the preceding item by

temporally asymmetrical synaptic associativity, possibly through a chunking process.

TEMPORAL ORDER MEMORY

It has been shown in humans that order judgments improve as the number of items in a sequence between the test items increases (Banks, 1978; Chiba et al., 1994; Madsen and Kesner, 1995). This phenomenon is referred to as a temporal distance effect (sometimes referred to as a temporal pattern separation effect; Kesner et al., 2004). The temporal distance effect is assumed to occur because there is more interference for temporally proximal events than for temporally distant events. To test for the temporal pattern separation effect in rodents, Gilbert et al. (2001) tested memory for the temporal order of items in a one-trial sequence learning paradigm in rodents. In the task, each rat was given one daily trial consisting of a sample phase followed by a choice phase. During the sample phase, the animal visited each arm of an eight-arm radial maze once in a randomly predetermined order and was given a reward at the end of each arm. The choice phase began immediately following the presentation of the final arm in the sequence. In the choice phase, two arms were opened simultaneously and the animal was allowed to choose between the arms. To obtain a food reward, the animal had to enter the arm that occurred earlier in the sequence that it had just followed. Temporal separations of 0, 2, 4, and 6 were randomly selected for each choice phase. These values represented the number of arms in the sample phase that intervened between the arms that were to be used in the test phase. After reaching criterion, rats received control, CA3 or CA1 lesions. The results indicated that control rats matched their preoperative performance across all temporal separations. In contrast, rats with CA1 lesions performed at chance across zero, two, or four temporal separations and a little better than chance in the case of a separation of six items. The results suggest that the CA3 and CA1 subregions are involved in memory for spatial location as a function of temporal separation of spatial locations, suggesting that lesions of the CA3 and CA1 decrease efficiency in temporal pattern separation. Using the same paradigm as described above for odors resulted in intact function for the dorsal CA1, but a deficit was observed for ventral CA1 (Kesner et al., 2010). There are no data available to suggest that the ventral CA3 may also produce a deficit. These results suggest CA3 can influence CA1 function and perhaps promote an inability to inhibit interference that may be associated with sequentially occurring events. The increase in temporal interference impairs the rat's ability to remember the order of specific events. Although CA1 lesions have been shown to produce a deficit in temporal pattern separation (Gilbert et al., 2001), some computational models (Levy, 1996; Wallenstein and Hasselmo, 1997; Lisman, 1999; Rolls and Kesner, 2006) have suggested that the CA3 region is an appropriate part of the hippocampus to form a sequence memory, for example, by utilizing synaptic associativity in the CA3–CA3 recurrent collaterals that entail a temporally asymmetrical component.

In a more recent experiment using an exploration paradigm described by Hannesson et al. (2004), it can be shown that temporal order information for visual objects is impaired only for CA1, but not for CA3 lesions (Hoge and Kesner, 2007). Thus, based on previous research, it has been suggested that the CA1 hippocampal subregion serves as a critical substrate for sequence learning and temporal order or temporal pattern separation. This position would be consistent with CA1 deficits in temporal order for spatial locations, odor, and visual objects (Hunsaker et al., 2008c). In addition, it appears that dorsal CA3 contributes to this temporal order sequential process whenever spatial location or odor are a factor; however, the CA3 region does not appear to play a role in these processes for visual object information (Hoge and Kesner, 2007; Hunsaker et al., 2008c). It is important to note that selective lesions of the NR1 subunit of the NMDA receptor in CA3 or CA1 resulted in a lack of any effect on temporal processing using the spontaneous exploration paradigm, which suggests that the NMDA receptor does not play an important role in temporal processing (Place et al., 2012).

ASSOCIATIONS ACROSS TIME

There is evidence implicating the hippocampus in mediating associations across time (Rawlins, 1985; Kesner, 1998). In particular, the CA1 subregion of the hippocampus may play a role in influencing the formation of associations whenever a time component (requiring a memory trace) is introduced between any stimuli that need to be associated. It has previously been shown that the acquisition of an object–odor association is not hippocampus-dependent (Gilbert and Kesner, 2003); however, it is unclear whether adding a temporal component would recruit the hippocampus and more specifically the CA1 region. To test this idea, rats were given CA1, CA3, or control lesions prior to learning an object–trace–odor task (Kesner et al., 2005). The task was conducted in a 115-cm linear box, in which the rat was presented with an object for 10 s, after which it was removed, followed by a 10-s trace period and by the presentation of an odor 50 cm away. If the odor and the object were paired, then the rat was to dig in the odor cup for a reward. If the odor and the object were unpaired, then the rat was to refrain from digging. Animals that had CA1 lesions were unable to make the association and never performed above chance, whereas animals that had CA3 lesions performed as well as control rats (Kesner et al., 2005). Furthermore, it can also be shown (MacDonald et al., 2011) that in the same paradigm neuronal activity from CA1 neurons fire during the trace interval reflecting location and ongoing behavior, which could also be based on the anticipation of the odor component of the task. However, no recordings were made of neurons within CA3. These results support the idea that the CA1 is involved in forming arbitrary associations that do not necessarily involve spatial information, as long as temporal processing is required. In support of this conclusion, it has been shown that both CA3 and CA1 lesions disrupt the acquisition of an object–trace–place paired-associate learning task, suggesting that the CA1 appears to be critical for mediating an associations with a temporal component, whereas the CA3 appears to contribute to temporal associations only when a spatial component is involved (Hunsaker et al., 2006). In an interesting study, McEchron et al. (2003) recorded from single cells in the CA1 region of the hippocampus during and after trace heart rate (fear) conditioning using either a 10- or 20-s trace interval. They reported that a significant number of cells showed maximal firing on CS-alone retention trials timed to the 10- or 20-s trace

after CS offset. This finding could reflect the transition from an attractor state implemented in CA3 with its recurrent collaterals that represents the CS to an attractor state that represents the conditioned response (CR; Rolls and Deco, 2002; Deco and Rolls, 2003, 2005). Computationally, one hypothesis would be that the CA3 system could provide the short-term memory necessary for hippocampus-dependent associations across time, and that the CA3 then influences the CA1 for this function to be implemented. The actual learning could involve holding one item active in CA3, but continuing firing in an attractor state until the next item in the sequence arrives, at which point it could be associated with the preceding item by temporally asymmetrical synaptic associativity (Rolls and Kesner, 2006). The computational suggestion is thus that associations across time could be implemented in the hippocampus by using shared functionality that may be used for sequence memory.

INTERMEDIATE MEMORY

In addition to the processing of temporal information, the CA1 subregion appears to entail cellular processes that match it to longer-term types of memory (intermediate-term memory) than that of CA3, which is thought to mediate short-term memory. To examine this idea rats with either CA3 or CA1 lesions were tested on a DNMP task in an eight-arm maze with a 10-s delay. Animals with CA3 lesions showed reliable acquisition impairments at the 10-s delay. Animals with CA1 lesions showed normal acquisition, suggesting that the CA1 region may not be necessary at short delay intervals (Lee and Kesner, 2003). Moreover, when transferred to a new maze in a different room and using a 10-s delay, similar impairments were observed for CA3- but not CA1-lesioned rats. Deficits for CA1 did not emerge until a 5-min delay was introduced. Interestingly, comparable deficits at a 5-min delay were also found for CA3-lesioned rats (Lee and Kesner, 2003). It should be noted that similar results as described for the lesion data were obtained following AP5 injections, which impaired transfer to the new environment when made into CA3, but not into CA1. At 5-min delays, AP5 injections into CA1 produced a sustained deficit in performance, whereas AP5 injections into CA3 did not produce a sustained deficit (Lee and Kesner, 2002, 2003). In a different study using a continuous recognition task for odors, Farovik et al. (2009) reported that with a 3-s interval between odors, rats with lesions of the dorsal CA3, but not dorsal CA1 disrupted memory for the order of odor information, but with a 10-s interval between odors, both CA1 and CA3 lesioned rats were impaired for odor information.

CONSOLIDATION AND LONG-TERM MEMORY

It has been suggested that the CA3 can influence the activity of CA1 by promoting a consolidation process resulting in long-term memory. To test this idea that the CA1 and CA3 region might be involved in retrieval after long (24 h) time delays, rats with CA1 or CA3 lesions were tested in a modified Hebb–Williams maze. The results indicated that CA3 lesioned rats were impaired in encoding (within-day tests), but with no deleterious effect on retrieval with a 24-h delay (across-day tests). In contrast, CA1-lesioned rats were impaired in retrieval with a 24-h delay (across-day tests), but they have no difficulty in encoding new information (i.e., within-day tests; Jerman et al., 2006; Vago et al., 2007). Using a spatial contextual fear-conditioning paradigm, rats with dorsal CA1, but not dorsal CA3, lesions were impaired relative to controls in retention (long-term memory) of contextual fear-conditioning (Lee and Kesner, 2004a,b; Hunsaker and Kesner, 2008). In a different study, Gall et al. (1998) demonstrated that c-fos gene expression was elevated selectively more in CA1 compared to CA3 only after overtraining in an olfactory discrimination task, whereas the same gene expression in CA3 compared to that in CA1 was selectively enhanced after the initial acquisition of the olfactory discrimination task. Furthermore, sustained neural activity over intervals of hours to days potentially promoting consolidation is mediated by CA1, but not CA3 neurons (Mankin et al., 2012). In a different task, Florian and Roullet (2004) showed that focal injections of diethyldithiocarbamate (DDC) into the CA3 region impaired the acquisition, but not recall of spatial information in the water maze. Also, injection of DDC into the CA3 region immediately after training in the water maze disrupted consolidation 24 h later. In a different study, Lassalle et al. (2000) also tested animals in the water maze and found that DDC injections into CA3 did not disrupt memory consolidation. The above-mentioned data suggest that the CA1 region may play an important role in supporting consolidation processes, but it appears that CA3 does not have a powerful modulatory effect on CA1 in affecting the consolidation process. Rather it is assumed that CA1 is important for consolidation of new information within the intermediate temporal memory framework by connecting with neocortical systems to promote consolidation.

INTERACTIONS AND DISSOCIATIONS BETWEEN CA1 AND CA3

The dominant view of the relationship between CA3 and CA1 and short-term and intermediate-term memory is that they operate as a feed-forward sequential processing system. There is evidence to suggest that, under certain task conditions, both the CA1 and CA3 interact in the processing of short-term and intermediate-term memory (Gilbert et al., 2001; Lee et al., 2005; Kesner et al., 2008; Farovik et al., 2009). However, based on more recent data, it is suggested that, for certain tasks, dissociations exist between short-term and intermediate-term memory mediated by the CA3 and CA1 subregions, respectively (Kesner, 2007). Moreover, evidence of parallel processing between the CA3 and CA1 implies possible functional independence of short-term and intermediate-term memory processes. One result that has been obtained when one compares the relationships between CA3 and CA1 is that there is a deficit following dysfunction of the CA3 subregion, but no concomitant deficit following dysfunction of the CA1 subregion. For example, lesions of the CA3, but not the CA1, subregion impair the acquisition of the DNMP task on an eight-arm maze with 10-s delays (Lee and Kesner, 2003) or novelty detection of a spatial location (Lee et al., 2005). Furthermore, CA3, but not CA1, lesions impair within-day learning (encoding) in a Hebb–Williams maze (Jerman et al., 2006; Vago et al., 2007). Taken together, these results suggest that short-term and intermediate-term memory can operate independently of each other. Is there an anatomical basis for this apparent parallel operation between CA3 and CA1 and short-term and intermediate-term episodic memory? Given that CA1

represents the primary output from the hippocampus, especially in light of the fact that CA3 does not have direct axonal projections to the subiculum or entorhinal cortex, how can information be transmitted to other neural regions outside the hippocampus once CA1 is ablated? Evidence presented in more detail elsewhere indicates that there is an important output from the CA3 to the septum via the fimbria and that lesions of the fimbria can mimic the CA3 lesion effects (Hunsaker et al., 2007b, 2008b). Further evidence of a functional dissociation between CA1 and CA3 can be observed on a number of tasks that produce a deficit in CA1, but no concomitant deficit following dysfunction of CA3. For example, intermediate-term memory in a delayed (5-min) non-matching-to-sample for a spatial location task is disrupted by AP5 injections into the CA1, but not into the CA3 subregion (Lee and Kesner, 2002). Furthermore, temporal order for a visual object (Hoge and Kesner, 2007), retrieval of information acquired in a Hebb–Williams maze (Jerman et al., 2006; Vago et al., 2007), and retention of contextual fear-conditioning are disrupted by CA1 but not CA3 lesions (Lee and Kesner, 2004a; Hunsaker and Kesner, 2008). These results also suggest that intermediate-term and short-term memory can operate independently of each other, begging the question whether there is a different anatomical basis for this apparent parallel operation between CA3 versus CA1 and short-term versus intermediate-term memory. In all these cases when there is a deficit following CA1 lesions, but not CA3 lesions, the possibility exists that the deficit is due to a faulty input from the direct perforant pathway to CA1, because the Schaffer collateral input is intact.

Based on the idea that *in vitro* dopamine injections into the CA1 region inhibit the direct perforant path projection to the CA1 region without affecting the Schaffer collateral projection into the CA1 region (Otmakhova and Lisman, 1999), rats were injected with apomorphine (a non-selective dopamine agonist) or vehicle control in the CA1 region in the delayed (5 min) non-matching-to-sample for a spatial location task, in the Hebb–Williams maze task, and in the contextual fear-conditioning task. The results showed that apomorphine injections into the CA1 disrupted performance in all of these tasks. Furthermore, apomorphine injections into CA1 did not disrupt encoding in the Hebb–Williams maze or transfer of short-term memory for a spatial location in a non-matching-to-sample task to a novel environment (a new maze), which represent processes that are not dependent on the CA1 region (Vago et al., 2007; Vago and Kesner, 2008). Apomorphine injections into the CA1 subregion produce the same pattern of deficits as are produced by CA1 but not CA3 lesions. Taken together, these results suggest that in situations where there is a CA1 but no CA3 lesion effect, the direct perforant path input into the CA1 region represents the main input for the integrity of intact performance, perhaps based on intermediate-term memory processing.

It can also be shown that in some tasks, there is an interaction between CA3 and CA1 in that one can observe a deficit following dysfunction of either the CA3 or CA1 subregion. For example, when multiple temporally organized sequential information is to be remembered within a short-term memory system, such as memory for multiple spatial locations, both CA3 and CA1 lesions produce impairments (Gilbert et al., 2001; Lee et al., 2005; Kesner et al., 2008). Thus, there is the implication that both regions are working cooperatively and that CA1 is likely to benefit from a feed-forward Schaffer collateral connection from CA3.

FUNCTIONAL ANALYSIS OF MOSSY FIBER VERSUS PERFORANT PATH INPUTS INTO CA3a,b

McNaughton and Morris (1987), Rolls and Treves (1998), and Rolls and Kesner (2006) have suggested that the dentate granule cell/mossy fiber pathway to CA3 may be important during the learning of new associations in the CA3 network, and that part of the way in which it is important is that it helps by pattern separation to produce relatively sparse and orthogonal representations in CA3. In addition, the theory proposes that the direct perforant path input to CA3 is important in initiating retrieval from the CA3 autoassociation network, especially with an incomplete retrieval cue.

In order to test the above mentioned ideas, a Hebb–Williams maze was used. In this task, rats were required to traverse a maze from the start to goal box in the most direct possible path. Learning across the final five trials of the first day compared to the first five trials of the first day of training was used as an index of encoding, and performance on the first 5 days of the second day compared to the last five trials of the first day was used as an index of retrieval. These operationally defined encoding and retrieval epochs were on average 10 min in length each. Using this task, it was found that lesions of the DG or CA3a,b (or a crossed lesion) disrupt within-day learning on the Hebb–Williams maze, but that retrieval of information at the start of the following day is not impaired (Lee and Kesner, 2004b; Jerman et al., 2006). In contrast, lesions of the perforant path input to CA3a,b from entorhinal cortex disrupt retrieval (i.e., initial performance on the following day), but not learning within a day (Lee and Kesner, 2004b). These findings support the hypothesis that the CA3 processes both inputs from the DG to support pattern separation and inputs from the entorhinal cortex via the perforant path to support pattern completion.

Furthermore, with respect to short-term memory, the DG and mossy fiber input into CA3 are not directly involved. This is illustrated by the observation that on a spatial pattern separation task, the performance of DG lesioned rats increased as a function of increased spatial separation between the target location and the foil location, whereas CA3 lesions were impaired across all spatial separations, indicating a potential impairment in short-term memory for spatial location information (Gilbert et al., 2001; Gilbert and Kesner, 2006).

Thus, from an anatomical perspective possible dissociations between DG and mossy fiber input into CA3 are primarily due to the observation that the CA3 subregion of the hippocampus has two major inputs with a direct connection from the DG via the mossy fibers and a direct input from the perforant path which bypasses the DG. In addition, short-term memory may be generated intrinsically in the CA3 region, but not in the DG.

A MODEL FOR BIASING CA3 TOWARD PATTERN SEPARATION OR PATTERN COMPLETION

A circuit between the hippocampus and medial septum/diagonal band of Broca has been characterized, as well as an efferent

pathway from the hippocampus to the lateral septum (Raisman et al., 1966; Swanson and Cowan, 1977, 1979; Wyss et al., 1980; Gaykema et al., 1991). Briefly, CA3 subcortical efferents in the fimbria terminate in the lateral septum, medial septum, and diagonal band of Broca that result in net medial septum/diagonal band of Broca inhibition. CA1 subcortical efferents in the dorsal fornix also terminate in the lateral septum, medial septum, and diagonal band of Broca that result in net medial septum/diagonal band of Broca excitation. These differential effects occur because the CA3 and CA1 projections synapse onto distinct neuron populations. The medial septum and diagonal band of Broca send cholinergic efferents via the fimbria into the hippocampus that have been implicated in the hippocampal theta rhythm and modulation of learning and memory (McLennan and Miller, 1974; Rawlins et al., 1979; McNaughton and Miller, 1986; Hasselmo and Bower, 1993; Hasselmo and Schnell, 1994; Hasselmo et al., 1995, 2002a,b; Hasselmo, 1999, 2005; Hasselmo and Fehlau, 2001; Hasselmo and McGaughy, 2004; Hasselmo and Giocomo, 2006). Critically, these studies also demonstrated that acetylcholine in the hippocampus acts presynaptically by inhibiting glutamate release, presumably through M4 muscarinic acetylcholine receptor activation primarily at synapses in the stratum radiatum. GABAergic inputs are involved in hippocampal function as well, but act too rapidly to modulate encoding and consolidation/retrieval as operationally defined in most studies (i.e., behavioral encoding and retrieval are measured in seconds or minutes as opposed to the millisecond time course of the GABAergic modulation within theta phase precession and similar processes; cf., Wallenstein and Hasselmo, 1997). It is suggested that these GABAergic projections are potentially involved in biasing pattern separation and pattern completion dynamics at millisecond timescales such as during theta cycles, and acetylcholine regulates these processes at longer time scales, such as the second to minute timescales encountered during cognitive testing. In CA1 and CA3, acetylcholine has a more robust inhibitory effect in stratum radiatum than stratum oriens, stratum lacunosum-moleculare or stratum lucidum in slice preparations. In the DG, there are dense cholinergic projections into the inner molecular layer as well as the hilus and acetylcholine effects to disinhibit granule neurons in the DG by reducing tonic inhibition.

The CA3 recurrent collaterals terminate primarily within the stratum radiatum, whereas the perforant path inputs terminate in the stratum lacunosum-moleculare and the mossy fibers terminate largely in the stratum lucidum with additional synapses onto thorny excrescences in the stratum oriens and stratum radiatum as well. Despite a partial overlap in connectivity among these input pathways, this pattern of connectivity suggests that the mossy fiber pathway (at least synapses in the stratum oriens and stratum lucidum) and perforant pathway inputs (in the stratum lacunosum-moleculare) are not as dramatically affected by acetylcholine influx as the recurrent collateral and Schaffer collateral inputs (which are presynaptically inhibited by acetylcholine via M4 receptors) – though they are bound to be affected to some degree, but this could arguably be beneficial and result in a high signal to noise ratio in the hippocampal system (cf., Hasselmo et al., 1995, 1996). These data suggest that acetylcholine modulates the hippocampus primarily by selectively altering the signal to noise ratio within the recurrent collaterals and Schaffer collaterals in the stratum radiatum by reducing synaptic transmission (Hasselmo and Schnell, 1994; Hasselmo et al., 1995, 1996).

An important additional effect of elevated acetylcholine levels in the hippocampus is the net result on DG granule neurons. Bilkey and Goddard (1985) demonstrated that activations of septal projections into the hippocampus resulted in disinhibition of granule neurons through inhibition of inhibitory interneurons that provide tonic inhibition to the granule neurons (i.e., disinhibition). Medial septal stimulation at magnitudes insufficient to result in evoked responses facilitated population spikes in the DG to medial perforant path stimulation *in vivo*. In other words, the tonic inhibition on the granule neurons from the inhibitory neurons in the hilus typically attenuating or shunting the activity levels of granule neurons is reduced by cholinergic influx – thereby increasing the levels of responsiveness to stimuli of the DG granule neurons under the same conditions that the influence of the recurrent collaterals in CA3 are minimized, supporting cholinergic models of encoding/retrieval dynamics in the hippocampus (cf., Hasselmo et al., 1996). Alternately, any reduction from the baseline levels of cholinergic influence in the DG would result in a net increase in inhibitory tone on granule neurons. This mechanism is important for models of hippocampal encoding and retrieval that require a relatively quiescent mossy fiber input to allow retrieval processes to be initiated via the perforant path projections from the entorhinal cortex (cf., Treves and Rolls, 1992, Treves and Rolls, 1994; Rolls, 1996).

It is important to note that the proposed mechanisms whereby the dentate gurus engages in pattern separation does not actually require low activity levels of granule neurons, but rather requires the sparseness of encoding – that is to say the divergent connections from the entorhinal cortex to the DG via the perforant path and the subsequent convergence of mossy fiber inputs to CA3 (Treves and Rolls, 1992, 1994; Rolls, 1996). In this case, the reduction of tonic inhibition in the DG would not result in reduced competitive inhibition, as the disinhibited granule neurons would be more likely to fire action potentials that excite the inhibitory interneurons that mediate competitive inhibition than they were when inhibited. What would be facilitated by disinhibition, however, is the responsiveness of the DG granule cells to perforant path inputs.

In other words, although the DG granule cells would be more responsive to entorhinal inputs, the cells would not sacrifice precision in their encoding because the following factors would remain unaltered: (1) the connectivity matrix with the entorhinal cortex would not be changed. (2) The competitive inhibition through local interneurons would be intact as the interneurons would still respond to mossy fiber inputs in the normal way. (3) CA3c is recruited in the dentate gurus network with the mossy cells in the hilus for pattern separation (cf., Myers and Scharfman, 2009, 2011) and these cells remain relatively unaffected by acetylcholine efflux (no recurrent collateral synapses in the stratum radiatum). When these three factors are not changed the net effect on the DG would actually be an increase in the overall competitive inhibition in the network but now with a lower threshold for initiation of these winner take all processes. This increased responsiveness to stimuli in the granule neurons, in concert with the reduced efficacy of the recurrent collateral synapses to activate CA3 pyramidal

cells would facilitate information transfer from the mossy fibers to the CA3 pyramidal cells with no net sacrifice of DG-dependent pattern separation.

Based on the models proposed by Hasselmo and Bower (1993), it is suggested that CA1 provides a feedback control over the cholinergic modulation of the hippocampus. It is proposed that CA1 sends a "mismatch" signal to the lateral septum, medial septum, and diagonal band of Broca in response to information that needs to be encoded – a process facilitated by pattern separation. This means that if information from the Schaffer collateral fiber pathway does not match the information in the perforant path projections, then CA1 signals the septum to raise levels of acetylcholine in the hippocampus to facilitate pattern separation processes and attenuate pattern completion processes by reducing recurrent collateral transmission while disinhibiting the granule neurons in the DG. The CA1 projections, importantly, are excitatory on cholinergic projection cells, overriding any effects of CA3 projections in the fimbria that serve a somewhat tonic inhibitory function. Conversely, in the absence of a CA1 mismatch signal, CA3 projections via the fimbria to the medial septum and diagonal band of Broca result in reduced acetylcholine levels, which facilitate pattern completion and retrieval of learned patterns. This means that if information from the perforant path matches the information in the Schaffer collaterals, then CA1 does not send excitatory signals the septum, which when combined with CA3 projections that inhibit the medial septum, serves to attenuate levels of acetylcholine in the hippocampus to facilitate pattern completion and retrieval and attenuate pattern separation processes (for a quantitative analysis of the computational models being described; cf., Hasselmo and Schnell, 1994; Hasselmo et al., 1995, 1996). The effects on the DG of the reduced acetylcholine levels would be that the granule neurons would be inhibited and less responsive to perforant path stimulation from the entorhinal cortex, thus providing the necessary reduction in DG activity levels required for retrieval processes to occur per the models posited by Treves and Rolls (1992, 1994). Additional evidence for an important role for acetylcholine is based on the observation that GABAergic interneurons, such as oriens-lacunosum-moleculare (OLM), can alter plasticity in the Schaffer collateral pathway and can alter the operation of CA1 and CA3 by gating information flow in CA1, facilitating CA3 transmission to CA1 and reducing the influence of perforant path inputs (Leão et al., 2012).

It has been clearly demonstrated that disrupting CA3a,b subcortical efferents in the fimbria disrupts encoding, but not retrieval, of spatial information during learning of the Hebb–Williams maze task (Hunsaker et al., 2008b). Rats with CA3a,b outputs to the septal nuclei via the fimbria disrupted were impaired for encoding or within-day learning, but showed intact abilities to perform between day retrieval. Rats with CA1 outputs to the septal nuclei via the dorsal fornix/alveus disrupted showed intact abilities to perform within-day encoding but were impaired for between day retrieval. Importantly, for these tasks the cholinergic inputs to the hippocampus via the fimbria were intact.

It is suggested that this effect is due to a critical role for cholinergic inputs to the hippocampus in biasing CA3a,b to pattern separation via silencing the recurrent collateral influence relative to the mossy fibers, since a disruption of these cholinergic projections would disrupts the ability of CA3a,b to encode spatial information (Hunsaker et al., 2007a,b, 2008b, 2009). The consequence of increasing the cholinergic projections to CA3a,b would be a decrease in the synaptic transmission of the recurrent collaterals and thus less recurrent activation relative to the mossy fiber inputs. Also, when acetylcholine levels increase in the DG, the inhibitory interneurons in the hilus are inhibited – thus reducing the amount of tonic inhibition on the granule neurons. The effect of this disinhibition is to increase mossy fiber neurotransmission (assuming increased transmission follows from increased responsiveness to stimulation), further biasing CA3a,b toward encoding information from the DG over recurrent activity from the recurrent collaterals.

Reducing acetylcholine by attenuating excitation of the medial septum/diagonal band of Broca cholinergic neurons would favor pattern completion and recall over pattern separation and encoding and push CA3a,b into the role of a working memory buffer by reducing the signal to noise level, and thus providing the best environment for the detection and completion of patterns from partial cues (Kesner and Rolls, 2001). As mentioned above, concurrent with the effects on CA3, reducing acetylcholine would reduce inhibitory tone on inhibitory interneurons in the hilus – thus increasing inhibition on the DG granule neurons, and subsequently reducing mossy fiber inputs to CA3a,b. Furthermore models also support this assertion by demonstrating decreased acetylcholine levels in a septo-hippocampal classical conditioning learning model result in overall reductions in the learning rate (Myers et al., 1996).

The pattern of results for scopolamine (a cholinergic antagonist) and physostigmine (a cholinergic agonist) infusions into CA3a,b is intriguing. Scopolamine, but not physostigmine, infusions, into CA3a,b disrupt encoding. In contrast, physostigmine, but not scopolamine infusions, into CA3 a,b, disrupt recall. This was observed during a spatial exploration paradigm (Hunsaker et al., 2007b), during Hebb–Williams maze learning (Rogers and Kesner, 2003), and during delay fear-conditioning (Rogers and Kesner, 2004). In another study, Pereira et al. (2005) showed that injections of 192IgG-saporin in the hippocampus, which produced a severe depletion of cholinergic cells in the medial septum, was sufficient to disrupt acquisition of the Hebb–Williams maze. These data suggest that cholinergic levels directly influence information processing in the hippocampus, supporting the assertion that acetylcholine levels are perfectly located in time and place to bias CA3a,b toward either pattern separation or pattern completion.

CONCLUSION

From a behavioral perspective the CA3a,b subregion of the hippocampus plays an important role in the encoding of new spatial information within short-term memory with a duration of seconds and minutes. This can easily be observed in tasks that require rapid encoding, novelty detection, one-trial short-term or working memory, and one-trial cued recall primarily for spatial information. These are tasks that have been assumed to reflect the operations of episodic memory and require interactions between CA3a,b and the DG via mossy fiber inputs into the CA3a,b. The CA3a,b is also important for encoding of spatial

information requiring the acquisition of arbitrary and relational associations. All these tasks are assumed to operate within an autoassociative network function of the CA3 region. The CA3a,b also supports retrieval of short-term memory information based on a spatial pattern completion process. Based on afferent inputs into CA3a,b from the DG via mossy fibers and afferents from the entorhinal cortex into CA3a,b as well as reciprocal connections with the septum, CA3a,b can bias the process of encoding utilizing the operation of spatial pattern separation and the process of retrieval utilizing the operation of pattern completion. The CA3a,b also supports sequential processing of information in cooperation with CA1 based on the Schaffer collateral output from CA3a,b to CA1. The CA3c function is in part based on modulation of the DG in supporting pattern separation processes.

REFERENCES

Amaral, D. G., and Witter, M. P. (1995). "The hippocampal formation," in *The Rat Nervous System*, ed. G. Paxinos (San Diego, CA: Academic Press), 443–493.

Banks, W. P. (1978). "Encoding and processing of symbolic information in comparative judgements," in *The Psychology of Learning and Motivation: Advances in Theory and Research*, ed. G. H. Bower (New York: Academic Press), 101–159.

Bilkey, D. K., and Goddard, G. V. (1985). Medial septal facilitation of hippocampal granule neuron activity is mediated by inhibition of inhibitory interneurons. *Brain Res.* 361, 99–106.

Breindl, A., Derrick, B. E., Rodriguez, S. B., and Martinez, J. L. Jr. (1994). Opioid receptor-dependent long-term potentiation at the lateral perforant path-CA3 synapse in rat hippocampus. *Brain Res. Bull.* 33, 17–24.

Buckmaster, P. S., and Schwartzkroin, P. A. (1994). Hippocampal mossy cell function: a speculative view. *Hippocampus* 4, 393–402.

Chiba, A. A., Kesner, R. P., and Reynolds, A. M. (1994). Memory for spatial location as a function of temporal lag in rats: role of hippocampus and medial prefrontal cortex. *Behav. Neural Biol.* 61, 123–131.

Colombo, M., Fernandez, T., Nakamura, K., and Gross, C. G. (1998). Functional differentiation along the anterior–posterior axis of the hippocampus in monkeys. *J. Neurophysiol.* 80, 1002–1005.

Cravens, C. J., Vargas-Pinto, N., Christian, K. M., and Nakazawa, K. (2006). CA3 NMDA receptors are crucial for rapid and automatic representation of context memory. *Eur. J. Neurosci.* 24, 1771–1780.

Day, M., Langston, R., and Morris, R. G. (2003). Glutamate-receptor-mediated encoding and retrieval of paired-associate learning. *Nature* 424, 205–209.

Debanne, D., Gahwiler, B. H., and Thompson, S. M. (1998). Long-term synaptic plasticity between pairs of individual CA3 pyramidal cells in rat hippocampal slice cultures. *J. Physiol.* 507, 237–247.

Deco, G., and Rolls, E. T. (2003). Attention and working memory: a dynamical model of neuronal activity in the prefrontal cortex. *Eur. J. Neurosci.* 18, 2374–2390.

Deco, G., and Rolls, E. T. (2005). Attention, short-term memory, and action selection: a unifying theory. *Prog. Neurobiol.* 76, 236–256.

DeCoteau, W. E., and Kesner, R. P. (2000). A double dissociation between the rat hippocampus and medial caudoputamen in processing two forms of knowledge. *Behav. Neurosci.* 114, 1096–1108.

Do, V. H., Martinez, C. O., Martinez, J. L. Jr., and Derrick, B. E. (2002). Long-term potentiation in direct perforant path projections to the hippocampal CA3 region in vivo. *J. Neurophysiol.* 87, 669–678.

Eichenbaum, H., and Cohen, N. J. (2001). *From Conditioning to Conscious Recollection: Memory Systems of the Brain.* New York: Oxford University Press.

Ekstrom, A. D., Meltzer, J., McNaughton, B. L., and Barnes, C. A. (2001). NMDA receptor antagonism blocks experience-dependent expansion of hippocampal "place fields". *Neuron* 31, 631–638.

Farovik, A., Dupont, L. M., and Eichenbaum, H. (2009). Distinct roles for dorsal CA3 and CA1 in memory for sequential nonspatial events. *Learn. Mem.* 17, 12–17.

Fellini, L., Florian, C., Courtey, J., and Roullet, P. (2009). Pharmacological intervention of hippocampal CA3 NMDA receptors impairs acquisition and long-term memory retrieval of spatial pattern completion task. *Learn. Mem.* 16, 387–394.

Ferbinteanu, J., Holsinger, R. M., and McDonald, R. J. (1999). Lesions of the medial or lateral perforant path have different effects on hippocampal contributions to place learning and on fear conditioning to context. *Behav. Brain Res.* 101, 65–84.

Florian, C., and Roullet, P. (2004). Hippocampal CA3-region is crucial for acquisition and memory consolidation in Morris water maze task in mice. *Behav. Brain Res.* 154, 365–374.

Gall, C. M., Hess, U. S., and Lynch, G. (1998). Mapping brain networks engaged by, and changed by, learning. *Neurobiol. Learn. Mem.* 70, 14–36.

Gaykema, R. P., van der Kuil, J., Hersh, L. B., and Luiten, P. G. (1991). Pattern of direct projections from the hippocampus to the medial septum-diagonal band complex: anterograde tracing with *Phaseolus vulgaris* leucoagglutinin combined with immunohistochemistry of choline acetyltransferase. *Neuroscience* 43, 349–360.

Gilbert, P. E., and Kesner, R. P. (2003). Localization of function within the hippocampus: the role of the dorsal CA3 subregion in paired-associate learning. *Behav. Neurosci.* 117, 1385–1394.

Gilbert, P. E., and Kesner, R. P. (2006). The role of dorsal CA3 hippocampal subregion in spatial working memory and pattern separation. *Behav. Brain Res.* 169, 142–149.

Gilbert, P. E., Kesner, R. P., and Lee, I. (2001). Dissociating hippocampal subregions: a double dissociation between the dentate gyrus and CA1. *Hippocampus* 11, 626–636.

Gold, A. E., and Kesner, R. P. (2005). The role of the CA3 subregion of the dorsal hippocampus in spatial pattern completion in the rat. *Hippocampus* 15, 808–814.

Hampson, R. E., Hedberg, T., and Deadwyler, S. A. (2000). Differential information processing by hippocampal and subicular neurons. *Ann. N.Y. Acad. Sci.* 911, 151–165.

Hannesson, D. K., Howland, J. G., and Phillips, A. G. (2004). Interaction between perirhinal and medial prefrontal cortex is required for temporal order but not recognition memory. *J. Neurosci.* 24, 4596–4603.

Hargreaves, E. L., Rao, G., Lee, I., and Knierim, J. J. (2005). Major dissociation between medial and lateral entorhinal input to dorsal hippocampus. *Science* 308, 1792–1794.

Harris, E. W., and Cotman, C. W. (1986). Long-term potentiation of guinea pig mossy fiber responses is not blocked by *N*-methyl D-aspartate antagonists. *Neurosci. Lett.* 70, 132–137.

Hasselmo, M. E. (1999). Neuromodulation: acetylcholine and memory consolidation. *Trends Cogn. Sci.* 3, 351–359.

Hasselmo, M. E. (2005). What is the function of hippocampal theta rhythm? – Linking behavioral data to phasic properties of field potential and unit recording data. *Hippocampus* 15, 936–949.

Hasselmo, M. E., Bodelon, C., and Wyble, B. P. (2002a). A proposed function for hippocampal theta rhythm: separate phases of encoding and retrieval enhance reversal of prior learning. *Neural Comput.* 14, 793–817.

Hasselmo, M. E., Hay, J., Ilyn, M., and Gorchetchnikov, A. (2002b). Neuromodulation, theta rhythm and rat spatial navigation. *Neural Netw.* 15, 689–707.

Hasselmo, M. E., and Bower, J. M. (1993). Acetylcholine and memory. *Trends Neurosci.* 16, 218–222.

Hasselmo, M. E., and Fehlau, B. P. (2001). Differences in time course of ACh and GABA modulation of excitatory synaptic potentials in slices of rat hippocampus. *J. Neurophysiol.* 86, 1792–1802.

Hasselmo, M. E., and Giocomo, L. M. (2006). Cholinergic modulation of cortical function. *J. Mol. Neurosci.* 30, 133–135.

Hasselmo, M. E., and McGaughy, J. (2004). High acetylcholine levels set circuit dynamics for attention and encoding and low acetylcholine levels set dynamics for consolidation. *Prog. Brain Res.* 145, 207–231.

Hasselmo, M. E., and Schnell, E. (1994). Laminar selectivity of the cholinergic suppression of synaptic transmission in rat hippocampal region CA1: computational modeling and brain slice physiology. *J. Neurosci.* 14, 3898–3914.

Hasselmo, M. E., Schnell, E., and Barkai, E. (1995). Dynamics of learning and recall at excitatory recurrent synapses and cholinergic modulation in rat hippocampal region CA3. *J. Neurosci.* 15, 5249–5262.

Hasselmo, M. E., and Wyble, B. P. (1997). Free recall and recognition in

a network model of the hippocampus: simulating effects of scopolamine on human memory function. *Behav. Brain Res.* 89, 1–34.

Hasselmo, M. E., Wyble, B. P., and Wallenstein, G. V. (1996). Encoding and retrieval of episodic memories: role of cholinergic and GABAergic modulation in the hippocampus. *Hippocampus* 6, 693–708.

Hoang, L. T., and Kesner, R. P. (2008). Dorsal hippocampus, CA3, and CA1 lesions disrupt temporal sequence completion. *Behav. Neurosci.* 122, 9–15.

Hoge, J., and Kesner, R. P. (2007). Role of CA3 and CA1 subregions of the dorsal hippocampus on the temporal processing of objects. *Neurobiol. Learn. Mem.* 88, 225–231.

Howard, M. W., Fotedar, M. S., Datey, A. V., and Hasselmo, M. E. (2005). The temporal context model in spatial navigation and relational learning: toward a common explanation of medial temporal lobe function across domains. *Psychol. Rev.* 112, 75–116.

Howard, M. W., and Natu, V. S. (2005). Place from time: reconstructing position from a distributed representation of temporal context. *Neural Netw.* 18, 1150–1162.

Hunsaker, M. R., Allan, K. D., and Kesner, R. P. (2007a). The role of dCA3 efferents via the fimbria in the acquisition of a delay-nonmatch to place task. *Hippocampus* 17, 494–502.

Hunsaker, M. R., Rogers, J. L., and Kesner, R. P. (2007b). Behavioral characterization of a transection of dorsal CA3 subcortical efferents: comparison with scopolamine and physostigmine infusions into dorsal CA3. *Neurobiol. Learn. Mem.* 88, 127–136.

Hunsaker, M. R., Mooy, G. G., Swift, J. S., and Kesner, R. P. (2007c). Dissociations of the medial and lateral perforant path projections into dorsal DG, CA3, and CA1 for spatial and nonspatial (visual object) information processing. *Behav. Neurosci.* 121,742–750.

Hunsaker, M. R., and Kesner, R. P. (2008). Dissociations across the dorsal–ventral axis of CA3 and CA1 for encoding and retrieval of contextual and auditory-cued fear. *Neurobiol. Learn. Mem.* 89, 61–69.

Hunsaker, M. R., and Kesner, R. P. (2013). The operation of pattern separation and pattern completion processes associated with different attributes or domains of memory. *Neurosci. Biobehav. Rev.* 37, 36–58.

Hunsaker, M. R., Rosenberg, J. S., and Kesner, R. P. (2008a). The role of the dentate gyrus, CA3a,b, and CA3c for detecting spatial and environmental novelty. *Hippocampus* 18, 1064–1073.

Hunsaker, M. R., Tran, G. T., and Kesner, R. P. (2008b). A double dissociation of subcortical hippocampal efferents for encoding and consolidation/retrieval of spatial information. *Hippocampus* 18, 699–709.

Hunsaker, M. R., Fieldsted, P. M., Rosenberg, J. S., and Kesner, R. P. (2008c). Dissociating the roles of dorsal and ventral CA1 for the temporal processing of spatial locations, visual objects, and odors. *Behav. Neurosci.* 122, 643–650.

Hunsaker, M. R., Thorup, J. A., Welch, T., and Kesner, R. P. (2006). The role of CA3 and CA1 in the acquisition of an object–trace–place paired associate task. *Behav. Neurosci.* 120, 1252–1256.

Hunsaker, M. R., Tran, G. T., and Kesner, R. P. (2009). A behavioral analysis of the role of CA3 and CA1 subcortical efferents during classical fear conditioning. *Behav. Neurosci.* 123, 624–630.

Jensen, O., and Lisman, J. E. (2005). Hippocampal sequence-encoding driven by a cortical multi-item working memory buffer. *Trends Neurosci.* 28, 67–72.

Jerman, T., Kesner, R. P., and Hunsaker, M. R. (2006). Disconnection analysis of CA3 and DG in mediating encoding but not retrieval in a spatial maze learning task. *Learn. Mem.* 13, 458–464.

Jinde, S., Zsiros, V., Jiang, Z., Nakao, K., Pickel, J., Kohno, K., et al. (2012). Hilar mossy cell degeneration causes transient dentate granule cell hyperexcitability and impaired pattern separation. *Neuron* 76, 1189–1200.

Jinde, S., Zsiros, V., and Nakazawa, K. (2013). Hilar mossy cell circuitry controlling dentate granule cell excitability. *Front. Neural Circuits* 7:14. doi: 10.3389/fncir.2013.00014

Kesner, R. P. (1998). Neural mediation of memory for time: role of hippocampus and medial prefrontal cortex. *Psychol. Bull. Rev.* 5, 585–596.

Kesner, R. P. (2007). Behavioral functions of the CA3 subregion of the hippocampus. *Learn. Mem.* 14, 771–781.

Kesner, R. P., Hunsaker, M. R., and Gilbert, P. E. (2005). The role of CA1 in the acquisition of an object–trace–odor paired associate task. *Behav. Neurosci.* 119, 781–786.

Kesner, R. P., Hunsaker, M. R., and Warthen, M. W. (2008). The CA3 subregion of the hippocampus is critical for episodic memory processing by means of relational encoding in rats. *Behav. Neurosci.* 122, 1217–1225.

Kesner, R. P., Hunsaker, M. R., and Ziegler, W. (2010). The role of the dorsal CA1 and ventral CA1 in memory for the temporal order of a sequence of odors. *Neurobiol. Learn. Mem.* 93, 111–116.

Kesner, R. P., Lee, I., and Gilbert, P. (2004). A behavioral assessment of hippocampal function based on a subregional analysis. *Rev. Neurosci.* 15, 333–351.

Kesner, R. P., and Rolls, E. T. (2001). Role of long-term synaptic modification in short-term memory. *Hippocampus* 11, 240–250.

Kesner, R. P., and Warthen, D. K. (2010). Implications of CA3 NMDA and opiate receptors for spatial pattern completion in rats. *Hippocampus* 20, 550–557.

Krug, M., Brödemann, R., and Wagner, M. (2001). Simultaneous activation and opioid modulation of long-term potentiation in the dentate gyrus and the hippocampal CA3 region after stimulation of the perforant pathway in freely moving rats. *Brain Res.* 913, 68–77.

Lassalle, J. M., Bataille, T., and Halley, H. (2000). Reversible inactivation of the hippocampal mossy fiber synapses in mice impairs spatial learning, but neither consolidation nor memory retrieval, in the Morris navigation task. *Neurobiol. Learn. Mem.* 73, 243–257.

Leão, R. N., Mikulovic, S., Leão, K. E., Munguba, H., Gezelius, H., Enjin, A., et al. (2012). OLM interneurons differentially modulate CA3 and entorhinal inputs to hippocampal CA1 neurons. *Nat. Neurosci.* 15, 1524–1532.

Lee, I., Jerman, T. S., and Kesner, R. P. (2005). Disruption of delayed memory for a sequence of spatial locations following CA1- or CA3-lesions of the dorsal hippocampus. *Neurobiol. Learn. Mem.* 84, 138–147.

Lee, I., and Kesner, R. P. (2002). Differential contribution of NMDA receptors in hippocampal subregions to spatial working memory. *Nat. Neurosci.* 5, 162–168.

Lee, I., and Kesner, R. P. (2003). Differential role of dorsal hippocampus subregions in spatial working memory with short versus intermediate delay. *Behav. Neurosci.* 117, 1044–1053.

Lee, I., and Kesner, R. P. (2004a). Differential contributions of dorsal hippocampal subregions to memory acquisition and retrieval in contextual fear-conditioning. *Hippocampus* 14, 301–310.

Lee, I., and Kesner, R. P. (2004b). Encoding versus retrieval of spatial memory: double dissociation between the dentate gyrus and the perforant path inputs into CA3 in the dorsal hippocampus. *Hippocampus* 14, 66–76.

Lee, I., Rao, G., and Knierim, J. J. (2004). A double dissociation between hippocampal subfields: differential time course of CA3 and CA1 place cells for processing changed environments. *Neuron* 42, 803–815.

Leutgeb, J. K., Leutgeb, S., Moser, M.-B., and Moser, E. I. (2007). Pattern separation in the dentate gyrus and CA3 of the hippocampus. *Science* 315, 961–966.

Leutgeb, J. K., Leutgeb, S., Treves, A., Meyer, R., Barnes, C. A., McNaughton, B. L., et al. (2005). Progressive transformation of hippocampal neuronal representations in "morphed" environments. *Neuron* 48, 345–358.

Levy, W. B. (1996). A sequence predicting CA3 is a flexible association that learns and uses context to solve hippocampal-like tasks. *Hippocampus* 6, 579–590.

Li, X.-G., Somogyi, P., Ylinen, A., and Buzsaki, G. (1994). The hippocampal CA3 network: an in vivo intracellular labeling study. *J. Comp. Neurol.* 339, 181–208.

Lisman, J. E. (1999). Relating hippocampal circuitry to function: recall of memory sequences by reciprocal dentate-CA3 interactions. *Neuron* 22, 233–242.

Lisman, J. E., and Grace, A. A. (2005). The hippocampal-VTA loop: controlling the entry of information into long-term memory. *Neuron* 46, 703–713.

Lisman, J. E., and Otmakhova, N. A. (2001). Storage, recall, and novelty detection of sequences by the hippocampus: elaborating on the SOCRATIC model to account for normal and aberrant effects of dopamine. *Hippocampus* 11, 551–568.

Lorente de Nó, R. (1934). Studies on the structure of the cerebral cortex II. Continuation of the study of the ammonic system. *J. Psychol. Neurol.* 46, 113–177.

MacDonald, C. J., Lepage, K. Q., Eden, U. T., and Eichenbaum, H. (2011). Hippocampal "time cells" bridge the gap in memory for discontiguous events. *Neuron* 71, 737–749.

Madsen, J., and Kesner, R. P. (1995). The temporal-distance effect in subjects with dementia of the Alzheimer type. *Alzheimer Dis. Assoc. Disord.* 9, 94–100.

Mankin, E. A., Sparks, F. T., Slayyeh, B., Sutherland, R. J., Leutgeb, S., and Leutgeb, J. K. (2012). Neuronal code for extended time in the hippocampus. *Proc. Natl. Acad. Sci. U.S.A.* 109, 19462–19467.

Marr, D. (1971). Simple memory: a theory for archicortex. *Proc. R. Soc. Lond. B. Biol. Sci.* 262, 23–81.

Martinez, C. O., Do, V. H., Martinez, J. L. Jr., and Derrick, B. E. (2002). Associative long-term potentiation (LTP) among extrinsic afferents of the hippocampal CA3 region in vivo. *Brain Res.* 940, 86–94.

McEchron, M. D., Tseng, W., and Disterhoft, J. F. (2003). Single neurons in CA1 hippocampus encode trace interval duration during trace heart rate (fear) conditioning in rabbit. *J. Neurosci.* 23, 1535–1547.

McLennan, H., and Miller, J. J. (1974). The hippocampal control of neuronal discharges in the septum of the rat. *J. Physiol.* 237, 607–624.

McNaughton, B. L., and Morris, R. G. (1987). Hippocampal synaptic enhancement and information storage within a distributed memory system. *Trends Neurosci.* 10, 408–415.

McNaughton, N., and Miller, J. J. (1986). Collateral specific long term potentiation of the output of field CA3 of the hippocampus of the rat. *Exp. Brain Res.* 62, 250–258.

Mehta, M. R., Barnes, C. A., and McNaughton, B. L. (1997). Experience-dependent, asymmetric expansion of hippocampal place fields. *Proc. Natl. Acad. Sci. U.S.A.* 94, 8918–8921.

Mehta, M. R., Lee, A. K., and Wilson, M. A. (2002). Role of experience and oscillations in transforming a rate code into a temporal code. *Nature* 417, 741–746.

Mizumori, S. J., Ragozzino, K. E., Cooper, B. G., and Leutgeb, S. (1999). Hippocampal representational organization and spatial context. *Hippocampus* 9, 444–451.

Morris, R. (2007). "Theories of hippocampal function," in *The Hippocampus Book*, eds P. Andersen, R. Morris, D. Amaral, T. Bliss, and J. O'Keefe (Oxford: Oxford University Press), 581–658.

Myers, C. E., Ermita, B. R., Harris, K., Hasselmo, M. E., Solomon, P., and Gluck, M. A. (1996). A computational model of cholinergic disruption of septohippocampal activity in classical eyeblink conditioning. *Neurobiol. Learn. Mem.* 66, 51–66.

Myers, C. E., and Scharfman, H. E. (2009). A role for hilar cells in pattern separation in the dentate gyrus: a computational approach. *Hippocampus* 19, 321–337.

Myers, C. E., and Scharfman, H. E. (2011). Pattern separation in the dentate gyrus: a role for the CA3 backprojection. *Hippocampus* 21, 1190–1215.

Nakazawa, K., Quirk, M. C., Chitwood, R. A., Watanabe, M., Yeckel, M. F., Sun, L. D., et al. (2002). Requirement for hippocampal CA3 NMDA receptors in associative memory recall. *Science* 297, 211–218.

Nakazawa, K., Sun, L. D., Quirk, M. C., Rondi-Reig, L., Wilson, M. A., and Tonegawa, S. (2003). Hippocampal CA3 NMDA receptors are crucial for memory acquisition of one-time experience. *Neuron* 38, 305–315.

Olton, D. S., Shapiro, M. L., and Hulse, S. H. (1984). "Working memory and serial patterns," in *Animal Cognition*, eds H. L. Roitblatt, T. G. Bever, and H. S. Terrace (Hillsdale, NJ: Lawrence Erlbaum Associates), 171–182.

O'Reilly, R. C., and McClelland, J. L. (1994). Hippocampal conjunctive encoding, storage, and recall: avoiding a trade-off. *Hippocampus* 4, 661–682.

O'Reilly, R. C., and Rudy, J. W. (2001). Conjunctive representations in learning and memory: principles of cortical and hippocampal function. *Psychol. Rev.* 108, 311–345.

Otmakhova, N. A., and Lisman, J. E. (1999). Dopamine selectively inhibits the direct cortical pathway to the CA1 hippocampal region. *J. Neurosci.* 19, 1437–1445.

Pereira, P. M., Cosquer, B., Schimchowitsch, S., and Cassel, J.-C. (2005). Hebb–Williams performance and scopolamine challenge in rats with partial immunotoxic hippocampal cholinergic deafferentation. *Brain Res. Bull.* 64, 381–394.

Place, R., Lykken, C., Beer, Z., Suh, J., McHugh, T. J., Tonegawa, S., et al. (2012). NMDA signaling in CA1 mediates selectively the spatial component of episodic memory. *Learn. Mem.* 19, 164–169.

Poucet, B. (1989). Object exploration, habituation, and response to a spatial change in rats following septal or medial frontal cortical damage. *Behav. Neurosci.* 103, 1009–1016.

Raisman, G., Cowan, M. W., and Powell, T. P. S. (1966). An experimental analysis of the efferent projection of the hippocampus. *Brain* 89, 83–108.

Rajji, T., Chapman, D., Eichenbaum, H., and Greene, R. (2006). The role of CA3 hippocampal NMDA receptors in paired associate learning. *J. Neurosci.* 26, 908–915.

Rawlins, J. N., Feldon, J., and Gray, J. A. (1979). Septo-hippocampal connections and the hippocampal theta rhythm. *Exp. Brain Res.* 37, 49–63.

Rawlins, J. N. P. (1985). Associations across time: the hippocampus as a temporary memory store. *Behav. Brain Sci.* 8, 479–496.

Risold, P. Y., and Swanson, L. W. (1997). Connections of the rat lateral septal complex. *Brain Res. Rev.* 24, 115–195.

Robertson, R. G., Rolls, E. T., and Georges-Francois, P. (1998). Spatial view cells in the primate hippocampus: effects of removal of view details. *J. Neurophysiol.* 79, 1145–1156.

Rogers, J. L., and Kesner, R. P. (2003). Cholinergic modulation of the hippocampus during encoding and retrieval. *Neurobiol. Learn. Mem.* 80, 332–342.

Rogers, J. L., and Kesner, R. P. (2004). Cholinergic modulation of the hippocampus during encoding and retrieval of tone/shock-induced fear conditioning. *Learn. Mem.* 11, 102–107.

Rolls, E. T. (1989a). "The representation and storage of information in neuronal networks in the primate cerebral cortex and hippocampus," in *The Computing Neuron*, eds R. Durbin, C. Miall, and G. Mitchison (Wokingham: Addison-Wesley), 125–159.

Rolls, E. T. (1989b). "Functions of neuronal networks I the hippocampus and neocortex in memory," in *Neural Models of Plasticity: Experimental and Theoretical Approaches*, eds J. H. Bryne and W. O. Berry (San Diego, CA: Academic Press), 240–265.

Rolls, E. T. (1996). A theory of hippocampal function in memory. *Hippocampus* 6, 601–620.

Rolls, E. T., and Deco, G. (2002). *Computational Neuroscience of Vision*. Oxford: Oxford University Press.

Rolls, E. T., and Kesner, R. P. (2006). A computational theory of hippocampal function, and empirical tests of the theory. *Prog. Neurobiol.* 79, 1–48.

Rolls, E. T., and Treves, A. (1998). *Neural Networks and Brain Function*. Oxford: Oxford University Press.

Rolls, E. T., Xiang, J.-Z., and Franco, L. (2005). Object, space and object–space representations in the primate hippocampus. *J. Neurophysiol.* 94, 833–844.

Samsonovich, A., and McNaughton, B. L. (1997). Path integration and cognitive mapping in a continuous attractor neural network model. *J. Neurosci.* 17, 5900–5920.

Scharfman, H. E. (2007). "The CA3 "backprojection" to the dentate gyrus," in *The Dentate Gyrus: A Comprehensive Guide to Structure, Functional and Clinical Implications*, Vol. 163, *Progress in Brain Research*, ed. H. E. Scharfman (Amsterdam: Elsevier Science), 627–638.

Skaggs, W. E., Knierim, J. J., Kudrimoti, H. S., and McNaugton, B. L. (1995). "A model of the neural basis of the rat's sense of direction," in *Advances in Neural Information Processing Systems*, Vol. 7, eds G. Tesauro, D. S. Touretzky, and T. K. Leen (Cambridge, MA: MIT Press), 173–180.

Swanson, L. W., and Cowan, W. M. (1977). An autoradiographic study of the organization of the efferent connections of the hippocampal formation of the rat. *J. Comp. Neurol.* 172, 49–84.

Swanson, L. W., and Cowan, W. M. (1979). The connections of the septal region in the rat. *J. Comp. Neurol.* 186, 621–656.

Tanila, H. (1999). Hippocampal place cells can develop distinct representations of two visually identical environments. *Hippocampus* 9, 235–246.

Treves, A., and Rolls, E. T. (1992). Computational constraints suggest the need for two distinct input systems to the hippocampal CA3 network. *Hippocampus* 2, 189–199.

Treves, A., and Rolls, E. T. (1994). Computational analysis of the role of the hippocampus in memory. *Hippocampus* 4, 374–391.

Vago, D. R., Bevan, A., and Kesner, R. P. (2007). The role of the direct perforant path input to the CA1 subregion of the dorsal hippocampus in memory retention and retrieval. *Hippocampus* 17, 977–987.

Vago, D. R., and Kesner, R. P. (2008). Disruption of the direct perforant path input to the CA1 subregion of the dorsal hippocampus interferes with spatial working memory and novelty detection. *Behav. Brain Res.* 189, 273–283.

Vazdarjanova, A., and Guzowski, J. F. (2004). Differences in hippocampal neuronal population responses

to modifications of an environmental context: evidence for distinct, yet complementary, functions of CA3 and CA1 ensembles. *J. Neurosci.* 24, 6489–6496.

Wallenstein, G. V., and Hasselmo, M. E. (1997). GABAergic modulation of hippocampal population activity: sequence learning, place field development, and the phase precession effect. *J. Neurophysiol.* 78, 393–408.

Watanabe, T., and Niki, H. (1985). Hippocampal unit activity and delayed response in monkeys. *Brain Res.* 325, 241–254.

Wirth, S., Yanike, M., Frank, L. M., Smith, A. C., Brown, E. N., and Suzuki, W. A. (2003). Single neurons in the monkeys hippocampus and learning of new associations. *Science* 300, 1578–1581.

Witter, M. P., Van Hoesen, G. W., and Amaral, D. G. (1989). Topographical organisation of the entorhinal projection to the dentate gyrus of the monkey. *J. Neurosci.* 9, 216–228.

Wyss, X., Swanson, I. W., and Cowan, W. M. (1980). The organization of the fimbria, dorsal fornix, and ventral hippocampal commissure in the rat. *Anat. Embryol.* 138, 303–316.

Zalutsky, R. A., and Nicoll, R. A. (1990). Comparison of two forms of long-term potentiation in single hippocampal neurons. *Science* 248, 1619–1624.

Conflict of Interest Statement: The author declares that the research was conducted in the absence of any commercial or financial relationships that could be construed as a potential conflict of interest.

Received: 28 March 2013; accepted: 08 May 2013; published online: 27 May 2013.

Citation: Kesner RP (2013) A process analysis of the CA3 subregion of the hippocampus. Front. Cell. Neurosci. ***7****:78. doi: 10.3389/fncel.2013.00078*

frontiers in
CELLULAR NEUROSCIENCE

REVIEW ARTICLE
published: 25 June 2013
doi: 10.3389/fncel.2013.00098

A quantitative theory of the functions of the hippocampal CA3 network in memory

Edmund T. Rolls [1,2]*

[1] Oxford Centre for Computational Neuroscience, Oxford, UK
[2] Department of Computer Science, University of Warwick, Coventry, UK

Edited by:
Enrico Cherubini, International School for Advanced Studies, Italy

Reviewed by:
Maria Passafaro, University of Milano, Italy
Alessandro Treves, Scuola Internazionale Superiore di Studi Avanzati, Italy

***Correspondence:**
Edmund T. Rolls, Department of Computer Science, University of Warwick, Coventry CV4 7AL, UK
e-mail: edmund.rolls@oxcns.org
www.oxcns.org

A quantitative computational theory of the operation of the hippocampal CA3 system as an autoassociation or attractor network used in episodic memory system is described. In this theory, the CA3 system operates as a single attractor or autoassociation network to enable rapid, one-trial, associations between any spatial location (place in rodents, or spatial view in primates) and an object or reward, and to provide for completion of the whole memory during recall from any part. The theory is extended to associations between time and object or reward to implement temporal order memory, also important in episodic memory. The dentate gyrus (DG) performs pattern separation by competitive learning to produce sparse representations suitable for setting up new representations in CA3 during learning, producing for example neurons with place-like fields from entorhinal cortex grid cells. The dentate granule cells produce by the very small number of mossy fiber (MF) connections to CA3 a randomizing pattern separation effect important during learning but not recall that separates out the patterns represented by CA3 firing to be very different from each other, which is optimal for an unstructured episodic memory system in which each memory must be kept distinct from other memories. The direct perforant path (pp) input to CA3 is quantitatively appropriate to provide the cue for recall in CA3, but not for learning. Tests of the theory including hippocampal subregion analyses and hippocampal NMDA receptor knockouts are described, and support the theory.

Keywords: hippocampus, attractor network, competitive network, episodic memory, spatial view neurons, object-place memory, recall, pattern separation

INTRODUCTION

In this paper a computational theory of how the hippocampal CA3 region operates and is involved in episodic memory is described. I consider how the network architecture of the hippocampal CA3 system may enable it to contribute to episodic memory, and to recall the whole of a memory when a partial retrieval cue is present using the recurrent collateral connections which I argue implement an autoassociation or attractor memory. I focus on a fundamental property of episodic memory, the ability to store and retrieve the memory of a particular single event involving an association between items such as the place and the object or reward seen at that place. Episodic memory in the sense of a series of linked events requires this type of event memory, and could be implemented by linking together a series of events. After the theory is presented, I then describe neurophysiological and related evidence that tests the theory. New hypotheses are described about the advantages of the diluted connectivity present in the CA3 network. The effects of the diluted connectivity of the CA3 recurrent collateral network, and the graded firing rates of hippocampal neurons, on the noise due to the randomness of the spiking times of CA3 neurons, and thus on the operation of an attractor system such as the CA3 network, are described. A hypothesis about why the connectivity in cortical networks is proposed. Factors that influence the stability of the CA3-CA3 recurrent collateral network are also considered, together with their possible implications for neuropsychiatric conditions such as schizophrenia.

Episodic memory, the memory of a particular episode, requires the ability to remember particular events, and to distinguish them from other events. An event consists of a set of items that occur together, such as seeing a particular object or person's face in a particular place. An everyday example might be remembering where one was for dinner, who was present, what was eaten, what was discussed, and the time at which it occurred. The spatial context is almost always an important part of an episodic memory (Dere et al., 2008), and it may be partly for this reason that episodic memory is linked to the functions of the hippocampal system, which is involved in spatial processing and memory.

In this paper I also show that the primate hippocampus including CA3 has a special representation of space that makes it particularly appropriate for episodic memory in primates including humans, for it is a representation of space "out there." This enables memories to be formed of what one has seen at a particular place, even if one has not been to the place. This is not possible with rodent place cells, which respond to the place where the rodent is located. I also show that the primate hippocampus has more than only a spatial representation, for it also represents objects that are seen at particular places, and rewards that are found at particular places in spatial scenes. I also show that primate hippocampal neurons are activated when a memory must

be recalled from a part of a memory, for example when the place at which an object was shown must be recalled when the object is seen alone. The ability to recall a whole memory from a partial cue is an important property of episodic memory.

SYSTEMS-LEVEL FUNCTIONS AND CONNECTIONS OF THE PRIMATE HIPPOCAMPUS

Any theory of the hippocampus must state at the systems level what is computed by the hippocampus. Some of the relevant evidence about the functions of the hippocampus in memory comes from the effects of damage to the hippocampus, the responses of neurons in the hippocampus during behavior, and the systems-level connections of the hippocampus, described in more detail elsewhere (Rolls and Kesner, 2006; Rolls and Xiang, 2006; Rolls, 2008, 2010b). Many of the memory functions are important in event or episodic memory, in which the ability to remember what happened where on typically a single occasion (or trial in a learning experiment) is important. It will be suggested below that an autoassociation memory implemented by the CA3 neurons enables event or episodic memories to be formed by enabling associations to be formed between spatial and other including object or reward representations.

Information stored in the hippocampus will need to be retrieved and affect other parts of the brain in order to be used. The information about episodic events recalled from the hippocampus could be used to help form semantic memories (Rolls, 1989b,c, 1990a; Treves and Rolls, 1994). For example, remembering many particular journeys could help to build a geographic cognitive map in the neocortex. The hippocampus and neocortex would thus be complementary memory systems, with the hippocampus being used for rapid, "on the fly," unstructured storage of information involving activity potentially arriving from many areas of the neocortex; while the neocortex would gradually build and adjust on the basis of much accumulating information, often recalled from the hippocampal unstructured store, the semantic representation (Rolls, 1989b; Treves and Rolls, 1994; McClelland et al., 1995; Moscovitch et al., 2005). The theory described below shows how information could be retrieved within the hippocampus, and how this retrieved information could enable the activity in neocortical areas that was present during the original storage of the episodic event to be reinstated, thus implementing recall, by using hippocampo-neocortical backprojections as described elsewhere (Treves and Rolls, 1994; Rolls, 1995, 1996b, 2008, 2010b) (see **Figure 1**).

To understand the functions of the primate hippocampus in event or episodic memory, it is necessary to understand which other parts of the brain it receives information from. Does it for example receive object as well as spatial information in terms of its connectivity? The primate hippocampus receives inputs via the entorhinal cortex (area 28) and the highly developed parahippocampal gyrus (areas TF and TH) as well as the perirhinal cortex from the ends of many processing streams of the cerebral association cortex, including the visual and auditory temporal lobe association cortical areas, the prefrontal cortex, and the parietal cortex (Van Hoesen, 1982; Amaral, 1987; Amaral et al., 1992; Suzuki and Amaral, 1994b; Witter et al., 2000; Lavenex et al., 2004; Rolls and Kesner, 2006; Rolls, 2008) (see **Figure 1**). The hippocampus is thus by its connections potentially able to associate together object and spatial representations. In addition, the entorhinal cortex receives inputs from the amygdala, and the orbitofrontal cortex, which could provide reward-related information to the hippocampus (Suzuki and Amaral, 1994a; Carmichael and Price, 1995; Stefanacci et al., 1996; Pitkanen et al., 2002).

The primary output from the hippocampus to neocortex originates in CA1 and projects to subiculum, entorhinal cortex, and parahippocampal structures (areas TF-TH) as well as prefrontal cortex (Van Hoesen, 1982; Witter, 1993; Delatour and Witter, 2002; Van Haeften et al., 2003) (see **Figure 1**), though there are other outputs (Rolls and Kesner, 2006). These are the pathways that are likely to be involved in the recall of information from the hippocampus.

A THEORY OF THE OPERATION OF THE HIPPOCAMPAL CA3 CIRCUITRY AS PART OF A MEMORY SYSTEM

In this section, I consider how event or episodic memories might be learned and retrieved by hippocampal circuitry, and in addition retrieved back into the neocortex. The theory has been developed through many stages (Rolls, 1987, 1989a,b,c, 1990a,b, 1991, 1995, 1996b, 2008, 2010b; Treves and Rolls, 1991, 1992, 1994; Rolls and Treves, 1998; Rolls and Kesner, 2006; Rolls and Deco, 2010), has as a predecessor developments made by Marr (1971; though he never identified the CA3 system as an autoassociation network), and has benefitted greatly from collaborations with many whose names appear below in the citations, including Alessandro Treves and Simon Stringer.

HIPPOCAMPAL CIRCUITRY

Projections from the entorhinal cortex layer 2 reach the granule cells (of which there are 10^6 in the rat) in the dentate gyrus (DG), via the perforant path (pp; Witter, 1993). The granule cells project to CA3 cells via the mossy fibers (MFs), which provide a *sparse* but possibly powerful connection to the $3{\cdot}10^5$ CA3 pyramidal cells in the rat. Each CA3 cell receives ∼46 MF inputs, so that the sparseness of this connectivity is thus 0.005%. By contrast, there are many more—possibly weaker—direct pp inputs also from layer 2 of the entorhinal cortex onto each CA3 cell, in the rat of the order of $4{\cdot}10^3$. The largest number of synapses (about $1.2{\cdot}10^4$ in the rat) on the dendrites of CA3 pyramidal cells is, however, provided by the (recurrent) axon collaterals of CA3 cells themselves (rc; see **Figure 2**). It is remarkable that the recurrent collaterals are distributed to other CA3 cells largely throughout the hippocampus (Amaral and Witter, 1989, 1995; Amaral et al., 1990; Ishizuka et al., 1990; Witter, 2007), so that effectively the CA3 system provides a single network, with a connectivity of ∼2% between the different CA3 neurons given that the connections are bilateral. The CA3-CA3 recurrent collateral system is even more extensive in macaques than in rats (Kondo et al., 2009). The neurons that comprise CA3, in turn, project to CA1 neurons via the Schaffer collaterals. In addition, projections that terminate in the CA1 region originate in layer 3 of the entorhinal cortex (see **Figure 1** and Amaral and Witter, 1989; Storm-Mathiesen et al., 1990; Amaral, 1993; Witter et al., 2000; Naber et al., 2001; Lavenex

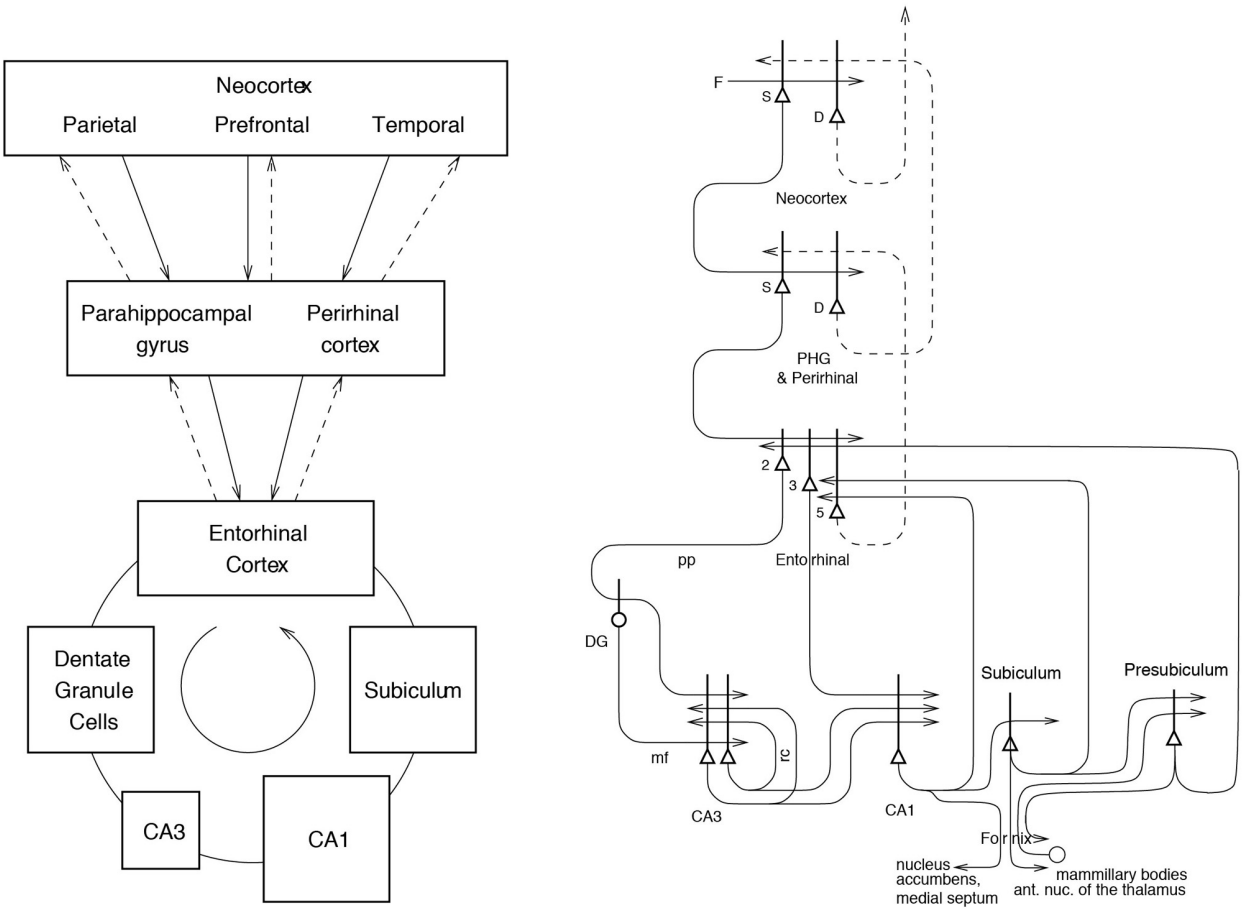

FIGURE 1 | Forward connections (solid lines) from areas of cerebral association neocortex via the parahippocampal gyrus and perirhinal cortex, and entorhinal cortex, to the hippocampus; and backprojections (dashed lines) via the hippocampal CA1 pyramidal cells, subiculum, and parahippocampal gyrus to the neocortex. There is great convergence in the forward connections down to the single network implemented in the CA3 pyramidal cells; and great divergence again in the backprojections. **Left:** block diagram. **Right:** more detailed representation of some of the principal excitatory neurons in the pathways. Abbreviations: D, Deep pyramidal cells; DG, Dentate Granule cells; F, Forward inputs to areas of the association cortex from preceding cortical areas in the hierarchy; mf, mossy fibers; PHG, parahippocampal gyrus and perirhinal cortex; pp, perforant path; rc, recurrent collateral of the CA3 hippocampal pyramidal cells; S, Superficial pyramidal cells; 2, pyramidal cells in layer 2 of the entorhinal cortex; 3, pyramidal cells in layer 3 of the entorhinal cortex; 5, pyramidal cells in layer 5 of the entorhinal cortex. The thick lines above the cell bodies represent the dendrites.

et al., 2004; Andersen et al., 2007; Witter, 2007; Kondo et al., 2009).

CA3 AS AN AUTOASSOCIATION OR ATTRACTOR MEMORY

Arbitrary associations, and pattern completion in recall

Many of the synapses in the hippocampus show associative modification as shown by long-term potentiation, and this synaptic modification appears to be involved in learning (see Morris, 1989, 2003; Morris et al., 2003; Nakazawa et al., 2003, 2004; Lynch, 2004; Andersen et al., 2007; Wang and Morris, 2010). On the basis of the evidence summarized above, Rolls (1987, 1989a,b,c, 1990a,b, 1991) and others (McNaughton and Morris, 1987; Levy, 1989; McNaughton, 1991) have suggested that the CA3 stage acts as an autoassociation memory which enables episodic memories to be formed and stored in the CA3 network, and that subsequently the extensive recurrent collateral connectivity allows for the retrieval of a whole representation to be initiated by the activation of some small part of the same representation (the cue). The crucial synaptic modification for this is in the recurrent collateral synapses. [A description of the operation of autoassociative networks is provided in detail elsewhere (Amit, 1989; Hertz et al., 1991; Rolls and Treves, 1998; Rolls and Deco, 2002, 2010; Rolls, 2010a) including *Memory, Attention, and Decision-Making* (Rolls, 2008)].

The architecture of an autoassociation network is shown in **Figure 3**, and the learning rule for the change in the synaptic weights is as shown in Equation 1 (Rolls and Treves, 1998; Rolls and Deco, 2002; Rolls, 2008).

$$\delta w_{ij} = k \cdot r_i \cdot r_j' \tag{1}$$

where k is a constant, r_i is the activation of the dendrite (the postsynaptic term), r_j' is the presynaptic firing rate, and δw_{ij} is the change in the synaptic weight w_{ij}. [w_{ij} refers to the j'th

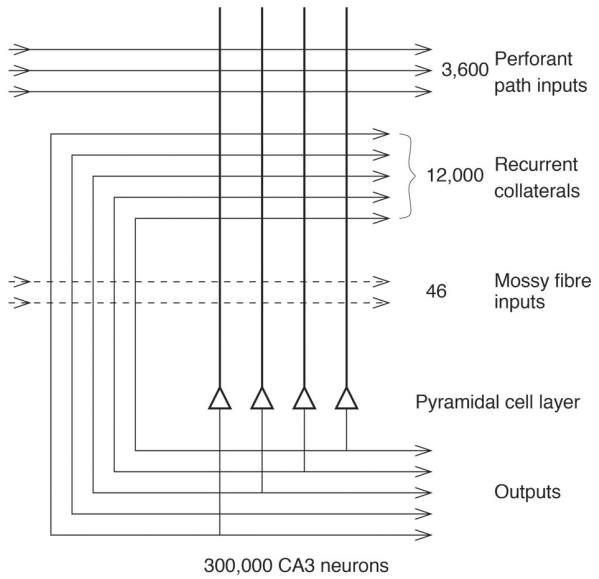

FIGURE 2 | The numbers of connections from three different sources onto each CA3 cell from three different sources in the rat (After Treves and Rolls, 1992; Rolls and Treves, 1998).

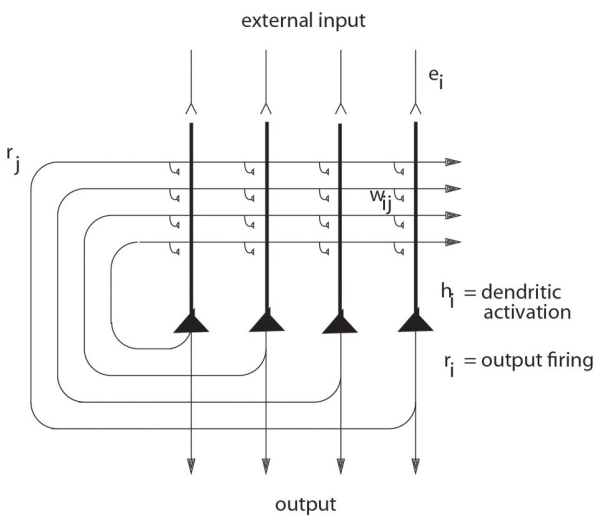

FIGURE 3 | The architecture of an autoassociation or attractor neural network (CANN) (see text).

synapse onto the *i*'th neuron. An introduction to autoassociation, competitive, and pattern association networks is provided in the Appendices of *Memory, Attention, and Decision-Making: A Unifying Computational Neuroscience Approach* (Rolls, 2008)].

The hypothesis is that because the CA3 operates effectively as a single network, it can allow arbitrary associations between inputs originating from very different parts of the cerebral cortex to be formed. These might involve associations between information originating in the temporal visual cortex about the presence of an object, and information originating in the parietal cortex about where it is. I note that although there is some spatial gradient in the CA3 recurrent connections, so that the connectivity is not fully uniform (Ishizuka et al., 1990; Witter, 2007), nevertheless the network will still have the properties of a single interconnected autoassociation network allowing associations between arbitrary neurons to be formed, given the presence of many long-range connections which overlap from different CA3 cells, and the ability of attractor networks to operate with diluted connectivity shown in our computational studies prompted by this issue (Treves, 1990; Treves and Rolls, 1991; Rolls, 2012a; Rolls and Webb, 2012).

Crucial issues include how many memories could be stored in this system (to determine whether the autoassociation hypothesis leads to a realistic estimate of the number of memories that the hippocampus could store); whether the whole of a memory could be completed from any part; whether the autoassociation memory can act as a short-term memory, for which the architecture is inherently suited; and whether the system could operate with spatial representations, which are essentially continuous because of the continuous nature of space. These and related issues are considered in the remainder of section CA3 as an Autoassociation or Attractor Memory and in more detail elsewhere (Rolls and Kesner, 2006; Rolls, 2008).

Storage capacity

We have performed quantitative analyses of the storage and retrieval processes in the CA3 network (Treves and Rolls, 1991, 1992; Webb et al., 2011; Rolls, 2012a; Rolls and Webb, 2012). We have extended previous formal models of autoassociative memory (see Amit, 1989) by analyzing a network with graded response units, so as to represent more realistically the continuously variable rates at which neurons fire, and with incomplete connectivity (Treves, 1990; Treves and Rolls, 1991; Rolls et al., 1997b; Webb et al., 2011). We have found that in general the maximum number $p_{\max}$ of firing patterns that can be (individually) retrieved is proportional to the number C^{RC} of (associatively) modifiable recurrent collateral synapses on to each neuron, by a factor that increases roughly with the inverse of the sparseness *a* of the neuronal representation. [Each memory is precisely defined in the theory: it is a set of firing rates of the population of neurons (which represent a memory) that can be stored and later retrieved, with retrieval being possible from a fraction of the originally stored set of neuronal firing rates.] The neuronal population sparseness *a* of the representation can be measured by extending the binary notion of the proportion of neurons that are firing to any one stimulus or event as,

$$a = \left(\sum_{i=1,n} r_i/N \right)^2 \Big/ \sum_{i=1,n} (r_i^2/N) \tag{2}$$

where r_i is the firing rate of the *i*'th neuron in the set of *N* neurons. The sparseness ranges from 1/*N*, when only one of the neurons responds to a particular stimulus (a local or grandmother cell representation), to a value of 1.0, attained when all the neurons are responding to a given stimulus. Approximately,

$$p_{\max} \cong \frac{C^{\mathrm{RC}}}{[a \ln(1/a)]} k \tag{3}$$

where k is a factor that depends weakly on the detailed structure of the rate distribution, on the connectivity pattern, etc., but is roughly in the order of 0.2-0.3 (Treves and Rolls, 1991). For example, for $C^{RC} = 12.000$ and $a = 0.02$, p_{max} is calculated to be ∼36,000. This analysis emphasizes the utility of having a sparse representation in the hippocampus, for this enables many different memories to be stored. [The sparseness a in this equation is strictly the population sparseness (Treves and Rolls, 1991; Franco et al., 2007). The population sparseness a^p would be measured by measuring the distribution of firing rates of all neurons to a single stimulus at a single time. The single neuron sparseness or selectivity a^s would be measured by the distribution of firing rates to a set of stimuli, which would take a long time. The selectivity or sparseness a^s of a single neuron measured across a set of stimuli often takes a similar value to the population sparseness a^p in the brain, and does so if the tuning profiles of the neurons to the set of stimuli are uncorrelated (Franco et al., 2007). These concepts are elucidated by Franco et al. (2007)]. (I note that the sparseness estimates obtained by measuring early gene changes, which are effectively population sparsenesses, would be expected to depend greatly on the range of environments or stimuli in which these were measured. If the environment was restricted to one stimulus, this would reflect the population sparseness. If the environment was changing, the measure from early gene changes would be rather undefined, as all the populations of neurons activated in an undefined number of testing situations would be likely to be activated.)

In order for most associative networks to store information efficiently, heterosynaptic Long-Term Depression (as well as LTP) is required (Rolls and Treves, 1990, 1998; Treves and Rolls, 1991; Fazeli and Collingridge, 1996; Rolls and Deco, 2002; Rolls, 2008). Simulations that are fully consistent with the analytic theory are provided by Rolls (1995, 2012a), Simmen et al. (1996) and Rolls et al. (1997b).

A number of points that arise, including measurement of the total amount of information (in bits per synapse) that can be retrieved from the network, the computational definition of a memory, the computational sense in which CA3 is an attractor network, and the possible computational utility of memory reconsolidation, are treated elsewhere (Rolls and Kesner, 2006; Rolls, 2008). Here I note that given that the memory capacity of the hippocampal CA3 system is limited, it is necessary to have some form of forgetting in this store, or other mechanism to ensure that its capacity is not exceeded. (Exceeding the capacity can lead to a loss of much of the information retrievable from the network.) Heterosynaptic LTD could help this *forgetting*, by enabling new memories to overwrite old memories (Rolls, 1996a, 2008). The limited capacity of the CA3 system does also provide one of the arguments that some transfer of information from the hippocampus to neocortical memory stores may be useful (see Treves and Rolls, 1994). Given its limited capacity, the hippocampus might be a useful store for only a limited period, which might be in the order of days, weeks, or months. This period may well depend on the acquisition rate of new episodic memories. If the animal were in a constant and limited environment, then as new information is not being added to the hippocampus, the representations in the hippocampus would remain stable and persistent. These hypotheses have clear experimental implications, both for recordings from single neurons and for the gradient of retrograde amnesia, both of which might be expected to depend on whether the environment is stable or frequently changing. They show that the conditions under which a gradient of retrograde amnesia might be demonstrable would be when large numbers of new memories are being acquired, not when only a few memories (few in the case of the hippocampus being less than a few hundred) are being learned.

It has been suggested that the feedforward connectivity from the entorhinal cortex via the pp to the CA3 neurons may act as a feedforward pattern association network that is more important than the CA3-CA3 recurrent collateral autoassociation system (Cheng, 2013). The quantitative properties of pattern association networks are described elsewhere (Rolls and Treves, 1990, 1998; Rolls, 2008). The analyses described in these sources shows that the capacity of pattern association networks (the maximum number of memories that can be stored and retrieved, here denoted by p_{max}) is approximately,

$$p_{max} \approx \frac{C^{PA}}{[a_0 \ln(1/a_0)]} \tag{4}$$

where C^{PA} is the number of feedforward associatively modifiable connections per neuron, and a_0 is the sparseness of the representation in the output neurons of the pattern associator (Rolls, 2008). Given that there are fewer feedforward (pp) synaptic connections onto CA3 neurons (3600) than recurrent synaptic connections between CA3 neurons (12,000 in the rat; see **Figure 2**), then the capacity of the feedforward system would be considerably smaller than that of the recurrent collateral CA3-CA3 system. (It is noted that the a_0 of Equation 4 would be the same number as the a of Equation (3), as that is just the sparseness of the firing of the population of CA3 neurons. The number of pp synapses is sufficiently large that it can act as a retrieval cue for even an incomplete pattern so that the CA3-CA3 connections can then complete the retrieval, given that the recall signal for the pp pattern associator is proportional to the square root of the number of pp synapses, as shown by Equation 17 of Treves and Rolls (1992). The feedforward hypothesis (Cheng, 2013) thus has a strong argument against it of storage capacity, which would be much less (approximately 3600/12,000) than that of the CA3-CA3 recurrent collateral system operating as an autoassociation memory. Another disadvantage of the feedforward hypothesis is that the attractor properties of the CA3-CA3 connections would be lost, and these potentially contribute to holding one or more items simultaneously active in short-term memory (Rolls, 2008; Rolls et al., 2013), and providing a basis for temporal order memory as described in section Temporal Order Memory in the Hippocampus, and Episodic Memory. Another disadvantage is that we have been able to show (Treves and Rolls, 1992) that an input of the pp type, alone, is unable to direct efficient information storage. Such an input is too weak, it turns out, to drive the firing of the cells, as the "dynamics" of the network is dominated by the randomizing effect of the recurrent collaterals. Another disadvantage of the feedforward hypothesis is that a pattern associator may not with an incomplete cue be able to recall

the exact pattern that was stored, whereas an attractor network has the property that it can fall into an attractor basin that can reflect perfect retrieval of the memory (Rolls and Treves, 1998; Rolls, 2008).

Recall and completion

A fundamental property of the autoassociation model of the CA3 recurrent collateral network is that the recall can be symmetric, that is, the whole of the memory can be retrieved and completed from any part (Rolls and Treves, 1998; Rolls and Kesner, 2006; Rolls, 2008). For example, in an object-place autoassociation memory, an object could be recalled from a place retrieval cue, and vice versa. In a test of this, Day et al. (2003) trained rats in a study phase to learn in one trial an association between two flavors of food and two spatial locations. During a recall test phase they were presented with a flavor which served as a cue for the selection of the correct location. They found that injections of an NMDA receptor blocker (AP5) or AMPA/kainate receptor blocker (CNQX) to the dorsal hippocampus prior to the study phase impaired encoding, but injections of AP5 prior to the test phase did not impair the place recall, whereas injections of CNQX did impair the place recall. The interpretation is that somewhere in the hippocampus NMDA receptors are necessary for learning one-trial odor-place associations, and that recall can be performed without further involvement of NMDA receptors.

Evidence that the CA3 system is not necessarily required during recall in a reference memory spatial task, such as the water maze spatial navigation for a single spatial location task, is that CA3 lesioned rats are not impaired during recall of a previously learned water maze task (Brun et al., 2002; Florian and Roullet, 2004). However, if completion from an incomplete cue is needed, then CA3 NMDA receptors are necessary (presumably to ensure satisfactory CA3-CA3 learning) even in a reference memory task (Nakazawa et al., 2002; Gold and Kesner, 2005). Thus, the CA3 system appears to be especially needed in rapid, one-trial object-place recall, and when completion from an incomplete cue is required (see further section Tests of the theory). Especially important though in assessing the implications of all such tests is that the theory sets out how the system operates when large numbers of memories, in the order of thousands, are to be stored and retrieved, and this is difficult to test adequately in behavioral experiments. Effects found when the storage and retrieval of just a few memories are tested may not reflect well the operation of the system when it is heavily loaded, as it is expected to be when operating in the natural environment.

Continuous, spatial, patterns, and CA3 representations

The fact that spatial patterns, which imply continuous representations of space, are represented in the hippocampus has led to the application of continuous attractor models to help understand hippocampal function. This has been necessary, because space is inherently continuous, because the firing of place and spatial view cells is approximately Gaussian as a function of the distance away from the preferred spatial location, because these cells have spatially overlapping fields, and because the theory is that these cells in CA3 are connected by Hebb-modifiable synapses. This specification would inherently lead the system to operate as a continuous attractor network. Continuous attractor network models have been studied by Amari (1977), Zhang (1996), Taylor (1999), Samsonovich and McNaughton (1997), Battaglia and Treves (1998), Stringer et al. (2002a,b, 2004), Stringer and Rolls (2002) and Rolls and Stringer (2005) (see Rolls and Deco, 2002; Rolls, 2008), and are described briefly next.

A "Continuous Attractor" neural network (CANN) can maintain the firing of its neurons to represent any location along a continuous physical dimension such as spatial view, spatial position, head direction, etc. It uses excitatory recurrent collateral connections between the neurons (as are present in CA3) to reflect the distance between the neurons in the state space of the animal (e.g., place or head direction). These networks can maintain the bubble or packet of neural activity constant for long periods wherever it is started to represent the current state (head direction, position, etc.) of the animal, and are likely to be involved in many aspects of spatial processing and memory, including spatial vision. Global inhibition is used to keep the number of neurons in a bubble or packet of actively firing neurons relatively constant, and to help to ensure that there is only one activity packet.

Continuous attractor networks can be thought of as very similar to autoassociation or discrete attractor networks (Rolls, 2008), and have the same architecture, as illustrated in **Figure 3**. The main difference is that the patterns stored in a CANN are continuous patterns, with each neuron having broadly tuned firing which decreases with for example a Gaussian function as the distance from the optimal firing location of the cell is varied, and with different neurons having tuning that overlaps throughout the space. Such tuning is illustrated in **Figure 4**. For comparison, autoassociation networks normally have discrete (separate) patterns (each pattern implemented by the firing of a particular subset of the neurons), with no continuous distribution of the patterns throughout the space (see **Figure 4**). A consequent difference is that the CANN can maintain its firing at any location in the trained continuous space, whereas a discrete attractor or autoassociation network moves its population of active neurons toward one of the previously learned attractor states, and thus implements the recall of a particular previously learned pattern from an incomplete or noisy (distorted) version of one of the previously learned patterns.

Space is continuous, and object representations are discrete. If these representations are to be combined in for example an object-place memory, then we need to understand the operation of networks that combine these representations. Rolls et al. (2002) have shown that attractor networks can store both continuous patterns and discrete patterns (as illustrated in **Figure 4**), and can thus be used to store for example the location in (continuous, physical) space (e.g., the place "out there" in a room represented by spatial view cells) where an object (a discrete item) is present. We showed this by storing associated continuous and discrete representations in the same single attractor network, and then showing that the representation in the continuous space could be retrieved by the discrete object that was associated with that spatial position; and that the representation of the discrete object could be retrieved by providing the position in the continuous representation of space.

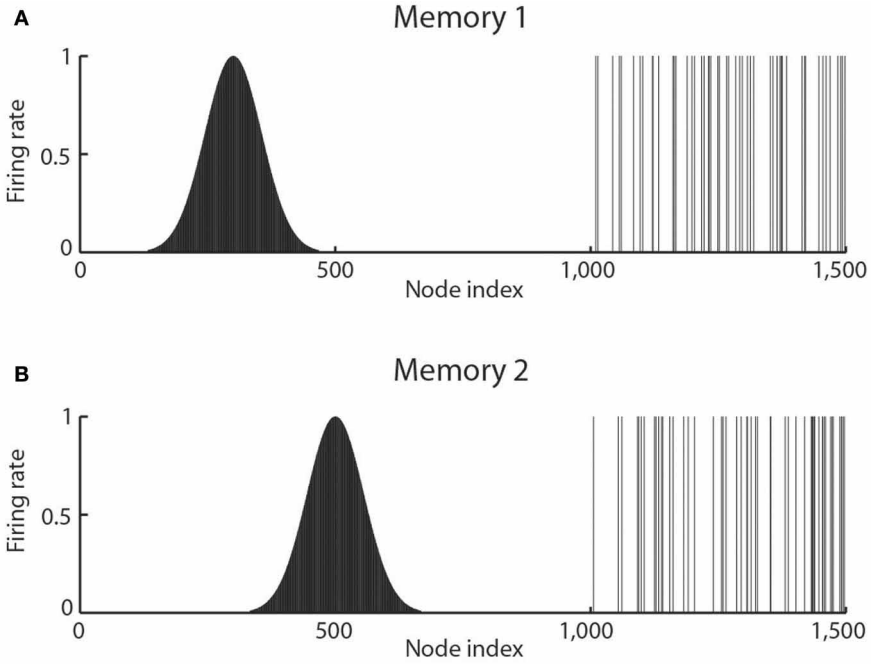

FIGURE 4 | The types of firing patterns stored in continuous attractor networks are illustrated for the patterns present on neurons 1–1000 for Memory 1 (when the firing is that produced when the spatial state represented is that for location 300), and for Memory 2 (when the firing is that produced when the spatial state represented is that for location 500). The continuous nature of the spatial representation results from the fact that each neuron has a Gaussian firing rate that peaks at its optimal location. This particular mixed network also contains discrete representations that consist of discrete subsets of active binary firing rate neurons in the range 1001–1500. The firing of these latter neurons can be thought of as representing the discrete events that occur at the location. Continuous attractor networks by definition contain only continuous representations, but this particular network can store mixed continuous and discrete representations, and is illustrated to show the difference of the firing patterns normally stored in separate continuous attractor and discrete attractor networks. For this particular mixed network, during learning, Memory 1 is stored in the synaptic weights, then Memory 2, etc., and each memory contains part that is continuously distributed to represent physical space, and part that represents a discrete event or object.

If spatial representations are stored in the hippocampus, the important issue arises in terms of understanding memories that include a spatial component or context of how many such spatial representations could be stored in a continuous attractor network. The very interesting result is that because there are in general low correlations between the representations of places in different maps or charts (where each map or chart might be of one room or locale), very many different maps of charts can be simultaneously stored in a continuous attractor network (Battaglia and Treves, 1998).

We have considered how spatial representations could be stored in continuous attractor networks, and how the activity can be maintained at any location in the state space in a form of short-term memory when the external (e.g., visual) input is removed. However, a property of some spatial representations is that they can be updated by self-motion, idiothetic, input, and mechanisms have been proposed for how this could be achieved (Samsonovich and McNaughton, 1997; Stringer et al., 2002a,b, 2005; Rolls and Stringer, 2005; Stringer and Rolls, 2006; Walters et al., 2013), including in the entorhinal cortex grid cell system (Kropff and Treves, 2008; Giocomo et al., 2011; Zilli, 2012). The ways in which path integration could be implemented in recurrent networks such as the CA3 system in the hippocampus or in related systems are described elsewhere (Samsonovich and McNaughton, 1997; Stringer et al., 2002a,b; McNaughton et al., 2006), and have been applied to primate spatial view cells by Rolls and colleagues (Stringer et al., 2004, 2005; Rolls and Stringer, 2005). Cognitive maps (O'Keefe and Nadel, 1978) can be understood by the operations of these attractor networks, and how they are updated by learning and by self-motion (Rolls, 2008). It has been argued that the bumpiness of the CA3 representation of space is more consistent with episodic memory storage, as argued in this paper, than with spatial path integration using the CA3 system as a continuous attractor network implementing path integration (Cerasti and Treves, 2013; Stella et al., 2013).

Mossy fiber inputs to the CA3 cells

We hypothesize that the MF inputs force efficient information storage by virtue of their strong and sparse influence on the CA3 cell firing rates (Rolls, 1987, 1989b,c; Treves and Rolls, 1992). [The strong effects likely to be mediated by the MFs were also emphasized by McNaughton and Morris (1987) and McNaughton and Nadel (1990)]. We (Rolls and Treves) (Rolls, 1987, 1989b,c, 1990b; Treves and Rolls, 1992; Rolls and Treves, 1998; Rolls, 2008) hypothesize that the MF input appears to be particularly appropriate in several ways. First, the fact that MF synapses are large

and located very close to the soma makes them relatively powerful in activating the postsynaptic cell. Second, the firing activity of dentate granule cells appears to be very sparse (Jung and McNaughton, 1993; Leutgeb et al., 2007) and this, together with the small number of connections on each CA3 cell, produces a sparse signal, which can then be transformed into sparse firing activity in CA3 by a threshold effect. The hypothesis is that the MF sparse connectivity solution performs the appropriate function to enable learning to operate correctly in CA3 (Treves and Rolls, 1992; Cerasti and Treves, 2010). The pp input would, the quantitative analysis shows, not produce a pattern of firing in CA3 that contains sufficient information for learning (Treves and Rolls, 1992) (see further section Perforant Path Inputs to CA3 Cells).

The particular property of the small number of MF connections onto a CA3 cell, ∼46 (see **Figure 2**), is that this has a **randomizing effect** on the representations set up in CA3, so that they are as different as possible from each other (Rolls, 1989c,b; Treves and Rolls, 1992; Rolls and Treves, 1998; Rolls and Kesner, 2006; Rolls, 2008). (This means for example that place cells in a given environment are well-separated to cover the whole space.) The result is that any one event or episode will set up a representation that is very different from other events or episodes, because the set of CA3 neurons activated for each event is random. This is then the optimal situation for the CA3 recurrent collateral effect to operate, for it can then associate together the random set of neurons that are active for a particular event (for example an object in a particular place), and later recall the whole set from any part. It is because the representations in CA3 are unstructured, or random, in this way that large numbers of memories can be stored in the CA3 autoassociation system, and that interference between the different memories is kept as low as possible, in that they are maximally different from each other (Hopfield, 1982; Treves and Rolls, 1991; Rolls and Treves, 1998; Rolls, 2008).

The requirement for a small number of MF connections onto each CA3 neuron applies not only to discrete (Treves and Rolls, 1992) but also to spatial representations, and some learning in these connections, whether associative or not, can help to select out the small number of MFs that may be active at any one time to select a set of random neurons in the CA3 (Cerasti and Treves, 2010). Any learning may help by reducing the accuracy required for a particular number of MF connections to be specified genetically onto each CA3 neuron. The optimal number of MFs for the best information transfer from dentate granule cells to CA3 cells is in the order of 35–50 (Treves and Rolls, 1992; Cerasti and Treves, 2010). The MFs also make connections useful for feedforward inhibition (Acsady et al., 1998).

On the basis of these and other points, we predicted that the MFs may be necessary for new learning in the hippocampus, but may not be necessary for the recall of existing memories from the hippocampus (Treves and Rolls, 1992; Rolls and Treves, 1998; Rolls, 2008). Experimental evidence consistent with this prediction about the role of the MFs in learning has been found in rats with disruption of the dentate granule cells (Lassalle et al., 2000) (section Tests of the theory).

We (Rolls and Kesner, 2006) have hypothesized that non-associative plasticity of MFs (see Brown et al., 1989, 1990) might have a useful effect in enhancing the signal-to-noise ratio, in that a consistently firing MF would produce non-linearly amplified currents in the postsynaptic cell, which would not happen with an occasionally firing fiber (Treves and Rolls, 1992). This plasticity, and also learning in the dentate, would also have the effect that similar fragments of each episode (e.g., the same environmental location) recurring on subsequent occasions would be more likely to activate the same population of CA3 cells, which would have potential advantages in terms of economy of use of the CA3 cells in different memories, and in making some link between different episodic memories with a common feature, such as the same location in space. Consistent with this, dentate neurons that fire repeatedly are more effective in activating CA3 neurons (Henze et al., 2002).

As acetylcholine turns down the efficacy of the recurrent collateral synapses between CA3 neurons (Hasselmo et al., 1995; Giocomo and Hasselmo, 2007), then cholinergic activation also might help to allow external inputs rather than the internal recurrent collateral inputs to dominate the firing of the CA3 neurons during learning, as the current theory proposes. If cholinergic activation at the same time facilitated LTP in the recurrent collaterals (as it appears to in the neocortex), then cholinergic activation could have a useful double role in facilitating new learning at times of behavioral activation (Hasselmo et al., 1995; Giocomo and Hasselmo, 2007), when presumably it may be particularly relevant to allocate some of the limited memory capacity to new memories.

Perforant path inputs to CA3 cells

By calculating the amount of information that would end up being carried by a CA3 firing pattern produced solely by the pp input and by the effect of the recurrent connections, we have been able to show (Treves and Rolls, 1992) that an input of the pp type, alone, is unable to direct efficient information storage. Such an input is too weak, it turns out, to drive the firing of the cells, as the "dynamics" of the network is dominated by the randomizing effect of the recurrent collaterals. On the other hand, an autoassociative memory network needs afferent inputs to apply the retrieval cue to the network. We have shown (Treves and Rolls, 1992) that the pp system is likely to be the one involved in relaying the cues that initiate retrieval in CA3. The concept is that to initiate retrieval, a numerically large input (the pp system, see **Figure 2**) is useful so that even a partial cue is sufficient [see Equationn 17 of Treves and Rolls (1992)]; and that the retrieval cue need not be very strong, as the recurrent collaterals (in CA3) then take over in the retrieval process to produce good recall (Treves and Rolls, 1992; Rolls, 2008). In contrast, during storage, strong signals, in the order of mV for each synaptic connection, are provided by the MF inputs to dominate the recurrent collateral activations, so that the new pattern of CA3 cell firing can be stored in the CA3 recurrent collateral connections (Treves and Rolls, 1992; Rolls, 2008).

Why is the CA3 recurrent collateral connectivity diluted?

Figure 2 shows that in the rat, there are ∼300,000 CA3 neurons, but only 12,000 recurrent collateral synapses per neuron. The dilution of the connectivity is thus 12,000/300,000 = 0.04. The

connectivity is thus not complete, and complete connectivity in an autoassociation network would make it simple, for the connectivity between the neurons would then be symmetric (i.e., the connection strength from any one neuron to another is matched by a connection of the same strength in the opposite direction), and this guarantees energy minima for the basins of attraction that will be stable, and a memory capacity than can be calculated (Hopfield, 1982). We have shown how this attractor type of network can be extended to have similar properties with diluted connectivity, and also with sparse representations with graded firing rates (Rolls and Treves, 1990; Treves, 1990, 1991; Treves and Rolls, 1991).

However, the question has recently been asked about whether there are any advantages to diluted autoassociation or attractor networks compared to fully connected attractor networks (Rolls, 2012a). One biological property that may be a limiting factor is the number of synaptic connections per neuron, which is 12,000 in the CA3-CA3 network just for the recurrent collaterals (see **Figure 2**). The number may be higher in humans, allowing more memories to be stored in the hippocampus than order 12,000. I note that the storage of large number of memories may be facilitated in humans because the left and right hippocampus appear to be much less connected between the two hemispheres than in the rat, which effectively has a single hippocampus (Rolls, 2008). In humans, with effectively two separate CA3 networks, one on each side of the brain, the memory storage capacity may be doubled, as the capacity is set by the number of recurrent collaterals per neuron in each attractor network (Equation 3). In humans, the right hippocampus may be devoted to episodic memories with spatial and visual components, whereas the left hippocampus may be devoted to memories with verbal/linguistic components, i.e., in which words may be part of the episode (e.g., who said what to whom and when; Barkas et al., 2010; Bonelli et al., 2010; Sidhu et al., 2013).

The answer that has been suggested to why the connectivity of the CA3 autoassociation network is diluted (and why neocortical recurrent networks are also diluted), is that this may help to reduce the probability of having two or more synapses between any pair of randomly connected neurons within the network, which it has been shown greatly impairs the number of memories that can be stored in an attractor network, because of the distortion that this produces in the energy landscape (Rolls, 2012a). In more detail, the hypothesis proposed is that the diluted connectivity allows biological processes that set up synaptic connections between neurons to arrange for there to be only very rarely more than one synaptic connection between any pair of neurons. If probabilistically there were more than one connection between any two neurons, it was shown by simulation of an autoassociation attractor network that such connections would dominate the attractor states into which the network could enter and be stable, thus strongly reducing the memory capacity of the network (the number of memories that can be stored and correctly retrieved), below the normal large capacity for diluted connectivity. Diluted connectivity between neurons in the cortex thus has an important role in allowing high capacity of memory networks in the cortex, and helping to ensure that the critical capacity is not reached at which overloading occurs leading to an impairment in the ability to retrieve any memories from the network (Rolls, 2012a). The diluted connectivity is thus seen as an adaptation that simplifies the genetic specification of the wiring of the brain, by enabling just two attributes of the connectivity to be specified (e.g., from a CA3 to another CA3 neuron chosen at random to specify the CA3 to CA3 recurrent collateral connectivity), rather than which particular neuron should connect to which other particular neuron (Rolls and Stringer, 2000; Rolls, 2012a). Consistent with this hypothesis, there are NMDA receptors with the genetic specification that they are NMDA receptors on neurons of a particular type, CA3 neurons (as shown by the evidence from CA3-specific vs. CA1-specific NMDA receptor knockouts; Rondi-Reig et al., 2001; Nakazawa et al., 2002, 2003, 2004). A consequence is that the vector of output neuronal firing in the CA3 regions, i.e., the number of CA3 neurons, is quite large (300,000 neurons in the rat). The large number of elements in this vector may have consequences for the noise in the system, as we will see below.

The dilution of the CA3-CA3 recurrent collateral connectivity at 0.04 may be greater dilution than that in a local neocortical area, which is in the order of 0.1 (Rolls, 2008, 2012a). This is consistent with the hypothesis that the storage capacity of the CA3 system is at a premium, and so the dilution is kept to a low value (i.e., great dilution), as then there is lower distortion of the basins of attraction and hence the memory capacity is maximized (Rolls, 2012a).

Noise and stability produced by the diluted connectivity and the graded firing rates in the CA3-CA3 attractor network

Many processes in the brain are influenced by the noise or variability of neuronal spike firing (Faisal et al., 2008; Rolls and Deco, 2010; Deco et al., 2013). The action potentials are generated in a way that frequently approximates a Poisson process, in which the spikes for a given mean firing rate occur at times that are essentially random (apart from a small effect of the refractory period), with a coefficient of variation (CV) of the interspike interval distribution near 1.0 (Rolls and Deco, 2010). The sources of the noise include quantal transmitter release, and noise in ion channel openings (Faisal et al., 2008). The membrane potential is often held close to the firing threshold, and then small changes in the inputs and the noise in the neuronal operations cause spikes to be emitted at almost random times for a given mean firing rate. Spiking neuronal networks with balanced inhibition and excitation currents and associatively modified recurrent synaptic connections can be shown to possess a stable attractor state where neuron spiking is approximately Poisson too (Amit and Brunel, 1997; Miller and Wang, 2006). The noise caused by the variability of individual neuron spiking which then affects other neurons in the network can play an important role in the function of such recurrent attractor networks, by causing for example an otherwise stable network to jump into a decision state (Wang, 2002; Deco and Rolls, 2006; Rolls and Deco, 2010). Attractor networks with this type of spiking-related noise are used in the brain for memory recall, and for decision-making, which in terms of the neural mechanism are effectively the same process (Rolls, 2008). Noise in attractor networks is useful for memory and decision-making, for it makes them non-deterministic, and this contributes to new

solutions to problems, and indeed to creativity (Rolls and Deco, 2010).

To investigate the extent to which this diluted connectivity affects the dynamics of attractor networks in the cerebral cortex (which includes the hippocampus), we simulated an integrate-and-fire attractor network taking decisions between competing inputs with diluted connectivity of 0.25 or 0.1 but the same number of synaptic connections per neuron for the recurrent collateral synapses within an attractor population as for full connectivity (Rolls and Webb, 2012). The results indicated that there was less spiking-related noise with the diluted connectivity in that the stability of the network when in the spontaneous state of firing increased, and the accuracy of the correct decisions increased. The decision times were a little slower with diluted than with complete connectivity. Given that the capacity of the network is set by the number of recurrent collateral synaptic connections per neuron, on which there is a biological limit, the findings indicate that the stability of cortical networks, and the accuracy of their correct decisions or memory recall operations, can be increased by utilizing diluted connectivity and correspondingly increasing the number of neurons in the network (which may help to smooth the noise), with little impact on the speed of processing of the cortex. Thus, diluted connectivity can decrease cortical spiking-related noise, and thus enhance the reliability of memory recall (Rolls and Webb, 2012).

Representations in the neocortex and in the hippocampus are often distributed with graded firing rates in the neuronal populations (Rolls and Treves, 2011). The firing rate probability distribution of each neuron to a set of stimuli is often exponential or gamma (Rolls and Treves, 2011). These graded firing rate distributed representations are present in the hippocampus, both for place cells in rodents and for spatial view cells in the primate (O'Keefe, 1979; McNaughton et al., 1983; O'Keefe and Speakman, 1987; Rolls et al., 1997a, 1998; Robertson et al., 1998; Georges-François et al., 1999; Rolls, 2008; Rolls and Treves, 2011). In processes in the brain such as memory recall in the hippocampus or decision-making in the cortex that are influenced by the noise produced by the close to random spike timings of each neuron for a given mean rate, the noise with this graded type of representation may be larger than with the binary firing rate distribution that is usually investigated. In integrate-and-fire simulations of an attractor decision-making network, we showed that the noise is indeed greater for a given sparseness of the representation for graded, exponential, than for binary firing rate distributions (Webb et al., 2011). The greater noise was measured by faster escaping times from the spontaneous firing rate state when the decision cues are applied, and this corresponds to faster decision or reaction times. The greater noise was also evident as less stability of the spontaneous firing state before the decision cues are applied. The implication is that spiking-related noise will continue to be a factor that influences processes such as decision-making, signal detection, short-term memory, and memory recall (including in the CA3 network) even with the quite large networks found in the cerebral cortex. In these networks there are several thousand recurrent collateral synapses onto each neuron. The greater noise with graded firing rate distributions has the advantage that it can increase the speed of operation of cortical circuitry (Webb et al., 2011).

DENTATE GRANULE CELLS

The theory is that the dentate granule cell stage of hippocampal processing which precedes the CA3 stage acts as a competitive network in a number of ways to produce during learning the sparse yet efficient (i.e., non-redundant) representation in CA3 neurons that is required for the autoassociation implemented by CA3 to perform well (Rolls, 1989b,c, 1990b; Treves and Rolls, 1992; Rolls and Kesner, 2006; Rolls et al., 2006). An important property for episodic memory is that the dentate by acting in this way would perform pattern separation (or orthogonalization) (Rolls, 1989b; Treves and Rolls, 1992; Rolls and Kesner, 2006; Rolls et al., 2006), enabling the hippocampus to store different memories of even similar events, and this prediction has been confirmed (Gilbert et al., 2001; Rolls and Kesner, 2006; Leutgeb and Leutgeb, 2007; McHugh et al., 2007; Goodrich-Hunsaker et al., 2008; Rolls, 2008; Kesner et al., 2012) (section Tests of the theory).

As just described, the dentate granule cells could be important in helping to build and prepare spatial representations for the CA3 network. The actual representation of space in the primate hippocampus includes a representation of spatial view (Rolls and Xiang, 2006), whereas in the rat hippocampus it is of the place where the rat is. The representation in the rat may be related to the fact that with a much less developed visual system than the primate, the rat's representation of space may be defined more by the olfactory and tactile as well as distant visual cues present, and may thus tend to reflect the place where the rat is. However, the spatial representations in the rat and primate could arise from essentially the same computational process as follows (Rolls, 1999; De Araujo et al., 2001). The starting assumption is that in both the rat and the primate, the dentate granule cells (and the CA3 and CA1 pyramidal cells) respond to combinations of the inputs received. In the case of the primate, a combination of visual features in the environment will, because of the fovea providing high spatial resolution over a typical viewing angle of perhaps 10–20°, result in the formation of a spatial view cell, the effective trigger for which will thus be a combination of visual features within a relatively small part of space. In contrast, in the rat, given the very extensive visual field subtended by the rodent retina, which may extend over 180–270°, a combination of visual features formed over such a wide visual angle would effectively define a position in space that is a place (De Araujo et al., 2001).

The entorhinal cortex contains grid cells, which have high firing in the rat in a two-dimensional spatial grid as a rat traverses an environment, with larger grid spacings in the ventral entorhinal cortex (Fyhn et al., 2004; Hafting et al., 2005). This may be a system optimized for path integration (McNaughton et al., 2006) which may self-organize during locomotion with longer time constants producing more widely spaced grids in the ventral entorhinal cortex (Kropff and Treves, 2008). How are the grid cell representations, which would not be suitable for association of an object or reward with a place to form an episodic memory, transformed into a place representation that would be appropriate for this type of episodic memory? I have proposed that this could be implemented by a competitive network (Rolls, 2008) in the DG

which operates to form place cells, implemented by each dentate granule cell learning to respond to particular combinations of entorhinal cortex cells firing, where each combination effectively specifies a place, and this has been shown to be feasible computationally (Rolls et al., 2006). The sparse representations in the DG, implemented by the mutual inhibition through inhibitory interneurons and competitive learning, help to implement this "pattern separation" effect (Rolls, 1989b,c; Rolls and Treves, 1998; Rolls, 2008).

In primates, there is now evidence that there is a grid-cell like representation in the entorhinal cortex, with neurons having grid-like firing as the monkey moves the eyes across a spatial scene (Killian et al., 2012). Similar competitive learning processes may transform these entorhinal cortex "spatial view grid cells" into hippocampal spatial view cells, and may help with the idiothetic (produced in this case by movements of the eyes) update of spatial view cells (Robertson et al., 1998). The presence of spatial view grid cells in the entorhinal cortex of primates (Killian et al., 2012) is of course predicted from the presence of spatial view cells in the primate CA3 and CA1 regions (Rolls et al., 1997a, 1998; Robertson et al., 1998; Georges-François et al., 1999; Rolls and Xiang, 2006; Rolls, 2008).

In primates, spatial view cells represent a scene view allocentrically, as described in section Systems-Level Neurophysiology of the Primate Hippocampus. How could such spatial view representations be formed, in which the relative spatial position of features in a scene is encoded? I have proposed that this involves competitive learning analogous to that used to form place cells in rats, but in primates operating on the representations of objects that reach the hippocampus from the inferior temporal visual cortex (Rolls et al., 2008b). We have shown that in complex natural scenes the receptive fields of inferior temporal cortex neurons become reduced in size and asymmetric with respect to the fovea (Aggelopoulos and Rolls, 2005; Rolls, 2009), and Rolls et al. (2008b) have demonstrated in a unifying computational approach that competitive network processes operating in areas such as the parahippocampal cortex, the entorhinal cortex, and/or the dentate granule cells could form unique views of scenes by forming a sparse representation of these object or feature tuned inferior temporal cortex ventral visual stream representations which have some spatial asymmetry.

CA1 CELLS

The CA3 cells connect to the CA1 cells by the Schaeffer collateral synapses. The associative modifiability in this connection helps the full information present in CA3 to be retrieved in the CA1 neurons (Treves and Rolls, 1994; Rolls, 1995; Treves, 1995; Schultz and Rolls, 1999). Part of the hypothesis is that the separate sub-parts of an episodic memory, which must be represented separately in CA3 to allow for completion, can be combined together by competitive learning in CA1 to produce an efficient retrieval cue for the recall via the backprojection pathways to the neocortex of memories stored in the neocortex (Rolls, 1989a,b; Treves and Rolls, 1994; Rolls, 1995, 1996b). Associative recall in the CA3 to CA1 feedforward connections is a prominent property (Rolls, 1995; Schultz et al., 2000).

BACKPROJECTIONS TO THE NEOCORTEX, AND MEMORY RECALL

The need for information to be retrieved from the hippocampus to affect other brain areas was noted in the Introduction. The way in which this could be implemented via backprojections to the neocortex is considered elsewhere (Treves and Rolls, 1994; Rolls, 1995, 1996b, 2008, 2010b) (see **Figure 1**).

TEMPORAL ORDER MEMORY IN THE HIPPOCAMPUS, AND EPISODIC MEMORY

There has for some time been evidence that the hippocampus plays a role in temporal order memory, even when there is no spatial component (Kesner et al., 2002; Rolls and Kesner, 2006; Hoge and Kesner, 2007). In humans, the hippocampus becomes activated when the temporal order of events is being processed (Lehn et al., 2009). If this is a function that can be implemented in the hippocampus, I now propose that this could be very important for understanding episodic memory, which often may comprise a temporal sequence of events. However, until recently it has not been clear how temporal order memory could be implemented in the hippocampus, or, for that matter, in other brain structures. However, the outline of a theory of temporal order memory, and how it could be implemented in the hippocampus, has now been developed (Rolls and Deco, 2010), as follows.

The approach is based on recent neurophysiological evidence of MacDonald et al. (2011) showing that neurons in the rat hippocampus have firing rates that reflect which temporal part of the task is current. In particular, a sequence of different neurons is activated at successive times during a time delay period. The tasks used included an object-odor paired associate non-spatial task with a 10 s delay period between the visual stimulus and the odor. The new evidence also shows that a large proportion of hippocampal neurons fire in relation to individual events in a sequence being remembered (e.g., a visual object or odor), and some to combinations of the event and the time in the delay period (MacDonald et al., 2011).

These interesting neurophysiological findings indicate that rate encoding is being used to encode time, that is, the firing rates of different neurons are high at different times within a trial, delay period, etc. (Rolls and Deco, 2010; MacDonald et al., 2011). This provides the foundation for a new computational theory of temporal order memory within the hippocampus (and also the prefrontal cortex) which I outline next, and which utilizes the slow transitions from one attractor to another which are a feature that arises at least in some networks in the brain due to the noise-influenced transitions from one state to another.

First, because some neurons fire at different times in a trial of a temporal order memory task or delay task, the time in a trial at which an object (e.g., a visual stimulus or odor) was presented could become encoded in the hippocampus by an association implemented in the CA3 recurrent collaterals between the neurons that represent the object [already known to be present in the hippocampus for tasks for which the hippocampus is required (Rolls et al., 2005; Rolls and Xiang, 2006)] and the "time encoding" neurons in the hippocampus (MacDonald et al., 2011). This would allow associations for the time at which the object was present to be formed.

Second, these associations would provide the basis for the recall of the object from the time in a trial, or vice versa. The retrieval of object or temporal information from each other would occur in a way that is analogous to that shown for recalling the object from the place, or the place from the object (Rolls et al., 2002), but substituting the details of the properties of the "time encoding" neurons (MacDonald et al., 2011) for what was previously the spatial (place) component. In addition, if the time encoding neurons simply cycled through their normal sequence during recall, this would enable the sequence of objects or events associated with each subset of time encoding neurons to be recalled correctly in the order in which they were presented.

Third, we need a theory of what the origin is of the temporal effect whereby different hippocampal (or potentially prefrontal cortex) neurons fire in different parts of a trial or delay period. The properties of the "time encoding neurons" (Rolls and Deco, 2010; MacDonald et al., 2011) are key here, and we need to understand how they are generated. Are they generated within the hippocampus, or elsewhere, and in any case, what is the mechanism by which different neurons have high firing rates at different times in a trial? The fundamentally new approach to hippocampal function I am taking here is that rate encoding is being used, that is, the firing rates of different neurons are high at different times within a trial (Rolls and Deco, 2010; MacDonald et al., 2011). This is a radically different approach to order encoding than that based on phenomena such a theta and gamma oscillations that has been investigated by Lisman and colleagues (Lisman and Redish, 2009).

We can consider three hypotheses about how the firing of the "time encoding" hippocampal neurons is produced. All utilize slow transitions between attractor states that can be a property of noisy attractor networks. The first hypothesis is that an attractor network with realistic dynamics (modeled at the integrate-and-fire level with a dynamical implementation of the neuronal membrane and synaptic current dynamics, and with synaptic or neuronal adaptation) can implement a sequence memory (Deco and Rolls, 2005). The hypothesis is that there are several different attractors, and that there are weak connections between the different attractors. In the model, adaptation produces effects whereby whatever sequence (order of stimuli) is presented on an individual trial that order can be replayed in the same sequence because as one attractor state dies as a result of the adaptation, the next attractor to emerge from the spontaneous firing because of the spiking-related noise is the one that has been active least recently, as it is the one that is least adapted (Deco and Rolls, 2005). The whole system operates at a rather slow timescale for the transitions between the attractors partly because of the time for the noise to drive the system from one attractor state to another, and the slow time course of the adaptation (Deco and Rolls, 2005; Rolls and Deco, 2010). This implements a type of order memory.

The second hypothesis is analogous, and is also implemented in a recurrently connected system such as the hippocampal CA3 system or local recurrent circuits in the neocortex (Rolls and Deco, 2010). This second theory is that again there are several attractors, but that each attractor is connected by slightly stronger forward than reverse synaptic weights to the next. In previous work, we have shown that with an integrate-and-fire implementation with spiking noise this allows slow transitions from one attractor state to the next (Deco and Rolls, 2003; Deco et al., 2005). During learning of the synaptic weights in the network, adaptation might lead to each "time encoding" population of neurons responding for only a limited period, helping to produce multiple sequentially activated populations of time encoding neurons (Rolls and Deco, 2010; MacDonald et al., 2011). In this scenario, an associative pool of neurons is unlikely to be helpful, and stronger forward that reverse weights between different attractors each consisting of a different population of "time encoding" neurons would be the essence. It will be of interest to investigate whether this system, because of the noise, is limited to transitions between up to perhaps 7 ± 2 different sequential firing rate states with different neuronal subpopulations for each state, and thus provides an account for the limit of the magical number 7 ± 2 on short-term memory and related types of processing (Miller, 1956), and for the recency part of short-term memory in which the items are naturally recalled in the order in which they were presented. This is the most likely model at present of short-term memory and its natural propensity to store and to recall items in the order in which they were received (Rolls and Deco, 2010).

A variation on this implementation that I have proposed would be to have short-term attractor memories with different time constants (for example of adaptation), but all started at the same time (Rolls and Deco, 2010). This could result in some attractors starting early in the sequence and finishing early, and with other attractors starting up a little later, but lasting for much longer in time. The neurons recorded in the rat (MacDonald et al., 2011) are not inconsistent with this possibility. This type of time-encoding representation could also be used to associate with items, to implement an item-order memory.

It is thus suggested that temporal order memory could be implemented in the hippocampus in this way, and could make an important contribution to episodic memory in which several events linked in the correct order might form an episode. The theory shows how items in a particular temporal order could be separated from each other, a property we have referred to as the temporal pattern separation effect (Rolls and Kesner, 2006). The theory of episodic memory described here shows how events and sequences of events could be recalled from the hippocampus to the neocortex, and there a longer-term more semantic representation of a recalled episode, such as what happened on one's fifth birthday, might be stored, and then accessed to describe the episode. For the order to be correctly implemented in the semantic neocortical store, a similar mechanism, involving for example stronger forward than reverse synaptic weights between long-term memory representations in attractors, could build an appropriate long-term order memory (Rolls and Deco, 2010).

The natural implementation of such temporal order memory would be in the hippocampal CA3-CA3 recurrent collateral network. It is therefore somewhat of a puzzle that some of the evidence implicates the CA1 region in temporal order memory (Rolls and Kesner, 2006; Hunsaker et al., 2008; Kesner et al., 2012). This issue remains to be clarified.

SYSTEMS-LEVEL NEUROPHYSIOLOGY OF THE PRIMATE HIPPOCAMPUS

The systems-level neurophysiology of the hippocampus shows what information could be stored or processed by the hippocampus. To understand how the hippocampus works it is not sufficient to state just that it can store information—one needs to know what information. The systems-level neurophysiology of the primate hippocampus has been reviewed by Rolls and Xiang (2006), and a summary is provided here because it provides a perspective relevant to understanding the function of the human hippocampus that is somewhat different from that provided by the properties of place cells in rodents, which have been reviewed elsewhere (McNaughton et al., 1983; O'Keefe, 1984; Muller et al., 1991; Jeffery et al., 2004; Jeffery and Hayman, 2004).

SPATIAL VIEW NEURONS IN THE PRIMATE HIPPOCAMPUS

We have shown that the primate hippocampus contains spatial cells that respond when the monkey looks at a certain part of space, for example at one quadrant of a video monitor while the monkey is performing an object-place memory task in which he must remember where on the monitor he has seen particular images (Rolls et al., 1989; Rolls, 1999). Approximately 9% of the hippocampal neurons have such spatial view fields, and about 2.4% combine information about the position in space with information about the object that is in that position in space (Rolls et al., 1989). The representation of space is for the majority of hippocampal neurons in allocentric not egocentric coordinates (Feigenbaum and Rolls, 1991). These spatial view cells can be recorded while monkeys move themselves round the test environment by walking (or running) on all fours (Rolls et al., 1997a, 1998; Robertson et al., 1998; Georges-François et al., 1999). These hippocampal "spatial view neurons" respond significantly differently for different allocentric spatial views and have information about spatial view in their firing rate, but do not respond differently just on the basis of eye position, head direction, or place. If the view details are obscured by curtains and darkness, then some spatial view neurons (especially those in CA1 and less those in CA3) continue to respond when the monkey looks toward the spatial view field, showing that these neurons can be updated for at least short periods by idiothetic (self-motion) cues including eye position and head direction signals (Rolls et al., 1997b; Robertson et al., 1998).

OBJECT-PLACE NEURONS IN THE PRIMATE HIPPOCAMPUS

A fundamental question about the function of the primate including human hippocampus in relation to episodic memory is whether object as well as allocentric spatial information is represented. To investigate this, Rolls et al. (2005) made recordings from single hippocampal formation neurons while macaques performed an object-place memory task that required the monkeys to learn associations between objects, and where they were shown in a room. Some neurons (10%) responded differently to different objects independently of location; other neurons (13%) responded to the spatial view independently of which object was present at the location; and some neurons (12%) responded to a combination of a particular object and the place where it was shown in the room. These results show that there are separate as well as combined representations of objects and their locations in space in the primate hippocampus. This is a property required in an episodic memory system, for which associations between objects and the places where they are seen, are prototypical. The results thus show that a requirement for a human episodic memory system, separate and combined neuronal representations of objects and where they are seen "out there" in the environment, are present in the primate hippocampus (Rolls et al., 2005).

What may be a corresponding finding in rats is that some rat hippocampal neurons respond on the basis of the conjunction of location and odor (Wood et al., 1999). Results consistent with our object-place neurons in primates are that Diamond and colleagues have now shown using the vibrissa somatosensory input for the "object" system that rat hippocampal neurons respond to object-place combinations, objects, or places, and there is even a reward-place association system in rats similar to that in primates described below (Itskov et al., 2011). This brings the evidence from rats closely into line with the evidence from primates of hippocampal neurons useful for object-place episodic associative memory.

Spatial view cells, and object-place cells, are also present in the parahippocampal areas (Rolls et al., 1997a, 1998, 2005; Robertson et al., 1998; Georges-François et al., 1999). There are backprojections from the hippocampus to the entorhinal cortex and thus to parahippocampal areas, and these backprojections could enable the hippocampus to influence the spatial representations found in the entorhinal cortex and parahippocampal gyrus. On the other hand, some of the spatial functions may be provided for in these parahippocampal areas, which will in turn influence the hippocampus. However, it is argued below that the hippocampus may be able to make a special contribution to event or episodic memory, by enabling in the CA3 network with its very widespread recurrent collateral connections an association between any one item with any other item to form an arbitrary association to represent an event.

RECALL-RELATED NEURONS IN THE PRIMATE HIPPOCAMPUS

It has now been possible to investigate directly, neurophysiologically, the hippocampal recall process in primates (Rolls and Xiang, 2006). We used a visual object-place memory task because this is prototypical of episodic memory. It has been shown that a one-trial odor-place recall memory task is hippocampal-dependent in rodents (Day et al., 2003). We designed a one-trial object-place recall task, in which the whole memory was recalled from a part of it. The task is illustrated in **Figure 5** and described in its legend. Images of new objects were used each day, and within a day the same objects were used, so that with non-trial unique objects within a day, the recall task is quite difficult.

Recordings were made from 347 neurons in the hippocampus of a macaque performing the object-place recall task. The following types of neurons were found in the task (Rolls and Xiang, 2006).

One type of neuron had responses that occurred to one of the objects used in the task. A number of these neurons had activity that was related to the recall process. An example of one of these neurons is shown in **Figure 6**. The neuron had activity that was greater to object one not only when it was shown in stages 1, 2,

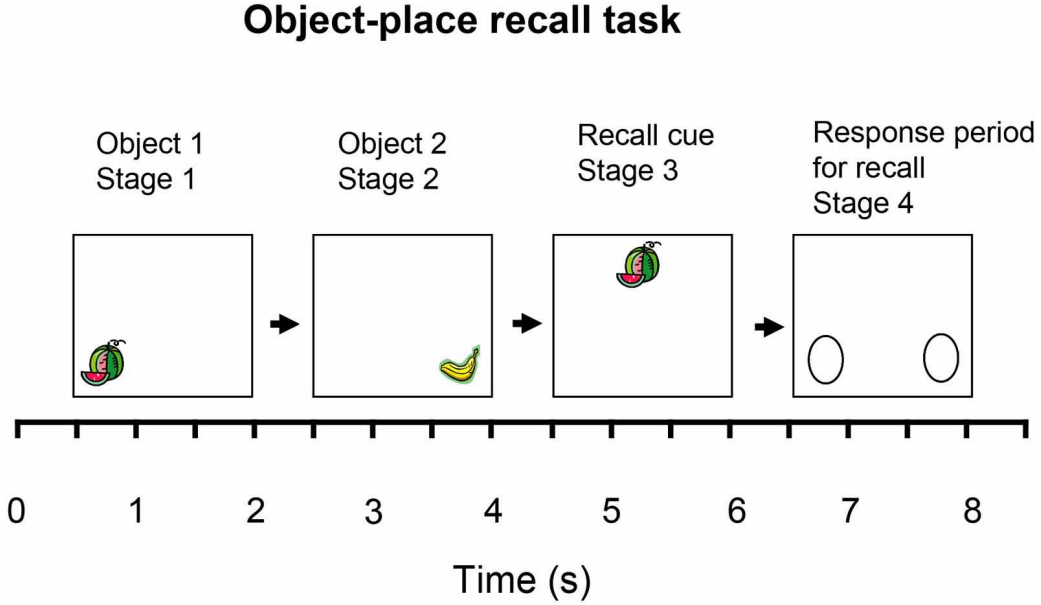

FIGURE 5 | The object-place recall task. One-trial is shown. After a 0.5 s tone to indicate the start of a trial, in Stage 1 one of two objects (O1) is shown at one of the places (P1). (The object and the place are chosen randomly on each trial.) To ensure that the monkey sees the stimulus, the monkey can touch the screen at the place to obtain one drop of juice reward by licking. After a 0.5 s delay, in Stage 2, the other of the two objects (O2) is shown at the other place (P2). (One drop of fruit juice was available as in Stage 1.) After a 0.5 s delay, in Stage 3, the recall cue, one of the objects chosen at random, is shown at the top of the screen in the middle. (One drop of fruit juice was available as in stage 1.) After a 0.5 s delay, in Stage 4, the macaque must then recall the place in which the object shown as the recall cue in stage 3 was presented, and must then touch that place on the screen to obtain 4 licks of fruit juice, thus indicating that he has recalled the location correctly. In stage 4 of the trials, the left and right positions (P1 and P2) have no image present, with the two possible locations for a response indicated by identical circles. The task requires the monkey to perform recall of the place from the object, within the period beginning at the presentation of the recall cue at the start of stage 3 and ending when the response is made in stage 4. Reward associations can not be used to solve the task, for the two objects and the two places are not differently associated with reward. Further details are provided by Rolls and Xiang (2006).

and 3 of the task, but also in the delay period following stage 3 when the object was no longer visible, and in stage 4, when also the object was no longer visible and the macaque was touching the remembered location of that object. Thus, while the location was being recalled from the object, this type of neuron continued to respond as if the object was present, that is it kept the representation of the object active after the object was no longer visible, and the place to touch was being recalled. Sixteen of the neurons responded in this way, and an additional 6 had object-related firing that did not continue following stage 3 of the task in the recall period. The difference of the firing rates of these 22 neurons to the different objects was in many cases highly statistically significant (e.g., $p < 10^{-6}$; Rolls and Xiang, 2006). None of these neurons had differential responses for the different places used in the object-place recall task.

A second type of neuron had responses related to the place (left or right) in which an object was shown in stages 1 or 2 of each trial. An example of one of these neurons is shown in **Figure 7**. The neuron responded more when an object was shown in the left position (P1) than in the right position (P2) on the screen. Interestingly, when the recall object was shown in stage 3 of the trial in the top center of the screen, the neuron also responded as if the left position (P1) was being processed on trials on which the left position had to be recalled. This firing continued in the delay period after the recall cue had been removed at the end of stage 3, and into stage 4. Thus, this type of neuron appeared to reflect the recall of the position on the screen at which the object had been represented. Analysis of trials on which errors were made indicated that the responses were not just motor response related, for if due to some response bias the monkey touched the incorrect side, the neuron could still respond according to the correct recalled location. [On these error trials, therefore, the neuronal responses reflected the correct memory, and not the incorrect motor response—see further Rolls and Xiang (2006)]. Thirteen neurons had differential responses to the different places P1 and P2, and continued to show place-related activity in the recall part of the task, stage 3. Five other neurons had left-right place-related responses without a memory recall component, in that they did not respond in stage 3 of the task, when a non-spatial recall stimulus was being shown, and a place should be being recalled (see **Table 1**). The population of 18 neurons as a population had statistically significant place-related responses (Rolls and Xiang, 2006). The new finding is that 13 of the neurons had place-related responses when a place was being recalled by an object cue.

The responses of the population of neurons recorded in one macaque are shown in **Table 1**. In addition to the neurons described above, 3 further neurons responded to particular

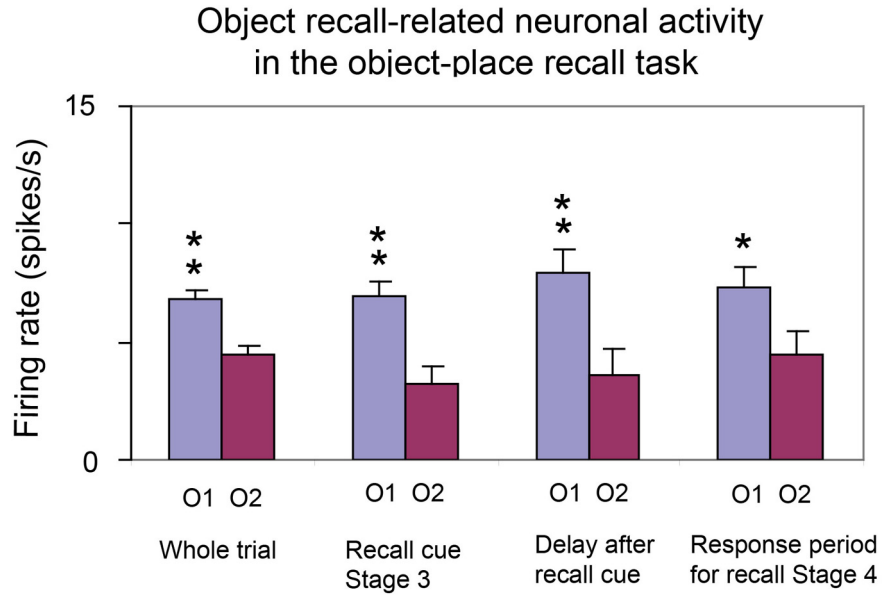

FIGURE 6 | Activity of a neuron with responses related to one of the objects used in the object-place recall task. The firing rate to object 1 (O1) and object 2 (O2) are shown (mean firing rate in spikes/s across trials ± sem). The first histogram pair (on the left) shows the responses to the two objects measured throughout the trial whenever object 1 or object 2 was on the screen. The second histogram pair shows the neuronal responses when the objects were being shown in stage 3 as the recall cue. The third histogram pair shows the neuronal responses in the 0.5 s delay period after one of the objects had been shown in stage 3 as the recall cue. The neuron continued to respond more after object 1 than after object 2 had been seen, in this recall period in which the place was being recalled from the object. The fourth histogram pair shows the neuronal responses in stage 4 when the macaque was recalling and touching the place at which the cue recall object had been shown. The responses of the neuron were object-related even when the object was not being seen, but was being used as a recall cue, in the delay after stage 3 of the task, and in stage 4. $^{**}p < 0.01$; $^{*}p < 0.05$ [After Rolls and Xiang (2006)].

combinations of objects and places, e.g., to object 1 when it was shown in place 1, but not to other combinations.

The recording sites of the object and of the place neurons were within the hippocampus proper (Rolls and Xiang, 2006). The mean firing rate of the population of responsive neurons (see **Table 1**) to the most effective object or place was 7.2 ± 0.6 spikes/s (±sem), and their mean spontaneous rate was 3.2 ± 0.6 spikes/s.

These findings (Rolls and Xiang, 2006) are the first we know in the primate hippocampus of neuronal activity that is related to recall. It is particularly interesting that the neurons with continuing activity to the object after it had disappeared in the recall phase of the task could reflect the operation of the object-place recall process that is hypothesized to take place in the CA3 cells. By continuing to respond to the object while the place is being recalled in the task, the object-related neurons could be part of the completion of the whole object-place combination memory from an autoassociation or attractor process in CA3 (Rolls and Kesner, 2006). Consistent with these findings, and with the computational theory, it has now been reported that human hippocampal neurons are activated during recall (Gelbard-Sagiv et al., 2008).

The neurons with recall-related activity in the object-place recall task also provide neurophysiological evidence on the speed of association learning in the hippocampal formation. Given that this is a one-trial object-place recall task, with the association between the object and its place being made in stages 1 and 2 of each trial (see **Figure 5**), it is clear that it takes just one-trial for the object-place associations to be formed that are relevant to the later recall on that trial. This is the speed of learning that is required for episodic memory, and this neurophysiological evidence shows that this type of rapid, one-trial, object-place learning is represented in the primate hippocampus.

REWARD-PLACE NEURONS IN THE PRIMATE HIPPOCAMPUS

The primate anterior hippocampus (which corresponds to the rodent ventral hippocampus) receives inputs from brain regions involved in reward processing such as the amygdala and orbitofrontal cortex (Pitkanen et al., 2002). To investigate how this affective input may be incorporated into primate hippocampal function, Rolls and Xiang (2005) recorded neuronal activity while macaques performed a reward-place association task in which each spatial scene shown on a video monitor had one location which if touched yielded a preferred fruit juice reward, and a second location which yielded a less preferred juice reward. Each scene had different locations for the different rewards. Of 312 hippocampal neurons analyzed, 18% responded more to the location of the preferred reward in different scenes, and 5% to the location of the less preferred reward (Rolls and Xiang, 2005). When the locations of the preferred rewards in the scenes were reversed, 60% of 44 neurons tested reversed the location to which they responded, showing that the reward-place associations could be altered by new learning in a few trials. The majority (82%) of these 44 hippocampal reward-place neurons tested did not respond to object-reward associations in a visual discrimination object-reward association task. Thus, the primate hippocampus

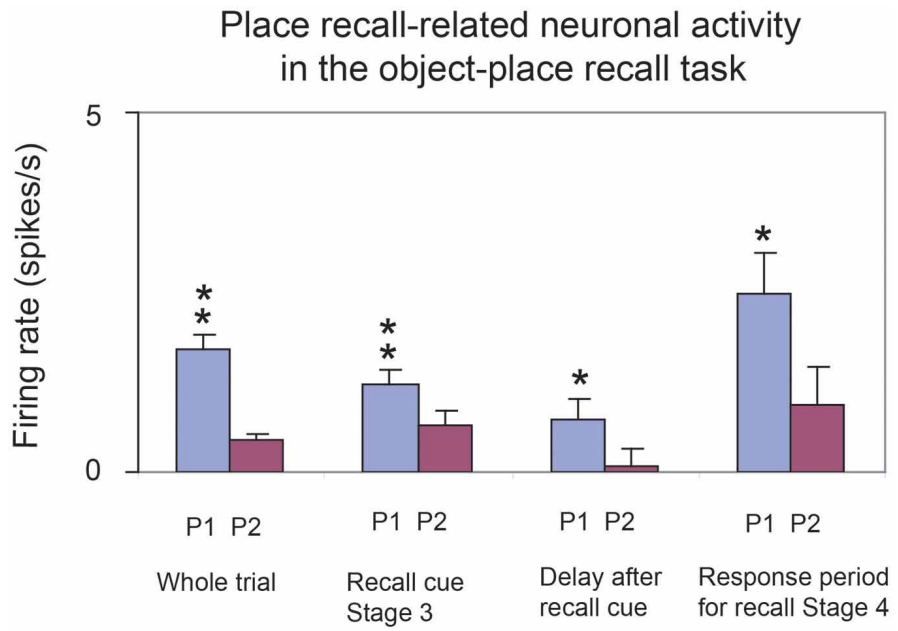

FIGURE 7 | Activity of a neuron with responses related to the left place (P1) in the object-place recall task. The firing rate to place 1 (P1) and place 2 (P2) are shown (mean firing rate in spikes/s across trials ± sem). The first histogram pair (on the left) shows the responses to the two places measured when a stimulus was on the screen in stage 1 or stage 2. The second histogram pair shows the neuronal responses when the objects were being shown in stage 3 as the recall cue, and depending on whether the place to be recalled was place 1 or place 2. The third histogram pair shows the neuronal responses in the 0.5 s delay period after one of the objects had been shown in stage 3 as the recall cue. The neuron responded more when place 1 was the correct place to be recalled on a trial. The fourth histogram pair shows the neuronal responses in stage 4 when the macaque was recalling and touching the place at which the cue recall object had been shown. The responses of the neuron were place-related even in stage 3 when the object being shown as a place recall cue was at the top of the screen, in the delay after stage 3 of the task, and in stage 4. $^{**}p < 0.01$; $^{*}p < 0.05$ [After Rolls and Xiang (2006)]. (recallplace2.eps).

contains a representation of the reward associations of places "out there" being viewed, and this is a way in which affective information can be stored as part of an episodic memory, and how the current mood state may influence the retrieval of episodic memories. There is consistent evidence that rewards available in a spatial environment can influence the responsiveness of rodent place neurons (Hölscher et al., 2003; Tabuchi et al., 2003).

TESTS OF THE THEORY

DENTATE GRANULE CELLS

The theory predicts that the dentate granule cell MF system of inputs to the CA3 neurons is necessary to store spatial memories, but not to recall them. Lassalle et al. (2000) have obtained evidence consistent with this in rats with damage to the MF system (Lassalle et al., 2000), and there is further evidence consistent with this (Lee and Kesner, 2004; Rolls and Kesner, 2006; Daumas et al., 2009).

The theory predicts that pattern separation is performed by the dentate granule cells. Evidence consistent with this has been found neurophysiologically in the small sparsely encoded place fields of dentate neurons (Jung and McNaughton, 1993; Leutgeb and Leutgeb, 2007) and their reflection in CA3 neurons (Leutgeb and Leutgeb, 2007). It has been shown that selective dentate lesions in rats (Gilbert et al., 2001; Gilbert and Kesner, 2003; Rolls and Kesner, 2006; Goodrich-Hunsaker et al., 2008; Rolls, 2008; Hunsaker and Kesner, 2013; Kesner, 2013) or dentate NMDA receptor knockouts in mice (McHugh et al., 2007) impair spatial, object-place (or reward-place: remembering where to find a reward) association tasks especially when the places are close together and require pattern separation before storage in CA3.

If adult neurogenesis in the DG does prove to be functionally relevant, its computational role could be to facilitate pattern separation for new patterns, by providing new dentate granule cells with new sets of random connections to CA3 neurons. Consistent with the dentate spatial pattern separation hypothesis (Rolls, 1989b,c; Treves and Rolls, 1992, 1994; Rolls, 1996b), in mice with impaired dentate neurogenesis, spatial learning in a delayed non-matching-to-place task in the radial arm maze was impaired for arms that were presented with little separation, but no deficit was observed when the arms were presented farther apart (Clelland et al., 2009). Consistently, impaired neurogenesis in the dentate also produced a deficit for small spatial separations in an associative object-in-place task (Clelland et al., 2009).

The theory predicts that the direct pp input from the entorhinal cortex to the CA3 cells (which bypasses the dentate granule cells) is involved in the recall of memory from the CA3 system, and Lee and Kesner (2004) have obtained evidence consistent with this in a Hebb–Williams maze recall task (Lee and Kesner, 2004).

Table 1 | Numbers of neurons in the hippocampus with different types of response during the object-place recall task.

Object with activity continuing after the recall cue	16
Object with activity not continuing after the recall cue	6
Place with activity during and after the recall cue	13
Place with activity during the recall cue	5
Object × Place	3
Total	347

CA3

The theory predicts that the CA3 is especially important in object-place or reward-place tasks in which associations must be formed between any spatial location and any object (referred to as **arbitrary associations**). There is much evidence from subregion analyses involving disruption of CA3 that CA3 is necessary for arbitrary associations between places and objects or rewards (Gilbert and Kesner, 2003; Rolls and Kesner, 2006). Similar impairments were obtained following deletion of CA3 NMDA receptors in mice in the acquisition of an odor-context paired associate learning task (Rajji et al., 2006). If place or time is not a component, associative tasks such as odor-object association are not impaired (Rolls and Kesner, 2006), underlining the fact that the hippocampus is especially involved in episodic types of associative memory which typically involve place and/or time.

The theory predicts that the CA3 is especially important in object-place or reward-place **completion** tasks, in which associations must be completed from a part of the whole. It has been shown that if completion from an incomplete cue is needed, then CA3 NMDA receptors are necessary (presumably to ensure satisfactory CA3-CA3 learning) even in a reference memory task (Nakazawa et al., 2002; Gold and Kesner, 2005).

The theory predicts that the CA3 system is especially needed in **rapid, one-trial object-place, learning, and recall**. It has been shown that hippocampal NMDA receptors (necessary for Long-Term Potentiation to occur) are needed for one-trial flavor-place association learning, and that hippocampal AMPA/kainate receptors are sufficient for the recall, though the hippocampal subregion involved was not tested (Day et al., 2003). In subregion studies, Kesner and colleagues have shown that CA3 lesions produce chance performance on a one-trial object-place recall task (Kesner et al., 2008) and other object-spatial tasks (Kesner and Rolls, 2001; Rolls and Kesner, 2006). For example, CA3 lesions produced chance performance on both a one-trial object-place recall and place-object recall task (Kesner et al., 2008). This is evidence that CA3 supports arbitrary associations as well as episodic memory based on 1-trial learning. A control fixed visual conditional to place task with the same delay was not impaired, showing that it is recall after one-trial (or rapid, episodic) learning that is impaired (Kesner et al., 2008). CA3 NMDA receptors are as predicted by the theory necessary for rapid/one-trial spatial learning, as shown by a mouse knockout study by Nakazawa and colleagues (Nakazawa et al., 2003, 2004; Tonegawa et al., 2003). As described in section Systems-Level Neurophysiology of the Primate Hippocampus, we have shown that hippocampal CA3 neurons reflect the computational processes necessary for one-trial object-place event memory, used as a model for episodic memory (Rolls and Xiang, 2006).

Another type of test of the autoassociation (or attractor) hypothesis for CA3 has been to train rats in different environments, e.g., a square and a circular environment, and then test the prediction of the hypothesis that when presented with an environment ambiguous between these, that hippocampoal neurons will fall in an attractor state that represents one of the two previously learned environments, but not a mixture of the two environments. Evidence consistent with the hypothesis has been found (Wills et al., 2005). In a particularly dramatic example, it has been found that within each theta cycle, hippocampal pyramidal neurons may represent one or other of the learned environments (Jezek et al., 2011). This is an indication, predicted by Rolls and Treves (1998), that autoassociative memory recall can take place sufficiently rapidly to be complete within one theta cycle (120 ms), and that theta cycles could provide a mechanism for a fresh retrieval process to occur after a reset caused by the inhibitory part of each theta cycle, so that the memory can be updated rapidly to reflect a continuously changing environment, and not remain too long in an attractor state.

The theory predicts that if primates including humans can form an episodic memory in which objects or people are seen at particular locations even though the observer viewing the space has never been to those locations "out there" in space, there should be a neural system in CA3 that can support such associations between places "out there" in a scene and objects. Exactly this is provided by the spatial view neurons Rolls and colleagues have discovered that are present in CA3 (Rolls et al., 1997a, 1998, 2005; Robertson et al., 1998; Georges-François et al., 1999; Rolls and Xiang, 2005, 2006). Place cells will not do for this type of episodic memory.

Many further tests of the theory are described elsewhere (Rolls and Kesner, 2006; Rolls, 2008; Kesner et al., 2012).

RECALL VIA CA1 TO NEOCORTEX

The theory shows quantitatively, analytically, how memories could be retrieved from the hippocampus to the neocortex (Treves and Rolls, 1994), and this has been shown by simulation of the multistage hippocampal system including the entorhinal cortex, dentate, CA3, CA1, and return to the entorhinal cortex to recall the memory to be quantitatively realistic (Rolls, 1995).

Many further tests of the theory are described elsewhere (Rolls and Kesner, 2006; Rolls, 2008, 2010b; Kesner et al., 2012).

DISCUSSION

The present theory holds that the hippocampus is used for the formation of episodic memories using autoassociation. This function is often necessary for successful spatial computation, but is not itself spatial computation. Instead, I believe that spatial computation is more likely to be performed in the neocortex (utilizing information if necessary for the particular task recalled from the hippocampus). Consistent with this view, hippocampal damage impairs the ability to learn new environments but not to perform spatial computations such as finding one's way to a place in a familiar environment, whereas damage to the parietal cortex and parahippocampal cortex can lead to problems such as

topographical and other spatial agnosias, in humans (see Kolb and Whishaw, 2003). This is consistent with spatial computations normally being performed in the neocortex. [In monkeys, there is evidence for a role of the parietal cortex in allocentric spatial computation. For example, monkeys with parietal cortex lesions are impaired at performing a landmark task, in which the object to be chosen is signified by the proximity to it of a "landmark" (another object; Ungerleider and Mishkin, 1982)].

A key aspect of the hippocampal theory, which relates it very closely to episodic memory, is that the hippocampal system has the dentate granule to MF to CA3 cell system, which with its sparse connectivity (46 synapses onto each CA3 neuron) has a randomizing effect on the representations set up in CA3, so that they are as different as possible from each other; and that this then enables each associative memory formed in the CA3 recurrent collaterals to be as different as possible from all the other event memories (see section Dentate Granule Cells). This is then the optimal situation for the CA3 recurrent collateral effect to operate, for it can then associate together the random set of neurons that are active for a particular event (for example an object in a particular place), and later recall the whole set from any part. It is because the representations in CA3 are unstructured, or random, in this way that large numbers of memories can be stored in the CA3 autoassociation system, and that interference between the different memories is kept as low as possible, in that they are maximally different from each other. This is the essence of the hippocampus as a memory system suitable for unstructured memories such as event or episodic memories, each of which should be kept as distinct from the others as possible.

In this theory, the entorhinal cortex grid cell to dentate/CA3 place cell transformation that can be achieved by competitive learning (Rolls et al., 2006) is necessary so that a sparse representation of a place with different representations for different places suitable for association with an object or reward can be made available for CA3. The grid cell representation does not have this property, in that the representations of different places by grid cells are too highly correlated to be useful in an associative memory (Rolls, 2008). The utility of the entorhinal grid cell system is likely to be its role in path integration (McNaughton et al., 2006): in the idiothetic (self-motion) update of location, where the location is represented as a series of ring attractors of different spatial sizes, with no beginning and no end to each ring continuous attractor. Because a ring is endless, and the packet of activity just keeps going round the ring as locomotion continues, the system can perform path integration beyond any known environment, and in the dark, where the spatial environmental cues are not known or cannot be seen, so allowing for example return to base.

Once place cell representations have been set up in the hippocampus, they form a continuous spatial attractor network because of associative synaptic modification during locomotion producing synapses that are stronger the nearer together two places are, and thus the more likely coactivity between CA3 pyramidal cells is (Stringer et al., 2002a, 2004, 2005; Stringer and Rolls, 2006; Rolls, 2008). Although this is a continuous representation, as it has to be because space is continuous, it is suitable for association with the representations of objects, which are discrete, to form an episodic memory (Rolls et al., 2002). An important property of this spatial system is that there can be many separate maps, or charts, each of a different environment, stored in the hippocampus (Battaglia and Treves, 1998), as each chart has low correlations with any other chart, due in part to the randomizing effect of the MFs. The essential property of the hippocampal CA3 system then may be that it is not specialized to perform the computations necessary for spatial navigation (McNaughton et al., 1991; O'Keefe, 1991; Burgess and O'Keefe, 1996; McNaughton et al., 1996), but instead is a memory system that inevitably contains some continuous representations of space because places, landmarks, etc., are being encoded as part of an episodic memory system, and space is inherently continuous. Having said this, the hippocampus according to the present (Rolls') theory does form memories of where objects, people, rewards, etc., have been found in space, and so may be useful when one is looking for a particular object or reward, for the place can be recalled from the hippocampal representation. Once recalled to the neocortex, the place may then be used in a neocortically organized system to enable actions to be performed to reach a place, which could involve spatial navigation, using landmark or body centered algorithms, but also actions such as getting on a boat or bus, taking a plane, etc.

The hippocampus is the only part of the brain I know with the type of sparse connectivity implemented in the MF to CA3 synaptic connections to set up randomly different representations. It sets up a fascinating comparison with the neocortex. In the neocortex, the connectivity is set up to emphasize feedforward connectivity from one area to the next that has large numbers of connections onto each neuron, in the order of several thousand. This enables the neocortex to form representations by competitive learning that represent combinations of the "features" present at an earlier stage, and which are separated apart in the space. Such a process operating over several stages of a hierarchy enables representations of different objects to be formed. Here the representations are not arbitrarily and randomly different, as in CA3, but instead represent converge of information over large information spaces (using many synapses onto each neuron) that together enables an object to be "diagnosed," that is, represented, as in Rolls' theory of invariant visual object recognition in the ventral cortical visual stream (Rolls, 1992, 2008, 2009, 2012c; Wallis and Rolls, 1997; Rolls and Stringer, 2006). In the neocortical system the local recurrent collateral connections between nearby cortical pyramidal cells play a largely different role to that in the hippocampal theory. In the neocortex they implement short-term memory which provides the basis for planning and attention; and decision-making including categorization (Rolls, 2008; Rolls and Deco, 2010).

A theory closely related to the present theory of how the hippocampus operates has been developed by McClelland et al. (1995). It is very similar to the theory we have developed (Rolls, 1987, 1989a,b,c, 2008, 2010b; Treves and Rolls, 1992, 1994) at the systems level, except that it takes a stronger position on the gradient of retrograde amnesia, emphasizes that recall from the hippocampus of episodic information is used to help build semantic representations in the neocortex, and holds that the last set of synapses that are modified rapidly during the learning of

each episode are those between the CA3 and the CA1 pyramidal cells, as described above (see **Figure 1**). It also emphasizes the important point that the hippocampal and neocortical memory systems may be quite different, with the hippocampus specialized for the rapid learning of single events or episodes, and the neocortex for the slower learning of semantic representations which may necessarily benefit from the many exemplars needed to shape the semantic representation.

We have developed an approach to the mechanisms of schizophrenia based on the stability of neuronal systems with stochastic dynamics (Loh et al., 2007; Rolls et al., 2008a; Rolls and Deco, 2011; Rolls, 2012b). The cognitive symptoms such as a failure to maintain attention are related to a decrease in the stability of prefrontal cortical networks related to lower firing rates produced by NMDA receptor down-regulation. The negative symptoms such as reduced emotion, motivation, and hedonia are related to a decrease in the firing rates of orbitofrontal cortex and related networks produced by NMDA receptor down-regulation. The positive symptoms of schizophrenia include bizarre trains of thoughts, hallucinations, and delusions (Liddle, 1987; Mueser and McGurk, 2004). Rolls et al. propose that owing to reduced currents through NMDAR-activated channels, the basins of attraction of the high-firing-rate attractor states are shallow (Rolls, 2005; Durstewitz, 2007; Loh et al., 2007) in the temporal lobe, which includes the semantic memory networks and the auditory association cortex. Because of the resulting statistical fluctuations in the states of the attractor networks, internal representations of thoughts and perceptions move too freely around in the energy landscape, from thought to weakly associated thought, leading to bizarre thoughts and associations, and to hallucinations. Such thoughts might eventually be associated together in semantic memory, leading to false beliefs and delusions (Rolls, 2005, 2008, 2012b).

In addition, Loh et al. (2007) propose that a reduction in GABA interneuron efficacy in schizophrenic patients may also contribute to the generation of positive symptoms: lower GABA-interneuron efficacy reduces the depth of the basin of attraction of the spontaneous state, making it more likely that a high firing-rate attractor state will emerge out of the spontaneous firing of the neurons. This type of instability in which a network jumps because of noise into a high firing rate state that is not triggered by an external input to the network contributes it is suggested to the positive symptoms of schizophrenia, including for example hallucinations, delusions, and feelings of lack of control or being controlled by others (Loh et al., 2007; Rolls et al., 2008a; Rolls, 2012b). Empirical evidence supports this computational proposal: markers indicating decreased inhibition by the GABA system are found in neocortical areas (Lewis et al., 2005) and in parts of the hippocampus (Benes, 2010).

In this paper we have thus seen that there is neurophysiological evidence that different representations of the type important in episodic memory, including object and place, and reward and place, are brought together in the primate hippocampus, and even that the whole representation can be completed from a partial retrieval cue in a one-trial object-place memory task. It appears to be a property of the hippocampus that it is involved in associations when one of the associates is place or time (Rolls and Kesner, 2006; Rolls, 2008; Rolls and Deco, 2010). We have moreover seen that the representation of space in the primate hippocampus provided by spatial view cells is appropriate for episodic memory in primates including humans, for it is a representation of space "out there," which is prototypical of the spatial representation that is involved in episodic memory in primates including humans. We have also described and updated a theory of how the hippocampal system could implement episodic memory (Rolls, 1987, 1989a,b,c, 1990a,b, 1991, 1995, 1996b, 2008, 2010b; Treves and Rolls, 1991, 1992, 1994; Rolls and Treves, 1998; Rolls and Kesner, 2006; Rolls and Deco, 2010), and shown how there is now considerable empirical support for the theory (Rolls and Kesner, 2006; Rolls, 2008; Kesner et al., 2012; Rolls, 2012b).

ACKNOWLEDGMENTS

Different parts of the research described here were supported by Programme Grants from the Medical Research Council; by a Human Frontier Science program grant; by an EEC BRAIN grant; by the MRC Oxford Interdisciplinary Research Centre in Cognitive Neuroscience; by the Oxford McDonnell-Pew Centre in Cognitive Neuroscience; and by the Oxford Centre for Computational Neuroscience. The author has performed the experimental and theoretical work which is incorporated in some of the ideas presented here on the hippocampus with many colleagues, including Alessandro Treves, Simon Stringer, Ray Kesner, Robert Robertson, Pierre Georges-François, Shane O'Mara, and Alain Berthoz, and their contributions are sincerely acknowledged. Pdfs of some of the papers cited are available at www.oxcns.org.

REFERENCES

Acsady, L., Kamondi, A., Sik, A., Freund, T., and Buzsaki, G. (1998). GABAergic cells are the major postsynaptic targets of mossy fibers in the rat hippocampus. *J. Neurosci.* 18, 3386–3403.

Aggelopoulos, N. C., and Rolls, E. T. (2005). Natural scene perception: inferior temporal cortex neurons encode the positions of different objects in the scene. *Eur. J. Neurosci.* 22, 2903–2916. doi: 10.1111/j.1460-9568.2005.04487.x

Amaral, D. G. (1987). "Memory: anatomical organization of candidate brain regions," in *Handbook of Physiology. Section 1, The Nervous System,* ed V. B. Mountcastle (Washington, DC: American Physiological Society), 211–294.

Amaral, D. G. (1993). Emerging principles of intrinsic hippocampal organisation. *Curr. Opin. Neurobiol.* 3, 225–229. doi: 10.1016/0959-4388(93)90214-J

Amaral, D. G., Ishizuka, N., and Claiborne, B. (1990). Neurons, numbers and the hippocampal network. *Prog. Brain Res.* 83, 1–11. doi: 10.1016/S0079-6123(08)61237-6

Amaral, D. G., Price, J. L., Pitkanen, A., and Carmichael, S. T. (1992). "Anatomical organization of the primate amygdaloid complex," in *The Amygdala,* ed J. P. Aggleton (New York, NY: Wiley-Liss), 1–66.

Amaral, D. G., and Witter, M. P. (1989). The three-dimensional organization of the hippocampal formation: a review of anatomical data. *Neuroscience* 31, 571–591. doi: 10.1016/0306-4522(89)90424-7

Amaral, D. G., and Witter, M. P. (1995). "The hippocampal formation," in *The Rat Nervous System,* ed G. Paxinos (San Diego, CA: Academic Press), 443–493.

Amari, S. (1977). Dynamics of pattern formation in lateral-inhibition type neural fields. *Biol. Cybern.* 27, 77–87. doi: 10.1007/BF00337259

Amit, D. J. (1989). *Modeling Brain Function.* Cambridge: Cambridge University Press.

Amit, D. J., and Brunel, N. (1997). Model of global spontaneous activity and local structured activity during delay periods in the cerebral cortex. *Cereb. Cortex* 7, 237–252. doi: 10.1093/cercor/7.3.237

Andersen, P., Morris, R. G. M., Amaral, D. G., Bliss, T. V. P., and O'keefe, J. (2007). *The Hippocampus Book*. London: Oxford University Press.

Barkas, L. J., Henderson, J. L., Hamilton, D. A., Redhead, E. S., and Gray, W. P. (2010). Selective temporal resections and spatial memory impairment: cue dependent lateralization effects. *Behav. Brain Res.* 208, 535–544. doi: 10.1016/j.bbr.2009.12.035

Battaglia, F. P., and Treves, A. (1998). Attractor neural networks storing multiple space representations: a model for hippocampal place fields. *Phys. Rev. E* 58, 7738–7753. doi: 10.1103/PhysRevE.58.7738

Benes, F. M. (2010). Amygdalocortical circuitry in schizophrenia: from circuits to molecules. *Neuropsychopharmacology* 35, 239–257. doi: 10.1038/npp.2009.116

Bonelli, S. B., Powell, R. H., Yogarajah, M., Samson, R. S., Symms, M. R., Thompson, P. J., et al. (2010). Imaging memory in temporal lobe epilepsy: predicting the effects of temporal lobe resection. *Brain* 133, 1186–1199. doi: 10.1093/brain/awq006

Brown, T. H., Ganong, A. H., Kairiss, E. W., Keenan, C. L., and Kelso, S. R. (eds.). (1989). *Long-Term Potentiation in Two Synaptic Systems of the Hippocampal Brain Slice*. San Diego, CA: Academic Press.

Brown, T. H., Kairiss, E. W., and Keenan, C. L. (1990). Hebbian synapses: biophysical mechanisms and algorithms. *Annu. Rev. Neurosci.* 13, 475–511. doi: 10.1146/annurev.ne.13.030190.002355

Brun, V. H., Otnass, M. K., Molden, S., Steffenach, H. A., Witter, M. P., Moser, M. B., et al. (2002). Place cells and place recognition maintained by direct entorhinal-hippocampal circuitry. *Science* 296, 2243–2246. doi: 10.1126/science.1071089

Burgess, N., and O'Keefe, J. (1996). Neuronal computations underlying the firing of place cells and their role in navigation. *Hippocampus* 6, 749–762.

Carmichael, S. T., and Price, J. L. (1995). Limbic connections of the orbital and medial prefrontal cortex in macaque monkeys. *J. Comp. Neurol.* 346, 403–434. doi: 10.1002/cne.903460306

Cerasti, E., and Treves, A. (2010). How informative are spatial CA3 representations established by the dentate gyrus. *PLoS Comput. Biol.* 6:e1000759. doi: 10.1371/journal.pcbi.1000759

Cerasti, E., and Treves, A. (2013). The spatial representations acquired in CA3 by self-organizing recurrent connections. *Front. Cell. Neurosci.*

Cheng, S. (2013). The CRISP theory of hippocampal function in episodic memory. *Front. Neural Circuits* 7:88. doi: 10.3389/fncir.2013.00088

Clelland, C. D., Choi, M., Romberg, C., Clemenson, G. D. Jr., Fragniere, A., Tyers, P., et al. (2009). A functional role for adult hippocampal neurogenesis in spatial pattern separation. *Science* 325, 210–213. doi: 10.1126/science.1173215

Daumas, S., Ceccom, J., Halley, H., Frances, B., and Lassalle, J. M. (2009). Activation of metabotropic glutamate receptor type 2/3 supports the involvement of the hippocampal mossy fiber pathway on contextual fear memory consolidation. *Learn. Mem.* 16, 504–507. doi: 10.1101/lm.1418309

Day, M., Langston, R., and Morris, R. G. (2003). Glutamate-receptor-mediated encoding and retrieval of paired-associate learning. *Nature* 424, 205–209. doi: 10.1038/nature01769

De Araujo, I. E. T., Rolls, E. T., and Stringer, S. M. (2001). A view model which accounts for the spatial fields of hippocampal primate spatial view cells and rat place cells. *Hippocampus* 11, 699–706. doi: 10.1002/hipo.1085

Deco, G., Ledberg, A., Almeida, R., and Fuster, J. (2005). Neural dynamics of cross-modal and cross-temporal associations. *Exp. Brain Res.* 166, 325–336. doi: 10.1007/s00221-005-2374-y

Deco, G., and Rolls, E. T. (2003). Attention and working memory: a dynamical model of neuronal activity in the prefrontal cortex. *Eur. J. Neurosci.* 18, 2374–2390. doi: 10.1046/j.1460-9568.2003.02956.x

Deco, G., and Rolls, E. T. (2005). Sequential memory: a putative neural and synaptic dynamical mechanism. *J. Cogn. Neurosci.* 17, 294–307. doi: 10.1162/0898929053124875

Deco, G., and Rolls, E. T. (2006). Decision-making and Weber's Law: a neurophysiological model. *Eur. J. Neurosci.* 24, 901–916. doi: 10.1111/j.1460-9568.2006.04940.x

Deco, G., Rolls, E. T., Albantakis, L., and Romo, R. (2013). Brain mechanisms for perceptual and reward-related decision-making. *Prog. Neurobiol.* 103, 194–213. doi: 10.1016/j.pneurobio.2012.01.010

Delatour, B., and Witter, M. P. (2002). Projections from the parahippocampal region to the prefrontal cortex in the rat: evidence of multiple pathways. *Eur. J. Neurosci.* 15, 1400–1407. doi: 10.1046/j.1460-9568.2002.01973.x

Dere, E., Easton, A., Nadel, L., and Huston, J. P. (eds.). (2008). *Handbook of Episodic Memory*. Amsterdam: Elsevier.

Durstewitz, D. (2007). "Dopaminergic modulation of prefrontal cortex network dynamics," in *Monoaminergic Modulation of Cortical Excitability,* eds K.-Y. Tseng and M. Atzori (New York, NY: Springer), 217–234. doi: 10.1007/978-0-387-72256-6_15

Faisal, A. A., Selen, L. P., and Wolpert, D. M. (2008). Noise in the nervous system. *Nat. Rev. Neurosci.* 9, 292–303. doi: 10.1038/nrn2258

Fazeli, M. S., and Collingridge, G. L. (eds.). (1996). *Cortical Plasticity: LTP and LTD*. Oxford: Bios.

Feigenbaum, J. D., and Rolls, E. T. (1991). Allocentric and egocentric spatial information processing in the hippocampal formation of the behaving primate. *Psychobiology* 19, 21–40.

Florian, C., and Roullet, P. (2004). Hippocampal CA3-region is crucial for acquisition and memory consolidation in Morris water maze task in mice. *Behav. Brain Res.* 154, 365–374. doi: 10.1016/j.bbr.2004.03.003

Franco, L., Rolls, E. T., Aggelopoulos, N. C., and Jerez, J. M. (2007). Neuronal selectivity, population sparseness, and ergodicity in the inferior temporal visual cortex. *Biol. Cybern.* 96, 547–560. doi: 10.1007/s00422-007-0149-1

Fyhn, M., Molden, S., Witter, M. P., Moser, E. I., and Moser, M. B. (2004). Spatial representation in the entorhinal cortex. *Science* 305, 1258–1264. doi: 10.1126/science.1099901

Gelbard-Sagiv, H., Mukamel, R., Harel, M., Malach, R., and Fried, I. (2008). Internally generated reactivation of single neurons in human hippocampus during free recall. *Science* 322, 96–101. doi: 10.1126/science.1164685

Georges-François, P., Rolls, E. T., and Robertson, R. G. (1999). Spatial view cells in the primate hippocampus: allocentric view not head direction or eye position or place. *Cereb. Cortex* 9, 197–212. doi: 10.1093/cercor/9.3.197

Gilbert, P. E., and Kesner, R. P. (2003). Localization of function within the dorsal hippocampus: the role of the CA3 subregion in paired-associate learning. *Behav. Neurosci.* 117, 1385–1394. doi: 10.1037/0735-7044.117.6.1385

Gilbert, P. E., Kesner, R. P., and Lee, I. (2001). Dissociating hippocampal subregions: double dissociation between dentate gyrus and CA1. *Hippocampus* 11, 626–636. doi: 10.1002/hipo.1077

Giocomo, L. M., and Hasselmo, M. E. (2007). Neuromodulation by glutamate and acetylcholine can change circuit dynamics by regulating the relative influence of afferent input and excitatory feedback. *Mol. Neurobiol.* 36, 184–200. doi: 10.1007/s12035-007-0032-z

Giocomo, L. M., Moser, M. B., and Moser, E. I. (2011). Computational models of grid cells. *Neuron* 71, 589–603. doi: 10.1016/j.neuron.2011.07.023

Gold, A. E., and Kesner, R. P. (2005). The role of the CA3 subregion of the dorsal hippocampus in spatial pattern completion in the rat. *Hippocampus* 15, 808–814. doi: 10.1002/hipo.20103

Goodrich-Hunsaker, N. J., Hunsaker, M. R., and Kesner, R. P. (2008). The interactions and dissociations of the dorsal hippocampus subregions: how the dentate gyrus, CA3, and CA1 process spatial information. *Behav. Neurosci.* 122, 16–26. doi: 10.1037/0735-7044.122.1.16

Hafting, T., Fyhn, M., Molden, S., Moser, M. B., and Moser, E. I. (2005). Microstructure of a spatial map in the entorhinal cortex. *Nature* 436, 801–806. doi: 10.1038/nature03721

Hasselmo, M. E., Schnell, E., and Barkai, E. (1995). Dynamics of learning and recall at excitatory recurrent synapses and cholinergic modulation in rat hippocampal region CA3. *J. Neurosci.* 15, 5249–5262.

Henze, D. A., Wittner, L., and Buzsaki, G. (2002). Single granule cells reliably discharge targets in the hippocampal CA3 network in vivo. *Nat. Neurosci.* 5, 790–795. doi: 10.1038/nn887

Hertz, J., Krogh, A., and Palmer, R. G. (1991). *An Introduction to the Theory of Neural Computation*. Wokingham: Addison-Wesley.

Hoge, J., and Kesner, R. P. (2007). Role of CA3 and CA1 subregions of the dorsal hippocampus on temporal processing of objects. *Neurobiol. Learn. Mem.* 88, 225–231. doi: 10.1016/j.nlm.2007.04.013

Hölscher, C., Jacob, W., and Mallot, H. A. (2003). Reward modulates neuronal activity in the hippocampus of the rat. *Behav. Brain Res.* 142, 181–191. doi: 10.1016/S0166-4328(02)00422-9

Hopfield, J. J. (1982). Neural networks and physical systems with emergent collective computational abilities. *Proc. Natl. Acad. Sci. U.S.A.* 79, 2554–2558. doi: 10.1073/pnas.79.8.2554

Hunsaker, M. R., and Kesner, R. P. (2013). The operation of pattern separation and pattern completion processes associated with different attributes or domains of memory. *Neurosci. Biobehav. Rev.* 37, 36–58. doi: 10.1016/j.neubiorev.2012.09.014

Hunsaker, M. R., Lee, B., and Kesner, R. P. (2008). Evaluating the temporal context of episodic memory: the role of CA3 and CA1. *Behav. Brain Res.* 188, 310–315. doi: 10.1016/j.bbr.2007.11.015

Ishizuka, N., Weber, J., and Amaral, D. G. (1990). Organization of intrahippocampal projections originating from CA3 pyramidal cells in the rat. *J. Comp. Neurol.* 295, 580–623. doi: 10.1002/cne.902950407

Itskov, P. M., Vinnik, E., and Diamond, M. E. (2011). Hippocampal representation of touch-guided behavior in rats: persistent and independent traces of stimulus and reward location. *PLos ONE* 6:e16462. doi: 10.1371/journal.pone.0016462

Jeffery, K. J., Anderson, M. I., Hayman, R., and Chakraborty, S. (2004). A proposed architecture for the neural representation of spatial context. *Neurosci. Biobehav. Rev.* 28, 201–218. doi: 10.1016/j.neubiorev.2003.12.002

Jeffery, K. J., and Hayman, R. (2004). Plasticity of the hippocampal place cell representation. *Rev. Neurosci.* 15, 309–331. doi: 10.1515/REVNEURO.2004.15.5.309

Jezek, K., Henriksen, E. J., Treves, A., Moser, E. I., and Moser, M.-B. (2011). Theta-paced flickering between place-cell maps in the hippocampus. *Nature* 278, 246–249. doi: 10.1038/nature10439

Jung, M. W., and McNaughton, B. L. (1993). Spatial selectivity of unit activity in the hippocampal granular layer. *Hippocampus* 3, 165–182. doi: 10.1002/hipo.450030209

Kesner, R. P. (2013). An analysis of the dentate gyrus function. *Behav. Brain Res*. doi: 10.1016/j.bbr.2013.01.012. [Epub ahead of print].

Kesner, R. P., Gilbert, P. E., and Barua, L. A. (2002). The role of the hippocampus in memory for the temporal order of a sequence of odors. *Behav. Neurosci.* 116, 286–290. doi: 10.1037/0735-7044.116.2.286

Kesner, R. P., Hunsaker, M. R., and Warthen, M. W. (2008). The CA3 subregion of the hippocampus is critical for episodic memory processing by means of relational encoding in rats. *Behav. Neurosci.* 122, 1217–1225. doi: 10.1037/a0013592

Kesner, R. P., Morris, A. M., and Weeden, C. S. S. (2012). "Spatial, temporal, and associative behavioral functions associated with different subregions of the hippocampus, Chapter 18," in *Oxford Handbook of Comparative Cognition,* eds T. R. Zentall and E. A. Wasserman (Oxford: Oxford University Press), 322–346.

Kesner, R. P., and Rolls, E. T. (2001). Role of long term synaptic modification in short term memory. *Hippocampus* 11, 240–250. doi: 10.1002/hipo.1040

Killian, N. J., Jutras, M. J., and Buffalo, E. A. (2012). A map of visual space in the primate entorhinal cortex. *Nature* 491, 761–764. doi: 10.1038/nature11587

Kolb, B., and Whishaw, I. Q. (2003). *Fundamentals of Human Neuropsychology*. New York, NY: Worth.

Kondo, H., Lavenex, P., and Amaral, D. G. (2009). Intrinsic connections of the macaque monkey hippocampal formation: II. CA3 connections. *J. Comp. Neurol.* 515, 349–377. doi: 10.1002/cne.22056

Kropff, E., and Treves, A. (2008). The emergence of grid cells: intelligent design or just adaptation. *Hippocampus* 18, 1256–1269. doi: 10.1002/hipo.20520

Lassalle, J. M., Bataille, T., and Halley, H. (2000). Reversible inactivation of the hippocampal mossy fiber synapses in mice impairs spatial learning, but neither consolidation nor memory retrieval, in the Morris navigation task. *Neurobiol. Learn. Mem.* 73, 243–257. doi: 10.1006/nlme.1999.3931

Lavenex, P., Suzuki, W. A., and Amaral, D. G. (2004). Perirhinal and parahippocampal cortices of the macaque monkey: intrinsic projections and interconnections. *J. Comp. Neurol.* 472, 371–394. doi: 10.1002/cne.20079

Lee, I., and Kesner, R. P. (2004). Encoding versus retrieval of spatial memory: double dissociation between the dentate gyrus and the perforant path inputs into CA3 in the dorsal hippocampus. *Hippocampus* 14, 66–76. doi: 10.1002/hipo.10167

Lehn, H., Steffenach, H. A., Van Strien, N. M., Veltman, D. J., Witter, M. P., and Haberg, A. K. (2009). A specific role of the human hippocampus in recall of temporal sequences. *J. Neurosci.* 29, 3475–3484. doi: 10.1523/JNEUROSCI.5370-08.2009

Leutgeb, J. K., Leutgeb, S., Moser, M. B., and Moser, E. I. (2007). Pattern separation in the dentate gyrus and CA3 of the hippocampus. *Science* 315, 961–966. doi: 10.1126/science.1135801

Leutgeb, S., and Leutgeb, J. K. (2007). Pattern separation, pattern completion, and new neuronal codes within a continuous CA3 map. *Learn. Mem.* 14, 745–757. doi: 10.1101/lm.703907

Levy, W. B. (1989). "A computational approach to hippocampal function," in *Computational Models of Learning in Simple Neural Systems,* eds R. D. Hawkins and G. H. Bower. (San Diego, CA: Academic Press), 243–305.

Lewis, D. A., Hashimoto, T., and Volk, D. W. (2005). Cortical inhibitory neurons and schizophrenia. *Nat. Rev. Neurosci.* 6, 312–324. doi: 10.1038/nrn1648

Liddle, P. F. (1987). The symptoms of chronic schizophrenia. A re-examination of the positive-negative dichotomy. *Br. J. Psychiatry* 151, 145–151. doi: 10.1192/bjp.151.2.145

Lisman, J., and Redish, A. D. (2009). Prediction, sequences and the hippocampus. *Philos. Trans. R. Soc. Lond. B Biol. Sci.* 364, 1193–1201. doi: 10.1098/rstb.2008.0316

Loh, M., Rolls, E. T., and Deco, G. (2007). A dynamical systems hypothesis of schizophrenia. *PLoS Comput. Biol.* 3:e228. doi: 10.1371/journal.pcbi.0030228

Lynch, M. A. (2004). Long-term potentiation and memory. *Physiol. Rev.* 84, 87–136. doi: 10.1152/physrev.00014.2003

MacDonald, C. J., Lepage, K. Q., Eden, U. T., and Eichenbaum, H. (2011). Hippocampal "time cells" bridge the gap in memory for discontiguous events. *Neuron* 71, 737–749. doi: 10.1016/j.neuron.2011.07.012

Marr, D. (1971). Simple memory: a theory for archicortex. *Philos. Trans. R. Soc. Lond. B Biol. Sci.* 262, 23–81. doi: 10.1098/rstb.1971.0078

McClelland, J. L., McNaughton, B. L., and O'Reilly, R. C. (1995). Why there are complementary learning systems in the hippocampus and neocortex: insights from the successes and failures of connectionist models of learning and memory. *Psychol. Rev.* 102, 419–457. doi: 10.1037/0033-295X.102.3.419

McHugh, T. J., Jones, M. W., Quinn, J. J., Balthasar, N., Coppari, R., Elmquist, J. K., et al. (2007). Dentate gyrus NMDA receptors mediate rapid pattern separation in the hippocampal network. *Science* 317, 94–99. doi: 10.1126/science.1140263

McNaughton, B. L. (1991). Associative pattern completion in hippocampal circuits: new evidence and new questions. *Brain Res. Rev.* 16, 193–220.

McNaughton, B. L., Barnes, C. A., Gerrard, J. L., Gothard, K., Jung, M. W., Knierim, J. J., et al. (1996). Deciphering the hippocampal polyglot: the hippocampus as a path integration system. *J. Exp. Biol.* 199, 173–185.

McNaughton, B. L., Barnes, C. A., and O'Keefe, J. (1983). The contributions of position, direction, and velocity to single unit activity in the hippocampus of freely-moving rats. *Exp. Brain Res.* 52, 41–49. doi: 10.1007/BF00237147

McNaughton, B. L., Battaglia, F. P., Jensen, O., Moser, E. I., and Moser, M.-B. (2006). Path integration and the neural basis of the 'cognitive map'. *Nat. Rev. Neurosci.* 7, 663–678. doi: 10.1038/nrn1932

McNaughton, B. L., Chen, L. L., and Markus, E. J. (1991). "Dead reckoning", landmark learning, and the sense of direction: a neurophysiological and computational hypothesis. *J. Cogn. Neurosci.* 3, 190–202. doi: 10.1162/jocn.1991.3.2.190

McNaughton, B. L., and Morris, R. G. M. (1987). Hippocampal synaptic enhancement and information storage within a distributed memory system. *Trends Neurosci.* 10, 408–415. doi: 10.1016/0166-2236(87)90011-7

McNaughton, B. L., and Nadel, L. (1990). "Hebb-Marr networks and the neurobiological representation of action in space," in *Neuroscience and Connectionist Theory,* eds M. A. Gluck and D. E. Rumelhart (Hillsdale, NJ: Erlbaum), 1–64.

Miller, G. A. (1956). The magic number seven, plus or minus two: some limits on our capacity for the processing of information. *Psychol. Rev.* 63, 81–93. doi: 10.1037/h0043158

Miller, P., and Wang, X. J. (2006). Inhibitory control by an integral feedback signal in prefrontal cortex: a model of discrimination between sequential stimuli. *Proc.*

Natl. Acad. Sci. U.S.A. 103, 201–206. doi: 10.1073/pnas.0508072103

Morris, R. G. (2003). Long-term potentiation and memory. *Philos. Trans. R. Soc. Lond. B Biol. Sci.* 358, 643–647. doi: 10.1098/rstb.2002.1230

Morris, R. G., Moser, E. I., Riedel, G., Martin, S. J., Sandin, J., Day, M., et al. (2003). Elements of a neurobiological theory of the hippocampus: the role of activity-dependent synaptic plasticity in memory. *Philos. Trans. R. Soc. Lond. B Biol. Sci.* 358, 773–786. doi: 10.1098/rstb.2002.1264

Morris, R. G. M. (1989). "Does synaptic plasticity play a role in information storage in the vertebrate brain?" in *Parallel Distributed Processing: Implications for Psychology and Neurobiology,* ed R. G. M. Morris (Oxford: Oxford University Press), 248–285.

Moscovitch, M., Rosenbaum, R. S., Gilboa, A., Addis, D. R., Westmacott, R., Grady, C., et al. (2005). Functional neuroanatomy of remote episodic, semantic and spatial memory: a unified account based on multiple trace theory. *J. Anat.* 207, 35–66. doi: 10.1111/j.1469-7580.2005.00421.x

Mueser, K. T., and McGurk, S. R. (2004). Schizophrenia. *Lancet* 363, 2063–2072. doi: 10.1016/S0140-6736(04)16458-1

Muller, R. U., Kubie, J. L., Bostock, E. M., Taube, J. S., and Quirk, G. J. (1991). "Spatial firing correlates of neurons in the hippocampal formation of freely moving rats," in *Brain and Space,* ed J. Paillard (Oxford: Oxford University Press), 296–333.

Naber, P. A., Lopes Da Silva, F. H., and Witter, M. P. (2001). Reciprocal connections between the entorhinal cortex and hippocampal fields CA1 and the subiculum are in register with the projections from CA1 to the subiculum. *Hippocampus* 11, 99–104. doi: 10.1002/hipo.1028

Nakazawa, K., McHugh, T. J., Wilson, M. A., and Tonegawa, S. (2004). NMDA receptors, place cells and hippocampal spatial memory. *Nat. Rev. Neurosci.* 5, 361–372. doi: 10.1038/nrn1385

Nakazawa, K., Quirk, M. C., Chitwood, R. A., Watanabe, M., Yeckel, M. F., Sun, L. D., et al. (2002). Requirement for hippocampal CA3 NMDA receptors in associative memory recall. *Science* 297, 211–218. doi: 10.1126/science.1071795

Nakazawa, K., Sun, L. D., Quirk, M. C., Rondi-Reig, L., Wilson, M. A., and Tonegawa, S. (2003). Hippocampal CA3 NMDA receptors are crucial for memory acquisition of one-time experience. *Neuron* 38, 305–315. doi: 10.1016/S0896-6273(03)00165-X

O'Keefe, J. (1979). A review of the hippocampal place cells. *Prog. Neurobiol.* 13, 419–439. doi: 10.1016/0301-0082(79)90005-4

O'Keefe, J. (1984). "Spatial memory within and without the hippocampal system," in *Neurobiology of the Hippocampus,* ed W. Seifert (London: Academic Press), 375–403.

O'Keefe, J. (1991). "The hippocampal cognitive map and navigational strategies," in *Brain and Space,* ed J. Paillard (Oxford: Oxford University Press), 273–295.

O'Keefe, J., and Nadel, L. (1978). *The Hippocampus as a Cognitive Map*. Oxford: Clarendon Press.

O'Keefe, J., and Speakman, A. (1987). Single unit activity in the rat hippocampus during a spatial memory task. *Exp. Brain Res.* 68, 1–27. doi: 10.1007/BF00255230

Pitkanen, A., Kelly, J. L., and Amaral, D. G. (2002). Projections from the lateral, basal, and accessory basal nuclei of the amygdala to the entorhinal cortex in the macaque monkey. *Hippocampus* 12, 186–205. doi: 10.1002/hipo.1099

Rajji, T., Chapman, D., Eichenbaum, H., and Greene, R. (2006). The role of CA3 hippocampal NMDA receptors in paired associate learning. *J. Neurosci.* 26, 908–915. doi: 10.1523/JNEUROSCI.4194-05.2006

Robertson, R. G., Rolls, E. T., and Georges-François, P. (1998). Spatial view cells in the primate hippocampus: effects of removal of view details. *J. Neurophysiol.* 79, 1145–1156.

Rolls, E. T. (1987). "Information representation, processing and storage in the brain: analysis at the single neuron level," in *The Neural and Molecular Bases of Learning,* eds J.-P. Changeux and M. Konishi (Chichester: Wiley), 503–540.

Rolls, E. T. (1989a). "Functions of neuronal networks in the hippocampus and cerebral cortex in memory," in *Models of Brain Function,* ed R. M. J. Cotterill (Cambridge: Cambridge University Press), 15–33.

Rolls, E. T. (1989b). "Functions of neuronal networks in the hippocampus and neocortex in memory," in *Neural Models of Plasticity: Experimental and Theoretical Approaches,* eds J. H. Byrne and W. O. Berry (San Diego, CA: Academic Press), 240–265.

Rolls, E. T. (1989c). "The representation and storage of information in neuronal networks in the primate cerebral cortex and hippocampus," in *The Computing Neuron,* eds R. Durbin, C. Miall, and G. Mitchison (Wokingham: Addison-Wesley), 125–159.

Rolls, E. T. (1990a). "Functions of the primate hippocampus in spatial processing and memory," in *Neurobiology of Comparative Cognition,* eds D. S. Olton and R. P. Kesner (Hillsdale, NJ: L.Erlbaum), 339–362.

Rolls, E. T. (1990b). Theoretical and neurophysiological analysis of the functions of the primate hippocampus in memory. *Cold Spring Harb. Symp. Quant. Biol.* 55, 995–1006. doi: 10.1101/SQB.1990.055.01.095

Rolls, E. T. (1991). Functions of the primate hippocampus in spatial and non-spatial memory. *Hippocampus* 1, 258–261. doi: 10.1002/hipo.450010310

Rolls, E. T. (1992). Neurophysiological mechanisms underlying face processing within and beyond the temporal cortical visual areas. *Philos. Trans. R. Soc. Lond. B Biol. Sci.* 335, 11–21. doi: 10.1098/rstb.1992.0002

Rolls, E. T. (1995). A model of the operation of the hippocampus and entorhinal cortex in memory. *Int. J. Neural Syst.* 6, 51–70.

Rolls, E. T. (1996a). "Roles of long term potentiation and long term depression in neuronal network operations in the brain," in *Cortical Plasticity,* eds M. S. Fazeli and G. L. Collingridge (Oxford: Bios), 223–250.

Rolls, E. T. (1996b). A theory of hippocampal function in memory. *Hippocampus* 6, 601–620.

Rolls, E. T. (1999). Spatial view cells and the representation of place in the primate hippocampus. *Hippocampus* 9, 467–480.

Rolls, E. T. (2005). *Emotion Explained*. Oxford: Oxford University Press. doi: 10.1093/acprof:oso/9780198570035.001.0001

Rolls, E. T. (2008). *Memory, Attention, and Decision-Making: A Unifying Computational Neuroscience Approach*. Oxford: Oxford University Press.

Rolls, E. T. (2009). "The neurophysiology and computational mechanisms of object representation," in *Object Categorization: Computer and Human Vision Perspectives,* eds S. Dickinson, M. Tarr, A. Leonardis, and B. Schiele (Cambridge: Cambridge University Press), 257–287. doi: 10.1017/CBO9780511635465.015

Rolls, E. T. (2010a). Attractor networks. *WIREs Cogn. Sci.* 1, 119–134.

Rolls, E. T. (2010b). A computational theory of episodic memory formation in the hippocampus. *Behav. Brain Res.* 205, 180–196. doi: 10.1016/j.bbr.2010.03.027

Rolls, E. T. (2012a). Advantages of dilution in the connectivity of attractor networks in the brain. *Biol. Inspired Cogn. Archit.* 1, 44–54.

Rolls, E. T. (2012b). Glutamate, obsessive-compulsive disorder, schizophrenia, and the stability of cortical attractor neuronal networks. *Pharmacol. Biochem. Behav.* 100, 736–751. doi: 10.1016/j.pbb.2011.06.017

Rolls, E. T. (2012c). Invariant visual object and face recognition: neural and computational bases, and a model, VisNet. *Front. Comput. Neurosci.* 6:35. doi: 10.3389/fncom.2012.00035

Rolls, E. T., and Deco, G. (2002). *Computational Neuroscience of Vision*. Oxford: Oxford University Press.

Rolls, E. T., and Deco, G. (2010). *The Noisy Brain: Stochastic Dynamics as a Principle of Brain Function*. Oxford: Oxford University Press. doi: 10.1093/acprof:oso/9780199587865.001.0001

Rolls, E. T., and Deco, G. (2011). A computational neuroscience approach to schizophrenia and its onset. *Neurosci. Biobehav. Rev.* 35, 1644–1653. doi: 10.1016/j.neubiorev.2010.09.001

Rolls, E. T., Dempere-Marco, L., and Deco, G. (2013). Holding multiple items in short term memory: a neural mechanism. *PLoS ONE* 8:e61078. doi: 10.1371/journal.pone.0061078

Rolls, E. T., and Kesner, R. P. (2006). A computational theory of hippocampal function, and empirical tests of the theory. *Prog. Neurobiol.* 79, 1–48. doi: 10.1016/j.pneurobio.2006.04.005

Rolls, E. T., Loh, M., Deco, G., and Winterer, G. (2008a). Computational models of schizophrenia and dopamine modulation in the prefrontal cortex. *Nat. Rev. Neurosci.* 9, 696–709. doi: 10.1038/nrn2462

Rolls, E. T., Tromans, J., and Stringer, S. M. (2008b). Spatial scene representations formed by self-organizing learning in a hippocampal extension of the ventral visual system. *Eur. J. Neurosci.* 28, 2116–2127. doi: 10.1111/j.1460-9568.2008.06486.x

Rolls, E. T., Miyashita, Y., Cahusac, P. M. B., Kesner, R. P., Niki,

H., Feigenbaum, J., et al. (1989). Hippocampal neurons in the monkey with activity related to the place in which a stimulus is shown. *J. Neurosci.* 9, 1835–1845.

Rolls, E. T., Robertson, R. G., and Georges-François, P. (1997a). Spatial view cells in the primate hippocampus. *Eur. J. Neurosci.* 9, 1789–1794. doi: 10.1111/j.1460-9568.1997.tb01538.x

Rolls, E. T., Treves, A., Foster, D., and Perez-Vicente, C. (1997b). Simulation studies of the CA3 hippocampal subfield modelled as an attractor neural network. *Neural Netw.* 10, 1559–1569. doi: 10.1016/S0893-6080(97)00092-0

Rolls, E. T., and Stringer, S. M. (2000). On the design of neural networks in the brain by genetic evolution. *Prog. Neurobiol.* 61, 557–579. doi: 10.1016/S0301-0082(99)00066-0

Rolls, E. T., and Stringer, S. M. (2005). Spatial view cells in the hippocampus, and their idiothetic update based on place and head direction. *Neural Netw.* 18, 1229–1241. doi: 10.1016/j.neunet.2005.08.006

Rolls, E. T., and Stringer, S. M. (2006). Invariant visual object recognition: a model, with lighting invariance. *J. Physiol. Paris* 100, 43–62. doi: 10.1016/j.jphysparis.2006.09.004

Rolls, E. T., Stringer, S. M., and Elliot, T. (2006). Entorhinal cortex grid cells can map to hippocampal place cells by competitive learning. *Network* 17, 447–465. doi: 10.1080/09548980601064846

Rolls, E. T., Stringer, S. M., and Trappenberg, T. P. (2002). A unified model of spatial and episodic memory. *Proc. Biol. Sci.* 269, 1087–1093. doi: 10.1098/rspb.2002.2009

Rolls, E. T., and Treves, A. (1990). The relative advantages of sparse versus distributed encoding for associative neuronal networks in the brain. *Network* 1, 407–421. doi: 10.1088/0954-898X/1/4/002

Rolls, E. T., and Treves, A. (1998). *Neural Networks and Brain Function*. Oxford: Oxford University Press.

Rolls, E. T., and Treves, A. (2011). The neuronal encoding of information in the brain. *Prog. Neurobiol.* 95, 448–490. doi: 10.1016/j.pneurobio.2011.08.002

Rolls, E. T., Treves, A., Robertson, R. G., Georges-François, P., and Panzeri, S. (1998). Information about spatial view in an ensemble of primate hippocampal cells. *J. Neurophysiol.* 79, 1797–1813.

Rolls, E. T., and Webb, T. J. (2012). Cortical attractor network dynamics with diluted connectivity. *Brain Res.* 1434, 212–225. doi: 10.1016/j.brainres.2011.08.002

Rolls, E. T., and Xiang, J.-Z. (2005). Reward-spatial view representations and learning in the hippocampus. *J. Neurosci.* 25, 6167–6174. doi: 10.1523/JNEUROSCI.1481-05.2005

Rolls, E. T., and Xiang, J.-Z. (2006). Spatial view cells in the primate hippocampus, and memory recall. *Rev. Neurosci.* 17, 175–200. doi: 10.1515/REVNEURO.2006.17.1-2.175

Rolls, E. T., Xiang, J.-Z., and Franco, L. (2005). Object, space and object-space representations in the primate hippocampus. *J. Neurophysiol.* 94, 833–844. doi: 10.1152/jn.01063.2004

Rondi-Reig, L., Libbey, M., Eichenbaum, H., and Tonegawa, S. (2001). CA1-specific N-methyl-D-aspartate receptor knockout mice are deficient in solving a nonspatial transverse patterning task. *Proc. Natl. Acad. Sci. U.S.A.* 98, 3543–3548. doi: 10.1073/pnas.041620798

Samsonovich, A., and McNaughton, B. L. (1997). Path integration and cognitive mapping in a continuous attractor neural network model. *J. Neurosci.* 17, 5900–5920.

Schultz, S., Panzeri, S., Rolls, E. T., and Treves, A. (2000). "Quantitive model analysis of a Schaffer collateral model," *in Information Theory and the Brain, Chapter 14*, ed P. Hancock, P. Földiák, and R. Baddeley (Cambridge, UK: Cambridge University Press), 257–272. doi: 10.1017/CBO9780511665516.019

Schultz, S., and Rolls, E. T. (1999). Analysis of information transmission in the Schaffer collaterals. *Hippocampus* 9, 582–598.

Sidhu, M. K., Stretton, J., Winston, G. P., Bonelli, S., Centeno, M., Vollmar, C., et al. (2013). A functional magnetic resonance imaging study mapping the episodic memory encoding network in temporal lobe epilepsy. *Brain*. 136, 1868–1888. doi: 10.1093/brain/awt099

Simmen, M. W., Treves, A., and Rolls, E. T. (1996). Pattern retrieval in threshold-linear associative nets. *Network* 7, 109–122. doi: 10.1088/0954-898X/7/1/007

Stefanacci, L., Suzuki, W. A., and Amaral, D. G. (1996). Organization of connections between the amygdaloid complex and the perirhinal and parahippocampal cortices in macaque monkeys. *J. Comp. Neurol.* 375, 552–582.

Stella, F., Cerasti, E., and Treves, A. (2013). Unveiling the metric structure of internal representations of space. *Front. Neural Circuits* 7:81. doi: 10.3389/fncir.2013.00081

Storm-Mathiesen, J., Zimmer, J., and Ottersen, O. P. (eds.). (1990). *Understanding the Brain through the Hippocampus.* Oxford: Elsevier.

Stringer, S. M., and Rolls, E. T. (2002). Invariant object recognition in the visual system with novel views of 3D objects. *Neural Comput.* 14, 2585–2596. doi: 10.1162/089976602760407982

Stringer, S. M., and Rolls, E. T. (2006). Self-organizing path integration using a linked continuous attractor and competitive network: path integration of head direction. *Network* 17, 419–445. doi: 10.1080/09548980601004032

Stringer, S. M., Rolls, E. T., and Trappenberg, T. P. (2004). Self-organising continuous attractor networks with multiple activity packets, and the representation of space. *Neural Netw.* 17, 5–27. doi: 10.1016/S0893-6080(03)00210-7

Stringer, S. M., Rolls, E. T., and Trappenberg, T. P. (2005). Self-organizing continuous attractor network models of hippocampal spatial view cells. *Neurobiol. Learn. Mem.* 83, 79–92. doi: 10.1016/j.nlm.2004.08.003

Stringer, S. M., Rolls, E. T., Trappenberg, T. P., and Araujo, I. E. T. (2002a). Self-organizing continuous attractor networks and path integration. Two-dimensional models of place cells. *Network* 13, 429–446. doi: 10.1088/0954-898X/13/4/301

Stringer, S. M., Trappenberg, T. P., Rolls, E. T., and Araujo, I. E. T. (2002b). Self-organizing continuous attractor networks and path integration: one-dimensional models of head direction cells. *Network* 13, 217–242.

Suzuki, W. A., and Amaral, D. G. (1994a). Perirhinal and parahippocampal cortices of the macaque monkey—cortical afferents. *J. Comp. Neurol.* 350, 497–533. doi: 10.1002/cne.903500402

Suzuki, W. A., and Amaral, D. G. (1994b). Topographic organization of the reciprocal connections between the monkey entorhinal cortex and the perirhinal and parahippocampal cortices. *J. Neurosci.* 14, 1856–1877.

Tabuchi, E., Mulder, A. B., and Wiener, S. I. (2003). Reward value invariant place responses and reward site associated activity in hippocampal neurons of behaving rats. *Hippocampus* 13, 117–132. doi: 10.1002/hipo.10056

Taylor, J. G. (1999). Neural "bubble" dynamics in two dimensions: foundations. *Biol. Cybern.* 80, 393–409. doi: 10.1007/s004220050534

Tonegawa, S., Nakazawa, K., and Wilson, M. A. (2003). Genetic neuroscience of mammalian learning and memory. *Philos. Trans. R. Soc. Lond. B Biol. Sci.* 358, 787–795. doi: 10.1098/rstb.2002.1243

Treves, A. (1990). Graded-response neurons and information encodings in autoassociative memories. *Phys. Rev. A* 42, 2418–2430. doi: 10.1103/PhysRevA.42.2418

Treves, A. (1991). Dilution and sparse coding in threshold-linear nets. *J. Phys. A* 24, 327–335. doi: 10.1088/0305-4470/24/1/038

Treves, A. (1995). Quantitative estimate of the information relayed by Schaffer collaterals. *J. Comput. Neurosci.* 2, 259–272. doi: 10.1007/BF00961437

Treves, A., and Rolls, E. T. (1991). What determines the capacity of autoassociative memories in the brain. *Network* 2, 371–397. doi: 10.1088/0954-898X/2/4/004

Treves, A., and Rolls, E. T. (1992). Computational constraints suggest the need for two distinct input systems to the hippocampal CA3 network. *Hippocampus* 2, 189–199. doi: 10.1002/hipo.450020209

Treves, A., and Rolls, E. T. (1994). A computational analysis of the role of the hippocampus in memory. *Hippocampus* 4, 374–391. doi: 10.1002/hipo.450040319

Ungerleider, L. G., and Mishkin, M. (1982). "Two cortical visual systems," in *Analysis of Visual Behavior*, eds D. J. Ingle, M. A. Goodale, and R. J. W. Mansfield (Cambridge, MA: MIT Press), 549–586.

Van Haeften, T., Baks-Te-Bulte, L., Goede, P. H., Wouterlood, F. G., and Witter, M. P. (2003). Morphological and numerical analysis of synaptic interactions between neurons in deep and superficial layers of the entorhinal cortex of the rat. *Hippocampus* 13, 943–952. doi: 10.1002/hipo.10144

Van Hoesen, G. W. (1982). The parahippocampal gyrus. New observations regarding its cortical connections in the monkey. *Trends Neurosci.* 5, 345–350. doi: 10.1016/0166-2236(82)90201-6

Wallis, G., and Rolls, E. T. (1997). Invariant face and object recognition in the visual system. *Prog. Neurobiol.* 51, 167–194. doi: 10.1016/S0301-0082(96)00054-8

Walters, D. M., Stringer, S. M., and Rolls, E. T. (2013). Path integration of head direction: updating a

packet of neural activity at the correct speed using axonal conduction delays. *PLoS ONE* 8:e58330. doi: 10.1371/journal.pone.0058330

Wang, S. H., and Morris, R. G. (2010). Hippocampal-neocortical interactions in memory formation, consolidation, and reconsolidation. *Annu. Rev. Psychol.* 61, 49–79, C41–44.

Wang, X. J. (2002). Probabilistic decision making by slow reverberation in cortical circuits. *Neuron* 36, 955–968. doi: 10.1016/S0896-6273(02)01092-9

Webb, T., Rolls, E. T., Deco, G., and Feng, J. (2011). Noise in attractor networks in the brain produced by graded firing rate representations. *PLoS ONE* 6:e23630. doi: 10.1371/journal.pone.0023630

Wills, T. J., Lever, C., Cacucci, F., Burgess, N., and O'Keefe, J. (2005). Attractor dynamics in the hippocampal representation of the local environment. *Science* 308, 873–876. doi: 10.1126/science.1108905

Witter, M. P. (1993). Organization of the entorhinal-hippocampal system: a review of current anatomical data. *Hippocampus* 3, 33–44.

Witter, M. P. (2007). Intrinsic and extrinsic wiring of CA3: indications for connectional heterogeneity. *Learn. Mem.* 14, 705–713. doi: 10.1101/lm.725207

Witter, M. P., Wouterlood, F. G., Naber, P. A., and Van Haeften, T. (2000). Anatomical organization of the parahippocampal-hippocampal network. *Ann. N.Y. Acad. Sci.* 911, 1–24. doi: 10.1111/j.1749-6632.2000.tb06716.x

Wood, E. R., Dudchenko, P. A., and Eichenbaum, H. (1999). The global record of memory in hippocampal neuronal activity. *Nature* 397, 613–616. doi: 10.1038/16564

Zhang, K. (1996). Representation of spatial orientation by the intrinsic dynamics of the head-direction cell ensemble: a theory. *J. Neurosci.* 16, 2112–2126.

Zilli, E. A. (2012). Models of grid cell spatial firing published 2005-2011. *Front. Neural Circuits* 6:16. doi: 10.3389/fncir.2012.00016

Conflict of Interest Statement: The author declares that the research was conducted in the absence of any commercial or financial relationships that could be construed as a potential conflict of interest.

Received: 22 April 2013; accepted: 05 June 2013; published online: 25 June 2013.

Citation: Rolls ET (2013) A quantitative theory of the functions of the hippocampal CA3 network in memory. Front. Cell. Neurosci. 7:98. doi: 10.3389/fncel.2013.00098

frontiers in
CELLULAR NEUROSCIENCE

ORIGINAL RESEARCH ARTICLE
published: 16 July 2013
doi: 10.3389/fncel.2013.00112

The spatial representations acquired in CA3 by self-organizing recurrent connections

Erika Cerasti [1,2†] ***and Alessandro Treves*** [1,3*†]

[1] *SISSA, Cognitive Neuroscience Sector, Trieste, Italy*
[2] *Collège de France, Paris, France*
[3] *Kavli Institute for Systems Neuroscience and Centre for the Biology of Memory, NTNU, Trondheim, Norway*

Edited by:
Enrico Cherubini, International School for Advanced Studies, Italy

Reviewed by:
Demian Battaglia, Max Planck Institute for Dynamics and Self-organization, Germany
Sandro Romani, Columbia University, USA

****Correspondence:***
Alessandro Treves, SISSA, Cognitive Neuroscience, via Bonomea 265, 34136 Trieste, Italy
e-mail: ale@sissa.it

†Present address:
Erika Cerasti, Dip. Di Fisiologia, Università La Sapienza, Roma, Italy; Alessandro Treves, Embassy of Italy, Science Office, Tel Aviv, Israel

Neural computation models have hypothesized that the dentate gyrus (DG) drives the storage in the CA3 network of new memories including, e.g., in rodents, spatial memories. Can recurrent CA3 connections self-organize, during storage, and form what have been called continuous attractors, or *charts*—so that they express spatial information later, when aside from a partial cue the information may not be available in the inputs? We use a simplified mathematical network model to contrast the properties of spatial representations self-organized through simulated Hebbian plasticity with those of charts pre-wired in the synaptic matrix, a control case closer to the ideal notion of continuous attractors. Both models form granular quasi-attractors, characterized by drift, which approach continuous ones only in the limit of an infinitely large network. The two models are comparable in terms of precision, but not of accuracy: with self-organized connections, the metric of space remains distorted, ill-adequate for accurate path integration, even when scaled up to the real hippocampus. While prolonged self-organization makes charts somewhat more informative about position in the environment, some positional information is surprisingly present also about environments never learned, borrowed, as it were, from unrelated charts. In contrast, context discrimination decreases with more learning, as different charts tend to collapse onto each other. These observations challenge the feasibility of the idealized CA3 continuous chart concept, and are consistent with a CA3 specialization for episodic memory rather than path integration.

Keywords: memory network, mossy fibers, associative plasticity, information theory, continuous attractors

INTRODUCTION

It has been suggested on the basis of network models (McNaughton and Morris, 1987; Treves and Rolls, 1992) that new CA3 memory representations may be primarily established by inputs from the dentate gyrus (DG), while the input coming from the entorhinal cortex (EC) serves as cue for the retrieval process.

This hypothesis is consistent with behavioral evidence from spatial learning in rodents (McNaughton et al., 1989; Lassalle et al., 2000; Lee and Kesner, 2004) that indicates that dentate inactivation and dentate lesions disproportionately affect the acquisition of new spatial memories, rather than their retention. In a previous study we have formulated a mathematical model that allows assessing, in quantitative detail, the storage of spatial memories that could result from DG inputs (Cerasti and Treves, 2010). The model demonstrates that a sparse and entirely structureless system of DG-CA3 projections can act effectively as a spatial random number generator, and impart considerable information content to distributions of CA3 place fields, by exploiting the very sparse activity seen across populations of granule cells (Chawla et al., 2005; Leutgeb et al., 2007). Intriguingly, much of this content has, however, a non-spatial character, due to the non-spatial and sparse nature of the connectivity. This non-spatial character is quantified in our study by the likelihood with which even distant locations in an environment can be confused with one another, when locations are decoded from the activity of a limited number of CA3 units.

Once the representation of a novel environment has been established in CA3, it is useful as a spatial memory if it allows the animal to reconstruct, from a partial cue, which environment it is in and/or its position within that environment (when both types of information are fully present in the inputs, there is no need for a memory system). An influential conceptual model (Samsonovich and McNaughton, 1997) posits that the CA3 recurrent network affords these abilities by using the DG-driven representations as continuous attractors. Among the N dimensions of its activity space, a continuous attractor based on N units spans a "chart" of only 1, or 2, or 3 dimensions, which correspond to those of physical space, e.g., 2 in the case of a planar environment. Along the other N-2 dimensions activity is attracted toward the chart, corresponding to the recognition of the environment, whereas activity can slide effortlessly along the 2 dimensions of the chart, guided e.g., by path integration, maintaining a memory of the current position. Learning arbitrary novel environments implies an ability to keep multiple charts in memory, in the same network.

Such a conceptual model is clear in principle, but is it realizable in practice? It is not yet understood, despite early studies (Samsonovich and McNaughton, 1997; Battaglia and Treves,

1998), how many multiple charts could be established and maintained by unsupervised synaptic plasticity on the recurrent CA3 connections. Even less, how close they would be to continuous attractors. Here, we use a simplified network model to show that what can be created by self-organization is considerably distant from a continuous attractor, and closer to a bundle of loosely organized discrete point-like attractors.

METHODS

BASIC MODEL

The model we consider is an extended version of the one used in our previous study (Cerasti and Treves, 2010), where the firing rate of a CA3 pyramidal cell, η_i, was determined, as the one informative component, by the firing rates $\{\beta\}$ of DG granule cells, which feed into it through mossy fiber (MF) connections. The model used for the neuron was a simple threshold-linear unit (Treves, 1990), so that the firing of the unit is produced by an activating current (which includes several non-informative components) which is compared to a threshold:

$$\eta_i(\vec{x}) = g\left[\sum_j c_{ij}^{\mathrm{MF}} J_{ij}^{\mathrm{MF}} \beta_j(\vec{x}) + \tilde{\delta}_i - \tilde{T}\right]^+ \quad (1)$$

where g is a gain factor, while $[\cdot]^+$ equals the sum inside the brackets if positive in value, and zero if negative. The effect of the current threshold for activating a cell, along with the effect of inhibition, and other non-informative components, are summarized into a single subtractive term, with a mean value across CA3 cells expressed as $\tilde{T}$, and a deviation from the mean for each particular cell i as $\tilde{\delta}_i$, which acts as a sort of noise; threshold and inhibition, in fact, while influencing the mean activity of the network, are supposed to have a minor influence on the coding properties of the system. In the earlier reduced model, however, $\tilde{T}$ and $\tilde{\delta}_i$ also included the effect of other cells in CA3, through recurrent collateral (RC) connections, and that of the perforant path (the input coming from the EC), both regarded as unspecific inputs—this based on the assumption that information is driven into a new CA3 representation solely by MF inputs. In this study, instead, since we are interested in the ability of the RC system to retrieve and express spatial representations, we separate out the RC contribution, and redefine $\tilde{T}$ and $\tilde{\delta}_i$ into T and δ_i—which sum the remaining unspecific inputs, including the perforant path, not analyzed here:

$$\eta_i(\vec{x}) = g\left[\sum_j c_{ij}^{\mathrm{MF}} J_{ij}^{\mathrm{MF}} \beta_j(\vec{x}) + \sum_k c_{ik}^{\mathrm{RC}} J_{ik}^{\mathrm{RC}} \eta_k(\vec{x}) + \delta_i - T\right]^+ \quad (2)$$

Connections between cells are indicated by the fixed binary matrices $\{c^{\mathrm{MF}}\}$, $\{c^{\mathrm{RC}}\}$, whose non-zero elements (which take value 1) represent the existence of anatomical synapses between two cells. The synaptic efficacies are instead indicated by the matrices of weights $\{J^{\mathrm{MF}}\}$, $\{J^{\mathrm{RC}}\}$, whose elements are allowed to take positive values. The notation is chosen to minimize differences with our previous analysis of other components of the hippocampal system (e.g., Treves, 1990; Kropff and Treves, 2008).

The firing rates of the various populations are all assumed to depend on the spatial position $\vec{x}$ of the animal; the time scale considered for evaluating the firing rate is of order the theta period, about a hundred msec, so the finer temporal dynamics over shorter time scales is neglected. Note that time is not explicitly included in the above equations, which only describe the end result of the dynamics at the theta scale. To be precise, in the simulations, we take a time step to correspond to 125 ms of real time, or a theta period. We assume in fact that the simulated rat moves at a speed of 20 cm/s, so during one step the rat moves by 2.5 cm. In support of the plausibility of this choice, recent evidence indicates that within each theta period only one spatial representation tends to be dynamically selected (Jezek et al., 2011).

THE STORAGE OF NEW REPRESENTATIONS

The important novel ingredient that was introduced by Cerasti and Treves (2010), and that makes the difference from previous models of self-organizing recurrent networks, is a realistic description of the patterns of firing in the inputs, i.e., in the DG. As the virtual rat explores the new environment, the activity $\beta_j(\vec{x})$ of DG unit j is determined by the position $\vec{x}$ of the animal, according to the expression:

$$\beta_j(\vec{x}) = \sum_{k=0}^{Q_j} \beta_0 e^{-(\vec{x}-\vec{x}_{jk})^2/2\sigma_f^2} \quad (3)$$

The firing rate of the granule cells is then a combination of Q_j Gaussian functions, resulting in "bumps," or fields in the firing map of the environment, centered at random points $\vec{x}_{jk}$. The environment is taken to have size A, and the fields are defined as all having the same effective size $\pi(\sigma_f)^2$ and height β_0. Q_j, which indicates the multiplicity of fields of DG cell j, is drawn from a Poisson distribution:

$$P(Q_j) = \frac{q^{Q_j}}{Q_j!} e^{-q} \quad (4)$$

with mean value q (and we take $q = 1.7$), which roughly fits the data reported by Leutgeb et al. (2007). According to the same experimental data, we assume that only a randomly selected fraction $p_{DG} << 1$ (here set at $p_{DG} = 0.033$) of the granule cells are active in a given environment. Hence population activity is sparse, but the firing map of individual active granule units need not be sparse (it would only be sparse if $q\,\pi(\sigma_f)^2/A << 1$, which we do not assume to be always the case).

The activity of DG units determines the probability distribution for the firing rate of any given CA3 pyramidal unit, once the connectivity level between the two layers has been fixed: $\left\{C_{ij}^{\mathrm{MF}}\right\} = 0, 1$ with $P\left(C_{ij}^{\mathrm{MF}} = 1\right) = \frac{C^{\mathrm{MF}}}{N_{\mathrm{DG}}} \equiv c^{\mathrm{MF}}$. In agreement with experimental data, we set $C^{\mathrm{MF}} = 50$, a value in the range of the ones providing an optimal information transmission from DG to CA3 (Cerasti and Treves, 2010). The MF synaptic weights are set to be uniform in value, $J_{ij}^{\mathrm{MF}} \equiv J$, and similarly $J_{ij}^{\mathrm{RC}} \equiv J_0^{\mathrm{RC}}$ initially. Subsequently, during the learning phase, RC weights are modified

according to the simulated learning process and under the influence of the input coming from the MF connections. Following the simplified hypothesis that the MFs carry all the information to be stored without contributing anything to the retrieval process, which is left to the RC, MF weights are kept fixed to their initial values J; note that we have found, in our earlier study, that MF connections appear to be inadequate, even when associatively plastic, to support retrieval of spatial representation (Cerasti and Treves, 2010).

The connectivity among CA3 cells is given by the matrix $\left\{C_{ij}^{\mathrm{RC}}\right\} = 0, 1$ with $P\left(C_{ij}^{\mathrm{RC}} = 1\right) = \frac{C^{\mathrm{RC}}}{N_{\mathrm{CA3}}} \equiv c^{\mathrm{RC}}$, where $C^{\mathrm{RC}} = 900$ in most simulations. The activity of the network is regulated by the constraint we impose on its mean and on its sparsity a_{CA3}, i.e., the fraction of the CA3 units firing significantly at each position, which is an important parameter affecting memory retrieval (Treves, 1990; more precisely, $a_{\mathrm{CA3}} = \langle \eta_i \rangle^2 / \langle \eta_i^2 \rangle$). Here we set the sparsity of each representations as $a_{\mathrm{CA3}} = 0.1$, in broad agreement with experimental data (Papp et al., 2007), and at each time step we regulate the threshold T accordingly, to fulfill such requirement, while keeping the mean activity $\langle \eta_i \rangle = 0.1$ by adjusting the gain g.

RECURRENT COLLATERAL PLASTICITY

During the learning phase, the activity of CA3 is driven by DG inputs, and RC connections contribute through weights uniformly set to their initial value J_0^{RC}. While the virtual rat explores the environment, RC weights are allowed to change according to an associative "Hebbian" learning rule, such that the total change in the synaptic weights is given as a sum of independent terms:

$$\Delta J_{ij}^{RC}(t) = \gamma \eta_i(t) \left(\eta_j(t) - \Lambda_j(t)\right) \tag{5}$$

where $\Delta J_{ij}(t)$ indicates the variation of the connection weight between cells i and j occurring at a given time step t, η_i, and η_j are the postsynaptic and presynaptic firing rate, while γ is the learning rate. This associative learning rule includes the contribution of a trace, Λ, of the recent past activity of the presynaptic cell, defined as:

$$\Lambda_j(t) = \frac{1}{\tau} \sum_{t_s=1}^{\tau} \eta_j(t - t_s) \tag{6}$$

where τ is taken equal to 14 time steps (1750 ms). RC weights are forced to be non-negative, so they are reset to zero each time they become negative. Moreover, the total of the synaptic weights afferent to a single postsynaptic CA3 cell is normalized at the end of the learning process, so that $\sum_{j=1}^{C^{\mathrm{RC}}} J_{ij}^{\mathrm{RC}} = 1$ per each CA3 cell. In words, the synaptic plasticity on recurrent connections allows the system to store the information about the current environment conveyed by MF inputs; such information is expressed in the form of place-like patterns of activity in CA3 units, and the Hebb-like learning rule strengthens the connections between units that show overlapping fields.

PRE-WIRED EXPONENTIAL CONNECTIVITY MODEL

In contrast to and as a control for this self-organizing connectivity, we also consider the case of a model network endowed with a pre-wired connectivity. The structure of connections is functional to the establishment of a quasi-continuous attractor surface, expressed by synaptic weights that follow an exponential decreasing function of the distance between place field centers (Tsodyks and Sejnowski, 1995; Samsonovich and McNaughton, 1997; Battaglia and Treves, 1998; Roudi and Treves, 2008). The weight of the connection between cell i and j is then written:

$$J_{ij}^{\mathrm{RC}} = e^{-\left|\vec{x}_i^c - \vec{x}_j^c\right| / \lambda} \tag{7}$$

if the two cells i and j both have place fields in the given environment with centers $\vec{x}_i^c$ and $\vec{x}_j^c$ (the largest field is chosen for each cell that has more than one), while $J_{ij} = 0$ if at least one of them has no place fields. We usually set here the characteristic spread of the connectivity to $\lambda = 5$ cm, and to $\lambda = 10$ cm in some control simulations, and the size of the environment is taken to be $A = 1 \times 1$ m; see below. The synaptic efficacies, in this control model, result from an artificial construction based on a precise and quite narrow exponential function; however, the distribution of place fields at the basis of such construction stems from the DG input, so that the place fields of CA3 units are randomly distributed in space, and not regularly arranged (Cerasti and Treves, 2010).

SIMULATIONS

The mathematical model described above was simulated with a network of typically 45000 DG units and 1500 CA3 units (although in the "quick" multi-chart simulations described below the number of DG units goes down to 15,000 and that of CA3 units to 500). A virtual rat explores a continuous two dimensional space, intended to represent a 1 sqm square environment but realized as a torus, with periodic boundary conditions. For the numerical estimation of mutual information, the environment is discretized in a grid of 20×20 locations, whereas trajectories are in continuous space, but in discretized time steps. In each time step (of 125 ms) the virtual rat moves 2.5 cm in a direction similar to the direction of the previous time step, with a small amount of noise. To allow construction of a full localization matrix with good statistics, simulations are run for typically 400,000 time steps (nearly 35 h of virtual rat time). Given the choice of periodic boundary conditions, made to avoid border effects, the longest possible distance between any two sampling locations is equal to 14.1 grid units, or 70 cm.

SCALING UP THE NETWORK

Different network sizes as used in **Figure 2** (where the number of units in the CA3 layer is indicated) are implemented in the simulations through the multiplication of the following parameters by a given factor: the total number of DG units, $N_{\mathrm{DG}}^{\mathrm{tot}}$, the total number of CA3 units, $N_{\mathrm{CA3}}^{\mathrm{tot}}$, the number of RC connections, C^{RC}. The multiplicative factors, relative to the reference model with 1500 CA3 units, are 1/3, 1, 5/3, 7/3, 10/3, 16/3. The connectivity between DG and CA3 stays unchanged, with always 50 MFs projecting to a single CA3 cell.

THRESHOLD SETTING IN CA3

CA3 units fire according to Equation (2), with the threshold T hypothesized to serve to adjust the sparsity a_{CA3} of CA3 activity to its required value. The sparsity is defined as:

$$a_{CA3} = \left(\sum \eta_i(\vec{x})\right)^2 \sum \eta_i^2(\vec{x}) \tag{8}$$

and it is set to $a_{CA3} = 0.1$. This implies that the activity of the CA3 cell population is under tight inhibitory control.

HEBBIAN LEARNING PROCESS

Before and during the learning session, all recurrent connections weights take the same value J_0^{RC}; after the learning phase, they take the values resulting from the sum of all modifications occurred during the session, and described by Equation (5), with learning rate γ. The trajectory of the virtual rat during the learning session is a random path, extended over a time long enough for it to effectively visit repeatedly all possible locations in space: 10,000 time steps to cover 400 locations (in each time step the rat is made to move half a grid unit). This is taken to correspond to about 20 min of exploration in real time. Such synaptic modifications start to have an effect on the CA3 firing rate only at the end of the learning session, when the RC weights are updated to their new values. In the "quick" multi-chart simulations below, the learning rate was sped up by a factor 20, $\gamma = 0.002$: in those simulations, each learning session (per each learned environment, or chart) lasted 3000 time steps, with the higher learning rate intended to partially compensate for the fewer time steps.

TURNING OFF THE DG INPUT

For simulations aimed at describing attractor properties, in each position of the virtual rat activity is allowed to reverberate for 15 iterations; with a full DG input during the first one, an input reduced to 1/3 during the second, and to 0 for the remaining 13 time steps. The final position is then inferred by comparing the population vector in the last iteration, i.e., the vector with components $[\eta_1(t), \ldots, \eta_i, (t) \ldots, \eta_N(t)]$ with the set of all templates, which are the population vectors corresponding to 400 possible locations in space (on a the 20×20 grid), measured when the DG input is on. The position relative to the template that is correlated the most with the actual population vector is taken to be the final position resulting from attractor dynamics elicited by the initial spatial input. Most correlated means having the smallest Euclidean vector distance. For simulations aimed at assessing the storage of multiple environments, for each position of the virtual rat the activity reverberates for only 5 iterations, to save CPU time; with the full DG input during the first 2, reduced to 1/3 on the third, and to 0 for the remaining 2 iterations.

Note that in order to assess the information content stored in the network, in this study we always probe the network by first presenting it with a full cue. Of course, the real memory capabilities of the CA3 network should be appreciated also by providing it with partial cues, possibly conveyed to the system by the direct PP input from EC, so that information is actually retrieved from the network and not merely relayed onwards. This can be the subject of future studies.

DECODING PROCEDURE AND INFORMATION EXTRACTION

At each time step, the firing vector of a sample of CA3 units is compared to each of the "template" vectors recorded, in previous test trials, at each position in the 20×20 grid, for the same sample of units. The position of the closest template, in the Euclidean distance sense, is taken to be the decoded position at that time step, for that sample. At the last iteration, this is taken to be the "final" position, reached through network dynamics, when the virtual rat is in a fixed position, corresponding to the "initial" one conveyed to the CA3 network by the MF inputs, as illustrated also in **Figure 2**. This procedure has been termed maximum likelihood Euclidean distance decoding (Rolls et al., 1997). The frequency of each pair of decoded and real positions are compiled in a so-called "confusion matrix," or localization matrix, that reflects the ensemble of conditional probabilities $\left\{P(\{\eta_i\}|\vec{x})\right\}$ for that set of units. All information measures from simulations are obtained constructing the full localization matrix $Q(\vec{x}, \vec{x}')$ (Cerasti and Treves, 2010). If the square environment is discretized into 20×20 spatial bins, this is a large 400×400 matrix, which requires of order 160,000 decoding events to be effectively sampled. We run simulations with trajectories of 400,000 steps. In all the information measures we report, we have also corrected for the limited sampling bias, as discussed by Treves and Panzeri (1995). In our case of spatial information, the bias is essentially determined by the spatial binning we used (20×20) and by the decoding method (Panzeri et al., 1999). Should decoding "work" in a perfect manner, in the sense of always detecting the correct position in space of the virtual rat, the confusion matrix would be the identity matrix. From the confusion matrix obtained at the end of the simulation, the amount of information is extracted, and plotted versus the number of CA3 units present in the sample. We average extensively over CA3 samples, as there are large fluctuations from sample to sample, i.e., for each given number of CA3 units we randomly pick several different groups of CA3 units and then average the mutual information values obtained.

The decoding and information extraction procedure is used similarly for the evaluation of context discrimination: at each time step a vector of a sample of CA3 units is compared to each of four "template" vectors recorded previously in four different environments at the same location, for the same sample of units. The environment corresponding to the closest template, in the Euclidean distance sense, is taken to be the decoded environment at that time step, for that sample.

FITTING

We fit the information curves obtained in simulations to exponentially saturating curves as a function of N, in order to get the values of the two most relevant parameters that describe their shape: the initial slope I_1 (i.e., the average information conveyed by the activity of individual units) and the total amount of information I_8 (i.e., the asymptotic saturation value). The function we used for the fit is:

$$I(N) = I_\infty \left(1 - e^{-NI_1 I_\infty}\right) \tag{9}$$

In most cases the fit was in excellent agreement with individual data points, as expected on the basis of previous analyses (Samengo and Treves, 2000).

RESULTS

We simulate a network of CA3 units, receiving input from DG units with multiple, disorderly arranged place fields. Recurrent connections are inserted and contribute to network dynamics either through a "self-organized" weight distribution resulting from an associative learning process or, as a control, through a "pre-wired" distribution manually set by using an exponential function of the place field distance, between pairs of CA3 units with a place field (in some analyses, we shall consider also, as further controls, recurrent weights fixed at their uniform initial value, or reshuffled one with the other). The dynamics is analyzed when the input coming from the DG units is either on, to characterize externally driven representations, or turned off after probing the network with a full cue, to characterize instead memory-driven "attractors." The noise level is kept very low ($\delta = 0.002$) in order to probe the microstructure of the spatial attractors, and is then raised ($\delta = 0.1$) to test their robustness. Parameters for the reference network are listed in **Table 1.**

SELF-ORGANIZED 2D ATTRACTORS ARE REASONABLY PRECISE, BUT NOT ACCURATE

Can the recurrent network in CA3 maintain a precise memory of the position in space of the animal, over realistic time scales, in the absence of afferent inputs? Neural activity in our CA3 model does indeed maintain a localized character, for quite some time after DG inputs are turned off, as illustrated by the examples in **Figures 1A,B**. The figure, however, indicates that the spatial code expressed by the model is rather far from the idealized notion of a smooth continuous attractor, which can sustain a distinct pattern of activity as a bell-shaped bump in each location of the environment. The control case of a pre-wired, finely tuned exponential connectivity, with DG inputs turned off, seems reasonably smooth (**Figure 1A**), while the self-organized bump in **Figure 1B** appears rather noisy. Bumps are in fact equally noisy also when the DG inputs are still on (not shown). Further, the example in **Figure 1C** indicates that the position of the bump drifts considerably when turning off the input. The idealized notion can only be crudely approximated with a network of finite size (Tsodyks and Sejnowski, 1995; Hamaguchi and Hatchett, 2006; Papp et al., 2007; Roudi and Treves, 2008). Are the irregularity and the drift merely finite size effects, due to the limited size of our simulations, which disappear for networks of real-brain size? **Figure 2** shows that the imprecision and the tendency to drift are reduced when the network is larger. To quantify the exact extent to which recurrent network dynamics approach the ideal notion of a continuous attractor, we study how the effective spatial resolution

Table 1 | Parameters.

Parameter	Symbol	Standard value
Number of DG units in the network	N_{DG}^{tot}	45000
Number of CA3 units in the network	N_{CA3}^{tot}	1500
Probability a DG unit is active in one environment	p_{DG}	0.033
Number of DG inputs to a CA3 unit	C^{MF}	50
Number of RC inputs to a CA3 unit	C^{RC}	$0.6 \times N_{CA3}^{tot}$
Mean number of fields per active DG unit	q	1.7
Mean number of fields activating a CA3 unit	μ	$C^{MF} \times p_{DG} \times q = 2.833$
Strength of MF inputs	J	1 (or $2.833/\mu$)
Initial strength of RC inputs	J_0^{RC}	$1/C^{MF}$
Noise affecting CA3 activity	δ	0.002 (in units in which $\beta_0 = 2.02$)
Sparsity of CA3 activity	a_{CA3}	0.1
Learning rate	γ	0.0001
Temporal trace window	τ	14 time steps (or 1750 ms)

Values used in the standard version of the model with recurrent collaterals.

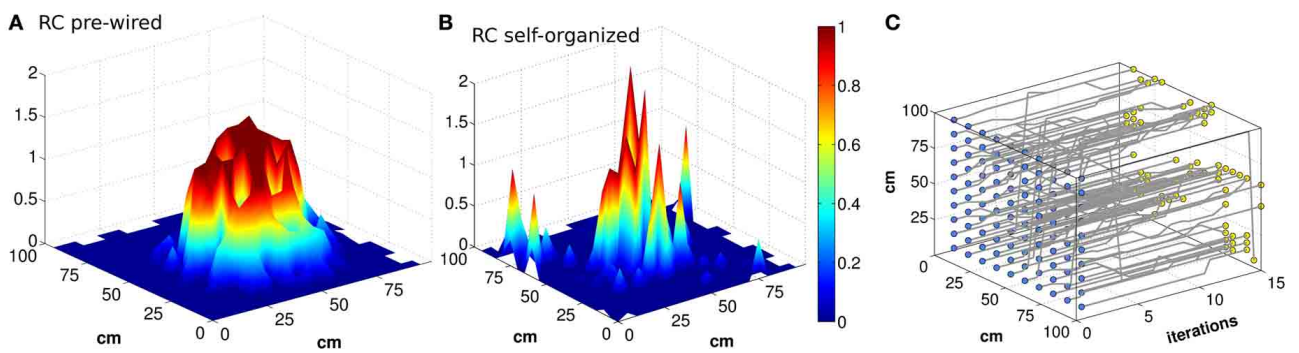

FIGURE 1 | Bumps of activity are rough, and tend to drift. Activity packets showing the localization of the firing pattern, when the virtual rat is in the position of coordinates $(x,y) = (55,45)$ (**A** and **B**). The firing rates of all the units active in the given environment, among $N_{CA3} = 1500$ units, are plotted in the position of their (main) place field centers, when noise is very low ($\delta = 0.002$). The attractor bump in a network with connectivity pre-wired following an exponential function **(A)** is much smoother than in a network with connectivity resulting from a Hebbian self-organizing process **(B)**, both expressed when the DG input is turned off. The trajectory of the activity bump over 16 iterations is outlined for each initial position **(C)** (the iterations are taken to be included within one 125 ms period during theta). The example in **(C)** is with pre-wired exponential connectivity.

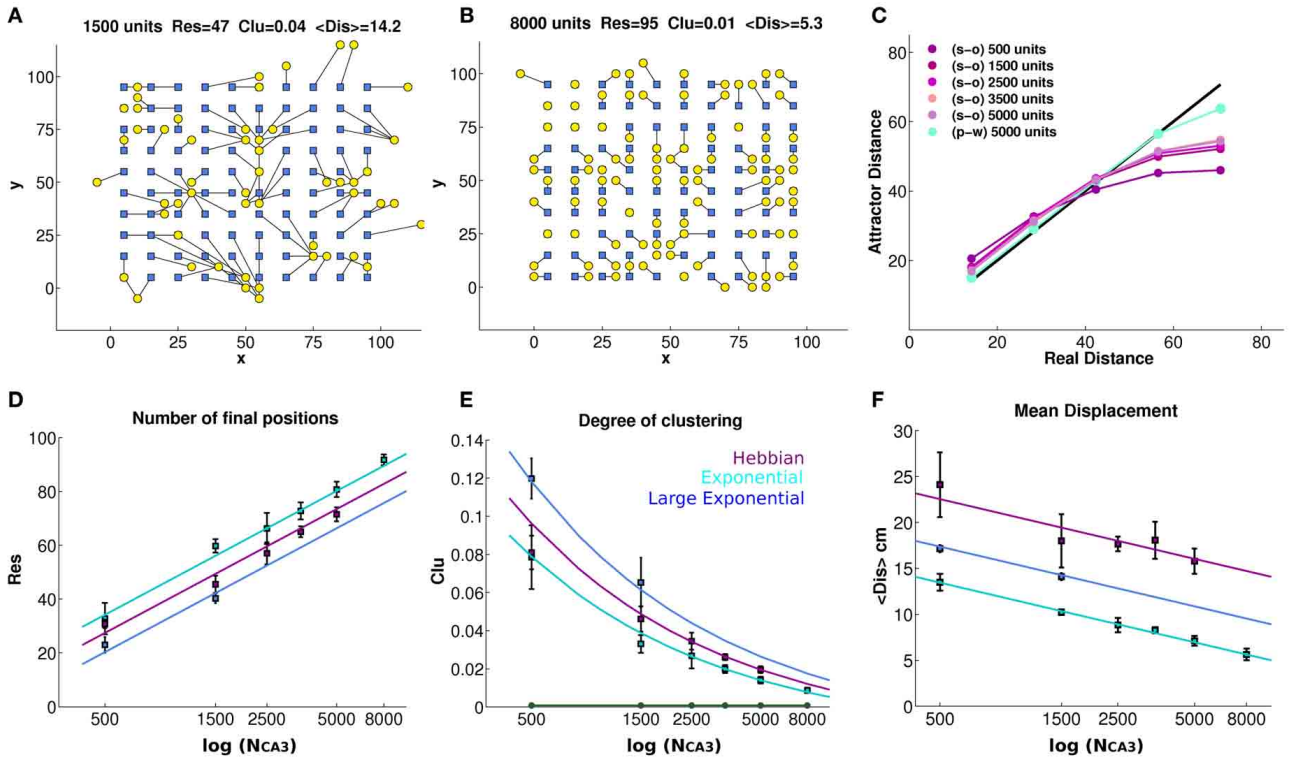

FIGURE 2 | Finite size effects eventually vanish, but the tendency to drift persists. The bump tends to drift from any initial position in the environment, encoded in the inputs, to the final position decoded from the complete CA3 activity vector in the self-sustaining attractor (**A** and **B**), even when noise is very low ($\delta = 0.002$). Each initial position (blue square) is connected to its final position (yellow circle) through a black line, showing strong drift of the bump as a result of turning off DG inputs, in a network of 1500 units with connectivity self-organized through Hebbian learning **(A)**, and much weaker drift in a network of 8000 units with pre-wired exponential connectivity and spread $\lambda = 1$ **(B)**. The panels **(A)** and **(B)** reports the number of distinct final positions *Res*, the degree of clustering *Clu* and the mean displacement from initial to final position $< Dis >$, whose average values over simulations with different network sizes are reported in the bottom row. **(C)** The average distance between final positions corresponding to a given input distance along the diagonal of the torus. As the network gets larger the global metric distortion of a self-organized net is reduced, approaching the black (identity) line, but very slowly. In contrast, a pre-wired network is much less distorted (light blue). **(D)** The mean number of final locations, obtained by providing 100 input locations, is plotted versus the size of the network (number of units in the CA3 layer) for networks with exponential pre-wired and with self-organized weights, when noise is very low ($\delta = 0.002$). The y-axis indicates the number of different final positions, after the removal of the input. Values are averaged over 4 different seeds, and standard errors of the mean are indicated. The cyan data points indicate the values obtained from a network with exponential weights, with the standard spatial decay constant equal to 1 grid unit (or 2 grid units for the blue data points) while the purple points indicate values obtained from a network with Hebbian learning. Data points are seen to approximate the logarithmic trends explained in the text. **(E)** Degree of clustering of the final positions. A measure of clustering is plotted as a function of network size, for networks with exponential pre-wired weights and with Hebbian learning (same color coding **D** as). The new green line indicates the same *Clu* measure for the initial locations that, by construction, are regularly arranged on a grid 10×10. **(F)** The mean displacement, following the removal of the input, between the initial position and the final position.

and spatial memory accuracy of the code change, when increasing in discrete steps the number of units in both the DG and the CA3 population, and the RC connectivity. Different network sizes are indicated in **Figure 2** by the number of units in the CA3 layer (see Methods).

Figure 2D quantifies spatial resolution by showing the number *Res* of different final positions obtained when the input is turned off, starting the network in 100 distinct initial positions. We can see that, already with 8000 units (**Figures 2B,D**), the spatial resolution of the pre-wired system can be quite high, failing to represent only about 5% of the initial locations, in the sense that the network reaches 95 distinct final positions. Note that the 100 initial positions are always taken as the positions at the vertices of a 10×10 grid (**Figures 2A,B**), embedded in the simulated 100×100 cm environment at every fourth node of the finer 20×20 grid used to produce population vector templates for decoding; and note that even distinct final positions do not, in general, coincide with the initial ones. As shown in **Figure 2D**, the spatial resolution of the attractor increases as the population of model CA3 neurons gets larger, both with pre-wired and with self-organized connectivity. This increase is intuitive; in fact with about a third of the CA3 cells active in the given environment, as a result of the DG input (Cerasti and Treves, 2010), an increase in population size implies an increase in the number of CA3 place fields randomly distributed over the environment. As a consequence, the firing level of units in the

activity packet, determined by RC weights, would approximate better a smooth decrease with distance from the center (necessary for a truly continuous attractor, Tsodyks and Sejnowski, 1995) if a larger number of fields is available. In the case of the smallest network in **Figure 2D**, 500 units, indeed the poor resolution is due to the fact that only around 150 place field are present to cover the environment. The network with pre-wired and finely tuned ($\lambda = 1$) connectivity appears to have only marginally better resolution, across sizes, than the self-organized one, which shows in turn slightly better resolution than the pre-wired but more coarsely tuned network ($\lambda = 2$). The **Figure 2D** also shows, as guides to the eye, the straight lines which on the semi-logarithmic scale of the graph correspond to the trends:

$$\mathrm{Res} = -90 + 46 \log_{10} \left(\frac{N_{CAs}}{\lambda} \right) \tag{10}$$

where the *Res* data-points for the self-organized network are reasonably well fit by taking an effective $\lambda = 1.4$. It is not clear at the stage whether these lines are just guides to the eye, or whether they really describe the scaling of finite size effects; this issue is left for future analysis. What they indicate is the size of the network for which *Res*∼100, that is, how large the CA3 network has to be, not to display the imprecision expressed by the collapsing together of the bumps of activity originated on a 10×10 grid of initial positions. We can extrapolate N_{CA3} ∼13,500 for the pre-wired network with finely tuned connectivity ($\lambda = 1$); N_{CA3} ∼27,000 with coarser connectivity ($\lambda = 2$); and N_{CA3} ∼18,900 with self-organized connectivity. Although approximately derived, such values are well below the size of the CA3 network in the rat, suggesting that lack of precision in representing distinct position may be a minor concern in the real rat brain.

To further test this hypothesis, we can also quantify fluctuations in the density of final positions, that is, the degree of clustering in their distribution, *Clu*, by calculating a weighted average for each pair *k, l* of final positions, and for each network realization, as follows:

$$\mathrm{Clu} = \frac{1}{S(S-1)} \sum_{k \neq l}^{S(S-1)} e^{-(\vec{x}_k - \vec{x}_i)^2} \tag{11}$$

where *S* is the total number of locations, 100 in our case. The *Clu* measure takes its minimum (optimal) value *Clu*∼0.00075 when the final positions are uniformly distributed in the environment, and its maximal (worst) value *Clu* = 1 when they are all clustered together. The values taken in our CA3 simulations are shown in **Figure 2E**, where the *Clu* value for the initial positions (the minimum one) is also indicated as a reference. The degree of clustering is much higher than the minimum reached for initial positions, indicating that several pairs of final positions do collapse onto each other or nearly so, yielding large contributions to the sum in Equation (6). The *Clu* measure thus quantifies the impression that final locations are not well distributed, and that the quasi-continuous attractor is locally distorted and "wrinkled." One sees that the distortion is progressively reduced, however, with increasing network size. Again, one can approximately fit to the data-points curves, which in this case describe the trends:

$$Clu = -0.016 + 2.12\sqrt{\lambda / N_{CA3}} \tag{12}$$

where for the self-organized network we can again take an effective value $\lambda = 1.4$. Again, we see that the pre-wired and finely tuned network leads to an attractor only marginally smoother than the self-organized one, which in turn is smoother than the more coarsely tuned pre-wired network. Extrapolating the curves to the optimal value *Clu*∼0.00075, we can extract approximate network sizes beyond which clustering effects disappear. They turn out to be N_{CA3} ∼16,000 for the pre-wired network with finely tuned connectivity ($\lambda = 1$); N_{CA3} ∼32,000 with coarser connectivity ($\lambda = 2$); and N_{CA3} ∼22,500 with self-organized connectivity. These values are similar, although somewhat larger, than those extrapolated from the resolution measures, again suggesting that for a real life rodent hippocampus spatial precision is not a major limitation. The network pre-wired with more coarsely tuned connections extending over double the distance ($\lambda = 2$) is significantly poorer, both in spatial resolution and in the degree of undesirable clustering, than the self-organized network (**Figures 2D,E**), indicating that the latter self-organizes rather precisely, and that the superiority of the control, exponentially pre-wired connections only arises due to their very finely tuned spatial coding.

Both the resolution and clustering measures of **Figures 2D,E** indicate a somewhat granular, but *locally* precise spatial code, able to discriminate neighboring position to a reasonable degree. They do not, however, tell us much about the *global* metric of the attractor surface, that is, whether the distance between any two real positions is reflected in the distance of the corresponding attractor representations. Such metric is distorted by bump drift. To graphically visualize what happens to a bump, we can look at **Figure 1C**; for each initial position, it is possible to follow the drift of the bump resulting from the turning off of the MF input and we can get an idea of the distortion the quasi-continuous attractor undergoes. This is expressed in **Figure 2F**, where the mean distance $<Dis>$ is shown between initial positions and positions reached after 10 iterations. Note that for a given network size distance $<Dis>$ tends to grow, approximately with the square root of the time elapsed since turning off the inputs (not shown), so those shown are not to be taken as the distances to any final, steady state position of the bump. Matching the trend of the spatial resolution, the average of the displacement drops to a value around 5 cm (one grid unit) for the largest network, but only for pre-wired connectivity with $\lambda = 1$. With $\lambda = 2$ $< Dis >$ is much larger, and in the case of the self-organized connectivity resulting from the simulated Hebbian process, the mean displacement is larger still, and not abated below about 16 cm (≈3 grid units), even for relatively large networks (the largest size was not used, because of the CPU time required). One can use in this case as guides to the eyes the logarithmic trends:

$$< Dis >= 6.2 - 1.3 \log_{10} \left(\frac{N_{CAs}}{\lambda^2} \right) \tag{13}$$

where one should note that the tuning width of the connectivity appears squared, λ^2, and still in order to fit the data for the self-organized network one has to use the larger effective value $\lambda = 5.0$. This leads to much larger extrapolated network sizes, beyond which global metric distortion vanishes, that is $<Dis> \sim 0$. One finds N_{CA3} ∼58,800 for the pre-wired network with finely tuned connectivity ($\lambda = 1$); N_{CA3} ∼235,000 with coarser connectivity ($\lambda = 2$); and N_{CA3} ∼1,470,000 with self-organized connectivity. The final positions in the self-organized network are considerably more displaced than those in the networks pre-wired with either λ value, and their mean displacement does not seem to decrease much with size (**Figure 2F**), not rapidly enough, at least, to become irrelevant to a real-life sized rodent CA3 network of a few hundred thousand units. This suggests therefore that, with Hebbian learning, the recurrent network self-organizes in a virtual space of its own, which maps into real space in a much more indirect, less accurate way than in the case of a pre-wired network, even though the mapping can be similarly precise. This global distortion is illustrated in **Figure 2C**, which shows that to nearby locations in real space correspond somewhat more distant bumps on the attractor, but to distant positions in space correspond much closer bumps, on average, on the attractor. The effect stems from the toroidal geometry, but it indicates that the global distortion is alleviated very slowly, when increasing the size of the network. Further, these results suggest that attractor drift may be an unavoidable feature of self-organized attractors.

RECURRENT CONNECTIONS CAN PRESERVE PART OF THE INPUT INFORMATION

The impression, conveyed by **Figures 2D–F**, of similarly precise spatial attractor codes expressed by networks with exponential weights and with weights shaped by learning, is confirmed by information measures. They are extracted from simulations, as described in the Methods (and see Cerasti and Treves, 2010), by decoding sub-samples of different sizes of CA3 units, randomly picked from the network, resulting in trends like those shown in **Figure 3A**. Those trends are fitted as detailed in Equation (9), yielding estimates of the average information I_1 conveyed

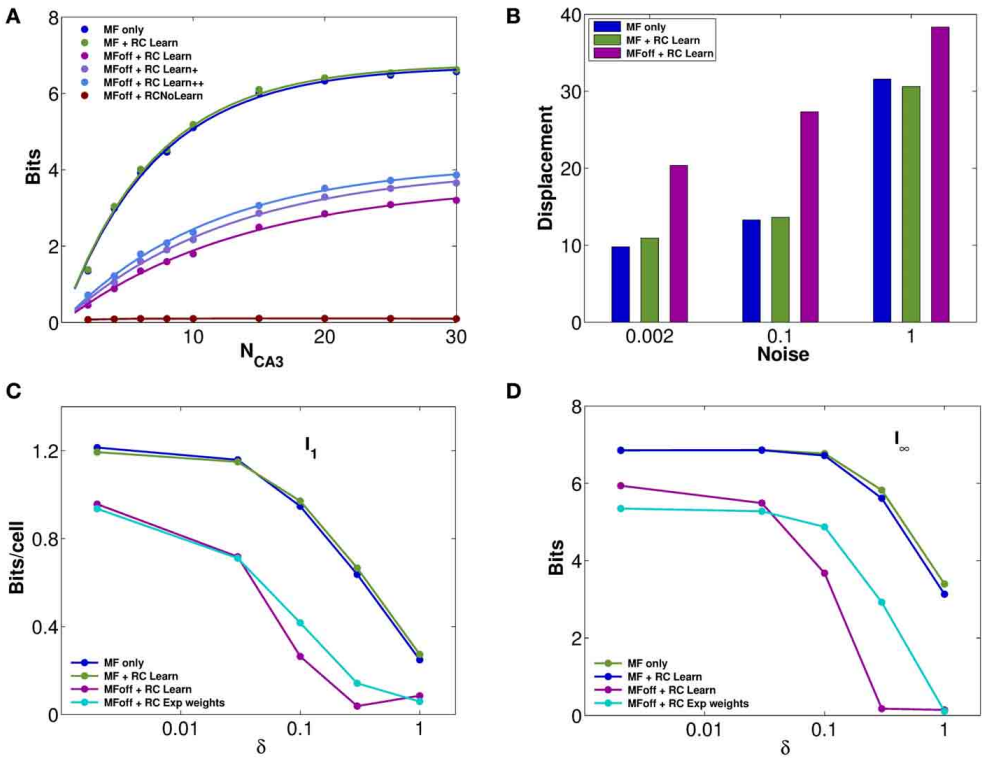

FIGURE 3 | Recurrent collaterals contribute little to the code, but sustain it, in part. (A) Information plotted versus the number of CA3 units in the sample. Fast noise $\delta = 0.1$. Blue curves refer to the DG-CA3 system without recurrent collaterals; adding the recurrent collaterals leads to the light green curves, and to the purple-light blue curves when mossy fiber inputs are turned off. The three purple to light blue curves refer to networks with DG inputs turned off, and recurrent connections self-organized with progressively more intense training, from bottom to top: simulations with 10,000 learning time steps and $\gamma = 0.0001$; with 10,000 training steps but $\gamma = 0.002$; and with $\gamma = 0.002$ but 20 × 10,000 training steps. The dark green curve (nearly flat) shows the spatial information present in the system when DG inputs are off, in the absence of any learning. **(B)** The bars show the mean displacement, as in **Figure 2F**, between the initial position and the final position for three values of fast noise, $\delta = 0.002$, $\delta = 0.1$, $\delta = 1$. Averages over 400,000 trials, started randomly in one of the 400 possible initial positions, while decoding samples of 10 CA3 units. The limited sample used in decoding results in a meaningful mean displacement also when the network is still driven by DG inputs. (**C** and **D**) Information plotted versus the fast noise δ values, on a semi-logarithmic scale, as measured by the slope parameter of the information curve I_1 **(C)** and by the saturation level I_8 (**D**; see text). Blue, light green, and purple curves as above. Cyan curves correspond also to DG inputs off, but for a network with standard pre-wired exponential weights.

by one unit, and of the information I_8 conveyed by the entire population. These estimates confirm that pre-wired networks do not encode a more informative map than self-organized ones, at least when fast noise (fast in the sense that it changes from one theta cycle to the next) is effectively absent (i.e., of the order of $\delta = 0.002$, the value used in **Figures 1**, **2**). **Figures 3C,D** shows, in fact, that the mutual information encoded by an exponential pre-wired connectivity, with inputs turned off (cyan lines) is similar the one encoded by a network with Hebbian weights (purple lines). It turns out, however, to be slightly more resistant to noise, so for larger noise values the pre-wired network is somewhat more informative (compare the cyan line with the purple line in **Figures 3C,D**.

A discrepancy then arises between what we might call the *precision* and the *accuracy* of self-organized spatial codes. The information results extend to a wider noise range the indication obtained with the resolution and clustering measures of **Figures 2D,F**, pointing at the reasonably precise spatial codes that can emerge from self-organizing weights. Their precision is comparable to that of the ones artificially wired with exact exponential connectivity. In contrast, the analysis of the distance between initial and final positions, i.e., the mean displacement in **Figure 2F**, indicates that self-organized codes are considerably less accurate, in mapping real space, than the pre-wired ones. In other words, distinct spatial positions are resolved to a similar degree for both codes, but while exponential connectivity minimizes drift, thus preserving distances, the self-organized one does not. The discrepancy can be conceptualized by stating that the attractor "manifold" established by Hebbian learning has a metric of its own, different from the one of real space, and much closer in nature, instead, to the rowdy metric established by DG inputs. **Figure 3B** in fact shows that our measure of displacement, if computed by decoding small ensembles of only 10 units, yields substantial values already for the spatial code produced by DG inputs alone. Adding reverberation along recurrent connections does not alter $<Dis>$ significantly. Once DG inputs are turned off, while a finely tuned prewired connectivity minimizes further drift by regularizing the attractor surface (not shown, but see **Figure 2F**), the self-organized connectivity adds substantial drift of its own (the higher purple bars in **Figure 3**, bottom right). An accurate metric map, however, is not necessary to maintain spatial knowledge in the network, with the result that the spatial information stored by the self-organized weights is not necessarily lower than with precisely wired weights. Such insight into the properties of these representations can be substantiated by applying information measures.

In terms of these measures, **Figure 3** further quantifies, in a network with self-organized recurrent connectivity, how different connections contribute to the amount of spatial information present in limited samples of CA3 units. Three different conditions can be contrasted. In the first, MF inputs are active, while RC activity enters only as random noise, as in Cerasti and Treves (2010), see **Table 1**; in the second, recurrent connections are added, with weights resulting from the learning process, and MF inputs are kept active; in the third condition, information is extracted from the CA3 population in the absence of DG inputs, from the self-organized attractor.

RC activity seems not to add information to the CA3 representation, when the input coming from the MFs is fully available, as shown in **Figures 3A–D** (cp. blue and green data, for the self-organized network). The same holds for the pre-wired network (not shown). One has to take into account the relative strength of the two inputs arriving to a CA3 cell: in fact, in the simulations shown here, the MF weights are much stronger than RC ones, with a total mean strength 5 times larger (averaged over the whole environment). However, a similar result holds even when the strength of RC weights is increased as much as to equal total mean MF strength (not shown). When the input is turned off, the scenario changes and RC activity is crucial. Recurrent connections are, in fact, able to convey information about the stored spatial representation, as it is clear from **Figures 3C,D**, provided the noise is not too high.

Considering the effect of learning strength, for a fixed level of noise, **Figure 3A** shows the corresponding information curves plotted versus CA3 sample size, in the case of $\delta = 0.1$. One can see the modest increase in the information due to a much higher learning rate, $\gamma = 0.002$, and to a much higher number of time steps, $20 \times 10{,}000$, in the model learning process. This indicates that protracted or intense learning (in terms of training time or learning rate) offers diminishing returns: most of the information structuring the attractor is acquired rapidly, even with minimal learning rates. The effect of the learning process on CA3 place fields can be seen in **Figure 4A**, where the firing maps in absence of MF inputs can be contrasted with the ones driven by them, with $\delta = 0.002$. When MF inputs are turned off, RC activity generates several new fields or amplifies existing ones, and suppresses others already present, usually the weaker ones. The fraction of CA3 units with at least one place field increases significantly, whereas the proportion of these with 2 or more fields does not change (**Figure 4B**). This effect could be tested experimentally in the real system.

MULTIPLE CHARTS LEAVE RESIDUAL SPATIAL INFORMATION

Having confirmed the ability of the RC network to retain spatial information about a given environment, we study how such information is affected by the storage of multiple "charts," i.e., representations of different environments. We allow the network, which in this case is comprised of 500 CA3 units, to store a different number of charts, each for an environment explored by the virtual rat for 3000 time steps. First, we consider the control case of exponential pre-wired efficacies (**Figures 5A,B**). In this case, all charts are encoded with equal strength. **Figure 5A** shows that a network of such limited size is overburdened already by the storage (i.e., the pre-wiring) of two charts: the mutual information that can be extracted about each from a given cell sample is below what can be extracted if only one chart is stored on the weights. There is a further decrease with the storage of four charts and, with six, the information in each of them is not more than what can be extracted about a chart that has *never* been stored. There is indeed significant information present in the network about positions in an environment that was not experienced in the simulations, and the amount becomes considerable when the noise level is low (**Figure 5B**). This apparently counterintuitive finding can be understood considering that information is not sensitive

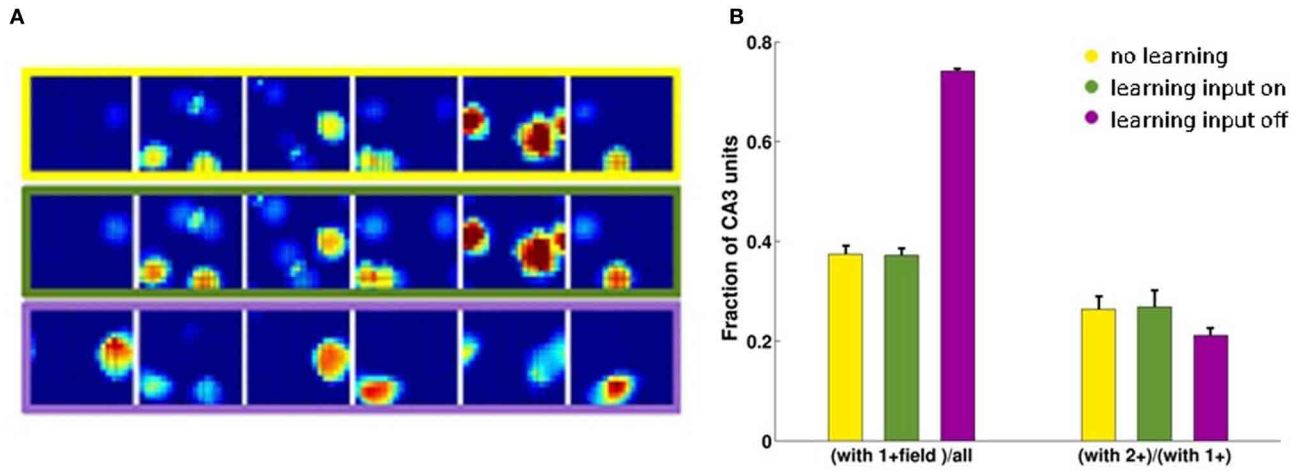

FIGURE 4 | CA3 place fields are refined by learning. Examples of CA3 firing maps in the DG-CA3 model network with MF and RC connections. **(A)** The top row shows CA3 place fields with no Hebbian learning; the middle row shows the same fields after learning; and the bottom row shows them after mossy fiber inputs are turned off. **(B)** Fraction of CA3 units with at least a place field (3-bars group on the left) and fraction of those with multiple fields among those with at least one (3-bars group on the right). Same color coding as in the frames of the **(A)**.

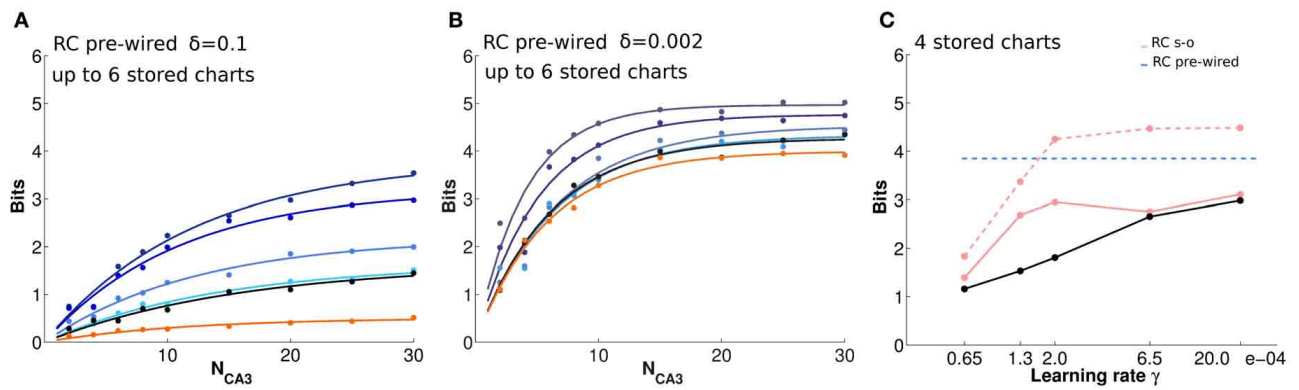

FIGURE 5 | The storage capacity for multiple charts is limited, but substantial residual information remains. (A and **B)** Information plotted versus the number of CA3 units in the sample, for a substantial noise level, $\delta = 0.1$ **(A)**, and for lower noise, $\delta = 0.002$ **(B)**. The two panels show the average amount of information retained through pre-wired recurrent collateral weights, in absence of the input, about position in one environment, after the storage of 1, 2, 4, and 6 charts, indicated by curves from purple to light blue, i.e., from top to bottom. The black curves indicate the amount of information retrieved through recurrent collaterals about a chart that had never been stored, when 6 other charts were learned, the "residual information." If no learning sessions had occurred, however, the curve would be flat at the bottom (not shown). The orange curve is the information retained after reshuffling synaptic weights, as explained in the text. Dots correspond to information values obtained from simulations, while the curves results from fits to the data points, as detailed in Methods. **(C)** Position information retrieved from the last (dashed pink) and first (pink) of 4 charts stored in a network with Hebbian learning, from 10 CA3 units, as a function of the learning rate. The dashed blue line is the reference level for 4 pre-wired charts. The black segments connect residual information datapoints. A full cue was provided to initiate retrieval. Limited plasticity (a small learning rate) is sufficient for effective storage of multiple chats, while increasing the rate, in this case beyond $\gamma = 0.0002$, adds only to the residual information.

to the logic of the mapping between actual position and position decoded from population activity, but solely to the precision of such mapping; it turns out, from our measures, that a precise mapping can be "inherited" from other charts.

This "residual" information is not due to specific encoding on the weights but to the disorder (or inhomogeneity) created in the network by cumulative encoding of other information of the same spatial nature. In fact, the information available when weights are set to their initial uniform values and no storage occurs at all is essentially at zero (not shown). Is any inhomogeneity in the weights sufficient to produce residual information, or is the weight distribution resulting from the storage of a spatial representation in any way special? To address this question, we reshuffled the weights produced by the storage of 6 charts, and again measured the amount of spatial information retrieved, either about that chart or about another, non-stored chart. The result is the same, and the corresponding curve (orange in **Figures 5A,B**) is below the amount of residual information, though for low values of noise (central panel) considerably above the vanishing amount present

with uniform weights. This indicates that a component of the residual information is merely due to the roughness of activity propagation in a recurrent network with generically inhomogeneous synaptic weights, while another component is due to the special spatial character of the inhomogeneity, due in turn to the storage of other charts, and not just to a sort of white noise. The difference between the two components probably lies in the variability of the distribution of weights presynaptic to any given unit, a point that requires further analysis.

These observations apply also to the case of self-organized representations. In this case, we run several simulations in which the network stores (self-organizes) representations of four different environments one after the other, and the degree of encoding is tested at the end for all charts, through decoding. The same length of exploration is used, but with different learning rates (**Figure 5C**). Obviously with such a procedure, the first chart to be stored is partially overwritten by the storage of successive charts; so that the amount of information about it is well below what can be retrieved about the last chart to be stored, especially with a high learning rate. For both, the encoding does not become stronger by using a learning rate above the intermediate value we used, $\gamma = 0.0002$, and information about the first and last chart "stabilizes" at amounts below and above the average across the four charts, which is roughly what can be retrieved from a pre-wired network (the horizontal line in **Figure 5C**; in the pre-wired case, obviously all charts are stored with statistically equal strength). This is the spatial equivalent of one-shot learning in episodic memory: virtually all there is to learn can be acquired with small modifications of the connection weights, and there is almost no return from more intense learning.

Interestingly, information about an environment that was never experienced, what we have called *residual* information, continues to grow a bit further with an increase in the learning rate, and approaches the amount relative to the first chart encoded for $\gamma = 0.00065$. From this rate of learning onward, the storage capacity of the network, with our parameters, is below 4 charts, and what is present about the first chart, which has been all but "forgotten," is just the residual information, which is however very substantial (when noise is low, $\delta = 0.002$).

This finding is broadly consistent with the notion, put forward over several years by Bruce McNaughton, that spatial charts are somehow prewired in the hippocampal system, and that spatial experience merely serves to associate locations in a pre-wired chart with configurations of sensory cues available in that location (Colgin et al., 2010). In McNaughton's view, the pre-existing chart is expressed by the path-integration system, which may well operate upstream of the hippocampus, e.g., in medial EC. Our model is not in conflict with this view, as it makes no distinction, in fact, between inputs to CA3 that relay path integration information vs. sensory information, e.g., between those on the medial vs. lateral perforant path that relay inputs from the medial and lateral EC to both DG and CA3. There is instead the distinction between (DG) inputs and recurrent connections. Still, the experimental evidence for the existence of prewired charts can be interpreted as also consistent with the considerable spatial information that, in a novel environment, may be available in recurrent weights modified by the charts of other environments—what we see in the model and have called residual information.

CONTEXT INFORMATION IS ALSO RETRIEVED AND PARTIALLY MAINTAINED IN THE ATTRACTOR

As we have discussed elsewhere (Stella et al., 2012), the specific contribution of the CA3 network can be argued to be in the formation of memories for specific spatio-temporal contexts, more than in retaining spatial information about a single context. So far we have quantified the amount of spatial information in one chart, either the only one or one among several stored concurrently, but one can also ask how much information the network can produce about which chart best matches the current environment, irrespective of exact position within it. Can CA3 tell a real rat not just where it is in one context, but also which context it is, among several competing possibilities? Can it retain this information in memory, and reactivate it from partial sensory cues? The question is made particularly relevant by the observation that the remarkable spatial code observed in the medial EC, expressed by grid cells, while providing exquisitely fine information about the position of the animal (Burak and Fiete, 2009) appears unable to discriminate between contexts (Fyhn et al., 2007).

We have addressed this question, again, by simulating the storage of 4 distinct charts, obtained by globally remapping the DG activity the drives the establishment of CA3 charts in the model, and again assessing both the representations activated by the inputs and those remaining active when the inputs are turned off. Self-organized charts can again be compared with those manually pre-wired.

Figure 6A shows that the model CA3 network can easily discriminate between 4 different contexts, even based on the activity of a limited sample of units, when DG inputs are still on. The discriminative capacity reaches close to the maximal value of 2 bits, irrespective of the noise level. When the inputs are turned off, the amount of retained context information becomes very sensitive to the noise level, and is minimal for relatively higher levels of noise. The interesting observation is that, for a given noise level, context information grows with the learning rate, which is intuitive, but only up to $\gamma = 0.0002$ (not shown); beyond that learning rate, less information can be retained the higher the learning rate. The three sets of mauve datapoints in **Figure 6A** correspond to the three larger learning rates of **Figure 5C**: $\gamma = 0.0002$, 0.00065, and 0.002 (see the legend of **Figure 6**). Thus multiplying the learning rate by 10, which brought no benefit to spatial information (**Figure 5C**), actually causes a loss of context information (**Figure 6A**). This is due to different charts collapsing onto each other, to some degree, so that individual fragments of one "stick" to those of another, and context discrimination is impaired. The model therefore suggests that self-organization cannot be "pushed" beyond its own limits: rather than smoothing out the granularity of the charts (which is there even when they are prewired) or stretching out their global metric (which is more

distorted in self-organized than in pre-wired charts) stronger self-organizations leads to gluing the charts with each other, like overcooked fettuccine.

Figure 6B shows which context is decoded from the activity of a sample of 10 units at successive positions along 300 time steps of a sample trajectory (when DG inputs are turned off): although the correct context is decoded more frequently than the other 3, the relative proportions are comparable, which makes the available context information low. **Figure 6C** shows one reason for such poor decoding performance: the overall activity of those 10 units, even when summed together, is sparse, in each of the 4 contexts. At many positions, there are no cells in the sample active, in a particular context. The other reason, of course, is related to the drift analysed previously. Interestingly, a pre-wired network appears to retain much less context information than a self-organized one, even when noise is low. This stands in contrast to the more accurate representation of spatial position expressed by the pre-wired network, and may be due to the way the pre-wiring procedure prevents the spontaneous development of context specific features of the spatial code.

DISCUSSION

The idealized notion of a continuous 2D attractor, a "chart," has been an important guide for theories of how the hippocampus operates in spatial memory (Samsonovich and McNaughton, 1997; Stringer and Rolls, 2002; Stringer et al., 2002; McNaughton et al., 2006). Simulating the formation of such charts in CA3, we find that what emerges is considerably distant from the idealized concept. Rather than "flaws" in the representation expressed by the network, the discrepancies from the ideal 2D spatial attractor point, in our view, at what CA3 is really meant to do: not merely recode spatial coordinates, but embed (some) spatial information into new memory representations.

We have compared a model network with self-organized connectivity with the control case of a network pre-wired with a connectivity dependent on the exact distance among the place fields produced by a randomizing dentate input, and focused on three distinct aspects to characterize CA3 attractors: their spatial precision; their accuracy; their informative content relative to one or more environments.

Networks of finite size cannot express a truly smooth continuous attractor manifold, but rather a quasi-continuous collection of discrete attractor points, characterized, in statistical physics parlance, as distinct valleys of the free-energy landscape. Left to their own recurrent dynamics, networks cannot settle into a pattern of activity that represents any possible position in space, but only a discrete, "granular" subset, leading to a decrease in spatial resolution; when driven by afferent inputs, the continuity is retrieved (Kali and Dayan, 2000). This "roughness of the free-energy," or imprecision in representing local continuity, had first been noted by Tsodyks and Sejnowski (1995), in a pre-wired one-dimensional model of a spatial attractor. Like Brunel and Trullier (1998), we find that also two-dimensional attractors "suffer" from these finite size effects; however, in both cases of pre-wired and self-organized networks, the roughness is seen to essentially disappear when reaching the size of a real rodent hippocampus (**Figures 2D–F**).

Moreover, the self-organization process turns out to be quite rapid (as in Nakazawa et al., 2003), effectively the spatial equivalent to one-shot learning in episodic memory: **Figure 3A** shows that more intense training brings very limited added value.

A pre-wired network with place fields regularly arranged on a grid would be much smoother, just like the entorhinal grid network, which is thought to express a single spatial representation (Fyhn et al., 2007) and to gradually smoothen it during development (McNaughton et al., 2006; Kropff and Treves, 2008). Such regular arrangement is however an artificial condition, particularly in the CA3 region, where providing strong, sparse and necessarily random inputs appears to be the raison d'être of the DG. Kali and Dayan (2000) consider a pre-wired and a self-organizing recurrent CA3 network like ours, and they also come to the conclusion that self-organized attractor manifolds can be similarly smooth as those determined by suitable pre-wired connectivity.

A second, conceptually distinct discrepancy from the idealized notion of a true representation of space is in the global geometry of the attractor manifold. This can be quantified indirectly by measuring the mean drift, i.e., the displacement, of the position decoded by the activity in the network from the position provided as input, which can be referred to as *global distortion* or *metric distortion*. In this respect, a self-organized attractor is considerably more distorted than a pre-wired one. Kali and Dayan (2000) discuss how the global distortion resulting from grossly uneven sampling of the environment can be effectively removed by modulating synaptic changes by a familiarity factor, which essentially reduces learning in areas that have been oversampled by the real or the virtual rat—typically, those at the center of the arena. The point they make is susceptible of experimental validation. In our simulation paradigm, however, the periodic boundary conditions do not give rise to gross oversampling of particular areas, so the global distortion in the attractor representation does not arise from that, but from random fluctuations. We find that the effect of such random fluctuations is not abated, as it might have been expected, in large self-organizing networks, which remain much more globally distorted than pre-wired networks in their spatial representations. Real-life networks may then suffer from a degree of metric distortion similar to the one observed here in a reduced model, although it is possible that the distortion be attenuated by additional mechanisms not considered here, such as short-term gain enhancement or synaptic facilitation (Roudi and Treves, 2008; Itskov et al., 2011). It could well be, as recently hypothesized by Romani and Tsodyks (2010), that the tendency to drift is expressed also as a propensity to replay and even preplay spatial trajectories, as observed in many experiments (e.g., Wilson and McNaughton, 1994; Foster and Wilson, 2006; Diba and Buzsáki, 2007; Karlsson and Frank, 2009; Dragoi and Tonegawa, 2010; Gupta et al., 2010). Replay would not reflect purposeful "thoughts" but rather uncontrolled drift along a randomly self-organized chart, whether relative to

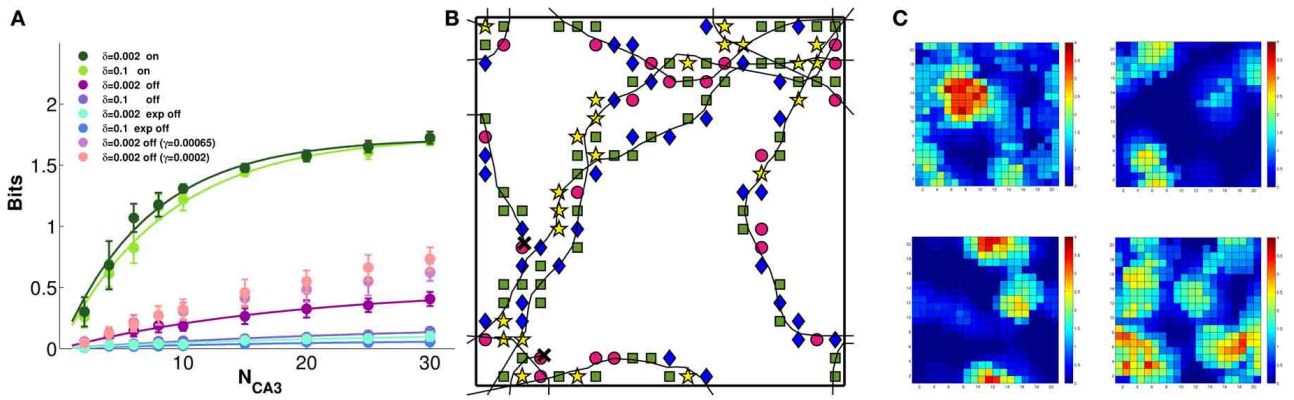

FIGURE 6 | Some context discrimination remains in memory, if self-organization is limited. The amount of information about which of 4 distinct environments is reflected in the DG inputs is extracted from subsamples of CA3 model units. **(A)** Decoding the activity driven by the inputs allows for good discrimination (the green curves, which are fitted to the data points as before), irrespective of noise. Turning the inputs off greatly reduces the context information retained in all cases, but more information remains when the network is allowed to self-organize, and noise is very low (purple curve). In contrast, pre-wired connectivity appears not to be suitable for context discrimination (light and dark blue curves). Importantly, context information decreases with more plasticity (pink to purple datapoints, top to bottom), indicating progressive attractor collapse. **(B)** A sample 300-time-step trajectory, with the environment decoded at each position, from a random sample of 10 units, shown by a different symbol (the green square is the correct environment). Some of the locations are superimposed on the 10 × 10 grid used for decoding. **(C)** The cumulated activity of the 10 units in each of the 4 environments, plotted in pseudo-colors. The correct environment is top left. Typically 3–4 of the units have a field in each environment, occasionally a double field. Hence overall activity remains sparse.

the current environment or residual from a previous environment. The difficulty with which (rapidly) self-organized representations come to reproduce global geometry contrasts with the beautiful, long-distance encoding of geometry by entorhinal grid cells (Hafting et al., 2005) which, again, presumably requires long developmental times to be established (Kropff and Treves, 2008). Once more, it appears how the CA3 network is not ideally suited to compute spatial relations *per se*, but rather to encode in memory spatial relations already computed upstream.

The spatial code expressed in the attractor is made inaccurate anyway by sampling only a small fragment of the entire population vector, as is the case with experimental recordings (Wilson and McNaughton, 1993). In fact, **Figure 3B** shows that populations of limited size are already quite inaccurate in the presence of the inputs, so that turning off the inputs, and letting activity to be sustained by the attractor, brings about only an additional degradation (e.g., doubling the mean displacement). In the light of our context information analysis, inaccurate spatial codes appear as a small price to pay in order to form arbitrary episodic memories with spatial content. In our simplified model, non-spatial aspects of such memories are not included explicitly, but still their episodic character emerges indirectly from the difference between the full and simplified localization matrices, the "dark information" discussed by Cerasti and Treves (2010).

The third dimension of discrepancy from the idealized notion requires, to be appreciated, information measures. Compared to the control, pre-wired network, **Figures 3C,D** show that a single environment can be encoded, in information terms, just as well with a self-organizing chart. Ideally, however, it should be possible to store multiple independent spatial attractors in the same recurrent network, to represent distinct environments with complete remapping from one to the other (Leutgeb et al., 2005), up to a capacity limit which has been studied analytically by Battaglia and Treves (1998). In our study, with the parameters we use and with the extra disorder of the irregular arrangement of the DG-induced fields, it appears that the weight modifications that encode a new chart, comprised of the cumulative granular "memory" of many different positions in the environment, are sufficient to almost wash out the information about a different environment learned in a previous session, even the one before. We say "almost," because of a paradoxical counter-effect. We find, in fact, that the network still encodes residual information about charts it has effectively "forgotten," and even about charts it has never stored in memory. Such "residual information" is limited when the noise, i.e., the temporal variability, is high (**Figure 5A**), but still it has to be taken into account when using decoding procedures also with real data. This effect can be explained by considering that, unlike temporal variability (noise), fixed or "quenched" spatial variability (disorder) causes reproducibility, which counter-intuitively confers information also to a random neuronal code. A component of this information even survives the reshuffling of all the synaptic weights.

Our overall conclusion is that, as a memory network, CA3 is clumsy at handling spatial information. If this runs against the intuition accrued from experiments, it may be because many of those experiments do not really probe memory function: they assess CA3 activity largely with "the inputs on." It is unclear to what extent DG inputs are reduced, during free exploration and foraging, even at their lowest theta phase. Nevertheless, it is important to analyze attractor dynamics as a function of theta phase, as in the study revealing brief, theta-paced "flickering"

memory dynamics in CA3 (Jezek et al., 2011). Even more important is to look at the information putatively retrieved from CA3 during sharp wave ripples (SWR). SWR events are thought to originate in CA3, presumably with no need for the dentate to trigger them with spatial information. Their statistical character is very different from what is observed during theta-modulated states, and they may have to do more with long-term memory formation elsewhere than with the active short-term retention of spatial information in hippocampal networks (Hoffman et al., 2007). They may be suited, therefore, to characterize attractors formed in CA3 during theta-modulated spatial exploration (Nakazawa et al., 2003).

ACKNOWLEDGMENTS

We are grateful for insightful discussions to Edmund Rolls, Kate Jeffery, and the whole Spacebrain collaboration.

REFERENCES

Battaglia, F. P., and Treves, A. (1998). Attractor neural networks storing multiple space representations: a model for hippocampal place fields. *Phys. Rev. E* 58, 7738–7753. doi: 10.1103/PhysRevE.58.7738

Brunel, N., and Trullier, O. (1998). Plasticity of directional place fields in a model of rodent CA3. *Hippocampus* 8, 651–665.

Burak, Y., and Fiete, I. R. (2009). Accurate path integration in continuous attractor network models of grid cells. *PLoS Comput. Biol.* 5:e1000291. doi: 10.1371/journal.pcbi.1000291

Cerasti, E., and Treves, A. (2010). How informative are spatial CA3 representations established by the dentate gyrus? *PLoS Comput. Biol.* 6:e1000759. doi: 10.1371/journal.pcbi.1000759

Chawla, M. K., Guzowski, J. F., Ramirez-Amaya, V., Lipa, P., Hoffman, K. L., Marriott, L. K., et al. (2005). Sparse, environmentally selective expression of arc rna in the upper blade of the rodent fascia dentata by brief spatial experience. *Hippocampus* 15, 579–586. doi: 10.1002/hipo.20091

Colgin, L. L., Leutgeb, S., Jezek, K., Leutgeb, J. K., Moser, E. I., McNaughton, B. L., et al. (2010). Attractor-map versus autoassociation based attractor dynamics in the hippocampal network. *J. Neurophysiol.* 104, 35–50. doi: 10.1152/jn.00202.2010

Diba, K., and Buzsáki, G. (2007). Forward and reverse hippocampal place-cell sequences during ripples. *Nat. Neurosci.* 10, 1241–1242. doi: 10.1038/nn1961

Dragoi, G., and Tonegawa, S. (2010). Prepay of future place cell sequences by hippocampal cellular assemblies. *Nature* 469, 397–401. doi: 10.1038/nature09633

Foster, D. J., and Wilson, M. A. (2006). Reverse replay of behavioural sequences in hippocampal place cells during the awake state. *Nature* 440, 680–683. doi: 10.1038/nature04587

Fyhn, M., Hafting, T., Treves, A., Moser, M. B., and Moser, E. I. (2007). Hippocampal remapping and grid realignment in entorhinal cortex. *Nature* 446, 190–194. doi: 10.1038/nature05601

Gupta, A. S., van der Meer, M. A., Touretzky, D. S., and Redish, A. D. (2010). Hippocampal replay is not a simple function of experience. *Neuron* 65, 695–705. doi: 10.1016/j.neuron.2010.01.034

Hafting, T., Fyhn, M., Molden, S., Moser, M. B., and Moser, E. I. (2005). Microstructure of a spatial map in the entorhinal cortex. *Science* 436, 801–806.

Hamaguchi, K., and Hatchett, J. P. L. (2006). Analytic solution of neural network with disordered lateral inhibition. *Phys. Rev. E Stat. Nonlin. Soft Matter Phys.* 73:051104. doi: 10.1103/PhysRevE.73.051104

Hoffman, K. L., Battaglia, F. P., Harris, K., MacLean, J. N., Marshall, L., and Mehta, M. R. (2007). The upshot of Up states in the neocortex: from slow oscillations to memory formation. *J. Neurosci.* 27, 11838–11841. doi: 10.1523/JNEUROSCI.3501-07.2007

Itskov, V., Hansel, D., and Tsodyks, M. (2011). Short-term facilitation may stabilize parametric working memory trace. *Front. Comput. Neurosci.* 5:40. doi: 10.3389/fncom.2011.00040

Jezek, K., Henriksen, E. J., Treves, A., Moser, E. I., and Moser, M.-B. (2011). Theta-paced flickering between place-cell maps in the hippocampus. *Nature* 478, 246–249. 246. doi: 10.1038/nature10439

Kali, S., and Dayan, P. (2000). The involvement of recurrent connections in area CA3 in establishing the properties of place fields: a model. *J. Neurosci.* 20, 7463–7477.

Karlsson, M. P., and Frank, L. M. (2009). Awake replay of remote experiences in the hippocampus. *Nat. Neurosci.* 12, 913–918. doi: 10.1038/nn.2344

Kropff, E., and Treves, A. (2008). The emergence of grid cells: intelligent design or just adaptation? *Hippocampus* 18, 1256–1269. doi: 10.1002/hipo.20520

Lassalle, J. M., Bataille, T., and Halley, H. (2000). Reversible inactivation of the hippocampal mossy fiber synapses in mice impairs spatial learning, but neither consolidation nor memory retrieval, in the Morris navigation task. *Neurobiol. Learn. Mem.* 73, 243–257. doi: 10.1006/nlme.1999.3931

Lee, I., and Kesner, R. P. (2004). Encoding versus retrieval of spatial memory: double dissociation between the dentate gyrus and the perforant path inputs into CA3 in the dorsal hippocampus. *Hippocampus* 14, 66–76. doi: 10.1002/hipo.10167

Leutgeb, S., Leutgeb, J. K., Barnes, C. A., Moser, E. I., McNaughton, B. L., and Moser, M. (2005). Independent codes for spatial and episodic memory in hippocampal neuronal ensembles. *Science* 309, 619–623. doi: 10.1126/science.1114037

Leutgeb, J. K., Leutgeb, S., Moser, M. B., and Moser, E. I. (2007). Pattern separation in the dentate gyrus and CA3 of the hippocampus. *Science* 315, 961–966. doi: 10.1126/science.1135801

McNaughton, B. L., Barnes, C. A., Meltzer, J., and Sutherland, R. J. (1989). Hippocampal granule cells are necessary for normal spatial learning but not for spatially-selective pyramidal cell discharge. *Exp. Brain Res.* 76, 485–496. doi: 10.1007/BF00248904

McNaughton, B. L., Battaglia, F. P., Jensen, O., Moser, E. I., and Moser, M.-B. (2006). Path integration and the neural basis of the 'cognitive map'. *Nat. Rev. Neurosci.* 7, 663–678. doi: 10.1038/nrn1932

McNaughton, B. L., and Morris, R. G. M. (1987). Hippocampal synaptic enhancement and information storage within a distributed memory system. *Trends Neurosci.* 10, 408–415. doi: 10.1016/0166-2236(87)90011-7

Nakazawa, K., Sun, L. D., Quirk, M. C., Rondi-Reig, L., Wilson, M. A., and Tonegawa, S. (2003). Hippocampal CA3 NMDA receptors are crucial for memory acquisition of one-time experience. *Neuron* 38, 305–315. doi: 10.1016/S0896-6273(03)00165-X

Panzeri, S., Treves, A., Schultz, S., and Rolls, E. T. (1999). On decoding the responses of a population of neurons from short time windows. *Neural Comput.* 11, 1553–1577. doi: 10.1162/089976699300016142

Papp, G., Witter, M. P., and Treves, A. (2007). The CA3 network as a memory store for spatial representations. *Learn. Mem.* 14, 732–744. doi: 10.1101/lm.687407

Rolls, E. T., Treves, A., and Tovee, M. J. (1997). The representational capacity of the distributed encoding of information provided by populations of neurons in primate temporal visual cortex. *Exp. Brain Res.* 114, 149–162. doi: 10.1007/PL00005615

Romani, S., and Tsodyks, M. (2010). Unified model of place fields and memory-related activity in the hippocampus. *FENS Abstr.* 130.69.

Roudi, Y., and Treves, A. (2008). Representing where along with what information in a model of a cortical patch. *PLoS Comput. Biol.* 4:e1000012. doi: 10.1371/journal.pcbi.1000012

Samengo, I., and Treves, A. (2000). Representational capacity of a set of independent neurons. *Phys. Rev. E Stat. Nonlin. Soft Matter Phys.* 63:011910.

Samsonovich, A., and McNaughton, B. L. (1997). Path integration and cognitive mapping in a continuous

attractor neural network model. *J. Neurosci.* 17, 5900–5920.

Stringer, S. M., and Rolls, E. T. (2002). Invariant object recognition in the visual system with novel views of 3D objects. *Neural Comput.* 14, 2585–2596. doi: 10.1162/089976602760407982

Stringer, S. M., Rolls, E. T., Trappenberg, T. P., and de Araujo, I. E. T. (2002). Self-organizing continuous attractor networks and path integration: two-dimensional models of place cells. *Network* 13, 429–446. doi: 10.1088/0954-898X/13/4/301

Stella, F., Cerasti, E., Si, B., Jezek, K., and Treves, A. (2012). Self-organization of multiple spatial and context memories in the hippocampus. *Neurosci. Biobehav. Rev.* 36, 1609–1625. doi: 10.1016/j.neubiorev.2011.12.002

Treves, A. (1990). Graded-response neurons and information encodings in autoassociative memories. *Phys. Rev. A* 42, 2418–2430. doi: 10.1103/PhysRevA.42.2418

Treves, A., and Panzeri, S. (1995). The upward bias in measures of information derived from limited data samples. *Neural Comput.* 7, 399–407. doi: 10.1162/neco.1995.7.2.399

Treves, A., and Rolls, E. T. (1992). Computational constraints suggest the need for two distinct input systems to the hippocampal CA3 network. *Hippocampus* 2, 189–199. doi: 10.1002/hipo.450020209

Tsodyks, M. V., and Sejnowski, T. (1995). Associative memory and hippocampal place cells. *Int. J. Neural Syst.* 6, 81–86.

Wilson, M. A., and McNaughton, B. L. (1993). Dynamics of the hippocampal ensemble code for space. *Science* 261, 1055–1058. doi: 10.1126/science.8351520

Wilson, M. A., and McNaughton, B. L. (1994). Reactivation of hippocampal ensemble memories during sleep. *Science* 265, 676–679. doi: 10.1126/science.8036517

Conflict of Interest Statement: The authors declare that the research was conducted in the absence of any commercial or financial relationships that could be construed as a potential conflict of interest.

Received: 30 March 2013; accepted: 26 June 2013; published online: 16 July 2013.

Citation: Cerasti E and Treves A (2013) The spatial representations acquired in CA3 by self-organizing recurrent connections. Front. Cell. Neurosci. 7:112. doi: 10.3389/fncel.2013.00112

frontiers in
CELLULAR NEUROSCIENCE

REVIEW ARTICLE
published: 04 March 2014
doi: 10.3389/fncel.2014.00064

Human neuroimaging studies on the hippocampal CA3 region – integrating evidence for pattern separation and completion

***Lorena Deuker*[1,2]*, *Christian F. Doeller*[2], *Juergen Fell*[1] and *Nikolai Axmacher*[1,3]**

[1] *Department of Epileptology, University of Bonn, Bonn, Germany*
[2] *Donders Institute for Brain, Cognition and Behaviour, Radboud University Nijmegen, Nijmegen, Netherlands*
[3] *German Center for Neurodegenerative Diseases, Bonn, Germany*

Edited by:
Richard Miles, Institut pour le Cerveau et la Moëlle Epinière, France

Reviewed by:
Enrico Cherubini, International School for Advanced Studies, Italy
Richard Miles, Institut pour le Cerveau et la Moëlle Epinière, France

***Correspondence:**
Lorena Deuker, Donders Institute for Brain, Cognition and Behaviour, Radboud University Nijmegen, Kapittelweg 29, 6525 EN Nijmegen, Netherlands
e-mail: lorenadeuker@gmail.com

Human functional magnetic resonance imaging (fMRI) studies have long investigated the hippocampus without differentiating between its subfields, even though theoretical models and rodent studies suggest that subfields support different and potentially even opposite functions. The CA3 region of the hippocampus has been ascribed a pivotal role both in initially forming associations during encoding and in reconstructing a memory representation based on partial cues during retrieval. These functions have been related to pattern separation and pattern completion, respectively. In recent years, studies using high-resolution fMRI in humans have begun to separate different hippocampal subregions and identify the role of the CA3 subregion relative to the other subregions. However, some of these findings have been inconsistent with theoretical models and findings from electrophysiology. In this review, we describe selected recent studies and highlight how their results might help to define different processes and functions that are presumably carried out by the CA3 region, in particular regarding the seemingly opposing functions of pattern separation and pattern completion. We also describe how these subfield-specific processes are related to behavioral, functional and structural alterations in patients with mild cognitive impairment and Alzheimer's disease. We conclude with discussing limitations of functional imaging and briefly outline possible future developments of the field.

Keywords: high-resolution fMRI, hippocampus, CA3, pattern separation, pattern completion

INTRODUCTION

The hippocampus is something of a lodestone for functional imaging studies in human memory research. Thousands of articles have been published investigating the exact role of the hippocampus (a Pubmed search on October 3rd 2013 for "hippocampus AND human AND memory AND fMRI" returned 2366 results). However, in addition to methodological shortcomings inherent to functional magnetic resonance imaging (fMRI) such as the indirect relationship to neuronal activity and the relatively low signal-to-noise ratio (SNR) and significant susceptibility artifacts in this region (Ojemann et al., 1997; Schacter and Wagner, 1999), many of these studies might also implicitly accept a flawed premise: That the hippocampus is a functional unit, and as such can be imaged and analyzed as a whole.

Everything we know from *in vitro* and animal studies points in the opposite direction. Not only is the hippocampus histologically heterogeneous, but electrophysiological recordings in subfields of the rodent hippocampus suggest a functional dissociation, and circumscribed lesions produce dissociable deficits (Lee and Kesner, 2004a; Lee et al., 2005; Andersen et al., 2006). Some of the hippocampal subfields might even be involved in contrary operations, which could easily lead to null results or opposite conclusions across studies.

Some studies in humans acknowledge a possible functional heterogeneity by considering the anterior and posterior hippocampus differentially (e.g., Ludowig et al., 2008; Chen et al., 2010; Libby et al., 2012; Poppenk et al., 2013), which in rodents maps onto the ventral-to-dorsal axis (Fanselow and Dong, 2010). However, the different subregions of the hippocampus (such as dentate gyrus (DG), and cornu ammonis (CA) regions CA3 and then CA1) extend along the longitudinal axis of the hippocampus and are still collapsed together in these analyses. As this review centers on region CA3, long-axis differentiation (see e.g., Moser and Moser, 1998; Poppenk et al., 2013) will not be further discussed here.

Theoretical models of the function of hippocampal subfields (see **Figure 1** for an overview of the structure) propose that during encoding, CA3 receives sparse, orthogonalized input via the mossy fibers from the DG, an area that in turn receives multimodal input from the entorhinal cortex (ERC; e.g., Lörincz and Buzsáki, 2000; van Strien et al., 2009). Orthogonalization here refers to

Abbreviations: AD, Alzheimer's disease; aMCI, amnesic mild cognitive impairment; BOLD, blood oxygen level dependent; CA, cornu ammonis; DG, dentate gyrus; DMS, delayed matching-to-sample; EEG, electroencephalography; ERC, entorhinal cortex; fMRI, functional magnetic resonance imaging; GLM, general linear model; MCI, mild cognitive impairment; MTL, medial temporal lobe; MVPA, multi-voxel pattern analysis; PHC, parahippocampal cortex; PRC, perirhinal cortex; SNR, signal-to-noise ratio; SUB, subiculum.

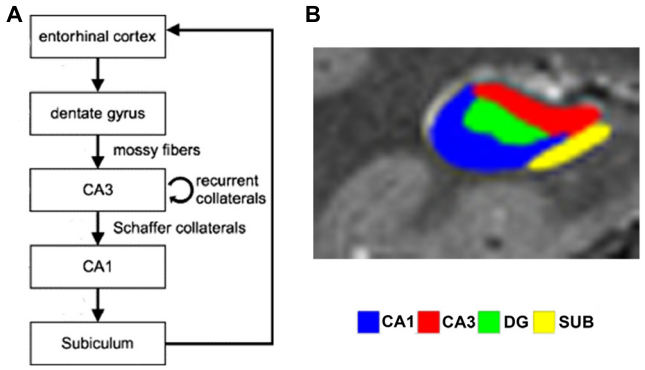

FIGURE 1 | (A) Simplified schematic depiction of entorhinal cortex and hippocampal subfields circuitry (modified from Axmacher et al., 2006). In the trisynaptic loop, the dentate gyrus receives input from entorhinal cortex via the perforant path and relays this to CA3 via the mossy fibers. CA3 transfers information to CA1 via Schaffer collaterals, which in turn projects to the subiculum, which routes back to entorhinal cortex. **(B)** Segmented high-resolution fMRI scan showing the different subfields (reproduced with permission from Bonnici et al., 2012).

a theoretical process by which neural patterns are rendered even more dissimilar than they originally were. In CA3, dense recurrent connections are hypothesized to promote rapid conjunctive representations of arbitrary coactive elements – i.e., of elements that are experienced together, but have not been previously linked to each other (Kesner et al., 2008). These anatomical properties are ideally suited to allow CA3 to effectively act as an autoassociative network (Grossberg, 1971; McClelland and Rumelhart, 1985; McNaughton and Morris, 1987). After encoding, CA3 is thought to be able to use a partial or degraded input pattern as a cue to retrieve and complete previously established memory traces, e.g., to retrieve an associated pair from one element of the pair only (O'Reilly and McClelland, 1994; Norman and O'Reilly, 2003; Kesner and Hopkins, 2006), a process called pattern completion (McNaughton and Morris, 1987; McClelland and Goddard, 1996; Colgin et al., 2008). Pattern separation, on the other hand, is the putative computational mechanism which renders partly overlapping neuronal patterns more dissimilar and thus prevents interference and allows novelty detection (Treves and Rolls, 1992; McClelland and Goddard, 1996; O'Reilly and Rudy, 2001). Hence, successful pattern completion depends on previous pattern separation. In other words, a sufficient separation of putatively interfering patterns is a necessary prerequisite for later accurate pattern completion. Rodent studies show that CA3 may promote both pattern completion and pattern separation depending on the degree of similarity or dissimilarity between contexts or learning material (Guzowski et al., 2004; see **Figure 2**). It has been proposed that CA1, in turn, uses the retrieved information from CA3 to compare it to perceptual input from the ERC, acting as a match/mismatch detector between CA3 predictions and EC perceptual input (Jensen and Lisman, 1996; Lee et al., 2004b; Lisman and Grace, 2005; Colgin et al., 2009).

A closer look at the experimental literature on *human* hippocampal subfield functions reveals a gap between these elaborate theoretical and computational models and electrophysiological results on the one hand and what has actually been confirmed in studies in humans on the other. This is mainly because, until recently, the vast majority of fMRI studies collapsed across these different subregions. This lack of discrimination with regard to hippocampal subfields in humans is due to the sheer difficulty to accurately differentiate subfields based on fMRI data in humans. The hippocampus is a relatively small structure, and its subfields are even smaller (on the order of only a few millimeters, with regions CA1, CA2 and CA3 together having an average volume of around 1 cm^3; see Malykhin et al., 2010). Standard 1.5T or 3T MRI with isotropic voxel sizes of 3–5 mm does not have the resolution to allow for reliable delineation of subfields. Intracranial electroencephalography (EEG) recordings, as they can for example be conducted in epilepsy patients, also cannot contribute because electrode positions usually cannot be determined with the necessary precision – and even if they could, the recorded electric fields are not restricted to the direct vicinity of an electrode, but likely reflect signals from more than one subfield. Microelectrodes have recently been employed in addition to clinically used macroelectrodes, and they record from small areas; often, single-cell activity can be identified (e.g., Suthana and Fried, 2012). However, the position of these microelectrodes often cannot be accurately ascribed to a specific subfield.

In the last decade, more powerful MR scanners with strong magnetic fields of 7T and beyond have become available. Together with scanning parameters specifically optimized for imaging medial temporal lobe structures (Weiskopf et al., 2006; Bakker et al., 2008; Doeller et al., 2008, 2010; Ekstrom et al., 2009; Bonnici et al., 2012), notorious for signal dropouts and low SNR, some studies have successfully extracted functional activity from hippocampal subfields. Another promising approach is the collection of multiple high-resolution structural scans and averaging them together for better signal quality (Bonnici et al., 2012; Newmark et al., 2013). Segmentation is most often done manually, based on specific landmarks (e.g., as described in Duvernoy, 2005) and can become difficult in the head and tail of the hippocampus. Therefore, only the body is segmented in many studies, while others do segmentation along the entire length. This can lead to differences across studies with regard to volumetry and to a skewed representation of subfields: the proportion of DG volume is lower in anterior than in posterior hippocampus whereas the proportion of CA1, CA2 and CA3 volume is higher in anterior than posterior hippocampus (Malykhin et al., 2010; Poppenk et al., 2013). Coregistration of subfields across participants is still a challenge, even though toolboxes have become available in the last years (e.g., ROI-AL, http://darwin.bio.uci.edu/~cestark/roial; see Yassa and Stark, 2009 for a review). Also, separation of CA3 from DG remains difficult and the two subregions are often collapsed, even though there is good reason to assume that they support different functions. However, some studies report reliable separation of CA3 from DG (Bonnici et al., 2012; Wisse et al., 2012). Recently, an initiative to standardize the procedures for subfield delineation has been founded, which will hopefully move the field towards studies with more easily comparable results (www.hippocampalsubfields.com).

In this review, we first summarize selected fMRI studies that aimed to differentiate between hippocampal subregions in healthy

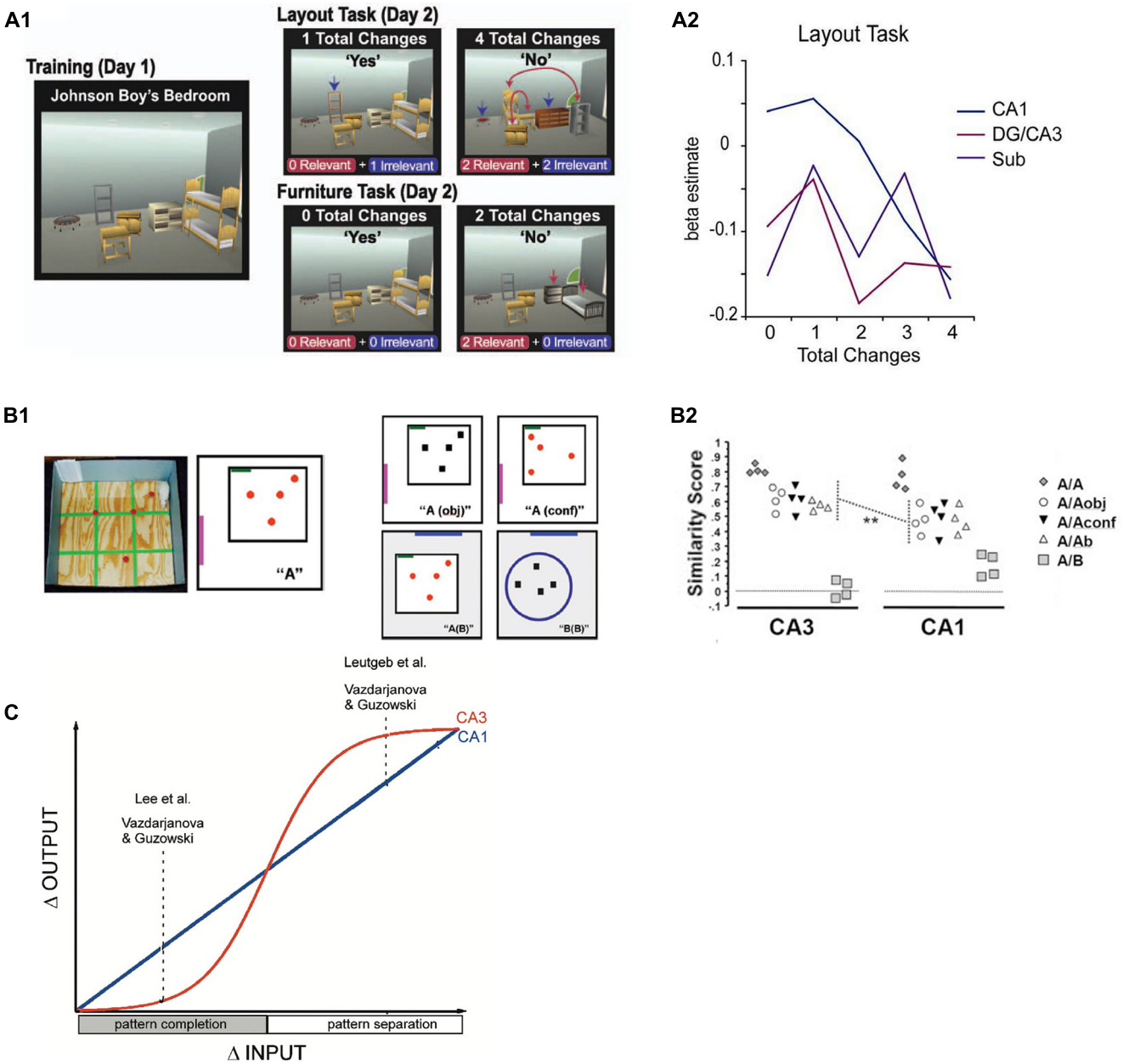

FIGURE 2 | (A) Design **(A1)** and results **(A2)** from a functional MRI study in humans (Duncan et al., 2012) in which participants were confronted with different numbers of relevant or irrelevant changes to highly familiar virtual room layouts. Whereas a more linear signal decrease with increasing number of changes was observed in CA1, there was a more sudden, step-like decrease of activity in DG/CA3. Reproduced with permission from Duncan et al. (2012), Copyright © 2011 Wiley Periodicals Inc. **(B)** Design **(B1)** and results **(B2)** from a study in rats (Vazdarjanova and Guzowski, 2004) that investigated the degree of overlap between neuronal ensembles that were active during a training environment **(A)** and a later test environment that was either identical (A/A), increasingly dissimilar (A/Aobj, A/Aconf and A/Ab), or completely different (A/B). Again, CA1 ensembles show linearly decreasing overlap (as captured by a similarity score) with increasing dissimilarity between training and test environment, whereas CA3 ensemble overlap remains fairly high and only drops rapidly in the most dissimilar condition. Reproduced with permission from Vazdarjanova and Guzowski (2004). **(C)** Schematic depiction of the results of three studies in rodents (Guzowski et al., 2004) in which a similar behavior as found in the Duncan et al. (2012) study is described: CA1 output changes linearly with increasing changes in input patterns, while CA3 changes its output more in a sigmoidal fashion (i.e., when a specific threshold is crossed), indicating a transition between pattern completion and pattern separation. Reproduced with permission from Guzowski et al. (2004).

participants. We discuss how these studies contribute to testing the theoretical models outlined above in terms of the processes thought to be performed by the CA3 subregion. We focus on CA3 and mention results on other subregions only where necessary for understanding the specific role of CA3. We then consider investigations in patient populations with subfield-specific damage. Finally, we conclude by discussing future developments which could potentially allow us to investigate the CA3 region in greater detail – possibly even resolving different subparts of this region. **Table 1** provides an overview of the main findings in selected recent studies and the subfields that have been delineated in them.

FUNCTIONAL IMAGING IN HEALTHY PARTICIPANTS

As mentioned above, a wealth of theories about the role of hippocampal subfields for memory exist (Marr, 1971; McNaughton and Morris, 1987; Treves and Rolls, 1992; McClelland and Goddard, 1996), in particular on the role of CA3. The most prevalent assumptions can be summarized as follows: (1) CA3 is important for memory encoding, (2) during encoding, CA3 processes orthogonalized input that likely is a result of pattern separation processes in DG and further supports pattern separation of these relatively dissimilar inputs, (3) CA3 promotes binding of dissociated elements, and during retrieval uses parts of a pattern to retrieve the entire pattern (pattern completion). In the following, we consider how recent studies in humans have contributed to shedding more light on these predictions.

CA3 IS IMPORTANT FOR MEMORY ENCODING

It has long been established that the hippocampus per se is critically important for memory formation (Scoville and Milner, 1957). But does subregion CA3 play a special role in encoding? As has been reviewed before (Carr et al., 2010a), some high-resolution studies on the hippocampus have found evidence that CA3 is more involved in encoding than retrieval (Zeineh et al., 2003; Suthana et al., 2011). Alternatively, it was shown that CA3 is more involved in encoding than other hippocampal subregions are. For example, a subsequent memory paradigm revealed that CA2/3/DG but not subiculum (SUB) predicted later memory success for pairs of line-drawing objects (Eldridge et al., 2005). In a delayed matching to sample (DMS) study, increased CA2/3/DG activity was observed during the sample and early delay phase (i.e., encoding related phases), whereas CA1 was more active during the delay and the test phase (Olsen et al., 2009). A more recent study found a subsequent memory effect in DG/CA2/3 that could not be detected in CA1 (Carr et al., 2013). However, some studies also find that encoding and novelty detection are not restricted to CA3 (Chen et al., 2011; Duncan et al., 2012).

It should be noted that in these studies, the fMRI signal from a combined region of CA2, CA3 and DG (CA2/3/DG) was analyzed, which limits interpretation. Also, the time between encoding and retrieval differs vastly, from 30 s (Olsen et al., 2009) to a week (Carr et al., 2010b). These differences should be considered in future studies because with very short time periods (e.g., in DMS tasks), one most likely investigates working memory maintenance, while only with longer periods, long-term memory processes are actually considered. Moreover, the involvement of CA2/3/DG appears to be related to the long-term stability of memories. This issue is illustrated in a study by Carr et al. (2010b) in which CA2/3/DG reflected successful encoding only for those items for which the memory lasted not only transiently (10 min) but also permanently (1 week).

CA3 SUPPORTS PATTERN SEPARATION OF DISSIMILAR INPUTS DURING ENCODING

Several fMRI studies have investigated the role of the CA3 region related to pattern separation and completion during memory encoding, for example two studies from Craig Stark's lab (Bakker et al., 2008; Lacy et al., 2011). In the first study (Bakker et al., 2008), the experimental task contained three types of trials: new items, repeated items or lures (new items which were very similar to already shown items). The authors then looked for repetition effects, i.e., attenuation of blood oxygen level dependent (BOLD) responses for novel, lure and repeated stimuli (Grill-Spector et al., 2006). The logic behind this is that lures are "intermediate" between novel items and repeated (identical) items and the authors used the presence or absence of BOLD attenuation during lure trials as an indication of whether the brain treated the lure stimuli more like novel or more like familiar stimuli. CA1 exhibited a tendency for pattern completion by showing repetition suppression for lures suggesting they were processed more like an already encountered object rather than a novel stimulus. DG/CA3 in contrast did not show repetition suppression for lures, which is indicative of pattern separation: the lure was treated more like a completely new object. In a follow-up study (Lacy et al., 2011), a linear modulation of repetition suppression in CA1 for increasingly dissimilar items (repeat, high similarity lure, low similarity lure, and new items) was found. In DG/CA3, attenuation of the BOLD response was more step-like: Only true repeat items were associated with repetition suppression, while neither high nor low similarity lures led to an attenuation of the BOLD response. These results are also consistent with a study by Duncan et al. (2012), in which participants were exposed to room layouts with different numbers of changes relative to previously learned rooms. CA1 was the only hippocampal subregion in which activation was linearly modulated by the number of changes. By contrast, DG/CA3 showed more of an abrupt, binary response, which might reflect a switch from pattern completion to pattern separation. This is, however, not discussed in this study, even though it complements a similar study in rodents using an immediate early gene brain imaging approach (Vazdarjanova and Guzowski, 2004) that investigated the degree of overlap of neuronal ensembles between learning and test environments. In this study, rats were familiarized with an environment and a set of objects. After 20 min, they were placed in environments that ranged from being very similar to very dissimilar to the original environment and set of objects. Only in the very dissimilar environment, the degree of overlap between neuronal ensembles decreased abruptly. This step-like response pattern was not seen in CA1 and it suggests that depending on the input dissimilarity, CA3 switches from pattern completion to pattern separation. However, another study in rodents reports that sudden, step-like like remapping of place cells in incrementally dissimilar environments can also occur in CA1 (Wills et al., 2005).

Table 1 | Overview of selected publications which have investigated the function of CA3 and other MTL and hippocampal subfields in humans.

Paper	ERC	PRC	PHC	CA1	CA2	CA3	DG	SUB	Results (CA3)
Bakker et al. (2008)		■	■	■		■	■	■	Pattern separation during encoding
Bonnici et al. (2012)				■	■	■	■	■	Pattern completion
Carr et al. (2010b)	■	■	■	■	■	■	■	■	Subsequent memory only for late recall
Chen et al. (2011)	■	■	■	■	■	■	■	■	Correct vs. incorrect retrieval
Dudukovic et al. (2011)	■	■	■	■	■	■	■	■	Pattern completion
Duncan et al. (2012)				■	■	■	■	■	Sigmoidal dependence on similarity
Eldridge et al. (2005)		■	■	■	■	■	■	■	Encoding > retrieval
Lacy et al. (2011)				■		■	■	■	Sigmoidal dependence on similarity
Mueller et al. (2007)	■			■	■	■	■	■	Preserved function in AD
Mueller et al. (2010)	■			■	■	■	■	■	Preserved function in MCI and AD
Newmark et al. (2013)	■	■	■	■		■	■	■	Pattern completion
Olsen et al. (2009)	■	■	■	■	■	■	■	■	Activation during DMS sample and delay
Schapiro et al. (2012)	■	■	■	■	■	■	■	■	Increased similarity via temporal proximity
Suthana et al. (2011)	■			■	■	■	■	■	Encoding > retrieval
Wisse et al. (2012)	■			■	■	■	■	■	Reliable manual segmentation
Yassa et al. (2010b)	■	■	■	■	■	■	■	■	Hyperactivity during pattern separation in aMCI
Zeineh et al. (2003)	■	■	■	■	■	■	■	■	Encoding > retrieval

ERC, entorhinal cortex; PRC, perirhinal cortex; PHC, parahippocampal cortex; CA1–CA3, cornu ammonis subregions 1–3, respectively; DG, dentate gyrus; SUB, subiculum. Gray boxes indicate the subfields that have been segmented in a given study; most studies combined subfields CA2, CA3, and dentate gyrus as indicated by gray boxes stretching several columns. The last column summarizes the main finding with regard to CA3 function.

That CA3 should be involved in pattern separation-like processes seems to be at odds with the notion that this subfield performs pattern completion (McNaughton and Morris, 1987; McClelland and Goddard, 1996; Colgin et al., 2008). One explanation for this apparent divergence of results from theoretical predictions could be that during the different stages of learning (e.g., encoding versus retrieval), the same region might support different processes, i.e., pattern separation during encoding and pattern completion during retrieval, as has been discussed before (Hunsaker and Kesner, 2013). Furthermore, it is not clear whether the BOLD response in a region reflects more synaptic input (e.g., from ERC) or processing in this region per se; see below in the discussion on the limitations of human subfield imaging studies.

In another high resolution fMRI study (Newmark et al., 2013), a DMS task was used. Participants were exposed to two face stimuli that either had overlapping features (same identity, different facial expression) or had non-overlapping features (different identity, different facial expression). Higher activity during working memory encoding in trials with overlapping samples was found in the right CA3/DG and in bilateral CA1. Higher activity for overlapping samples during the 8 s of maintenance was found in right CA1 and SUB only. Similarly, Dudukovic et al. (2011) report more activation in CA1 and CA3/DG during the test phase in a DMS task when the tested item matched the sample than when the tested item did not match the sample. They interpret this "match enhancement" as an indication for pattern completion.

The studies described thus far used classical univariate approaches to data analysis, investigating whether BOLD activity systematically differs between conditions, usually modeled within the general linear model (GLM) framework. However, these approaches are limited in elucidating the functional role of different hippocampal subfields, because many theoretical models conceptualize the subfields in terms of information content rather than activation level. Therefore, multivariate pattern analysis (MVPA) approaches may not only uncover differences that would not be detected in classical GLMs, but may be conceptually better suited to address predictions from these models. Bonnici et al. (2012) performed pattern classification analyses on voxels belonging to different hippocampal subfields while participants viewed scenes that were either purely scene A or scene B or ambiguous scenes which were morphed continuously between scenes A and B. Participants had to decide whether the presented scene was scene A or scene B, which was easy for the pure scenes (with which participants were presented during the first part of the study), but was more difficult or completely arbitrary for the morphed scenes, with which participants were confronted during the second part of the study. In this study, in addition to CA1 and SUB, CA3 and DG were delineated as separate subfields. Interestingly, classifier accuracy was better when classifying subjects' responses to morphed scenes (i.e., trials with high perceptual ambiguity) than to "pure scenes", and in these ambiguous trials, CA1 and CA3 had better classification accuracy than DG and SUB. Higher classification accuracy for ambiguous stimuli was interpreted by the authors as evidence for a pattern completion process due to the stronger need to retrieve internal representations in these trials. This result supports the idea that CA1, together with information from CA3, acts as a mismatch detector between

stored information and perceptual input from the ERC (Fries, 2009).

In summary, recent studies have provided evidence for both pattern separation and pattern completion-like processes in hippocampal subfield CA3 during working and long-term memory operations, even though these results are not always specific for CA3 but are sometimes also reported for CA1. Which of the two processes is observed in CA3 likely depends on a variety of factors such as the degree of similarity or dissimilarity of inputs and whether the stimulus material in general is novel (as in Bakker et al., 2008; Lacy et al., 2011) or highly familiar (as, for example, in Duncan et al., 2012; Newmark et al., 2013), because different processes are likely involved in processing these two types of stimuli (for example, encoding versus retrieval, as discussed above).

CA3 PROMOTES BINDING DURING ENCODING AND PATTERN COMPLETION DURING RETRIEVAL

A key function that is attributed to CA3 is the binding of previously not associated elements. An MVPA approach was used by Schapiro et al. (2012) to investigate how representational similarity (i.e., pattern similarity in fMRI scans) for unfamiliar, unrelated fractal pictures would change if they were presented repeatedly in a temporally structured manner. First, they presented abstract fractal pictures in random order. Then, the fractals were presented again with some fractals forming pairs in which one always followed the other (strong pairs) or followed the other in a third of all cases (weak pairs). Finally, fractals were shown in a random order again, and representational similarity independent of temporal proximity between the pairs was compared between the initial and the final scanning. Similarity for strong pairs relative to non-pairs and weak pairs increased in SUB, CA1 and combined CA2/CA3/DG, thereby showing that a temporal association between items increases the similarity of their representations, but only CA2/3/DG did so in a forward-looking, predictive manner (the first of a pair leading to reinstatement of the second part of the pair, but not the other way around). This study provides support for both the notion that CA3 is involved in forming arbitrary associations (e.g., between previously unrelated fractals), but also suggests that after encoding, CA3 uses parts of the newly formed association to retrieve the complete pattern, i.e., pattern completion.

In a similar vein as Schapiro et al. (2012), Chen et al. (2011) let participants study house-face pairs and during recall presented them with only one part of the pair. Participants had to covertly recall the associated house or face. After 7.5 s, participants were presented with a probe which was either a match (the correct partner of the pair) or a foil (belonging to another pair). Activation in an anatomical CA2/CA3/DG ROI was higher during the covert retrieval phase if participants subsequently responded correctly to the probe, which would be consistent with CA3 retrieving the associated pair.

Investigating how hippocampal subfields react to pairs of stimuli is a promising approach. On the one hand, this line of research allows one to test the hypothesis that the CA3 region promotes rapid binding of disparate elements. MVPA approaches might in future be used to track the "learning" process of such associative pairing (i.e., how similarity changes over the course of a learning process). On the other hand, paired associative studies also allow testing the assumption that CA3 uses parts of a memory trace to reinstate or retrieve the complete trace. In pair-association studies, it would be especially interesting to separate DG from CA3 because these two regions in such tasks likely perform different or even opposite operations, which may make it difficult to observe significant findings for the regions in the first place.

STRUCTURAL AND FUNCTIONAL ALTERATIONS IN ALZHEIMER'S DISEASE AND MILD COGNITIVE IMPAIRMENT

Investigations into the function of hippocampal subfields in humans may also benefit from studies in patient populations in whom these functions are disturbed. Accordingly, the link between changes in hippocampal subfields and psychiatric and neurological diseases has been intensively investigated (for a review, see Small et al., 2011). Of special interest here is Alzheimer's disease (AD), not only because it is primarily a memory disorder, but also because of its high prevalence, making it a major medical issue in an increasingly aging population. Mild cognitive impairment (MCI) has also been the target of many studies because MCI patients often progress to AD (Petersen et al., 1999), especially in case of the amnesic subtype which is characterized by subjective and objective unusual impairment in memory in the presence of preserved general cognitive abilities and function in daily activities (Petersen, 2004). Studies on amnesic MCI (aMCI) patients therefore offer the possibility to detect early symptoms and alterations in the memory system.

Healthy aging and AD are associated with different morphological changes in the hippocampal formation: In AD, volume loss occurs rather in ERC, CA1 and SUB than in CA3 or DG (Mueller et al., 2007, 2010). By contrast, in healthy aged as compared to healthy young humans the perforant pathway which connects ERC and hippocampus is specifically degraded, and the degree of fiber loss is correlated with the degree of behavioral memory deficits (Yassa et al., 2010a). Furthermore, perforant path degradation was associated with diminished pattern separation abilities on a behavioral level and to a lack of pattern separation-like activity in DG/CA3 on a functional MRI level (Yassa et al., 2011).

It has been suggested that one of the first behavioral deficits in patients with aMCI is a reduced ability to separate patterns (i.e., to recognize differences between very similar events), and that this basic deficit accounts for many of the amnesic symptoms (Yassa et al., 2010b). To address this question, Yassa et al. (2010b) investigated patients with aMCI. In addition to differences in volume and shape of hippocampal subfields in patients, they found reduced activity in the ERC during an encoding task that employed highly similar "lure" items and thus required pattern separation for successful performance. They found behavioral deficits in pattern separation compared to healthy controls and hyperexcitability of the CA3/DG region during the task. Interestingly, this corresponds well to results from Wilson et al. (2005) who reported increased firing in CA3 place cells in healthy aged rats. This hyperactivity could be a sign for a computational shift from pattern separation to pattern completion (Yassa et al., 2010b). In contrast to Mueller et al. (2010), the study by Yassa et al. (2010b) also found smaller CA3/DG volumes in aMCI patients. One possible explanation for these conflicting findings might relate to the different segmentation methods used in the studies, especially

with regard to the longitudinal extent in which subfields were delineated.

A pattern separation deficit in aMCI, associated with decreased volume and hyperexcitability in CA3/DG, seems to be at odds with the notion that CA3/DG is relatively spared in patients with AD (assuming that some of the aMCI patients are on the way to developing the disease). Differences in segmentation methods could be one explanation for the different conclusions. In addition, patients with aMCI also exhibit abnormal activity in the ERC, which could lead to altered downstream DG and CA3 function even in the absence of structural alterations in CA3 itself (Yassa et al., 2010b).

Clearly, more research is needed to investigate the specific behavioral deficits of patients with aMCI and relate them to structural and functional changes in CA3. Paradigms asking participants to differentiate between highly similar stimulus material provide a good model for the investigation of pattern separation processes, but they should be complemented by experiments which require participants to retrieve paired associates, which is another major function ascribed to CA3. The field will also benefit from studies that look at healthy young populations who have a genetic risk for developing AD such as carriers of the epsilon4 subtype of the apolipoprotein E gene (Corder et al., 1993).

OUTLOOK – NEW METHODS

Taken together, recent high-resolution MRI and fMRI studies have provided support for theoretical models with regard to pattern completion and pattern separation functions of CA3, its key role in forming new associations and relevance for retrieval of complete patterns based on only some parts of a memory trace. It has become clear from the studies described above that it is essential to use well designed studies that control factors such as incidental versus instructed encoding, whether novel or highly familiar stimuli are used and whether working memory or long-term memory processes are investigated.

It also seems to be important to develop methods for reliable separation of CA3 from DG. Combining these two subfields may lead to conflicting results. Also, the extent of subfield delineation along the longitudinal axis of the hippocampus should be more consistent across studies, especially because the relative proportion of CA3 and DG volume might be affected by the different portions of the hippocampus that are included (Poppenk et al., 2013).

Despite the many interesting findings that research on hippocampal subfields in humans has yielded so far, interpretation should always be careful. Even when stepping from theoretical models to rodent studies, some discrepancies can be observed between model and data, which are likely due to both methodological difficulties as well as the challenge of operationalizing specific memory processes. In humans, especially with fMRI imaging, these problems increase further. The BOLD response is a coarse signal when compared to single cell activity, both in time and in space. It is not possible to unequivocally attribute the BOLD signal to input, output or local processes within a subregion (Buzsáki et al., 2007; Logothetis, 2008), which will not be fixed even by higher resolution scanning, and signal "spill-over" between regions also has to be expected, even if difficult-to-delineate subfield such as CA3 and DG should one day be successfully and routinely segmented.

An integrative approach is required to bring together data from different modalities (such as animal research, intracranial EEG, lesion studies, volumetry studies in patient populations and high resolution functional MRI) with refined theoretical models and well-conceived standard paradigms. We expect that in the next decade, availability of high-field MRI scanners and the development of new scanning protocols will allow vastly improved delineation of subfields. Studies using 7T report resolutions as fine as in 0.8 mm, optimized for resolution of individual cell layers, in fMRI (De Martino et al., 2013) and temporal resolution may also be decreased to 700 ms for fMRI (Smith et al., 2013) or even 50 ms with Generalized iNverse imaging (GiN; Boyacioğlu and Barth, 2012), albeit at the expense of spatial specificity or SNR. New protocols might also allow better structural scanning in 1.5T or 3T scanners, which is especially important for good localization in patients with intracranial electrodes who cannot be scanned at higher magnetic field strengths. This might allow us to draw conclusions about specific subfields in these valuable participants as well. Also, multivariate approaches are an exciting new possibility to investigate hippocampal subfields, because they can assess information content rather than BOLD activity level and might allow for the detection of differences that would be missed with classical univariate methods. This method might also be used to track the emergence of associations between the two parts of a pair and test whether, during retrieval, parts of a pair induce reinstatement of the complete trace, which is one of the main processes attributed to CA3. For elucidating the exact role of CA3 in encoding and retrieval and whether CA3 supports pattern separation, pattern completion or both in different parts of the learning process, it is critical to carefully choose a paradigm that permits investigating the purported functions in detail and to integrate results from different research techniques and questions. Importantly, paradigms which approach the goal of process purity as close as possible should be applied. As Hunsaker and Kesner (2013) argue, in many cases encoding and retrieval processes are mingled due to the use of everyday objects, representations of which are likely already stored and will be retrieved at the time of experimental encoding, thereby further increasing the difficulty of dissociating pattern separation and pattern completion. This problem might be circumvented by using abstract, never-before-seen objects during encoding for which no prior associations have been formed.

Taken together, improved scanning and stronger experimental control might, in the future, lead to better understanding, more accurate diagnosis and even targeted treatment of memory disorders.

AUTHOR CONTRIBUTIONS

Lorena Deuker, Christian F. Doeller, Juergen Fell, and Nikolai Axmacher wrote the manuscript.

ACKNOWLEDGMENT

The authors thank Alejandro Vicente Grabovetsky for helpful suggestions for the manuscript. Christian F. Doeller is supported

by the European Research Council (ERC-StG 261177). Lorena Deuker and Christian F. Doeller are supported by the Netherlands Organisation for Scientific Research (NWO-Vidi 452-12-009). Nikolai Axmacher received funding via a DFG Emmy Noether grant (AX82/2) and via the SFB 1089. Juergen Fell was supported via SFB 1089 and via DFG grant FE366/6.

REFERENCES

Andersen, P., Morris, R., Amaral, D., Bliss, T., and O'Keefe, J. (2006). *The Hippocampus Book*. New York: Oxford University Press. doi: 10.1093/acprof:oso/9780195100273.001.0001

Axmacher, N., Mormann, F., Fernández, G., Elger, C. E., and Fell, J. (2006). Memory formation by neuronal synchronization. *Brain Res. Rev.* 52, 170–182. doi: 10.1016/j.brainresrev.2006.01.007

Bakker, A., Kirwan, C. B., Miller, M., and Stark, C. E. L. (2008). Pattern separation in the human hippocampal CA3 and dentate gyrus. *Science* 319, 1640–1642. doi: 10.1126/science.1152882

Bonnici, H. M., Chadwick, M. J., Kumaran, D., Hassabis, D., Weiskopf, N., and Maguire, E. A. (2012). Multi-voxel pattern analysis in human hippocampal subfields. *Front. Hum. Neurosci.* 6:290. doi: 10.3389/fnhum.2012.00290

Boyacioğlu, R., and Barth, M. (2012). Generalized iNverse imaging (GIN): ultrafast fMRI with physiological noise correction. *Magn. Reson. Med.* 70, 962–971. doi: 10.1002/mrm.24528

Buzsáki, G., Kaila, K., and Raichle, M. (2007). Inhibition and brain work. *Neuron* 56, 771–783. doi: 10.1016/j.neuron.2007.11.008

Carr, V. A., Engel, S. A., and Knowlton, B. J. (2013). Top-down modulation of hippocampal encoding activity as measured by high-resolution functional MRI. *Neuropsychologia* 51, 1829–1837. doi: 10.1016/j.neuropsychologia.2013.06.026

Carr, V. A., Rissman, J., and Wagner, A. D. (2010a). Imaging the human medial temporal lobe with high-resolution fMRI. *Neuron* 65, 298–308. doi: 10.1016/j.neuron.2009.12.022

Carr, V. A., Viskontas, I. V., Engel, S. A., and Knowlton, B. J. (2010b). Neural activity in the hippocampus and perirhinal cortex during encoding is associated with the durability of episodic memory. *J. Cogn. Neurosci.* 22, 2652–2662. doi: 10.1162/jocn.2009.21381

Chen, J., Olsen, R. K., Preston, A. R., Glover, G. H., and Wagner, A. D. (2011). Associative retrieval processes in the human medial temporal lobe: hippocampal retrieval success and CA1 mismatch detection. *Learn. Mem.* 18, 523–528. doi: 10.1101/lm.2135211

Chen, K. H., Chuah, L. Y., Sim, S. K., and Chee, M. W. (2010). Hippocampal region-specific contributions to memory performance in normal elderly. *Brain Cogn.* 72, 400–407. doi: 10.1016/j.bandc.2009.11.007

Colgin, L. L., Denninger, T., Fyhn, M., Hafting, T., Bonnevie, T., Jensen, O., et al. (2009). Frequency of gamma oscillations routes flow of information in the hippocampus. *Nature* 462, 353–357. doi: 10.1038/nature08573

Colgin, L. L., Moser, E. I., and Moser, M.-B. (2008). Understanding memory through hippocampal remapping. *Trends Neurosci.* 31, 469–477. doi: 10.1016/j.tins.2008.06.008

Corder, E. H., Saunders, A. M., Strittmatter, W. J., Schmechel, D. E., Gaskell, P. C., Small, G. W., et al. (1993). Gene dose of apolipoprotein E type 4 allele and the risk of Alzheimer's disease in late onset families. *Science* 261, 921–923. doi: 10.1126/science.8346443

De Martino, F., Zimmermann, J., Muckli, L., Ugurbil, K., Yacoub, E., and Goebel, R. (2013). Cortical depth dependent functional responses in humans at 7T: improved specificity with 3D GRASE. *PLoS ONE* 8:e60514. doi: 10.1371/journal.pone.0060514

Doeller, C. F., Barry, C., and Burgess, N. (2010). Evidence for grid cells in a human memory network. *Nature* 463, 657–661. doi: 10.1038/nature08704

Doeller, C. F., King, J. A., and Burgess, N. (2008). Parallel striatal and hippocampal systems for landmarks and boundaries in spatial memory. *Proc. Natl. Acad. Sci. U.S.A.* 105, 5915–5920. doi: 10.1073/pnas.0801489105

Dudukovic, N. M., Preston, A. R., Archie, J. J., Glover, G. H., and Wagner, A. D. (2011). High-resolution fMRI reveals match enhancement and attentional modulation in the human medial temporal lobe. *J. Cogn. Neurosci.* 23, 670–682. doi: 10.1162/jocn.2010.21509

Duncan, K., Ketz, N., Inati, S. J., and Davachi, L. (2012). Evidence for area CA1 as a match/mismatch detector: a high-resolution fMRI study of the human hippocampus. *Hippocampus* 22, 389–398. doi: 10.1002/hipo.20933

Duvernoy, H. M. (2005). *The Human Hippocampus*, 3rd Edn. Berlin, Heidelberg: Springer-Verlag.

Ekstrom, A. D., Bazih, A. J., Suthana, N. A., Al-Hakim, R., Ogura, K., Zeineh, M., et al. (2009). Advances in high-resolution imaging and computational unfolding of the human hippocampus. *Neuroimage* 47, 42–49. doi: 10.1016/j.neuroimage.2009.03.017

Eldridge, L. L., Engel, S. A., Zeineh, M. M., Bookheimer, S. Y., and Knowlton, B. J. (2005). A dissociation of encoding and retrieval processes in the human hippocampus. *J. Neurosci.* 25, 3280–3286. doi: 10.1523/JNEUROSCI.3420-04.2005

Fanselow, M. S., and Dong, H.-W. (2010). Are the dorsal and ventral hippocampus functionally distinct structures? *Neuron* 65, 7–19. doi: 10.1016/j.neuron.2009.11.031

Fries, P. (2009). The model- and the data-gamma. *Neuron* 64, 601–602. doi: 10.1016/j.neuron.2009.11.024

Grill-Spector, K., Henson, R., and Martin, A. (2006). Repetition and the brain: neural models of stimulus-specific effects. *Trends Cogn. Sci.* 10, 14–23. doi: 10.1016/j.tics.2005.11.006

Grossberg, S. (1971). Pavlovian pattern learning by nonlinear neural networks. *Proc. Natl. Acad. Sci. U.S.A.* 68, 828–831. doi: 10.1073/pnas.68.4.828

Guzowski, J. F., Knierim, J. J., and Moser, E. I. (2004). Ensemble dynamics of hippocampal regions CA3 and CA1. *Neuron* 44, 581–584. doi: 10.1016/j.neuron.2004.11.003

Hunsaker, M. R., and Kesner, R. P. (2013). The operation of pattern separation and pattern completion processes associated with different attributes or domains of memory. *Neurosci. Biobehav. Rev.* 37, 36–58. doi: 10.1016/j.neubiorev.2012.09.014

Jensen, O., and Lisman, J. E. (1996). Hippocampal CA3 region predicts memory sequences: accounting for the phase precession of place cells. *Learn. Mem.* 3, 279–287. doi: 10.1101/lm.3.2-3.279

Kesner, R. P., and Hopkins, R. O. (2006). Mnemonic functions of the hippocampus: a comparison between animals and humans. *Biol. Psychol.* 73, 3–18. doi: 10.1016/j.biopsycho.2006.01.004

Kesner, R. P., Hunsaker, M. R., and Warthen, M. W. (2008). The CA3 subregion of the hippocampus is critical for episodic memory processing by means of relational encoding in rats. *Behav. Neurosci.* 122, 1217–1225. doi: 10.1037/a0013592

Lacy, J. W., Yassa, M. A., Stark, S. M., Muftuler, L. T., and Stark, C. E. L. (2011). Distinct pattern separation related transfer functions in human CA3/dentate and CA1 revealed using high-resolution fMRI and variable mnemonic similarity. *Learn. Mem.* 18, 15–18. doi: 10.1101/lm.1971111

Lee, I., Hunsaker, M. R., and Kesner, R. P. (2005). The role of hippocampal subregions in detecting spatial novelty. *Behav. Neurosci.* 119, 145–153. doi: 10.1037/0735-7044.119.1.145

Lee, I., and Kesner, R. P. (2004a). Encoding versus retrieval of spatial memory: double dissociation between the dentate gyrus and the perforant path inputs into CA3 in the dorsal hippocampus. *Hippocampus* 14, 66–76. doi: 10.1002/hipo.10167

Lee, I., Rao, G., and Knierim, J. J. (2004b). A double dissociation between hippocampal subfields: differential time course of CA3 and CA1 place cells for processing changed environments. *Neuron* 42, 803–815. doi: 10.1016/j.neuron.2004.05.010

Libby, L. A., Ekstrom, A. D., Ragland, J. D., and Ranganath, C. (2012). Differential connectivity of perirhinal and parahippocampal cortices within human hippocampal subregions revealed by high-resolution functional imaging. *J. Neurosci.* 32, 6550–6560. doi: 10.1523/JNEUROSCI.3711-11.2012

Lisman, J. E., and Grace, A. A. (2005). The hippocampal-VTA loop: controlling the entry of information into long-term memory. *Neuron* 46, 703–713. doi: 10.1016/j.neuron.2005.05.002

Logothetis, N. K. (2008). What we can do and what we cannot do with fMRI. *Nature* 453, 869–878. doi: 10.1038/nature06976

Lörincz, A., and Buzsáki, G. (2000). Two-phase computational model training long-term memories in the entorhinal-hippocampal region. *Ann. N. Y. Acad. Sci.* 911, 83–111. doi: 10.1111/j.1749-6632.2000.tb06721.x

Ludowig, E., Trautner, P., Kurthen, M., Schaller, C., Bien, C. G., Elger, C. E., et al. (2008). Intracranially recorded memory-related potentials reveal higher posterior than anterior hippocampal involvement in verbal encoding and retrieval. *J. Cogn. Neurosci.* 20, 841–851. doi: 10.1162/jocn.2008.20507

Malykhin, N. V., Lebel, R. M., Coupland, N. J., Wilman, A. H., and Carter, R. (2010). In vivo quantification of hippocampal subfields using 4.7 T fast spin echo imaging. *Neuroimage* 49, 1224–1230. doi: 10.1016/j.neuroimage.2009.09.042

Marr, D. (1971). Simple memory: a theory for archicortex. *Philos. Trans. R. Soc. Lond. B Biol. Sci.* 262, 23–81. doi: 10.1098/rstb.1971.0078

McClelland, J. L., and Goddard, N. H. (1996). Considerations arising from a complementary learning systems perspective on hippocampus and neocortex. *Hippocampus* 6, 654–665. doi: 10.1002/(SICI)1098-1063(1996)6:6<654::AID-HIPO8>3.0.CO;2-G

McClelland, J. L., and Rumelhart, D. E. (1985). Distributed memory and the representation of general and specific information. *J. Exp. Psychol. Gen.* 114, 159–197. doi: 10.1037/0096-3445.114.2.159

McNaughton, B., and Morris, R. (1987). Hippocampal synaptic enhancement and information storage within a distributed memory system. *Trends Neurosci.* 10, 408–415. doi: 10.1016/0166-2236(87)90011-7

Moser, M. B., and Moser, E. I. (1998). Functional differentiation in the hippocampus. *Hippocampus* 8, 608–619. doi: 10.1002/(SICI)1098-1063(1998)8:6<608::AID-HIPO3>3.0.CO;2-7

Mueller, S. G., Schuff, N., Yaffe, K., Madison, C., Miller, B., and Weiner, M. W. (2010). Hippocampal atrophy patterns in mild cognitive impairment and Alzheimer's disease. *Hum. Brain Mapp.* 31, 1339–1347. doi: 10.1002/hbm.20934

Mueller, S., Stables, L., Du, A., Schuff, N., Truran, D., Cashdollar, N., et al. (2007). Measurement of hippocampal subfields and age-related changes with high resolution MRI at 4T. *Neurobiol. Aging* 28, 719–726. doi: 10.1016/j.neurobiolaging.2006.03.007

Newmark, R. E., Schon, K., Ross, R. S., and Stern, C. E. (2013). Contributions of the hippocampal subfields and entorhinal cortex to disambiguation during working memory. *Hippocampus* 23, 467–475. doi: 10.1002/hipo.22106

Norman, K. A., and O'Reilly, R. C. (2003). Modeling hippocampal and neocortical contributions to recognition memory: a complementary-learning-systems approach. *Psychol. Rev.* 110, 611–646. doi: 10.1037/0033-295X.110.4.611

Ojemann, J. G., Akbudak, E., Snyder, A. Z., McKinstry, R. C., Raichle, M. E., and Conturo, T. E. (1997). Anatomic localization and quantitative analysis of gradient refocused echo-planar fMRI susceptibility artifacts. *Neuroimage* 6, 156–167. doi: 10.1006/nimg.1997.0289

Olsen, R. K., Nichols, E. A., Chen, J., Hunt, J. F., Glover, G. H., Gabrieli, J. D. E., et al. (2009). Performance-related sustained and anticipatory activity in human medial temporal lobe during delayed match-to-sample. *J. Neurosci.* 29, 11880–11890. doi: 10.1523/JNEUROSCI.2245-09.2009

O'Reilly, R. C., and McClelland, J. L. (1994). Hippocampal conjunctive encoding, storage, and recall: avoiding a trade-off. *Hippocampus* 4, 661–682. doi: 10.1002/hipo.450040605

O'Reilly, R. C., and Rudy, J. W. (2001). Conjunctive representations in learning and memory: principles of cortical and hippocampal function. *Psychol. Rev.* 108, 311–345. doi: 10.1037/0033-295X.108.2.311

Petersen, R. C. (2004). Mild cognitive impairment as a diagnostic entity. *J. Intern. Med.* 256, 183–94. doi: 10.1111/j.1365-2796.2004.01388.x

Petersen, R. C., Smith, G. E., Waring, S. C., Ivnik, R. J., Tangalos, E. G., and Kokmen, E. (1999). Mild cognitive impairment: clinical characterization and outcome. *Arch. Neurol.* 56, 303–308. doi: 10.1001/archneur.56.3.303

Poppenk, J., Evensmoen, H. R., Moscovitch, M., and Nadel, L. (2013). Long-axis specialization of the human hippocampus. *Trends Cogn. Sci.* 17, 230–240. doi: 10.1016/j.tics.2013.03.005

Schacter, D. L., and Wagner, A. D. (1999). Medial temporal lobe activations in fMRI and PET studies of episodic encoding and retrieval. *Hippocampus* 9, 7–24. doi: 10.1002/(SICI)1098-1063(1999)9:1<7::AID-HIPO2>3.0.CO;2-K

Schapiro, A. C., Kustner, L. V., and Turk-Browne, N. B. (2012). Shaping of object representations in the human medial temporal lobe based on temporal regularities. *Curr. Biol.* 22, 1622–1627. doi: 10.1016/j.cub.2012.06.056

Scoville, W. B., and Milner, B. (1957). Loss of recent memory after bilateral hippocampal lesions. *J. Neuropsychiatry Clin. Neurosci.* 12, 103–113. doi: 10.1136/jnnp.20.1.11

Small, S. A., Schobel, S. A., Buxton, R. B., Witter, M. P., and Barnes, C. A. (2011). A pathophysiological framework of hippocampal dysfunction in ageing and disease. *Nat. Rev. Neurosci.* 12, 585–601. doi: 10.1038/nrn3085

Smith, S. M., Beckmann, C. F., Andersson, J., Auerbach, E. J., Bijsterbosch, J., Douaud, G., et al. (2013). Resting-state fMRI in the human connectome project. *Neuroimage* 15, 144–168. doi: 10.1016/j.neuroimage.2013.05.039

Suthana, N., Ekstrom, A., Moshirvaziri, S., Knowlton, B., and Bookheimer, S. (2011). Dissociations within human hippocampal subregions during encoding and retrieval of spatial information. *Hippocampus* 21, 694–701. doi: 10.1002/hipo.20833

Suthana, N., and Fried, I. (2012). Percepts to recollections: insights from single neuron recordings in the human brain. *Trends Cogn. Sci.* 16, 427–436. doi: 10.1016/j.tics.2012.06.006

Treves, A., and Rolls, E. T. (1992). Computational constraints suggest the need for two distinct input systems to the hippocampal CA3 network. *Hippocampus* 2, 189–199. doi: 10.1002/hipo.450020209

van Strien, N. M., Cappaert, N. L. M., and Witter, M. P. (2009). The anatomy of memory: an interactive overview of the parahippocampal–hippocampal network. *Nat. Rev. Neurosci.* 10, 272–282. doi: 10.1038/nrn2614

Vazdarjanova, A., and Guzowski, J. F. (2004). Differences in hippocampal neuronal population responses to modifications of an environmental context: evidence for distinct, yet complementary, functions of CA3 and CA1 ensembles. *J. Neurosci.* 24, 6489–6496. doi: 10.1523/JNEUROSCI.0350-04.2004

Weiskopf, N., Hutton, C., Josephs, O., and Deichmann, R. (2006). Optimal EPI parameters for reduction of susceptibility-induced BOLD sensitivity losses: a whole-brain analysis at 3 T and 1.5 T. *Neuroimage* 33, 493–504. doi: 10.1016/j.neuroimage.2006.07.029

Wills, T. J., Lever, C., Cacucci, F., Burgess, N., and O'Keefe, J. (2005). Attractor dynamics in the hippocampal representation of the local environment. *Science* 308, 873–876. doi: 10.1126/science.1108905

Wilson, I. A., Ikonen, S., Gallagher, M., Eichenbaum, H., and Tanila, H. (2005). Age-associated alterations of hippocampal place cells are subregion specific. *J. Neurosci.* 25, 6877–6886. doi: 10.1523/JNEUROSCI.1744-05.2005

Wisse, L. E. M., Gerritsen, L., Zwanenburg, J. J. M., Kuijf, H. J., Luijten, P. R., Biessels, G. J., et al. (2012). Subfields of the hippocampal formation at 7 T MRI: in vivo volumetric assessment. *Neuroimage* 61, 1043–1049. doi: 10.1016/j.neuroimage.2012.03.023

Yassa, M. A., Mattfeld, A. T., Stark, S. M., and Stark, C. E. L. (2011). Age-related memory deficits linked to circuit-specific disruptions in the hippocampus. *Proc. Natl. Acad. Sci. U.S.A.* 108, 8873–8878. doi: 10.1073/pnas.1101567108

Yassa, M. A., Muftuler, L. T., and Stark, C. E. L. (2010a). Ultrahigh-resolution microstructural diffusion tensor imaging reveals perforant path degradation in aged humans in vivo. *Proc. Natl. Acad. Sci. U.S.A.* 107, 12687–12691. doi: 10.1073/pnas.1002113107

Yassa, M. A., Stark, S. M., Bakker, A., Albert, M. S., Gallagher, M., and Stark, C. E. (2010b). High-resolution structural and functional MRI of hippocampal CA3 and dentate gyrus in patients with amnestic mild cognitive impairment. *Neuroimage* 51, 1242–1252. doi: 10.1016/j.neuroimage.2010.03.040

Yassa, M. A., and Stark, C. E. L. (2009). A quantitative evaluation of cross-participant registration techniques for MRI studies of the medial temporal lobe. *Neuroimage* 44, 319–327. doi: 10.1016/j.neuroimage.2008.09.016

Zeineh, M. M., Engel, S. A., Thompson, P. M., and Bookheimer, S. Y. (2003). Dynamics of the hippocampus during encoding and retrieval of face-name pairs. *Science* 299, 577–580. doi: 10.1126/science.1077775

Conflict of Interest Statement: The authors declare that the research was conducted in the absence of any commercial or financial relationships that could be construed as a potential conflict of interest.

Received: 17 October 2013; accepted: 13 February 2014; published online: 04 March 2014.

Citation: Deuker L, Doeller CF, Fell J and Axmacher N (2014) Human neuroimaging studies on the hippocampal CA3 region – integrating evidence for pattern separation and completion. Front. Cell. Neurosci. ***8****:64. doi: 10.3389/fncel.2014.00064*

This article was submitted to the journal Frontiers in Cellular Neuroscience.

frontiers in
CELLULAR NEUROSCIENCE

ORIGINAL RESEARCH ARTICLE
published: 25 December 2013
doi: 10.3389/fncel.2013.00263

Frequency dependence of CA3 spike phase response arising from h-current properties

Melodie Borel[1†], Simone Guadagna[1†], Hyun Jae Jang[2], Jeehyun Kwag[2]* and Ole Paulsen[1]*

[1] *Department of Physiology, Development and Neuroscience, University of Cambridge, Cambridge, UK*
[2] *Department of Brain and Cognitive Engineering, Korea University, Seoul, Korea*

Edited by:
Enrico Cherubini, International School for Advanced Studies, Italy

Reviewed by:
Norbert Hajos, Hungarian Academy of Sciences, Hungary
Majid Mohajerani, University of British Columbia, Canada

***Correspondence:**
Jeehyun Kwag, Department of Brain and Cognitive Engineering, Korea University, 145 Anam-ro, Seongbuk-gu, Seoul, 136-701, Korea
e-mail: jkwag@korea.ac.kr;
Ole Paulsen, Physiological Laboratory, Department of Physiology, Development and Neuroscience, University of Cambridge, Downing Street, Cambridge CB2 3EG, UK
e-mail: op210@cam.ac.uk
† *These authors have contributed equally to this work.*

The phase of firing of hippocampal neurons during theta oscillations encodes spatial information. Moreover, the spike phase response to synaptic inputs in individual cells depends on the expression of the hyperpolarization-activated mixed cation current (I_h), which differs between CA3 and CA1 pyramidal neurons. Here, we compared the phase response of these two cell types, as well as their intrinsic membrane properties. We found that both CA3 and CA1 pyramidal neurons show a voltage sag in response to negative current steps but that this voltage sag is significantly smaller in CA3 cells. Moreover, CA3 pyramidal neurons have less prominent resonance properties compared to CA1 pyramidal neurons. This is consistent with differential expression of I_h by the two cell types. Despite their distinct intrinsic membrane properties, both CA3 and CA1 pyramidal neurons displayed bidirectional spike phase control by excitatory conductance inputs during theta oscillations. In particular, excitatory inputs delivered at the descending phase of a dynamic clamp-induced membrane potential oscillation delayed the subsequent spike by nearly 50 mrad. The effect was shown to be mediated by I_h and was counteracted by increasing inhibitory conductance driving the membrane potential oscillation. Using our experimental data to feed a computational model, we showed that differences in I_h between CA3 and CA1 pyramidal neurons could predict frequency-dependent differences in phase response properties between these cell types. We confirmed experimentally such frequency-dependent spike phase control in CA3 neurons. Therefore, a decrease in theta frequency, which is observed in intact animals during novelty, might switch the CA3 spike phase response from unidirectional to bidirectional and thereby promote encoding of the new context.

Keywords: theta oscillation, phase response, I_h, resonance, hippocampus, CA3, CA1

1. INTRODUCTION

During spatial exploration, the rodent hippocampus exhibits a distinctive rhythmic slow network activity, during which the extracellularly recorded local field potential shows oscillations at theta frequency (4–12 Hz; Vanderwolf, 1969; O'Keefe and Recce, 1993; Buzsáki, 2002). During theta oscillations in anaesthetized rats, the membrane potential of hippocampal pyramidal neurons is driven by rhythmic perisomatic inhibition (Soltész and Deschenes, 1993; Kamondi et al., 1998). As a consequence, their spike probability distribution is phase locked to the ongoing theta rhythm (Kamondi et al., 1998). However, pyramidal neurons are not fully synchronized and the phase relative to theta oscillation at which each of them is active carries information, as shown by the phase precession of place cell firing when an animal moves through an environment (O'Keefe and Recce, 1993). The hyperpolarization-activated current, I_h, mediated by HCN1 channels, confers to hippocampal neurons a frequency preference to inputs in the theta range (Hu et al., 2002). Nevertheless, theta power is increased in the hippocampus of animals with a genetic knockout of HCN1 channels (Nolan et al., 2004), suggesting that h-channels are more important for spike phase control in individual neurons, rather than contributing to the synchronization of neuronal firing during theta activity.

Several lines of experimental evidence suggest that hippocampal theta oscillations are important for memory processes: (i) Theta activity occurs during learning: the theta power increases during a water maze task when the rat has to learn the location of a hidden platform and not when it can see it (Olvera-Cortés et al., 2002). (ii) The power of theta oscillation correlates with performance: rabbits develop eyeblink conditioning twice as fast if stimuli are delivered when the hippocampus displays theta oscillations (Seager et al., 2002). Moreover, during food foraging on a hole-board, theta power is stronger when animals have the possibility of learning the position of baited/unbaited holes. This activity is associated with learning as demonstrated by a decrease in the rate of visiting unbaited holes (Woldeit and Korz, 2010). (iii) Theta activity is required for performance: suppression of rhythmic neuronal activity in rat hippocampus, resulting from a lesion (Winson, 1978) or pharmacological inactivation (McNaughton et al., 2006) of the medial

septum, prevents them from learning the target position of a circular maze or water maze, respectively. (iv) Restoration of theta oscillations rescues performance: a rhythmic electrical stimulation of the septohippocampal fibres, while the medial septum is inactivated, partially restores theta-like activity in the rat hippocampus and considerably improves performance in the Morris water maze task (McNaughton et al., 2006). Finally, (v) theta activity also occurs during rapid eye movement (REM) sleep (Jouvet et al., 1959), which appears to be involved in memory consolidation: the duration of REM sleep increases specifically after a rat is trained in a water maze task (Smith and Rose, 1997), and place cells reactivate during REM episodes following exposure to the corresponding place field (Pavlides and Winson, 1989). A rat that is deprived of REM sleep for 12 hours after its first training session in a water maze task takes longer time to find the hidden platform in a second session (Smith and Rose, 1996). Interestingly, an enhancement of REM sleep following the training of rats in a footshock-motivated discrimination task improves their performance (Wetzel et al., 2003).

The mechanism by which theta oscillations contribute to memory is unknown but might involve plasticity of synaptic transmission. Huerta and Lisman (1993) reported that field excitatory post-synaptic potentials (EPSPs) recorded in the *stratum radiatum* of CA1 are potentiated in hippocampal slices when the Schaffer collateral pathway is stimulated at low frequency during carbachol-induced theta oscillations. In particular, the magnitude of the potentiation correlates with the amplitude of the oscillation (Huerta and Lisman, 1993). This long-lasting and activity-dependent strengthening of synaptic transmission also occurs in rats under anaesthesia during spontaneous or pinched-induced theta oscillation (Hölscher et al., 1997). Importantly, electrical stimulation of the afferent path induces long term potentiation only when it occurs at the positive phase of the field theta oscillation. Such a synaptic input, given the relationship between the field theta cycle and the spike distribution of pyramidal neurons (Kamondi et al., 1998), occurs slightly before pyramidal neurons are the most likely to fire an action potential. This form of synaptic plasticity has been reproduced at the single neuron level *in vitro* (Kwag and Paulsen, 2009b) and Schaffer collateral stimulation at the ascending phase of the membrane potential oscillation potentiates EPSPs when the post-synaptic cell fires at the peak of the oscillation. In contrast, synaptic stimulation at the descending phase of the membrane potential oscillation, after the action potential at the peak of the oscillation, depresses the EPSPs. Interestingly, a phase shift of the post-synaptic action potential influences the direction of the synaptic plasticity due to the time dependence between pre- and post-synaptic activity (Kwag and Paulsen, 2009b). Therefore, control of the post-synaptic spike phase could determine the direction and extent of synaptic plasticity.

Evidence of such spike phase control by synaptic inputs has previously been reported in rats in both CA3 (Lengyel et al., 2005) and CA1 pyramidal neurons (Kwag and Paulsen, 2009a). However, CA3 and CA1 differ considerably anatomically and are likely to have distinct functions in memory processes. While both CA3 and CA1 pyramidal neurons receive direct information from the entorhinal cortex, they also receive major inputs via the tri-synaptic circuit from the dentate gyrus to CA3 and then CA1 (Amaral and Witter, 1989). Because of its abundant recurrent connections, CA3 is thought to support autoassociative memory and to encode context (McNaughton and Morris, 1987). Rats with specific lesions of the CA3 subfield, although perfectly able to detect the novelty of an object they never have encountered before, fail to detect the spatial novelty if a familiar object is moved (Lee et al., 2005). The CA1, which receives the internally encoded input from CA3 and direct information from the entorhinal cortex, is thought to support heteroassociative memory of novelty (McNaughton and Morris, 1987). The quantification of c-fos protein expression in CA1 of rats exposed to an environment was shown to be positively correlated to the degree of novelty (VanElzakker et al., 2008). Interestingly, training of an animal in a navigation task induces a backward shift in place fields of hippocampal cells (Mehta et al., 1997). This asymmetric expansion of place fields is NMDAR-dependent (Ekstrom et al., 2001), and is reduced in HCN1 knockout mice (Hussaini et al., 2011). Moreover, CA3 and CA1 place cells have distinct properties with regard to this experience-dependent change of activity (Lee et al., 2004).

Here, we compared the intrinsic membrane properties of mouse CA3 and CA1 pyramidal neurons and analyzed the consequence of their differences on spike phase control by synaptic input.

2. MATERIALS AND METHODS

2.1. PREPARATION OF THE BIOLOGICAL MATERIAL

Animals used in this study were C57BL/6 mice (Harlan, Wyton, UK; $n = 51$) of both sexes, aged 2 to 5 weeks. To investigate the effect of the hyperpolarization-activated current I_h, some experiments were carried out on mice with a genetic knockout of the hyperpolarization-activated cyclic nucleotide-gated channel 1 (HCN1 KO; B6.129S-Hcn1^{tm2Kndl}/J, The Jackson Laboratory, Bar Harbor, Maine, USA; $n = 3$). All animal care and experimental procedures were in accordance with the UK Animals (Scientific Procedures) Act of 1986.

Horizontal hippocampal slices (350 μm) were prepared from the left hemisphere in cold (0–3 °*C*), oxygenated (95% O_2, 5% CO_2), sucrose-based cutting solution (in mM: KCl 3, NaH_2PO_4 1.25, $MgSO_4$ 2, $MgCl_2$ 1, $CaCl_2$ 1, $NaHCO_3$ 26.4, glucose 10, sucrose 206, ascorbic acid 0.40, kynurenic acid 1) using a vibrating microtome (VT1200S, Leica Micro-systems, Milton Keynes, UK). Slices were stored at room temperature in a submerged-style holding chamber with oxygenated artificial cerebrospinal fluid (aCSF; in mM: NaCl 126, KCl 3, NaH_2PO_4 1.25, $MgSO_4$ 2, $CaCl_2$ 2, $NaHCO_3$ 26.4, glucose 10) for at least 1 h. Kynurenic acid (0.5 mM; Abcam, Cambridge, UK) was added to standard aCSF for the first 30 min of their recovery.

Slices were then individually placed in a recording chamber, superfused with oxygenated, standard aCSF at 30 °*C* at a flow-rate of approximately 3.5 mL·min^{-1}. For some experiments, the I_h blocker ZD7288 (10 μM; Sigma Aldrich, Dorset, UK) was added to the superfusate 20 min prior to starting recordings.

2.2. RECORDING AND STIMULATION

2.2.1. Whole-cell recording

Whole-cell patch-clamp recordings of CA3 and CA1 pyramidal neurons were performed with a Multiclamp 700B amplifier (Molecular Devices, Foster City, California, USA) in current clamp mode under visual guidance by infrared differential interference contrast video microscopy. Patch electrodes (4–7 MΩ) were pulled from borosilicate glass capillaries and filled with a solution containing (in mM): K gluconate 110, HEPES 40, NaCl 4, ATP-Mg 4, GTP-NaCl 0.3; the pH was adjusted to 7.2 with KOH. Amplified signals were filtered at 4 kHz and digitized at 8 kHz (Instrutech ITC-18, Port Washington, New York, USA). Customized procedures within Igor Pro Software (WaveMetrics, Lake Oswego, Oregon, USA) were used to generate command signals, and for data collection and analysis.

2.2.2. Dynamic clamp

Cells were recorded in dynamic clamp mode (Robinson and Kawai, 1993; Prinz et al., 2004) to allow stimulations mimicking physiological synaptic inputs. The injected current (I_{inj}) was calculated as:

$$I_{\text{inj}}(t) = g(t) \times [V_m(t) - E_{\text{Rev}}] \quad (1)$$

where $g(t)$ is the conductance as a function of time, $V_m(t)$ is the measured membrane potential and E_{Rev} is the reversal potential of the synaptic input to be mimicked. The reversal potential was set to −70 mV for inhibitory inputs and to 0 mV for excitatory inputs.

Occasionally, the experiments required the membrane potential of the cell to be clamped using dynamic clamp mode. The reversal potential was then set to the clamp value and $g(t)$ was set to be constant at its maximal value (5 nS).

Table 1 | Morphology and passive membrane properties of CA3 and CA1 pyramidal cell (PC) models.

		CA3 PC	CA1 PC
Soma	Length (μm)	75	60
	Diameter (μm)	60	60
Resting potential (mV)		−60	−60
Membrane capacitance (μF·cm^{-2})		1.0	1.0
Membrane resistance (kΩ·cm^2)		200	100
Axial resistance (Ω·cm)		50	50

Table 2 | Maximal conductance of voltage-gated conductance in CA1 and CA3 pyramidal neuron model.

	Conductance (mS·cm^{-2})
g_{Leak}	0.01
g_{Na}	9
g_{KDR}	6
g_{KA}	36

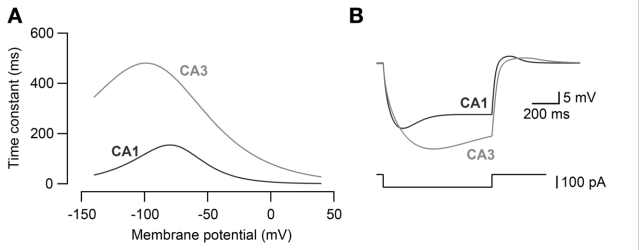

FIGURE 1 | Modeling of I_h kinetics. (A) The activation time constants of h-channel conductance for CA3 pyramidal neuron model and CA1 pyramidal neuron model. **(B)** Voltage response to −100 pA current steps (bottom) in CA3 and CA1 neuron models. CA3 and CA1 neuron models were fit to the voltage response recorded in CA3 and CA1 pyramidal neurons to −100 pA current steps *in vitro*.

2.3. EXPERIMENTAL DESIGN

Pyramidal neurons from the CA3 and CA1 subfields were identified on the basis of location, as well as morphological and electrical properties.

2.3.1. Characterization of the cell

The cell resting membrane potential (RMP) was defined as the average potential recorded over 1250 ms without any injected current. Cells with RMP positive to −50 mV were discarded. The sag amplitude, reflecting the activation of I_h, was measured at the soma from the membrane potential response to a negative current step (−100 pA, 800 ms), from a steady state membrane potential of −60 mV.

$$\text{Sag} = \frac{V_{\text{peak}} - V_{\text{steady}}}{V_{\text{peak}} - \text{RMP}} \quad (2)$$

The resonance properties of the membrane were studied using an impedance (Z) amplitude profile (ZAP) protocol as previously described (Pike et al., 2000). An oscillatory current of constant peak-to-peak amplitude (40 pA) and increasing frequency (from 0 to 20 Hz) was delivered at the soma held close to −60, −70, or −80 mV by superimposing a constant current. Both the stimulation current command and the voltage response were subjected to a discrete Fourier transform (FFT). The ratio of the response FFT over the stimulation FFT determines the impedance of the cell (Puil et al., 1986). A resonance frequency was found when the impedance reached a frequency-specific peak (Z_{res}). The strength of the resonance was calculated as the "Q-value" which was estimated as the ratio of Z_{res} over $Z_{0.5\ Hz}$ (Hu et al., 2002).

2.3.2. Characterization of the spike phase control

An 11 s-long oscillatory current was delivered at the soma from a sinusoidal inhibitory conductance using dynamic clamp (5 Hz, either 3 or 1 nS). A tonic current was superimposed on the oscillatory input so that one action potential was triggered at the peak of each cycle of the oscillation. Five dynamic clamp-induced artificial excitatory post-synaptic conductances (aEPSGs) per trial were modeled using an alpha function:

$$\text{aEPSG}(t) = g_{\max} \times \alpha t \times e^{(1-\alpha t)} \quad (3)$$

Table 3 | Passive membrane properties and resonance properties of CA3 and CA1 pyramidal neurons.

	CA3	CA1	
RMP (mV)	−54 ± 1 (40)	−57 ± 1 (21)	n.s.
Rin (MΩ)	248 ± 10 (40)	212 ± 16 (21)	n.s.
Sag	0.16 ± 0.01 (40)	0.30 ± 0.02 (21)	***
F_{Res} (Hz)	1.19 ± 0.09 (15)	2.49 ± 0.17 (19)	***
Q-value	1.06 ± 0.01 (15)	1.15 ± 0.01 (19)	***

*Data are presented as mean ± SEM; numbers in parenthesis represent number of cells. Cells were recorded at 30 °C. RMP, resting membrane potential; Sag measured at −60 mV; Frequency preference (F_{Res}) and resonance strength (Q-value) measured at −70 mV. ***$p < 0.001$, n.s.: $p > 0.05$, unpaired two-sample Student's t-test.*

with $g_{max} = 1$ nS and $\alpha = 260$. They occurred at 20 different phases of the oscillation over 40 trials within the time intervals: [2,2.4], [4,4.4], [6,6.4], [8,8.4], and [10,10.4] s.

The four cycles immediately preceding each aEPSG were used as a control period from which to calculate the average spike phase, which was used as a reference. The phase of each aEPSG and that of the subsequent spike were compared to this reference. The phase responses were averaged in 20 bins of 0.1π rad. The effect of the aEPSG on the subsequent spike has been reported as phase responses in the text. In some figure panels the spike time response has been plotted as a function of input phase.

A related protocol was designed to study the phase response specifically to inputs at the descending phase of the membrane potential oscillation. In this protocol, the dynamic clamp-induced 5 nS oscillation at either 5 or 4 Hz lasted for 7 s. Each trial included a perturbation whose duration was set to half of the duration of the descending phase (between 0.3π and 0.8π rad). Subthreshold excitation and inhibition were mimicked by clamping the membrane potential for this duration just negative to the spike threshold or at the trough of the oscillation, respectively. A third, control, condition measured the variation of spike phase in the absence of any induced perturbation. These three conditions were alternated, 15 trials of each were recorded and the response presented as the average phase response.

2.4. STATISTICAL ANALYSIS

Conventional and circular statistics (Berens, 2009) were used as detailed in the Results section. As a test of normality, the D'Agostino–Pearson omnibus test ($p > 0.05$) was used prior to applying a Student's *t*-test. A circular one-sample mean angle test was applied to compare the spike phase distribution from a reference value. Differences between two independent spike phase distributions were tested using the Watson–Williams test. Comparison of spike phase shifts in several conditions per cell were tested using the Moore's paired test. A *p*-value < 0.05 was considered statistically significant.

2.5. COMPUTATIONAL MODEL

Hippocampal CA3 and CA1 pyramidal neurons were modeled as a single compartment neuron model using the NEURON program [Version 7.2, Hines and Carnevale, 1997]. CA3 and CA1 neurons were modeled to have the passive membrane properties as shown in **Table 1** and CA3 neurons were modeled to have a larger surface area than CA1 neurons (Ishizuka et al., 1995; Morellini et al., 2010).

All voltage-gated conductances were modeled using Hodgkin-Huxley style kinetics (Hodgkin and Huxley, 1952). Leak (I_{Leak}), fast sodium (I_{Na}), delayed-rectifier potassium (I_{KDR}) and A-type potassium (I_{KA}) currents were modeled (Morse et al., 2010) in both the CA3 and CA1 models, each with a maximal conductance as shown in **Table 2**.

2.5.1. Activation kinetics of CA3 and CA1 h-channels

The kinetics of I_h in CA3 and CA1 models (Morse et al., 2010) were adjusted (**Figure 1A**) so that the voltage sag amplitude in response to steps of current reflected the experimental recordings of the CA3 and CA1 neurons *in vitro* (**Figure 1B**). The maximal h-channel conductance (g_h) of CA3 was 2.0×10^{-3} mS·cm^{-2} and that of CA1 neuron was 4.5×10^{-3} mS·cm^{-2}. The activation kinetics of h-channels for CA3 and CA1 pyramidal neuron models were adopted from Morse et al. (2010; Equations 4–5):

$$\frac{dm}{dt} = \left[1 - \left(\frac{1}{1 + e^{-(V_m+73)/8}} - m\right)\right] \times \frac{1}{\tau_{\{CA1,CA3\}}} \quad (4)$$

where m was the gating variable, V_m was the membrane potential and τ was the time constant with:

$$\tau_{CA3} = 942 \times e^{-(V_m+90)/37} \quad (5)$$

and

$$\tau_{CA1} = 303 \times e^{-(V_m+75)/20} \quad (6)$$

Time constants were modified for CA3 (Equation 5) and CA1 neuron model (Equation 6) to fit the voltage response to hyperpolarizing current steps obtained experimentally in CA3 and CA1 neurons (**Figure 1B**).

2.5.2. Simulation conditions and analysis

Oscillation of the membrane potential was simulated with an oscillatory inhibitory conductance at 5 Hz or 4 Hz (1 s, 4 nS), and a step current (1 s, 20.0 − 24.3 pA) was superimposed so that the model elicited one spike at the peak of each oscillation cycle. To simulate artificial synaptic input onto the cell, an excitatory or inhibitory conductance step (5 nS) was delivered on the descending phase of the oscillation (0.3 − 0.8π rad). The spike phase response to excitatory or inhibitory perturbation was calculated in the CA3 and CA1 models, compared to the spike phase before perturbation. All NEURON simulations were conducted with a time step of 25 μs and the total duration of a simulation was 1000 ms.

3. RESULTS

3.1. PASSIVE AND RESONANCE PROPERTIES OF CA3 AND CA1 PYRAMIDAL NEURONS

In order to compare the intrinsic membrane properties of CA1 and CA3 pyramidal neurons, whole-cell recordings were made

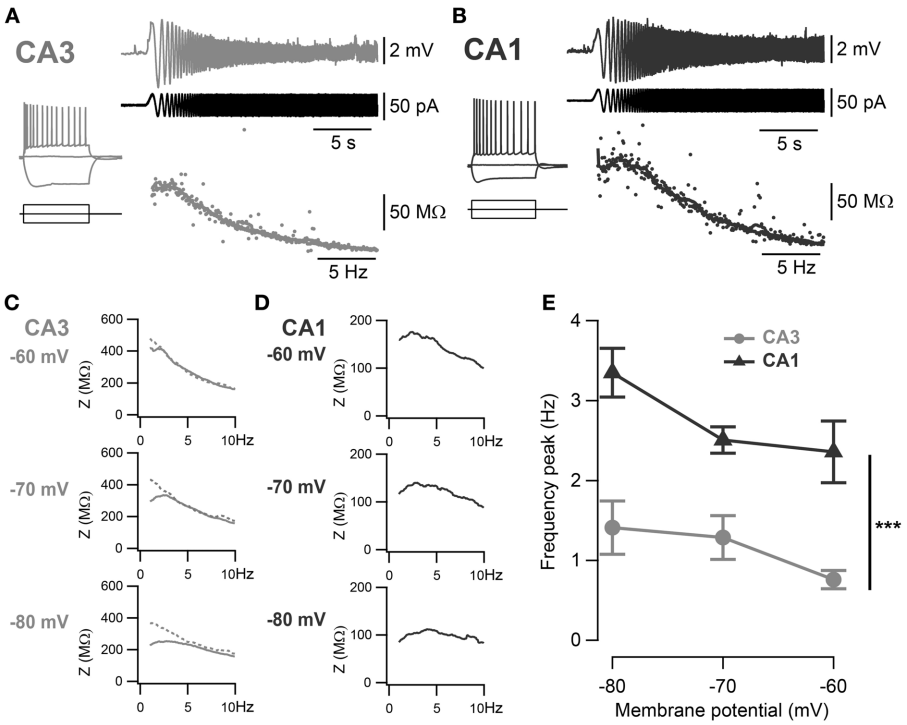

FIGURE 2 | Frequency preference of CA3 and CA1 pyramidal neurons. **(A,B)** Representative ZAP recordings of CA3 and CA1 cells, respectively. Voltage responses (upper traces) to a sinusoidal current of increasing frequency (0–20 Hz, middle traces) were recorded and relative impedances (lower traces) were calculated. A peak in the impedance curve indicates a frequency preference of the cell. Representative impedance magnitudes of CA3 **(C)** and CA1 **(D)** pyramidal neurons at −60, −70 and −80 mV holding potentials. Some cells in CA3 did not show detectable frequency preference (dotted line) and a frequency preference could not be detected. **(E)** Average frequency preference of CA3 cells with resonance peak above 1 Hz ($n = 7$) and all CA1 cells ($n = 12$). Preferred frequency increased at more negative holding potentials and was significantly greater in CA1 than in CA3 cells (***$p < 0.001$, One-Way ANOVA with Bonferroni *post-hoc* test).

in mouse hippocampal slices. The RMP of CA3 and CA1 pyramidal neurons (CA3: -54 ± 1 mV, $n = 40$; CA1: -57 ± 1 mV, $n = 21$; $p = 0.06$, unpaired two-sample Student's *t*-test; **Table 3**), as well as their input resistance (CA3: 248 ± 10 MΩ, $n = 40$; CA1: 212 ± 16 MΩ, $n = 21$; $p = 0.07$, unpaired two-sample Student's *t*-test; **Table 3**) were comparable. However, CA3 and CA1 neurons showed distinct sag amplitudes in response to negative current steps (see representative traces in **Figures 2A,B**). When recorded at −60 mV, the sag ratio in CA1 (0.30 ± 0.02, $n = 21$) was twice that in CA3 neurons (0.16 ± 0.01, $n = 40$; $p < 10^{-4}$, unpaired two-sample Student's *t*-test; **Table 3**).

The voltage-dependent activation of the conductance(s) responsible for this sag has commonly been associated with resonance properties. Therefore, resonance properties of CA3 and CA1 pyramidal neurons were estimated from a standard ZAP protocol (Hutcheon and Yarom, 2000; Pike et al., 2000). Briefly, a 40 pA peak-to-peak oscillatory current of increasing frequency from 0 to 20 Hz was applied to the cell and the impedance was calculated from the membrane potential response as a function of the frequency (**Figures 2A,B**). A frequency preference could be determined when the impedance reached a peak in 15 out of 40 CA3 cells and in 19 out of 21 CA1 cells (**Table 3**). CA3 pyramidal neurons were separated into two groups according to their frequency preference: cells with resonance at a frequency higher than 1 Hz and cells with resonance at lower frequency or not measurable (**Figures 2D,E**). For most CA1 cells and CA3 cells with resonance above 1 Hz, the frequency preference increased with hyperpolarization of the membrane holding potential (**Figures 2C–E**). When compared at −70 mV, CA1 pyramidal neurons showed resonance at both a higher frequency (CA3: 1.19 ± 0.09 Hz, $n = 15$; CA1: 2.49 ± 0.17 Hz, $n = 19$; $p < 10^{-4}$, unpaired two-sample Student's *t*-test; **Table 3**) and with greater Q-value (CA3: 1.06 ± 0.01, $n = 15$; CA1: 1.15 ± 0.01, $n = 19$; $p < 10^{-4}$, unpaired two-sample Student's *t*-test; **Table 3**) than CA3 pyramidal neurons.

3.2. BIDIRECTIONAL PHASE RESPONSE CURVE IN CA3 AND CA1 PYRAMIDAL NEURONS

In order to compare the spike timing response between mouse CA3 and CA1 pyramidal neurons, their phase response curves were measured using dynamic clamp. Artificial conductances were applied at the soma of the pyramidal neurons to mimic the inhibitory theta oscillation (3 nS) and excitatory inputs (aEPSGs, 1 nS). The aEPSGs were delivered at different phases of the induced 5 Hz oscillation and their effect on the successive spike phase was measured, compared to a control spike phase averaged from the four immediately preceding cycles. As previously described in rat CA3 (Lengyel et al., 2005), aEPSGs advanced

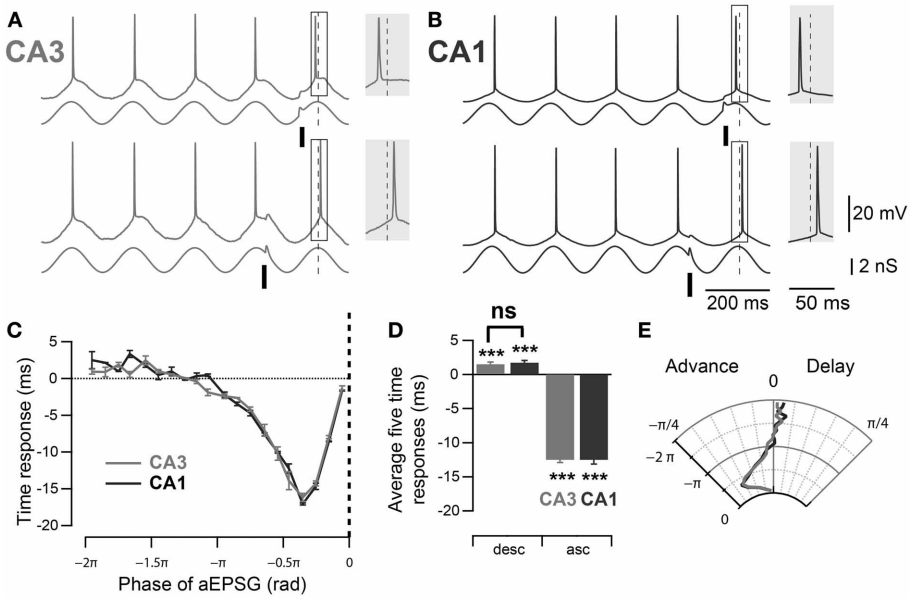

FIGURE 3 | Comparable PRCs measured at the soma of mouse CA3 and CA1 pyramidal neurons. (A,B) Representative traces, in CA3 and CA1 respectively, of spike phase shift in response to excitatory input (aEPSG) delivered at different phases of a theta oscillation imposed by dynamic clamp. When aEPSG was delivered at ascending phases, the following spike was advanced compared to the average spike phase over the four preceding cycles (top traces). In contrast, when aEPSG was delivered at descending phases, the following spike was delayed compared to the control spike phase (bottom traces). The spike phase shifts (boxes) are enlarged in the shaded insets. **(C)** Spike time response curve: plot of spike time shift as a function of aEPSG phase relative to the imposed theta oscillation. **(D)** Average spike time response induced by aEPSGs at five descending and ascending phases. Neurons in both CA3 and CA1 showed significant delay after excitatory input at the descending phase of theta oscillation. **(E)** Polar graph of the phase response curve. Data are shown as mean ± SEM, $n = 32$ for CA3 and 11 for CA1. $^{***}p < 0.001$, one-sample mean angle test; ns: Watson–Williams test; rad, radian; asc, ascending phases; desc, descending phases.

the subsequent spike when delivered at the ascending phase of the theta oscillation (**Figures 3A,C–E**, ascending phases: -0.39 ± 0.01 rad, $n = 32$, $p < 10^{-4}$, one-sample mean angle test) and led to a significant delay of the following spike when delivered at the descending phase (**Figures 3A–E**; descending phases: 0.04 ± 0.01 rad, $n = 32$, $p = 10^{-4}$, one-sample mean angle test). Moreover, as suggested by previous work (Kwag and Paulsen, 2009a), a similar effect was seen in CA1 pyramidal neurons (**Figures 3B–E**; ascending phases: -0.39 ± 0.02 rad, $n = 11$, $p < 10^{-4}$; descending phases: 0.05 ± 0.01 rad, $n = 11$, $p < 10^{-4}$; one-sample mean angle test). We then quantitatively compared the phase response curves between CA3 and CA1 (**Figures 3C–E**). Quantifications were done by averaging spike phase responses for stimulations occurring in the first descending $\pi/2$ rad and the last ascending $\pi/2$ rad of theta cycles. There was no significant difference in spike phase delay induced by stimulation at descending phases of the theta oscillation between CA3 and CA1 (descending phases CA3 *vs.* CA1: $p = 0.98$, Watson–Williams test); nor was there a difference in spike phase advance in response to aEPSGs delivered at ascending phases (ascending phases CA3 *vs.* CA1: $p = 1$, Watson–Williams test).

3.3. EFFECT OF THE CONDUCTANCE MAGNITUDE OF THE IMPOSED OSCILLATION

As the neuronal phase response to aEPSGs is likely to reflect the interaction of intrinsic properties and imposed oscillation, we next investigated the effect of the magnitude of the imposed oscillatory conductance in CA1 cells. By decreasing it from 3 to 1 nS (**Figure 4A**), the average spike phase delay and advancement measured for aEPSGs delivered during $\pi/2$ rad of the ascending and descending oscillation, respectively, tended to increase (**Figures 4B–D**; ascending phases of 1 nS oscillation: -0.63 ± 0.07 rad, $p = 0.001$; descending phases of 1 nS oscillation: 0.12 ± 0.03 rad, $p = 0.03$; $n = 5$, Watson–Williams test). Interestingly, the profile of the phase response curve (PRC) was altered as spikes were advanced in response to aEPSGs delivered at earlier phases of the oscillation (**Figures 4A,C**; phase of the aEPSGs producing the maximal phase advance: during 3 nS oscillation: $-0.38 \pm 0.02\pi$ rad, $n = 11$; during 1 nS oscillation: $-0.61 \pm 0.06\pi$ rad, $n = 5$; $p = 0.001$, Watson–Williams test).

3.4. ROLE OF H-CURRENT IN SPIKE PHASE RESPONSE

Given the differences in intrinsic membrane properties between CA3 and CA1 pyramidal neurons (**Table 3**), it appeared surprising that we were unable to detect any significant difference in phase response properties between the two cell types. We therefore designed a new protocol to maximize possible differences between CA3 and CA1 pyramidal neurons. To this end, the oscillation was driven by dynamic clamp with a 5 nS inhibitory conductance. Moreover, perturbations were optimized for descending phases of the oscillation by increasing their duration to one quarter of an oscillatory cycle (between -1.8π and

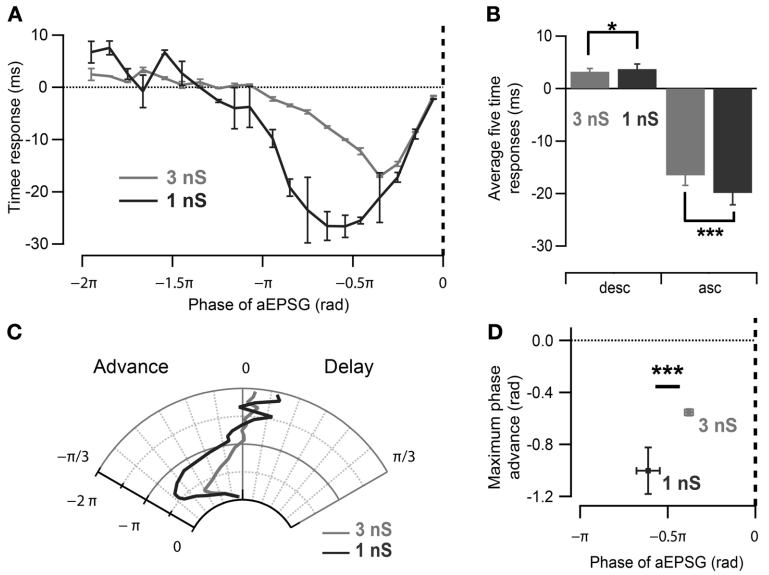

FIGURE 4 | Effect of oscillation strength on the phase response curve. **(A)** Spike time response curve of CA1 pyramidal neurons measured for strong (3 nS) and weak (1 nS) induced oscillation. Note differences in the input phase for maximum spike time advance as well as the magnitude of time advance. **(B)** Spikes have a tendency to be more advanced and delayed by aEPSGs delivered at 0.5π rad of the ascending and descending slope of 1 nS than 3 nS-induced oscillation respectively. $^{*}p < 0.05$, $^{***}p < 0.001$, Watson–Williams test. **(C)** Polar representation of the phase response curves in **(A)**. **(D)** Maximal spike phase advance occurs significantly earlier with excitatory inputs during oscillations with smaller maximum conductance in CA1 pyramidal neurons. Data are shown as mean ± SEM, $n = 11$ for 3 nS and $n = 5$ for 1 nS oscillatory inhibition; $^{***}p < 0.001$, Watson–Williams test; rad, radian; asc, ascending phases; desc, descending phases.

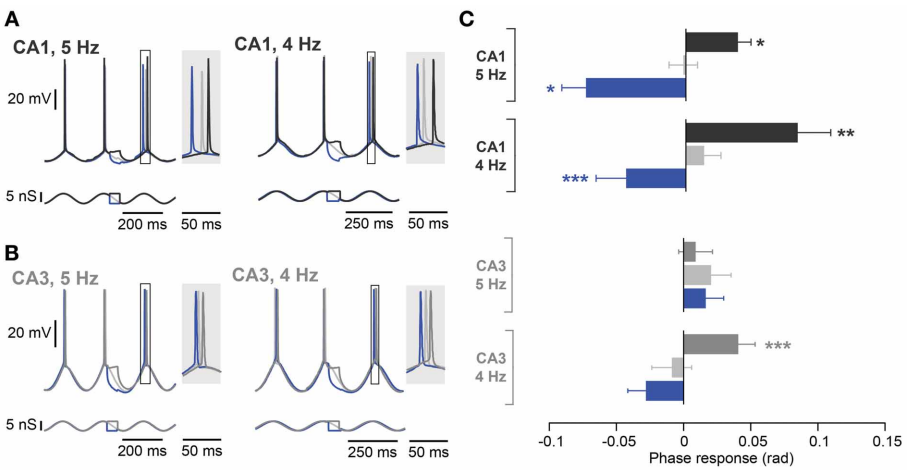

FIGURE 5 | Frequency dependence of spike phase control recorded at 5 Hz and 4 Hz. **(A)** Representative responses of a CA1 neuron (top traces) to inputs optimized for modulating I_h during induced oscillation (bottom traces) at 5 Hz (left panel) and 4 Hz (right panel). The spike phase shifts (boxes) are enlarged in the shaded insets. **(B)** Same as in **(A)** but from a CA3 neuron with a resonance peak > 1 Hz. **(C)** Average phase responses of CA1 and CA3 pyramidal neurons for both a 5 and 4 Hz oscillation. In CA1, a depolarizing step delayed the following spike, whereas a hyperpolarizing step advanced the following spike compared to the control condition at both oscillation frequencies. CA3 neurons, however, even with a resonance peak > 1 Hz, failed to show phase delay and advance with stimulation during descending phases of an ongoing 5 Hz oscillation. The spike phase delay is partially rescued when the frequency of the imposed oscillation is lowered to 4 Hz ($n = 4$). Data are shown as mean ± SEM. $^{*}p < 0.05$, $^{**}p < 0.001$, $^{***}p < 0.0001$, Moore's test; rad, radian.

−1.3π rad). The effect of excitation and inhibition were estimated as the spike phase response to subthreshold depolarizing and hyperpolarizing steps compared to a control condition when no perturbation was added (**Figures 5A,B**). As expected (Kwag and Paulsen, 2009a), depolarizing steps led to a delay and hyperpolarizing steps led to advancement of the subsequent spike in CA1 during the 5 Hz oscillation (**Figure 5C**; control: -0.02 ± 0.01 rad; depolarization: 0.04 ± 0.01 rad, $p = 0.02$;

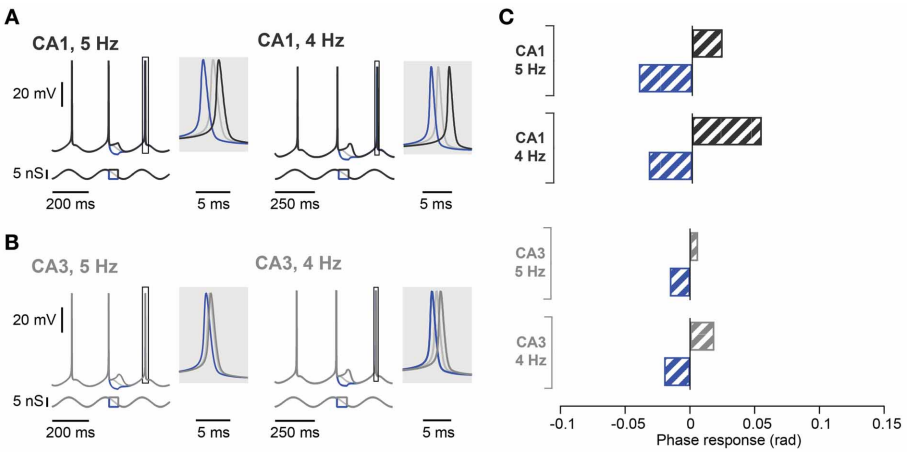

FIGURE 6 | Spike phase control in computational models of hippocampal CA1 and CA3 pyramidal neurons. (A) Voltage response of CA1 neuron model (top traces) in response to excitatory and inhibitory perturbation of an oscillatory input (bottom traces) at 5 Hz (left panel) or 4 Hz (right panel). The voltage response around the control spike is expanded to display spike phase responses. The spike phase shifts (boxes) are enlarged in the shaded insets. **(B)** Same as in **(A)** but in CA3 neuron model with h-channel kinetics adjusted to reproduce the voltage sag seen in CA3 neurons. **(C)** Summary spike phase changes elicited in CA1 and CA3 neuron model by excitatory and inhibitory step inputs during 5 and 4 Hz oscillation. rad, radian.

hyperpolarization: -0.07 ± 0.02 rad, $p = 0.02$; $n = 5$, Moore's test). This effect was prevented by the I_h blocking drug ZD7288 (10 μM, $n = 5$; control: 0.02 ± 0.01 rad; depolarization: 0.00 ± 0.02 rad, $p = 0.67$; hyperpolarization: 0.09 ± 0.04 rad, $p = 0.25$; $n = 5$, Moore's test; data not shown) and was absent in mice with a genetic deletion of h-channels (HCN1 KO, $n = 5$; control: 0.0 ± 0.01 rad; depolarization: -0.01 ± 0.02 rad, $p = 0.67$; hyperpolarization: 0.04 ± 0.04 rad, $p = 0.45$; $n = 5$, Moore's test; data not shown).

In contrast to the effect in CA1, during a 5 Hz oscillation this protocol failed to induce any significant phase response from CA3 pyramidal neurons, even those selected for their resonance properties (**Figure 5C**; control: 0.02 ± 0.01 rad; depolarization: 0.01 ± 0.01 rad, $p = 0.62$; hyperpolarization: 0.02 ± 0.01 rad, $p = 0.99$; $n = 5$, Moore's test). Since not only the strength of resonance but also the frequency preference differed between CA3 and CA1 pyramidal neurons (**Table 3**), we next investigated the influence of the I_h kinetics. To that aim, a computational model of CA3 and CA1 pyramidal neurons was generated in which the main distinction was I_h activation time constants and maximal conductance. I_h kinetics were modified according to experimental data so that CA3 model cells had half the sag in response to a negative step of current compared to the CA1 model (**Table 3**; **Figure 1B**). With those parameters, the model demonstrated a more prominent spike phase response during 5 Hz oscillation in CA1 than in CA3 neuron models (**Figures 6A–C**). The model also suggested that decreasing the oscillatory frequency to 4 Hz would increase the spike phase response in CA3 cells (**Figures 6B,C**).

Experimentally, we confirmed that the spike phase delay resulting from subthreshold steps during the descending phase of an oscillation was rescued in CA3 cells with resonance peak exceeding 1 Hz by reducing the oscillation frequency to 4 Hz (**Figure 5C**; control: -0.01 ± 0.01 rad; depolarization: 0.04 ± 0.01 rad, $p < 10^{-4}$; hyperpolarization: -0.03 ± 0.01 rad, $p = 0.35$; $n = 4$, Moore's test). A reduction in oscillation frequency had only a minor effect on CA1 cells (**Figure 5C**; control: 0.01 ± 0.01 rad; depolarization: 0.08 ± 0.02 rad, $p = 0.001$; hyperpolarization: -0.04 ± 0.02 rad, $p = 0.0004$; $n = 10$, Moore's test).

4. DISCUSSION

This study revealed a frequency-dependent difference between CA3 and CA1 spike phase responses based on differential properties of the I_h current in these two cell classes. The stronger expression and faster kinetics of I_h in CA1 pyramidal neurons was reflected by a larger voltage sag ratio in response to injection of negative current steps, compared to CA3, together with a more prominent resonance peak than that in CA3 cells. Low conductance oscillations promoted precise temporal spike pattern of CA3 and CA1 pyramidal neurons, bidirectionally controlled by their inputs. The involvement of I_h in the spike phase shift induced by inputs at descending phases of the membrane potential oscillation was confirmed by the impairment of the response when I_h was blocked by a selective blocker or by a genetic knockout of HCN1 channels. Moreover, the active spike phase response was reduced by a strong oscillatory conductance. As predicted by a computational model, and consistent with the kinetics of I_h activation in the two cell types, the active spike phase response was much reduced in CA3 pyramidal neurons at 5 Hz but rescued at a lower frequency. Our results support the view that intrinsic properties of hippocampal cells allow temporal control of their output by the interaction of inputs with active membrane properties during oscillatory network activity.

CA3 and CA1 pyramidal neurons display different membrane properties consistent with differential expression of I_h. This conclusion is supported by two independent measurements, namely the sag ratio and the resonance frequency of the two cell types, and is in agreement with previous reports. In CA1

pyramidal neurons, our data are consistent with previous reports concerning the sag ratio (Zemankovics et al., 2010), the frequency preference (Hu et al., 2002) and the magnitude of the resonance (Hu et al., 2002; Zemankovics et al., 2010). In CA3 pyramidal neurons, the more modest sag ratio and resonance properties are consistent with the work of Vasilyev and Barish (2002), measuring a slower and smaller I_h in CA3 compared to CA1 cells. This can explain why only a subpopulation of pyramidal neurons in CA3 had a detectable resonance peak.

Despite different membrane properties, CA3 and CA1 pyramidal neurons have similar spike phase responses. This similarity reflects their comparable passive membrane properties and especially R_{in}. The active component of their response, however, although based on I_h activation, is surprisingly similar despite differences in I_h between the two cell types. This could be accounted for by the experimental design, which drives the membrane potential oscillation and mimics artificial inputs with relatively low conductances using dynamic clamp. This allows the smaller I_h conductance in CA3 neurons to influence spike timing. Bidirectional spike phase responses have previously been reported in both CA3 (Lengyel et al., 2005) and CA1 (Kwag and Paulsen, 2009a) pyramidal neurons. Differences in the magnitude of the delay effects between the studies most likely result from differences in the species used, the strength of the oscillation imposed, and in the analysis procedures, particularly in the handling of directly activated spikes. In view of these results, the place field stability described by Hussaini et al. (2011) in HCN1 KO animals could result from the impairment of spike phase shift responsible for the appropriate experience-dependent changes in synaptic weights.

An interaction between the injected conductance and the intrinsic conductances was seen when the membrane potential oscillation of CA1 pyramidal neurons was driven with a weaker conductance. In this case, the passive and active spike phase responses (based on artificially injected and I_h-activated conductances respectively) are more prominent. The larger I_h in CA1 pyramidal neurons allows an active spike phase control even for strong oscillation of the membrane potential. With a more modest expression of I_h, in contrast, CA3 pyramidal neurons appear to fail to activate the I_h conductance sufficiently to overcome the injected oscillatory conductance. Interestingly, the gradient expression of I_h along the dendritic tree (Magee, 1998) predicts stronger spike phase control resulting from extracellular stimulation in apical dendritic layers. Inputs would yield different control of spike phase depending on their location and the local I_h, although additional synaptic conductances may also contribute (Kwag and Paulsen, 2009b).

The differences in I_h properties between CA3 and CA1 pyramidal neurons involve not only the total conductance but also the activation kinetics, and the spike phase response in CA3 pyramidal neurons was rescued during slower oscillations. This effect was predicted by computational modeling of the two cell types based on known morphological differences (Ishizuka et al., 1995; Morellini et al., 2010) and the recorded intrinsic membrane properties. The model was designed as a single compartment and conformed to our *in vitro* experiments for which current injection, conductance simulation, and membrane potential recordings were done at the soma. It has to be noted, nonetheless, that this model did not explicitly model the spatial recruitment of the dendritic conductances (Káli and Zemankovics, 2012). The activation kinetics for I_h, although modified to fit our data, remain close to the source equation originating from Morse et al. (2010). The frequency-dependence of CA3 pyramidal neuron spike phase control could be of functional importance with regards to information processing. The slower oscillation used in this study, namely 4 Hz, is in the lower range of the theta band. Interestingly, a reduction of theta frequency accompanies novelty *in vivo* (Jeewajee et al., 2008). I_h expression in CA3 pyramidal neurons might therefore account for a separation between encoding and retrieval states in this subfield and internal associational connections storing previous experiences could then be strengthened before being reconnected to primary sensory information in CA1.

ACKNOWLEDGMENTS

FUNDING

This work was supported by the Biotechnology and Biological Sciences Research Council and the Wellcome Trust. Hyun Jae Jang and Jeehyun Kwag were supported by the Basic Science Research Program (NRF-2011-0014481) through the National Research Foundation of Korea funded by the Ministry of Education, Science, and Technology.

REFERENCES

Amaral, D. G., and Witter, M. P. (1989). The three-dimensional organization of the hippocampal formation: a review of anatomical data. *Neuroscience* 31, 571–591. doi: 10.1016/0306-4522(89)90424-7

Berens, P. (2009). CircStats: a MATLAB toolbox for circular statistics. *J. Stat. Softw.* 31, 1–21.

Buzsáki, G. (2002). Theta oscillations in the hippocampus. *Neuron* 33, 325–340. doi: 10.1016/S0896-6273(02)00586-X

Ekstrom, A. D., Meltzer, J., McNaughton, B. L., and Barnes, C. A. (2001). NMDA receptor antagonism blocks experience-dependent expansion of hippocampal "place field". *Neuron* 31, 631–638. doi: 10.1016/S0896-6273(01)00401-9

Hines, M. L., and Carnevale, N. T. (1997). The NEURON simulation environment, *Neural Comput.*, 9, 1179–1209

Hodgkin, A. L., and Huxley, A. F. (1952). A quantitative description of membrane current and its application to conduction and excitation in nerve. *J. Physiol.* 117, 500–544.

Hölscher, C., Anwyl, R., and Rowan, M. J. (1997). Stimulation on the positive phase of hippocampal theta rhythm induces long-term potentiation that can be depotentiated by stimulation on the negative phase in area CA1 *in vivo*. *J. Neurosci.* 17, 6470–6477.

Hu, H., Vervaeke, K., and Storm, J. F. (2002). Two forms of electrical resonance at theta frequencies, generated by M-current, h-current and persistent Na^+ current in rat hippocampal pyramidal cells. *J. Physiol.* 545, 783–805. doi: 10.1113/jphysiol.2002.029249

Huerta, P. T., and Lisman, J. E. (1993). Heightened synaptic plasticity of hippocampal CA1 neurons during a cholinergically induced rhythmic state. *Nature* 364, 723–725. doi: 10.1038/364723a0

Hussaini, S. A., Kempadoo, K. A., Thuault, S. J., Siegelbaum, S. A., and Kandel, E. R. (2011). Increased size and stability of CA1 and CA3 place fields in HCN1 knockout mice. *Neuron* 72, 643–653. doi: 10.1016/j.neuron.2011.09.007

Hutcheon, B., and Yarom, Y. (2000). Resonance, oscillation and the intrinsic frequency preferences of neurons. *Trends Neurosci.* 23, 216–222. doi: 10.1016/S0166-2236(00)01547-2

Ishizuka, N., Cowan, W. M., and Amaral, D. G. (1995). A quantitative analysis of the dendritic organization of pyramidal cells in the rat hippocampus. *J. Comp. Neurol.* 362, 17–45. doi: 10.1002/cne.903620103

Jeewajee, A., Lever, C., Burton, S., O'Keefe, J., and Burgess, N. (2008). Environmental novelty is signaled by reduction of the hippocampal theta frequency. *Hippocampus* 18, 340–348. doi: 10.1002/hipo.20394

Jouvet, M., Michel, F., and Courjon, J. (1959). Sur un stade d'activité électrique cérébrale rapide au cours du sommeil physiologique [On a stage of rapid cerebral electrical activity in the course of physiological sleep]. *C. R. Soc. Biol.* 153, 1024–1028.

Káli, S., and Zemankovics, R. (2012). The effect of dendritic voltage-gated conductances on the neuronal impedance: a quantitative model. *J. Comput. Neurosci.* 33, 257–284. doi: 10.1007/s10827-012-0385-9

Kamondi, A., Acsády, L., Wang, X.-J., and Buzsáki, G. (1998). Theta oscillations in somata and dendrites of hippocampal pyramidal cells *in vivo*: activity-dependent phase-precession of action potentials. *Hippocampus* 261, 244–261. doi: 10.1002/(SICI)1098-1063(1998)8:3<244::AID-HIPO7>3.0.CO;2-J

Kwag, J., and Paulsen, O. (2009a). Bidirectional control of spike timing by $GABA_A$ receptor-mediated inhibition during theta oscillation in CA1 pyramidal neurons. *Neuroreport* 20, 1209–1213. doi: 10.1097/WNR.0b013e32832f5cc7

Kwag, J., and Paulsen, O. (2009b). The timing of external input controls the sign of plasticity at local synapses. *Nat. Neurosci.* 12, 1219–1221. doi: 10.1038/nn.2388

Lee, I., Hunsaker, M. R., and Kesner, R. P. (2005). The role of hippocampal subregions in detecting spatial novelty. *Behav. Neurosci.* 119, 145–153. doi: 10.1037/0735-7044.119.1.145

Lee, I., Rao, G., and Knierim, J. J. (2004). A double dissociation between hippocampal subfields: differential time course of CA3 and CA1 place cells for processing changed environments. *Neuron* 42, 803–815. doi: 10.1016/j.neuron.2004.05.010

Lengyel, M., Kwag, J., Paulsen, O., and Dayan, P. (2005). Matching storage and recall: hippocampal spike timing-dependent plasticity and phase response curves. *Nat. Neurosci.* 8, 1677–1683. doi: 10.1038/nn1561

Magee, J. C. (1998). Dendritic hyperpolarization-activated currents modify the integrative properties of hippocampal CA1 pyramidal neurons. *J. Neurosci.* 18, 7613–7624.

McNaughton, B. L., and Morris, R. G. M. (1987). Hippocampal synaptic enhancement and information storage within a distributed memory system. *Trends Neurosci.* 10, 408–415. doi: 10.1016/0166-2236(87)90011-7

McNaughton, N., Ruan, M., and Woodnorth, M.-A. (2006). Restoring theta-like rhythmicity in rats restores initial learning in the Morris water maze. *Hippocampus* 16, 1102–1110. doi: 10.1002/hipo.20235

Mehta, M. R., Barnes, C. A., and McNaughton, B. L. (1997). Experience-dependent, asymmetric expansion of hippocampal place fields. *Proc. Natl. Acad. Sci. U.S.A.* 94, 8918–8921. doi: 10.1073/pnas.94.16.8918

Morellini, F., Sivukhina, E., Stoenica, L., Oulianova, E., Bukalo, O., Jakovcevski, I., Dityatev, A., et al. (2010). Improved reversal learning and working memory and enhanced reactivity to novelty in mice with enhanced GABAergic innervation in the dentate gyrus. *Cereb. Cortex* 20, 2712–2727. doi: 10.1093/cercor/bhq017

Morse, T. M., Carnevale, N. T., Mutalik, P. G., Migliore, M., and Shepherd, G. M. (2010). Abnormal excitability of oblique dendrites implicated in early Alzheimer's: a computational study. *Front. Neural Circuits* 4:16. doi: 10.3389/fncir.2010.00016

Nolan, M. F., Malleret, G., Dudman, J. T., Buhl, D. L., Santoro, B., Gibbs, E., et al. (2004). A behavioral role for dendritic integration: HCN1 channels constrain spatial memory and plasticity at inputs to distal dendrites of CA1 pyramidal neurons. *Cell* 119, 719–732. doi: 10.1016/j.cell.2004.11.020

O'Keefe, J., and Recce, M. L. (1993). Phase relationship between hippocampal place units and the EEG theta rhythm. *Hippocampus* 3, 317–330. doi: 10.1002/hipo.450030307

Olvera-Cortés, M. E., Cervantes, M., and González-Burgos, I. (2002). Place-learning, but not cue-learning training, modifies the hippocampal theta rhythm in rats. *Brain Res. Bull.* 58, 261–270. doi: 10.1016/S0361-9230(02)00769-4

Pavlides, C., and Winson, J. (1989). Influences of hippocampal place cell firing in the awake state on the activity of these cells during subsequent sleep episodes. *J. Neurosci.* 9, 2907–2918.

Pike, F. G., Goddard, R. S., Suckling, J. M., Ganter, P., Kasthuri, N., and Paulsen, O. (2000). Distinct frequency preferences of different types of rat hippocampal neurones in response to oscillatory input currents. *J. Physiol.* 529, 205–213. doi: 10.1111/j.1469-7793.2000.00205.x

Prinz, A. A., Abbott, L. F., and Marder, E. (2004). The dynamic clamp comes of age. *Trends Neurosci.* 27, 218–224. doi: 10.1016/j.tins.2004.02.004

Puil, E., Gimbarzevsky, B., and Miura, R. M. (1986). Quantification of membrane properties of trigeminal root ganglion neurons in guinea pigs. *J. Neurophysiol.* 55, 995–1016.

Robinson, H. P., and Kawai, N. (1993). Injection of digitally synthesized synaptic conductance transients to measure the integrative properties of neurons. *J. Neurosci. Methods* 49, 157–165. doi: 10.1016/0165-0270(93)90119-C

Seager, M. A., Johnson, L. D., Chabot, E. S., Asaka, Y., and Berry, S. D. (2002). Oscillatory brain states and learning: impact of hippocampal theta-contingent training. *Proc. Natl. Acad. Sci. U.S.A.* 99, 1616–1620. doi: 10.1073/pnas.032662099

Smith, C. T., and Rose, G. M. (1996). Evidence for a paradoxical sleep window for place learning in the Morris water maze. *Physiol. Behav.* 59, 93–97. doi: 10.1016/0031-9384(95)02054-3

Smith, C. T., and Rose, G. M. (1997). Posttraining paradoxical sleep in rats is increased after spatial learning in the Morris water maze. *Behav. Neurosci.* 111, 1197–1204. doi: 10.1037/0735-7044.111.6.1197

Soltész, I., and Deschenes, M. (1993). Low- and high-frequency membrane potential oscillations during theta activity in CA1 and CA3 pyramidal neurons of the rat hippocampus under ketamine-xylazine anesthesia. *J. Neurophysiol.* 70, 97–116.

Vanderwolf, C. H. (1969). Hippocampal electrical activity and voluntary movement in the rat. *Electroencephalogr. Clin. Neurophysiol.* 26, 407–418. doi: 10.1016/0013-4694(69)90092-3

VanElzakker, M., Fevurly, R. D., Breindel, T., and Spencer, R. L. (2008). Environmental novelty is associated with a selective increase in fos expression in the output elements of the hippocampal formation and the perirhinal cortex. *Learn. Mem.* 15, 899–908. doi: 10.1101/lm.1196508

Vasilyev, D. V., and Barish, M. E. (2002). Postnatal development of the hyperpolarization-activated excitatory current I_h in mouse hippocampal pyramidal neurons. *J. Neurosci.* 22, 8992–9004.

Wetzel, W., Wagner, T., and Balschun, D. (2003). REM sleep enhancement induced by different procedures improves memory retention in rats. *Eur. J. Neurosci.* 18, 2611–2617. doi: 10.1046/j.1460-9568.2003.02890.x

Winson, J. (1978). Loss of hippocampal theta rhythm results in spatial memory deficit in the rat. *Science* 201, 160–163. doi: 10.1126/science.663646

Woldeit, M. L., and Korz, V. (2010). Theta oscillations during holeboard training in rats: different learning strategies entail different context-dependent modulations in the hippocampus. *Neuroscience* 165, 642–653. doi: 10.1016/j.neuroscience.2009.11.002

Zemankovics, R., Káli, S., Paulsen, O., Freund, T. F., and Hájos, N. (2010). Differences in subthreshold resonance of hippocampal pyramidal cells and interneurons: the role of h-current and passive membrane characteristics. *J. Physiol.* 588, 2109–2132. doi: 10.1113/jphysiol.2009.185975

Conflict of Interest Statement: The authors declare that the research was conducted in the absence of any commercial or financial relationships that could be construed as a potential conflict of interest.

Received: 29 October 2013; accepted: 03 December 2013; published online: 25 December 2013.

Citation: Borel M, Guadagna S, Jang HJ, Kwag J and Paulsen O (2013) Frequency dependence of CA3 spike phase response arising from h-current properties. Front. Cell. Neurosci. 7:263. doi: 10.3389/fncel.2013.00263

This article was submitted to the journal Frontiers in Cellular Neuroscience.

frontiers in
CELLULAR NEUROSCIENCE

ORIGINAL RESEARCH ARTICLE
published: 25 July 2013
doi: 10.3389/fncel.2013.00117

Amyloid-β induces synaptic dysfunction through G protein-gated inwardly rectifying potassium channels in the fimbria-CA3 hippocampal synapse

Mauricio O. Nava-Mesa[1,2], Lydia Jiménez-Díaz[1], Javier Yajeya[2] and Juan D. Navarro-Lopez[1]*

[1] *Laboratorio Neurofisiología y Comportamiento, Facultad de Medicina de Ciudad Real, Universidad de Castilla-La Mancha, Ciudad Real, Spain*
[2] *Department of Fisiología y Farmacología, Universidad de Salamanca, Salamanca, Spain*

Edited by:
Enrico Cherubini, International School for Advanced Studies, Italy

Reviewed by:
Lisa Topolnik, Laval University, Canada
Claudia Lodovichi, Venetian Institute of Molecular Medicine, Italy

***Correspondence:**
Juan D. Navarro-López, Neurophysiology and Bahavior Lab, School of Medicine of Ciudad Real, University of Castilla-La Mancha, Paseo Moledores s/n, 13071-Ciudad Real, Spain
e-mail: juan.navarro@uclm.es

Last evidences suggest that, in Alzheimer's disease (AD) early stage, Amyloid-β (Aβ) peptide induces an imbalance between excitatory and inhibitory neurotransmission systems resulting in the functional impairment of neural networks. Such alterations are particularly important in the septohippocampal system where learning and memory processes take place depending on accurate oscillatory activity tuned at fimbria-CA3 synapse. Here, the acute effects of Aβ on CA3 pyramidal neurons and their synaptic activation from septal part of the fimbria were studied in rats. A triphasic postsynaptic response defined by an excitatory potential (EPSP) followed by both early and late inhibitory potentials (IPSP) was evoked. The EPSP was glutamatergic acting on ionotropic receptors. The early IPSP was blocked by $GABA_A$ antagonists whereas the late IPSP was removed by $GABA_B$ antagonists. Aβ perfusion induced recorded cells to depolarize, increase their input resistance and decrease the late IPSP. Aβ action mechanism was localized at postsynaptic level and most likely linked to $GABA_B$-related ion channels conductance decrease. In addition, it was found that the specific pharmacological modulation of the $GABA_B$ receptor effector, G-protein-coupled inward rectifier potassium (GirK) channels, mimicked all Aβ effects previously described. Thus, our findings suggest that Aβ altering GirK channels conductance in CA3 pyramidal neurons might have a key role in the septohippocampal activity dysfunction observed in AD.

Keywords: septohippocampal system, fimbria-CA3 synapse, amyloid-β_{25-35} peptide, $GABA_B$, GirK channels, Alzheimer's disease, brain slices, intracellular recordings

INTRODUCTION

Being still lack of effective treatments for Alzheimer's disease (AD), current research efforts have focused on finding the relationships between amyloid-β peptide (Aβ) functions and toxic mechanisms to understand the development of AD (Huang and Mucke, 2012). Memory deficits and disorientation appear as the first symptoms of AD (McKhann et al., 1984; Swanberg et al., 2004) and, among the different regions early affected, damages found in septum and hippocampus could explain these cognitive deficits (Moreno et al., 2007; Palop et al., 2007; Villette et al., 2010; Rubio et al., 2012). Both structures are reciprocally interconnected through fimbria/fornix, and are functionally coupled to form the septohippocampal system (Bland and Colom, 1993), which is critical in generating certain oscillatory activity, such as *theta* rhythm, necessary for fundamental processes in learning and memory (Stewart and Fox, 1990; Bland and Oddie, 2001; Buzsaki, 2002; Sotty et al., 2003; Colom, 2006; Colom et al., 2010; Rubio et al., 2012). *Theta* oscillation coordinates septohippocampal network and depends on interconnections, which include well known cholinergic and GABAergic (Lynch et al., 1977; Kohler et al., 1984; Bland and Colom, 1993) as well as glutamatergic (Sotty et al., 2003; Huh et al., 2010) projections.

In animal models of AD, septohippocampal network dysfunction has extensively been reported (Colom, 2006; Palop and Mucke, 2010; Peña et al., 2010; Villette et al., 2010, 2012; Rubio et al., 2012; Verret et al., 2012). At the synaptic level, dysfunction induced by Aβ on inhibitory neurotransmission causes aberrant patterns of activity in its associated neural circuits, destabilizes neuronal networks and impairs oscillatory activity. This scenario, ultimately, seems to be responsible for the early alteration of the processes implicated in learning and memory tasks observed in AD patients (Palop and Mucke, 2010; Huang and Mucke, 2012). However, the specific mechanisms involving inhibitory neurotransmission at the molecular level, synaptic circuits or systems that consistently explain Aβ neurotoxic effects and associated neurological deficits remain unknown.

γ-aminobutyric acid (GABA) is the main inhibitory neurotransmitter in the mammalian central nervous system and is involved in the regulation of many physiological processes. GABA mediates the inhibitory neurotransmission and accordingly, regulates excitatory activity preventing hyperexcitation, actions especially relevant to maintain neural network stability and oscillatory activity (Palop and Mucke, 2010). GABA metabotropic type receptors ($GABA_B$) are coupled to intracellular signal transduction mechanisms via G proteins (Mott and

Lewis, 1994; Kaupmann et al., 1998) and mediate slow and prolonged synaptic inhibition mainly by postsynaptic G protein-coupled activated inwardly-rectifying potassium (GirK) channels (Luscher et al., 1997; Kaupmann et al., 1998). Thus, GirK channels act as key players in the control of cellular and network excitability by modulating synaptic activity (Lujan and Ciruela, 2012).

In this study, we aimed to characterize Aβ effects on septohippocampal fimbria/CA3 synapsis. To address this question, we used an *in vitro* preparation taking advantage of the specific septo-hippocampal projection to CA3 pyramidal neurons, and evoked a characteristic complex synaptic response in CA3 recorded neurons by stimulating the septal part of the fimbria. For the first time, we provide evidence that Aβ decreased $GABA_B$ neurotransmission through altering GirK channel conductance.

MATERIALS AND METHODS

ANIMALS

Experiments were carried out on male and female rats (80–100 g) raised in the Salamanca University Animal House (Salamanca, Spain). All animal procedures were reviewed and approved by the Ethical Committee for Use of Laboratory Animals of the University of Salamanca and University of Castilla-La Mancha, and followed the European Communities Council (86/609/EEC).

PREPARATION OF SLICES

Animals were deeply anesthetized with halothane and decapitated. The brain was excised and rapidly immersed in oxygenated ice-cold (4–6°C) artificial cerebrospinal fluid (ACSF), with sucrose (234 mM) replacing the NaCl (117 mM) to maintain osmolarity. In order to preserve the optimal connectivity from fimbria fibers on CA3 pyramidal neurons (Gloveli et al., 2005; Bischofberger et al., 2006), horizontal slices containing the septal part of the fimbria, i.e., lateral fimbria (Alonso and Kohler, 1984; Amaral and Lavenex, 2007), and the hippocampus (350 μm-thick) were cut in cold oxygenated Ringer solution using a vibratome (Leica VT 1000S, Wetzlar, Germany) and placed in an incubation chamber, where they were maintained for at least 2 h at room temperature (22°C) before the recordings. Further details of this *in vitro* preparation have been described elsewhere (Yajeya et al., 2000).

SHARP ELECTRODE RECORDINGS

For recordings, a single septohippocampal slice was transferred to an interface recording chamber (BSC-HT and BSC-BU; Harvard Apparatus, Holliston, US) and perfused continuously with ACSF comprising (in mM) 117 NaCl, 4.7 KCl, 2.5 $CaCl_2$, 1.2 $MgCl_2$, 25 $NaHCO_3$, 1.2 NaH_2PO_4, and 11 glucose. The ACSF was bubbled with carbogen gas (95%O_2–5%CO_2) and maintained at room temperature during the recordings.

Intracellular sharp electrode recordings from CA3 pyramidal neurons were obtained with borosilicate glass microelectrodes (140–180 MΩ; WPI, Sarasota, US) filled with a potassium acetate solution (3 M) and connected to the headstage of an intracellular recording amplifier (Bio-logic VF180, Claix, France). Only data from neurons with both, stable resting membrane potential (RMP) with values ≤ -60 mV in the absence of direct current (DC) holding currents, and presenting overshooting action potentials, were collected for analysis. Spike amplitude, afterdepolarization and afterhyperpolarizing potentials were measured relative to threshold.

Excitatory and inhibitory postsynaptic potentials (EPSP and IPSP, respectively) were elicited orthodromically by stimulating the lateral fimbria where septal afferents to CA3 hippocampal neurons are mainly found (Alonso and Kohler, 1984; Amaral and Lavenex, 2007). For that purpose a monopolar stainless steel electrode (2 MΩ of effective resistance; WPI, Sarasota, US) and a programmable stimulator (MASTER-8, A8, A.M.P.I., Jerusalem, Israel) were used. Single, cathodal, square-wave pulses of 100–200 μs duration and 100–500 μA intensity were adjusted to subthreshold values for orthodromic spike generation. Postsynaptic potentials were characterized according to their amplitude (as a function of the RMP) and latency. Since horizontal slices were obtained at different level and angle, sometimes the location of the electrode along lateral fimbria had to be changed to evoke the characteristic triphasic response.

IDENTIFICATION OF STIMULATION AND RECORDING SITES

Recorded neurons were identified following procedures described elsewhere (Navarro-Lopez et al., 2004). Briefly, selected neurons were stained by the intracellular injection of biocytin diluted in a 2 M potassium acetate solution, using positive current pulses of 0.2 nA for 6 min. Slices were fixed, and cut in sections (40 μm) using a freezing microtome (HM400R, Microm, Heidelberg, Germany). Sections were incubated with avidin-biotin-peroxidase complex (ABC, Vector Labs., Burlingame, US). 3,3′-Diaminobenzidine was used as chromogen for visualization of the biocytin complex. Sections were counterstained with cresyl violet. Neuron was reconstructed from serial sections using a graphic design software. Photographs were superimposed and orientated to obtain the best fit between the corresponding sectioned elements.

DRUGS

All chemicals used in this study were purchased from Sigma (Poole, UK) and Tocris (Biogen Científica, Spain) and applied by superfusion in the ACSF. The chemicals used were amyloid-β peptides ($Aβ_{25–35}$ and the reverse $Aβ_{35–25}$), 6-cyano-nitroquinoxaline-2,3-dione (CNQX; a potent, competitive AMPA-kainate receptor antagonist), 2-amino-5-phosphonovalerate (APV; a specific blocker of NMDA receptors), Bicuculline Methiodide (specific blocker of $GABA_A$ receptors), (RS)-3-Amino-2-(4-chlorophenyl) propylphosphonic acid (Saclofen; blocker of $GABA_B$ receptors), (RS)-4-Amino-3-(4-chlorophenyl) butanoic acid (Baclofen; agonist of $GABA_B$ receptors), Tetrodotoxine (TTX; voltage dependent sodium channel blocker), Tertiapin-Q (selective blocker of GirK channels) and 2-methyl-2,4-pentanediol (MPD, agonist of GirK channels).

PREPARATION OF Aβ PEPTIDES SOLUTIONS

$Aβ_{25–35}$ and $Aβ_{35–25}$ peptides were prepared as previously (Ashenafi et al., 2005; Santos-Torres et al., 2007). Briefly, the peptides were dissolved to 1 mM in bidistilled water and stored in aliquots at −20°C. Then aliquots were diluted in ACSF to

required concentration and incubated for 24 h at 37°C before experiments were performed (Peña et al., 2010; Leao et al., 2012).

DATA STORAGE AND STATISTICAL ANALYSIS

Sharp electrode data were acquired online with the help of a CED 1401 interface (CED, Cambridge, UK), and stored on a personal computer (sample frequency 12.5 kHz). Analysis in both cases was performed using the MiniAnalysis Program, version 6.0.3 (Synaptosoft, Decatur, US). Unless otherwise indicated, the electrophysiological data are always expressed as mean ± standard error of the mean (SEM), and n represents the number of averaged neurons. Synaptic potentials were averaged (≥5) before quantitative analysis. Statistical analysis of collected data was performed using either Student's *t*-test or non-parametric test (Mann-Whitney *U*-test), accordingly with data distribution. When necessary, one-way ANOVA or equivalent non parametric test (Kruskal-Wallis test) and *post-hoc* analysis were performed. Statistical significance was determined at a level of $p \leq 0.05$.

RESULTS

ELECTROPHYSIOLOGICAL CHARACTERIZATION OF RECORDED NEURONS AND THEIR SYNAPTIC RESPONSE TO FIMBRIA STIMULATION

This study comprises 110 intracellular recordings from pyramidal CA3 neurons (**Figure 1**), selected on the basis of their RMP (≤ −60 mV) and monosynaptic activation from the fimbria. Recorded neurons did not exhibit action potentials spontaneously at RMP values (−72.5 ± 1.8 mV). The input resistance (Ri) of the neurons was 113.4 ± 6.7 MΩ and the membrane time constant was 77.2 ± 25.4 ms. The direct activation of these neurons by depolarizing current injections (0.1–0.6 nA ; 300 ms) evoked a series of two to five spikes with marked spike frequency adaptation and decreased amplitude and longer duration of the second spike relative to the first one (**Figure 1B**). The spike amplitude was 101.1 ± 3.2 mV. These characteristics, together with neuronal morphology (**Figure 1D**) and other electrophysiological properties such as the presence of triphasic afterhyperpolarization (fAHP: 5.6 ± 0.8 mV; mAHP: 10.5 ± 1.5 mV; sAHP: 17.6 ± 1.3 mV) or afterdepolarization (ADP: 3.6 ± 0.5 mV), characterize the principal pyramidal-like neurons widely described in the hippocampus (Spruston and Johnston, 1992; Wittner et al., 2007). The location of selected neurons ($n = 10$) filled with biocytin is illustrated in **Figure 1A**. The morphology corresponds to pyramidal neurons in CA3 region of the hippocampus. The cell body is located into the *stratum pyramidale* and the visible basal dendrites on *stratum oriens* (**Figure 1D**).

Single subthreshold stimulation of the fimbria evoked stereotyped triphasic synaptic responses in CA3 pyramidal cells (**Figure 2**). The initial response was a fast EPSP, which occurred at a latency of 6.5 ± 0.6 ms following stimulus offset, suggesting the monosynaptic nature of the connection. The size of the EPSP was graded with the stimulus intensity and it increased in amplitude when elicited at progressively more negative membrane potentials (**Figure 2A**). The EPSP was followed by a rapidly developing hyperpolarization (early IPSP, **Figures 2A,B**) that reached its peak amplitude 30.4 ± 1.4 ms ($n = 11$) following fimbria stimulation. Finally a second hyperpolarization (late IPSP, **Figures 2A,B**)

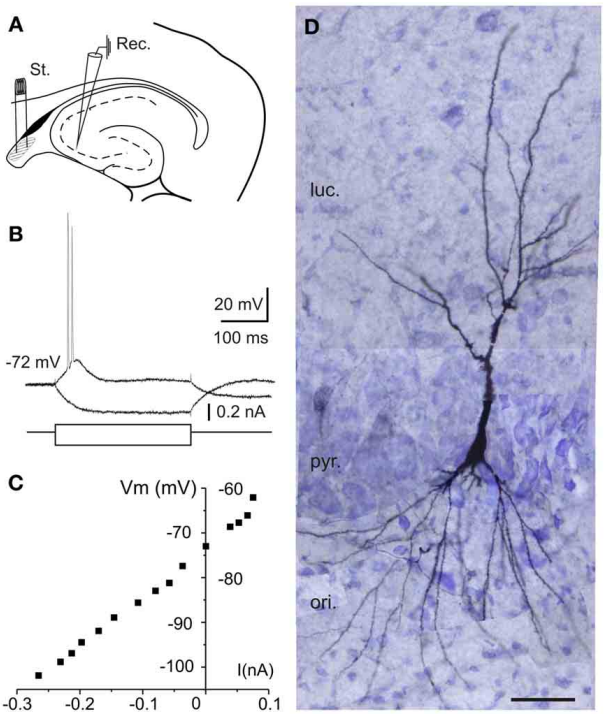

FIGURE 1 | Location and electrophysiological characterization of the recorded neurons in hippocampal slices. (A) Experimental design. Diagram of stimulation and recording sites in an hippocampal horizontal section. Schematic location of recording (Rec.) and stimulating (St.) electrodes is shown. Stimuli were applied to the lateral part of the fimbria (shaded area). **(B)** Response of a CA3 neuron to depolarizing pulses consisted of two to five spikes with marked spike frequency adaptation with a depolarizing current pulse (100 pA, 300 ms) while hyperpolarizing current pulse injection (−160 pA, 300 ms) induced a hyperpolarizing response that allowed us monitoring the input resistance during the experiments. **(C)** Current-voltage (*I-V*) relationships for the pyramidal neuron recorded in **(B)**. **(D)** Reconstruction of the CA3 neuron recorded in **(B,C)** labeled with biocytin after intracellular recording from 40-μm-thick serial sections. Note the pyramidal morphology of the injected hippocampal cell. ori, *stratum oriens*; pyr, *stratum pyramidale*; luc, *stratum lucidum*; Scale bar 50 μm.

following the early IPSP, had a latency to peak amplitude of 247.4 ± 6.6 ms ($n = 44$). The amplitudes of both, IPSPs and EPSP, varied with membrane potential (**Figures 2A,B**), allowing us to determine the approximate reversal potential for both inhibitory components (early −61.1 mV and late −80.0 mV).

In order to determine the nature of the complex response, a pharmacological dissection of the postsynaptic potential components was performed (**Figure 3**). The early IPSP was blocked by bicuculline (10 μM, $n = 6$), a specific blocker of $GABA_A$ receptors (**Figures 3A,C–E**) whereas late IPSP was removed by saclofen (200 μM; $n = 5$), a specific blocker of $GABA_B$ receptors (**Figures 3B,E**). The excitatory component was increased by early IPSP block with bicuculline ($n = 9$; **Figures 3A,C–E**) and presented a glutamatergic nature acting mainly on non-NMDA ($n = 5$; **Figure 3D**) receptors, since although its complete elimination required CNQX (10 μM) and APV (50 μM)

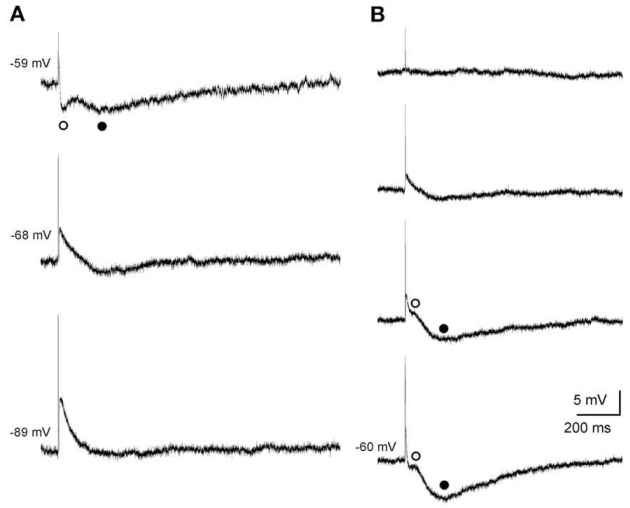

FIGURE 2 | Postsynaptic septohippocampal response in CA3 pyramidal neurons. (A) Effect of membrane potential variations on the amplitude of the early and late IPSPs evoked by orthodromic activation in a pyramidal CA3 neuron. Stimulation of the fimbria elicited an EPSP followed by an early (open circles) and late (closed circles) IPSP. Traces shown are the average of five responses. **(B)** Effect of varying the intensity of fimbria stimulation on the complex postsynaptic response recorded in another neuron at a membrane potential of −60 mV. From top to bottom, traces represent synaptic responses which were evoked by progressive increments in fimbria stimulation. Stimulation of the fimbria at a low intensity evoked only EPSP followed by an early (○, open circles) IPSP. Delivery of stimulation at higher intensities resulted in the elicitation of a subsequent late (●, closed circles) IPSP. The approximate reversal potential for both inhibitory components was early −61.1 mV and late −80.0 mV.

the cells were held at −75 mV (a membrane potential where NMDA receptor-mediated currents are null). However, when recorded cells were held at more positive values than RMP ($n = 4$; **Figure 3C**), NMDA channels were entirely functional and perfusion with APV decreased both bicuculline-enhanced responses, EPSP and late IPSP (**Figure 3E**), suggesting the participation of NMDA receptors in the response. As previously, complete blockage of EPSP also required CNQX (**Figure 3C**). In this regard, the pharmacological elimination of glutamatergic responses with CNQX plus APV also abolished the inhibitory response (**Figures 3C,D**) suggesting that IPSPs were produced by interneurons activation.

On the other hand, when both inhibitory components were removed an epileptiform-like discharge was generated (**Figures 3F,G**). This response could reach a firing frequency of 90 Hz and showed a glutamatergic nature acting mainly on non-NMDA receptors, since CNQX completely abolished it (**Figure 3F**) whereas APV only could block it partially (**Figure 3G**).

These results indicate that the triphasic complex response involves excitatory and inhibitory neurotransmission mediated by glutamate and GABA receptors activation, suggesting that a precise tuning is required for information processing at this synapse.

$A\beta_{25–35}$ DIFFERENTIAL EFFECTS ON MEMBRANE PROPERTIES

In all cases, the recordings were stabilized for at least 10 min. During this time, characterization of firing pattern, membrane potential, Ri and synaptic responses were performed. The specificity of the $A\beta_{25–35}$ peptide action was confirmed by the use, as negative control, of the reverse sequence $A\beta_{35–25}$ (1.5 μM), without any noticeable effect (**Figures 4A,C**). Then, slices were perfused with increasing concentrations of $A\beta_{25–35}$ (0.5, 1.0, and 1.5 μM) for at least another 10 min at each concentration.

No significant differences were found in spike amplitude [$F_{(3,\ 50)} = 2.62$, $p = 0.062$], threshold [$F_{(3,\ 50)} = 2.14$, $p = 0.108$], ADP [$F_{(3,\ 22)} = 0.576$, $p = 0.638$], fAHP [$F_{(3,\ 31)} = 1.22$, $p = 0.320$], or sAHP [$F_{(3,\ 33)} = 1.625$, $p = 0.204$] after perfusion with $A\beta_{25–35}$ at increasing concentrations. However, as shown in **Figures 4B,C**, a significant depolarization was observed when $A\beta_{25–35}$ was applied (1 μM; 4.3 ± 2.3 mV; $n = 4$; and 1.5 μM; 6.2 ± 1.6 mV; $n = 10$). The membrane potential of the recorded neurons was maintained at its RMP value by DC holding current injection to cancel out the depolarization induced by $A\beta_{25–35}$ (**Figure 4D**). These variations in current injection were statistically significant at 1.0 μM ($t = 2.557$, $p = 0.021$) and 1.5 μM ($t = 4.301$, $p < 0.001$) concentrations and no difference was observed at 0.5 μM concentrations ($t = 0.842$, $p = 0.412$). Additionally, $A\beta_{25–35}$ also produced a significant increase in the relative Ri (% = Ri recorded/Ri control *100; $n = 16$) (**Figures 4D–F**) at 1.0 μM concentration ($t = -2.635$, $p = 0.018$) and 1.5 μM ($t = -3.236$, $p = 0.007$) whereas no differences were found at 0.5 μM (Mann–Whitney U Statistic = 10.000, $p = 0.690$) (**Figures 4E,F**).

To determine the synaptic location of these $A\beta_{25–35}$ effects, slices were perfused with TTX and any afferent synaptic activity was blocked. In these conditions, superfusion of the slice with $A\beta_{25–35}$ was able to evoke both, depolarization and Ri increasing (**Figure 4D**) of intracellularly recorded CA3 pyramidal neurons, suggesting a postsynaptic location for the $A\beta_{25–35}$ action mechanism ($n = 5$).

DIFFERENTIAL EFFECTS OF $A\beta_{25–35}$ ON FIMBRIA-CA3 SYNAPTIC RESPONSE

Since Aβ has widely shown to exert its effects through septohippocampal network impairing, we examined whether this peptide altered the fimbria-CA3 complex postsynaptic response ($n = 20$). In the experiment shown in **Figure 5A**, superfusion of $A\beta_{25–35}$ produced a significant decrease of the late IPSP component (1 μM; $t = 2.532$, $p = 0.030$ and 1.5 μM; $t = 2.519$, $p = 0.036$) that was neither observed at 0.5 μM ($t = 1.133$, $p = 0.295$) nor on early IPSP ($H = 2.578$; $p = 0.461$). However, the late IPSP reduction was associated with an increase in the excitatory response observed at concentration of 1.5 μM ($t = -2.503$, $p = 0.046$) but not at lower concentrations (**Figures 5B,C**). These results indicate a possible mechanism to imbalance the particular excitatory/inhibitory tuning in the septohippocampal system, and therefore a differential $A\beta_{25–35}$ effect, according to the specific neurotransmission system involved.

Due to this differential $A\beta_{25–35}$ effect on both inhibitory components, the late component reduction may not be attributable to a decreased neurotransmitter release since $GABA_A$ component

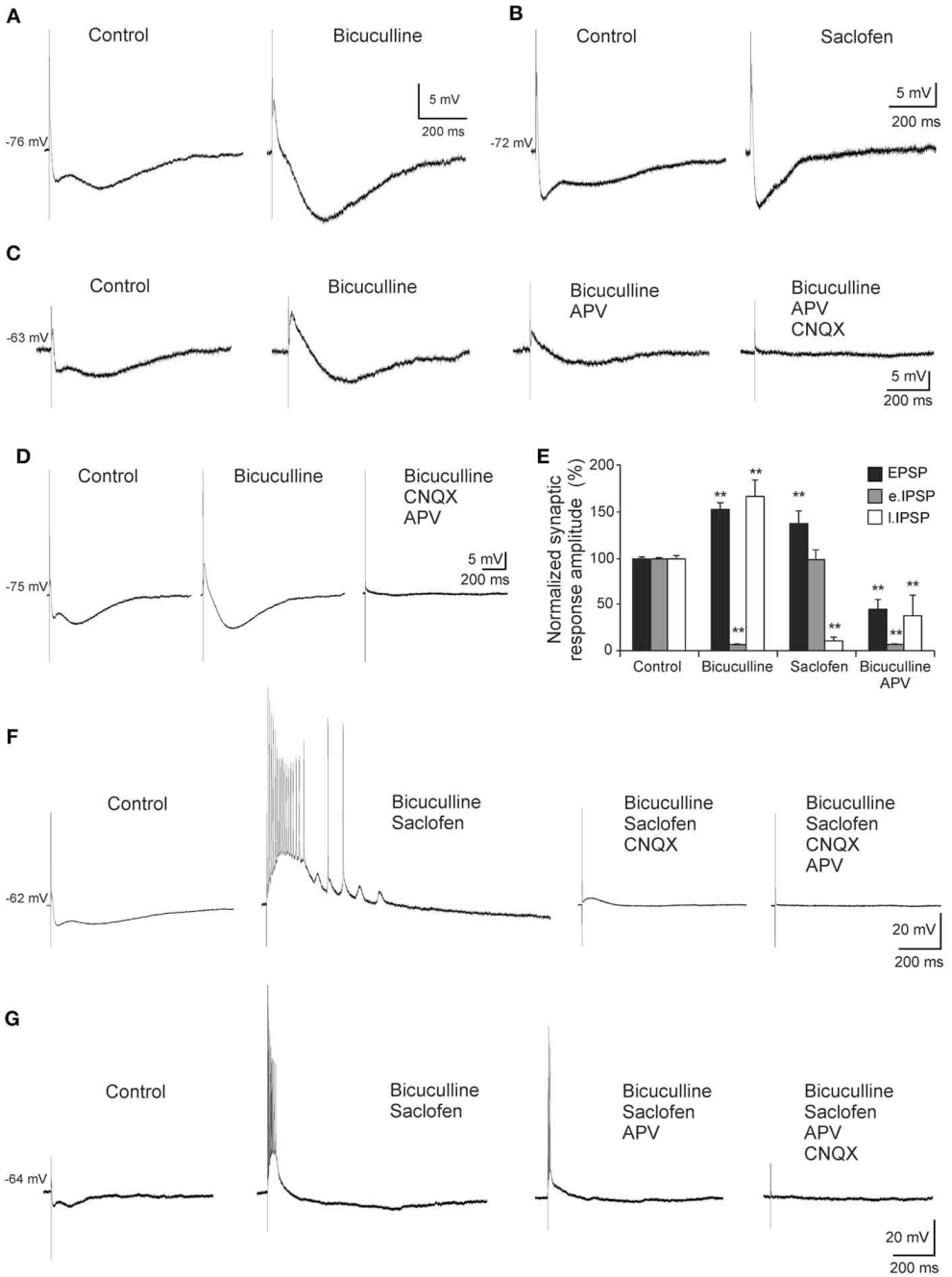

FIGURE 3 | Pharmacological characterization of septohippocampal synaptic response. (A) Recordings from a pyramidal CA3 neuron illustrating a marked reduction of the early IPSP after perfusion with bicuculline (10 μM; specific blocker of $GABA_A$ receptors). **(B)** Blocking of the late IPSP after perfusion with saclofen (200 μM; blocker of $GABA_B$ receptor) was accompanied by a mild increase of the early IPSP and EPSP. **(C)** The increase in the amplitude of EPSP and late IPSP produced by perfusion of bicuculline was reduced by APV application (50 μM; specific blocker of NMDA receptor). Membrane potential was maintained at values more positives than resting membrane potential to assure NMDA receptors functionality. Synaptic response was completely removed with the addition of CNQX (10 μM; competitive non-NMDA receptor antagonist). **(D)** Blockade of the early IPSP with bicuculline ($n = 4$) was associated with a marked increase in amplitude of EPSP and late IPSP. Excitatory and inhibitory responses were blocked by CNQX and APV. The cells were held at −75 mV (a membrane potential where NMDA receptor-mediated currents are null). **(E)** Histograms with relative mean amplitude as percentage of control of the different components of the complex synaptic response (EPSP; early, e.IPSP; and late, l.IPSP) under pharmacological conditions described in **(A–D)** (** $p < 0.001$). **(F)** Both, early and late IPSPs were blocked by bicuculline and saclofen, respectively, while a large repetitive burst of action potential appeared ($n = 4$). At membrane potential values that assured NMDA activation, this epileptic-like activity could be removed by CNQX. Finally, residual excitatory NMDA response was eliminated by APV perfusion. **(G)** During the epileptic-like activity induced by both inhibitory components elimination, and at membrane potential values that led NMDA receptor activation, APV perfusion reduced the size of the epileptic response that had to be removed by addition of CNQX ($n = 4$).

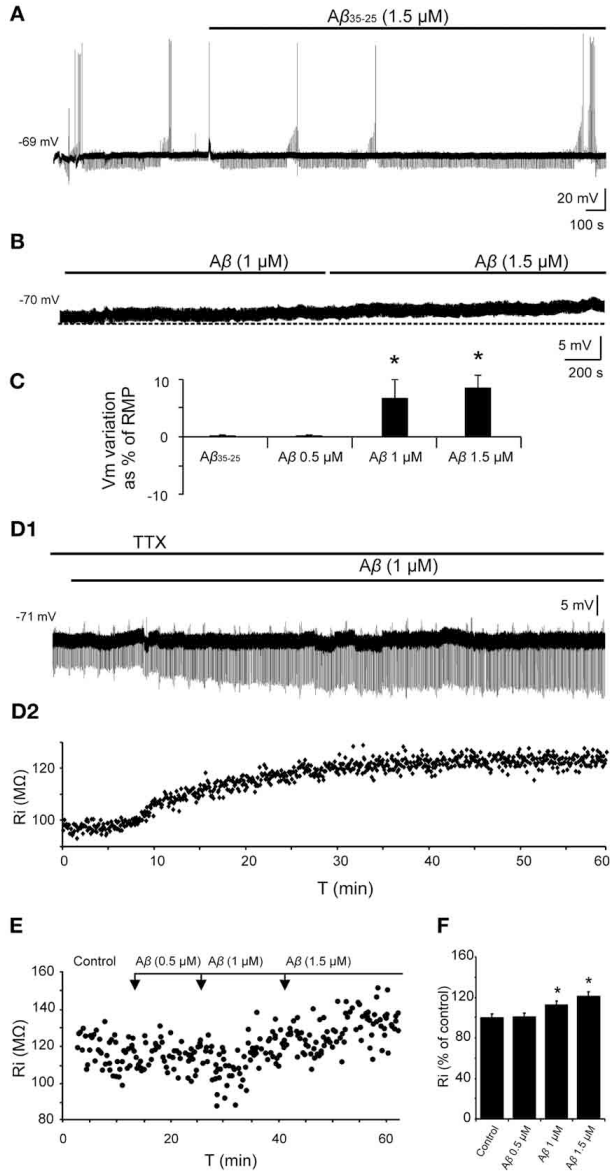

FIGURE 4 | Effects of $A\beta_{25–35}$ on membrane potential and Ri of CA3 neurons. (A) Recording of a CA3 pyramidal neuron during the perfusion of the reverse sequence of the peptide, $A\beta_{35–25}$, used as negative control ($n = 4$). **(B)** Depolarization of membrane potential induced by perfusion of Aβ in a recorded pyramidal CA3 neuron ($n = 10$). **(C)** Plot of the membrane potential variations as a percentage of resting membrane potential (RMP). Perfusion of $A\beta_{35–25}$ 1 μM or $A\beta_{25–35}$ 0.5 μM did not induce any significant change in the membrane potential or Ri. $A\beta_{25–35}$ higher concentrations induced the cells to depolarize (1 μM; 6.8 ± 3.2 %, $n = 4$; 1.5 μM, 8.6 ± 2.2 %, $n = 10$). **(D1)** Time course of Aβ effects on Ri in a CA3 pyramidal neuron after perfusion with TTX. The membrane potential was held at its RMP value by direct current (DC) holding current injection to cancel out the depolarization. **(D2)** For the same neuron, each point represents the Ri during the recording in **(D1)**. Membrane potential was held at −71 mV. **(E)** Plot showing the time course of the effects of $A\beta_{25–35}$ concentration increase on the Ri of a CA3 pyramidal neuron. Note that recordings last for a very long time. **(F)** Histogram with mean values in percentage for Ri ($n = 10$) at different $A\beta_{25–35}$ concentration ($^*p < 0.05$).

amplitude was maintained. This result pointed out to a selective postsynaptic action on $GABA_B$ complex.

$A\beta_{25–35}$ EFFECTS CAN BE EXPLAINED BY A REDUCTION IN THE CONDUCTANCE OF GirK CHANNELS COUPLED TO $GABA_B$ RECEPTOR

Depolarization caused by $A\beta_{25–35}$ was associated to Ri increase and therefore, linked to a possible decrease in membrane conductance, which may very likely involve in ion channels closing. Given the correlation between reduction in $GABA_B$ component and Ri increase shown in **Figure 5D**, we investigated whether these $A\beta_{25–35}$ effects could be mediated by conductance reduction of $GABA_B$ effector, GirK channel. We found that GirK blockade by its selective antagonist, tertiapin-Q (0.5 μM), not only removed the $GABA_B$ component (late IPSP; **Figures 6A,B**) of the synaptic response, but also induced a significant increase in Ri (**Figures 6C,D**; $122.5 \pm 5.4\%$; $t = -3.264$; $p = 0.022$) as well as membrane depolarization (**Figure 6E**; 9.1 ± 2.6 mV; $n = 5$; $t = 8.69$, $p < 0.001$), therefore mimicking all $A\beta_{25–35}$ effects previously described.

To determine the mechanism involved in the postsynaptic reduction of the late IPSP amplitude and Ri increase, pharmacological blockage of different receptors/channels was performed and effects of increasing $A\beta_{25–35}$ concentrations on Ri were evaluated (**Figure 7**). The blockade of synaptic transmission by TTX did not produce significant changes in Ri (Mann-Whitney U, $p = 0.700$) compared to control (**Figures 7A–C**, Exp. 1–3). Then, $A\beta_{25–35}$ perfusion produced a significant increase in Ri ($n = 4$) at high concentrations (**Figure 7**, Exp. 1; 1.0 μM, $t = -7.424$; $p = 0.018$ and 1.5 μM, $t = -7.519$; $p = 0.002$), which was not observed at 0.5 μM (Mann-Whitney U, $p = 1.00$). These results indicate a postsynaptic $A\beta_{25–35}$ mechanism that quite likely involves a reduction in ion channels conductance.

On the other hand, since saclofen perfusion prevented $A\beta_{25–35}$-induced changes on Ri ($n = 6$; $H = 3.964$, $p = 0.411$; **Figure 7**, Exp. 2), an interaction with $GABA_B$ receptors might be assumed. However, although saclofen also induced a reduction on late IPSP amplitude (see **Figures 3B,E**), in the presence of TTX it did not exhibit any noticeable effect on membrane potential (1.7 ± 2.8 mV; $t = -0.541$; $p = 0.617$; non illustrated) or Ri (**Figure 7**, Exp. 2; $94.5 \pm 7.3\%$; $t = 1.198$; $p = 0.285$), in contrast to $A\beta_{25–35}$. Altogether, these results suggest that $A\beta_{25–35}$ exerts its effects acting preferentially on postsynaptic GirK channels, instead of $GABA_B$ receptors.

In accordance with this hypothesis, $A\beta_{25–35}$ was found to be unable to generate additional increase on Ri after postsynaptic blockage of GirK channels by tertiapin-Q [**Figure 7**, Exp. 3; $n = 6$; $F_{(3,\ 21)} = 0.129$, $p = 0.941$], suggesting that Aβ-induced Ri increase may be associated to a reduction in GirK channel conductance. However, because conductance depends, among others, on the number of channels, their open probability or membrane voltage, the methodology used in the present study has some limitations to determine the exact mechanism for Aβ-mediated Ri increase. In addition, in some experiments, it was necessary to inject DC to maintain a stable membrane potential and to prevent depolarization. Previous studies had reported that depolarization mechanisms induced by Aβ might involve activation of glutamatergic receptors (Blanchard et al., 2002a,b). In order to

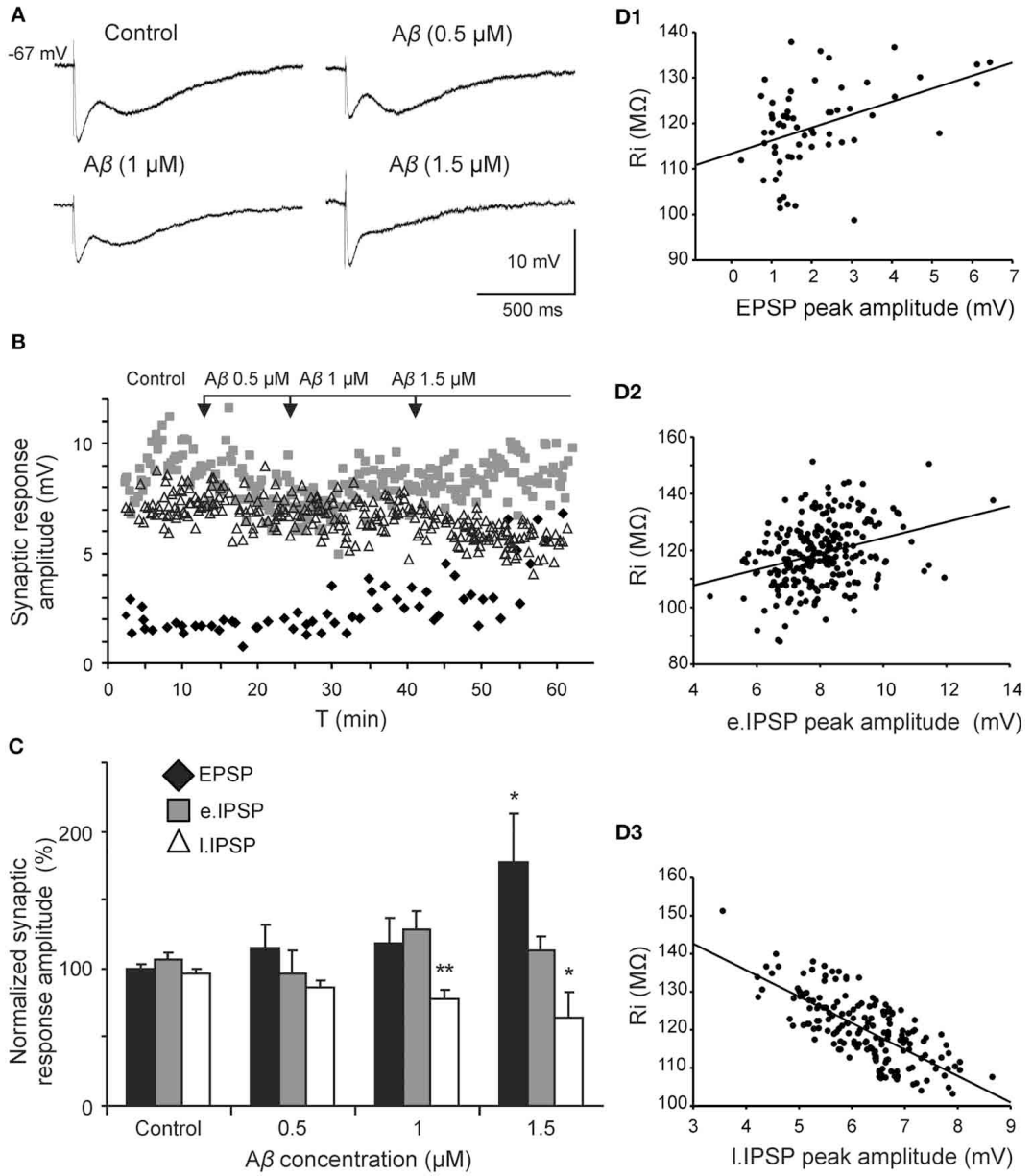

FIGURE 5 | Selective effect of $A\beta_{25-35}$ on different components of the complex postsynaptic response recorded in CA3 pyramidal neurons by fimbria stimulation. (A) Evoked responses obtained in a pyramidal CA3 neuron by fimbria orthodromic stimulation (control) and during perfusion of different concentrations of $A\beta_{25-35}$ (0.5, 1, and 1.5 μM). The reduction of the late IPSP after perfusion with $A\beta_{25-35}$ has been shown to be concentration-dependent. **(B)** Plot displaying the time course of $A\beta_{25-35}$ perfusion effects on the amplitude (in mV) of the different components of the complex response (EPSP, black diamonds; early IPSP, gray squares; late IPSP, white triangles; see color code in **C**). **(C)** Histograms with relative mean amplitude ($n = 20$) of the different components of the complex synaptic response (EPSP; early, e.IPSP; and late, I.IPSP) 10 min after $A\beta_{25-35}$ perfusion (0.5, 1, and 1.5 μM). Significant differences were found for EPSP at 1.5 μM $A\beta_{25-35}$ and for late IPSP at 1–1.5 μM $A\beta_{25-35}$. **(D)** Correlation analysis of $A\beta_{25-35}$ perfusion on different components of the complex postsynaptic response vs. Ri values. Data showed a higher correlation between Aβ-induced Ri increase and late IPSP amplitude ($R = -0.73$, $p < 0.001$; **D3**) than Aβ-induced Ri increase and EPSP ($R = 0.42$, $p < 0.001$; **D1**) or early IPSP ($R = 0.31$, $p < 0.01$; **D2**)(*$p < 0.05$; **$p < 0.01$).

control these variables, tertiapin-Q was perfused together with glutamatergic antagonists CNQX (10 μM) and APV (50 μM). This protocol not only prevented the Aβ-mediated increase in Ri, but also abolished the dependence of DC injection to compensate membrane depolarization ($n = 4$; H = 3.709, $p = 0.447$; non illustrated). In contrast, perfusion with CNQX, APV and the $GABA_A$ blocker, bicuculline (10 μM), was not able to prevent the Ri increase induced by $A\beta_{25-35}$ ($n = 4$; H = 21.681; $p < 0.001$; non illustrated) further suggesting an effect of $A\beta_{25-35}$ on GirK channels.

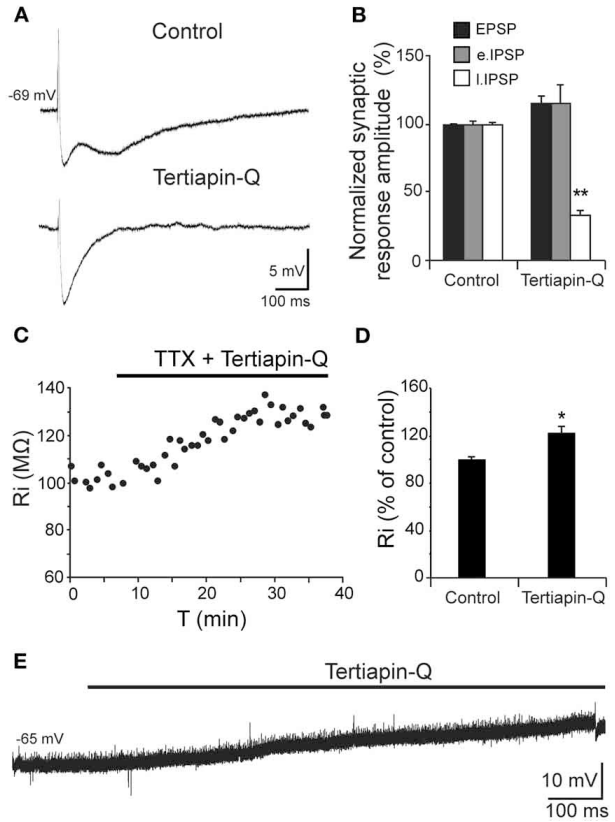

FIGURE 6 | Effects of the selective GirK channel antagonist tertiapin-Q on CA3 pyramidal neurons complex response to fimbria stimulation. **(A)** Selective blockade by tertiapin-Q of the late IPSP recorded in CA3 pyramidal neurons after fimbria stimulation. Superfusion of the GirK antagonist tertiapin-Q (0.5 μM; selective blocker of GirK channels) selectively blocked the late IPSP but did not reduce the early IPSP that was elicited by fimbria stimulation. **(B)** Histograms with relative mean amplitude ($n = 5$) of the different components of the complex synaptic response (EPSP; early, e.IPSP; and late, l.IPSP) 40 min after tertiapin-Q perfusion. Significant differences were found for late IPSP. **(C)** Results of an experiment in another neuron designed to assess the postsynaptic effects of tertiapin-Q on Ri of CA3 pyramidal neurons. Perfusion of TTX ($n = 5$; 1 μM; voltage-dependent sodium channel blocker) blocked afferent neurotransmission and therefore any effect of tertiapin-Q took place at postsynaptic location. Note the significant Ri increase after 30 min. **(D)** Histogram with mean values in percentage for Ri ($n = 6$) after tertiapin-Q perfusion during 40 min ($^*p < 0.05$). **(E)** Effect of tertiapin-Q on CA3 pyramidal neurons membrane potential ($n = 5$). Chart record shows that superfusion of tertiapin-Q (0.5 μM) produced a marked depolarization when applied at resting membrane potential (−65 mV). $^{**}p < 0.01$.

EFFECTS OF $A\beta_{25–35}$ ON THE HYPERPOLARIZATION MEDIATED BY $GABA_B$-GirK ACTIVATION

Given that, Ri changes may depend on multiple factors and might be affected by Aβ acting on different ion channels and receptors, we designed a protocol to specifically evaluate the effects of $A\beta_{25–35}$ on $GABA_B$ response. To verify whether $A\beta_{25–35}$ affects the postsynaptic response mediated by $GABA_B$ receptor activation, we used a drug cocktail including: TTX to block synaptic transmission, bicuculline to block $GABA_A$ receptors activation and baclofen to stimulate $GABA_B$ receptors (**Figure 8**). Cocktail application in the slice produced a postsynaptic membrane hyperpolarization in recorded CA3 pyramidal neurons (**Figures 8A,D**; $-9.5 \pm 2.8\%$ of the RMP value). When membrane potential was stabilized, $A\beta_{25–35}$ perfusion induced a pronounced depolarization (**Figures 8A,D**; 15.5 ± 4.3 % of the RMP value; $n = 4$), which confirms that $A\beta_{25–35}$ reduces the postsynaptic $GABA_B$ response in a concentration and time dependent manner. But $A\beta_{25–35}$ action on this $GABA_B$ response might also be explained by an effect on its final effector, GirK, which would also underlie the already described $A\beta_{25–35}$ effects on Ri and membrane depolarization.

In order to validate this hypothesis and evaluate the effect of $A\beta_{25–35}$ on GirK response, we used a GirK channel agonist, MPD (Aryal et al., 2009). Bath application of the previous drugs cocktail together with MPD (50 mM) induced the cell to hyperpolarize by two postsynaptic mechanisms, $GABA_B$ receptor activation and direct increase in GirK conductance (**Figure 9**; $-11.2 \pm 3.8\%$ of the RMP value; $n = 15$). Then, perfusion of $A\beta_{25–35}$ (1–1.5 μM) removed the hyperpolarization mediated by $GABA_B$-GirK stimulation (**Figures 9A,E**; $5.9 \pm 2.7\%$; $n = 3$, **Figures 9B,E**; $4.2 \pm 2.4\%$, $n = 4$), while this effect was not evident at 0.5 μM (**Figures 9C,E**; $-7.2 \pm 4.8\%$ $n = 4$). In fact, the hyperpolarization could be eliminated when the cocktail was washed (**Figure 9C**). Finally, Aβ-induced depolarization was mimicked by tertiapin-Q, the specific antagonist of GirK channels (**Figures 9D,E**; $5.5 \pm 1.5\%$; $n = 4$), indicating that $A\beta_{25–35}$ directly affects GirK channels conductance.

DISCUSSION

Despite the importance that rhythms as an emergent property of neural network seem to have, few studies have investigated how Aβ induces injury and how it may contribute to impair septohippocampal oscillatory activity, which in turn may underlie the early symptoms typically observed in AD patients (Colom, 2006; Palop and Mucke, 2010; Villette et al., 2010; Rubio et al., 2012; Verret et al., 2012). The present study identifies alterations in GirK channels conductance of fimbria-CA3 synapse as a putative mechanism of Aβ-induced synaptic dysfunction observed in the septohippocampal system activity.

SEPTOHIPPOCAMPAL SYSTEM AND $A\beta_{25–35}$ NEUROTOXICITY

Previously, it has been proposed that $A\beta_{25–35}$ constitutes the biologically active fragment of Aβ (Millucci et al., 2010), and has been shown to induce major neuropathological signs related to early stages of AD in rats (Klementiev et al., 2007). In addition, $A\beta_{25–35}$ is reported to be more soluble and presents toxic effects more rapidly than the parent peptide $A\beta_{1–42}$ (Varadarajan et al., 2001), and has widely been used as a very useful tool to explore acutely the pathophysiological events related with neuronal dysfunction induced by soluble Aβ forms (Ashenafi et al., 2005; Santos-Torres et al., 2007; Peña et al., 2010; Leao et al., 2012). But the most important advantage for present work is that $A\beta_{25–35}$ does not form ion-permeable pores in neuronal membrane (Jang et al., 2010; Chang et al., 2011; Leao et al., 2012) which could alter our protocols, especially input resistance measurements.

From neuroanatomical and electrophysiological points of view, hippocampus receives different projections from the medial

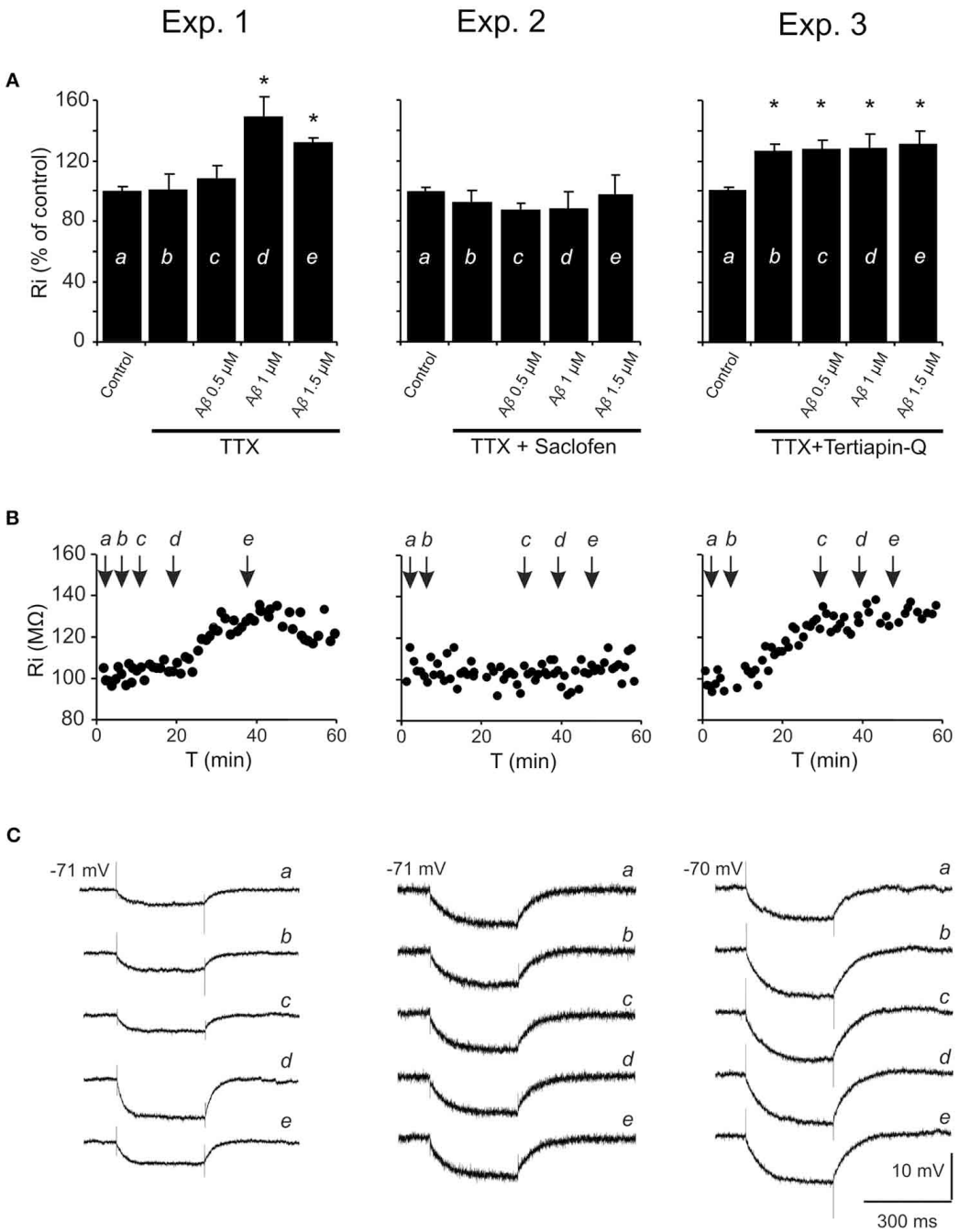

FIGURE 7 | Histograms with Ri mean values in CA3 pyramidal neurons for increasing $A\beta_{25-35}$ concentrations. (A) Normalized mean value of Ri as % of control after perfusion with three different $A\beta_{25-35}$ concentrations in three different experimental conditions (Exp. 1–3). In all cases, TTX pre-treatment (1 μM; voltage-dependent sodium channel blocker) was unable to prevent $A\beta_{25-35}$ effects on Ri, suggesting a postsynaptic location for $A\beta_{25-35}$ action. Exp. 1: Significant increase on Ri was recorded after 1 and 1.5 μM $A\beta_{25-35}$ perfusion ($n = 16$), even in the presence of TTX. Exp. 2: After perfusion of both TTX and saclofen (to block postsynaptic $GABA_B$ receptors), $A\beta_{25-35}$ was unable to evoke any significant modification in Ri ($n = 6$). Exp. 3: As in the experiment showed in **Figure 6B**, TTX perfusion together with the selective antagonist of GirK channels, tertiapin-Q (0.5 μM), induced a significant increase in Ri compared to control values. However, when tertiapin-Q was perfused and GirK channels blocked, $A\beta_{25-35}$ became unable to induce any additional Ri increase ($n = 6$). Control value for Ri was normalized to 100%. Data show mean ± SEM. $^*p < 0.05$. Lower-case letters (*a–e*) indicate the five pharmacological conditions during each experimental treatment. **(B)** Representative examples for time course of Ri recorded in experimental conditions (Exp. 1–3). The arrows indicate the time point at which drugs were applied during the recordings. **(C)** Representative examples of recordings were expanded in time to show the changes in membrane potential during the presentation of hyperpolarizing pulses. This protocol allowed us to monitor Ri during the whole recording and to study the effect of different pharmacological treatments represented by lower-case letters (*a–e*).

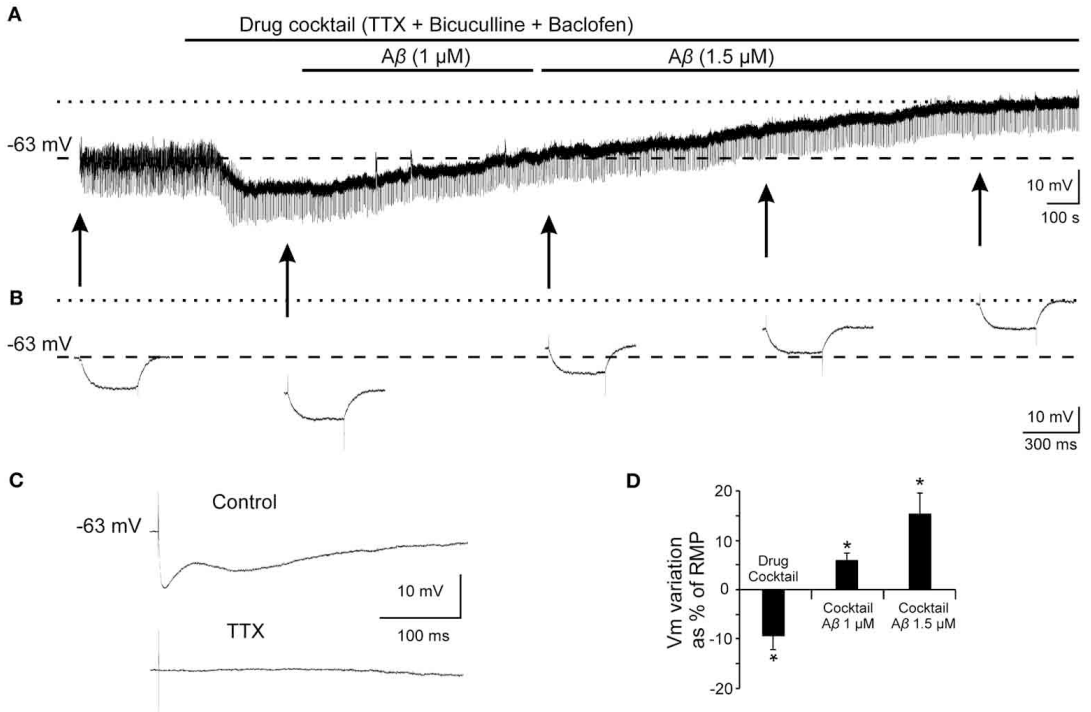

FIGURE 8 | Effects of $A\beta_{25–35}$ on postsynaptic hyperpolarization induced by activation of $GABA_B$ receptors. (A) Membrane potential recording from a CA3 neuron (top) after perfusion with TTX (1 μM; voltage-dependent sodium channels blocker), bicuculline (10 μM; specific blocker of $GABA_A$ receptor) and baclofen (15 μM; agonist of $GABA_B$ receptor). This treatment ($n = 4$) produced a membrane hyperpolarization depending on $GABA_B$ postsynaptic receptors activation. Perfusion with $A\beta_{25–35}$ (1 and 1.5 μM) markedly induced the membrane to depolarize. **(B)** Intracellular hyperpolarizing current pulses. The arrows indicate the time points at which recordings were expanded in time to show the changes in the membrane potential during the presentation of hyperpolarizing pulses. This protocol allowed us to monitor Ri during the whole recording and check the viability of the neurons. Dashed lines in **(A)** and **(B)** indicate membrane resting potential. Maximum membrane potential evoked by $A\beta_{25–35}$ superfusion is indicated by dotted lines. **(C)** In the same neuron, fimbria stimulation elicited the characteristic triphasic postsynaptic response before drugs cocktail perfusion. This complex postsynaptic potential was completely removed by TTX (1 μM; voltage-dependent sodium channels blocker) perfusion. **(D)** Plot of the membrane potential variations as a percentage of resting membrane potential (RMP) under pharmacological conditions presented in **(A)**. TTX, bicuculline and baclofen (drug cocktail) induced pyramidal neurons to hyperpolarize while $A\beta_{25–35}$ produced a noticeable depolarization ($n = 4$; 21.4 ± 5.9 mV). $^*p < 0.05$.

septum diagonal broca band mainly through lateral fimbria (Wyss et al., 1980; Alonso and Kohler, 1984; Colom, 2006; Amaral and Lavenex, 2007). Cholinergic neurons innervate pyramidal neurons and interneurons (Widmer et al., 2006), GABAergic fibers project onto interneurons (Freund and Antal, 1988; Chamberland et al., 2010) and glutamatergic projections contact with CA3 pyramidal cells (Huh et al., 2010). These septo-hippocampal circuits are involved in both, generating hippocampal *theta* rhythm, as well as in learning and memory processes. To maintain these high-level functions, a precise septohippocampal network activity requires of finely regulated excitatory and inhibitory neurotransmission (Buzsaki, 2002; Sotty et al., 2003; Borhegyi et al., 2004; Colom, 2006) whose alteration could lead to impairments that would be consistent with the deficits described for AD initial stages (Bland and Colom, 1993; Palop and Mucke, 2010). In this sense, it has been reported that in hippocampus, Aβ mainly induces aberrant inhibitory septohippocampal network activity (Palop et al., 2007; Villette et al., 2010, 2012). Therefore, although an Aβ effect on inhibitory neurotransmission might be expected, the putative mechanism to detune the network coordination of this system remains unclear.

$A\beta_{25–35}$ was found not to affect the active properties of CA3 pyramidal recorded neurons suggesting that $A\beta_{25–35}$ does not modify the conductances that mediate active membrane properties such as sodium or potassium voltage-gated channels for spike amplitude (Hille, 2001), BK/SK channels for AHPs (Sah and Faber, 2002) or R-type calcium channels for ADP (Metz et al., 2005). Similar results have also been shown in other AD related regions as amygdala (Ashenafi et al., 2005), septum (Santos-Torres et al., 2007), or cortex (Wang et al., 2009).

On the other hand, $A\beta_{25–35}$ induced an Ri increase associated with membrane depolarization. We have previously showed that $A\beta_{25–35}$ exerts variable effects on membrane potential and Ri in amygdalar pyramidal neurons, possibly due to a presynaptic mechanism (Ashenafi et al., 2005) and in septal neurons, depending on pre- and postsynaptic actions (Santos-Torres et al., 2007). In the present study, TTX was not able to prevent $A\beta_{25–35}$ effects suggesting a direct effect of $A\beta_{25–35}$ on CA3 pyramidal neurons membrane.

Previous research has shown that neurotransmission in the septohippocampal system is affected by Aβ through altering the *theta* oscillatory activity (Colom et al., 2010; Rubio et al., 2012),

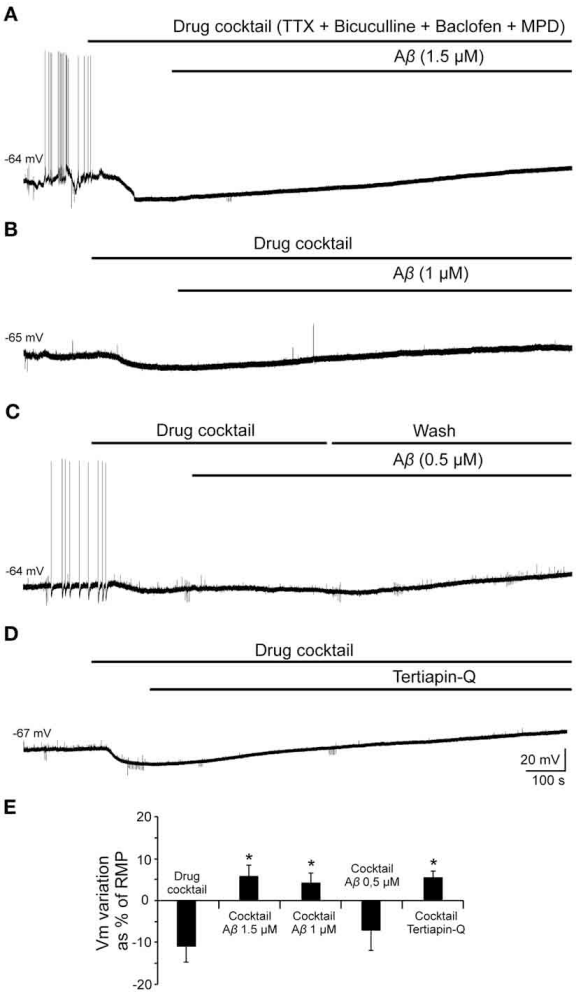

FIGURE 9 | Effects of $A\beta_{25–35}$ perfusion on the response evoked by pharmacological co-activation of GirK channels and $GABA_B$ receptors. **(A,B)** GirK/$GABA_B$ postsynaptic hyperpolarization was induced ($n = 15$) by perfusion of drugs cocktail including TTX (1 μM; voltage-dependent sodium channels blocker), bicuculline (10 μM; specific blocker of $GABA_A$ receptors), baclofen (15 μM; agonist of $GABA_B$ receptors), and MPD (50 mM; GirK channel agonist) perfusion. $A\beta_{25–35}$ 1.5 μM ($n = 3$) and 1.0 μM ($n = 4$)(**A** and **B,** respectively) evoked a postsynaptic depolarization. **(C)** Using the same protocol, $A\beta_{25–35}$ 0.5 μM was not able to produce this depolarization. The cocktail hyperpolarizing effect on membrane potential disappeared after cell washing with bathing solution ($n = 4$). **(D)** Tertiapin-Q ($n = 4$; 0.5 μM; selective blocker of GirK channels), the specific antagonist of GirK channels, induced a depolarization of the postsynaptic hyperpolarization mediated by GirK/$GABA_B$ activation, reproducing $A\beta_{25–35}$ effects. **(E)** Plot showing the membrane potential changes as a percentage of resting membrane potential (RMP) under pharmacological conditions presented in **(A–D)**. $^*p < 0.05$.

but studies at the synaptic level on the mechanisms underlying this alteration have not been exhaustively performed. Thus, the possibility of studying in a single preparation and in a particular synapse, excitatory and inhibitory neurotransmission, presents fimbria-CA3 synapse preparation as an excellent model for dissecting the possible mechanisms involved in Aβ action on different septohippocampal neurotransmission systems.

A biphasic (glutamatergic, non-NMDA, and GABAergic, $GABA_A$) response in CA3 region after fimbria stimulation (Schneiderman et al., 1992) has previously been reported. However, we found a complex synaptic response comprising three phases: an ionotropic glutamatergic EPSP (Huh et al., 2010) followed by two IPSPs, early ($GABA_A$), and late ($GABA_B$). This complex response has also been described in pyramidal neurons of basolateral amygdaloid nucleus (Washburn and Moises, 1992a), in CA3 pyramidal cells after hilus and mossy fibers stimulation (Malouf et al., 1990; Scanziani et al., 1991). In our study, the inhibitory feedback seems to be mediated by activation of GABAergic interneurons and depends on glutamatergic activation, since the block of EPSP also eliminated both IPSPs. The loss of $GABA_A$ inhibition led to an increase in EPSP and late IPSP amplitudes whereas complete GABAergic component block induced an epileptic-like response mainly mediated by non-NMDA receptors, although NMDA antagonist reduced the response partially. Very similar results have been shown in neurons from CA3 hippocampal region (Scanziani et al., 1991) or frontal cortex (Sutor and Luhmann, 1998) possibly caused by an increased excitation of interneurons arising from disinhibited excitatory neurons, and disinhibition of interneurons due to block of $GABA_A$ receptors on the inhibitory cell. This machinery has been suggested as a self-protective mechanism for the control of recurrent activity when an imbalance of the system occurs (Scanziani et al., 1991; Sutor and Luhmann, 1998).

On the other hand, although it has been reported that cholinergic septal neurons innervate pyramidal CA3 neurons and interneurons (Widmer et al., 2006), it is also known that cholinergic axons must be activated by train stimulation (>30 Hz) (Washburn and Moises, 1992b; Faber and Sah, 2002; Navarro-Lopez et al., 2004). It can therefore be suggested that cholinergic axons projecting onto CA3 neurons were not activated during single stimulation of the fimbria.

$A\beta_{25–35}$ EFFECTS ON THE COMPLEX FIMBRIA-CA3 SYNAPTIC RESPONSE

In the present study, pharmacological characterization of the complex septohippocampal synaptic response revealed the glutamatergic nature of the EPSP. Glutamatergic septohippocampal neurons (Colom et al., 2005; Huh et al., 2010) have shown spontaneous firing at *theta* frequencies and Aβ increases this frequency (Leao et al., 2012), suggesting Aβ to be likely to impair septohippocampal excitatory and network activity through more than one mechanism.

We found $A\beta_{25–35}$ to increase the EPSP. This result may be explained because excitatory response is strongly braked by the $GABA_B$ activity (Otmakhova and Lisman, 2004; Chen and Johnston, 2005), and $A\beta_{25–35}$ diminished late IPSP. Since late IPSP was generated by $GABA_B$ receptors stimulation, an $A\beta_{25–35}$ effect on such receptors, on its intracellular signaling mechanism, or on its final effector, GirK channels, could be hypothesized. Assuming that the early $GABA_A$ component is not affected by $A\beta_{25–35}$, the reduction of $GABA_B$ component would not be due to an inhibition of GABA release or other presynaptic mechanism. Together with Ri increase and membrane depolarization, our

results lead to a reduction of the conductance of potassium channels coupled to $GABA_B$ receptor.

Binding studies in postmortem AD patients have shown a reduction in GABA receptors density in the hippocampus (Chu et al., 1987). More recently, the 17A polymerase has been described to be responsible for generating alternative splicing of $GABA_{B2}$ subunit in AD patients (Massone et al., 2011). This modification affects intracellular signaling pathway and activation of GirK channels, and is also associated with an increased secretion of Aβ, suggesting a relationship between the metabolism of APP protein and dysfunction in the $GABA_B$ receptor signaling.

$Aβ_{25–35}$ ACTION ON GirK CHANNELS

When fimbria is stimulated, GABAergic interneurons activate $GABA_B$ receptors of CA3 pyramidal cells; $Aβ_{25–35}$ behaves as a selective antagonist and reduces late IPSP. However, the $GABA_B$ system has a very low tonic activity in basal conditions, and only when the system is activated pharmacologically or by afferent stimulation, the antagonist effect becomes obvious (Bowery and Smart, 2006) as occurs, for example, in chronic pain (Malcangio and Bowery, 1994). For this reason, blocking $GABA_B$ receptors induces little effects on membrane properties, i.e., membrane potential or Ri (Lambert et al., 1989; Emri et al., 1996), so $GABA_B$ receptor antagonism would not explain all the effects induced by $Aβ_{25–35}$.

Another aspect to consider is that both, $GABA_B$ receptors and GirK channels are coupled and co-expressed in the postsynaptic membrane of CA3 pyramidal neurons (Luscher et al., 1997; Kulik et al., 2003; Lujan et al., 2009) conforming an oligomeric stable molecular complex (Lujan et al., 2009; Ciruela et al., 2010). Therefore, $Aβ_{25–35}$ action on the membrane should include the effector coupled to $GABA_B$ receptor. GirK channels exhibit a tonic basal activity, even without receptor signaling, due to their direct binding to the Gα subunit of G proteins (Lujan et al., 2009). Hence, administration of GirK channel selective antagonist (tertiapin-Q) simulates all the effects of $Aβ_{25–35}$ on the postsynaptic membrane, i.e., late IPSP reduction, Ri increase and membrane depolarization, even in the presence of GirK and $GABA_B$ agonists. Furthermore, $Aβ_{25–35}$ was found to be unable to generate an additional significant increase in Ri after pharmacological blocking of GirK channels. These results not only suggest that GirK channels are functional in the basal state, but also that $Aβ_{25–35}$ action seems to be more evident when these GirK channels are activated.

GirK channels activity alteration may have multiple implications for synaptic activity and neuronal network function. Numerous studies have emphasized its role in several pathological processes in the nervous system such as epilepsy, pain, addiction, Parkinson or Down syndrome (Luscher and Slesinger, 2010). Deletion studies of GirK channels have revealed their role in learning and memory processes. GIRK4 knock-out mice exhibited impaired performance in spatial learning and memory test (Wickman et al., 2000). Moreover, mutations in GIRK2 subunit reduced LTP and increased LTD in hippocampus (Sago et al., 1998; Siarey et al., 1999; Luscher and Slesinger, 2010) and it is especially relevant in Down syndrome, where cerebral Aβ accumulation is greatly accelerated and leads to invariant early-onset AD neuropathology (Lott and Head, 2005; Moncaster et al., 2010; Cooper et al., 2012).

The present study proposes a putative synaptic mechanism for neural network hyperactivity, which is considered as an early event in AD pathogenesis and is associated with early Aβ deposition in non-demented humans with or without mild cognitive impairment (Sperling et al., 2009). An alteration in GirK channel conductance of pyramidal CA3 neurons might underlie this hyperactivity and the impaired inhibition which has been related to network dysfunction and alteration of rhythm generation required for information processing and memory storage in the septohippocampal system (Palop et al., 2007; Palop and Mucke, 2010; Villette et al., 2010, 2012; Rubio et al., 2012; Verret et al., 2012). Our data could be in accordance to the notion that reducing network hyperactivity would have beneficial effects on cognitive functions (Palop and Mucke, 2010; Verret et al., 2012). Subsequently, the present work shows GirK channel as a new target to study Aβ pathophysiology in early and mild cognitive impairment in AD. Since cholinergic or glutamatergic treatments in AD have shown limited success, therapies combining modulators of different neurotransmission systems seem to be a more promising tool for the treatment, and overall prevention, of this dementia.

ACKNOWLEDGMENTS

This work was supported by Spanish MINECO Grants BFU2009-07341 (Javier Yajeya) and SAF2010-14878, BFU2011-22740 (Juan D. Navarro-Lopez). The research leading to these results also received funding (Juan D. Navarro-Lopez) from Fundación Eugenio Rodríguez Pascual. Juan D. Navarro-Lopez held a *Ramón y Cajal* Research Fellow (RYC-2009-03827). We thank Drs. A. Munera and D. Soto for their enlightening comments about this work, N. Gonzalez for her excellent technical assistance and Eureka-science for its help in manuscript editing.

REFERENCES

Alonso, A., and Kohler, C. (1984). A study of the reciprocal connections between the septum and the entorhinal area using anterograde and retrograde axonal transport methods in the rat brain. *J. Comp. Neurol.* 225, 327–343. doi: 10.1002/cne.902250303

Amaral, D. G., and Lavenex, P. (2007). "Hippocampal neuroanatomy," in *The Hippocampus Book,* eds P. Andersen, R. Morris, D. G. Amaral, T. Bliss, and J. O'Keefe (New York, NY: Oxford University Press), 37–114.

Aryal, P., Dvir, H., Choe, S., and Slesinger, P. A. (2009). A discrete alcohol pocket involved in GIRK channel activation. *Nat. Neurosci.* 12, 988–995. doi: 10.1038/nn.2358

Ashenafi, S., Fuente, A., Criado, J. M., Riolobos, A. S., Heredia, M., and Yajeya, J. (2005). Beta-Amyloid peptide 25–35 depresses excitatory synaptic transmission in the rat basolateral amygdala "*in vitro*". *Neurobiol. Aging* 26, 419–428. doi: 10.1016/j.neurobiolaging.2004.05.008

Bischofberger, J., Engel, D., Li, L., Geiger, J. R., and Jonas, P. (2006). Patch-clamp recording from mossy fiber terminals in hippocampal slices. *Nat. Protoc.* 1, 2075–2081. doi: 10.1038/nprot.2006.312

Blanchard, B. J., Stockwell, B. R., and Ingram, V. M. (2002a). Eliminating membrane depolarization caused by the Alzheimer peptide Abeta(1-42, aggr.). *Biochem. Biophys. Res. Commun.* 293, 1204–1208. doi: 10.1016/S0006-291X(02)00290-5

Blanchard, B. J., Thomas, V. L., and Ingram, V. M. (2002b). Mechanism of membrane depolarization caused by the Alzheimer Abeta1-42 peptide. *Biochem. Biophys. Res. Commun.* 293, 1197–1203. doi: 10.1016/S0006-291X(02)00346-7

Bland, B. H., and Colom, L. V. (1993). Extrinsic and intrinsic properties underlying oscillation and synchrony in limbic cortex. *Prog. Neurobiol.* 41, 157–208. doi: 10.1016/0301-0082(93)90007-F

Bland, B. H., and Oddie, S. D. (2001). Theta band oscillation and synchrony in the hippocampal formation and associated structures: the case for its role in sensorimotor integration. *Behav. Brain Res.* 127, 119–136. doi: 10.1016/S0166-4328(01)00358-8

Borhegyi, Z., Varga, V., Szilagyi, N., Fabo, D., and Freund, T. F. (2004). Phase segregation of medial septal GABAergic neurons during hippocampal theta activity. *J. Neurosci.* 24, 8470–8479. doi: 10.1523/JNEUROSCI.1413-04.2004

Bowery, N. G., and Smart, T. G. (2006). GABA and glycine as neurotransmitters: a brief history. *Br. J. Pharmacol.* 147 (Suppl. 1), S109–S119. doi: 10.1038/sj.bjp.0706443

Buzsaki, G. (2002). Theta oscillations in the hippocampus. *Neuron* 33, 325–340. doi: 10.1016/S0896-6273(02)00586-X

Chamberland, S., Salesse, C., Topolnik, D., and Topolnik, L. (2010). Synapse-specific inhibitory control of hippocampal feedback inhibitory circuit. *Front. Cell. Neurosci.* 4:130. doi: 10.3389/fncel.2010.00130

Chang, Z., Luo, Y., Zhang, Y., and Wei, G. (2011). Interactions of Abeta25–35 beta-barrel-like oligomers with anionic lipid bilayer and resulting membrane leakage: an all-atom molecular dynamics study. *J. Phys. Chem. B* 115, 1165–1174. doi: 10.1021/jp107558e

Chen, X., and Johnston, D. (2005). Constitutively active G-protein-gated inwardly rectifying K+ channels in dendrites of hippocampal CA1 pyramidal neurons. *J. Neurosci.* 25, 3787–3792. doi: 10.1523/JNEUROSCI.5312-04.2005

Chu, D. C., Penney, J. B. Jr., and Young, A. B. (1987). Quantitative autoradiography of hippocampal GABAB and GABAA receptor changes in Alzheimer's disease. *Neurosci. Lett.* 82, 246–252. doi: 10.1016/0304-3940(87)90264-3

Ciruela, F., Fernandez-Duenas, V., Sahlholm, K., Fernandez-Alacid, L., Nicolau, J. C., Watanabe, M., et al. (2010). Evidence for oligomerization between GABAB receptors and GIRK channels containing the GIRK1 and GIRK3 subunits. *Eur. J Neurosci.* 32, 1265–1277. doi: 10.1111/j.1460-9568.2010.07356.x

Colom, L. V. (2006). Septal networks: relevance to theta rhythm, epilepsy and Alzheimer's disease. *J. Neurochem.* 96, 609–623. doi: 10.1111/j.1471-4159.2005.03630.x

Colom, L. V., Castaneda, M. T., Banuelos, C., Puras, G., Garcia-Hernandez, A., Hernandez, S., et al. (2010). Medial septal beta-amyloid 1-40 injections alter septo-hippocampal anatomy and function. *Neurobiol. Aging* 31, 46–57. doi: 10.1016/j.neurobiolaging.2008.05.006

Colom, L. V., Castaneda, M. T., Reyna, T., Hernandez, S., and Garrido-Sanabria, E. (2005). Characterization of medial septal glutamatergic neurons and their projection to the hippocampus. *Synapse* 58, 151–164. doi: 10.1002/syn.20184

Cooper, A., Grigoryan, G., Guy-David, L., Tsoory, M. M., Chen, A., and Reuveny, E. (2012). Trisomy of the G protein-coupled K+ channel gene, Kcnj6, affects reward mechanisms, cognitive functions, and synaptic plasticity in mice. *Proc. Natl. Acad. Sci. U.S.A.* 109, 2642–2647. doi: 10.1073/pnas.1109099109

Emri, Z., Turner, J. P., and Crunelli, V. (1996). Tonic activation of presynaptic GABA(B) receptors on thalamic sensory afferents. *Neuroscience* 72, 689–698. doi: 10.1016/0306-4522(95)00590-0

Faber, E. S., and Sah, P. (2002). Physiological role of calcium-activated potassium currents in the rat lateral amygdala. *J. Neurosci.* 22, 1618–1628.

Freund, T. F., and Antal, M. (1988). GABA-containing neurons in the septum control inhibitory interneurons in the hippocampus. *Nature* 336, 170–173. doi: 10.1038/336170a0

Gloveli, T., Dugladze, T., Rotstein, H. G., Traub, R. D., Monyer, H., Heinemann, U., et al. (2005). Orthogonal arrangement of rhythm-generating microcircuits in the hippocampus. *Proc. Natl. Acad. Sci. U.S.A.* 102, 13295–13300. doi: 10.1073/pnas.0506259102

Hille, B. (2001). *Ion Channels of Excitable Membranes*. Sunderland, MA: Sinauer associates.

Huang, Y., and Mucke, L. (2012). Alzheimer mechanisms and therapeutic strategies. *Cell* 148, 1204–1222. doi: 10.1016/j.cell.2012.02.040

Huh, C. Y., Goutagny, R., and Williams, S. (2010). Glutamatergic neurons of the mouse medial septum and diagonal band of Broca synaptically drive hippocampal pyramidal cells: relevance for hippocampal theta rhythm. *J. Neurosci.* 30, 15951–15961. doi: 10.1523/JNEUROSCI.3663-10.2010

Jang, H., Arce, F. T., Ramachandran, S., Capone, R., Azimova, R., Kagan, B. L., et al. (2010). Truncated beta-amyloid peptide channels provide an alternative mechanism for Alzheimer's Disease and Down syndrome. *Proc. Natl. Acad. Sci. U.S.A.* 107, 6538–6543. doi: 10.1073/pnas.0914251107

Kaupmann, K., Schuler, V., Mosbacher, J., Bischoff, S., Bittiger, H., Heid, J., et al. (1998). Human gamma-aminobutyric acid type B receptors are differentially expressed and regulate inwardly rectifying K+ channels. *Proc. Natl. Acad. Sci. U.S.A.* 95, 14991–14996. doi: 10.1073/pnas.95.25.14991

Klementiev, B., Novikova, T., Novitskaya, V., Walmod, P. S., Dmytriyeva, O., Pakkenberg, B., et al. (2007). A neural cell adhesion molecule-derived peptide reduces neuropathological signs and cognitive impairment induced by Abeta25–35. *Neuroscience* 145, 209–224. doi: 10.1016/j.neuroscience.2006.11.060

Kohler, C., Chan-Palay, V., and Wu, J. Y. (1984). Septal neurons containing glutamic acid decarboxylase immunoreactivity project to the hippocampal region in the rat brain. *Anat. Embryol. (Berl.)* 169, 41–44. doi: 10.1007/BF00300585

Kulik, A., Vida, I., Lujan, R., Haas, C. A., Lopez-Bendito, G., Shigemoto, R., et al. (2003). Subcellular localization of metabotropic GABA(B) receptor subunits GABA(B1a/b) and GABA(B2) in the rat hippocampus. *J. Neurosci.* 23, 11026–11035.

Lambert, N. A., Harrison, N. L., Kerr, D. I., Ong, J., Prager, R. H., and Teyler, T. J. (1989). Blockade of the late IPSP in rat CA1 hippocampal neurons by 2-hydroxy-saclofen. *Neurosci. Lett.* 107, 125–128. doi: 10.1016/0304-3940(89)90803-3

Leao, R. N., Colom, L. V., Borgius, L., Kiehn, O., and Fisahn, A. (2012). Medial septal dysfunction by Abeta-induced KCNQ channel-block in glutamatergic neurons. *Neurobiol. Aging* 33, 2046–2061. doi: 10.1016/j.neurobiolaging.2011.07.013

Lott, I. T., and Head, E. (2005). Alzheimer disease and Down syndrome: factors in pathogenesis. *Neurobiol. Aging* 26, 383–389. doi: 10.1016/j.neurobiolaging.2004.08.005

Lujan, R., and Ciruela, F. (2012). GABAB receptors-associated proteins: potential drug targets in neurological disorders? *Curr. Drug Targets* 13, 129–144. doi: 10.2174/138945012798868425

Lujan, R., Maylie, J., and Adelman, J. P. (2009). New sites of action for GIRK and SK channels. *Nat. Rev. Neurosci.* 10, 475–480. doi: 10.1038/nrn2668

Luscher, C., Jan, L. Y., Stoffel, M., Malenka, R. C., and Nicoll, R. A. (1997). G protein-coupled inwardly rectifying K+ channels (GIRKs) mediate postsynaptic but not presynaptic transmitter actions in hippocampal neurons. *Neuron* 19, 687–695. doi: 10.1016/S0896-6273(00)80381-5

Luscher, C., and Slesinger, P. A. (2010). Emerging roles for G protein-gated inwardly rectifying potassium (GIRK) channels in health and disease. *Nat. Rev. Neurosci.* 11, 301–315. doi: 10.1038/nrn2834

Lynch, G., Rose, G., and Gall, C. (1977). Anatomical and functional aspects of the septo-hippocampal projections. *Ciba Found. Symp.* 58, 5–24.

Malcangio, M., and Bowery, N. G. (1994). Spinal cord SP release and hyperalgesia in monoarthritic rats: involvement of the GABAB receptor system. *Br. J. Pharmacol.* 113, 1561–1566. doi: 10.1111/j.1476-5381.1994.tb17174.x

Malouf, A. T., Robbins, C. A., and Schwartzkroin, P. A. (1990). Phaclofen inhibition of the slow inhibitory postsynaptic potential in hippocampal slice cultures: a possible role for the GABAB-mediated inhibitory postsynaptic potential. *Neuroscience* 35, 53–61. doi: 10.1016/0306-4522(90)90119-O

Massone, S., Vassallo, I., Fiorino, G., Castelnuovo, M., Barbieri, F., Borghi, R., et al. (2011). 17A, a novel non-coding RNA, regulates GABA B alternative splicing and signaling in response to inflammatory stimuli and in Alzheimer disease. *Neurobiol. Dis.* 41, 308–317. doi: 10.1016/j.nbd.2010.09.019

McKhann, G., Drachman, D., Folstein, M., Katzman, R., Price, D., and Stadlan, E. M. (1984). Clinical diagnosis of Alzheimer's disease: report of the NINCDS-ADRDA Work Group under the auspices of Department of Health and Human Services Task Force on Alzheimer's Disease. *Neurology* 34,

939–944. doi: 10.1212/WNL.34.7.939

Metz, A. E., Jarsky, T., Martina, M., and Spruston, N. (2005). R-type calcium channels contribute to afterdepolarization and bursting in hippocampal CA1 pyramidal neurons. *J. Neurosci.* 25, 5763–5773. doi: 10.1523/JNEUROSCI.0624-05.2005

Millucci, L., Ghezzi, L., Bernardini, G., and Santucci, A. (2010). Conformations and biological activities of amyloid beta peptide 25–35. *Curr. Protein Pept. Sci.* 11, 54–67. doi: 10.2174/138920310790274626

Moncaster, J. A., Pineda, R., Moir, R. D., Lu, S., Burton, M. A., Ghosh, J. G., et al. (2010). Alzheimer's disease amyloid-beta links lens and brain pathology in Down syndrome. *PLoS ONE* 5:e10659. doi: 10.1371/journal.pone.0010659

Moreno, H., Wu, W. E., Lee, T., Brickman, A., Mayeux, R., Brown, T. R., et al. (2007). Imaging the Abeta-related neurotoxicity of Alzheimer disease. *Arch. Neurol.* 64, 1467–1477. doi: 10.1001/archneur.64.10.1467

Mott, D. D., and Lewis, D. V. (1994). The pharmacology and function of central GABAB receptors. *Int. Rev. Neurobiol.* 36, 97–223. doi: 10.1016/S0074-7742(08)60304-9

Navarro-Lopez, J. D., Alvarado, J. C., Marquez-Ruiz, J., Escudero, M., Delgado-Garcia, J. M., and Yajeya, J. (2004). A cholinergic synaptically triggered event participates in the generation of persistent activity necessary for eye fixation. *J. Neurosci.* 24, 5109–5118. doi: 10.1523/JNEUROSCI.0235-04.2004

Otmakhova, N. A., and Lisman, J. E. (2004). Contribution of Ih and GABAB to synaptically induced afterhyperpolarizations in CA1: a brake on the NMDA response. *J. Neurophysiol.* 92, 2027–2039. doi: 10.1152/jn.00427.2004

Palop, J. J., Chin, J., Roberson, E. D., Wang, J., Thwin, M. T., Bien-Ly, N., et al. (2007). Aberrant excitatory neuronal activity and compensatory remodeling of inhibitory hippocampal circuits in mouse models of Alzheimer's disease. *Neuron* 55, 697–711. doi: 10.1016/j.neuron.2007.07.025

Palop, J. J., and Mucke, L. (2010). Amyloid-beta-induced neuronal dysfunction in Alzheimer's disease: from synapses toward neural networks. *Nat. Neurosci.* 13, 812–818. doi: 10.1038/nn.2583

Peña, F., Ordaz, B., Balleza-Tapia, H., Bernal-Pedraza, R., Marquez-Ramos, A., Carmona-Aparicio, L., et al. (2010). Beta-amyloid protein (25–35) disrupts hippocampal network activity: role of Fyn-kinase. *Hippocampus* 20, 78–96.

Rubio, S. E., Vega-Flores, G., Martinez, A., Bosch, C., Perez-Mediavilla, A., Del, R. J., et al. (2012). Accelerated aging of the GABAergic septohippocampal pathway and decreased hippocampal rhythms in a mouse model of Alzheimer's disease. *FASEB J.* 26, 4458–4467. doi: 10.1096/fj.12-208413

Sago, H., Carlson, E. J., Smith, D. J., Kilbridge, J., Rubin, E. M., Mobley, W. C., et al. (1998). Ts1Cje, a partial trisomy 16 mouse model for Down syndrome, exhibits learning and behavioral abnormalities. *Proc. Natl. Acad. Sci. U.S.A.* 95, 6256–6261. doi: 10.1073/pnas.95.11.6256

Sah, P., and Faber, E. S. (2002). Channels underlying neuronal calcium-activated potassium currents. *Prog. Neurobiol.* 66, 345–353. doi: 10.1016/S0301-0082(02)00004-7

Santos-Torres, J., Fuente, A., Criado, J. M., Riolobos, A. S., Heredia, M., and Yajeya, J. (2007). Glutamatergic synaptic depression by synthetic amyloid beta-peptide in the medial septum. *J. Neurosci. Res.* 85, 634–648. doi: 10.1002/jnr.21150

Scanziani, M., Gahwiler, B. H., and Thompson, S. M. (1991). Paroxysmal inhibitory potentials mediated by GABAB receptors in partially disinhibited rat hippocampal slice cultures. *J. Physiol.* 444, 375–396.

Schneiderman, J. H., Cairns, A., and Sterling, C. A. (1992). Evoked CA3 field potentials corresponding to both EPSPs and IPSPs in hippocampal slice. *Brain Res.* 569, 287–294. doi: 10.1016/0006-8993(92)90641-L

Siarey, R. J., Carlson, E. J., Epstein, C. J., Balbo, A., Rapoport, S. I., and Galdzicki, Z. (1999). Increased synaptic depression in the Ts65Dn mouse, a model for mental retardation in Down syndrome. *Neuropharmacology* 38, 1917–1920. doi: 10.1016/S0028-3908(99)00083-0

Sotty, F., Danik, M., Manseau, F., Laplante, F., Quirion, R., and Williams, S. (2003). Distinct electrophysiological properties of glutamatergic, cholinergic and GABAergic rat septohippocampal neurons: novel implications for hippocampal rhythmicity. *J. Physiol.* 551, 927–943. doi: 10.1113/jphysiol.2003.046847

Sperling, R. A., LaViolette, P. S., O'Keefe, K., O'Brien, J., Rentz, D. M., Pihlajamaki, M., et al. (2009). Amyloid deposition is associated with impaired default network function in older persons without dementia. *Neuron* 63, 178–188. doi: 10.1016/j.neuron.2009.07.003

Spruston, N., and Johnston, D. (1992). Perforated patch-clamp analysis of the passive membrane properties of three classes of hippocampal neurons. *J. Neurophysiol.* 67, 508–529.

Stewart, M., and Fox, S. E. (1990). Do septal neurons pace the hippocampal theta rhythm? *Trends Neurosci.* 13, 163–168. doi: 10.1016/0166-2236(90)90040-H

Sutor, B., and Luhmann, H. J. (1998). Involvement of GABA(B) receptors in convulsant-induced epileptiform activity in rat neocortex *in vitro*. *Eur. J Neurosci.* 10, 3417–3427. doi: 10.1046/j.1460-9568.1998.00351.x

Swanberg, M. M., Tractenberg, R. E., Mohs, R., Thal, L. J., and Cummings, J. L. (2004). Executive dysfunction in Alzheimer disease. *Arch. Neurol.* 61, 556–560. doi: 10.1001/archneur.61.4.556

Varadarajan, S., Kanski, J., Aksenova, M., Lauderback, C., and Butterfield, D. A. (2001). Different mechanisms of oxidative stress and neurotoxicity for Alzheimer's A beta(1–42) and A beta(25–35). *J. Am. Chem. Soc.* 123, 5625–5631. doi: 10.1021/ja010452r

Verret, L., Mann, E. O., Hang, G. B., Barth, A. M., Cobos, I., Ho, K., et al. (2012). Inhibitory interneuron deficit links altered network activity and cognitive dysfunction in Alzheimer model. *Cell* 149, 708–721. doi: 10.1016/j.cell.2012.02.046

Villette, V., Poindessous-Jazat, F., Bellessort, B., Roullot, E., Peterschmitt, Y., Epelbaum, J., et al. (2012). A new neuronal target for beta-amyloid peptide in the rat hippocampus. *Neurobiol. Aging* 33, 1126–1114. doi: 10.1016/j.neurobiolaging.2011.11.024

Villette, V., Poindessous-Jazat, F., Simon, A., Lena, C., Roullot, E., Bellessort, B., et al. (2010). Decreased rhythmic GABAergic septal activity and memory-associated theta oscillations after hippocampal amyloid-beta pathology in the rat. *J. Neurosci.* 30, 10991–11003. doi: 10.1523/JNEUROSCI.6284-09.2010

Wang, Y., Zhang, G., Zhou, H., Barakat, A., and Querfurth, H. (2009). Opposite effects of low and high doses of Abeta42 on electrical network and neuronal excitability in the rat prefrontal cortex. *PLoS ONE* 4:e8366. doi: 10.1371/journal.pone.0008366

Washburn, M. S., and Moises, H. C. (1992a). Inhibitory responses of rat basolateral amygdaloid neurons recorded *in vitro*. *Neuroscience* 50, 811–830. doi: 10.1016/0306-4522(92)90206-H

Washburn, M. S., and Moises, H. C. (1992b). Muscarinic responses of rat basolateral amygdaloid neurons recorded *in vitro*. *J. Physiol.* 449, 121–154.

Wickman, K., Karschin, C., Karschin, A., Picciotto, M. R., and Clapham, D. E. (2000). Brain localization and behavioral impact of the G-protein-gated K+ channel subunit GIRK4. *J. Neurosci.* 20, 5608–5615.

Widmer, H., Ferrigan, L., Davies, C. H., and Cobb, S. R. (2006). Evoked slow muscarinic acetylcholinergic synaptic potentials in rat hippocampal interneurons. *Hippocampus* 16, 617–628. doi: 10.1002/hipo.20191

Wittner, L., Henze, D. A., Zaborszky, L., and Buzsaki, G. (2007). Three-dimensional reconstruction of the axon arbor of a CA3 pyramidal cell recorded and filled *in vivo*. *Brain Struct. Funct.* 212, 75–83. doi: 10.1007/s00429-007-0148-y

Wyss, J. M., Swanson, L. W., and Cowan, W. M. (1980). The organization of the fimbria, dorsal fornix and ventral hippocampal commissure in the rat. *Anat. Embryol. (Berl.)* 158, 303–316. doi: 10.1007/BF00301819

Yajeya, J., De La Fuente, A., Criado, J. M., Bajo, V., Sanchez-Riolobos, A., and Heredia, M. (2000). Muscarinic agonist carbachol depresses excitatory synaptic transmission in the rat basolateral amygdala *in vitro*. *Synapse* 38, 151–160.

Conflict of Interest Statement: The authors declare that the research was conducted in the absence of any commercial or financial relationships that could be construed as a potential conflict of interest.

Received: 19 April 2013; accepted: 05 July 2013; published online: 25 July 2013.
Citation: Nava-Mesa MO, Jiménez-Díaz L, Yajeya J and Navarro-Lopez JD (2013) Amyloid-β induces synaptic dysfunction through G protein-gated inwardly rectifying potassium channels in the fimbria-CA3 hippocampal synapse. Front. Cell. Neurosci. 7:117. doi: 10.3389/fncel.2013.00117